

**ROMP-Derived Alkylating Reagents and Scavengers:
Application in Library Development and Sequestration**

By

Saqib Faisal

Submitted to the graduate degree program in Department of Chemistry and the
Graduate Faculty of the University of Kansas in partial fulfillment of the
requirements of the degree of Doctor of Philosophy

Paul R. Hanson, Chair

Jon A. Tunge

Michael Rubin

Thomas E. Prisinzano

Helena C. Malinakova

Date Defended: October 19th 2016

The Dissertation Committee for Saqib Faisal certifies that this is
the approved version of the following dissertation:

**ROMP-Derived Alkylating Reagents and Scavengers:
Application in Library Development and Sequestration**

Paul R. Hanson, chair

Date Approved: October 19th 2016

Abstract

Saqib Faisal

Department of Chemistry

University of Kansas, Oct. 19th 2016

The overarching goal of this dissertation is the development and utilization of (ring-opening metathesis polymerization) ROMP-derived high load phosphorus- and sulfur-based soluble, silica and magnetic alkylating reagents and scavengers. Chapter one begins with a brief introduction of solid phase and solution phase organic synthesis, and next describes the advances in soluble-, silica- and magnetic-immobilized reagents, with a few applications in flow chemistry. Chapter one also outlines the advances in ROMP technology for the synthesis of polymeric soluble, silica and magnetic materials for use as reagents, scavengers and catalysts.

Chapter 2 begins with a brief review of immobilized alkylating reagents and next describes the development and utilization of soluble high load ROMP-derived oligomeric triazole phosphates (OTP_n) for the efficient (triazolyl)methylation of nucleophilic species in purification free protocols. Chapter 2 finishes with a description of library efforts using a purification-free route that combines MACOS scale-out and ROMP-derived oligomeric triazole phosphates (OTP_n) for the generation of a 106-member library of triazole-containing benzothioxazepine-1,1-dioxides.

In Chapter 3, the first section describes the use of ROMP technology to aid in the development of high-load hybrid silica oligomeric phosphates based alkylating reagents, and their applications for facile benzylation and (triazolyl)methylating of *N*-, *O*- and *S*-

containing nucleophilic species. The surface initiated ROMP reaction of Nb-tagged silica particles and functionalized Nb-tagged monomers efficiently yields high-load, hybrid Si-ROMP benzylating (Si-OBP) and (triazolyl)methylating (Si-OTP) reagents. The second section, describes the application of the developed silica-immobilized alkylating reagents in one-pot sequential protocols for diversification of benzothioxazepine-1,1-dioxides analogues. The last section of Chapter 3 outlines the synthesis of high-load, hybrid silica-immobilized heterocyclic benzyl phosphate (Si-OHBP) and triazolyl phosphate (Si-OHTP) alkylating reagents for efficient hetero-benzylation and hetero-(triazolyl)methylation and their application in purification-free protocols, which diversify various nucleophilic species.

Chapter 4 describes the development and utilization of recyclable magnetic ROMP-derived alkylating reagents and scavengers, immobilized on Co/C magnetic nanoparticles via surface-initiated ROM polymerization. The first section 4.1 outlines the development and application of a high-load magnetic Co/C ROMP-derived oligomeric benzenesulfonate ester Co/C-OBSE_n, as an efficient methylating reagent for a variety of carboxylic acids. In addition, an in situ method of methylation/alkylation was developed using Co/C benzenesulfonyl chloride Co/C-OBSC_n and corresponding ROH. The desired alkylated products were isolated by simple magnetic decantation and filtration and the spent byproduct magnetic benzenesulfonic acid Co/C-OBSA_n was successfully recycled and re-used up to ten times without considerable loss of magnetic material.

Section 4.2 details the synthesis and utilization of high-load hybrid magnetic oligomeric phosphonyl dichloride Co/C-OPC_n as an efficient scavenger of amines. The magnetic Co/C-OPC_n scavenger is employed in amide formations, sulfonylations and

urea formations using a variety of amines (used in excess). The coupling products were isolated by simple magnetic decantation and filtrations of reaction mixture. The spent magnetic scavenger was easily isolated by external magnetic decantation and its regeneration is in progress.

In dedication to my Parents and Family for their Prayers and Support

Acknowledgments

First, I would like to thank my God for providing me good health to achieve the goals of my life. I would like to thank my family members; especially mother, father, brothers and sisters for their prayers and kind support throughout this entire journey. Their encouragement and support helped me to move forward through out my entire career. This was an incredible journey of learning and renewal of my long-time passion for the sciences. I would like to thank my respectable wife Muzna for her love, support, caring, making delicious foods almost everyday, and helping me stay focused on my graduate studies in the last 5 years. I would like to thank my son Ashaz for providing me enjoyment and keeping me fresh everyday.

I would especially like to thank my advisor Professor Paul R. Hanson for his kind support and guidance for everything during the years at KU. Paul you taught me many things, and I am very grateful for everything that you have done for me and still doing it. I am so glad that I worked with you as my Ph.D. advisor and Thank you for teaching me not to give up under any circumstances. I will always remember your motivations and encouragements during numerous regular or emergency meetings and I learned a lot in these meetings. It has been a great experience to work with you in a group of diverse peoples, where I learned many skills from you as well as from different cultures. I would also like to thank Dr. Yumi for being very kind and supportive during my PhD. and she taught me many scientific and professional skills. In addition, I would also like to thank her for providing us fish or Veg. foods during thanksgiving, Christmas and other parties at home. I would also like to acknowledge Paul's parents for treating us as a family.

I would also like to acknowledge my thesis committee members: Professors Jon Tunge, Michael Rubin, Helena Malinakova and Thomas E. Prisinzano for their help and guidance during my Ph.D. In addition, I would also like to thank other research groups in Malott Hall, including all of the Tunge, Rubin, Malinakova, Clift, Givens, Prisinzano and Altman group members.

I would like to thank all of the past and current Hanson group members for their support. I would like to thank current post docs including Qing Zang, Jessica Torres, and Jung Ho, for their help, guidance and providing me useful feedback during my practice talks, oral proposal and reviewing thesis. I would like to thank Dr. Pradip K. Maity for his cooperation, teamwork and help regarding my entire research at KU. I would like to thank all current students in Hanson group including, Salim Javed, Andie, Maria, Gihan, Corn, Arghya, Viena and Jay (for reviewing my thesis chapters) and for useful discussion in all aspects of chemistry and lab work. I would like also to thank all the former group members including Alan Rolfe, Thiwanka B. Samarakoon, Toby Long, Chris Thomas, Naeem Asad, Ryan Kurtz, Rambabu and Mahipal, Kashif, Moon, and Phanindra for their guidance and help during my PhD. I would like to thank my undergrad Robby Sourk for his hard work and contribution to my research.

I would especially like to thank Dr. Patrick Kearney for his kind help with so many things and for his useful suggestion and guidance during ROMP meetings. I really appreciate what you have done for me, regarding research ideas as well as during my research talk and thesis dissertation. I would also like to thank Dr. Diana Stoianova for her useful suggestion, guidance and contribution to my research. Also I would like to acknowledge Materia Inc. for providing us metathesis catalyst.

I would especially like to thank and acknowledge Professor Dr. Fatima Bahsa and Dr. Anwar Basha, for providing me opportunities to contribute in the research at KU. Its all become possible because of their kind help and support in all aspect of my career. I would also like to thank all Professors at HEJ research institute especially Professor Dr. Iqbal Choudhary for providing me scientific opportunities at HEJ research institute. I would like to thank all Professors at Chemistry Department Karachi University.

Lastly, a special thanks to Dr. Justin Douglas and Sarah Neuenswander for their help in NMR experiments and data interpretation and Dr. Gerald Lushington, Patrick Porubsky and Ben Neuenswander for providing tremendous help with both purification and in-silico-analysis of my compounds. I would like to acknowledge Dr. Prem Thapa and Ms. Heather Shinogle for carrying out SEM analysis. I would like to acknowledge our front office staffs, Susan, Beth, Beverly, Ruben, Deanne, Elaine, Elizabeth, Jan, Danny and Donnie for their help. I would like to acknowledge the staffs of HBC grant service. I would like to acknowledge the cricket club members providing us a fun activity every Sunday.

ROMP-Derived Alkylating Reagents and Scavengers: Application in Library Development and Sequestration

TABLE OF CONTENTS	Page #
Abstract	iii
Dedication Page	vi
Acknowledgments	vii
Table of Contents	x
Abbreviations	xiv
Chapter 1: Advances in Immobilized Reagents, Scavengers and Catalysts:	
Applications in Chemical Synthesis	1
1.1 Introduction	2
1.1.1 Solid-Phase and Solution Phase Synthesis	3
1.2 Advances in Immobilized Reagents and their Application in Flow Chemistry	4
1.3 Advances in Silica-Supported Reagents and Catalysts	9
1.4 Advances in Magnetic Reagents and Catalysts	14
1.5 ROMP-Derived Oligomeric Reagents, Scavengers and Catalyst	19
1.6 Conclusion	32
References	34
Chapter 2: High Load Soluble ROMP-Derived Oligomeric Alkylating Reagents and their Application in Library Synthesis	54
Section: 2.1	
“Click”-Capture, Ring-Opening Metathesis Polymerization (ROMP), Release: Facile Triazolation Utilizing ROMP-Derived Oligomeric Phosphates	
2.1.1 Introduction	55
2.1.2 Results and Discussion	58

Section: 2.2

Facile (Triazolyl)methylation of MACOS-derived Benzofused Sultams Utilizing ROMP-derived OTP Reagents.

2.2.1 Introduction	63
2.2.2 Results and Discussion	64
2.2.3 Special Acknowledgment	71
References	72

Chapter 3: High Load Hybrid Si-ROMP Alkylating Reagents: Development and Applications in Library Synthesis and One-Pot Protocols 80**Section 3.1**

Synthesis and Development of Si-OBP and Si-OPT as Alkylating Reagents

3.1.1 Introduction	81
3.1.2 Results and Discussion	83

Section: 3.2

Application of Silica-Supported Alkylating Reagents in a One-Pot Protocol for the Synthesis of Diverse Benzoxathiazepine 1,1-Dioxides.

3.2.1 Introduction	91
3.2.2 Results and Discussion	93

Section 3.3

Synthesis of High-load, Hybrid Silica-immobilized Heterocyclic Benzyl Phosphate (Si-OHBP) and Triazolyl Phosphate (Si-OHTP) Alkylating Reagents.

3.3.1 Introduction	97
3.3.2 Results and Discussion	98
3.3.3 Special Acknowledgment	104
References	105

Chapter 4: High Load Hybrid Co/C-Magnetic ROMP-Derived Alkylating Reagents and Scavengers 121

Section: 4.1

Recyclable Magnetic Co/C Hybrid ROMP Benzenesulfonate Ester (Co/C-OBSE) and Benzenesulfonyl Chloride (Co/C-OBSC) Nanoparticles as Facile Methylating/Alkylating Reagent: Development and Applications

4.1.1 Introduction 120

4.1.2 Results and Discussion 124

Section: 4.2

Synthesis of High-load, Hybrid Co/C-Oligomeric Phosphonyl Dichloride: Application to Scavenging Amines

4.2.1 Introduction 132

4.2.2 Results and Discussion 133

4.3 Special Acknowledgment 136

References 137

Chapter 5: Experimentals and Spectra for Chapter 2–4

5.1 General Experimental Methods 144

5.2 Experimentals for Chapter 2.1 146

5.3 Spectra for Chapter 2.1 174

5.4 Experimental for Chapter 2.2 216

5.5 Spectra for Chapter 2.2 234

5.5.1 Library Data Set –Thiadiazepin-1,1-dioxide 4-ones 250

5.6 Experimental for Chapter 3.1 253

5.7 Spectra for Chapter 3.1 270

5.8 Experimental for Chapter 3.2 295

5.9 Spectra for Chapter 3.2 311

5.10 Experimental for Chapter 3.3 326

5.11 Spectra for Chapter 3.3 338

5.12 Experimental for Chapter 4.1 357

5.13 Spectra for Chapter 4.1 363

5.14 Experimental for Chapter 4.2	373
5.15 Spectra for Chapter 4.2	378

Abbreviations

AAS	atomic absorption spectroscopy
Ar	aryl
Bn	benzyl
BOC	<i>tert</i> -butoxycarbonyl
Cat	catalyst
CDI	carbodiimide
CM	cross-metathesis
Co/C	cobalt/carbon
Cy	cyclohexyl
DCC	1,3-dicyclohexylcarbodiimide
DCE	dichloroethane
DEAD	diethyl azodicarboxylate
DMAP	4-dimethylaminopyridine
DME	1,2-dimethoxyethane
DMF	<i>N,N</i> -dimethylformamide
DMSO	dimethylsulfoxide
ee	enantiomeric excess
equiv	equivalent
EVE	ethyl vinyl ether
GC	gas chromatography
G-I	first generation Grubbs catalysts
G-II	second generation Grubbs catalysts
HPLC	high-performance liquid chromatography
MACOS	microwave-assisted, continuous flow organic synthesis
<i>m</i> -CPBA	metachloroperoxy benzoic acid
Mes	mesityl
MS	mass spectrometry
Nb	norbornene
NMI	<i>N</i> -methylimidazole
NMR	nuclear magnetic resonance

NPs	nanoparticle
OACC	oligomeric alkyl cyclohexyl carbodiimide
OBAC	
OBP	oligomeric benzyl phosphate
OBSA	oligomeric benzenesulfonic acid
OBSC	oligomeric benzenesulfonyl chloride
OBSE	oligomeric benzenesulfonate ester
OHBP	oligomeric heterobenzyl phosphates
OHTP	heterotriazolyl phosphates
OPC	oligomeric phosphonyl dichloride
OTP	oligomeric triazole phosphate
OTPP	oligomeric triphenylphosphine
PASP	polymer-assisted solution phase
PEG	polyethylene glycol
PEPPSI [™]	Pyridine-Enhanced Precatalyst Preparation Stabilization and Initiation.
PS	polystyrene
quant	quantitative
RCM	ring-closing metathesis
ROM	ring-opening metathesis
ROMP	ring-opening metathesis polymerization
rt	room temperature
SEM	scanning electron microscopy
S _N 2	bimolecular nucleophilic substitution
SPE	solid-phase extraction
SPOS	solid-phase organic synthesis
SPION	superparamagnetic iron oxide nanoparticles
TEM	transmission electron microscopy
TFA	trifluoroacetic acid
TFAA	trifluoroacetic anhydride
THF	tetrahydrofuran
TLC	thin layer chromatography
TMS	trimethylsilyl

Chapter 1

Advances in Immobilized Reagents, Scavengers and Catalysts:
Applications in Chemical Synthesis

1.1 Introduction

The development of new green technologies that enable the facile assembly of small molecules in an economical and safe manner is a key factor in driving modern synthesis and drug discovery and development efforts.¹ In particular, development and utilization of immobilized technologies for carrying out synthesis in a more sustainable manner, which minimize the use of toxic reagents and facilitate recovery and recycling of expensive reagents, is an important and continually emerging area of modern day synthesis.² Immobilized platforms have not only enabled automated synthesis, but also more recently have had a major impact in flow-through technologies.³ A wide range of immobilized reagents and scavengers have been developed for the facilitated synthesis of small molecules. Despite these advancements, limitations exist, and improvement in load levels, synthetic efficiency, recyclability, and cost-effectiveness continues to drive innovation in the field.

It is the purpose of this introductory chapter to highlight recent advancements in the area of polymer-supported technologies, with an emphasis on immobilized reagents, including silica and magnetic reagents, scavengers and catalysts. Chapter 1 will be concluded with an introduction to ring-opening metathesis (ROMP) technologies that are at the heart of this dissertation work. Chapter 2, 3 and 4 will detail work carried out in this dissertation regarding the use of ROM polymerization to generate soluble, silica supported and magnetic alkylating agents and scavenging agents, respectively. In addition, throughout chapters 1–4, employment of these reagents in generating molecular libraries will be discussed.

1.1.1 Solid-Phase and Solution Phase Synthesis

The introduction of solid-phase synthesis by Bruce Merrifield and coworkers in 1963,⁴ has impacted a number of fields, including organic chemistry, medicinal chemistry, and automated technologies.⁵ This pioneering work of Merrifield not only enabled new facilitated approaches in peptide chemistry,⁶ but also played a significant role in the generation of complex natural products⁷ and new synthetic materials.⁸

Conventional solid-phase synthesis offers many benefits, which include: (i) enabling use of excess reagents to drive reactions to completion, (ii) elimination of chromatographic separations for compound purification via simple filtration, (iii) the safer handling of toxic materials through immobilization onto solid supports, and (iv) automation of optimized high-utility chemical reactions (Figure 1.1.1).

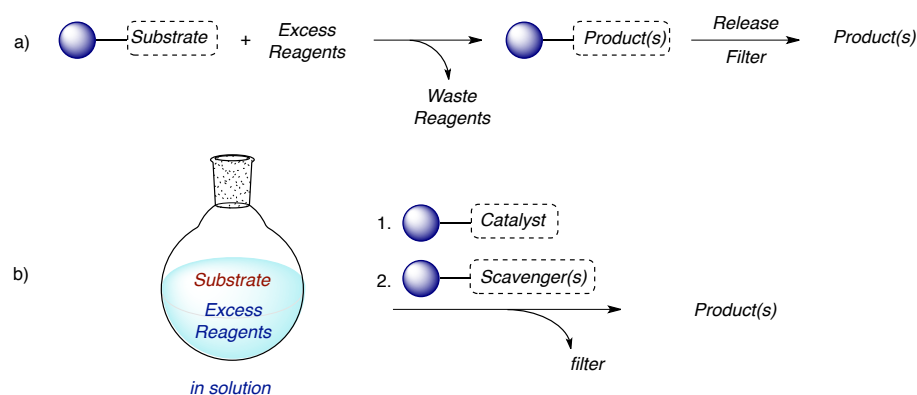


Figure 1.1.1: (a) *Solid Phase Organic Synthesis* (b) *Polymer-Assisted Solution Phase Synthesis*

In addition to aforementioned advantages, polymer-assisted solution phase (PASP) synthesis⁹ has disclosed a new paradigm shift in drug discovery. Compared to solid-phase synthesis, reagent-supported solution-phase synthesis offers benefits that allow simplification of synthetic processes including, heterogeneous reaction

conditions (improved reaction kinetics), reaction monitoring, as well as isolation and purification of intermediates and products.¹⁰ These attributes allow the expanded use of nearly the entire repertoire of organic reactions, and have several ideal features, including: (i) ease of reaction monitoring using conventional techniques such as TLC, NMR, and LC-MS; (ii) no additional steps are needed to attach and cleave substrate from solid support; (iii) overcoming the limitations of non-linear reaction kinetics; (iv) commercial availability of immobilized reagents, catalysts, and scavengers;¹¹ (v) facilitate cleaner and safer reactions through immobilization of toxic materials;¹² (vi) possible recovery of the spent reagent; and (vii) enabling of the synthesis of libraries of small molecules in desirable quantities.¹³ Immobilized reagents have been extensively used in flow-through processes to perform multistep reactions.

1.2 Advances in Immobilized Reagents and their Application in Flow Chemistry

The application of polymer-supported reagents has steadily increased over the last several decades and has become persistent to play a key role in facilitated synthesis of small-molecules. A variety of platforms have been developed for immobilization including, polystyrene resins,¹⁴ silicas,¹⁵ fluororous-tagged compounds,¹⁶ monoliths,¹⁷ and soluble polyethylene glycol (PEG)¹⁸ to remove impurities and excess reagents from reaction mixtures. These immobilized reagents and scavengers have provided ease of synthesis to eliminate time-consuming chromatographic separations and have been used frequently in the arena of facilitated synthesis and high-throughput chemistry,¹⁹ as well as in the scale-up of advanced pharmaceutical intermediates.²⁰ Again, limitations continue to drive improvement,

such as: (i) enhancing the load, (ii) increasing the synthetic efficiency and thus reducing the reaction time, (iii) removing toxic reagents/metals, (iv) ensuring recyclability of reagents, (v) the cost-effectiveness of the process, and (vi) utilization in one-pot processes.

Polymer-supported reagents are continuing to make a significant impact in flow-through technologies, whereby a variety of polymer-supported reagents, catalysts, and scavengers have been employed through the use of micro-scale reactors for the preparation of small molecules and natural products, and thus become quite popular in both academia and the pharmaceutical industry.³ Among several seminal players, Ley,²¹ Kirschning,²² Baxendale,²³ Seeberger,²⁴ Kobayashi,²⁵ and Jamison²⁶ are among the most prolific, and have demonstrated a wide array of polymer-assisted solution phase (PASP) based techniques via continuous-flow synthetic methodologies as outlined in Figure 1.2.1. A number of beautifully written reviews and thematic issues have highlighted the myriad advancements in the field^{27,3} and five representative examples are noted below.

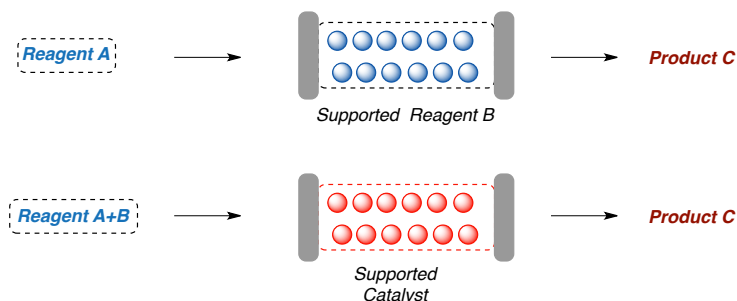
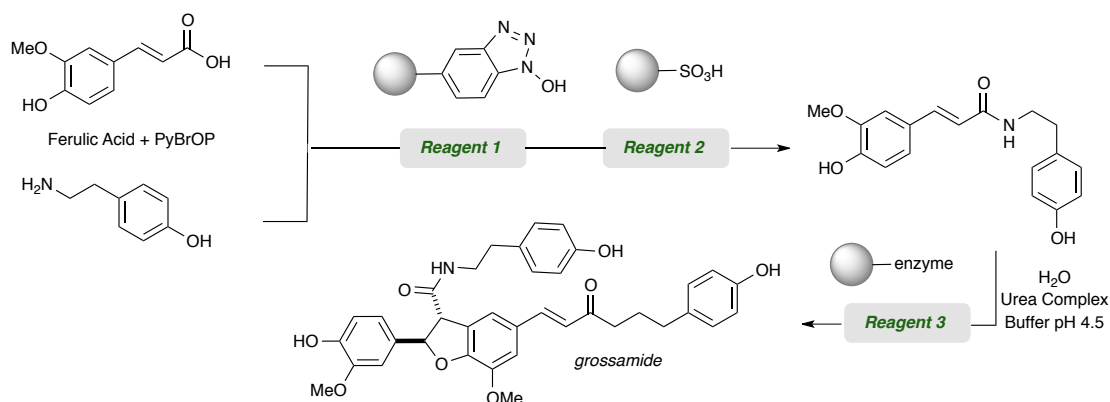


Figure 1.2.1 *Application of Supported Reagents and Catalyst in Continuous Flow Systems.*

In 2006, Ley and coworkers reported the use of flow-chemistry in the first total synthesis of the neolignan natural product grossamide²⁸ (Scheme 1.2.1). This early synthesis was achieved via amide-bond coupling of ferulic acid with tyramine using a pre-packed column of polymer-supported HOBt (PS-HOBt), and the use of sulfonic acid resin to scavenge out excess amine.

Scheme 1.2.1 *Flow-through Synthesis of Grossamide.*



In 2010, Reiser and coworker reported the first example of immobilized magnetic Co/C nanoparticles for the kinetic resolution of racemic 1,2-diphenylethane-1,2-diol via asymmetric monobenzylation.²⁹ The carbon-coated Co/C nanoparticles were tagged with azabis(oxazoline)-Cu(II) complexes utilizing a CuI-catalyzed azide/alkyne cycloaddition reaction. The semi-heterogeneous catalyst was employed under batch conditions as well as in continuous flow processes (Figure 1.2.2). The magnetic decantation of nano-beads allowed recycling of magnetic reagent not only in the batch reactions, but also in the continuous flow-reactor system.

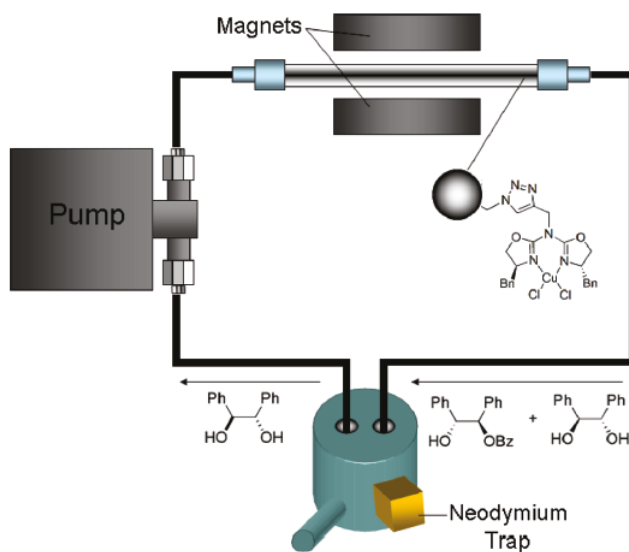


Figure 1.2.2 Representation of a Closed Circuit Type Reactor For the Asymmetric Monobenzylation of Racemic Diol.

In 2012, Ley and coworkers developed a novel monolith-supported synthetic procedure,³⁰ taking advantage of flow processing, to allow facile access to a useful family of 2-aminopyrimidine analogues (Figure 1.2.3). This “Catch-React-Release” process has been successfully applied to generate a key precursor en route to the kinase inhibitor Imatinib (Ar = 3-pyridyl, R¹ = 2-methyl-5-nitrobenzyl, R² = H).

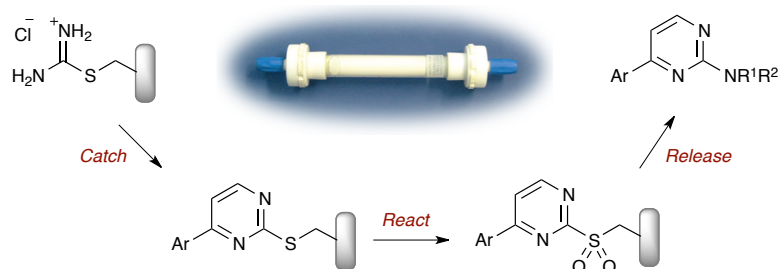
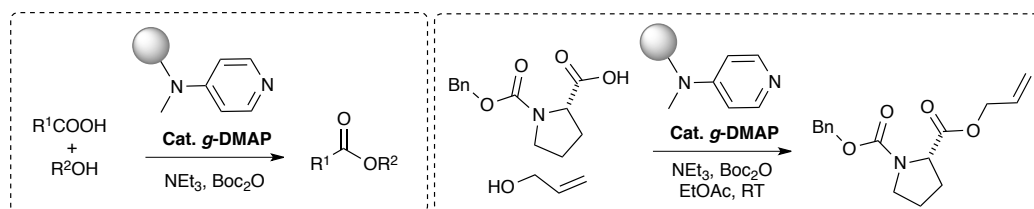


Figure 1.2.3 Synthesis of 2-aminopyrimidines Using Monolith-Supported Flow Systems.

In 2015, Takeda and coworkers reported an application of polyethylene-g-polyacrylic acid-immobilized dimethylaminopyridine (g-DMAP) as a catalyst in a continuous-flow system for decarboxylative esterification (Scheme 1.2.2).³¹ This

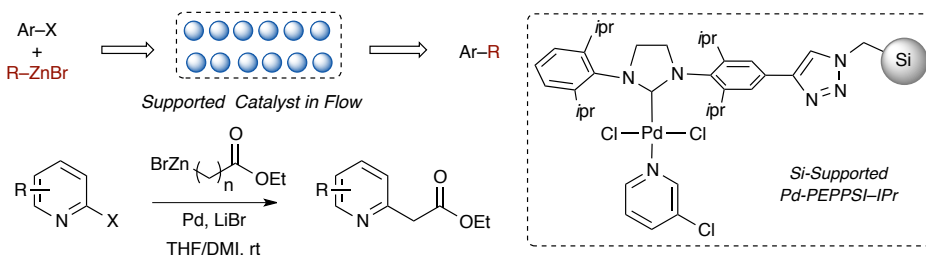
example described a convenient and simple esterification using *di-tert*-butyl anhydride (Boc_2O) as a coupling reagent in a continuous-flow system, which afforded decarboxylative esterification with carboxylic acids and alcohols. The reaction time was reduced in this esterification reaction in continuous-flow conditions, because of the use of polymer-supported catalyst.

Scheme 1.2.2 *Supported (g-DMAP) Catalyst in Continuous-flow System for Decarboxylative Esterification*



In 2016, Organ and coworkers reported continuous flow Negishi cross-couplings employing silica-supported Pd-PEPPSI-IPr precatalyst (Scheme 1.2.3).³² The prepared triethoxysilyl functionalized Pd-PEPPSI-IPr complex was found to be active in Negishi cross-coupling reactions under batch and continuous flow conditions. The supported-catalyst afforded moderate to excellent yields of coupled product with various functionalized alkyl zinc reagents and aryl halides. The catalyst was successfully recycled at least five times with minimal loss in activity.

Scheme 1.2.3 *Negishi Cross Couplings Employing Si-Supported Pd-PEPPSI-IPr Pre-Catalyst in Flow.*



Overall, flow-technology is very adaptable to integration with various immobilized platforms, including, polymer supported reagents, scavengers or catalysts for multistep synthesis of scaffolds. This combination is continually evolving and enabling the development of fully automated processes with an increased efficiency and improved sustainability in many synthetic approaches. The utilization of supported components packed into simple columns or reactor cartridges, makes it possible to perform multistep organic sequences with the benefit of purifications.

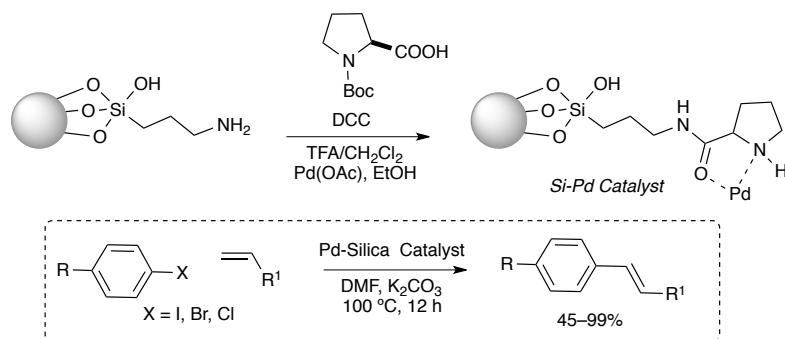
1.3 Advances in Silica-Supported Reagents and Catalysts:

Silica-supported technologies for the immobilization of reagents and catalysts have also emerged as an attractive source of attachment for the development of hybrid silica (SiO_2) supported materials.³³ The reaction with tris(alkoxy)silanes not only provides a practical route to silica-immobilized reagents/scavengers/catalysts, but also serves to provide linkers for a variety of desired functional handles.³⁴ A range of commercial materials has shown the use of silica as a prominent solid-phase support, and impressive progress has been reported regarding silica-supported reagents in the last decade.¹⁵ Efforts in this area have highlighted a number of benefits regarding purification, filtration, easy separation, and stability of supported materials.

In 2008, Li and coworkers demonstrated an efficient and recyclable Pd-catalyst hybrid material anchored on a silica surface, and employed this catalyst in a Heck coupling reaction (Scheme 1.3.1).³⁵ The corresponding cross-coupling

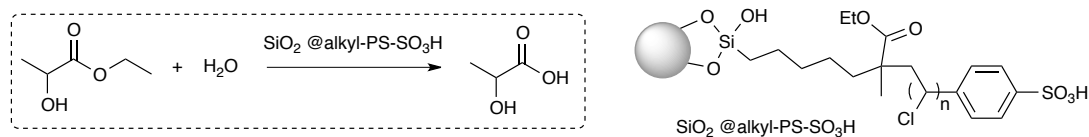
products were achieved in good to excellent yields under phosphine- and amine-free reaction conditions. Furthermore, the silica-supported Pd-catalyst was recovered by simple filtration of the reaction solution and reused for several consecutive trials without considerable loss of its catalytic activity.

Scheme 1.3.1: *Synthesis and Utilization of Silica-Supported Pd-Catalyst.*



In 2011, Jones and coworkers reported polymer-oxide hybrid materials based on nonporous silica-supported sulfonic acid-containing polymer for their application in ester hydrolysis.³⁶ The catalysts were evaluated for the hydrolysis of ethyl lactate, with the hybrid sulfonic acid materials having the same activity as a homogeneous catalyst, *p*-toluenesulfonic acid, and observed more activity than acidic polymer resin (Amberlyst 15). The heterogeneous nature of the catalyst facilitated recovery and recycling of the spent reagent (Scheme 1.3.2).

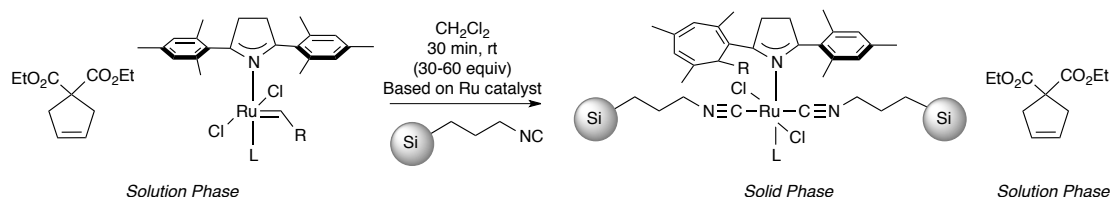
Scheme 1.3.2: *Silica-Supported Sulfonic Acid-Containing Polymer*



In 2013, Diver and coworkers reported a novel silica gel-supported isocyanide ligand to destroy active metathesis catalysts and to remove ruthenium byproducts

from metathesis reactions (Scheme 1.3.3).³⁷ This isocyanide-grafted silica gel successfully reduced the concentration of remaining ruthenium from the reaction mixture for several alkene and enyne metathesis reactions, requiring simply filtration, in combination with chromatography, to further reduce the levels of residual Ru.

Scheme 1.3.3: *Silica-Supported Isocyanide Ligand.*



In 2013, Davies and coworkers demonstrated a silica-supported dirhodium(II) tetraproline catalyst (Figure 1.3.1) for enantioselective carbenoid reactions.³⁸ This catalyst was prepared from L-proline and used for various enantioselective transformations of donor/acceptor carbenoids, which include cyclopropanation, cyclopropanation, tandem ylide formation [2,3] sigmatropic rearrangement, and C–H functionalization reactions. The products were obtained in comparable yields to those produced with the homogeneous counterpart, $\text{Rh}_2(\text{S-DOSP})_4$. In addition, the silica-immobilized chiral dirhodium $\text{Rh}_2(\text{S-DOSP})_4$ was successfully recycled.

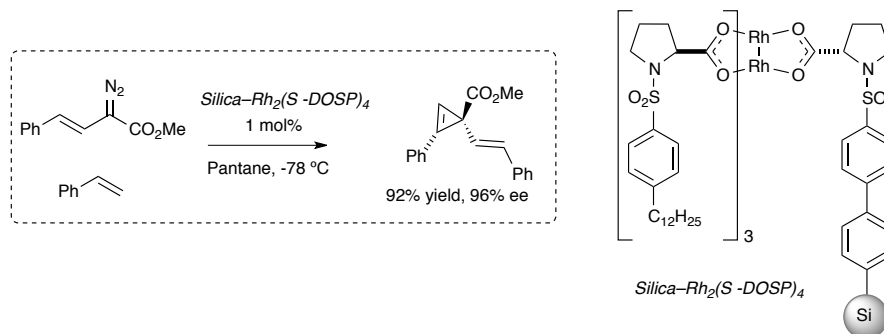


Figure 1.3.1: *Silica-Supported Dirhodium(II) Tetraproline Catalyst.*

In 2013, Schrock and coworkers reported, a silica-supported tungsten oxo-alkylidene complex (Figure 1.3.2) for its application as an alkene metathesis catalyst.³⁹ The well-defined oxo-alkylidene surface complex $[(\equiv\text{SiO})\text{W}(=\text{O})(=\text{CHtBu})\text{OAr}]$ is prepared by surface organometallic chemistry and displayed unprecedented activity at room temperature in the metathesis of alkenes. This catalyst was found to be the most active heterogeneous metathesis catalysts in the self-metathesis of *cis*-4-nonene and ethyl oleate.

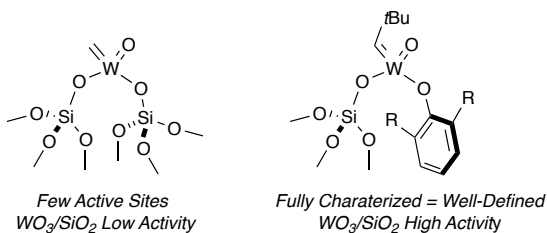
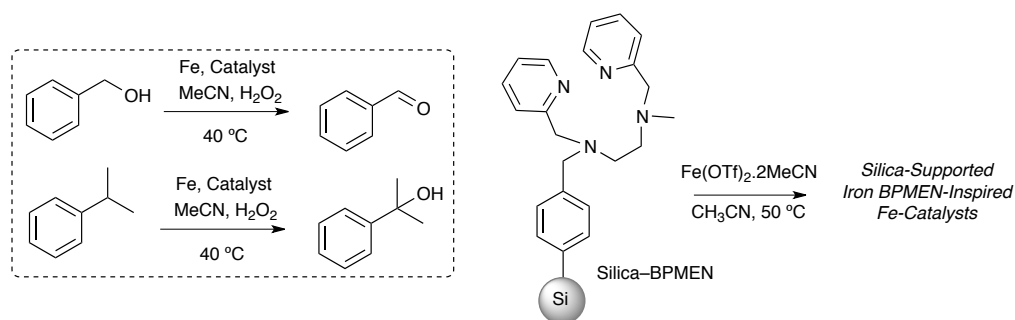


Figure 1.3.2: Silica-Supported Tungsten Oxo Alkylidene Complex.

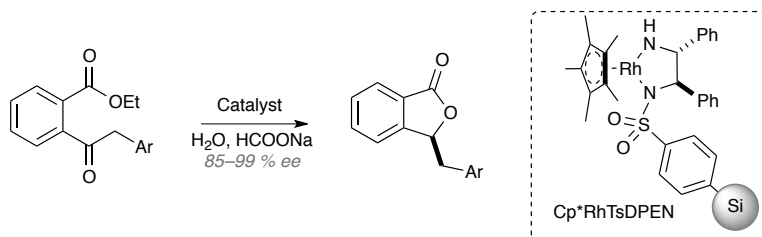
In 2014, Jones and coworkers reported polymer- and silica-supported iron BPMEN-catalysts (Scheme 1.3.4) for C–H bond functionalization reactions.⁴⁰ These catalysts were synthesized and evaluated for catalytic C–H functionalization reactions, using cyclohexane, cyclohexene, cyclo-octane, adamantane, benzyl alcohol, and cumene in the presence of aqueous hydrogen peroxide. The product yields were found to be better with silica-supported catalysts as compared to polymer-supported catalysts.

Scheme 1.3.4: *Silica-Supported Iron BPMEN-Catalysts.*



In 2016, Liu and coworkers reported a silica-supported rhodium/diamine (Scheme 1.3.5) for controllable reaction switching in enantioselective tandem reduction–lactonization of ethyl 2-acylarylcarboxylates.⁴¹ The observation demonstrated that the extended form of the polymer coating of this catalyst at 40 °C facilitates highly efficient tandem asymmetric catalysis, however the closed form at 15 °C terminates the reaction. This silica-supported heterogeneous catalyst was easily recovered and reused up to eight times without any loss of enantioselectivity.

Scheme 1.3.5: *Silica-Supported Rhodium/Diamine*



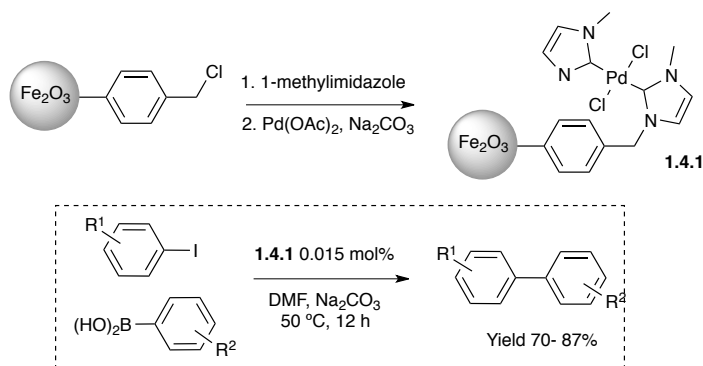
1.4 Advances in Magnetic Reagents and Catalysts:

Magnetic nanoparticles have recently received considerable attention as an attractive source for grafting of functional handles and useful scaffolds, to rapidly purify products from reaction mixtures with the aid of an external magnetic field. In particular, there has been increased interest in air-stable core-shell magnetic nanoparticles.⁴² These magnetic materials can combine the useful magnetic properties of the core-shell with feasible surface functionalization. In this section, discussion will focus on the main attributes of magnetic supports, as well as highlight recent advancements in the area of magnetic reagents, scavengers and catalysts.

Seminal efforts by many in the field reported use of core-shell assemblies based on super paramagnetic iron oxide NPs [magnetite (Fe_3O_4) and maghemite ($\gamma\text{-Fe}_2\text{O}_3$)],⁴³ which lack magnetic remanence ("magnetic memory") in the absence of an external magnetic field. This property is especially beneficial in order to enhance the ability to disperse nanomagnets. However, this advantage is offset by a relatively low saturation moment of ferrites (M_S , bulk ≤ 92 emu/g), which is further diminished through additional use of a protective shell.⁴⁴ As a consequence, for effective magnetic separation, hybrid materials that rely on iron oxide NPs demand a high metal content, thus limiting the total load capacity of other functional materials in the composite. Therefore, NPs derived from pure metals have been developed and exhibit superior magnetic properties to metal oxides; however, their synthesis has been limited.⁴⁵

In 2005, Gao and coworkers examined emulsion polymerization for the synthesis of an iron oxide nanoparticle-supported catalyst for Suzuki cross-coupling reactions (Scheme 1.4.1).⁴⁶ In this report, styrene, 4-vinylbenzene chloride and 1,4-divinylbenzene chloride were copolymerized to allow immobilization of 1-methylimidazole, which further generated N-heterocyclic carbenes. The coordination of Pd with NHCs afforded the desired magnetic iron oxide-Pd complex, which was subsequently applied for Suzuki Miyaura coupling reactions of aryl halides with aryl boronic acids. Recovery of catalysts was achieved by applying a permanent magnet externally and the isolated Pd-catalyst was reused without significant loss in catalytic activity.

Scheme 1.4.1. *Synthesis of Polymer-Coated Iron oxide Nanoparticles with Pd-NHC Complexes, for Application in Suzuki couplings.*



In 2007, Grass-Stark and coworkers reported⁴⁷ the one-step, large-scale production of carbon-coated nano-magnets (Figure 1.4.1) with increased air and thermal stabilities in a continuous process using a technique called reducing flame-spray pyrolysis.⁴⁸ A key feature of these Co/C nanoparticles is the graphene layer, which provides an extremely high level of chemical and thermal stability and prevents oxidation of the Co metal core.⁴² Moreover, the carbon layer deposited on

the Co-core has no detrimental effect on magnetization (158 emu/g).⁴⁹ Cobalt-carbon magnetic beads display excellent magnetic properties and high stability in air at temperatures up to 190 °C. The core-shell particles were functionalized through the use of diazonium chemistry, which afforded *Cl*-, *NO*₂-, and *NH*₂-functionalized magnetic nanoparticles (Scheme 1.4.2).

Scheme 1.4.2. *Functionalization of Carbon-Coated Magnetic Nanobeads:*

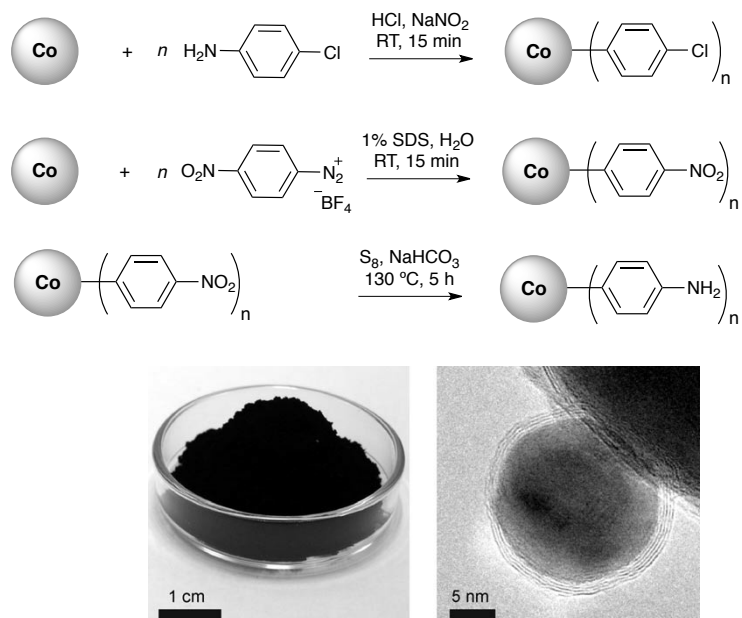
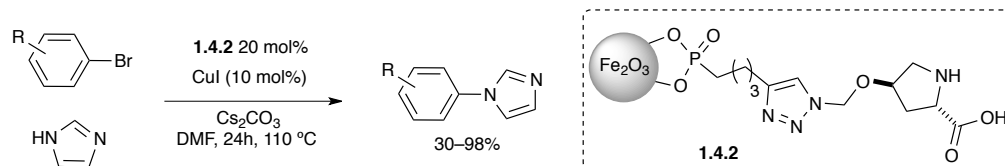


Figure 1.4.1. *Left: Carbon-Coated Nanomaterial. Right: Transmission Electron Microscopic image of Graphene Layers Coating of Metallic Cobalt Core.*

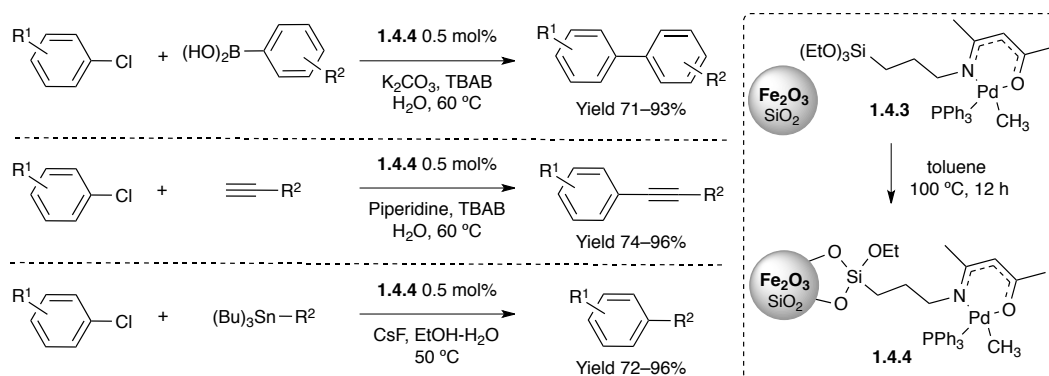
In 2007, Alper and coworkers, reported a magnetic-supported proline ligand⁵⁰ **1.4.2**, which was utilized in CuI-catalyzed Ullmann-type coupling reactions of aryl/hetero-aryl bromides with several nitrogen heterocycles to generate the corresponding N-aryl products (Scheme 1.4.3). This magnetic proline ligand could be readily separated using an external magnet and reused up to four times without any significant loss in efficiency of the catalyst.

Scheme 1.4.3. Utilization of Magnetic Nanoparticle Supported Proline Ligand.



In 2010, Lee and coworkers reported a heterogeneous Pd-catalyst for Suzuki, Sonogashira, and Stille coupling reactions of unreactive aryl chlorides.⁵¹ A silylated Pd-complex was immobilized on the surface of Fe₃O₄ coated with a thin layer of silica (SiO₂). A range of normally unreactive aryl chlorides afforded coupling products under mild conditions (Scheme 1.4.4). This magnetic/SiO₂ hybrid Pd-catalyst was successfully reused and retained its performance without significant loss of activity.

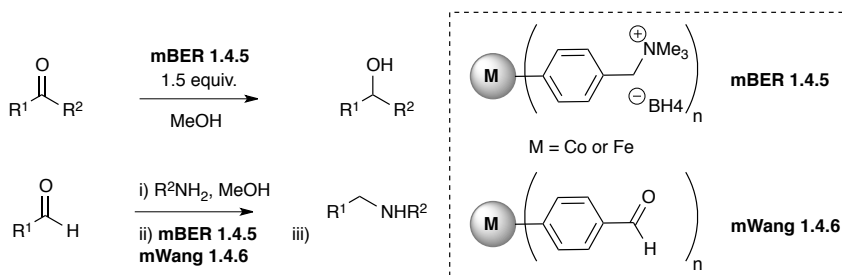
Scheme 1.4.4. Synthesis and Utilization of Magnetic Pd-Catalyst for Suzuki, Sonogashira, and Stille Couplings.



In 2013, Reiser and coworkers reported a magnetic amine resin, a magnetic Wang aldehyde (mWang) as a viable scavenger, and a magnetic borohydride exchange resin (Fe/C-mBER) for the reduction of various aldehydes, ketones and α,β -unsaturated substrates (Scheme 1.4.5).⁵² A small library of ureas and thioureas

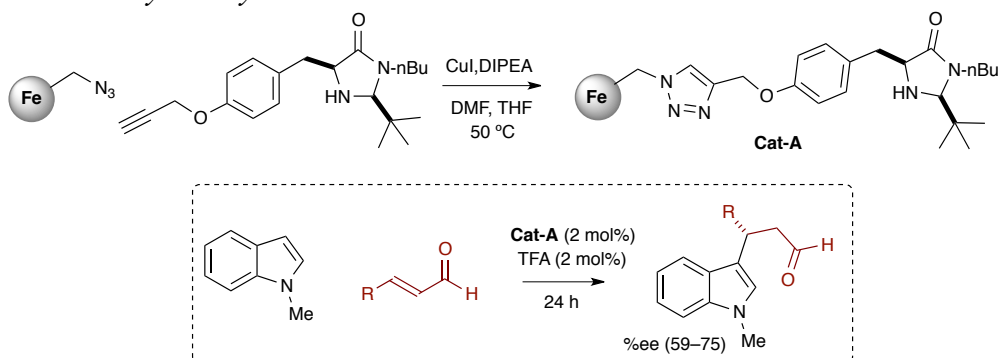
was prepared by the combination of these magnetic resins. The reductive amination of aromatic and aliphatic aldehydes was carried out with a magnetic mBER and the excess amine needed to complete the reaction was subsequently scavenged by the mWang. Simple magnetic decantation afforded secondary amines in good yields and purities. In all cases, the spent magnetic resins were successfully regenerated and reused for subsequent runs.

Scheme 1.4.5 *Synthesis and Utilization of Magnetic mBER and mWang.*



In 2016, Pericàs and coworkers reported magnetic versions of the second-generation MacMillan organo-catalyst⁵³ supported on 1% DVB Merrifield resin (0.6 mmol/g) and iron oxide Fe_3O_4 MNPs (Scheme 1.4.6). This catalyst was immobilized on Fe_3O_4 magnetic nanoparticles through a copper catalyzed alkyne–azide cycloaddition (CuAAC) reaction (0.72 mmol/g). The resulting catalytic materials were applied to the asymmetric Friedel-Crafts alkylation of indoles with α,β -unsaturated aldehydes. The immobilized catalysts were easily recovered and reused.

Scheme 1.4.6 *Synthesis and Utilization for FC-Alkylation of Indoles with Enals Mediated by Catalyst A*



1.5 ROMP-Derived Oligomeric Reagents, Scavengers and Catalyst:

A large number of immobilized reagents and scavengers have been developed and are commercially available. Moreover, extensive applications have been shown in organic synthesis and the production of combinatorial libraries.^{2,54} Despite huge advances in this area, limitations in non-linear reaction kinetics (heterogeneous reactions), low resin-load capacities, means of distributing reagents, and solution-phase automation technology continue to warrant the development of designer polymers for library production.⁵⁵ These limitations (i.e. non-linear kinetics and load) motivated the development of new polymer technologies to address them. In this regard, Buchmeiser,⁵⁶ Bolm,⁵⁷ Barrett,⁵⁸ Hanson,⁵⁹ and others⁶⁰ have demonstrated significant advancements in area by generating a wide range of ROMPgel (Figure 1.5.1) materials using ring-opening metathesis polymerization (ROMP) of functionalized norbornene (Nb-tagged) monomers.

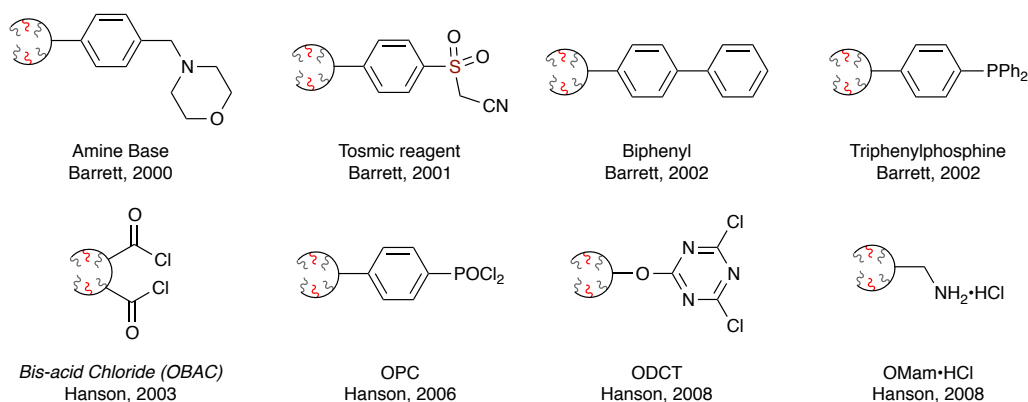


Figure 1.5.1. *Polymers Using ROMP of Nb-tagged Monomers.*

ROM polymerization is suitable for strained norbornene or 7-oxanorbornene-based monomers.^{56,59} These functionalized, olefin-based cyclic Nb-tagged monomers are easily prepared from low-cost commercial starting materials. The synthesis of Nb-tagged monomers is achieved either by a Diels–Alder reaction between cyclopentadiene (or furan) with a suitable dienophile or from a Pd-catalyzed, reductive Heck reaction with commercially available norbornadiene (Figure 1.5.2). A variety of functionalized Nb-tagged monomers can be constructed on large scale because of the low cost and commercial availability of starting materials.

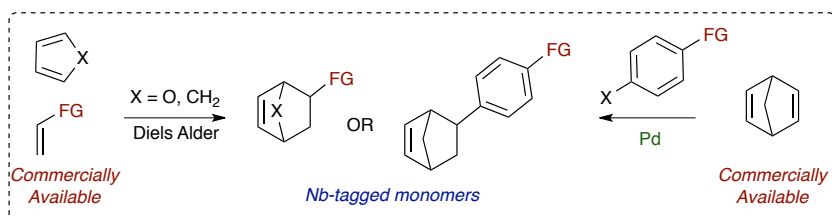


Figure 1.5.2. *Synthesis of Nb-Tagged Monomers.*

The first- and second-generation Grubbs catalysts (Figure 1.5.3) are more commonly used in ROM polymerization of Nb-tagged monomers. A number of

kinetic studies have been carried out by Grubbs and coworkers with $(\text{PCy}_3)_2(\text{Cl})_2\text{Ru}=\text{CHPh}$ (G-I)⁶¹ and $(\text{ImMesH}_2)(\text{PCy}_3)(\text{Cl})_2\text{Ru}=\text{CHPh}$ (G-II)⁶² to

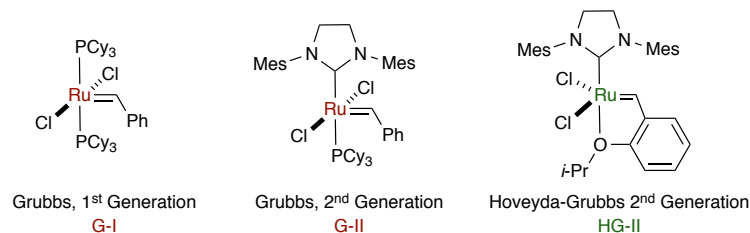


Figure 1.5.3. *Most Commonly Used Olefin-Metathesis Catalysts for ROMP.*

elaborate on the mechanism of ROM polymerization (Figure 1.5.4). The first step involves the dissociation of a phosphine ligand from the pre-catalyst, **1.5.1**. The resulting 14-electron complex **1.5.2** undergoes a [2+2] cyclo-addition reaction with functionalized Nb-tagged monomer **1.5.3** to generate metalla-cyclobutane intermediate **1.5.4**. The rapid [2+2] cyclo-reversion of intermediate **1.5.4** generates ring-opened product **1.5.5**. The highly ring-strained Nb-tagged monomers favor the ring-opened cycle due to the relief of ring strain. Active intermediate Ru-alkylidene **1.5.5** goes through repeating cycles until monomer **1.5.3** is consumed. The polymerization is quenched by the addition of ethyl vinyl ether (EVE), which afforded the desired ROMP-polymer **1.5.8**.

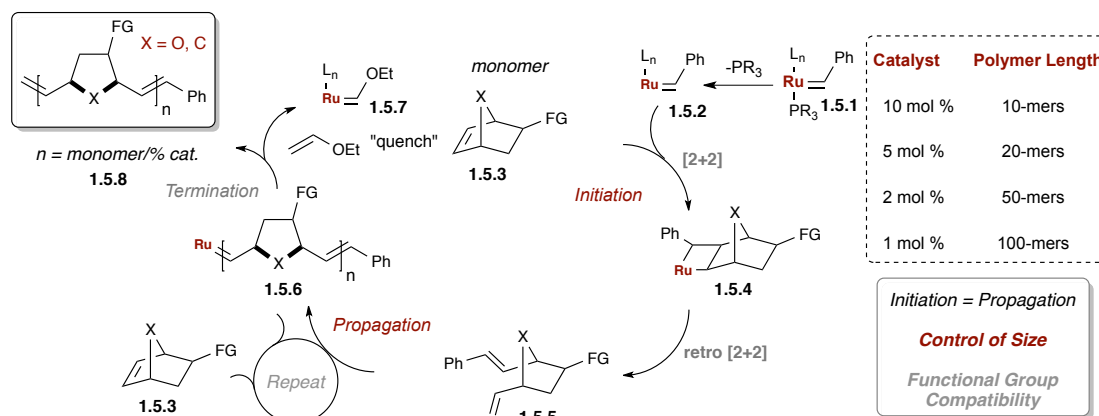


Figure 1.5.4. Mechanism of Ring-Opening Metathesis Polymerization (ROMP).

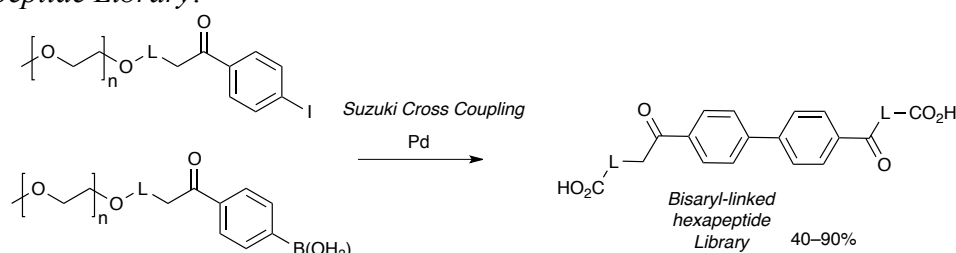
The authors^{59d} observed that the rate of initiation is similar to the rate of propagation. As a result, 10 mol % of catalyst (10:1 monomer:catalyst) predominantly generates 10-mers, and 5 mol % of catalyst (20:1 monomer:catalyst) mainly produces 20-mers, etc. The chain length of oligomers in this process can be conveniently controlled by the amount of catalyst. Higher amounts of catalyst generate shorter oligomers, and smaller amounts of catalyst generate longer oligomers.^{59d} ROM polymerization reactions can be carried out in round bottom flasks, screw-cap vials, and pressure tubes, either inside or outside of a glove box. In addition, ROM polymerizations can be conducted from milligram to kilogram scale. The length of the ROMP-derived oligomer has considerable effect on its solubility profile. The shorter length oligomers show more solubility in common solvents as compared to higher chain length oligomers.

In 2002, Barrett and coworkers synthesized ROM polymers as solid supported reagents for their application in various key transformations and parallel synthesis (Figure 1.5.1).⁵⁸ The benefit of ROMPgel supports is their ease of synthesis from

cheap and commercially available starting materials. The major benefit of ROM polymerization results in a ROMPgel in which every repeating unit is functionalized with the desired reagent functionality. The synthesized ROMP polymers have reasonably high loading and variable physical properties, which can be easily tuned and optimized.

In 2003, Janda and coworkers reported the first soluble polymer-supported convergent parallel synthesis library⁶³ of a PEG-supported tripeptide aryl iodides and PEG-supported tripeptide arylboronic acids reacted smoothly in a multi-polymer Pd-catalyzed Suzuki coupling reaction to generate a library of bisaryl-linked hexapeptides (Scheme 1.5.1). This convergent parallel synthesis demonstrated the utilization of soluble polymers as supports in library synthesis and illustrated the synthesis of an 81-membered library of bisaryl-linked hexapeptides.

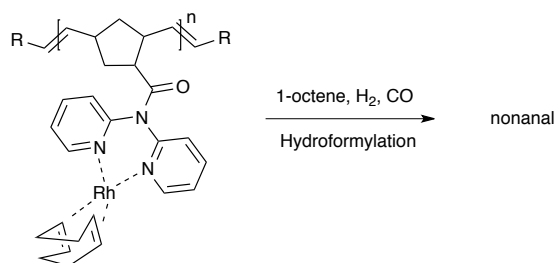
Scheme 1.5.1. *Polymer-supported Convergent Approach to the Bisaryl-linked hexapeptide Library.*



In 2010, Buchmeiser and coworkers reported, an amphiphilic block copolymer bearing chelating ligands *N,N*-dipyrid-2-ylamide via ROMP using a Mo-based Schrock initiator (Scheme 1.5.2).⁶⁴ Chelation with Rh(I) afforded a polymer-bound catalyst that was used for the hydroformylation of 1-octene. From the hydroformylation data obtained with the polymer-bound catalyst as well as with the

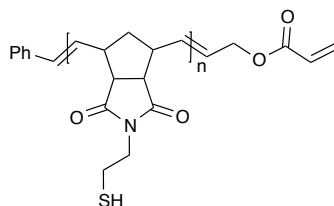
model catalyst, it becomes clear that the use of a micellar catalyst favors the formation of the n-aldehyde by suppressing the isomerization propensity of a catalyst. Apparently, the higher concentration of the starting alkene inside the micelle effectively prevents β -hydride elimination, an effect that can be further enhanced by adding free ligand that again accumulates inside the micelle. Further advantages in favor of a micellar setup are the low metal contamination of the products, as well as the possibility of reuse.

Scheme 1.5.2. *Hydroformylation Using Polymeric Rh-Catalyst.*



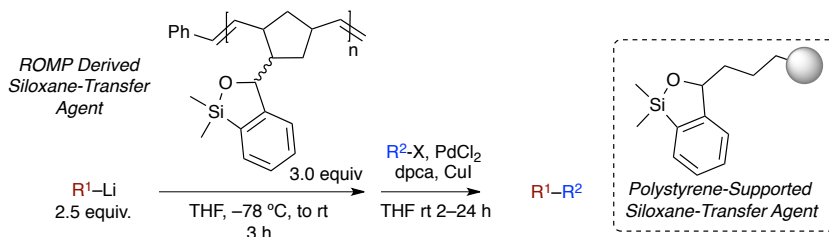
In 2013, Zhu and coworkers reported the facile synthesis of thiol-functionalized long-chain highly branched (LCHBPs) ROMP-derived polymers and its surface was decorated with gold nanoparticles.⁶⁵ Synthesis of thiol-functionalized long-chain highly branched polymers was achieved via combination of ring-opening metathesis polymerization (ROMP) and thiol-Michael addition click reaction. The thiol containing ROMP polymer with a terminal acrylate and groups is first prepared through, and then subsequent thiol-ene reaction between acrylate and thiol, afforded LCHBPs. Further Au nanoparticles were fabricated onto the surface of thiol-functionalized LCHBP to generate novel hybrid nanostructures (Scheme 1.5.3).

Scheme 1.5.3. *Synthesis of Thiol-Functionalized Long-Chain Highly Branched ROMP Polymers.*



In 2013, Smith and coworkers reported the synthesis and validation of a recyclable soluble ROMP-derived polymer supported siloxane transfer agents for use in Pd-catalyzed cross coupling reactions (Scheme 1.5.4).⁶⁶ The soluble nature of this polymer allows facile product purification as well as afforded recycling without significant loss in cross-coupling activity. In addition, another insoluble polystyrene-supported siloxane-transfer agent was prepared in 2014, for Pd-catalyzed cross-coupling reactions, which further simplified product purification and reused with various nucleophiles and electrophiles.

Scheme 1.5.4. *Polymer-Supported Siloxane Transfer Agents for Pd-Catalyzed Cross-Coupling Reactions.*

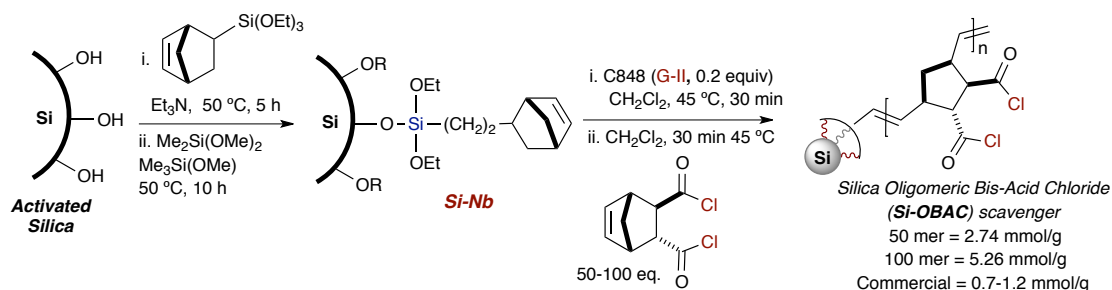


Surface functionalization of nanoparticles^{67,68} represents a well-established method for the generation of polymeric hybrid materials. Hybrid nanomaterials integrate the physical properties of the inorganic shell (particle size, pore and shape) with the tunable properties of the grafted organic polymer.⁶⁹ Key reports have described the utilization of surface-initiated ROM polymerization as a useful method

for grafting of organic-polymers from inorganic nanoparticles,⁷⁰ metal surfaces,⁷¹ carbon nanotubes,⁷² and resins.⁷³ Amongst the many grafted-hybrid materials,⁷⁴ Si-polymer hybrids are the most commonly reported in the literature for their application as heterogeneous supported catalysts,⁷⁵ and their utilization in consumer industry.⁷⁶

In 2010, the Hanson group reported the application of surface-initiated, ROMP to generate high-load immobilized silica reagents and scavengers.⁷⁷ The synthesis of three high load Si-ROMP reagents was successfully achieved which include (i) Si-immobilized bis-acid chloride (Si-OBAC) as scavenger, (ii) Si-immobilized dichlorotriazine (Si-ODCT) for amide coupling reactions and (iii) Si-immobilized triphenylphosphine Si-OTPP. The combination of Nb-tagged silica particles with functionalized Nb-tagged monomers using surface-initiated ROM polymerization generated these high-load, hybrid Si-ROMP reagents (Scheme 1.5.5).

Scheme 1.5.5 *Synthesis of Silica Oligomeric Bis-Acid Chloride (Si-OBAC)*



The hybrid Si-OBAC₅₀ material was utilized for the scavenging of excess alcohol efficiently, whereby a variety of alcohols were benzoylated to generate the corresponding esters. Additional synthesis of materials Si-ODCT₅₀ and Si-OTPP₅₀ was successfully achieved via the grafting of the corresponding Nb-tagged

dichlorotriazine,^{59a} and Nb-tagged triphenylphosphine^{59g} (Figure 1.5.5) utilizing the same protocol.

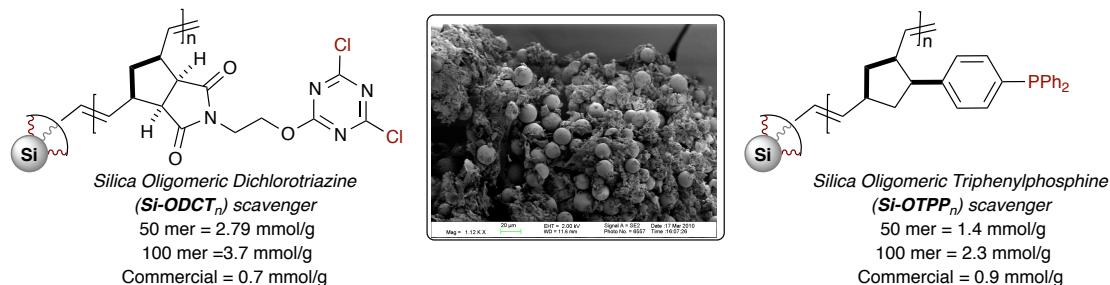
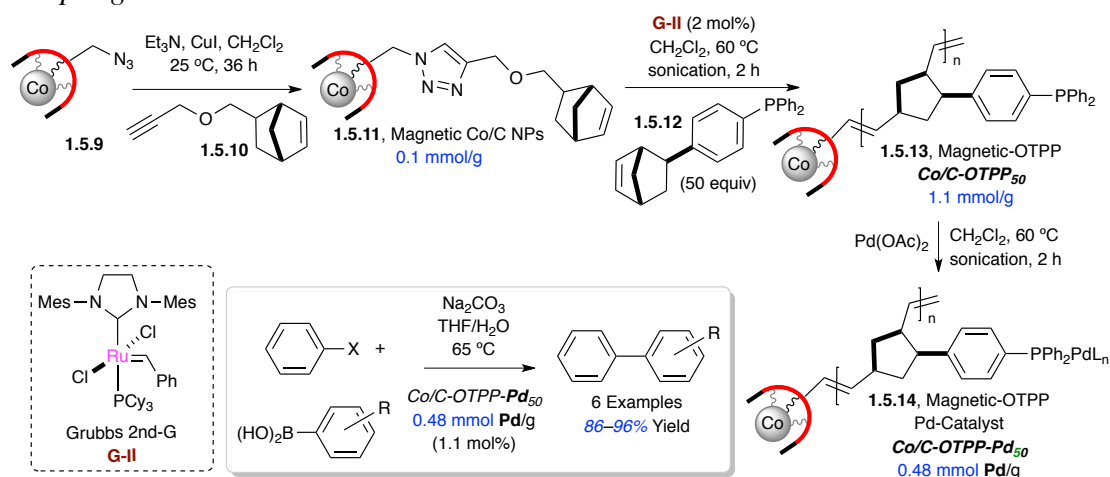


Figure 1.5.5 Silica-grafted Oligomeric Dichlorotriazine and (Si-ODCT₅₀) and Triphenylphosphine (Si-OTPP₅₀)

In 2010, Hanson-Reiser reported the utilizing the aforementioned surface-initiated ROMP, and developed a Co/C-immobilized, recyclable Pd-catalyst possessing a load of 0.48 mmol Pd/g (Scheme 1.5.6).⁷⁸ Initially magnetic Co/C NPs **1.5.9** are synthesized using Nb-tagged propargylic ether **1.5.10** via “click” attachment to the azido Co/C NP **1.5.11**. The Nb-tagged triphenylphosphine (Nb-TPP) monomer **1.5.4** was prepared and immobilized onto highly magnetic Co/C NPs **1.5.9** (0.1 mmol/g), using second-generation Grubbs catalyst [G-II], followed by the addition of the Nb-TPP monomer **1.5.12** (50 equiv.), afforded immobilized ROMP-derived Co/C-OTPP **1.5.13** possessing increased load (1.1 mmol/g). In a single step, the Co/C-OTPP ligand was utilized to afford the corresponding Co/C Pd-catalyst **1.5.14** possessing a load of 0.48 mmol/g. The Co/C-OTPP-Pd hybrid material was successfully employed in the construction of biaryl compounds in a Suzuki-Miyaura coupling reaction, where the catalyst was recycled and used 6 times without significant loss in activity.

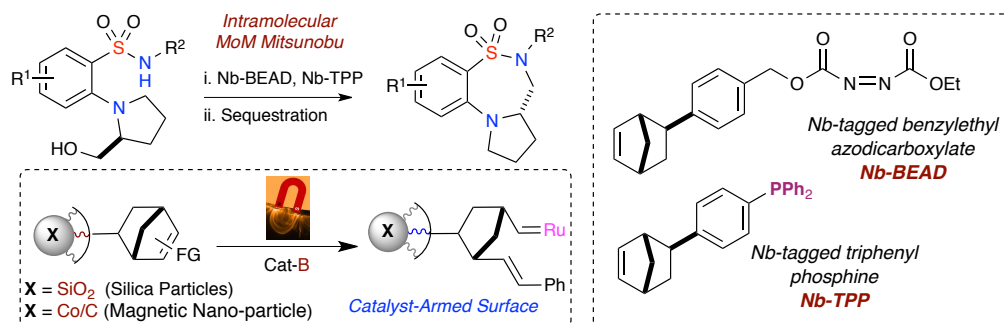
Scheme 1.5.6 *Co/C Oligomeric TPP-Pd Catalyst Utilized in Suzuki-Miyaura Biaryl Couplings.*



In 2010–2011, Hanson, Reiser and coworkers reported a sequestration protocol as a variant of the Mitsunobu reaction utilizing Nb-tagged reagents in conjunction with Nb-tagged Co/C NPs to sequester all by-products in the reaction.⁷⁹ In this impurity annihilation method,⁸⁰ termed *monomer-on-monomer* (MoM) Mitsunobu, purification was rapidly achieved by reacting the Nb-tagged Co/C NPs **1.5.11** via addition of the G-II catalyst in a surface-initiated polymerization process, which subsequently sequestered all Nb-tagged entities. To consider the biological importance of benzofused thiadiazepine-dioxides, in 2011, Hanson and Reiser utilized (MoM) Mitsunobu protocol for the synthesis of variable benzofused thiadiazepine-dioxides.⁸¹ The intramolecular Mitsunobu reaction has been widely applied for the cyclization of various molecules in natural product synthesis.⁸² In this process, facile sequestration of the utilized and excess reagents was achieved by three methods such as: (i) free catalyst in solution, (ii) surface-initiated catalyst-armed silica, and (iii) surface-initiated catalyst-armed carbon-coated (Co/C) magnetic

nanoparticles (Nps) [Scheme 1.5.7]. All three methods were found to work well with free catalyst in solution, silica surface-initiated ROMP, or Co/C NP surface-initiated ROMP, the latter being the most economical and efficient.

Scheme 1.5.7. Catalyst-armed Silica- and Co/C Magnetic Nanoparticles



Building on these results, substrate scope for the synthesis of benzofused thiadiazepine-dioxides analogues were investigated using all three-sequestration purification protocols. Thus, MoM Mitsunobu cyclization's (Figure 1.5.6) were employed to generate benzofused thiadiazepine-dioxides using free cat-**B**, Nb-tagged Co/C magnetic particles and Nb-tagged Silica particles.

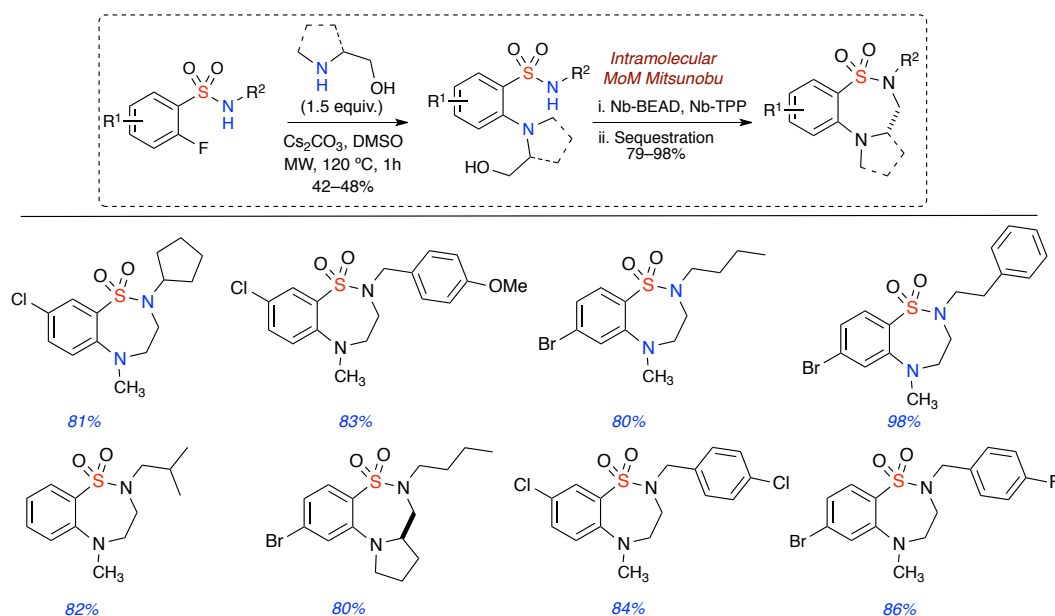
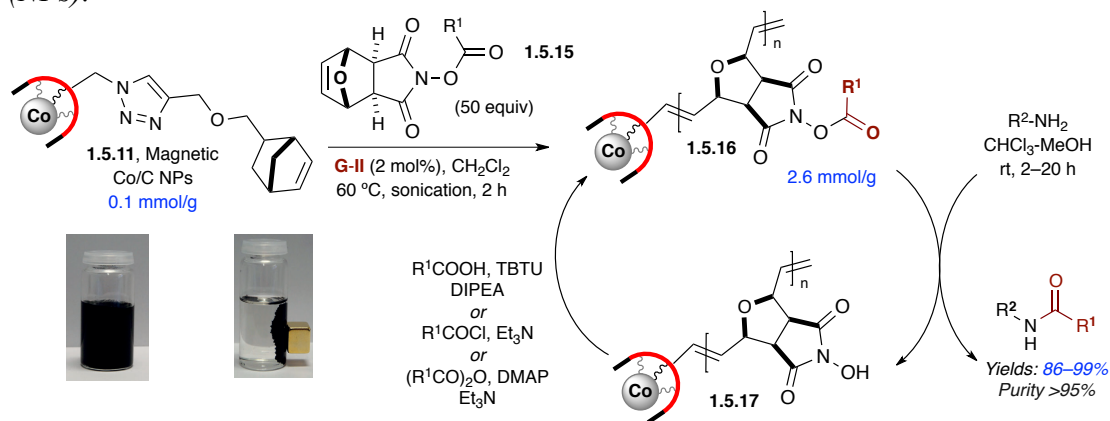


Figure 1.5.6. Synthesis of Benzofused Thiadiazepine-dioxides Analogues.

In 2013, Reiser and coworkers in collaboration with Hanson group reported efforts on an operationally simple method for the acylation of amines utilizing carbon-coated cobalt (Co/C) and iron (Fe/C) nanobeads as recyclable supports (Scheme 1.5.8).⁸³ Magnetic Co/C-NPs **1.5.11** was grafted with Nb-tagged acylated *N*-hydroxysuccinimide **1.5.15** monomers through surface initiated ROMP using G-II catalyst. The high loading hybrid material **1.5.16** (up to 2.6 mmol/g) was utilized for the acylation of various 1° and 2° amines in high yields (86–99%) and excellent purities after rapid magnetic decantation and simple evaporation of the solvents. The spent *N*-hydroxysuccinimide NPs **1.5.17** were successfully re-acylated via acid chlorides, anhydrides, and acids and reused for up to five cycles without considerable loss of activity.

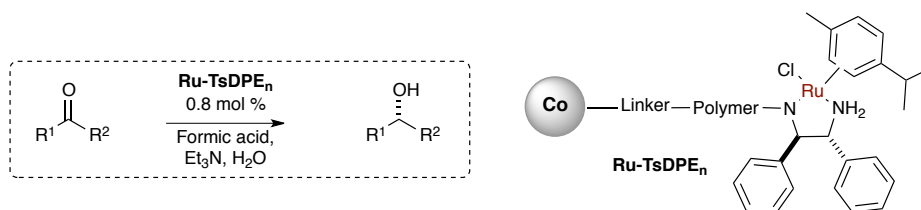
Scheme 1.5.8 *Recyclable, Magnetic Co/C Hybrid ROMP Acylation Nanoparticles (NPs).*



In 2016, Reiser and coworkers, reported synthesis and application of a magnetic Noyori-type ruthenium catalysts (Scheme 1.5.9) for an asymmetric transfer hydrogenation reactions in water.⁸⁴ The synthesized polymeric Noyori-type

ruthenium catalysts were immobilized on carbon-coated cobalt nanoparticles and were evaluated for asymmetric transfer hydrogenation of various ketones. The spent catalysts were recovered and directly reused without further reactivation treatment in 10 consecutive runs, using advantage of the magnetic decantation of the polymeric material.

Scheme 1.5.9 *Recyclable, Magnetic Co/C hybrid Noyori-type Ruthenium Catalysts.*



Overall, ROMP-derived oligomers possess unique physical properties, which make them a robust and useful approach for immobilization of a variety of soluble, silica and magnetic reagents, scavengers, and catalysts. The main advantages of ROMP technology include (a) various functional groups (Nb-FG) can be incorporated before polymerization, however in case of incompatibility with catalyst, post-polymerization can be achieved, (b) several attractive synthetic routes to functionalized norbornene and oxa-norbornene derivatives, (Nb-FG) are available for the generation of inexpensive immobilized reagents, (c) physical properties can be finely tuned. Chapter 2, 3 and 4 will detail work carried out in this dissertation regarding the use of ROM polymerization to generate soluble, silica and magnetic alkylating reagents and scavengers. The soluble ROMP polymers are air stable, high-load free flowing non-toxic solids, which are easy to handle and purification of products could be achieved via simple precipitation/filtration. The silica supported

ROMP derived polymers afforded the desired products via simple filtration. However magnetic polymers could be isolated by simple magnetic decantation, which further simplified the purification process (Figure 1.5.7).

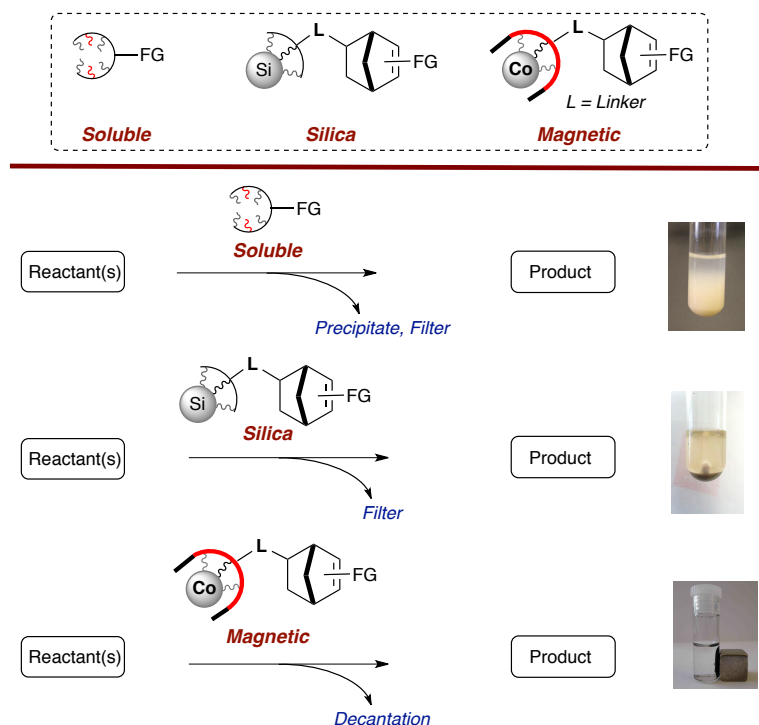


Figure 1.5.7: ROMP-Derived Soluble, Silica and Magnetic reagents.

1.6 Conclusion

The prime examples in recent years have shown significant developments for immobilized soluble, silica and magnetic reagents/scavengers/catalysts. Immobilized platforms have not only enabled automated synthesis, but also more recently have had a major impact in flow-through technologies. In addition, advances in ROMP-derived polymers, brings a robust and convenient approach of immobilization for a variety of soluble, silica and magnetic reagents/scavengers and catalyst. The combination of these ROMP derived technologies, because of there inherent physical properties can

play a key role in facilitating complex reaction processes. Taking the combine advantages of polymer-assisted solution phase precipitation, silica-supported filtration and magnetic-decantation, the frame of work discussed herein represent the front lines for future advancement in natural product synthesis and small-molecule library development. Since its discovery, ROMP has advanced as a general and viable means of immobilizing reagents/scavengers and catalysts and will undoubtedly continue to expand beyond these borders. It is reasonable to expect a variety of more useful immobilized polymers to be introduced in the future.

References

- [1] (a) Dolle, R. E.; Bourdonnec, B. L.; Worm, K.; Morales, G. A.; Thomas, C. J.; Zhang, W. Comprehensive Survey of Chemical Libraries for Drug Discovery and Chemical Biology: 2009 *J. Comb. Chem.* **2010**, *12*, 765–806. (b) Schreiber, S. L. Organic synthesis toward small-molecule probes and drugs *Proc. Natl. Acad. Sci. U. S. A.* **2011**, *108*, 6699–6702. (c) Chatterjee, A. K. Cell-Based Medicinal Chemistry Optimization of High-Throughput Screening (HTS) Hits for Orally Active Antimalarials. Part 1: Challenges in Potency and Absorption, Distribution, Metabolism, Excretion/Pharmacokinetics (ADME/PK *J. Med. Chem.* **2013**, *56*, 7741–7749.
- [2] For reviews concerning soluble polymers, see: (a) Gravert, D. J.; Janda, K. D. Organic Synthesis on Soluble Polymer Supports: Liquid-Phase Methodologies *Chem. Rev.* **1997**, *97*, 489–509. (b) Toy, P. H.; Janda, K. D. Soluble Polymer-Supported Organic Synthesis *Acc. Chem. Res.* **2000**, *33*, 546–554. (c) Dickerson, T. J.; Reed, N. N.; Janda, K. D. Soluble Polymers as Scaffolds for Recoverable Catalysts and Reagents *Chem. Rev.* **2002**, *102*, 3325–3344. (d) Haag, R. Dendrimers and Hyperbranched Polymers as High-Loading Supports for Organic Synthesis *Chem. Eur. J.* **2001**, *7*, 327–335. (e) Haag, R.; Sunder, A.; Hebel, A.; Roller, S. Dendritic Aliphatic Polyethers as High-Loading Soluble Supports for Carbonyl Compounds and Parallel Membrane Separation Techniques *J. Comb. Chem.* **2002**, *4*, 112–119. (f) Bergbreiter, D. E. Using Soluble Polymers To Recover Catalysts and Ligands *Chem. Rev.* **2002**, *102*, 3345–3384. (g) Bergbreiter, D. E.; Tian, J.; Hongfa, C. Using Soluble Polymer Supports To Facilitate Homogeneous Catalysis *Chem. Rev.* **2009**, *109*, 530–582. (h) Bergbreiter, David E. Soluble Polymers as Tools in Catalysis *ACS Macro Letters* **2014**, *3*, 260–265.
- [3] (a) Fletcher, P. D. I.; Haswell, S. J.; Pombo-Villar, E.; Warrington, B. H.; Watts, P.; Wong, S. Y. F.; Zhang, X., Micro reactors: principles and applications in organic synthesis. *Tetrahedron* **2002**, *58*, 4735–4757. (b) Pastre, J. C.; Browne, D. L.; Ley, S. V. Flow chemistry syntheses of natural products *Chem. Soc. Rev.* **2013**, *42*, 8849–8869. Myers, R. M.; Fitzpatrick, D. E.; Turner, R. M.; Ley, S. V. *Chem. Eur. J.* **2014**, *20*, 12348–12366 (c) Baumann, M.; Baxendale, I. R. The synthesis of active

- pharmaceutical ingredients (APIs) using continuous flow chemistry *Beilstein J. Org. Chem.* **2015**, *11*, 1194–1219. (d) Porta, R.; Benaglia, M.; Puglisi, A.; Flow Chemistry: Recent Developments in the Synthesis of Pharmaceutical Products, *Org. Process Res. Dev.* **2016**, *20*, 2–25.
- [4] (a) Merrifield, R. B. Solid phase peptide synthesis. I. The synthesis of a tetrapeptide. *J. Am. Chem. Soc.* **1963**, *85*, 2149–2154. (b) Merrifield, R. B. Solid phase peptide synthesis. II. Synthesis of bradykinin. *J. Am. Chem. Soc.* **1964**, *86*, 304–305. (c) Mitchell, A. R.; Kent, S. B. H.; Engelhard, M.; Merrifield, R. B. A new synthetic route to tert-butyloxycarbonylaminoacyl-4-(oxymethyl)phenylacetamidomethyl-resin, an improved support for solid-phase peptide synthesis. *J. Org. Chem.* **1978**, *43*, 2845–2852.
- [5] (a) Koppitz, M.; Eis, K. Automated medicinal chemistry. *Drug Discov. Today* **2006**, *11*, 561–568. (b) Koppitz, M., Maximizing Efficiency in the Production of Compound Libraries *J. Comb. Chem.* **2008**, *10*, 573–579 (c) Hird, N. W. Automated synthesis: new tools for the organic chemist. *Drug Discov. Today* **1999**, *4*, 265–274.
- [6] (a) Baxendale, I. R.; Ley, S. V.; Smith, C. D.; Tranmer, G. K. A flow reactor process for the synthesis of peptides utilizing immobilized reagents, scavengers and catch and release protocols. *Chem. Commun.* **2006**, *46*, 4835–4837. (b) France, S.; Bernstein, D.; Weatherwax, A.; Lectka, T. Performing the Synthesis of a Complex Molecule on Sequentially Linked Columns: Toward the Development of a "Synthesis Machine". *Org. Lett.* **2005**, *7*, 3009–3012. (c) Collins, J. M.; Porter, K. A.; Singh, S. K.; Vanier, G. S. High-Efficiency Solid Phase Peptide Synthesis (HE-SPPS) *Org. Lett.* **2014**, *16*, 940–943. (d) Palomo, J. M. Solid-phase peptide synthesis: an overview focused on the preparation of biologically relevant peptides *RSC Adv.*, **2014**, *4*, 32658–32672. (e) Elashal, H. E.; Cohen, R. D.; Raj, M. Fmoc solid-phase synthesis of C-terminal modified peptides by formation of a backbone cyclic urethane moiety. *Chem. Commun.* **2016**, *52*, 969–9702.
- [7] (a) Winssinger, N.; Barluenga, S.; Dakas, P.-Y. High-throughput synthesis of natural products. In *Power of Functional Resins in Organic Synthesis*. Wiley-VCH Verlag

- Gmb H&Co. KGaA, Weinheim, Germany, 2008; pp 613–640. Mentel, M.; Breinbauer, R., Combinatorial solid-phase natural product chemistry. *Top. Curr. Chem.* **2007**, 278 (Combinatorial Chemistry on Solid Supports), 209–241. (b) Ganesan, A. Solid-phase synthesis in the twenty-first century. Mini-Reviews in Medicinal Chemistry **2006**, 6, 3–10. (c) Baxendale, I. R.; Ley, S. V. Synthesis of alkaloid natural products using solid-supported reagents and scavengers. *Curr. Org. Chem.* **2005**, 9, 1521–1534. (d) Nandy, J. P.; Prakesch, M.; Khadem, S.; Reddy, P. Thirupathi, S., U.; Arya, P. Advances in Solution- and Solid-Phase Synthesis toward the Generation of Natural Product-like Libraries. *Chem. Rev.* **2009**, 109, 1999–2060. (e) Arndt, H.-D.; Rizzo, S.; Nçcker, C.; Wakchaure, V. N.; Milroy, L.-G.; Bieker, V.; Calderon, A.; Tran, T. T. N.; Brand, S.; Dehmelt, L.; Waldmann, H. Divergent Solid-Phase Synthesis of Natural Product-Inspired Bipartite Cyclodepsipeptides: Total Synthesis of Seragamide A *Chem. Eur. J.* **2015**, 21, 5311–5316.
- [8] (a) Schultz, P. G.; Xiang, X.-D., Combinatorial approaches to materials science. *Curr. Opin. Solid St. M.* **1998**, 3, 153–158. (b) Meier, M. A. R.; Schubert, U. S. Combinatorial polymer research and high-throughput experimentation: powerful tools for the discovery and evaluation of new materials. *J. Mater. Chem.* **2004**, 14, 3289–3299. (c) Petro, M.; Nguyen, S. H.; Liu, M.; Kolosov, O. Combinatorial exploration of polymeric transport agents for targeted delivery of bioactives to human tissues. *Macromol. Rapid Comm.* **2004**, 25, 178–188. (d) Krajcovicova, S.; Soural, M. Solid-Phase Synthetic Strategies for the Preparation of Purine Derivatives *ACS Comb. Sci.*, **2016**, 18, 371–386 (e) St-Pierre, G.; Hanessian, S.; Solution and Solid-Phase Stereo controlled Synthesis of 1,2-*cis*-Glycopyranosides with Minimally Protected Glycopyranosyl Donors Catalyzed by BF_3 -*N,N*-Dimethylformamide Complex *Org. Lett.* **2016**, 18, 3106–3109.
- [9] (a) Flynn, D. L.; Devraj, R. V.; Naing, W.; Parlow, J. J.; Weidner, J. J.; Yang, S. Polymer-assisted solution phase (PASP) chemical library synthesis. *Med. Chem. Res.* **1998**, 8, 219–243. (b) Parlow, J. J. Polymer-assisted solution-phase chemical library synthesis. *Curr. Opin. Drug Disc.* **2005**, 8, 757–775. (c) Ley, S. V.; Ladlow, M.;

- Vickerstaffe, E. The use of polymer-assisted solution-phase synthesis and automation for the high-throughput preparation of biologically active compounds *Exp. Chem. Div. Dr. Disc.* **2006**, 3–32.
- [10] (a) Salimi, H.; Rahimi, A.; Pourjavadi A. Applications of Polymeric Reagents in Organic Synthesis. *Monatshefte fur Chemie* **2007**, 138, 363–379. (b) Boldt, G. E.; Dickerson, T. J.; Janda, K. D. Emerging chemical and biological approaches for the preparation of discovery libraries. *Drug Discov. Today* **2006**, 11, 143–148. (c) Colombo M.; Peretto, I. Chemistry strategies in early drug discovery: an overview of recent trends. *Drug Discov. Today* **2008**, 13, 677–684. (d) Kennedy, J. P.; Williams, L.; Bridges, T. M.; Daniels, R. N.; Weaver, D.; Lindsley, C. W. Application of Combinatorial Chemistry Science on Modern Drug Discovery. *J. Comb. Chem.* **2008**, 10, 345–354.
- [11] (a) Rademann, J. Advanced polymer reagents based on activated reactants and reactive intermediates: powerful novel tools in diversity-oriented synthesis. *Method. Enzymol.* **2003**, 369 (Combinatorial Chemistry, Part B), 366–390. (b) Bhattacharyya, S. New developments in polymer-supported reagents, scavengers and catalysts for organic synthesis. *Curr. Opin. Drug Disc.* **2004**, 7, 752–764. (c) Cherkupally, P.; Ramesh, S.; Torre, B. G.; Govender, T.; Kruger, H. G.; Albericio, F. Immobilized Coupling Reagents: Synthesis of Amides/Peptides *ACS Comb. Sci.* **2014**, 16, 579–601.
- [12] (a) Sinfelt, J. H.; Yates, D. J. C. Studies of ethane hydrogenolysis over Group VIII metals: supported osmium and iron. *J. Catal.* **1968**, 10, 362–367. (b) Lee, B. S.; Mahajan, S.; Janda, K. D. Asymmetric dihydroxylation catalyzed by ionic polymer-supported osmium tetroxide. *Tetrahedron Lett.* **2005**, 46, 4491–4493. (c) Keshavarz, M.; Iravani, N.; Ghaedi, A.; Zarei, A.; Vafaei-Nezhad, A. M.; Karimi, S.; Macroporous polymer supported azide and nanocopper (I): efficient and reusable reagent and catalyst for multicomponent click synthesis of 1,4-disubstituted-1*H*-1,2,3-triazoles from benzyl halides *SpringerPlus* **2013**, 2:64. (d) Albéniz, A. C.; Carrera, N. Polymers for Green C–C Couplings *Eur. J. Inorg. Chem.* **2011**, 2347–2360.
- [13] (a) Li, K.; Tunge, J. A. Chemical Libraries via Sequential C-H Functionalization of

- Phenols. *J. Comb. Chem.* **2008**, *10*, 170–174. (b) Faisal, S.; Ullah, F.; Maity, P. K.; Rolfe, A.; Samarakoon, T. B.; Porubsky, P.; Neuenswander, B.; Lushington, G. H.; Basha, F. Z.; Organ, M. G.; Hanson, P. R. Facile (Triazolyl)methylation of MACOS-derived Benzofused Sultams Utilizing ROMP-derived OTP Reagents *ACS Comb. Sci.* **2012**, *14*, 268–272. (c) Gerard, B.; Duvall, J. R.; Lowe, J. T.; Murillo, T.; Wei, J.; Akella, L. B.; Marcaurelle, L. A.; Synthesis of a Stereochemically Diverse Library of Medium-Sized Lactams and Sultams via S_NAr Cycloetherification. *ACS. Combi. Sci.* **2011**, *13*, 365–374. (d) Chen, W.; Li, Z.; Ou, L.; Giulianott, M. A.; Houghten, R. A.; Yu, Y. Solid-phase synthesis of skeletally diverse benzofused sultams via palladium-catalyzed cyclization. *Tetrahedron Lett.* **2011**, *52*, 1456–1458. (e) Fenster, E.; Long, T.; Zang, Q.; Hill, D.; Neunswander, B.; Lushington, G.; Zhao, A.-H.; Santini, C.; Hanson, P. R. Automated Synthesis of a 184-Member Library of Thiadiazepan-1,1-dioxide-4-ones. *ACS Combi. Sci.* **2011**, *13*, 244–250.
- [14] (a) Lu, J.; Toy, P. H. Organic Polymer Supports for Synthesis and for Reagent and Catalyst Immobilization. *Chem. Rev.* **2009**, *109*, 815–838. (b) Storer, R. I.; Takemoto, T.; Jackson, P. S.; Brown, D. S.; Baxendale, I. R.; Ley, S. V. Multi-Step Application of Immobilized Reagents and Scavengers: A Total Synthesis of Epothilone C. *Chem. Eur. J.* **2004**, *10*, 2529–2547. (c) Baxendale, I. R.; Ley, S. V. Piutti, C. Total Synthesis of the Amaryllidaceae Alkaloid (+)-Plicamine and Its Unnatural Enantiomer by Using Solid-Supported Reagents and Scavengers in a Multistep Sequence of Reactions. *Angew. Chem., Int. Ed.* **2002**, *41*, 2194–2197. (d) Roller, S.; Türk, H.; Stumbé, J.-F.; Rapp, W.; Haag, R. Polystyrene-graft-Polyglycerol Resins: A New Type of High-Loading Hybrid Support for Organic Synthesis. *J. Comb. Chem.* **2006**, *8*, 350–354. (e) Takashima, H.; Vigneaud, V. D.; Merrifield, R. B. Synthesis of deaminooxytocin by the solid phase method *J. Am. Chem. Soc.* **1968**, *90*, 1323–1325.
- [15] (a) Guillier, F.; Orain, D.; Bradley, M. Linkers and cleavage strategies in solid-phase organic synthesis and combinatorial chemistry. *Chem. Rev.* **2000**, *100*, 2091–2157. (b) Polshettiwar, V.; Len, C.; Fihri, A. Silica-supported palladium: Sustainable catalysts for cross-coupling reactions. *Coord. Chem. Rev.* **2009**, *253*, 2599–2626. (c) Moreno, J.; Iglesias, J.; Meleroa, J. A.; Sherrington, D. C. Synthesis and characterisation of

- (hydroxypropyl)-2-aminomethyl pyridine containing hybrid polymer–silica SBA-15 materials supporting Mo(VI) centres and their use as heterogeneous catalysts for oct-1-ene epoxidation. *J. Mater. Chem.* **2011**, *21*, 6725–6735. (d) Fihri, A.; Bouhrara, M.; Patil, U.; Cha, D.; Saih, Y.; Polshettiwar, V. Fibrous nano-silica supported ruthenium (KCC-1/Ru): A sustainable catalyst for the hydrogenolysis of alkanes with good catalytic activity and lifetime. *ACS Cat.* **2012**, *2*, 1425–1431.
- [16] (a) Curran, D. P. Parallel synthesis with fluorous reagents and reactants. *Med. Res. Rev.* **1999**, *19*, 432–438. (b) Curran, D. P. Organic Synthesis with Light-Fluorous Reagents, Reactants, Catalysts, and Scavengers. *Aldrichimica Acta* **2006**, *39*, 3–11. (c) Dandapani, S.; Curran, D. P. Second Generation Fluorous DEAD Reagents Have Expanded Scope in the Mitsunobu Reaction and Retain Convenient Separation Features. *J. Org. Chem.* **2004**, *69*, 8751–8757. (d) Zhang, W. Fluorous linker-facilitated chemical synthesis. *Chem. Rev.* **2009**, *109*, 749–795. (e) Sugiyama, Y.; Ishihara, K.; Masuda, Y.; Kobayashi, Y.; Hamamoto, H.; Matsugi, M. Fluorous mixture synthesis of fluorous-Fmoc reagents using a one-pot double tagging strategy. *Tetrahedron Lett.* **2013**, *54*, 2060–2062. (f) Kim, J.; Lee, W. S.; Koo, J.; Lee, J.; Park, S. B. Synthesis and Library Construction of Privileged Tetra-Substituted Δ^5 -2-Oxopiperazine as β -Turn Structure Mimetics. *ACS Comb. Sci.* **2014**, *16*, 24–32.
- [17] (a) Mayr, M.; Mayr, B.; Buchmeiser, M. R. Monolithic Materials: New High-performance Supports for Permanently Immobilized Metathesis Catalysts. *Angew. Chem. Int. Ed.* **2001**, *40*, 3839–3842 (b) Bandari, R.; Knolle, W.; Prager-Duschke, A.; Buchmeiser, M. R. Ring-Opening Metathesis Polymerization Based Post-Synthesis Functionalization of Electron Beam Curing Derived Monolithic Media. *Macromolecules* **2007**, *28*, 2090–2094. (c) Moitra, N.; Ichii, S.; Kamei, T.; Kanamori, K.; Zhu, Y.; Takeda, K.; Nakanishi, K.; Shimada, T. Surface Functionalization of Silica by Si–H Activation of Hydrosilanes. *J. Am. Chem. Soc.* **2014**, *136*, 11570–11573. (d) Anderson, E. B.; Buchmeiser, M. R. Catalysts Immobilized on Organic Polymeric Monolithic Supports: From Molecular Heterogeneous Catalysis to Biocatalysis. *ChemCatChem* **2012**, *4*, 30–41.

- [18] (a) Crauste, C.; Périgaud, C.; Peyrottes, S. Synthesis of 2',3'-Dideoxynucleoside Phosphoesters Using H-Phosphonate Chemistry on Soluble Polymer Support. *J. Org. Chem.* **2011**, *76*, 997–1000. (b) Adams, J. H.; Cook, R. M.; Hudson, D.; Jammalamadaka, V.; Lyttle, M. H.; Songster, M. F. A Reinvestigation of the Preparation, Properties, and Applications of Aminomethyl and 4-Methylbenzhydrylamine Polystyrene Resins. *J. Org. Chem.* **1998**, *63*, 3706–3716. (c) Gooding, O. W.; Baudart, S.; Deegan, T. L.; Heisler, K.; Labadie, J. W.; Newcomb, W. S.; Porco, J. A., Jr.; Eikeren, P. V. On the Development of New Poly(styrene-oxyethylene) Graft Copolymer Resin Supports for Solid-Phase Organic Synthesis. *J. Comb. Chem.* **1999**, *1*, 113–122. (d) Lee, J. W.; Fuchs, P. L. Axially Chiral Amidinium Ions as Inducers of Enantioselectivity in Diels–Alder Reactions. *Org. Lett.* **1999**, *1*, 179–181. (e) Kalinina, I.; Worsley, K.; Lugo, C.; Mandal, S.; Bekyarova, E.; Haddon, R. C. Synthesis, Dispersion, and Viscosity of Poly(ethylene glycol)-Functionalized Water-Soluble Single-Walled Carbon Nanotubes. *Chem. Mater.* **2011**, *23*, 1246–1253. (f) Dalvi, P. B.; Lin, S.-F.; Paik, V.; Sun, C.-M. Microwave-Assisted Multicomponent Synthesis of Dihydroquinoxalinones on Soluble Polymer Support. *ACS Comb. Chem.* **2015**, *17*, 421–425.
- [19] (a) Kirschning, A.; Monenschein, H.; Wittenberg, R. Functionalized polymers—emerging versatile tools for solution-phase chemistry and automated parallel synthesis. *Angew. Chem. Int. Ed.* **2001**, *40*, 650–679. (b) Booth, R. J.; Hodges, J. C. Solid-Supported Reagent Strategies for Rapid Purification of Combinatorial Synthesis Products. *Acc. Chem. Res.* **1999**, *32*, 18–26. (c) Ley, S. V.; Baxendale, I. R.; Bream, R. N.; Jackson, P. S.; Leach, A. G.; Longbottom, D. A.; Nesi, M.; Scott, J. S.; Storer, R. I.; Taylor, S. J. Multi-step organic synthesis using solid-supported reagents and scavengers: a new paradigm in chemical library generation. *J. Chem. Soc., Perkin Trans. 1* **2000**, 3815–4195. (d) Strohmeier, G. A.; Kappe, C. O. Combinatorial Synthesis of Functionalized 1,3-Thiazine Libraries Using a Combined Polymer-Supported Reagent/Catch-and-Release Strategy. *Angew. Chem. Int. Ed.* **2004**, *43*, 621–624.

- [20] (a) Hudson, D. Matrix Assisted Synthetic Transformations: A Mosaic of Diverse Contributions. I. The Pattern Emerges *J. Comb. Chem.* **1999**, *1*, 333–360. (b) Polshettiwar, V.; Varma, R. S. Microwave-Assisted Organic Synthesis and Transformations using Benign Reaction Media *Acc. Chem. Res.* **2008**, *41*, 629–639.
- [21] (a) Hopkin, M. D.; Baxendale, I. R.; Ley, S. V. A flow-based synthesis of Imatinib: the API of Gleevec. *Chem. Commun.* **2010**, *46*, 2450–2452. (b) Hartwig, J.; Metternich, J. B.; Nikbin, N.; Kirschning, A.; Ley, S. V. Continuous flow chemistry: a discovery tool for new chemical reactivity patterns. *Org. Biomol. Chem.* **2014**, *12*, 3611–3615.
- [22] Wegner, J.; Ceylan, S.; Kirschning A. Flow Chemistry - A Key Enabling Technology for (Multistep) Organic Synthesis *Adv. Synth. Catal.* **2012**, *354*, 17–57.
- [23] Baxendale, I. R.; Ley, S. V.; Smith, C. D.; Tamborini, L.; Voica, A.-F. A Bifurcated Pathway to Thiazoles and Imidazoles Using a Modular Flow Microreactor. *J. Comb. Chem.* **2008**, *10*, 851–857.
- [24] Seeberger, P. H. Scavengers in full flow, *Nature Chem.* **2009**, *1*, 259–260. (b) McQuade D. T.; Seeberger, P. H.; Applying Flow Chemistry: Methods, Materials, and Multistep Synthesis *J. Org. Chem.* **2013**, *78*, 6384–6389.
- [25] (a) Tsubogo, T.; Oyamada, H.; Kobayashi, S. Multistep continuous-flow synthesis of (R)- and (S)-rolipram using heterogeneous catalysts. *Nature*. **2015**, *520*, 329–331. (b) Koboyashi, S.; Flow “Fine” Synthesis: High Yielding and Selective Organic Synthesis by Flow Methods. *Chem. Asia J.* **2016**, *11*, 425–436.
- [26] (a) Dai, C.; Snead, D. R.; Zhang, P. “Continuous Flow Synthesis and Purification of Atropine with Sequential In-Line Separations of Structurally Similar Impurities,” *J. Flow Chem.* **2015**, *5*, 133–138. (b) Snead, D.; Jamison, T.F. "A Three-Minute Synthesis and Purification of Ibuprofen: Pushing the Limits of Continuous-Flow Processing" *Angew. Chem. Int. Ed.* **2015**, *54*, 983–987. (c) Andrade, L.H.; Kroutil, W.; Jamison, T. F. “Continuous Flow Synthesis of Chiral Amines in Organic Solvents: Immobilization of E. coli Cells Containing Both ω -Transaminase and PLP” *Org. Lett.* **2014**, 6092–6095.

- [27] (a) Geyer, K.; Codee, J. D. C.; Seeberger, P. H. Microreactors as Tools for Synthetic Chemists—The Chemists' Round-Bottomed Flask of the 21st Century? *Chem. Eur. J.* **2006**, *12*, 8434–8442. (b) Tsubogo, T.; Ishiwata, T.; Kobayashi, S.; Asymmetric Carbon–Carbon Bond Formation under Continuous-Flow Conditions with Chiral Heterogeneous *Angew. Chem. Int. Ed.* **2013**, *52*, 6590–6604. (c) Malet-Sanz, L.; Susanne, F. Continuous Flow Synthesis. A Pharma Perspective *J. Med. Chem.* **2012**, *55*, 4062–4098.
- [28] Baxendale, I. R.; Griffiths-Jones, C. M.; Ley, S. V.; Tranmer, G. K. Preparation of the neolignan natural product grossamide by a continuous-flow process. *Synlett* **2006**, 427–430.
- [29] Schatz, A.; Grass, R. N.; Kainz, Q.; Stark, W. J.; Reiser, O. Cu(II)–azabis(oxazoline) complexes immobilized on magnetic Co/C nanoparticles: kinetic resolution of 1,2-diphenylethane-1,2-diol under batch and continuous-flow conditions *Chem. Mater.* **2010**, *22*, 305–310.
- [30] Ingham, R. J.; Riva, E.; Nikbin, N.; Baxendale, I. R.; Ley, S. V.; A “Catch_React_Release” Method for the Flow Synthesis of 2-Aminopyrimidines and Preparation of the Imatinib Base *Org. Lett.* **2012**, *14*, 3920–3923.
- [31] Okuno, Y.; Isomura, S.; Sugamata, A.; Tamahori, K.; Fukuhara, A.; Kashiwagi, M.; Kitagawa, Y.; Kasai, E.; Takeda, K. A Convenient and Simple Esterification in Continuous-Flow Systems using g-DMAP *ChemSusChem* **2015**, *8*, 3587–3589.
- [32] Price, G. A.; Bogdan, A. R.; Aguirre, A. L.; Iwai, T.; Djuric, S. W.; Organ, M. G. Continuous flow Negishi cross-couplings employing silica-supported Pd-PEPPSI-IPr precatalyst. *Cata. Sci. & Tech.* **2016**, *6*, 4733–4742.
- [33] Timoftea, R. S.; Woodward, S. Preparation of silane-grafted pellets: silica bound reagents in a very convenient form *Tet. Lett.* **2004**, *45*, 39–42.
- [34] Carpino, L. A.; Ismail, M.; Truran, G. A.; Mansour, E. M. E.; Iguchi, S.; Ionescu, D.; El-Faham, A.; Riemer, C.; Warrass, R. The 1,1-Dioxobenzo[*b*]thiophene-2-ylmethoxycarbonyl (Bsmoc) Amino-Protecting Group *J. Org. Chem.* **1999**, *64*,

4324–4338.

- [35] Lei, H.; Wang, L.; Li, P. Highly Efficient and Recyclable Palladium Catalyst Anchored on Organic–Inorganic Hybrid Material: Application in the Heck Reaction *Synthesis*, **2008**, 2405–2411.
- [36] Long, W.; Jones, C. W. Hybrid Sulfonic Acid Catalysts Based on Silica-Supported Poly(Styrene Sulfonic Acid) Brush Materials and Their Application in Ester Hydrolysis *ACS Catal.* **2011**, *1*, 674–681.
- [37] French, J. M.; Caras, C. A.; Diver, S. T. Removal of Ruthenium Using a Silica Gel Supported Reagent. *Org. Lett.* **2013**, *15*, 5416–5419.
- [38] Chepiga, K. M.; Feng, Y.; Brunelli, N. A.; Jones, C. W.; Davies, H. M. L. Silica-Immobilized Chiral Dirhodium(II) Catalyst for Enantioselective Carbenoid Reactions. *Org. Lett.* **2013**, *15*, 6136–6139.
- [39] Conley, M. P.; Mougél, V.; Peryshkov, D. V.; Forrest, W. P.; Gajan, D. J.; Lesage, A.; Emsley, L.; Coperet, C.; Schrock, R. R. A Well-Defined Silica-Supported Tungsten Oxo Alkylidene Is a Highly Active Alkene Metathesis Catalyst. *J. Am. Chem. Soc.* **2013**, *135*, 19068–19070.
- [40] Feng, Y.; Moschetta, E. G.; Jones, C. W. Polymer- and Silica-Supported Iron BPMEN-Inspired Catalysts for C-H Bond Functionalization Reactions *Chem. Asian J.* **2014**, *9*, 3142–3152.
- [41] Kong, L.; Zhao, J.; Cheng, T.; Lin, J.; Liu, G. Polymer-Coated Rhodium/Diamine-Functionalized Silica for Controllable Reaction Switching in Enantioselective Tandem Reduction Lactonization of Ethyl 2 Acylarylcarboxylates *ACS Catal.* **2016**, *6*, 2244–2249.
- [42] (a) Schatz, A.; Reiser, O.; Stark, W. J.; Nanoparticles as Semi-Heterogeneous Catalyst Supports *Chem. Eur. J.* **2010**, *16*, 8950–8967. (b) Polshettiwar, V.; Luque, R.; Fihri, A.; Zhu, H.; Bouhrara, M.; Basset, J.-M. Magnetically Recoverable Nanocatalysts. *Chem. Rev.* **2011**, *111*, 3036–3075. (c) Olson, C. A.; Nie, J.; Diep, J.; Al-Shyoukh, I.; Takahashi, T. T.; Al-Mawsawi, L. Q.; Bolin, J. M.; Elwell, A. L.; Swanson, S.;

- Stewart, R.; Thomson, J. A.; Soh, H. T.; Roberts, R. W.; Sun, R. Single-Round, Multiplexed Antibody Mimetic Design through mRNA Display. *Angew. Chem. Int. Ed.* **2012**, *51*, 12449–12453. (d) Gawande, M. B.; Branco, P. S.; Varma, R. S. Nanomagnetite (Fe₃O₄) as a support for recyclable catalysts in the development of sustainable methodologies. *Chem. Soc. Rev.* **2013**, *42*, 3371–3393. (e) Girija, D.; Bhojya Naik, H. S.; Vinay, B. K.; Sudhamani, C. N.; Harish, K. N. New Green, Recyclable Magnetic Nanoparticles Supported Amino Acids as Simple Heterogeneous Catalysts for Knoevenagel Condensation. *Lett. in Org. Chem.* **2013**, *10*, 468–477. (f) Varma, R. S.; Branco, P. S. Gawande, M. B.; Rathi, A. K.; Nogueira, I. D. Magnetite-supported sulfonic acid: a retrievable nanocatalyst for the Ritter reaction and multicomponent reactions. *Green Chem.* **2013**, *15*, 1895–1899. (g) Nasir-Baig, R. B.; Varma, R. S. Organic synthesis via magnetic attraction: benign and sustainable protocols using magnetic nanoferrites. *Green Chem.* **2013**, *15*, 398–417. (h) Chng, L. L.; Erathodiyil, N.; Ying, J. Y. Nanostructured Catalysts for Organic Transformations. *Acc. Chem. Res.* **2013**, *46*, 1825–1837.
- [43] (a) Abu-Reziq, R.; Alper, H.; Wang, D.; Post, M. L. Metal Supported on Dendronized Magnetic Nanoparticles: Highly Selective Hydroformylation Catalysts. *J. Am. Chem. Soc.* **2006**, *128*, 5279–5282. (b) Lu, A. H.; Salabas, E. L.; Schuth, F. Magnetic Nanoparticles: Synthesis, Protection, Functionalization, and Application. *Angew. Chem. Int. Ed.* **2007**, *46*, 1222–1244. (c) Shokouhimehr, M.; Piao, Y.; Kim, J.; Jang, Y.; Hyeon, T. A Magnetically Recyclable Nanocomposite Catalyst for Olefin Epoxidation. *Angew. Chem. Int. Ed.* **2007**, *119*, 7169–7173. (d) Gleeson, O.; Tekoriute, R.; Gun'ko, Y. K.; Connon, S. J. The first magnetic nanoparticle-supported chiral DMAP analogue: highly enantioselective acylation and excellent recyclability. *Chem. Eur. J.* **2009**, *15*, 5669–5673. (e) Rosario-Amorin, D.; Wang, X.; Gaboyard, M.; Clerac, R.; Nlate, S.; Heuze, K. Dendron-functionalized core-shell superparamagnetic nanoparticles: magnetically recoverable and reusable catalysts for Suzuki C-C cross-coupling reactions. *Chem. Eur. J.* **2009**, *15*, 12636–12643. (f) Hua, D.; Tang, J.; Dai, L.; Pu, Y.; Cao, X.; Zhu, X. A Strategy for Synthesis of Magnetic Nanoparticles with "Well-Defined" Polymers via Reversible Addition Fragmentation Chain Transfer

- Polymerization Under Ultrasonic Irradiation. *J. Nanosci. Nanotechnol.* **2009**, *9*, 6681–6687. (g) Jin, M.-J.; Lee, D.-H. A Practical Heterogeneous Catalyst for the Suzuki, Sonogashira, and Stille Coupling Reactions of Unreactive Aryl Chlorides. *Angew. Chem.* **2010**, *122*, 1137–1140.
- [44] (a) Sun, Y.; Duan, L.; Guo, Z.; Mu, Y. D.; Ma, M.; Xu, L.; Zhang, Y.; Gu, N. An improved way to prepare superparamagnetic magnetite-silica core-shell nanoparticles for possible biological application. *J. Magn. Magn. Mater.* **2005**, *285*, 65–70. (c) Deng, Y.-H.; Wang, C.-C.; Hu, J.-H.; Yang, W.-L.; Fu, S.-K. Investigation of formation of silica-coated magnetite nanoparticles via sol–gel approach. *Colloids Surf., A* **2005**, *26*, 87–93. (d) Lee, J.; Lee, Y.; Youn, J. K.; Na, H. B.; Yu, T.; Kim, H.; Lee, S.-M.; Koo, Y.-M.; Kwak, J. H.; Park, H. G.; Chang, H. N.; Hwang, M.; Park, J.-G.; Kim, J.; Hyeon, T. Simple Synthesis of Functionalized Superparamagnetic Magnetite/Silica Core/Shell Nanoparticles and their Application as Magnetically Separable High-Performance Biocatalysts. *Small* **2008**, *4*, 143–152.
- [45] (a) Saito, Y. Nanoparticles and filled nanocapsules. *Carbon* **1995**, *33*, 979–988. (b) Scott, J. H. J.; Majetich, S. A. Morphology, structure, and growth of nanoparticles produced in a carbon arc. *Phys. Rev. B* **1995**, *52*, 12564–12571. (c) Wang, Z. H.; Choi, C. J.; Kim, B. K.; Kim, J. C.; Zhang, Z. D. Characterization and magnetic properties of carbon-coated cobalt nanocapsules synthesized by the chemical vapor-condensation process. *Carbon* **2003**, *41*, 1751–1758. (d) Senapati, K. K.; Roy, S.; Borgohain, C.; Phukan, P. Palladium nanoparticle supported on cobalt ferrite: An efficient magnetically separable catalyst for ligand free Suzuki coupling. *J. Mol. Cat. A: Chemical* **2012**, *352*, 128–134. (e) Nasir Baig, R. B.; Varma, R. S. A highly active and magnetically retrievable nanoferrite-DOPA-copper catalyst for the coupling of thiophenols with aryl halides. *Chem. Commun.* **2012**, *48*, 2582–2584.
- [46] Stevens, P. D.; Fan, J.; Gardimalla, H. M. R.; Yen, M.; Gao, Y.; Superparamagnetic Nanoparticle-Supported Catalysis of Suzuki Cross-Coupling Reactions *Org. Lett.* **2005**, *11*, 2085–2088.

- [47] (a) Grass, R. N.; Stark, W. J. Gas phase synthesis of fcc-cobalt nanoparticles. *J. Mater. Chem.* **2006**, *16*, 1825–1830. (b) Grass, R. N.; Athanassiou, E. K.; Stark, W. J. Covalently Functionalized Cobalt Nanoparticles as a Platform for Magnetic Separations in Organic Synthesis. *Angew. Chem. Int. Ed.* **2007**, *46*, 4909–4912. (c) Herrmann, I. K.; Grass, R. N.; Mazunin, D.; Stark, W. J. Synthesis and Covalent Surface Functionalization of Nonoxidic Iron Core–Shell Nanomagnets. *Chem. Mater.* **2009**, *21*, 3275–3281. (d) Wittmann, S.; Schätz, A.; Grass, R. N.; Stark, W. J.; Reiser, O. A Recyclable Nanoparticle-Supported Palladium Catalyst for the Hydroxycarbonylation of Aryl Halides in Water. *Angew. Chem. Int. Ed.* **2010**, *49*, 1867–1870.
- [48] Stark, W. J.; Madler, L.; Maciejewski, M.; Pratsinis, S. E.; Baiker, A. Flame synthesis of nanocrystalline ceria–zirconia: effect of carrier liquid. *Chem. Commun.* **2003**, 588–589.
- [49] (a) Schätz, A.; Grass, R. N.; Stark, W. J.; Reiser, O. TEMPO Supported on Magnetic C/Co-Nanoparticles: A Highly Active and Recyclable Organocatalyst. *Chem. Eur. J.* **2008**, *18*, 8262–8266. (b) Michalek, F.; Lagunas, A.; Jimeno, C.; Pericàs, M. A. Synthesis of functional cobalt nanoparticles for catalytic applications: Use in asymmetric transfer hydrogenation of ketones. *J. Mater. Chem.* **2008**, *18*, 4692–4697.
- [50] Chouhan, G.; Wangb, D.; Alper, H. Magnetic nanoparticle-supported proline as a recyclable and recoverable ligand for the CuI catalyzed arylation of nitrogen. *Chem. Commun.* **2007**, 4809–4811.
- [51] Jin, M.-J.; and Lee, D. -H. A Practical Heterogeneous Catalyst for the Suzuki, Sonogashira, and Stille Coupling Reactions of Unreactive Aryl Chlorides. *Angew. Chem. Int. Ed.* **2010**, *49*, 1119–1122.
- [52] Kainz, Q. M.; Zeltner, M.; Rossier, M.; Strak, W. J.; Reiser, O. Synthesis of Trisubstituted Ureas by a Multistep Sequence Utilizing Recyclable Magnetic Reagents and Scavengers. *Chem. Eur. J.* **2013**, *19*, 10038–10045.

- [53] Ranjbar, S.; Riente, P.; Rodríguez-Escrich, C.; Yadav, J.; Ramineni, K.; Perica, M. A.; Polystyrene or Magnetic Nanoparticles as Support in Enantioselective Organocatalysis? A Case Study in Friedel–Crafts Chemistry *Org. Lett.* **2016**, *18*, 1602–1605.
- [54] (a) Eames, J.; Watkinson, M. Polymeric Scavenger Reagents in Organic Synthesis. *Eur. J. Org. Chem.* **2001**, 1213–1224. (b) Bergbreiter, D. E. Introduction to Facilitated Synthesis. *Chem. Rev.*, **2009**, *109*, 257–258 (c) Basu, S.; Waldmann, H. Polymer supported synthesis of a natural product-inspired oxepane library *Bioorg. Med. Chem.* **2014**, *22*, 4430–4444.
- [55] (a) Studer, A.; Curran, D. P. A strategic alternative to solid phase synthesis: Preparation of a small isoxazoline library by “fluorous synthesis” *Tetrahedron* **1997**, *53*, 6681–6696. (b) Hjerten, S.; Li, Y.-M.; Liao, J. L.; Mankazato, K.; Mohammad, J.; Pettersson, G. Continuous beds: high-resolving, cost-effective chromatographic matrices. *Nature* **1992**, *356*, 810–811. (c) Baumann, M.; Baxendale, I. R.; Ley, S. V.; Nikbin, N.; Smith, C. D. A modular flow reactor for performing Curtius rearrangements as a continuous flow process *Org. Biomol. Chem.* **2008**, *6*, 1577–1586.
- [56] (a) Buchmeiser, M. R.; Atzl, N.; Bonn, G. K. Ring-Opening-Metathesis Polymerization for the Preparation of Carboxylic-Acid-Functionalized, High-Capacity Polymers for Use in Separation Techniques. *J. Am. Chem. Soc.* **1997**, *119*, 9166–9174. (b) Buchmeiser, M. R. Homogeneous Metathesis Polymerization by Well-Defined Group VI and Group VIII Transition-Metal Alkylidenes: Fundamentals and Applications in the Preparation of Advanced Materials. *Chem. Rev.* **2000**, *100*, 1565–1604. (c) Buchmeiser, M. R. Heterogeneous C–C coupling and polymerization catalysts prepared by ROMP. *Bioorg. Med. Chem. Lett.* **2002**, *12*, 1837–1840. (d) Buchmeiser, M. R. In *Handbook of Metathesis*, Vol. 3, Grubbs, R. H., Ed.: Wiley-VCH: Weinheim, 2003. pp 226–254. (e) Lubbad, S. H.; Bandari, R.; Buchmeiser, M. R. Ring-opening metathesis polymerization-derived monolithic strong anion exchangers for the separation of 5-phosphorylated oligodeoxythymidylic acids fragments. *J. Chromatogr. A* **2011**, *1218*, 8897–8902. (f) Wang, D.; Unold, J.; Bubrin, M.; Frey, W.; Kaim, W.; Buchmeiser, M. R. Ruthenium(IV)–Bis(methallyl) Complexes as UV-Latent Initiators for Ring-Opening Metathesis Polymerization *ChemCatChem* **2012**, *4*, 1808–1812. (g)

- Buchmeiser, M. R. Edited by Schlueter, D. A.; Hawker, C. J.; Sakamoto, J. In *Synthesis of Polymers*. 2012, Vol. 2, 547–586. (h) Buchmeiser, M. R. Tandem Ring-Opening Metathesis / Vinyl Insertion Polymerization-Derived Poly (Olefin)s. *Curr. Org. Chem.* **2013**, *17*, 2764–2775. (i) Naumann, S.; Schmidt, F. G.; Frey, W.; Buchmeiser, M. R. Protected N-heterocyclic carbenes as latent pre-catalysts for the polymerization of ϵ -caprolactone *Polymer Chemistry* **2013**, *4*, 4172–4181.
- [57] (a) Bolm, C.; Dinter, C. L.; Seger, A.; Höcker, H.; Brozio, J. Synthesis of Catalytically Active Polymers by Means of ROMP: An Effective Approach toward Polymeric Homogeneously Soluble Catalysts *J. Org. Chem.* **1999**, *64*, 5730–5731. (b) Bolm, C.; Dinter, C. L.; Schiffrers, I.; Defrere, L. Living Ring-Opening Metathesis Polymerization of Enantiopure Norbornene-type β -Amino Acid Derivatives. *Synlett* **2001**, 1875–1877. (c) Bolm, C.; Tanyeli, C.; Grenz, A.; Dinter, C. L. *Adv. Synth. Catal.* **2002**, *344*, 649–656.
- [58] For reviews concerning ROMP reagents, see: (a) Barrett, A. G. M.; Hopkins, B. T.; Köbberling, J.; ROMPgel Reagents in Parallel Synthesis. *Chem. Rev.* **2002**, *102*, 3301–3324. (b) Barrett, A. G. M.; Hopkins, B. T.; Love, A. C.; Tedeschi, L. Parallel Synthesis of Terminal Alkynes Using a ROMPgel-Supported Ethyl 1-Diazo-2-oxopropylphosphonate. *Org. Lett.* **2004**, *6*, 835–837. (c) Arstad, E.; Barrett, A. G. M.; Tedeschi, L. ROMPgel-supported tris(triphenylphosphine)rhodium(I) chloride: a selective hydrogenation catalyst for parallel synthesis. *Tetrahedron Lett.* **2003**, *44*, 2703–2707. (d) Fuchter, M. J.; Hoffman, B. M.; Barrett, A. G. M. Ring-Opening Metathesis Polymer Sphere-Supported *s* eco-Porphyrazines: Efficient and Recyclable Photooxygenation Catalysts. *J. Org. Chem.* **2006**, *71*, 724–729.
- [59] (a) Rolfe, A.; Probst, D. A.; Volp, K.; Omar, I.; Flynn, D.; Hanson, P. R. High-load, Oligomeric dichlorotriazine (ODCT): A Versatile ROMP-derived Reagent and Scavenger. *J. Org. Chem.* **2008**, *73*, 8785–8790. (b) Stoianova, D. S.; Yao, L.; Rolfe, A.; Samarakoon, T.; Hanson, P. R. High-load, Oligomeric Monoamine Hydrochloride: Facile Generation via ROM Polymerization and Application as an Electrophile Scavenger. *Tetrahedron Lett.* **2008**, *49*, 4553–4555. For reviews concerning ROMP

- reagents (c) Flynn, D. L.; Hanson, P. R.; Berk, S. C.; Makara, G. M. New Developments in Chemical Library Synthesis. Norbornenyl Tags for Use in Phase-Switching, Sequestration, Capture-Release and Soluble Support Applications. *Curr. Opin. Drug Discovery Dev.* **2002**, *5*, 571–579. (d) Harned, A. M.; Zhang, M.; Vedantham, P.; Mukherjee, S.; Herpel, R. H.; Flynn, D. L.; Hanson, P. R. ROM Polymerization in Facilitated Synthesis. *Aldrichim. Acta* **2005**, *38*, 3–16. (e) Harned, A. M.; He H. S.; Toy, P. H.; Flynn, D. L.; Hanson, P. R. Multipolymer Solution-Phase Reactions: Application to the Mitsunobu Reaction. *J. Am. Chem. Soc.* **2005**, *127*, 52–53.
- [60] (a) Roberts, R. S. ROMPgel beads in IRORI format: acylations revisited. *J. Comb. Chem.* **2005**, *7*, 21–32. (b) Nguyen, M. H.; Smith III, A. B. Copper-catalyzed electrophilic amination of organolithiums mediated by recoverable siloxane transfer agents. *Org. Lett.* **2013**, *15*, 4872–4875. (c) Harned, A. M.; Probst, D. A.; Hanson, P. R. The Use of Olefin Metathesis in Combinatorial Chemistry: Supported and Chromatography-Free Syntheses. In *Handbook of Metathesis*; Grubbs, R. H., Ed.: Wiley-VCH: Weinheim, Germany, 2003; pp 361–402.
- [61] (a) Schwab, P.; Grubbs, R. H.; Ziller, J. W. Synthesis and Applications of $\text{RuCl}_2(=\text{CHR}')(\text{PR}_3)_2$: The Influence of the Alkylidene Moiety on Metathesis Activity. *J. Am. Chem. Soc.* **1996**, *118*, 100–110. (b) Schwab, P.; France, M. B.; Ziller, J. W.; Grubbs, R. H. A Series of Well-Defined Metathesis Catalysts-Synthesis of $[\text{RuCl}_2(=\text{CHR}')(\text{PR}_3)_2]$ and Its Reactions. *Angew. Chem. Int. Ed.* **1995**, *34*, 2039–2041.
- [62] Scholl, M.; Ding, S.; Lee, C. W.; Grubbs, R. H. Synthesis and Activity of a New Generation of Ruthenium-Based Olefin Metathesis Catalysts Coordinated with 1,3-Dimesityl-4,5-dihydroimidazol-2-ylidene Ligands. *Org. Lett.* **1999**, *1*, 953–956.
- [63] Ahn, J-M.; Wentworth, Jr. P.; Janda, K. D.; Soluble polymer-supported convergent parallel library synthesis *Chem. Comm.* **2003**, 480–481.
- [64] Pawar, G. M.; Weckesser, J.; Blechert, S.; Buchmeiser, M. R. Ring opening metathesis polymerization-derived block copolymers bearing chelating ligands: synthesis, metal

immobilization and use in hydroformylation under micellar conditions *Beilstein J. Org. Chem.* **2010**, *6*, No. 28.

- [65] Ding, L.; Qiu, J.; Zhu, Z. Facile Synthesis of Thiol-Functionalized Long-Chain Highly Branched ROMP Polymers and Surface-Decorated with Gold Nanoparticles. *Macromol. Rapid Commun.* **2013**, *34*, 1635–1641.
- [66] Nguyen, M. H.; Smith, III. A. B. Polymer-Supported Siloxane Transfer Agents for Pd-Catalyzed Cross-Coupling Reactions. *Org. Lett.* **2013**, *15*, 4258–4261.
- [67] (a) Graf, C.; Vossen, D. I. J.; Imhof, A.; van Blaaderen, A. A General Method To Coat Colloidal Particles with Silica. *Langmuir* **2003**, *19*, 6693–6700. (b) Schneider, G.; Decher, G. From Functional Core/Shell Nanoparticles Prepared via Layer-by-Layer Deposition to Empty Nanospheres. *Nano Lett.* **2004**, *4*, 1833–1839.
- [68] (a) Ambrose, D.; Fritz, J. S.; Buchmeiser, M. R.; Altz, N.; Bonn, G. K. New, high-capacity carboxylic acid functionalized resins for solid-phase extraction of a broad range of organic compounds. *J. Chromatography. A* **1997**, *786*, 259–268. (b) Buchmeiser, M. R.; Sinner, F.; Mupa, M.; Wurst, K. Ring-Opening Metathesis Polymerization for the Preparation of Surface-Grafted Polymer Supports. *Macromolecules* **2000**, *33*, 32–39. (c) Eder, K.; Reichel, E.; Schottenberger, H.; Huber, C. G.; Buchmeiser, M. R. Alkyne Metathesis Graft Polymerization: Synthesis of Poly(ferricinium)-Based Silica Supports for Anion-Exchange Chromatography of Oligonucleotides. *Macromolecules* **2001**, *34*, 4334–4341.
- [69] Kim, N. Y.; Jeon, N. L.; Choi, I. S.; Takami, S.; Harada, Y.; Finnie, K. R.; Girolami, G. S.; Nuzzo, R. G.; Whitesides, G. M.; Laibinis, P. E. Surface-Initiated Ring-Opening Metathesis Polymerization on Si/SiO₂. *Macromolecules* **2000**, *33*, 2793–2795.
- [70] (a) Kong, B.; Lee, J. K.; Choi, I. S. Surface-Initiated, Ring-Opening Metathesis Polymerization: Formation of Diblock Copolymer Brushes and Solvent-Dependent Morphological Changes. *Langmuir* **2007**, *23*, 6761–6765. (b) Faulkner, C. J.; Fischer, R. E.; Jennings, G. K. Surface-Initiated Polymerization of 5-(Perfluoro-n-alkyl)norbornenes from Gold Substrates. *Macromolecules* **2010**, *43*, 1203–1209.

- [71] Rutenberg, I. M.; Scherman, O. A.; Grubbs, R. H.; Jiang, W.; Garfunkel, E.; Bao, Z. Synthesis of Polymer Dielectric Layers for Organic Thin Film Transistors via Surface-Initiated Ring-Opening Metathesis Polymerization. *J. Am. Chem. Soc.* **2004**, *126*, 4062–4063.
- [72] Jeong, W.; Kessler, M. R. Toughness Enhancement in ROMP Functionalized Carbon Nanotube/Polydicyclopentadiene Composites. *Chem. Mater.* **2008**, *20*, 7060–7068.
- [73] (a) Le, D.; Montembault, V.; Soutif, J.-C.; Rutnakornpituk, M.; L. Fontaine. L. Fontaine. Synthesis of Well-Defined ω -Oxanorbornenyl Poly(ethylene oxide) Macromonomers via Click Chemistry and Their Ring-Opening Metathesis Polymerization. *Macromolecules* **2010**, *43*, 5611–5617. (b) Barrett, A. G. M.; Cramp, S. M.; Roberts, R. S.; ROMP-Spheres: A Novel High-Loading Polymer Support Using Cross Metathesis between Vinyl Polystyrene and Norbornene Derivatives. *Org. Lett.* **1999**, *1*, 1083–1086.
- [74] (a) Heckel, A.; Seebach, D. Preparation and characterization of TADDOLs immobilized on hydrophobic controlled-pore-glass silica gel and their use in enantioselective heterogeneous catalysis. *Chem. Eur. J.* **2002**, *8*, 559–572. (b) Lim, H.; Lee, J.; Jin, S.; Kim, J.; Yoon, J.; Hyeon, T. Highly active heterogeneous Fenton catalyst using iron oxide nanoparticles immobilized in alumina coated mesoporous silica. *Chem. Commun.* **2006**, 463–465. (c) Sharma, R. K.; Yukti, M. Silica encapsulated magnetic nanoparticles-supported Zn(II) nanocatalyst: A versatile integration of excellent reactivity and selectivity for the synthesis of azoxyarenes, combined with facile catalyst recovery and recyclability. *App. Cat. A: General* **2013**, *454*, 1–10.
- [75] (a) Elias, X.; Pleixats, R.; Man, M. W. C. Hybrid silica materials derived from Hoveyda–Grubbs ruthenium carbenes. Electronic effects of the nitro group on the activity and recyclability as diene and enyne metathesis catalysts. *Tetrahedron* **2008**, *64*, 6770–6781. (b) Mayr, M.; Buchmeiser, M. R.; Wurst, K. Synthesis of a Silica-Based Heterogeneous Second Generation Grubbs Catalyst. *Adv. Synth. Catal.* **2002**, *344*, 712–719. (c) Krause, J. O.; Lubbad, S.; Muyken, O.; Buchmeiser, M. R.

- Monolith- and Silica-Supported Carboxylate-Based Grubbs-Herrmann-Type Metathesis Catalysts. *Adv. Synth. Catal.* **2003**, *345*, 996–1004.
- [76] Garcie, M.; Zyl, W. E.; Cate, M. G. J.; Stouwdam, J. W.; Verweij, H.; Pimplapure, M. S.; Weickert, G. Novel Preparation of Hybrid Polypropylene/Silica Nanocomposites in a Slurry-Phase Polymerization Reactor. *Ind. Engl. Chem. Res.* **2003**, *42*, 3750–3757.
- [77] Rolfe, A.; Loh, J. K.; Maity, P. K.; Hanson, P. R. High-load, hybrid Si-ROMP reagents. *Org. Lett.* **2011**, *13*, 4–7.
- [78] Schätz, A.; Long, T. R.; Grass, R. N.; Stark, W. J.; Hanson, P. R.; Reiser, O. Immobilization on a Nanomagnetic Co/C Surface using ROM Polymerization: Generation of a Novel Hybrid Material as Support for a Recyclable Palladium Catalyst. *Adv. Func. Mat.* **2010**, *20*, 4323–4328.
- [79] Maity, P. K.; Rolfe, A.; Samarakoon, T. B.; Faisal, S.; Kurtz, R. D.; Long, T. R.; Schatz, A.; Flynn, D. L.; Grass, R. N.; Stark, W. J.; Reiser, O.; Hanson, P. R. Monomer-on-Monomer (MoM) Mitsunobu Reaction: Facile Purification Utilizing Surface-Initiated Sequestration. *Org. Lett.* **2011**, *13*, 8–10.
- [80] (a) Barrett, A. G. M.; Smith, M. L.; Zecri, F. J. Impurity annihilation; a strategy for solution phase combinatorial chemistry with minimal purification. *Chem. Commun.* **1998**, 2317–2318. (b) Ball, C. P.; Barrett, A. G. M.; Poitout, L. F.; Smith, M. L.; Thorn, Z. E. Polymer backbone disassembly: polymerizable templates and vanishing supports in high loading parallel synthesis. *Chem. Commun.* **1998**, 2453–2454. (c) Barrett, A. G. M.; Roberts, R. S.; Schröder, J. Impurity annihilation: chromatography-free parallel Mitsunobu reactions. *Org. Lett.* **2000**, *2*, 2999–3001. (d) Asad, N.; Hanson, P. R.; Long, T. R.; Rayabarapu, D. K.; Rolfe, A. Synthesis of epoxybenzo[d]isothiazole 1,1-dioxides: ROMP purification via sequestration of excess oxa-norbornene sultams. *Chem. Commun.* **2011**, *47*, 9528–9530.
- [81] Maity, P. K.; Kainz, Q. M.; Faisal, S.; Rolfe, A.; Samarakoon, T. B.; Basha, F. Z.; Reiser, O.; Hanson, P. R. Intramolecular Monomer-on-Monomer (MoM) Mitsunobu Cyclization for the Synthesis of Thiadiazepine-dioxides. *Chem. Commun.* **2011**, *47*, 12524–12526.

- [82] (a) Ottesen, L. K.; Olsen, C. A.; Witt, M.; Jaroszewski, J. W.; Franzyk, H. Selectively N-protected enantiopure 2,5-disubstituted piperazines: Avoiding the pitfalls in solid-phase Fukuyama-Mitsunobu cyclizations. *Chem. Eur. J.*, **2009**, *15*, 2966–2978. (b) Arya, P.; Wei, C.-Q.; Barnes, M. L.; Daroszewska, M. A Solid Phase Library Synthesis of Hydroxyindoline-Derived Tricyclic Derivatives by Mitsunobu Approach. *J. Comb. Chem.* **2004**, *6*, 65–72. (c) Banfi, L.; Basso, A.; Giardini, L.; Riva, R.; Rocca, V.; Guanti, G. Tandem Ugi MCR/Mitsunobu Cyclization as a Short, Protecting-Group-Free Route to Benzoxazinones with Four Diversity Points *Eur. J. Org. Chem.* **2011**, 100–109. (d) Samanta K.; Srivastava N.; Saha S.; Panda G. Inter- and intramolecular Mitsunobu reaction and metal complexation study: synthesis of *S*-amino acids derived chiral 1,2,3,4-tetrahydroquinoxaline, benzo-annulated [9]-N₃ peraza, [12]-N₄ peraza-macrocycles *Organic & biomolecular chemistry* **2012**, *10*, 1553–1564.
- [83] For a related paper on Capture-ROMP-release, see: Harned, A. M.; Hanson, P. R. Capture-ROMP-Release: Application for the Synthesis of *O*-Alkyl Hydroxylamines. *Org. Lett.* **2002**, *4*, 1007–1110.
- [84] Eichenseer, C. M.; Kast, B.; Perica, M. A.; Hanson, P. R.; Reiser, O. Synthesis and application of magnetic Noyori-Type ruthenium catalysts for asymmetric transfer hydrogenation reactions in water *ACS Sustainable Chem. Eng.* **2016**, *4*, 2698–2705.

Chapter 2

High Load Soluble ROMP-Derived Alkylating Reagents and their Application in Library Synthesis

Section 2.1 “Click”-Capture, Ring-Opening Metathesis Polymerization (ROMP), Release: Facile Triazolation Utilizing ROMP-Derived Oligomeric Phosphates

2.1.1 Introduction

In Chapter 1, recent advances in the area of immobilized reagents for the production of libraries for high-throughput screening (HTS) and automated technologies were highlighted. In addition, the end of Chapter 1 summarized advances in ring-opening metathesis polymerization (ROMP) technology for immobilization of a variety of soluble, silica and magnetic reagents/scavengers and catalysts. In Chapter 2 (Section 2.1) we report the development and utilization of high-load, soluble oligomeric triazole phosphates for direct triazolation of *N*-, *O*- and *S*-nucleophilic species in a “Click”-capture, ROMP, release protocol that exploits the innate properties of phosphate-based alkylating agents. To the best of our knowledge, these reagents represent the first phosphate-based oligomeric/polymeric reagents in the literature.

Alkylations of simple nitrogen, oxygen, and sulfur nucleophiles are highly prevalent and significant reactions in organic synthesis, medicinal chemistry and drug discovery.¹ Moreover, benzylation of amines and alcohols are the most commonly used protecting group strategies in organic synthesis, due to the ease of benzyl incorporation and cleavage, which can be achieved under a variety of conditions.² In addition, benzylation is a useful diversification reaction in medicinal chemistry, high-throughput chemistry, and diversity-oriented synthesis (DOS).³ The most common reagents to attain this operation are benzyl bromides, which usually severe lachrymators and present both safety and toxicity issues. In this regard, a number of alternative methods for alkylation/benzylation⁴ and polymer-supported⁵ reagents have been developed.

In 1998, Reitz and coworkers reported the first example of solid-supported resin bound arylsulfonate esters as an alkylating reagent (Figure 2.1.1).⁶ In 2004, Hanson and coworkers reported the development of high-load, soluble oligomeric sulfonate esters (OSC_n) as a free-flowing solids using ring-opening metathesis polymerization (ROMP) technology and demonstrated their utilization for facile benzylation of a variety of amines⁷ (Figure 2.1.1). Later, in 2007, Hanson and coworkers reported oligomeric benzylsulfonium salts, which were generated via ROMP⁸ (Figure 2.1.1). These oligomeric sulfonium salts were utilized for facile benzylations of various nucleophiles via simple precipitation/filtration to deliver products in excellent yields and purities.

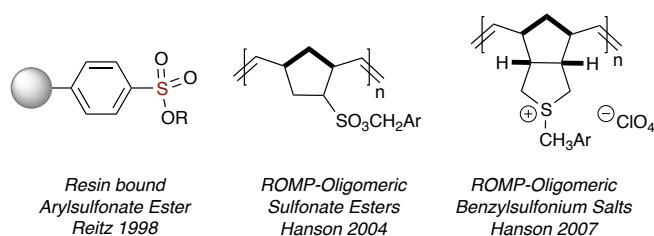
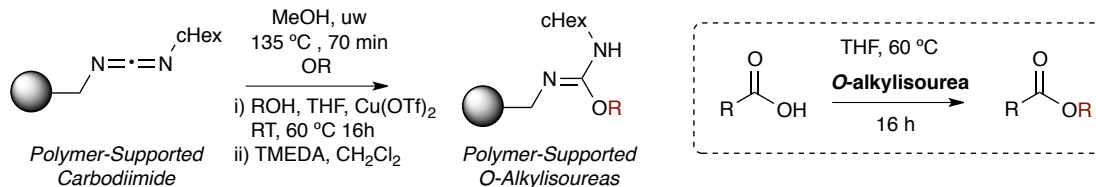


Figure 2.1.1: *Polymer Supported and ROMP-Derived Alkylating Reagents*

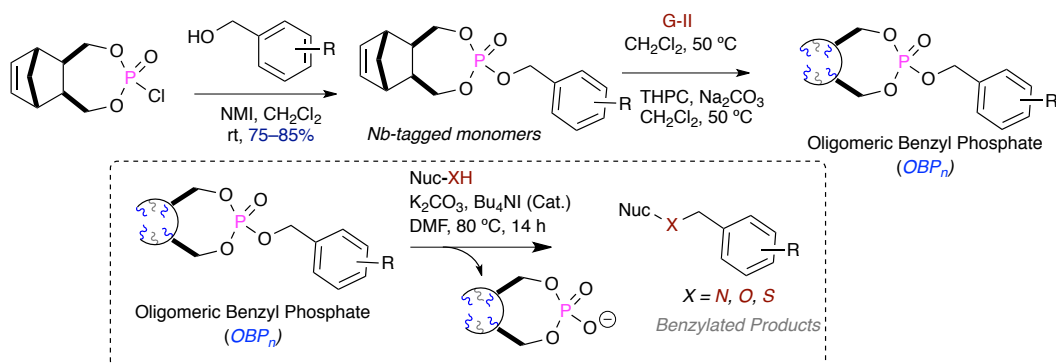
During the period 2002–2009, several reports from Linclau and coworkers demonstrated the application of polymer supported *O*-alkylisoureas⁹ for the alkylation of various carboxylic acids. This reagent was prepared from commercially available polymer supported carbodiimide (Scheme 2.1.1). The prepared *o*-methylisourea reagent was successfully used for the preparation of methyl esters of the corresponding carboxylic acids. In addition, *O*-alkylisoureas were utilized to transform carboxylic acids into the corresponding benzyl, allyl, and *p*-nitrobenzyl esters in high yields and purities after simple resin filtration and solvent evaporation.

Scheme 2.1.1: Synthesis and Utilization of Polymer-Supported *O*-Alkylisoureas



In 2010, Hanson and coworkers reported soluble ROMP-derived oligomeric benzyl phosphates (OBP_n) for the application in facile benzylation in purification free protocols (Scheme 2.1.2).¹⁰ The innate property of phosphate as a leaving group,^{11,12} including stability, multiple valency/oxidation states, and variable pKa can be harnessed to generate these oligomeric phosphate reagents for the benzylation of *N*, *O* and *S*-nucleophilic species. The oligomeric benzyl phosphates OBP were synthesized via ROMP of Nb-tagged phosphate monomers and were utilized for efficient benzylation of a variety of nucleophiles.

Scheme 2.1.2: ROMP-Derived Oligomeric Benzyl Phosphate (OBP), Benzylation of *N*-, *O*-, and *S*-Nucleophiles.



A variety of cyclic and acyclic amines were subjected to benzylation and were found to proceed smoothly toward the desired benzylated products. Additionally, benzylation of *N*-, *O*- and *S*-nucleophiles was achieved successfully in excellent yields and purities. In all cases, the resulting polymer was precipitated, and subsequent filtration

using a silica SPE cartridge, followed by the evaporation of solvent afforded the desired benzylated products in excellent yields and high purities. In this section, we will discuss the development and utilization of a new ROMP-derived oligomeric triazole phosphate (OTP) for application as a soluble, efficient triazolating reagent of *N*-, *O*- and *S*-nucleophilic species.

2.1.2 Results and Discussion

Triazoles and their derivatives have demonstrated a wide variety of biological profiles, which include antifungal,¹³ antibacterial¹⁴ and anticancer activities.¹⁵ Despite this activity, the utilization of solution-phase or immobilized reagents to directly triazolate nucleophilic species in a one-step protocol has been limited to reports of a two-step, one-pot propargylation-click protocol which, while very powerful, has limitations in the potential storage of sub-libraries which would be comprised of reactive alkynes and azides.¹⁶ In this chapter, we demonstrate the synthesis of ROMP-derived triazolating reagents (OTP) for application in purification free diversifications of nucleophilic species using the title method, termed “Click”-Capture, ROMP, Release.¹⁷ This method utilizes a propargyl-tagged norbornenyl-phosphate to capture an azide in a classical “click” reaction, followed by ROM polymerization to generate the desired soluble oligomeric triazole reagent (OTP). Subsequent release via S_N2 displacement with nucleophilic species yields triazolated products along with the spent oligomeric phosphate that is readily sequestered via precipitation (Figure 2.1.2).

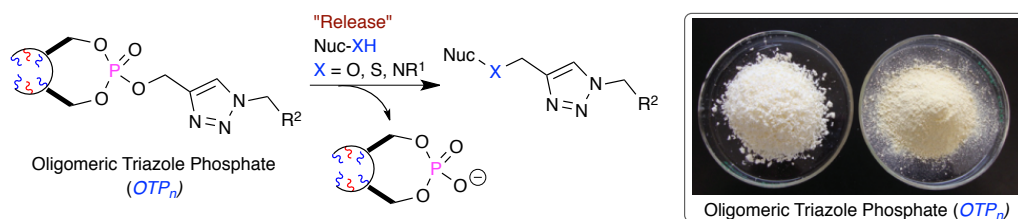
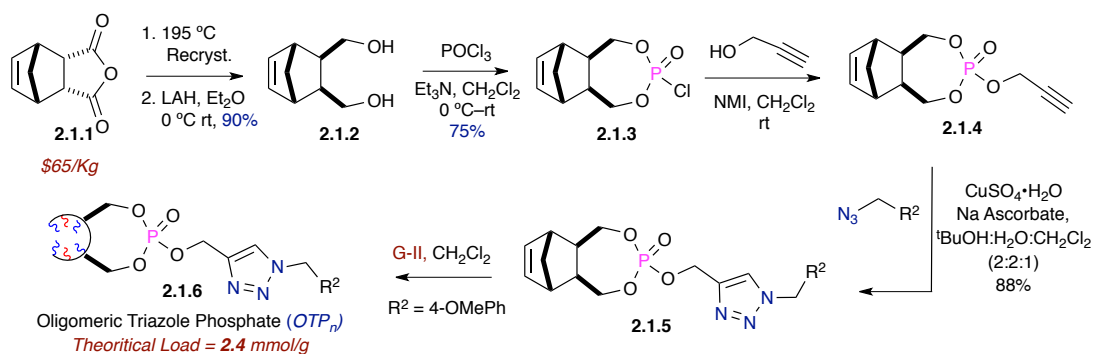


Figure 2.1.2 Utilization of Oligomeric Triazole Phosphate (OTP_n)

The synthesis of the oligomeric triazole phosphate bearing a p-methoxy benzyl group **OTP 2.1.5**, starts with the exo-norbornenyl tagged (Nb-tagged) phosphonyl chloride **2.1.3** utilized in the synthesis of previously reported ROMP-derived benzylating reagent OBP.^{10,18} Phosphorylation of propargyl alcohol with Nb-tagged phosphonyl chloride **2.1.3**, followed by a “Click”-capture event of the corresponding azide, yields the desired monomer **2.1.5** in an efficient fashion. ROM polymerization of monomer **2.1.5** was achieved with $RuCl_2(PCy_3)_2=CHPh$ (G-II), followed by basic workup utilizing the Pederson protocol.^{19,20} Precipitation via dropwise addition into anhydrous Et_2O , afforded the corresponding oligomeric triazole phosphate (OTP_{20}) **2.1.6** as a free-flowing white solid possessing a theoretical load of 2.4 mmol/g (Scheme 2.1.3).

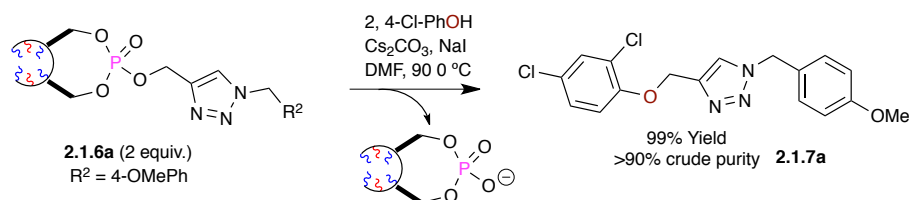
Scheme 2.1.3. Synthesis of Oligomeric Triazole Phosphate (OTP) **2.1.6**



Investigation into the utilization of **OTP 2.1.6** as a direct triazolating reagent was next studied using reaction conditions reported for the application of OBP (Scheme 2.1.4). After optimization of reaction conditions for the (triazolyl)methylation of 2,4-

dichlorophenol utilizing OTP **2.1.6a**, the corresponding triazole ether **2.1.7a**, was isolated in excellent yield (98%) and crude purity (>90%) using simple filtration through a Celite® SPE (Table 2.1.2).

Scheme 2.1.4. Utilization of Oligomeric Triazole Phosphate (OTP) **2.1.6a**



The application of OTP **2.1.6a** as an efficient triazolating reagent was extended to a variety of *N*-, *O*- and *S*-nucleophilic species (Table 2.1.1). Initially, a variety of phenols were utilized (Table 2.1.1, entries 1–3) though reduced yields were observed for sterically hindered naphthalene-1-ol. In addition to phenols, thiophenols (Table 2.1.1, entry 5) and a variety of amines (Table 2.1.1, entries 6–10) were successfully utilized to release the corresponding triazole in >90 % crude purity.

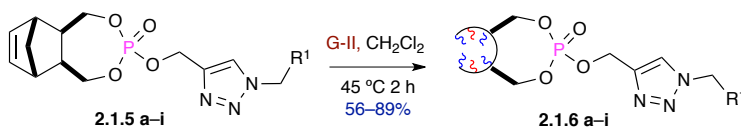
Table 2.1.1. (Triazolyl)methylation of *N*-, *O*-, and *S*-Nucleophiles Using OTP₂₀ **2.1.6a**

Entry	Nucleophile	Pdt	Yield (%)
1	2,4-dichlorophenol	2.1.7a	98
2	4-fluorophenol	2.1.7b	92
3	4-(tert-butyl)phenol	2.1.7c	90
4	naphthalene-1-ol	2.1.7d	69
5	4-(methylthio)benzenethiol	2.1.7e	60
6	Morpholine	2.1.7f	72
7	Thiomorpholine	2.1.7g	75
8	1-phenylpiperazine	2.1.7h	95
9	Indoline	2.1.7i	88
10	<i>N</i> -ethylnaphthalen-1-amine	2.1.7j	62

^[a] Purities >90% observed for all reactions using both GC and ¹H NMR. ^[b] OTP **2.7a** utilized as a 20-mer.

Building on the success of OTP **2.1.6a**, a variety of additional OTP derivatives **2.1.6b–i** were synthesized as free-flowing powders on gram scale from ROM polymerization of their corresponding monomers utilizing the **G-II** catalyst (Table 2.1.2).

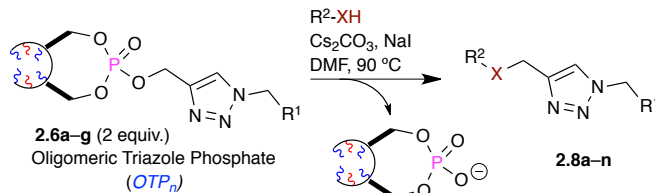
Table 2.1.2. *Synthesis of Various OTP_n Analogues*



Monomer	R ¹	pdt	Yield (%) ^a
2.1.5a	4-OMe-C ₆ H ₄	2.1.6a	82
2.1.5b	4-Me-C ₆ H ₄	2.1.6b	88
2.1.5c	2-Me-C ₆ H ₄	2.1.6c	77
2.1.5d	4-Cl-C ₆ H ₄	2.1.6d	71
2.1.5e	4-F-C ₆ H ₄	2.1.6e	74
2.1.5f	4-CF ₃ -C ₆ H ₄	2.1.6f	73
2.1.5g	Cylohexyl	2.1.6g	70
2.1.5h	4-Br-C ₆ H ₄	2.1.6h	89
2.1.5i	2-Furyl	2.1.6i	56

^aYields corresponding to metathesis of corresponding monomers.

With a variety of OTP derivatives in hand, the (triazolyl)methylation of both naphthalene-1-ol and *N*-ethylnaphthalen-1-amine with OTP derivatives **2.1.6a–g** was investigated (Table 2.1.3). All reactions proceeded with good yields with >90% crude purity after Celite[®] SPE to remove the spent oligomer.

Table 2.1.3 Triazolylation Utilizing OTP derivatives 2.1.6a–g

entry	Nucleophile	OTP	Pdt	Yield (%) ^a
1	naphthalene-1-ol	2.1.6a	2.1.8a	72
2	naphthalene-1-ol	2.1.6b	2.1.8b	90
3	naphthalene-1-ol	2.1.6c	2.1.8c	55
4	naphthalene-1-ol	2.1.6d	2.1.8d	68
5	naphthalene-1-ol	2.1.6e	2.1.8e	70
6	naphthalene-1-ol	2.1.6f	2.1.8f	65
7	naphthalene-1-ol	2.1.6g	2.1.8g	49
8	<i>N</i> -ethylnaphthalen-1-amine	2.1.6a	2.1.8h	62
9	<i>N</i> -ethylnaphthalen-1-amine	2.1.6b	2.1.8i	52
10	<i>N</i> -ethylnaphthalen-1-amine	2.1.6c	2.1.8j	63
11	<i>N</i> -ethylnaphthalen-1-amine	2.1.6d	2.1.8k	51
12	<i>N</i> -ethylnaphthalen-1-amine	2.1.6e	2.1.8l	50
13	<i>N</i> -ethylnaphthalen-1-amine	2.1.6f	2.1.8m	60
14	<i>N</i> -ethylnaphthalen-1-amine	2.1.6g	2.1.8n	66

^[a] Purities >90% observed for all reactions using both GC and ¹H NMR. ^[b] OTP **4a–g** utilized as a 20-mer.

Overall, we have developed and demonstrated the synthesis and utilization of oligomeric triazole phosphates for direct (triazolyl)methylation of *N*-, *O*- and *S*-nucleophilic species in a “Click”-capture, ROMP, release protocol. These oligomeric reagents are readily synthesized on multi-gram scale from commercially available materials as soluble, high-load, free-flowing powders. These oligomeric reagents are easy to handle, non-toxic, air stable and can be easily stored for long-term at room temperature. The application of OTP in the diversification of core scaffolds for the synthesis of diverse collections of small molecules will be discussed in the next section.

Section: 2.2 Facile (Triazolyl)methylation of MACOS-derived Benzofused Sultams Utilizing ROMP-derived OTP Reagents

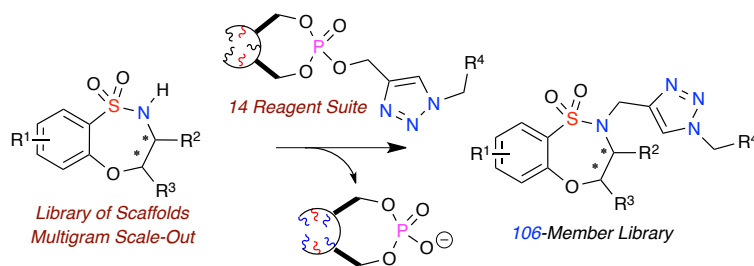
2.2.1 Introduction

Enabling technologies that allow for the assembly of diverse small molecule collections where synthesis, diversification and purification are integrated into one parallel process can play a valuable role in fast paced early drug discovery efforts. Classical synthetic approaches to small molecule libraries have suffered from multistep processes requiring costly and time-consuming solvent/compound transfer and purification at every stage. In addition, issues relating to low yielding or unreliable reactions for the preparation of compounds and key intermediates have a negative effect on early stage drug discovery.²¹ In recent years, a variety of enabling technologies have been developed to address these limitations, giving rapid access to small molecule HTS collections.²² One such technology has been the development and utilization of continuous flow synthesis platforms, which can carry out multistep processes, combined with inline diversification/purification, utilizing immobilized reagents/scavengers.²³ In addition to inline purification,²⁴ the ability for automation,²⁵ safe, in situ generation of reactive intermediates,²⁶ and rapid reaction optimization and multigram scale-out makes this a powerful enabling tools in early stage drug discovery.²⁷

This section of Chapter 2 describes the utilization of a microwave-assisted, continuous flow organic synthesis (MACOS) platform in combination with soluble oligomeric triazole phosphates (OTP) reagents derived from ROMP for the rapid, purification-free synthesis of a 106-member library of benzothioxazepine-1,1-dioxides.²⁸

In the recent years, sultams (cyclic sulfonamide analogues) have emerged in as important targets in drug discovery due to their extensive chemical and biological profiles.²⁹ A variety of core sultam scaffolds prepared via MACOS³⁰ could be quickly diversified in a facile, purification-free process utilizing a suite of ROMP-derived reagents.³¹ A number of synthetic methods have been developed to give access to diverse sultam libraries.³² Building on these efforts, the utilization of MACOS in combination with ROMP-derived oligomeric reagents for the library synthesis of benzothioxazepine-1,1-dioxides will be described here (Scheme 2.2.1).²⁸

Scheme 2.2.1. MACOS-“Click”-Capture, ROMP, Release 108-Member Library

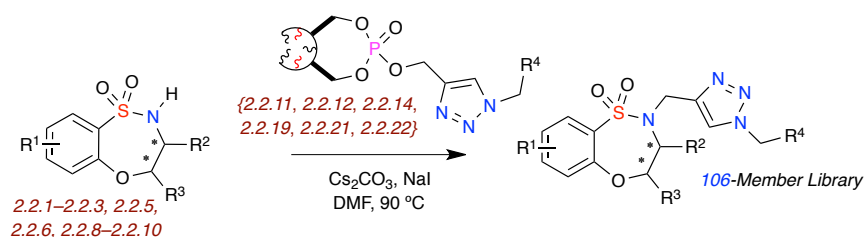


2.2.2 Result and Discussion

The corresponding core scaffolds benzothioxazepine-1,1-dioxide were synthesized using a MACOS platform³³ in collaboration with Organ and coworkers. In a concerted effort, a suite of soluble, high-load ROMP-derived oligomeric triazole phosphates were generated in our laboratory for the facile, purification-free diversification of nucleophilic small molecules.¹⁷ These ROMP-derived OTP reagents were found to be bench stable, free flowing solids that are readily soluble in a variety of solvents (CH₂Cl₂, CHCl₃, DMF) to generate stock solutions, making them well-suited for parallel synthesis. With these reagents in hand, the (triazolyl)methylation of core benzothioxazepine-1,1-dioxide scaffolds **2.2.1–2.2.10** scaled-out on the MACOS platform were investigated with a suite

of oligomeric triazole phosphate (OTP) reagents {2.2.11–2.2.24}. Initially a 16-member prototype library was investigated for the generation of triazole containing benzothiazepine-1,1-dioxides (Table 2.2.1).

Table 2.2.1. Prototype Library Demonstrating Utilization of Scaffolds **2.2.1–2.2.3**, **2.2.5**, **2.2.6**, **2.2.8–2.2.10** with OTP₂₀ Oligomers {2.2.11; 2.2.12; 2.2.14; 2.2.19; 2.2.21; 2.2.22}



entry ^a	scaffold	OTP ₂₀ {X}	yield %	entry ^a	scaffold	OTP ₂₀ {X}	yield %
1	2.2.1	{2.2.21}	85	9	2.2.9	{2.2.11}	63
2	2.2.2	{2.2.22}	62	10	2.2.9	{2.2.12}	89
3	2.2.3	{2.2.21}	97	11	2.2.9	{2.2.14}	82
4	2.2.3	{2.2.22}	92	12	2.2.9	{2.2.19}	79
5	2.2.5	{2.2.22}	70	13	2.2.10	{2.2.11}	68
6	2.2.6	{2.2.21}	98	14	2.2.10	{2.2.12}	75
7	2.2.8	{2.2.21}	98	15	2.2.10	{2.2.14}	72
8	2.2.8	{2.2.22}	94	16	2.2.10	{2.2.19}	75

^a Reaction conditions: OTP₂₀ (1.5 equiv.), NaI (0.2 equiv.), Cs₂CO₃ (3 equiv.), dry DMF (0.2 M) and sultam **2.2.1–2.2.10** (1 equiv.). Reaction heated at 90 °C for 2–14 h (TLC analysis).

Utilizing reported conditions for the (triazolyl)methylation of a variety of nucleophilic species,¹⁷ the generation of a 16-member prototype library was successfully achieved in good yield and crude purity (85–100%, ¹H NMR), demonstrating both substrate and reagent scope. With the synthesis of a 16-member prototype library, a 96-

member library was designed with benzothiazepine-1,1-dioxide scaffolds **2.2.1–2.2.10** and OTP₂₀ oligomers {2.2.11–2.2.24}.

Library Design. A *full-matrix* library was designed using in silico analysis, literature precedence, and observed synthetic results.³⁴ A virtual library incorporating all possible building block combinations of sultam scaffolds **2.2.1–2.2.10** (Figure 2.2.2) with OTP reagents {2.2.11–2.2.24} (Figure 2.2.3) was evaluated. Physicochemical property filters were applied, guiding the elimination of undesirable combinations that led to products with undesirable in-silico properties. These metric filters included standard Lipinski Rule of 5 parameters (molecular weight <500, ClogP <5.0, number of H-acceptors <10, and number of H-donors <5), in addition to consideration of the number of rotatable bonds (<5) and polar surface area. Absorption, distribution, metabolism and excretion (ADME) properties were calculated along with diversity analysis using standard H-aware 3D BCUT descriptors compared against the MLSMR screening set (~7/2010; ~330,000 unique chemical structures). Guided by this library design analysis, a 96-member library was designed.

Benzothiazepine-1,1-dioxide Scaffolds **2.2.1–2.2.10**

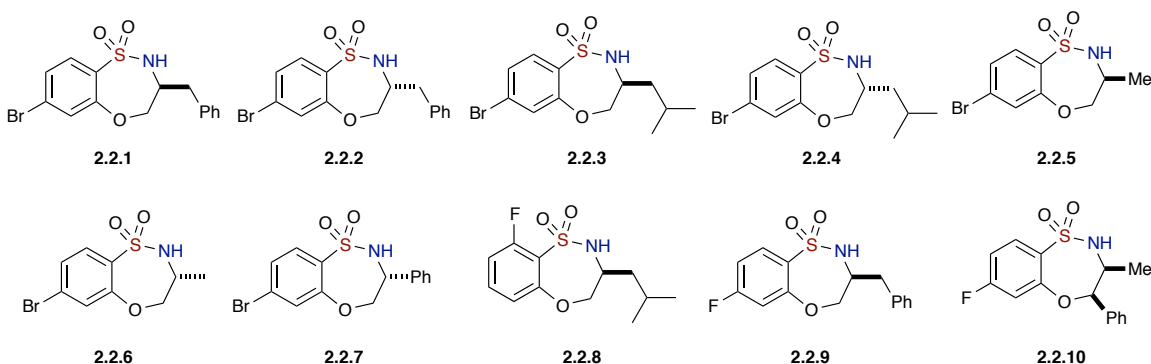


Figure 2.2.2. Scaffolds (**2.2.1–2.2.10**) for Library Building Blocks.

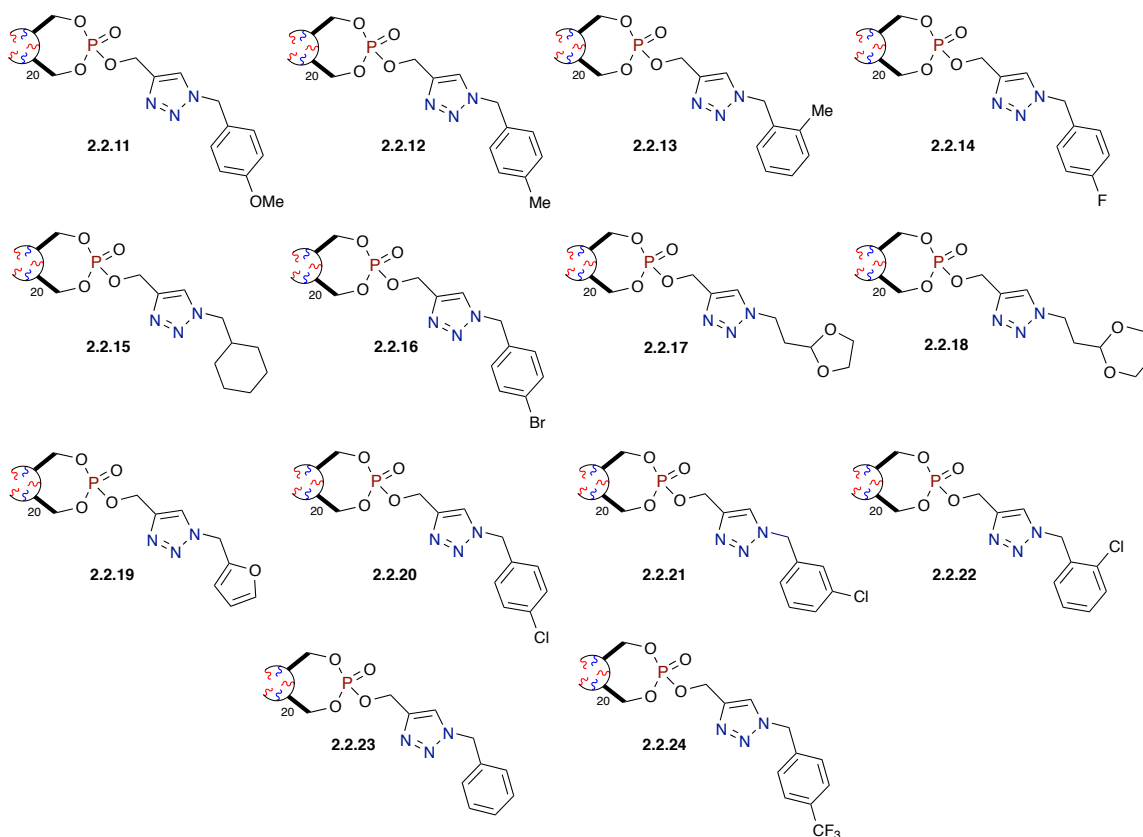
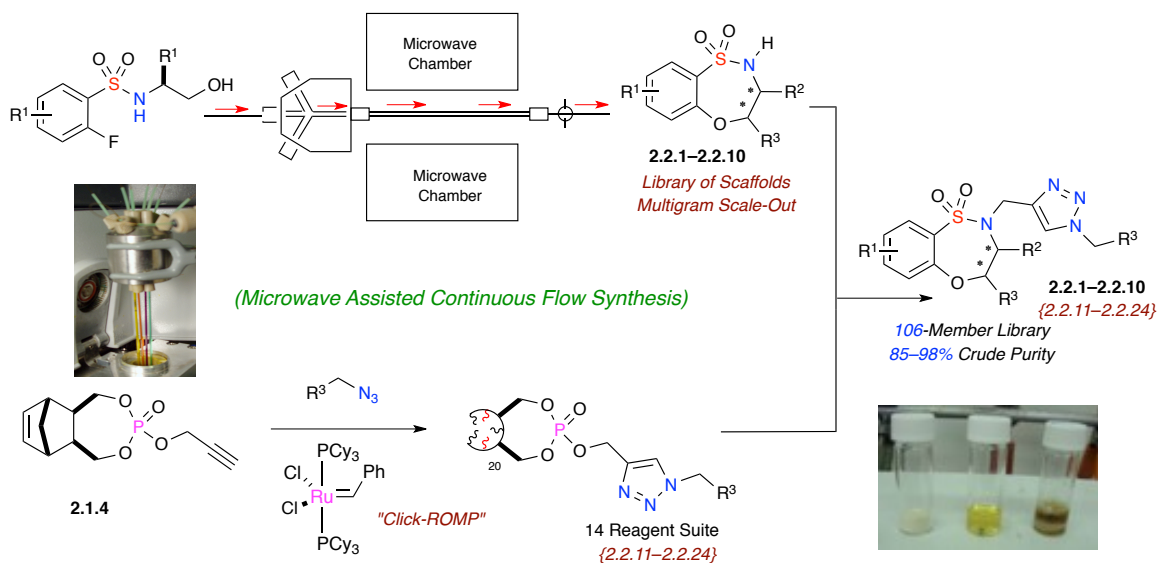


Figure 2.2.3. *OTP*₂₀ Reagents {2.2.11–2.2.24} for Library Building Blocks.

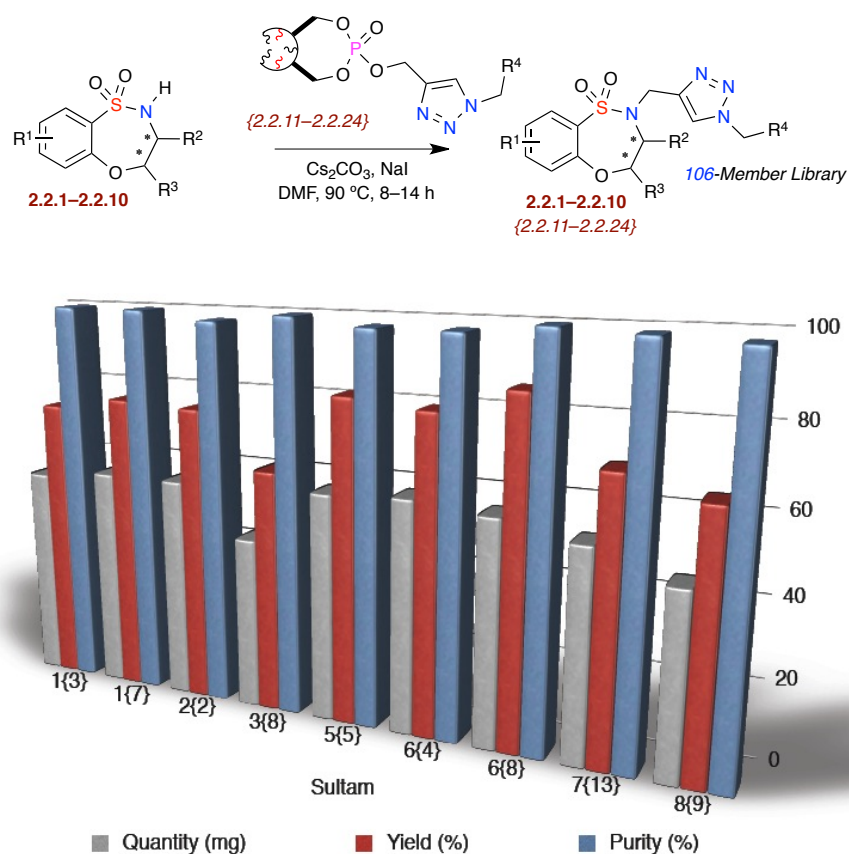
Microwave-assisted continuous flow organic synthesis (MACOS) has emerged as a powerful technology for libraries production of compounds in a scale suitable for biological screening purposes.²⁷ The use of microreactors technology can reduce reaction times as well as the quantity of waste produced such as solvents, because the method efficiently delivers desired quantities of material that are necessary for early stage biological screening. The MACOS approach addresses safety, as the quantities of toxic compounds are minimized, and reactions performed using this methodology are cleaner and higher yielding as compared to typical solution phase approach.³⁵ The combination of MACOS platform and ROMP-derived oligomeric triazole phosphates (OTP_n) were

successfully utilized for the library preparation of triazole containing benzothiazepine-1,1-dioxides.

Scheme 2.2.2. *Facile Library Generation Utilizing MACOS Scale-out Combined with Triazolation and ROMP-derived OTP_n*



Library Generation. The proposed 96-member library was prepared in 1-dram vials via a mix-and-match approach using stock solutions of scaffold (2.2.1-2.2.10) and OTP₂₀ reagents {2.2.11-2.2.24}. Crude purity analysis of the 96-member library demonstrated that 66 compounds had crude purities of 80-99%, 16 compounds at 70-80% and 8 compounds with <70% (Scheme 2.2.2). Final analysis of this library after purification by automated mass-directed LCMS resulted in the successful synthesis of 90 compounds with 84/90 compounds possessing >90% final purity (Graph 2.2.1).



Graph 2.2.1. Final Mass, Purity and Yield Analysis for Benzothiazoxazepine-1,1-dioxide Library.

In conclusion, a 90-member library of triazole containing benzothiazoxazepine-1,1-dioxides was successfully prepared combining two enabling technologies, namely MACOS platform and ROMP-derived OTP reagents. Utilization of a suite of soluble OTP_n reagents **{2.2.11–2.2.24}**, 10 MACOS-derived sultam scaffolds **2.2.1–2.2.10** were successfully diversified in a purification-free parallel process amenable for automation. Taken collectively, a total of 106 out of 112 sultams were successfully generated (95% success rate) with 100/112 (89% rate) possessing purities >90%. The compound libraries have been submitted to the University of Kansas Center for Chemical Methodologies and Library Development (KU-CMLD) for delivery to the NIH Molecular Library Small

Molecule Repository (MLSMR) for distribution and broad screening for biological activity within the MLPCN screening network.

Special Acknowledgment

The author acknowledges that portions of this chapter, including the preliminary Introduction and Results and Discussion sections, are reprinted, in part, or adapted from the following publications, with permission from the corresponding publishers:

- [1] Long, T. R.; Faisal, S.; Maity, P. K.; Rolfe, A.; Kurtz, R.; Klimberg, S. V.; Najjar, R.; Basha, F. Z.; Hanson, P. R. “Click”-Capture, Ring-Opening Metathesis Polymerization (ROMP), Release: Facile Triazolation Utilizing ROMP-Derived Oligomeric Phosphates. *Org. Lett.* **2011**, *13*, 2038–2041. Copyright 2011, with permission from American Chemical Society publications.

- [2] Faisal, S.; Ullah, F.; Maity, P. K.; Rolfe, A.; Samarakoon, T. B.; Porubsky, P.; Neuenswander, B.; Lushington, G. H.; Basha, F. Z.; Organ, M. G.; Hanson, P. R. Facile (Triazolyl)methylation of MACOS-derived Benzofused Sultams Utilizing ROMP-derived OTP Reagents. *ACS Comb. Sci.* **2012**, *14*, 268–272. Copyright 2016, with permission from American Chemical Society publications.

References

- [1] (a) Albinia, P. A.; Dudley, G. B. New Reagents for the Synthesis of Arylmethyl Ethers and Esters. *Synlett* **2010**, 6, 841–851. (b) Enyong, A. B.; Moasser, B. Ruthenium-Catalyzed N-Alkylation of Amines with Alcohols under Mild Conditions Using the Borrowing Hydrogen Methodology *J. Org. Chem.* **2014**, 79, 7553–7563. (c) Andrew J. A. Watson, Aoife C. Maxwell, and Jonathan M. J. Williams. *J. Org. Chem.* **2011**, 76, 2328–2331. (d) Nishimoto, Y.; Okita, A.; Yasuda, M.; Baba, A. Synthesis of a Wide Range of Thioethers by Indium Triiodide Catalyzed Direct Coupling between Alkyl Acetates and Thiosilanes. *Org. Lett.* **2012**, 14, 1846–1849. (d) Faisal; S.; Basha; A. F.; Siddiqui; H.; Basha. F. Z.; O-Alkylation of Menthone Oxime: Synthesis and ^{13}C NMR Studies of a Series of Novel Oxime Ethers. *Synth. Comm.* **2010**, 40, 3101–3108.
- [2] (a) Paquette, L. A. In *Encyclopedia of Reagents for Organic Synthesis*, 1st ed.; John Wiley and Sons: New York, 1995; pp 316–318. (b) March, J. *Advanced Organic Chemistry*, 4th ed.; Wiley: New York, 1991. (c) Greene, T. W.; Wuts, P. G. M. In *Protective Groups in Organic Synthesis*, 4th ed.; John Wiley and Sons: New York, 2007; pp 102–148.
- [3] (a) Dolle, R. E.; Bourdonnec, B. L. Goodman, A. J.; Morales, G. A.; Thomas, C. J.; Zhang, W. Comprehensive Survey of Chemical Libraries for Drug Discovery and Chemical Biology: 2008. *J. Comb. Chem.* **2009**, 11, 739–790. (b) Fenster, E.; Rayabarapu, D. K.; Zhang, M.; Mukherjee, S.; Hill, D.; Neuenswander, B.; Schoenen, F.; Hanson, P. R.; Aubé, J. Three-Component Synthesis of 1,4-Diazepin-5-ones and the Construction of γ -Turn-like Peptidomimetic Libraries. *J. Comb. Chem.* **2008**, 10, 230–234.
- [4] (a) Shieh, W.-C.; Lozanov, M.; Loo, M.; Repic, O.; Blacklock, T. J. DABCO- and DBU-accelerated green chemistry for N-, O-, and S-benzylation with dibenzyl carbonate. *Tetrahedron Lett.* **2003**, 44, 4563–4565. (b) Loris, A.; Perosa, A.; Selva, M.; Tundo, P. J. Selective *N,N*-Di-benylation of Primary Aliphatic Amines with Dibenzyl Carbonate in the Presence of Phosphonium Salts. *Org. Chem.* **2004**, 69,

- 3953–3956. (c) Poon, K. W. C.; House, S. E.; Dudley, G. B. A bench-stable organic salt for the benzylation of alcohols. *Synlett* **2005**, 20, 3142–3144. (d) Lopez, S. S.; Dudley, G. B. Convenient method for preparing benzyl ethers and esters using 2-benzyloxypyridine. *Beilstein J. Org. Chem.* **2008**, 4, No. 44.
- [5] (a) Hanessian, S.; Huynh, H. K. Solution and solid-phase *p*-alkoxybenzylation of alcohols under neutral conditions. *Tetrahedron Lett.* **1999**, 40, 671–674. (b) Rueter, J. K.; Nortey, S. O.; Baxter, E. W.; Leo, G. C.; Reitz, A. B. Arylsulfonate esters in solid phase organic synthesis. I. Cleavage with amines, thiolate, and imidazole. *Tetrahedron Lett.* **1998**, 39, 975–978. (c) Prakash, G. K. S.; Weber, C.; Chacko, S.; Olah, G. A. New Solid-Phase Bound Electrophilic Difluoromethylating Reagent. *J. Comb. Chem.* **2007**, 9, 920–923.
- [6] (a) Baxter, E. W.; Rueter, J. K.; Nortey, S. O.; Reitz, A. B. Arylsulfonate esters in solid phase organic synthesis. II. Compatibility with commonly-used reaction condition *Tetrahedron Lett.* **1998**, 39, 979–982. (b) Yoshino, T.; Togo, H. Facile Preparation of Polymer-Supported Methyl Sulfonate and its Recyclable Use for Methylation of Carboxylic Acids and Amines *Synlett* **2005**, 517–519.
- [7] Zhang, M.; Moore, J. D.; Flynn, D. L.; Hanson, P. R. Development of High-Load, Soluble, Oligomeric Sulfonate Esters via ROM Polymerization: Applications to the Benzylation of Amines. *Org. Lett.* **2004**, 6, 2657–2660.
- [8] Zhang, M.; Flynn, D. L.; Hanson, P. R. Oligomeric Benzylsulfonium Salts: Facile Benzylation via High-Load ROMP Reagents. *J. Org. Chem.* **2007**, 72, 3194–3198.
- [9] (a) Crosignani, S.; White, P. D.; Linclau, B. Polymer-Supported *O*-Methylisourea: A New Reagent for the *O*-Methylation of Carboxylic Acids. *Org. Lett.* **2002**, 4, 1035–1037. (b) Crosignani, S.; White, P. D.; Linclau, B. Polymer-Supported *O*-Alkylisoureas: Useful Reagents for the *O*-Alkylation of Carboxylic Acids. *J. Org. Chem.* **2004**, 69, 5897–5905. (c) Chighine, A.; Crosignani, S.; Arnal, M.-C.; Bradley, M.; Linclau, B. Microwave-Assisted Ester Formation Using *O*-Alkylisoureas: A Convenient Method for the Synthesis of Esters with Inversion of Configuration. *J. Org. Chem.* **2009**, 74, 4753–4762.

- [10] Long, T.; Maity, P. K.; Rolfe, A.; Hanson, P. R. ROMP-Derived Oligomeric Phosphates for Application in Facile Benzylation. *Org. Lett.* **2010**, *12*, 2904–2907.
- [11] (a) Manfredini, T.; Pellacani, G. C.; Pozzi, P.; Corradi, A. B. Monomeric and oligomeric phosphates as deflocculants of concentrated aqueous clay suspensions *Applied Clay Science* **1990**, *5*, 193–201. (b) Best, M. D.; Zhang, H.; Prestwich, G. D.; Inositol polyphosphates, diphosphoinositol polyphosphates and phosphatidylinositol polyphosphate lipids: Structure, synthesis, and development of probes for studying biological activity. *Nat. Prod. Rep.* **2010**, *27*, 1403–1430. (c) Fylaktakidou, K. C.; Duarte, C. D.; Koumbis, A. E.; Nicolau, C.; Lehn, J-M. *Chem. Med. Chem.* **2011**, *6*, 153–168 and references cited therein.
- [12] (a) Nicolaou, K. C.; Shi, G. Q.; Gunzner, J. L.; Gaertner, P.; Yang, Z. Palladium-Catalyzed Functionalization of Lactones via Their Cyclic Ketene Acetal Phosphates. Efficient New Synthetic Technology for the Construction of Medium and Large Cyclic Ethers. *J. Am. Chem. Soc.* **1997**, *119*, 5467–5468. (b) La Cruz, T. E.; Rychnovsky, S. D. A Reductive Cyclization Approach to Attenol A *J. Org. Chem.* **2007**, *72*, 2602–2611. (c) Lapointe, D.; Fagnou, K. Palladium-Catalyzed Benzylation of Heterocyclic Aromatic Compounds *Org. Lett.* **2009**, *11*, 4160–4163. (d) Westheimer, F. H. *Science* **1987**, *236*, 1173–1178. (e) Thomas, C. D.; Hanson, P. R. *Metathesis in Natural Product Synthesis*, Cossy, J.; Areniyadis, S.; Meyer, C. Ed.: Wiley-VCH: Weinheim, 2010. pp 129–144. (f) Beaucage, S. L.; Caruthers, M. H. *Bioorganic Chemistry: Nucleic Acids*, S. M. Hecht, Ed.: Oxford University Press: New York, 1996. Chapter 2, pp. 36–74.
- [13] (a) Cronin, S.; Chandrasekar, P. H. Safety of triazole antifungal drugs in patients with cancer *J. Antimicrob. Chemother.* **2010**, *65*, 410–416. (b) Nivoix, Y.; Ubeaud-Sequier, G.; Engel, P.; Leveque, D.; Herbrecht, R. Drug-drug interactions of triazole antifungal agents in multimorbid patients and implications for patient care *Curr. Drug Metab.* **2009**, *10*, 395–409. (c) Peyton, L. R.; Gallagher, S.; Hashemzadeh, M. Triazole antifungals: A review. *Drugs Today* **2015**, *51*, 705–718.
- [14] (a) Kushwaha, K.; Kaushik, N.; Jain, L. S. C. Design and synthesis of novel 2H-chromen-2-one derivatives bearing 1,2,3-triazole moiety as lead antimicrobials.

- Bioorg. Med. Chem. Lett.* **2014**, *24*, 1795–1801. (b) Behbehani, H.; Ibrahim, H. M.; Makhseed, S.; Mahmoud, H.; Applications of 2-arylhydrazononitriles in synthesis: preparation of new indole containing 1,2,3-triazole, pyrazole and pyrazolo[1,5-a]pyrimidine derivatives and evaluation of their antimicrobial activities, *Eur. J. Med. Chem.* **2011**, *46*, 1813–1820. (c) Thomas, K. D.; Adhikari, A. V.; Shetty, N. S. Design, synthesis and antimicrobial activities of some new quinoline derivatives carrying 1,2,3-triazole moiety. *Eur. J. Med. Chem.* **2010**, *45*, 3803–3810.
- [15] (a) Xia, Y.; Qu, F.; Peng, L. Triazole Nucleoside Derivatives Bearing Aryl Functionalities on the Nucleobases Show Antiviral and Anticancer Activity. *Mini Rev. Med. Chem.* **2010**, *10*, 806–821. (b) Kraljevic, T. G.; Harej, A.; Sedic, M.; Pavelic, S. K.; Stepanic, V.; Drenjancevic, D.; Talapko, J.; Raic-Malic, S. Synthesis, *in vitro* anticancer and antibacterial activities and *in silico* studies of new 4-substituted 1,2,3-triazole–coumarin hybrids. *Eur. J. Med. Chem.* **2016**, *124*, 794–808.
- [16] (a) Inverarity, I. A.; Hulme, A. N. Marked small molecule libraries: a truncated approach to molecular probe design. *Org. Biomol. Chem.* **2007**, *5*, 636–643. (b) Smith, G.; Glaser, M.; Perumal, M.; Nguyen, Q-D.; Shan, B.; Aarstad, E.; Aboagye, E. O. Design, Synthesis, and Biological Characterization of a Caspase 3/7 Selective Isatin Labeled with 2-[¹⁸F]fluoroethylazide. *J. Med. Chem.* **2008**, *51*, 8057–8067.
- [17] Long, T. R.; Faisal, S.; Maity, P. K.; Rolfe, A.; Kurtz, R.; Klimberg, S. V.; Najjar, R.; Basha, F. Z.; Hanson, P. R. “Click”-Capture, Ring-Opening Metathesis Polymerization (ROMP), Release: Facile Triazolation Utilizing ROMP-Derived Oligomeric Phosphates. *Org. Lett.* **2011**, *13*, 2038–2041.
- [18] Craig, D. The rearrangement of endo-3,6-Methylene-1,2,3,6-tetrahydro-cis-phthalic anhydride. *J. Am. Chem. Soc.* **1951**, *73*, 4889–4892.
- [19] Schwab, P.; Grubbs, R. H.; Ziller, J. W. Synthesis and Applications of RuCl₂(=CHR')(PR₃)₂: The Influence of the Alkylidene Moiety on Metathesis Activity. *J. Am. Chem. Soc.* **1996**, *118*, 100–110.

- [20] Pederson, R. L.; Fellows, I. M.; Ung, T. A.; Ishihara, H.; Hajela, S. P. Applications of Olefin Cross Metathesis to Commercial Products. *Adv. Synth. Catal.* **2002**, *344*, 728–735.
- [21] (a) Bonander, N.; Bill, R. M. Relieving the first bottleneck in the drug discovery pipeline: Using array technologies to rationalize membrane protein production. *Expert Rev. Proteomic* **2009**, *6*, 501–505. (b) Seeberger, P. H. Organic Synthesis Scavengers in full flow. *Nat. Chem.* **2009**, *1*, 258–260
- [22] (a) Gershell, L. J.; Atkins, J. H. A brief history of novel drug discovery technologies. *Nature Rev. Drug Discov.* **2003**, *2*, 321–327. (b) Kappe, C. O.; Dallinger, D. The Impact of Microwave Synthesis on Drug Discovery. *Nature Rev. Drug Discov.* **2006**, *5*, 51–63. (c) O'Brien, M.; Denton, R.; Ley, S. V. Lesser-Known Enabling Technologies for Organic Synthesis. *Synthesis* **2011**, *8*, 1157–1192. (d) Hanson, P. R.; Samarakoon, T.; Rolfe, A. The Power of Functional Resins in Organic Synthesis. (F. Albericio, J. Tulla-Puche, Eds), Wiley-VCH: Weinheim, Germany, 2008. (e) Kappe, C. O.; Dallinger, D. Controlled Microwave Heating in Modern Organic Synthesis. Highlights from the 2004-2008 Literature. *Mol. Diversity* **2009**, *13*, 71–193.
- [23] (a) Baumann, M.; Baxendale, I. R.; Kuratli, C.; Ley, S. V.; Martin, R. E.; Schneider, J. Synthesis of a Drug-Like Focused Library of Trisubstituted Pyrrolidines Using Integrated Flow Chemistry and Batch Methods. *ACS Combi. Sci.* **2011**, *13*, 405–413. (b) Roberge, D. M.; Zimmermann, B.; Rainone, F.; Gottsponer, M.; Eyholzer, M.; Kockmann, N. Microreactor Technology and Continuous Processes in the Fine Chemical and Pharmaceutical Industry: Is the Revolution Underway. *Org. Process Res. Dev.* **2008**, *12*, 905–910. (c) Wiles, C.; Watts, P. Improving Chemical Synthesis Using Flow Reactors. *Expert Opinion on Drug Discovery* **2007**, *2*, 1487–1503.
- [24] (a) Carter, C. F.; Baxendale, I. R.; Pavey, J. B. J.; Ley, S. V. The continuous flow synthesis of butane-2,3-diacetal protected building blocks using microreactors. *Org. Biomol. Chem.* **2010**, *8*, 1588–1595. (b) Wiles, C.; Watts, P.; Haswell, S. J. The use of solid-supported reagents for the multi-step synthesis of a combinatorial

array of analytically pure alpha, beta-unsaturated compounds in miniaturized flow reactors. *Lab Chip* **2007**, *7*, 322–330.

- [25] (a) Lange, H.; Carter, C. F.; Hopkin, M. D.; Burke, A.; Goode, J. G.; Baxendale, I. R.; Ley, S. V. A Breakthrough Method for the Accurate Addition of Reagents in Multi-step Segmented Flow Processing. *Chem. Sci.* **2011**, *2*, 765–769. (b) Smith, C. J.; Baxendale, I. R.; Lange, H.; Ley, S. V. Fully Automated, Multistep Flow Synthesis of 5-Amino-4-cyano-1,2,3-triazoles. *Org. Biomol. Chem.* **2011**, *9*, 1938–1947. (c) Hopkin, M. D.; Baxendale, I. R.; Ley, S. V. An Automated Flow-Based Synthesis of Imatinib: the API of Gleevec. *Chem. Commun.* **2010**, *46*, 2450–2452.
- [26] (a) Brandt, J. C.; Wirth, T. Controlling hazardous chemicals in microreactors: Synthesis with iodine azide. *Beilstein J. Org. Chem.* **2009**, *5*, No. 30. (b) Wang, W.; Huang, Y.; Liu, J.; Xie, Y.; Zhao, R.; Xiong, S.; liu, G.; Chen, Y.; Ma, H. Integrated SPPS on continuous-flow radial microfluidic chip. *Lab Chip* **2011**, *11*, 929–935. (c) Panke, G.; Schwalbe, T.; Stirner, W.; Taghavi-Moghadam, S.; Wille, G. High Energetic Nitration Reactions in Microreactors. *Synthesis* **2003**, *18*, 2827–2830. (d) Polyzos, A.; O'Brien, M.; Pugaard-Petersen, T.; Baxendale, I. R.; Ley, S. V. The Continuous Flow Synthesis of Carboxylic Acids using CO₂ in a Tube-in-Tube Gas Permeable Membrane Reactor. *Angew. Chem. Int. Ed.* **2011**, *50*, 1190–1193.
- [27] (a) Price, G. A.; Bogdan, A. R.; Aguirre, A. L.; Iwai, T. Djuric, S. W.; Organ, M. G. Continuous flow Negishi cross-couplings employing silica-supported Pd-PEPPSI-IPr precatalyst. *Cata. Sci. & Tech.* **2016**, *6*, 4733–4742. (b) Organ, M. G.; Hanson, P. R.; Rolfe, A.; Samarakoon, T. B.; Ullah, F. Accessing Stereochemically Rich Sultams via Microwave-Assisted, Continuous Flow Organic Synthesis (MACOS) Scale-out. *J. Flow Chem.* **2011**, *1*, 32–39. (c) Zang, Q.; Javed, S.; Ullah, F.; Zhou, A.; Knudtson, C. A.; Bi, D.; Basha, F. Z.; Organ, M. G.; Hanson, P. R. Application of a Double aza-Michael Reaction in a “Click, Click, Cy-Click” Strategy: From Bench to Flow. *Synthesis* **2011**, 2743–2750. (d) Ullah, F.; Samarakoon, T. B.; Rolfe, A.; Kurtz, R. D.; Hanson, P. R.; Organ, M. G. Scaling Out by Microwave-Assisted, Continuous Flow Organic Synthesis

- (MACOS): Multi-Gram Synthesis of Bromo- and Fluoro-benzofused sultams Benzothioxazepine-1,1-dioxides. *Chem. Eur. J.* **2010**, 10959–10962. (e) Moseley, J. D.; Woodman, E. K. Scaling-Out Pharmaceutical Reactions in an Automated Stop-Flow Microwave Reactor. *Org. Process Res. Dev.* **2008**, 12, 967–981. (f) Styring, P.; Parracho, A. I. R. From discovery to production: Scale-out of continuous flow meso reactors. *Belstein. J. Org. Chem.* **2009**, 5, No. 29.
- [28] Faisal, S.; Ullah, F.; Maity, P. K.; Rolfe, A.; Samarakoon, T. B.; Porubsky, P.; Neuenswander, B.; Lushington, G. H.; Basha, F. Z.; Organ, M. G.; Hanson, P. R. Facile (Triazolyl)methylation of MACOS-derived Benzofused Sultams Utilizing ROMP-derived OTP Reagents. *ACS Comb. Sci.* **2012**, 14, 268–272.
- [29] (a) Drews, J. Drug Discovery: A Historical Perspective. *Science* **2000**, 287, 1960–1964. (b) Navia, M. A. A Chicken in Every Pot, Thanks to Sulfonamide Drugs. *Science* **2000**, 288, 2132–2133. (c) Page, M. I. β -Sultams Mechanism of Reactions and Use as Inhibitors of Serine Proteases. *Acc. Chem. Res.* **2004**, 37, 297–303. For an extensive list of biologically active sultams see (d) Rolfe, A.; Young, K.; Hanson, P. R. Domino Heck-Aza-Michael Reactions: A One-pot, Multi-Component Approach to 1,2-Benzisothiazoline-3-acetic acid 1,1-dioxides. *Eur. J. Org. Chem.* **2008**, 5254–5262.
- [30] (a) Rolfe, A.; Samarakoon, T. B.; Klimberg, S. V.; Brzozowski, M.; Neuenswander, B.; Lushington, G. H.; Hanson, P. R. S_NAr -Based, Facile Synthesis of a Library of Benzothioxazepine-1,1'-dioxides. *J. Comb. Chem.* **2010**, 12, 850–854.
- [31] (a) Anderson, E. B.; Buchmeiser, M. R. Catalysts Immobilized on Organic Polymeric Monolithic Supports: From Molecular Heterogeneous Catalysis to Biocatalysis. *ChemCatChem* **2012**, 4, 30–41. (b) Buchmeiser, M. R. Ring-opening metathesis polymerization-derived materials for separation science, heterogeneous catalysis and tissue engineering. *Macromolecular Symposia* **2010**, 298, 17–24. (c) Sutthasupa, S.; Shiotsuki, M.; Sanda, F. Recent advances in ring-opening metathesis polymerization, and application to synthesis of functional materials. *Polymer Journal* **2010**, 42, 905–915. (d) Rolfe, A.; Loh, J. K.; Maity, P.

- K.; Hanson, P. R. High-Load, Hybrid Si-ROMP Reagents. *Org. Lett.* **2011**, *13*, 4–7. (e) Rolfe, A.; Probst, D.; Volp, K.; Omar, I.; Flynn, D.; Hanson, P. R. High-load, Oligomeric dichlorotriazine (ODCT): A Versatile ROMP-derived Reagent and Scavenger. *J. Org. Chem.* **2008**, *73*, 8785–8790.
- [32] (a) Gerard, B.; Duvall, J. R.; Lowe, J. T.; Murillo, T.; Wei, J.; Akella, L. B.; Marcaurelle, L. A.; Synthesis of a Stereochemically Diverse Library of Medium-Sized Lactams and Sultams via S_NAr Cycloetherification. *ACS. Combi. Sci.* **2011**, *13*, 365–374. (b) Chen, W.; Li, Z.; Ou, L.; Giulianotti, M. A.; Houghton, R. A.; Yu, Y. Solid-phase synthesis of skeletally diverse benzofused sultams via palladium-catalyzed cyclization. *Tetrahedron Lett.* **2011**, *52*, 1456–1458. (c) Fenster, E.; Long, T.; Zang, Q.; Hill, D.; Neunswander, B.; Lushington, G.; Zhao, A.-H.; Santini, C.; Hanson, P. R. Automated Synthesis of a 184-Member Library of Thiadiazepan-1,1-dioxide-4-ones. *ACS Combi. Sci.* **2011**, *13*, 244–250. (d) Pizzirani, D.; Kaya, T.; Clemons, P. A.; Schreiber, S. L. Stereochemical and Skeletal Diversity Arising from Amino Propargylic Alcohols. *Org. Lett.* **2010**, *12*, 2822–2825. (e) Rolfe, A.; Lushington, G. H.; Hanson, P. R. Reagent Based DOS: A Click, Click, Cyclize Strategy to Probe Chemical Space. *Org. Biomol. Chem.* **2010**, *8*, 2198–2203. (f) Rolfe, A.; Samarakoon, T. B.; Hanson, P. R. Formal [4+3] Epoxide Cascade Reaction via a Complementary Ambiphilic Pairing Strategy. *Org. Lett.* **2010**, *12*, 1216–1219.
- [33] (a) Wang, T.-W.; Intaranukulkit, T.; Rosana, M. R.; Slegers, R.; Simon, J.; Dudley, G. B. Microwave-assisted benzyl-transfer reactions of commercially available 2-benzyloxy-1-methylpyridinium triflate. *Org. Biomol. Chem.* **2011**, *10*, 248–250.
- [34] Akella, L. B.; Marcaurelle, L. A. Application of a Sparse Matrix Design Strategy to the Synthesis of DOS Libraries. *ACS Comb. Sci.* **2011**, *13*, 357–364.
- [35] Morschhäuser, R.; Krull, M.; Kayser, C.; Boberski, C.; Bierbaum, R.; Püschner, P. A.; Glasnov, T. N.; Kappe, C.; O. Microwave-assisted continuous flow synthesis on industrial scale *Green Process Synth* **2012**, 281–290.

Chapter 3

High Load Hybrid Si-ROMP Alkylating Reagents: Development and Applications in Library Synthesis and One-Pot Sequential Protocols

Section 3.1: Synthesis and Development of Si-OBP and Si-OPT as Alkylating Reagents.

3.1.1 Introduction

The need to rapidly synthesize a wide variety of small molecules in desired quantities with high purities and yields is an important challenge facing drug discovery and developmental chemistry.¹ To help address this need, immobilized reagents^{2,3} and scavengers have been developed to provide ease of synthesis and to eliminate time-consuming chromatographic separation protocols. In this chapter we describe our efforts to expand the family of ROMP-derived oligomeric materials that have been grafted onto the surface of silica. A metathesis catalyst-armed surface (CAS)-initiated polymerization was key to functionalization of units on the silica particle surface. In Chapter 3 (Section 3.1), we report the development and utilization of Silica-immobilized oligomeric benzyl phosphate (Si-OBP_n) and triazole phosphate (Si-OTP_n),⁴ which we previously discussed in Chapter 2 as soluble alkylating reagents for enabling library generation.⁵

Silica-immobilized reagents^{6,7,8} are frequently used for enabling synthesis and automated flow through technologies. Some of the more recent advances include, silica-supported isocyanide ligands for scavenging ruthenium,⁹ mesocellular silica-supported boronic acids as direct amidation catalysts,¹⁰ silica-supported rhodium catalysts,¹¹ *N*-heterocyclic carbenes,¹² iron BPMEN-inspired catalysts,¹³ sulfonic acid catalysts,¹⁴ tungsten oxo-alkylidene,¹⁵ TEMPO,¹⁶ Pd-, Mn- and Cu(I)-catalysts,¹⁷ peracid,¹⁸ phosphines,¹⁹ prolinol, and TADDOLs.²⁰ However, despite significant advantages over resin-based systems, silica-based immobilized reagents are often limited by several factors, including (i) low load levels (ii) heterogeneous reaction kinetics and non-surface

diffusion-controlled processes, (iii) immobilized reagent swelling, and (iv) poor solvent tolerance. Inspired by the seminal work of Buchmeister and coworkers,²¹ our efforts were focused on the synthesis and study of a number of hybrid materials that graft several ROMPgel materials onto the surface of silica particles.²² Through this grafting process, the resulting immobilized ROMP reagents can be removed from solution by simple filtration, thus eliminating the precipitation step. In this regard, silica-supported ROMPgel acid chloride, dichlorotriazine, and triphenylphosphine reagents were generated and found to have properties nearly identical to the equivalent soluble ROMPgel oligomeric reagents.

Our lab has previously examined a variety of soluble, high-load, oligomeric reagents and scavengers derived through the use of ring-opening metathesis polymerization (ROMP) of functionalized norbornene and 7-oxanorbornene monomers.²³ These materials, known as ROMPgels, are built on the pioneering efforts of Barrett,²⁴ Buchmeiser,²⁵ Bolm,²⁶ and others;²⁷ and they have effectively been used to mediate a number of chemical reactions. Our soluble ROMPgel materials behave equivalently to traditional homogeneous reagents and catalysts, and are generally removed from solution via precipitation. However, the need to precipitate can at times limit their use in pharmaceutical applications.

Benzylation and triazolation are useful diversification reactions in medicinal chemistry, high-throughput chemistry, and diversity-oriented synthesis (DOS).²⁸ The benzylation of amines and alcohols also serves as one of the most utilized protecting group strategies in organic synthesis due to its easy incorporation and removal.²⁹ While these uses have spurred development of a number of alternative approaches to

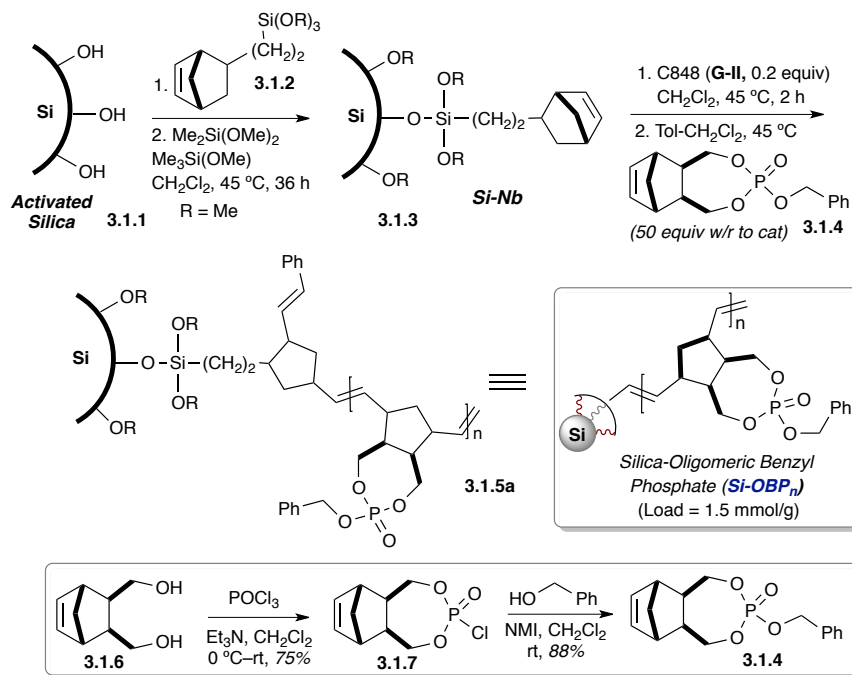
benzylation³⁰ and triazolation, we believe that the generation of the analogous silica-oligomeric benzyl phosphate (Si-OBP_n) and triazole phosphate (Si-OTP_n) reagents could find efficient, safe, and cost effective applications in chemical synthesis and library production. Key advantages of these reagents include: (i) their stability at room temperature, (ii) safety in handling when compared to commercially available benzyl bromides or iodides, and (iii) ease of purification via simple filtration.

3.1.2 Results and Discussion

Initial efforts were centered on the synthesis of the silica-grafted oligomeric benzyl phosphate reagent, as outlined in Scheme 3.1.1, using a modification of the procedure reported by Buchmeiser.³¹ The activated silica **3.1.1** (60 Å, 20 μm) was tagged with commercially available norbornene silyl reagent [(MeO)₃Si-(CH₂)₂-Nb (**3.1.2**)] followed by capping with trimethoxymethylsilane and dimethoxydimethylsilane to afford the norbornene-functionalized silica (Si-Nb) **3.1.3**. It was observed that the use of (MeO)₃Si-(CH₂)₂-Nb (**3.1.2**) dramatically increased the norbornene load of Si-Nb (**3.1.3**) compared to 5-(bicycloheptenyl)-triethoxysilane [Nb-Si(OEt)₃], which was previously used for silica tagging.²² By this optimized method, we prepared norbornene-functionalized silica **3.1.3** (Si-Nb) on gram scale with 0.4 mmol/g loading (determined by a modified bromine titration method).³² With this Si-tagged nanoparticle (**3.1.3**) in hand, a metathesis catalyst-armed surface-initiated polymerization was established using the C848 catalyst (Grubbs 2nd generation catalyst, **G-II**)³³ (20 mol%, based on Si-Nb load) in CH₂Cl₂ and toluene as solvents, followed by addition of the Nb-tagged benzyl phosphate monomer **3.1.4** to rapidly generate the desired hybrid material (Si-OBP_n) **3.1.5a**. The benzyl phosphate monomer **3.1.4** was easily synthesized in good yield and purity

according to previously reported methods.⁴ Norbornene *exo*-diol **3.1.6** was reacted with POCl₃ and Et₃N in the presence of catalytic DMAP to generate the Nb-tagged monochlorophosphate compound **3.1.7** in moderate yields as a white solid (Scheme 3.1.1). This material was then reacted with benzyl alcohol in NMI and CH₂Cl₂ at room temperature to yield **3.1.4**.

Scheme 3.1.1. *Synthesis of Silica-supported Oligomeric Benzyl Phosphate (Si-OBP_n).*



The scale-up synthesis of the monomeric reagent, as well as Si-OBP_n, have been carried out on gram scale as stable, free-flowing powders. The scanning electron microscopy (SEM) images of Si-OBP_n and Si-OTP_n silica hybrid materials demonstrate the grafting of the corresponding monomer on silica surface and inherent morphology of hybrid materials (Figure 3.1.1).

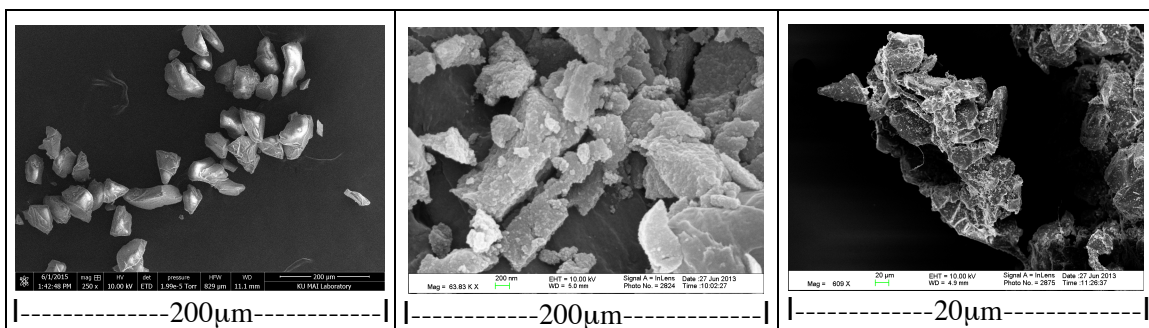


Figure 3.1.1. SEM images of *Si-Nb* (left), *Si-OBP_n* (middle) and *Si-OTP_n* (right).

The utilization of silica oligomeric benzyl phosphate **3.1.5a** (Si-OBP_n) for benzylation with various *N*-, *O*-, and *S*-nucleophiles, including anilines, amines, phenols, thiols, and sulfonamides (Table 3.1.1), was examined. The reactions were carried out in a sealed pressure tube with different nucleophiles (1 equiv.), Si-OBP_n (1.5 equiv.), Cs₂CO₃ (3.0 equiv.), and NaI (0.2 equiv.) in THF at 80 °C (oil bath temperature) to yield the products after simple filtration via Celite® SPE to remove the Si-phosphate byproduct. Initially, a variety of amines and phenols (Table 3.1.1, entry 1–4) were utilized, and were next extended to thiophenols and sulfonamides (Table 3.1.1, entry 5–8). The corresponding benzylated analogs **3.1.8a–3.1.8h** were isolated in excellent purities (>90%, determined by LC-MS) and yields (>90%).

Table 3.1.1. Benzylation of *N*-, *O*- and *S*-nucleophiles utilizing Si-OBP_n.

1) R²-X^H, Cs₂CO₃, NaI
THF, 80 °C, 14 h
2) Celite SPE

Nucleophile	Pdt	Yield (%)	Nucleophile	Pdt	Yield (%)
		97			98
		95			98
		97			99
		98			97

With these results in hand, an expanded set of Si-OBP_n derivatives was next examined (Figure 3.1.2). These high load reagents (**3.1.5b–3.1.5d**) were synthesized in an analogous fashion to the Si-OBP_n reagent and were also obtained on gram scales as free-flowing powders. Utilization of these reagents in substitution reactions with *O*- and *S*-nucleophiles were next carried out to afford benzylated products (**3.1.8i–3.1.8n**) in good yields (>90%) and excellent purity after Celite[®] SPE filtration (Table 3.1.2). Diversification of the Si-OBP_n reagents by using different electron withdrawing and electron donating group substituents on the aryl moiety were next examined. In all cases, analogous results to Table 3.1.1 were obtained (Table 3.1.2).

Figure 3.1.2: Various Silica-supported Oligomeric Benzyl Phosphate (Si-OBP_n) analogs.

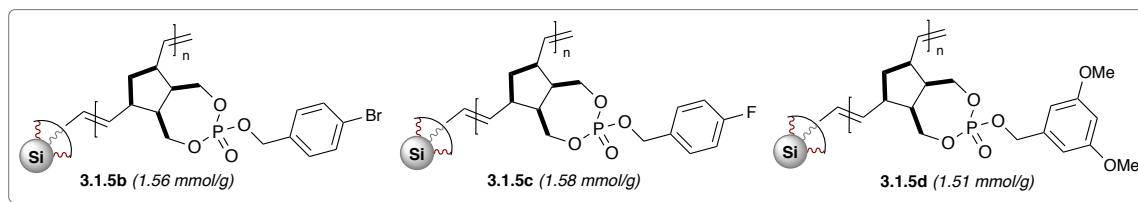


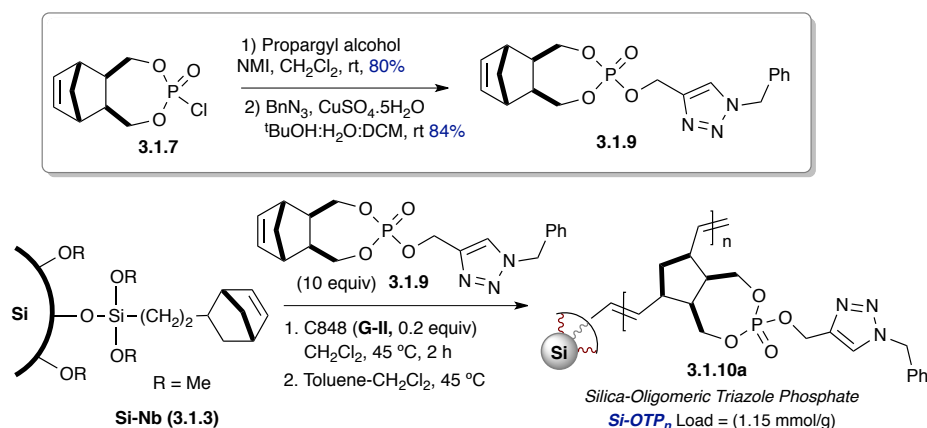
Table 3.1.2. Benzylation of *N*-, *O*- and *S*-nucleophiles utilizing various Si-OBP_n analogs.

Entry	Si-OBP _n	Nucleophile	Pdt	Yield (%)
1	3.1.5b	2,4-dichlorophenol	3.1.8i	98
2	3.1.5b	2,4,6-trichlorobenzenethiol	3.1.8j	94
3	3.1.5c	2,4-dichlorophenol	3.1.8k	96
4	3.1.5c	2,4,6-trichlorobenzenethiol	3.1.8l	95
5	3.1.5d	2,4-dichlorophenol	3.1.8m	98
6	3.1.5d	2,4,6-trichlorobenzenethiol	3.1.8n	94

Attention was next placed on the gram-scale generation of silica oligomeric triazole phosphate hybrid reagents (Si-OTP_n). Triazoles and their derivatives have demonstrated a wide variety of biological activities.³⁴ We previously reported soluble oligomeric triazole phosphates to construct a wide array of triazole-containing compounds.⁴ Silica-immobilized oligomeric triazole phosphate **3.1.10a** (Si-OTP_n) was synthesized via grafting of the Nb-tagged benzyl triazole phosphate monomer **3.1.9** onto the surface of norbornene-functionalized silica (Si-Nb) **3.1.3**. The synthesis was accomplished through the same protocol discussed for the synthesis of Si-OBP_n in

Scheme 3.1.1. The product, **3.1.10a** (Si-OTP_n), was isolated as a free flowing solid with a high-load value (1.15 mmol/g) (Scheme 3.1.2). The triazole phosphate monomer **3.1.9** was synthesized in good yield and purity according to previously reported methods.⁵ Phosphorylation of propargyl alcohol with Nb-tagged phosphonyl chloride **3.1.7**, followed by a “Click”-capture event of the corresponding azide, efficiently yielded the desired monomer **3.1.9** (Scheme 3.1.2). The triazole phosphate monomer and the silica oligomeric triazole phosphate reagents (Si-OTP_n) were synthesized on gram scale as stable, free-flowing solids.

Scheme 3.1.2. *Synthesis of Silica-Supported Oligomeric Triazole Phosphate (Si-OTP_n).*



With Si-OTP_n **3.1.10a** in hand, the hybrid material was evaluated for the ability to (triazolyl)methylate a variety of nucleophiles, including amines, phenols, thiophenols and sulfonamides, in good yields and high purity with chromatography-free purification. The reaction was carried out overnight in a pressure tube with different nucleophiles (1 equiv.), Si-OTP_n (1.5 equiv.), Cs₂CO₃ (3.0 equiv.), and NaI (0.2 equiv.) in DMF at 90 °C. The reaction mixture was diluted with EtOAc and filtered through a pad of Celite to furnish the corresponding (triazolyl)methylated products. Optimal results were achieved in DMF compared to THF. A variety of *N*-, *O*-, and *S*-nucleophiles were utilized for

nucleophilic substitution reactions with Si-OTP_n, which afforded the desired (triazolyl)methylated products (**3.1.11a–3.1.11g**) in excellent yield and high purity (>85%, determined by LC-MS) (Table 3.13). In all cases, similar results were obtained as compared to Si-OBP_n in THF in Table 3.1.2.

Table 3.1.3. Triazolation utilizing Si-OTP_n with *O*-, *N*- and *S*-nucleophiles.

Reaction scheme: **3.1.10a** (Si-OTP_n reagent) reacts with **1) R²-XH, Cs₂CO₃, NaI, DMF, 90 °C, 14 h** and **2) Celite SPE** to yield **3.1.11a-g** (triazolyl)methylated products.

Nucleophile	Pdt	yield (%)	Nucleophile	Pdt	yield (%)
		84			92
		83			92
		91			94
		90			89

Building on these results, the project was expanded to the synthesis of additional variants of Si-OTP_n hybrid reagents (**3.1.10b–3.1.10d**, Figure 3.1.3) on gram scales as free-flowing powders in an analogous fashion to the Si-OTP_n reagent in Scheme 3.1.2. These Si-OTP_n hybrid reagents were utilized for (triazolyl)methylation of *O*- and *S*-nucleophiles. In all cases, (triazolyl)methylated products (**3.1.11h–3.1.11m**) were isolated in excellent yields and high purities after passing through a Celite[®] SPE (Table 3.1.4).

Figure 3.1.3: Various Silica-Supported Oligomeric Triazole Phosphate (Si-OTP_n) analogs.

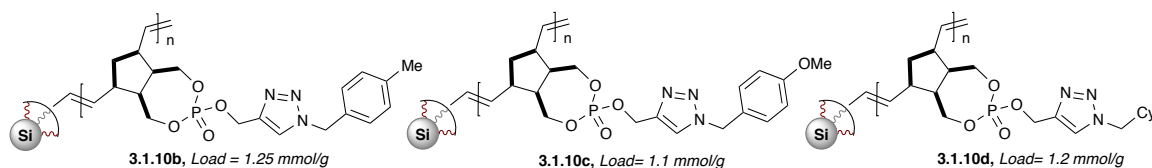


Table 3.1.4. Triazolation of *N*-, *O*- and *S*-nucleophiles utilizing various Si-OTP_n analogs.

Entry	Si-OTP_n	Nucleophile ($\text{R}^5\text{-XH}$)	Pdt	Yield (%)
1	3.1.10b , $\text{R}^4 = 4\text{-Me-C}_6\text{H}_4$	4-bromophenol	3.1.11h	85
2	3.1.10b , $\text{R}^4 = 4\text{-Me-C}_6\text{H}_4$	2,4,6-trichlorobenzenethiol	3.1.11i	87
3	3.1.10c , $\text{R}^4 = 4\text{-OMe-C}_6\text{H}_4$	4-bromophenol	3.1.11j	89
4	3.1.10c , $\text{R}^4 = 4\text{-OMe-C}_6\text{H}_4$	2,4,6-trichlorobenzenethiol	3.1.11k	86
5	3.1.10d , $\text{R}^4 = \text{cyclohexyl}$	4-bromophenol	3.1.11l	86
6	3.1.10d , $\text{R}^4 = \text{cyclohexyl}$	2,4,6-trichlorobenzenethiol	3.1.11m	88

Overall, this section demonstrated the synthesis and utilization of silica-supported, hybrid Si-ROMP benzylating and (triazolyl)methylating reagents. A metathesis catalyst-armed surface (CAS)-initiated polymerization was key to functionalization of units off the silica particle surface. With this technology, the developed Si-immobilized were synthesized on gram scale as stable, free-flowing powders. The resulting Si-immobilized ROMP reagents can be removed by simple filtration, thus eliminating the precipitation step. SEM imaging was utilized to demonstrate the grafting of the corresponding oligomer and the inherent morphology of the hybrid materials. Utilization of these reagents in one-pot protocols for the synthesis of diverse small molecule is demonstrated in the next section 3.2.

Section: 3.2 Application of Silica-Supported Alkylating Reagents in a One-Pot Protocol for the Synthesis of Diverse Benzoxathiazepine 1,1-Dioxides.

3.2.1 Introduction

The utilization of immobilized reagents in one-pot protocols can further integrate synthesis, diversification, and purification into one parallel process to rapidly expand efforts in early stage drug discovery.^{2,35} In this section, we report expanded applications of our developed silica-immobilized benzyl phosphate Si-OBP_n and triazole phosphate Si-OTP_n reagents (discussed in section 3.1),^{4,36} in the establishment of one-pot, sequential protocols for facile library synthesis of diverse benzothioxazepine-1,1-dioxides (Figure 3.2.1).³⁷

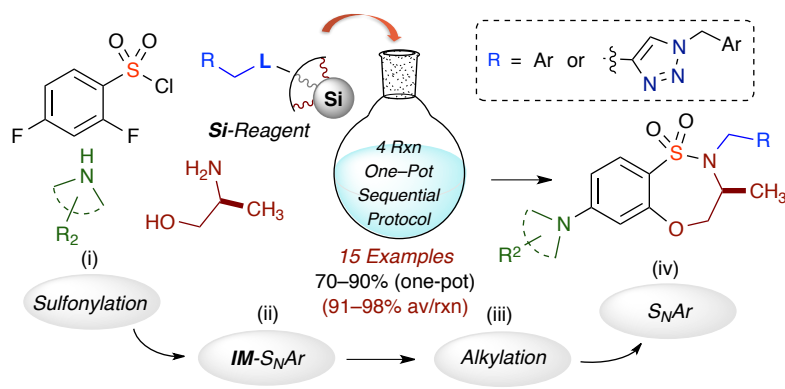


Figure 3.2.1. *Benzothioxazepine-1,1-Dioxides in a One-Pot Protocol.*

Multi-component reactions in one-pot processes provide efficient pathways to synthesize complex heterocyclic scaffolds from simple building blocks.³⁸ One-pot strategies enable the formation of multiple bonds and stereocenters in one synthetic step, as well as reducing purification resources, time, and waste. This process minimizes the need of work-up and chromatographic separations of intermediary reactions. Among several literature reports, elegant efficient efforts by Hayashi³⁹ have demonstrated the power of consecutive one-pot, sequential procedures to complete multi-step syntheses.

Benzothiazoxazepine-1,1-dioxides are unique scaffolds,⁴⁰ that have shown a broad range of bioactivities, including inhibition of a variety of enzymes.⁴¹ Substituted benzothiazoxazepine-1,1-dioxides have shown activity as antipsychotic agents,⁴² modulators of histamine H₃-receptor,⁴³ glucokinase activators,⁴⁴ modulators of AMPA receptors⁴⁵ and monoacidic inhibitors of KEAP1⁴⁶ (Figure 3.2.2). The current demand is to develop step-economical methods to facilitate the synthesis of these biologically inspired sultams in a desirable fashion. In light of our recent approaches for the synthesis of scaffolds containing benzothiazoxazepine-1,1-dioxides,⁴⁷ we herein elaborate the importance of 2-difluoroarylsulfonyl chloride (**3.2.4**) as an attractive building block for the generation of these scaffolds.

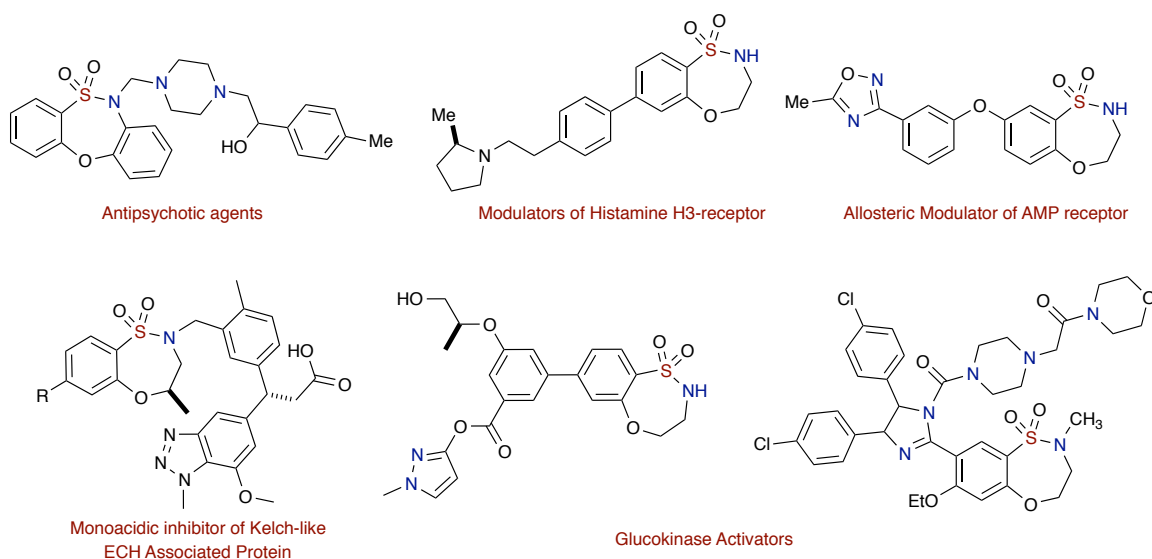
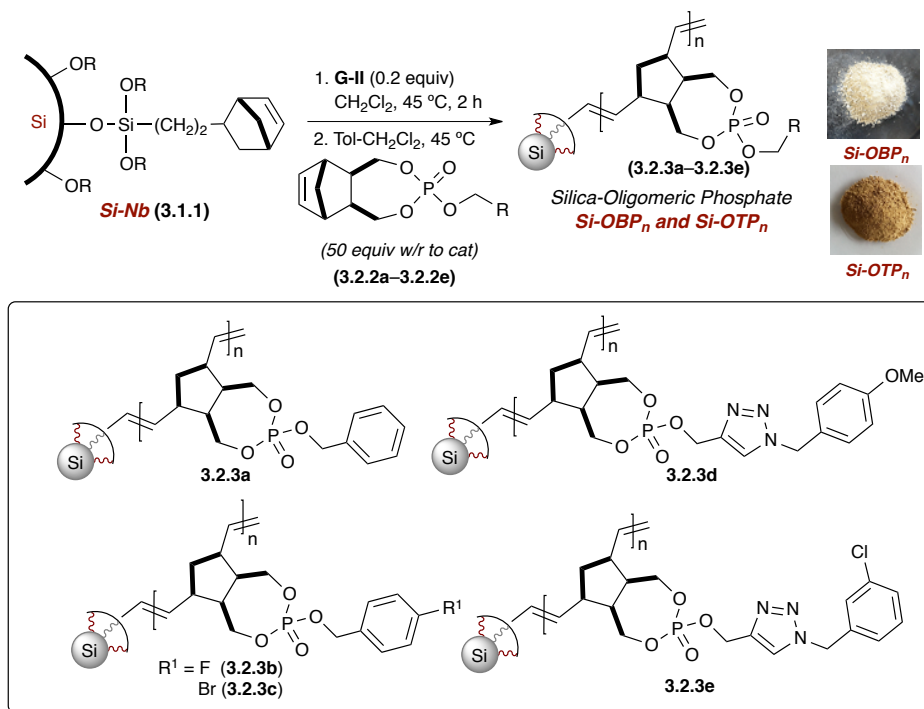


Figure 3.2.2. Biologically active benzothiazoxazepine-1,1-dioxide-containing sultams.

3.2.2 Results and Discussion

The titled silica phosphate reagents, Si-OBP_n and Si-OTP_n, were synthesized from norbornenyl-functionalized silica (Si-Nb) **3.1.1** and Nb-tagged phosphate monomers **3.2.2a–3.2.2e** using a similar protocol to that described in section 3.1 (Scheme 3.1.1). Surface-initiated polymerization of these monomers onto the surface of silica was achieved using the Grubbs second-generation catalyst (G-II) in toluene-CH₂Cl₂.³³ Following the reported procedure, the desired Si-ROMP benzylating Si-OBP_n **3.2.3a–3.2.3c** (n ~ 50) and triazolating Si-OTP_n **3.2.3d–3.2.3e** (n ~ 50) reagents were furnished as free-flowing solids on gram-scale.

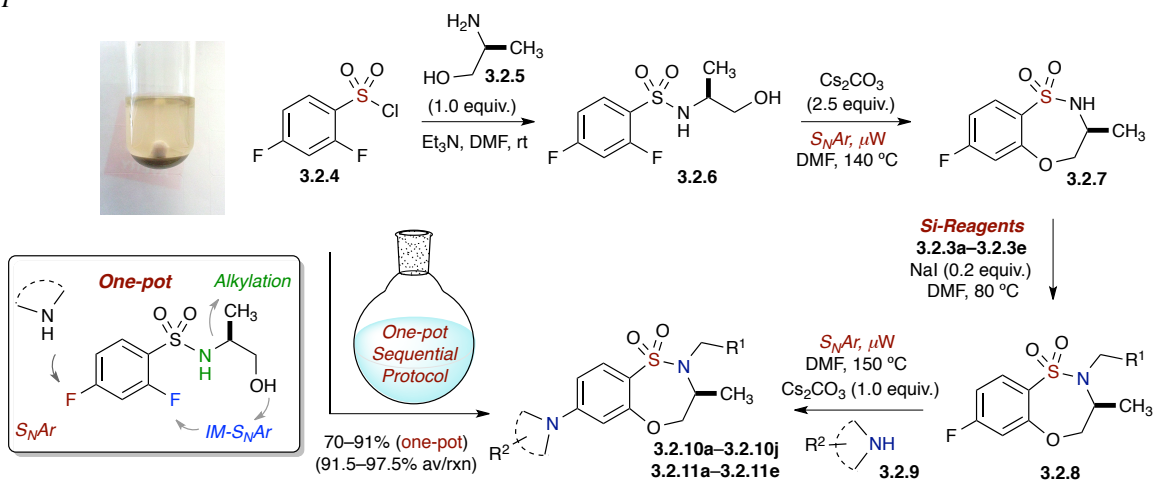
Scheme 3.2.1. Synthesis of Si-Supported Oligomeric Benzyl (Si-OBP_n) and Triazole (Si-OTP_n) Phosphates.



With Si-OBP_n reagents **3.2.3a–3.2.3c** and (triazolyl)methylating reagents Si-OTP_n **3.2.3d–3.2.3e** in hand, we directed our attention to their utilization in the titled one-pot sequential process. Thus, we planned to achieve sulfonylation, intramolecular

nucleophilic aromatic substitution (IM-S_NAr), alkylation (Si-OBP_n and Si-OTP_n), and intermolecular S_NAr reactions using the same solvent (DMF) in an overall one-pot protocol. The synthesis started with commercially available 2,4-difluorobenzenesulfonyl chloride (**3.2.4**) and a simple chiral amino alcohol **3.2.5** to achieve sulfonylation at room temperature using Et₃N in DMF. The resulting sulfonamide **3.2.6** next underwent facile IM-S_NAr cyclization using microwave conditions at 140 °C in the same pot to furnish benzothioxazepine-1,1-dioxide **3.2.7** (Scheme 3.2.2). Further diversification of **3.2.7** was achieved through use of Si-OBP_n or Si-OTP_n for benzylation and (triazolyl)methylation, respectively. Successful benzylations using Si-OBP_{n **3.2.3a** of the corresponding cyclic sulfonamides were achieved in the same pot by heating the reaction mixture to 80 °C for 10–12 hours. The final intermolecular S_NAr reaction (150 °C under microwave irradiation) with a variety of cyclic five- or six-membered secondary/aromatic amines afforded diverse benzofused sulfonamides **3.2.10a–3.2.10e** in the same pot (Table 3.2.1, entries 1–5).}

Scheme 3.1.2. *Synthesis of benzothioxazepine-1,1-dioxides in a one-pot, sequential protocol.*



In the next stage, different variants of silica-immobilized benzylating reagents **3b–3c** were employed in one-pot procedures, and the desired *N*-benzylated benzoxathiazepine 1,1-dioxides **10f–10j** were achieved after the final intermolecular S_NAr reactions (DMF, 150 °C under microwave irradiation), using a variety of cyclic five-membered secondary/aromatic amines (Table 3.2.1, entries 6–10).

Table 3.2.1. One-pot Synthesis of Benzothiazoxazepine-1,1-Dioxides Utilizing Various Si-OBP Reagents.

Entry	Amines (R ²)	Si-OBP	Product	Yield (%)	Entry	Amines (R ²)	Si-OBP	Product	Yield (%)
1		3.2.3a		71	6		3.2.3b		90
2		3.2.3a		90	7		3.2.3b		90
3		3.2.3a		79	8		3.2.3c		72
4		3.2.3a		90	9		3.2.3c		84
5		3.2.3a		91	10		3.2.3c		70

We next studied diversifications via sulfonamide *N*-(triazolyl)methylation utilizing Si-OTP reagents **3.2.3d–3.2.3e** as summarized in Table 3.2.2. These efforts

were driven by the biological importance of 1,2,3-triazole-containing scaffolds,³⁴ as well as their effective mimicry of *trans*-amide bonds due to similarities in size, planarity, dipole, and H-bonding capabilities.⁴⁸

Table 3.2.2. One-pot Synthesis of Benzofused Sultams Utilizing Variable Si-OTP Reagents

Entry	Amines (R ²)	Si-OTP	Product	Yield (%)
1		3.2.3d		70
2		3.2.3d		72
3		3.2.3d		73
4		3.2.3e		80
5		3.2.3e		92

To consider the biological importance of benzoxathiazepine 1,1-dioxides (Figure 3.2.1), we planned to design a small library of diverse *N*-(triazolyl)methylated benzoxathiazepine 1,1-dioxides derivatives using a similar one-pot protocol as described above.⁴⁹ Subsequent intermolecular S_NAr reaction in the same pot using various cyclic

amines afforded the desired *N*-(triazolyl)methylated benzoxathiazepine 1,1-dioxides **3.2.11a–3.2.11e** in high yield, 70–92% over four sequential steps, representing average yields of 92.5–98% per reaction (av/rxn) (Table 3.2.2).

Overall, this section demonstrated the applications of silica-immobilized reagents (Si-OBP_n and Si-OTP_n) reagents in the diversification of core scaffolds to achieve the synthesis of a variety of unique benzoxathiazepine 1,1-dioxides in a one-pot, sequential protocol. Efforts to expand the scope of these reagents to various drug-related molecules, and improvement in synthesis and scale-up are continued for application in diversity-oriented synthesis.

Section 3.3: Synthesis of High-load, Hybrid Silica-immobilized Heterocyclic Benzyl Phosphate (Si-OHBP) and Triazolyl Phosphate (Si-OHTP) Alkylating Reagents.

3.3.1 Introduction

Heterocycles are prevalent in small molecule drugs and natural compounds⁵⁰ and often they are used to manipulate structural and electronic properties of small molecules that are key to regulating molecular lipophilicity, polarity, and hydrogen bonding capacity.⁵¹ Despite these attributes, introduction of *N*-heterocyclic functionality into core structures can be problematic in subsequent purification stages due to increased polarity and basicity in combinatorial synthesis. Immobilized reagents offer many advantages that can potentially circumvent these issues. As noted previously, compared to traditional solution-phase synthesis, solid-phase techniques⁵² have shown advantages in simplifying the purification process, especially in flow-through chemistry and automated synthesis.⁵³ In the previous sections (3.1, 3.2), we reported the development and utilization of silica-immobilized benzyl phosphate Si-OBP_n and triazole phosphate Si-OTP_n as efficient

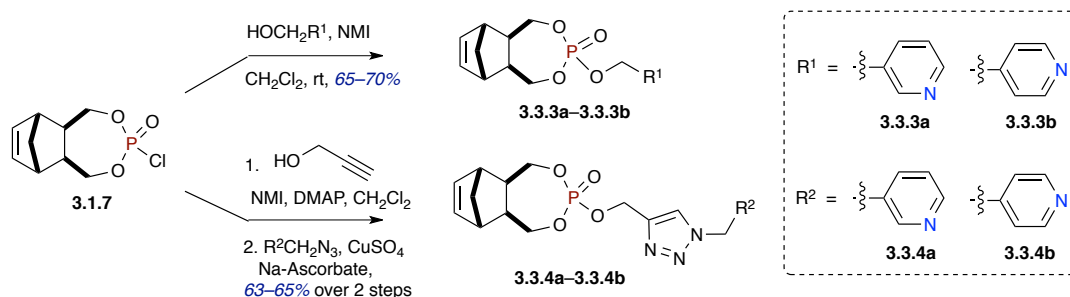
alkylating reagents, as well as their applications in one-pot protocols.³⁷ In this section we report the development of hybrid silica-immobilized oligomeric hetero-benzyl phosphates (Si-OHBP_n) and hetero-triazolyl phosphate (Si-OHTP_n) as efficient alkylating reagents.⁵⁴ We envision that these high load ROMP-derived reagents are highly applicable in purification-free protocols to install heterocycles, namely pyridines and pyridine-substituted triazoles in *N*-, *O*-, and *S*-nucleophilic species, in the synthesis of complex molecules. In addition to these benefits, the titled Si-OHBP_n and Si-OHTP_n reagents are bench stable, environmental friendly, and have ease of purification via simple filtration through Celite. Furthermore, the low cost, commercial availability of the starting pyridine methanol derivatives, as compared to their corresponding bromomethyl pyridines, is another advantage that inspired us to produce the titled silica-supported phosphate analogs. Taken collectively, these examples have showcased the development of high-load, ROMP-derived silica-immobilized reagents and their utilization in a variety of organic reactions.

3.3.2 Results and Discussion

The route to the titled phosphates began with reduction of *exo*-norbornenyl carbic anhydride (readily-derived from commercially available *endo*-norbornenyl carbic anhydride)⁵ to the corresponding diol using LiAlH₄, followed by phosphorylation of the norbornenyl (Nb) *exo*-diol using freshly distilled POCl₃ and Et₃N, to afford the Nb-phosphorochloridate **3.1.7** described in section 3.1 (Scheme 3.1.1) as a white solid in 73% yield. This reagent was conveniently stored for several months as a solid under argon in a desiccator for use in preparing various phosphate monomer analogs. Addition of **3.1.7** into a solution containing hetero-benzyl alcohol, NMI, and CH₂Cl₂ at room

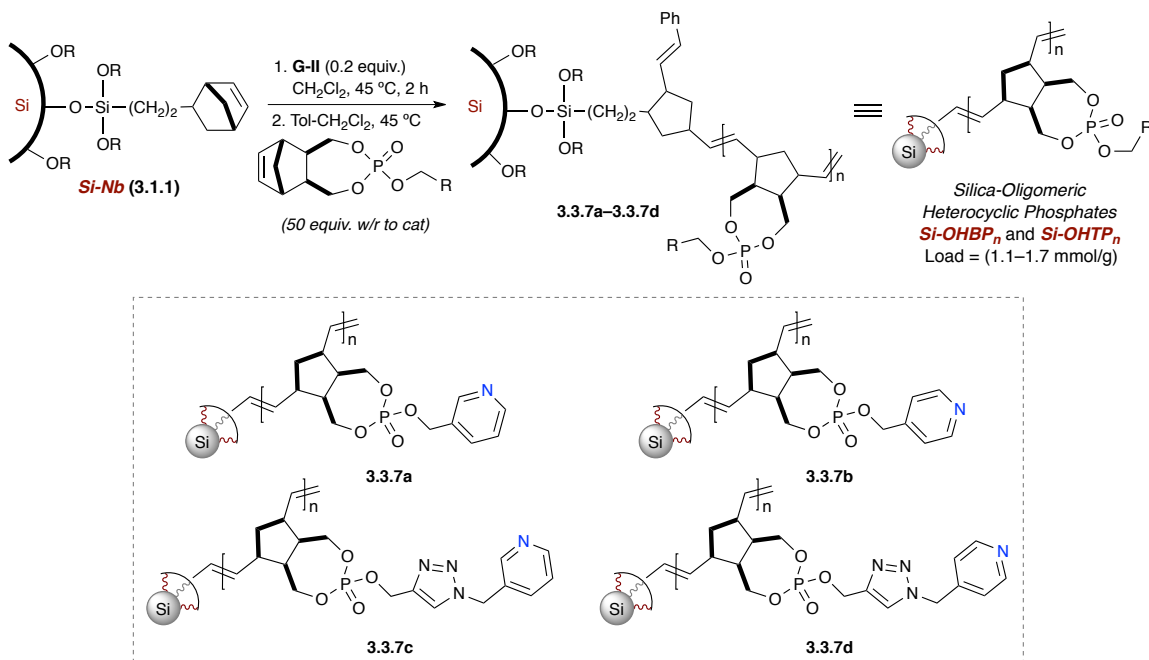
temperature cleanly afforded hetero-benzylic phosphates **3.3.3a–3.3.3b** in good yields (65–70%). Similarly, phosphorylation of Nb-tagged phosphorochloridate **3.1.7** with propargyl alcohol, followed by a “Click”-capture event of an azidomethyl pyridine, afforded the corresponding hetero-benzylic triazole phosphate monomers **3.3.4a–3.3.4b** in good yields (63–65% over two steps).

Scheme 3.3.1: *Synthesis of Hetero-benzyl and Hetero-triazole Phosphate Monomers.*



Utilizing a similar protocol demonstrated in the previous section 3.1,⁴ $(\text{MeO})_3\text{Si}-(\text{CH}_2)_2-(\text{Nb})$ **3.1.1** was synthesized. With these Nb-tagged silica particles in hand, surface-initiated polymerization of Nb-tagged phosphate monomers **3.3.3a–3.3.3b** and **3.3.4a–3.3.4b** onto the silica surface was achieved using the Grubbs second-generation catalyst (**G-II**), followed by washing with CH_2Cl_2 , to furnish the desired silica-tagged heterocyclic phosphates as free-flowing solids possessing experiment loads of 1.1–1.7 mmol/g (Scheme 3.3.2).

Scheme 3.3.2: Synthesis of Silica-Supported Oligomeric Hetero-benzyl (Si-OHBP_n) and Hetero-triazole (Si-OHTP_n) Phosphates.



Gram-scale syntheses were next carried out for both Si-ROMP hetero-benzylating (Si-OHBP_n) and hetero-(triazolyl)methylating (Si-OHTP_n) reagents, **3.3.7a–3.3.7b** and **3.3.7c–3.3.7d**, respectively.

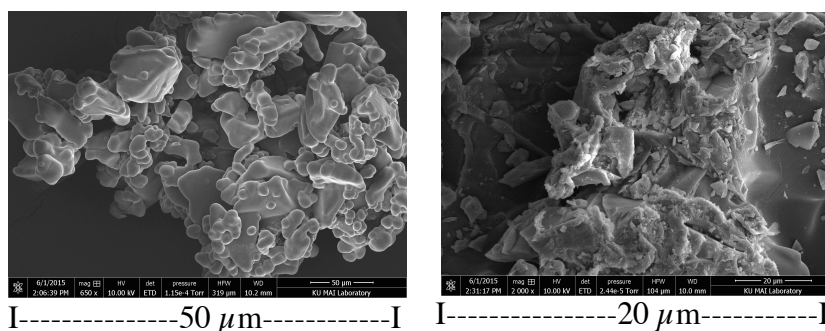


Figure 3.3.1. SEM images of Si-OHBP_n (left) and Si-OHTP_n (right).

The SEM images of Si-OHBP_n and Si-OHTP_n are shown in Figure 3.3.1 and depict grafting of the corresponding monomer onto the silica surface and the inherent morphology of the new hybrid Si-ROMP materials.

With the hybrid Si-ROMP materials in hand, efforts were focused on utilization of Si-OHBP_n **3.3.7a–3.3.7b** as hetero-benzylating reagents. After investigating various reagent stoichiometry ratios, an optimized condition was established. The reactions proceeded by using nucleophiles (1 equiv.), Si-OHBP_n (1.5 equiv.), Cs₂CO₃ (3.0 equiv.), and NaI (0.2 equiv.) in 0.1 M THF at 80 °C (oil bath temperature) in a sealed pressure tube. With these optimized conditions, the hetero-benzylation of a variety of *N*-, *O*-, and *S*-nucleophiles was achieved using two silica oligomeric hetero-benzyl phosphates (Si-OHBP_n, **3.3.7a**, **3.3.7b**) (Table 3.3.1).

Table 3.3.1: Hetero-benzylation of *N*-, *O*- and *S*-nucleophiles Utilizing Si-OHBP_n

Reaction conditions: 1) R²-XH (1.0 equiv.), Cs₂CO₃ (3.0 equiv.), NaI (0.2 equiv.), THF, 80 °C, 12 h; 2) Celite SPE.

Nucleophile (R ² -XH)	Product	Yield (%)	Nucleophile (R ² -XH)	Product	Yield (%)
		97			99
		72			84
		70			96
		97			72
		97			

Various phenols and thiophenols, as well as more complex sulfonamides, were successfully alkylated to afford the corresponding hetero-benzylated products **3.3.8a–3.3.8i** (Table 3.3.1). In all cases, simple filtration through a Celite® SPE allowed the products to be isolated in good to excellent yields (70–99%) and desired crude purity (>90%, calculated by UV area percent from HPLC analysis).

With the hybrid Si-ROMP materials in hand, efforts were focused on utilization of Si-OHBP_n **3.3.7a–3.3.7b** as hetero-benzylating reagents. After investigating various reagent stoichiometry ratios, an optimized condition was established. The reactions proceeded by using nucleophiles (1 equiv.), Si-OHBP_n (1.5 equiv.), Cs₂CO₃ (3.0 equiv.), and NaI (0.2 equiv.) in 0.1 M THF at 80 °C (oil bath temperature) in a sealed pressure tube. With these optimized conditions, the hetero-benzylation of a variety of *N*-, *O*-, and *S*-nucleophiles was achieved using two silica oligomeric hetero-benzyl phosphates (Si-OHBP_n, **3.3.7a**, **3.3.7b**) (Table 3.3.1). Various phenols and thiophenols, as well as more complex sulfonamides, were successfully alkylated to afford the corresponding hetero-benzylated products **3.3.8a–3.3.8i** (Table 3.3.1). In all cases, simple filtration through a Celite® SPE allowed the products to be isolated in good to excellent yields (70–99%) and desired crude purity (>90%, calculated by UV area percent from HPLC analysis).

In the next step, silica-immobilized triazole phosphate derivatives **3.3.7c–3.3.7d** were synthesized on gram scale with a load of 1.1–1.3 mmol/g as free-flowing powders. Use of these reagents in nucleophilic substitution reactions with *N*-, *O*-, and *S*-nucleophiles afforded (triazolyl)methylated products **3.3.9a–3.3.9f** in excellent yields (81–93%) and purities (>90%, calculated by UV area percent from HPLC analysis) using simple filtration through a Celite® SPE (Table 3.3.2).

Table 3.3.2: Hetero-(triazolyl)methylation of *N*-, *O*- and *S*-nucleophiles Utilizing *Si-OHTP_n*

$R^1 =$ **3.3.7c**
3.3.7d

Silica-Oligomeric
3.3.7c–3.3.7d Hetero-triazole Phosphates
(Si-OHTP_n)
 Load 1.1–1.3 mmol/g

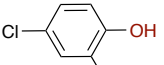
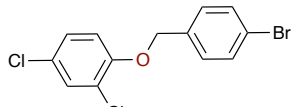
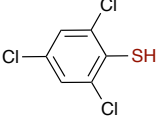
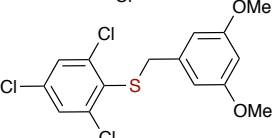
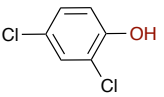
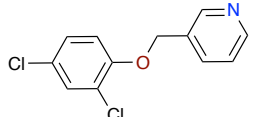
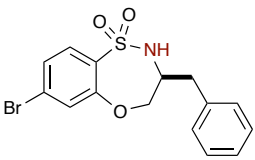
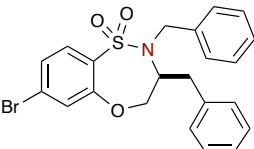
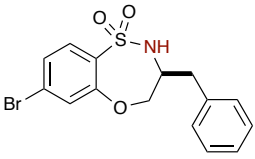
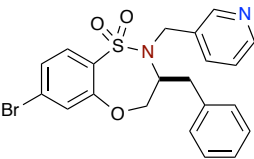
1) R^2-XH (1.0 equiv.)
 Cs_2CO_3 (3.0 equiv.)
 NaI (0.2 equiv.)
 DMF , 80 °C, 12 h
 2) Celite SPE

3.3.9a–3.3.9f

Nucleophile (R^2-XH)	Product	Yield (%)	Nucleophile (R^2-XH)	Product	Yield (%)
		88			84
		93			89
		81			87

Efforts to expand the scope of these reagents in multicomponent reactions (one-pot processes) towards drug-related heterocycles, and improvement in scale-up are continued for further applications in diversity-oriented synthesis. These efforts and the gathering of corresponding results continue, and will be reported in due course. The crude purities of selected products utilizing silica-supported alkylating reagents were also monitored by LC/HRMS analysis shown in table 3.3.3.

Table 3.3.3: *Crude Purity analysis by LC/HRMS.*

Nucleophile	Product	Crude Purity (%)
		97
		98
		99
		99
		95

In conclusion, grafting of Nb-tagged silica particles with functionalized Nb-tagged heterocyclic phosphate monomers using ROM polymerization efficiently yields high-load, hybrid Si-immobilized oligomeric hetero-benzyl (Si-OHBP_n) and triazolyl phosphates (Si-OHTP_n). The application of these ROMP-derived oligomeric heterocyclic phosphate reagents have been demonstrated for diversification of various *N*-, *O*- and *S*-nucleophilic species, for efficient hetero-benzylation and (triazolyl)methylation in purification-free protocols.

3.3.3 Special Acknowledgment

The author acknowledges that portions of this chapter, including the preliminary Introduction and Results and Discussion sections, are reprinted, in part, or adapted from the following publications, with permission from the corresponding publishers:

- [1] Maity, P. K.; Faisal, S.; Rolfe, A.; Stoianova, D.; Hanson, P. R. Silica-Supported Oligomeric Benzyl Phosphate (Si-OBP) and Triazole Phosphate (Si-OTP) Alkylating Reagents. *J. Org. Chem.* **2015**, *80*, 9942–9950. Copyright 2015, with permission from American Chemical Society publications.

- [2] Faisal, S.; Maity, P. K.; Zang, Q.; Samarakoon, T. B.; Sourk, R. L.; Hanson, P. R. Application of Silica-Supported Alkylating Reagents in a One-Pot, Sequential Protocol to Diverse Benzoxathiazepine 1,1-Dioxides. *ACS Comb. Sci.* **2016**, *18*, 387–393. Copyright 2016, with permission from American Chemical Society publications.

- [3] Faisal, S.; Maity, P. K.; Zang, Q.; Rolfe, A.; Hanson, P. R. Synthesis of High-Load, Hybrid Silica-Immobilized Heterocyclic Benzyl Phosphate (Si-OHBP) and Triazolyl Phosphate (Si-OHTP) Alkylating Reagents. *ACS Comb. Sci.* **2016**, *18*, 394–398. Copyright 2016, with permission from American Chemical Society publications.

3.4 References

- [1] (a) Gallop, M. A.; Barrett, R. W.; Dower, W. J.; Fodor, S. P. A.; Gordon, E. M. Applications of combinatorial technologies to drug discovery. 1. Background and peptide combinatorial libraries. *J. Med. Chem.* **1994**, *37*, 1233–1251. (b) Musonda, C. C.; Chibale, K. Application of combinatorial and parallel synthesis chemistry methodologies to antiparasitic drug discovery. *Curr. Med. Chem.* **2004**, *11*, 2519–2533. (c) Dolle, R. E.; Bourdonnec, B. L.; Worm, K.; Morales, G. A.; Thomas, C. J.; Zhang, W. Comprehensive survey of chemical libraries for drug discovery and chemical biology: 2009. *J. Comb. Chem.* **2010**, *12*, 765–806. (d) Schreiber, S. L. Organic synthesis toward small-molecule probes and drugs. *Proc. Natl. Acad. Sci. U. S. A.* **2011**, *108*, 6699–6702. (e) Chatterjee, A. K. Cell-based medicinal chemistry optimization of high-throughput screening (HTS) hits for orally active antimalarials. Part 1: challenges in potency and absorption, distribution, metabolism, excretion/pharmacokinetics (ADME/PK) *J. Med. Chem.* **2013**, *56*, 7741–7749.
- [2] (a) Kirschning, A.; Monenschein, H.; Wittenberg, R. Functionalized polymers—emerging versatile tools for solution-phase chemistry and automated parallel synthesis. *Angew. Chem. Int. Ed.* **2001**, *40*, 650–679. (b) Eames, J.; Watkinson, M. Polymeric scavenger reagents in organic synthesis. *Eur. J. Org. Chem.* **2001**, 1213–1224. (c) Booth, R. J.; Hodges, J. C. Solid-Supported Reagent Strategies for Rapid Purification of Combinatorial Synthesis Products *Acc. Chem. Res.* **1999**, *32*, 18–26. (d) Ley, S. V.; Baxendale, I. R.; Bream, R. N.; Jackson, P. S.; Leach, A. G.; Longbottom, D. A.; Nesi, M.; Scott, J. S.; Storer, R. I.; Taylor, S. J. Multi-step organic synthesis using solid-supported reagents and scavengers: a new paradigm in chemical library generation. *J. Chem. Soc., Perkin Trans. 1* **2000**, 3815–4195. (e) Strohmeier, G. A.; Kappe, C. O. Combinatorial Synthesis of Functionalized 1,3-Thiazine Libraries Using a Combined Polymer-Supported Reagent/Catch-and-Release Strategy. *Angew. Chem. Int. Ed.* **2004**, *43*, 621–624.

- [3] (a) Gravert, D. J.; Janda, K. D. Organic Synthesis on Soluble Polymer Supports: Liquid-Phase Methodologies. *Chem. Rev.* **1997**, *97*, 489–509. (b) Haag, R. Dendrimers and Hyperbranched Polymers as High-Loading Supports for Organic Synthesis *Chem. Eur. J.* **2001**, *7*, 327–335. (c) Haag, R.; Sunder, A.; Hebel, A.; Roller, S. Dendritic Aliphatic Polyethers as High-Loading Soluble Supports for Carbonyl Compounds and Parallel Membrane Separation Techniques. *J. Comb. Chem.* **2002**, *4*, 112–119. (d) Toy, P. H.; Janda, K. D. Soluble Polymer-Supported Organic Synthesis. *Acc. Chem. Res.* **2000**, *33*, 546–554. (e) Dickerson, T. J.; Reed, N. N.; Janda, K. D. Soluble Polymers as Scaffolds for Recoverable Catalysts and Reagents. *Chem. Rev.* **2002**, *102*, 3325–3344. (f) Bergbreiter, D. E. Using Soluble Polymers To Recover Catalysts and Ligands. *Chem. Rev.* **2002**, *102*, 3345–3384. (g) Bergbreiter, D. E.; Tian, J.; Hongfa, C. Using Soluble Polymer Supports To Facilitate Homogeneous Catalysis. *Chem. Rev.* **2009**, *109*, 530–582.
- [4] Maity, P. K.; Faisal, S.; Rolfe, A.; Stoianova, D.; Hanson, P. R. Silica-Supported Oligomeric Benzyl Phosphate (Si-OBP) and Triazole Phosphate (Si-OTP) Alkylating Reagents. *J. Org. Chem.* **2015**, *80*, 9942–9950.
- [5] (a) Long, T.; Maity, P. K.; Samarakoon, T. B.; Hanson, P. R. ROMP-Derived Oligomeric Phosphates for Application in Facile Benzylation. *Org. Lett.* **2010**, *12*, 2904–2907. (b) Long, T. R.; Faisal, S.; Maity, P. K.; Rolfe, A.; Kurtz, R. D.; Klimberg, S. V.; Najjar, M. R.; Basha, F. Z.; Hanson, P. R. “Click”-Capture, Ring-Opening Metathesis Polymerization (ROMP), Release: Facile Triazolation Utilizing ROMP-Derived Oligomeric Phosphates. *Org. Lett.* **2011**, *13*, 2038–2041. (c) Faisal, S.; Ullah, F.; Maity, P. K.; Rolfe, A.; Samarakoon, T. B.; Porubsky, P.; Neuenswander, B.; Lushington, G. H.; Basha, F. Z.; Organ, M. G.; Hanson, P. R. Facile (Triazolyl)methylation of MACOS-derived Benzofused Sultams Utilizing ROMP-derived OTP Reagents. *ACS Comb. Sci.* **2012**, *14*, 268–272.
- [6] (a) Guillier, F.; Orain, D.; Bradley, M. Linkers and cleavage strategies in solid-phase organic synthesis and combinatorial chemistry. *Chem. Rev.* **2000**, *100*, 2091–2157. (b) Polshettiwar, V.; Len, C.; Fihri, A. Silica-supported palladium: Sustainable catalysts for cross-coupling reactions. *Coord. Chem. Rev.* **2009**, *253*,

- 2599–2626. (c) Moreno, J.; Iglesias, J.; Melero, J. A.; Sherrington, D. C. Synthesis and characterisation of (hydroxypropyl)-2-aminomethyl pyridine containing hybrid polymer–silica SBA-15 materials supporting Mo(VI) centres and their use as heterogeneous catalysts for oct-1-ene epoxidation. *J. Mater. Chem.* **2011**, *21*, 6725–6735. (d) Fihri, A.; Bouhrara, M.; Patil, U.; Cha, D.; Saih, Y.; Polshettiwar, V. Fibrous nano-silica supported ruthenium (KCC-1/Ru): A sustainable catalyst for the hydrogenolysis of alkanes with good catalytic activity and lifetime. *ACS Cat.* **2012**, *2*, 1425–1431.
- [7] (a) Elias, X.; Pleixats, R.; Man, M. W. C. Hybrid silica materials derived from Hoveyda–Grubbs ruthenium carbenes. Electronic effects of the nitro group on the activity and recyclability as diene and enyne metathesis catalysts. *Tetrahedron* **2008**, *64*, 6770–6781. (b) Mayr, M.; Buchmeiser, M. R.; Wurst, K. Synthesis of a Silica-Based Heterogeneous Second Generation Grubbs Catalyst. *Adv. Synth. Catal.* **2002**, *344*, 712–719. (c) Krause, J. O.; Lubbad, S.; Muyken, O.; Buchmeiser, M. R. Monolith- and Silica-Supported Carboxylate-Based Grubbs-Herrmann-Type Metathesis Catalysts. *Adv. Synth. Catal.* **2003**, *345*, 996–1004.
- [8] Garcie, M.; Zyl, W. E.; Cate, M. G. J.; Stouwdam, J. W.; Verweij, H.; Pimplapure, M. S.; Weickert, G. Novel Preparation of Hybrid Polypropylene/Silica Nanocomposites in a Slurry-Phase Polymerization Reactor. *Ind. Engl. Chem. Res.* **2003**, *42*, 3750–3757.
- [9] French, J. M.; Caras, C. A.; Diver, S. T. Removal of Ruthenium Using a Silica Gel Supported Reagent. *Org. Lett.* **2013**, *15*, 5416–5419.
- [10] Gu, L.; Lim, J.; Cheong, J. L.; Lee, S. S. MCF-supported boronic acids as efficient catalysts for direct amide condensation of carboxylic acids and amines *Chem. Commun.* **2014**, *50*, 7017–7019.
- [11] (a) Chepiga, K. M.; Feng, Y.; Brunelli, N. A.; Jones, C. W.; Davies, H. M. L. Silica-Immobilized Chiral Dirhodium(II) Catalyst for Enantioselective Carbenoid Reactions. *Org. Lett.* **2013**, *15*, 6136–6139. (b) Kong, L.; Zhao, J.; Cheng, T.; Lin, J.; Liu, G.; Polymer-Coated Rhodium/Diamine-Functionalized Silica for

Controllable Reaction Switching in Enantioselective Tandem Reduction Lactonization of Ethyl 2 Acylarylcarboxylates *ACS Catal.* **2016**, *6*, 2244–2249.

- [12] Ghiaci, M.; Zarghani, M.; Khojastehnezhad, A.; Moeinpour, F. Preparation, characterization and first application of silica supported palladium-*N*-heterocyclic carbene as a heterogeneous catalyst for C–C coupling reactions *RSC Adv.* **2014**, *4*, 15496–15501.
- [13] Feng, Y.; Moschetta, E. G.; Jones, C. W. Polymer- and Silica-Supported Iron BPMEN-Inspired Catalysts for C–H Bond Functionalization Reactions. *Chem. Asian J.* **2014**, *9*, 3142–3152.
- [14] Long, W.; Jones, C. W. Hybrid Sulfonic Acid Catalysts Based on Silica-Supported Poly (Styrene Sulfonic Acid) Brush Materials and Their Application in Ester Hydrolysis. *ACS Catal.* **2011**, *1*, 674–681.
- [15] (a) Conley, M. P.; Mougél, V.; Peryshkov, D. V.; Forrest, W. P.; Gajan, D. J.; Lesage, A.; Emsley, L.; Coperet, C.; Schrock, R. R. A Well-Defined Silica-Supported Tungsten Oxo Alkylidene Is a Highly Active Alkene Metathesis Catalyst. *J. Am. Chem. Soc.* **2013**, *135*, 19068–19070. (b) Ong, T.-C.; Liao, W.-C.; Mougél, V.; Gajan, D.; Lesage, A.; Emsley, L.; Coperet, C. Atomistic Description of Reaction Intermediates for Supported Metathesis Catalysts Enabled by DNP SENS. *Angew. Chem. Int. Ed.* **2016**, *55*, 4743–4747. (c) Pucino, M.; Mougél, V.; Schowner, R.; Fedorov, A.; Buchmeiser, M. R.; Coperet, C.; Schrock, R. R. Cationic Silica-Supported *N*-Heterocyclic Carbene Tungsten OxoAlkylidene Sites: Highly Active and Stable Catalysts for Olefin Metathesis *Angew. Chem. Int. Ed.* **2016**, *55*, 4300–4302.
- [16] Shakir, A. J.; Paraschivescu, C.; Matache, M.; Tudose, M.; Mischie, A.; Spafiu, F.; Ionita, I.; A convenient alternative for the selective oxidation of alcohols by silica supported TEMPO using dioxygen as the final oxidant *Tetrahedron Letters* **2015**, *56*, 6878–6881.
- [17] (a) Alesi, S.; Di Maria, F.; Melucci, M.; Macquarrie, D. J.; Luque, R.; Barbarella, G. Microwave-assisted synthesis of oligothiophene semiconductors in aqueous

- media using silica and chitosan supported Pd catalysts *Green Chem.* **2008**, *10*, 517–523. (b) Opanasenko, M.; Stepnicka, P.; Cejka, J. Heterogeneous Pd catalysts supported on silica matrices. *RSC Adv.* **2014**, *4*, 65137–65162. (c) Miao, T.; Wang, L. Regioselective Synthesis of 1,2,3-Triazoles by Use of a Silica-Supported Copper(I) Catalyst *Synthesis* **2008**, 363–368. (c) Martina, K.; Baricco, F.; Caporaso, M.; Berlier, G.; Cravotto, G. Cyclodextrin-Grafted Silica-Supported Pd Nanoparticles: An Efficient and Versatile Catalyst for Ligand-Free C-C Coupling and Hydrogenation *ChemCatChem* **2016**, *8*, 1176–1184. (d) Cao, S.; Duan, W.; Microwave assisted solvent-free C–H amination by silica-supported manganese dioxide *Tetrahedron Letters* **2016**, *57*, 2390–2394.
- [18] Mello, R.; Alcalde-Aragónés, A.; Núñez, M. E. G.; Asensio, G. Epoxidation of Olefins with a Silica-Supported Peracid in Supercritical Carbon Dioxide under Flow. *J. Org. Chem.* **2012**, *77*, 4706–4710.
- [19] (a) Iwai, T.; Harada, T.; Tanaka, R.; Sawamura, M. Silica-supported Tripod Triarylphosphines: Application to Palladium Catalyzed Borylation of Chloroarenes. *Chem. Lett.* **2014**, *43*, 548–586. (b) Tsiavalariis, G.; Haubrich, S.; Merckle, C.; Blümel, J. New Bifunctional Chelating Phosphine Ligands for Immobilization of Metal Complexes on Oxidic Supports *Synlett* **2001**, 391–393.
- [20] (a) Altava, B.; Burguete, M. I.; Garcia-Verdugo, E.; Luis, S. V.; Vicent, M. J. FT-Raman as a simple tool for the fast monitoring of reactions on silica-supported reagents and catalysts: application to silica-bound prolinol and TADDOLs *Tetrahedron. Lett.* **2001**, *42*, 8459–8462. (b) Heckel, A.; Seebach, D. Preparation and Characterization of TADDOLs Immobilized on Hydrophobic Controlled-Pore-Glass Silica Gel and Their Use in Enantioselective Heterogeneous Catalysis *Chem. Eur. J.* **2002**, *8*, 559–572.
- [21] (a) Buchmeiser, M. R. Polymer-Supported Well-Defined Metathesis Catalysts. *Chem. Rev.*, **2009**, *109*, 303–321. (b) Zou, H.; Wu, S.; Shen, J. Review Polymer/Silica Nanocomposites: Preparation, Characterization, Properties, and Applications *Chem. Rev.* **2008**, *108*, 3893–3957. (c) Timofte, R. S.; Woodward, S. Preparation of silane-grafted pellets: silica bound reagents in a very convenient

- form *Tetrahedron Lett.* **2004**, *45*, 39–42. (d) Butterworth, A. J.; Clark, J. H.; Walton, P. H.; Barlow, S. J. Environmentally friendly catalysis using supported reagents: catalytic epoxidation using a chemically modified silica gel. *Chem. Commun.* **1996**, 1859–1860.
- [22] Rolfe, A.; Loh, J. K.; Maity, P. K.; Hanson, P. R. High-Load, Hybrid Si-ROMP Reagents. *Org. Lett.* **2011**, *13*, 4–7.
- [23] (a) Maity, P. K.; Kainz, Q. M.; Faisal, S.; Rolfe, A.; Samarakoon, T. B.; Basha, F. Z.; Reiser, O.; Hanson, P. R. Intramolecular monomer-on-monomer (MoM) Mitsunobu cyclization for the synthesis of benzofused thiadiazepine-dioxides. *Chem. Commun.* **2011**, *47*, 12524–12526. (b) Rolfe, A.; Probst, D.; Volp, K.; Omar, I.; Flynn, D.; Hanson, P. R. High-load, Oligomeric dichlorotriazine (ODCT): A Versatile ROMP-derived Reagent and Scavenger. *J. Org. Chem.* **2008**, *73*, 8785–8790. (c) Stoianova, D. S.; Yao, L.; Rolfe, A.; Samarakoon, T.; Hanson, P. R. High-load, Oligomeric Monoamine Hydrochloride: Facile Generation via ROM Polymerization and Application as an Electrophile Scavenger *Tetrahedron Lett.* **2008**, *49*, 4553–4555. (d) Herpel, R. H.; Vedantham, P.; Flynn, D. L.; Hanson, P. R. High-load, Oligomeric Phosphonyl Dichloride: Facile Generation via ROM Polymerization and Applications to Scavenging Amines. *Tetrahedron Lett.* **2006**, *47*, 6429–6432. (e) Harned, A. M.; He Song, H.; Toy, P. H.; Flynn, D. L.; Hanson, P. R. Multipolymer Solution-Phase Reactions: Application to the Mitsunobu Reaction. *J. Am. Chem. Soc.* **2005**, *127*, 52–53. (f) Zhang, M.; Moore, J. D.; Flynn, D. L.; Hanson, P. R. Development of High-Load, Soluble, Oligomeric Sulfonate Esters via ROM Polymerization: Applications to the Benzylation of Amines. *Org. Lett.* **2004**, *6*, 2657–2660. (g) Asad, N.; Hanson, P. R.; Long, T. R.; Rayabarapu, D. K.; Rolfe, A. Synthesis of epoxybenzo[d]isothiazole 1,1-dioxides: ROMP purification via sequestration of excess oxa-norbornene sultams. *Chem. Commun.* **2011**, *47*, 9528–9530. (h) Maity, P. K.; Rolfe, A.; Samarakoon, T. B.; Faisal, S.; Kurtz, R. D.; Long, T. R.; Schatz, A.; Flynn, D. L.; Grass, R. N.; Stark, W. J.; Reiser, O.; Hanson, P. R. Monomer-on-Monomer (MoM) Mitsunobu Reaction: Facile Purification Utilizing Surface-Initiated Sequestration. *Org. Lett.* **2011**, *13*, 8–

10. (i) Kainz, Q. M.; Linhardt, R.; Maity, P. K.; Hanson, P. R.; Reiser, O. Ring-Opening Metathesis Polymerization-based Recyclable Magnetic Acylation Reagents *ChemSusChem* **2013**, *6*, 721–729. (j) Harned, A. M.; Zhang, M.; Vedantham, P.; Mukherjee, S.; Herpel, R. H.; Flynn, D. L.; Hanson, P. R. ROM Polymerization in Facilitated Synthesis. *Aldrichimica Acta* **2005**, *38*, 3–16.
- [24] (a) Barrett, A. G. M.; Hopkins, B. T.; Love, A. C.; Tedeschi, L. Parallel Synthesis of Terminal Alkynes Using a ROMPgel-Supported Ethyl 1-Diazo-2-oxopropylphosphonate. *Org. Lett.* **2004**, *6*, 835–837. (b) Arstad, E.; Barrett, A. G. M.; Tedeschi, L. ROMPgel-supported tris(triphenylphosphine)rhodium(I) chloride: a selective hydrogenation catalyst for parallel synthesis *Tetrahedron Lett.* **2003**, *44*, 2703–2707. (c) Barrett, A. G. M.; Cramp, S. M.; Roberts, R. S. ROMP-Spheres: A Novel High-Loading Polymer Support Using Cross Metathesis between Vinyl Polystyrene and Norbornene Derivatives. *Org. Lett.* **1999**, *1*, 1083–1086. (d) Fuchter, M. J.; Hoffman, B. M.; Barrett, A. G. M. Ring-Opening Metathesis Polymer Sphere-Supported *s*eco-Porphyrazines: Efficient and Recyclable Photooxygenation Catalysts. *J. Org. Chem.* **2006**, *71*, 724–729. (e) Barrett, A. G. M.; Hopkins, B. T.; Köbberling, J. ROMPgel Reagents in Parallel Synthesis. *Chem. Rev.* **2002**, *102*, 3301–3324.
- [25] (a) Buchmeiser, M. R.; Atzl, N.; Bonn, G. K. Ring-Opening-Metathesis Polymerization for the Preparation of Carboxylic-Acid-Functionalized, High-Capacity Polymers for Use in Separation Techniques. *J. Am. Chem. Soc.* **1997**, *119*, 9166–9174. (b) Buchmeiser, M. R. Homogeneous Metathesis Polymerization by Well-Defined Group VI and Group VIII Transition-Metal Alkylidenes: Fundamentals and Applications in the Preparation of Advanced Materials. *Chem. Rev.* **2000**, *100*, 1565–1604. (c) Buchmeiser, M. R. Heterogeneous C–C coupling and polymerization catalysts prepared by ROMP *Bioorg. Med. Chem. Lett.* **2002**, *12*, 1837–1840. (d) Buchmeiser, M. R. *In Handbook of Metathesis, Vol. 3*, Grubbs, R. H., Ed.: Wiley-VCH: Weinheim, 2003. pp 226-254. (e) Lubbad, S. H.; Bandari, R.; Buchmeiser, M. R. Ring-opening metathesis polymerization-derived monolithic strong anion exchangers for the separation of 5'-phosphorylated

- oligodeoxythymidylic acids fragments. *J. Chromatogr. A* **2011**, *1218*, 8897–8902.
- (f) Wang, D.; Unold, J.; Bubrin, M.; Frey, W.; Kaim, W.; Buchmeiser, M. R. Ruthenium(IV)–Bis(methallyl) Complexes as UV-Latent Initiators for Ring-Opening Metathesis Polymerization *ChemCatChem* **2012**, *4*, 1808–1812. (g) Buchmeiser, M. R. Edited by Schlueter, D. A.; Hawker, C. J.; Sakamoto, J. In *Synthesis of Polymers*. 2012, Vol. 2, 547–586. (h) Naumann, S.; Schmidt, F. G.; Frey, W.; Buchmeiser, M. R. Protected N-heterocyclic carbenes as latent pre-catalysts for the polymerization of ϵ -caprolactone. *Polymer Chemistry* **2013**, *4*, 4172–4181.
- [26] (a) Bolm, C.; Dinter, C. L.; Seger, A.; Höcker, H.; Brozio, J. Synthesis of Catalytically Active Polymers by Means of ROMP: An Effective Approach toward Polymeric Homogeneously Soluble Catalysts. *J. Org. Chem.* **1999**, *64*, 5730–5731. (b) Bolm, C.; Dinter, C. L.; Schiffers, I.; Defrere, L. Living Ring-Opening Metathesis Polymerization of Enantiopure Norbornene-type β -Amino Acid Derivatives. *Synlett* **2001**, 1875–1877.
- [27] (a) Roberts, R. S. ROMPgel beads in IRORI format: acylations revisited. *J. Comb. Chem.* **2005**, *7*, 21–32. (b) Nguyen, M. H.; Smith III, A. B. Polymer-supported siloxane transfer agents for Pd-catalyzed cross-coupling reactions. *Org. Lett.* **2013**, *15*, 4258–4261. (c) Nguyen, M. H.; Smith III, A. B. Copper-catalyzed electrophilic amination of organolithiums mediated by recoverable siloxane transfer agents. *Org. Lett.* **2013**, *15*, 4872–4875. (d) Flynn, D. L.; Hanson, P. R.; Berk, S. C.; Makara, G. M. New developments in chemical library synthesis. Norbornenyl tags for use in phase-switching, sequestration, capture-release and soluble support applications. *Curr. Opin. Drug Discovery Dev.* **2002**, *5*, 571–579. (e) Harned, A. M.; Probst, D. A.; Hanson, P. R. In *Handbook of Metathesis*; Grubbs, R. H., Ed.: Wiley-VCH: Weinheim, Germany, 2003; pp 361–402.
- [28] (a) Dolle, R. E.; Le Bourdonnec, B.; Goodman, A. J.; Morales, G. A.; Thomas, C. J.; Zhang, W. Comprehensive survey of chemical libraries for drug discovery and chemical biology: 2008. *J. Comb. Chem.* **2009**, *11*, 739–790. (b) Fenster, E.; Rayabarapu, D. K.; Zhang, M.; Mukherjee, S.; Hill, D.; Neuenswander, B.;

- Schoenen, F.; Hanson, P. R.; Aube', J. Three-component synthesis of 1,4-diazepin-5-ones and the construction of gamma-turn-like peptidomimetic libraries. *J. Comb. Chem.* **2008**, *10*, 230–234.
- [29] (a) Paquette, L. A. In *Encyclopedia of Reagents for Organic Synthesis*, 1st ed.; John Wiley and Sons: New York, 1995; pp 316-318. (b) March, J. *Advanced Organic Chemistry*, 4th ed.; Wiley: New York, 1991. (c) Greene, T. W.; Wuts, P. G. M. In *Protective Groups in Organic Synthesis*, 4th ed.; John Wiley and Sons: New York, 2007; pp 102–148.
- [30] (a) Lopez, S. S.; Dudley, G. B. Convenient method for preparing benzyl ethers and esters using 2-benzyloxypyridine. *Beilstein J. Org. Chem.* **2008**, *4*, No. 44.
- [31] (a) Buchmeiser, M. R.; Sinner, F.; Mupa, M.; Wurst, K. Ring-Opening Metathesis Polymerization for the Preparation of Surface-Grafted Polymer Supports *Macromolecules* **2000**, *33*, 32–39. (b) Eder, K.; Reichel, E.; Schottenberger, H.; Huber, C. G.; Buchmeiser, M. R. Alkyne Metathesis Graft Polymerization: Synthesis of Poly(ferricinium)-Based Silica Supports for Anion-Exchange Chromatography of Oligonucleotides *Macromolecules* **2001**, *34*, 4334–4341.
- [32] Johnson, H. L.; Clark, R. A. Determination of Bromine Number of Olefinic Hydrocarbons *Anal. Chem.* **1947**, *19*, 869–872.
- [33] (a) Nguyen, S. T.; Johnson, L. K.; Grubbs, R. H.; Ziller, J. W. Ring-opening metathesis polymerization (ROMP) of norbornene by a Group VIII carbene complex in protic media. *J. Am. Chem. Soc.* **1992**, *114*, 3974–3975. (b) Schwab, P.; France, M. B.; Ziller, J. W.; Grubbs, R. H. A Series of Well-Defined Metathesis Catalysts-Synthesis of $[\text{RuCl}_2(=\text{CHR}')(\text{PR}_3)_2]$ and Its Reactions. *Angew. Chem. Int. Ed.* **1995**, *34*, 2039–2041. (c) Schwab, P.; Grubbs, R. H.; Ziller, J. W. Synthesis and Applications of $\text{RuCl}_2(=\text{CHR}')(\text{PR}_3)_2$: The Influence of the Alkylidene Moiety on Metathesis Activity. *J. Am. Chem. Soc.* **1996**, *118*, 100–110. (d) Scholl, M.; Ding, S.; Lee, C. W.; Grubbs, R. H. Synthesis and Activity of a New Generation of Ruthenium-Based Olefin Metathesis Catalysts Coordinated with 1,3-Dimesityl-4,5-dihydroimidazol-2-ylidene Ligands. *Org. Lett.* **1999**, *1*, 953–956. (e)

- Vougioukalakis, G. C.; Grubbs, R. H. Ruthenium-Based Heterocyclic Carbene-Coordinated Olefin Metathesis Catalysts. *Chem. Rev.* **2010**, *110*, 1746–1787.
- [34] (a) Xia, Y.; Qu, F.; Peng, L. Triazole nucleoside derivatives bearing aryl functionalities on the nucleobases show antiviral and anticancer activity *Rev. Med. Chem.* **2010**, *10*, 806–821. (b) Cronin, S.; Chandrasekar, P. H. J. Safety of triazole antifungal drugs in patients with cancer. *Antimicrob. Chemother.* **2010**, *65*, 410–416. (c) Nivoix, Y.; Ubeaud-Sequier, G.; Engel, P.; Leveque, D.; Herbrecht, R. Drug-drug interactions of triazole antifungal agents in multimorbid patients and implications for patient care. *Curr. Drug Metab.* **2009**, *10*, 395–409.
- [35] (a) Parlow, J. J.; Naing, W.; South, M. S.; Flynn, D. L. In Situ Chemical Tagging: Tetrafluorophthalic anhydride as a "Sequestration Enabling Reagent" (SER) in the Purification of Solution Phase Combinatorial Libraries. *Tetrahedron Lett.* **1997**, *38*, 7959–7963. (b) Miller II, A. L.; Bowden, N. B. A Materials Approach to the Dual Site-Isolation of Catalysts Bonded to Linear Polymers and Small, Ionic Molecules for Use in One-Pot Cascade Reactions. *Adv. Mater.* **2008**, *20*, 4195–4199.
- [36] For additional benzylation reagents, see: (a) Crosignani, S.; White, P. D.; Linclau, B. Polymer-Supported O-Alkylisoureas: Useful Reagents for the O-Alkylation of Carboxylic Acids. *J. Org. Chem.* **2004**, *69*, 5897–5905. (b) Poon, K. W. C.; House, S. E.; Dudley, G. B. A Bench-Stable Organic Salt for Benzylation of Alcohols. *Synlett* **2005**, 3142–3144. (c) Poon, K. W. C.; Dudley, G. B. Mix-and-Heat Benzylation of Alcohols Using a Bench-Stable Pyridinium Salt, *J. Org. Chem.* **2006**, *71*, 3923–3927 and references cited therein. (d) Zhang, M.; Flynn, D. L.; Hanson, P. R. Oligomeric Benzylsulfonium Salts: Facile Benzylation via High-Load ROMP Reagents. *J. Org. Chem.* **2007**, *72*, 3194–3198.
- [37] Faisal, S.; Maity, P. K.; Zang, Q.; Samarakoon, T. B.; Sourk, R. L.; Hanson, P. R. Application of Silica-Supported Alkylating Reagents in a One-Pot, Sequential Protocol to Diverse Benzoxathiazepine 1,1-Dioxides. *ACS Comb. Sci.* **2016**, *18*, 387–393.

- [38] For excellent reviews on this topic, see: (a) Dömling, A.; Wang, W.; Wang, K. Chemistry and Biology of Multicomponent Reactions. *Chem. Rev.* **2012**, *112*, 3083–3135. (b) Malinakova, H. C. Recent advances in the discovery and design of multicomponent reactions for the generation of small-molecule libraries. *Reports in Organic Chemistry* **2015**, *5*, 75–90. (c) Rotstein, B. H.; Zaretsky, S.; Rai, V.; Yudin, A. K. Small Heterocycles in Multicomponent Reactions *Chem. Rev.* **2014**, *114*, 8323–8359. (d) Hong, B.-C.; Raja, A.; Sheth, V. M. Asymmetric Synthesis of Natural Products and Medicinal Drugs through One-Pot-Reaction Strategies *Synthesis* **2015**, *47*, 3257–3285. (e) Armstrong, R. M.; Combs, A. P.; Tempest, P. A.; Brown, S. D.; Keating, T. A. Multiple-Component Condensation Strategies for Combinatorial Library Synthesis. *Acc. Chem. Res.* **1996**, *29*, 123–131.
- [39] (a) Hayashi, Y. Pot economy and one-pot synthesis. *Chem. Sci.* **2016**, *7*, 866–880. (b) Ishikawa, H.; Suzuki, T.; Hayashi, Y. High-yielding synthesis of the anti-influenza neuramidase inhibitor (–)-oseltamivir by three "One-Pot" operations. *Angew. Chem. Int. Ed.* **2009**, *48*, 1304–1307. (c) Ishikawa, H.; Suzuki, T.; Orita, H.; Uchimarui, T.; Hayashi, Y. High-Yielding Synthesis of the Anti-Influenza Neuraminidase Inhibitor (–)-Oseltamivir by Two "One-Pot" Sequences. *Chem. Eur. J.* **2010**, *16*, 12616–12626.
- [40] (a) René, O.; Fauber, B. P.; Malhotra, S.; Yajima, H. Palladium-Catalyzed α -Arylation of Sultams with Aryl and Heteroaryl Iodides. *Org. Lett.* **2014**, *16*, 3468–3471. (b) Debnath, S.; Mondal, S. One-Pot Sonogashira Coupling–Cyclization toward Regioselective Synthesis of Benzosultams. *J. Org. Chem.* **2015**, *80*, 3940–3948. (c) Asad, N.; Samarakoon, T. B.; Zang, Q.; Loh, J. K.; Javed, S.; Hanson, P. R. Rapid, Scalable Assembly of Stereochemically Rich, Mono- and Bicyclic Acyl Sultams. *Org. Lett.* **2014**, *16*, 82–85. (d) Organ, M. G.; Hanson, P. R.; Rolfe, A.; Samarakoon, T. B.; Ullah, F. Accessing Stereochemically Rich Sultams via Microwave-Assisted, Continuous Flow Organic Synthesis (MACOS) Scale-out. *J. Flow Chem.* **2011**, *1*, 32–39. (e) Samarakoon, T. B.; Loh, J. K.; Rolfe, A.; Le, L. S.; Yoon, S. Y.; Lushington, G. H.; Hanson, P. R. A Modular Reaction

- Pairing Approach to the Diversity-Oriented Synthesis of Fused- and Bridged-Polycyclic Sultams. *Org. Lett.* **2011**, *13*, 5148–5151. (f) Jiménez-Hopkins, M.; Hanson, P. R. An RCM Strategy to Stereodiverse δ -Sultam Scaffolds. *Org. Lett.* **2008**, *10*, 2223–2226. (g) Majumdar, K. C.; Mondal, S. Recent Developments in the Synthesis of Fused Sultams. *Chem. Rev.* **2011**, *111*, 7749–7773.
- [41] (a) Kim, S. H.; Ramu, R.; Kwon, S. W.; Lee, S. H.; Kim, C. H.; Kang, S. K.; Rhee, S. D.; Bae, M. A.; Ahn, S. H.; Ha, D. C.; Cheon, H. G.; Kim, K. Y.; Ahn, J. H. Discovery of cyclic sulfonamide derivatives as 11β -hydroxysteroid dehydrogenase 1 inhibitors. *Bioorg. Med. Chem. Lett.* **2010**, *20*, 1065–1069. (b) Supuran, C. T. Carbonic anhydrases: novel therapeutic applications for inhibitors and activators. *Nat. Rev. Drug Discovery* **2008**, *7*, 168–181. (c) Brzozowski, F.; Saczewski, F.; Neamati, N. Synthesis and anti-HIV-1 activity of a novel series of 1,4,2-benzodithiazine-dioxides. *Bioorg. Med. Chem. Lett.* **2006**, *16*, 5298–5302. (d) Silvestri, R.; Marfe, G.; Artico, M.; La Regina, G.; Lavecchia, A.; Novellino, E.; Morgante, M.; Di Stefano, C.; Catalano, G.; Filomeni, G.; Abruzzese, E.; Ciriolo, M. R.; Russo, M. A.; Amadori, S.; Cirilli, R.; La Torre, F.; Salimei, P. S. Pyrrolo[1,2-b][1,2,5]benzothiadiazepines (PBTDS): A New Class of Agents with High Apoptotic Activity in Chronic Myelogenous Leukemia K562 Cells and in Cells from Patients at Onset and Who Were Imatinib-Resistant. *J. Med. Chem.* **2006**, *49*, 5840–5844.
- [42] Rocher, J.-P. Preparation of Diarylsultam Derivatives As Anti-psychotic Agents. PCT Int. Appl. WO 9730038 A1 19970821, 1997.
- [43] Santora, V. J.; Covell, J. A.; Ibarra, J. B.; Semple, G. Smith, B.; Smith, J.; Weinhouse, M. I.; Schultz, J. A. Biphenylsulfonamides as Modulators of the Histamine H₃-Receptor Useful for the Treatment of Disorders Related Thereto and Their Preparation. PCT Int. Appl. WO 2008005338 A1 20080110, 2008.
- [44] (a) McKerrecher, D.; Pike, K. G.; Waring, M. J. Preparation of Heteroaryl Benzamide Derivatives for Use As Glucokinase Activators in the Treatment of Type 2 Diabetes. PCT Int. Appl. WO 2006125972 A1 20061130, 2006.

- (b) Campbell, L.; Pike, K. G.; Suleman, A.; Waring, M. J. Preparation of Benzoyl Amino Heterocyclyl Compounds as Glucokinase Activators for Treating Type 2 Diabetes and Other Dis-eases Mediated By GLK. PCT Int. Appl. WO 2008050101 A2 20080502, 2008.
- [45] Duan, J.; Chen, L.; Cherney, R. J.; Decicco, C. P.; Voss, M. E.; W.O. Patent 1, 994, 126 Aug 19, 1988.
- [46] Davies, T. G.; Wixted, W. E.; Coyle, J. E.; Griffiths-Jones, C.; Hearn, K.; McMenamin, R.; Norton, D.; Rich, S. J.; Richardson, C.; Kerns, J. K. et.al. Monoacidic Inhibitors of the Kelch-like ECH-Associated Protein 1: Nuclear Factor Erythroid 2-Related Factor 2 (KEAP1:NRF2) Protein-Protein Interaction with High Cell Potency Identified by Fragment-Based Discovery. *J. Med. Chem.* **2016**, *59*, 3991–4006
- [47] (a) Rolfe, A.; Samarakoon, T. B.; Klimberg, S. V.; Brzozowski, M.; Neuenswander, B.; Lushington, G. H.; Hanson, P. R. S_NAr-Based, Facile Synthesis of a Library of Benzothioxazepine-1,1'-dioxides. *J. Comb. Chem.* **2010**, *12*, 850–854. (b) Rolfe, A.; Ullah, F.; Samarakoon, T. B.; Kurtz, R. D.; Porubsky, P.; Neunswander, B.; Lushington, G.; Santini, C.; Organ, M. G.; Hanson, P. R. Synthesis of Amino-Benzothioxazepine-1,1-dioxides Utilizing a Microwave-Assisted, S_NAr Protocol. *ACS Comb. Sci.* **2011**, *13*, 653–658. (c) Loh, J. K.; Asad, N. A.; Samarakoon, T. B.; Hanson, P. R. Modular, One-Pot, Sequential Aziridine Ring Opening–S_NAr Strategy to 7-,10-, and 11-Membered Benzo-Fused Sultams. *J. Org. Chem.* **2015**, *80*, 9926–9941.
- [48] Valverde, I. E.; Bauman, A.; Kluba, C. A.; Vomstein, S.; Walter, M. A.; Mindt, T. L. 1,2,3-Triazoles as Amide Bond Mimics: Triazole Scan Yields Protease-Resistant Peptidomimetics for Tumor Targeting *Angew. Chem., Int. Ed.* **2013**, *52*, 8957–8960.
- [49] It should be noted that the typical manner of installing a triazole group requires a two-step protocol, such as the alkylation of propargyl bromide (a severe lachrymator) followed by a click reaction with a corresponding azide. The

developed Si-alkylating reagent avoids the use of these toxic reagents and provides a more modular way of installing a triazole group onto the complex-substrates in a one-pot protocol. Moreover, the developed Si-alkylating reagents are free flowing solids, bench stable and can be stored for longer time at room temperature and successfully utilized for alkylation reactions in a one-pot protocol. In addition, once made they can be shipped under safer conditions as compared to the corresponding benzyl bromides.

- [50] (a) Vitaku, E.; Smith, D. T.; Njardarson, J. T. Analysis of the Structural Diversity, Substitution Patterns, and Frequency of Nitrogen Heterocycles among U.S. FDA Approved Pharmaceuticals *J. Med. Chem.* **2014**, *57*, 10257–10274. (b) Baumann, M.; Baxendale, I. R. An overview of the synthetic routes to the best selling drugs containing 6-membered heterocycles. *Beilstein J. Org. Chem.* **2013**, *9*, 2265–2319. (c) Michlik, S.; Kempe, R. Regioselectively functionalized pyridines from sustainable resources *Angw. Chem., Int. Ed.*, **2013**, *52*, 6326–6329. (d) Dua, R.; Shrivastava, S.; Sonwane, S. K.; Srivastava, S. K. Pharmacological Significance of Synthetic Heterocycles Scaffold: A Review. *Adv. Bio. Res.* **2011**, *5*, 120–144.
- [51] Gomtsyan A. Heterocycles in drugs and drug discovery. *Chem. Heterocycl. Compd.* **2012**, *48*, 7–10.
- [52] For general concepts of solid-phase techniques: (a) Toy, P. H.; Lam, Y. Solid-Phase Organic Synthesis: Concepts, Strategies, and Applications; John Wiley & Sons, Inc., Hoboken, New Jersey, 2012. (b) Choi, S.; Amajjahe, S.; Ritter, H. Polymerization of included monomers and behavior of resulting polymers From Advances in Polymer Science. In *Inclusion Polymers* Gerhard W.; Ed.; Springer-Verlag Berlin Heidelberg 2009, 222, pp 175–203.
- [53] Myers, R. M., Roper, K. A., Baxendale, I. R. and Ley, S. V. The Evolution of Immobilized Reagents and their Application in Flow Chemistry for the Synthesis of Natural Products and Pharmaceutical Compounds. In *Modern Tools for the Synthesis of Complex Bioactive Molecules* Cossy, J.; Arseniyadis, S.; Eds.; John Wiley & Sons, Inc.: New Jersey, 2012; pp 359–393.

- [54] Faisal, S.; Maity, P. K.; Zang, Q.; Rolfe, A.; Hanson, P. R. Synthesis of High-Load, Hybrid Silica-Immobilized Heterocyclic Benzyl Phosphate (Si-OHBP) and Triazolyl Phosphate (Si-OHTP) Alkylating Reagents. *ACS Comb. Sci.* **2016**, *18*, 394–398.

Chapter 4

High Load Hybrid Co/C-Magnetic ROMP-Derived Alkylating Reagents and Scavengers

Section: 4.1 Recyclable Magnetic Co/C Hybrid ROMP Benzenesulfonate Ester (Co/C-OBSE) and Benzenesulfonyl Chloride (Co/C-OBSC) Nanoparticles as Facile Methylating/Alkylating Reagent: Development and Applications.

4.1.1 Introduction

Growing material consumption has resulted in an increasing need for the development of sustainable technologies in the production of chemical entities. Recovery and recycling of expensive reagents in a more sustainable manner is an important area in minimizing environmental impact. The advances in the area of immobilized reagents and ring-opening metathesis polymerization (ROMP) for immobilization for a variety of soluble, silica and magnetic reagents/scavengers and catalyst were summarized in Chapter 1. In Chapter 2 and Chapter 3 we report the development and utilization of soluble and silica supported alkylating reagent respectively. In Chapter 4 (Section 4.1) we describe the synthesis and utilization of Co/C ROMP-derived oligomeric benzene sulfonate ester and benzene sulfonyl chloride (Co/C-OBSC_n) as efficient methylating/alkylating reagents for various carboxylic acids.

Among many grafted-hybrid materials, magnetic-immobilized nanoparticle (NPs) reagents and catalysts have emerged recently as a powerful approach combining the high-load nature of grafted-polymers with the adventitious isolation and recyclability.¹ The synthesis of hybrid materials, which combine the properties of Co/C magnetic nanoparticles with a high-load functionalized material, are well suited to address the limitations of traditional immobilized reagents (e.g functionalized silicas and polystyrene resins). In this regard,² recent developments in our laboratories in collaboration with Oliver Reiser (University of Regensburg), Robert Grass (TurboBead), and Materia, Inc.

(Pasadena, CA) have demonstrated advancements in grafting high load ROMP-derived oligomeric reagents and scavengers onto SiO_2 ³ and magnetic Co/C surfaces⁴ for application in facilitated synthesis and sequestration protocols.

Previous efforts in the Hanson group have demonstrated a sequestration protocol as a variant of the Mitsunobu reaction⁵ utilizing Nb-tagged reagents in conjunction with Nb-tagged Silica and Co/C NPs to sequester all by-products in the reaction (Figure 4.1.1).^{4c} Several variants of the Mitsunobu reaction have been developed for facile purification of the desired product from unwanted by-products, which include tagged, immobilized and water-soluble reagents.⁶ In this protocol, facile sequestration of the utilized and excess reagents was achieved by three methods such as: (i) free catalyst in solution, (ii) surface-initiated catalyst-armed silica,⁷ or (iii) surface-initiated catalyst-armed carbon-coated (Co/C) magnetic nanoparticles (Nps).⁸ In, 2013, using the same protocol, Hanson and coworkers reported an intramolecular Mitsunobu cyclization^{4d} for the synthesis of various benzofused thiadiazepine-dioxides analogs (Figure 4.1.1).

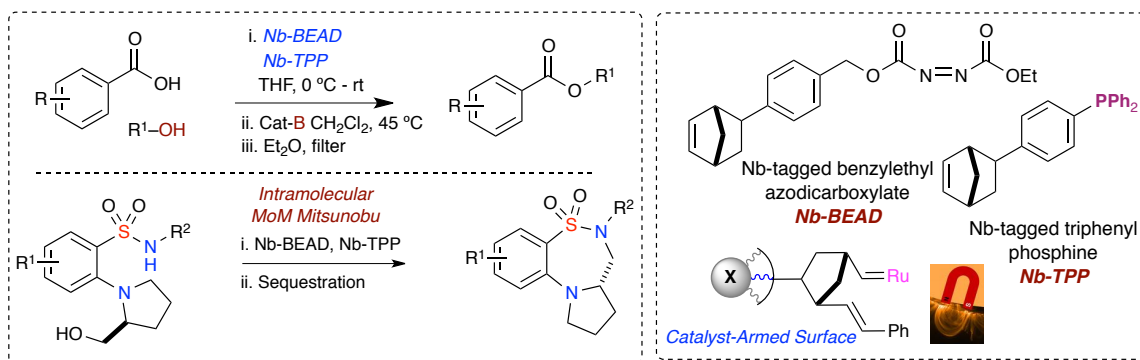


Figure 4.1.1 Norbornenyl-tagged Reagents Nb-TPP and Nb-DEAD and Co/C Np's for MoM Mitsunobu Reactions.

In continuation to our recent interest for the development of Co/C based ROMP derived magnetic nano-supports, we aimed to synthesize a recyclable magnetic support

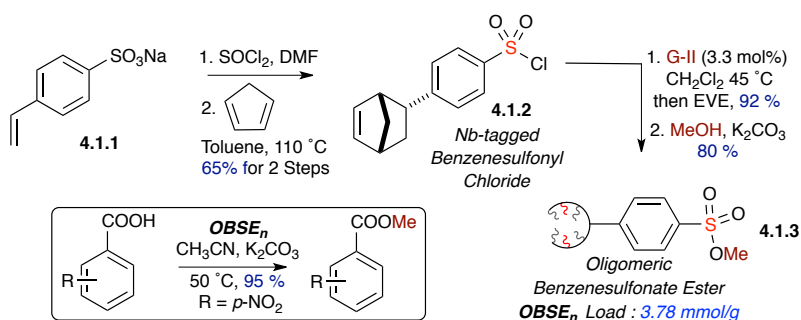
for conducting methylation/alkylation reactions. Common methylating reagents, such as dimethyl sulfate, methyl iodide and diazomethane are extensively used in organic and medicinal chemistry, but have undesirable physical characteristics that pose safety issues when used for routine synthesis, such as toxicity, carcinogenicity and their explosive nature.⁹ Alternative, safe, bench stable, polymer-supported and recyclable methylating or alkylating reagents represent a better platform with enhanced safety/toxicity profiles for routine synthetic transformations.¹⁰ In this section of Chapter 4, we demonstrate the synthesis of magnetic Co/C ROMP-derived oligomeric benzenesulfonate ester (Co/C-OBSE_n) and the in situ use of benzenesulfonyl chloride (Co/C-OBSC_n)/ROH as efficient methylating/alkylating reagents for various carboxylic acids in purification free protocols.

4.1.2 Result and Discussion

Starting with the previously reported soluble ROMP-derived oligomeric sulfonyl chloride OSC reagent¹¹ sulfonate ester¹² and benzenesulfonyl chloride OBSC,¹³ efforts were directed towards the development of the first example of high load magnetic Co/C ROMP-derived oligomeric benzenesulfonate ester (Co/C-OBSE_n), and benzenesulfonyl chloride (Co/C-OBSC_n)/ROH (in situ) as efficient methylating/alkylating reagents for various carboxylic acids. The alkylated ester reaction products were obtained by simple decantation/filtration, evaporation procedure, which makes this method suitable for automated parallel synthesis. For this purpose, we first synthesized the soluble OBSE_n using our previously reported procedure,¹³ (Scheme 4.1.1), where commercially available sodium 4-styrenesulfonate **4.1.1** is treated with thionyl chloride to form sulfonyl chloride. ROM polymerization of monomer **4.1.2** is achieved with use of the Grubbs-II catalyst

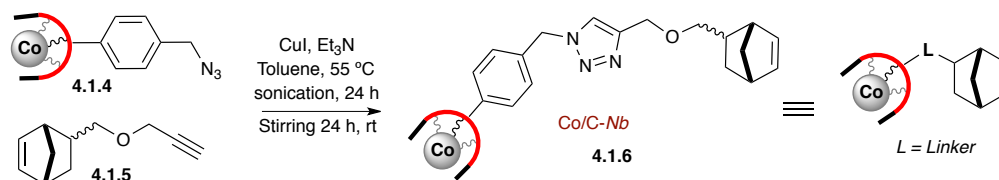
(**G-II**) and further grinding of resulting oligomeric sulfonyl chloride in wet MeOH afforded the desired oligomeric sulfonate ester OBSE **4.1.3**. The desired methylations of carboxylic acids were achieved in greater than 90% yield, when oligomeric benzenesulfonate ester is treated with carboxylic acid in the presence of potassium carbonate. However the isolation and regeneration of the spent polymeric reagent is generally tedious after filtration with SPE cellite or silica.

Scheme 4.1.1. Synthesis of Soluble Oligomeric Benzenesulfonate Ester (OBSE)



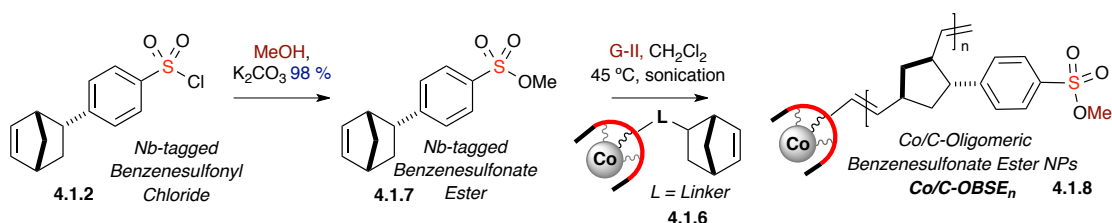
To synthesize the magnetic version of oligomeric benzenesulfonate ester Co/C-OBSE, we first generated the Nb-tagged magnetic linker (Co/C-Nb) **4.1.6**, which has been found to be a suitable precursor for the surface-initiated ROMP of various Nb-tagged monomers.⁴ The synthesis of Co/C-Nb **4.1.6** is achieved by copper(I)-catalyzed alkyne/azide cyclo-addition reaction using commercially available Co/C-azide **4.1.4** and the propargylated bicycle[2.2.1]hept-5-en-2-ylmethanol **4.1.5**, (Scheme 4.1.2). The reaction was performed under sonication/stirring for 48 hours then Nb-tagged Co/C Nps were recovered from the reaction mixture with the aid of a neodymium-based magnet.

Scheme 4.1.2. Synthesis of Nb-tagged Co/C Nanoparticles (Co/C-Nb).



In the next step, Nb-tagged benzenesulfonate ester monomer **4.1.7** is synthesized by grinding Nb-tagged sulfonyl chloride **4.1.2** in wet MeOH to afford the desired compound **4.1.7** in excellent yield and high purity without column chromatography (Scheme 4.1.3).

Scheme 4.1.3. Magnetic Co/C Hybrid ROMP Benzene Sulfonate Ester NPs (Co/C-OBSE)



Utilizing our previously reported protocol⁴ to generate an active ruthenium carbene species on the surface of Nb-tagged Co/C nanobeads, Material **4.1.6** is sonicated with Grubbs-II catalyst (**G-II**, 1.0 equiv. with respect to the loading of Co/C-Nb **4.1.6**) at 45 °C. Next, Nb-tagged sulfonate **4.1.7** (50 equiv.) monomer was added in solution and sonication was carried out further for 6-8 hours to afford the desired ROMPgel-grafted onto the surface of the Co/C nano-beads. After quenching with ethyl vinyl ether (EVE), the solvent was decanted, and the resulting magnetic solid gel was dried rigorously under vacuum, and next crushed for further use. Based on the gain in mass of magnetic polymer **4.1.8**, more than 95% of monomer **4.1.7** was incorporated into the hybrid material, resulting in magnetic NPs with a load of 2.1–2.2 mmol/g. For utilization, initial studies were focused on the methylation of simple carboxylic acid substrates. The reagent Co/C-OBSE_n **4.1.8** was successfully utilized for methylation of various carboxylic acids

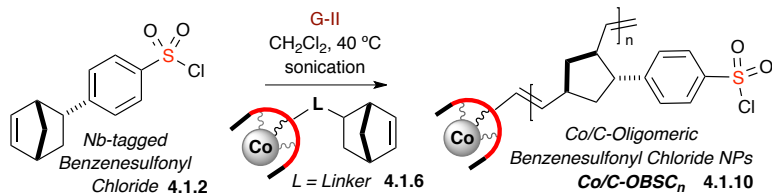
4.1.9a–4.1.9e (shown in Table 4.1.2), which afforded excellent yield (88-95%) and purity after celite SPE filtration. The spent Co/C-OBSE reagent was isolated with the help of a neodymium magnet.

Table 4.1.2. *Methylation of Various Carboxylic Acids Utilizing Magnetic Co/C-OBSE.*

Entry	RCOOH	Product	Yield (%)
1		 4.1.9a	93
2		 4.1.9b	89
3		 4.1.9c	95
4		 4.1.9d	93
5		 4.1.9e	88

Efforts were next directed towards in situ generation from the magnetic benzenesulfonyl chloride, Co/C-OBSC_n, which could subsequently be used for direct alkylations of carboxylic acid in the presence of alcohols. As a result, we focused our attention towards the synthesis and utilization of magnetic sulfonyl chloride Co/C-OBSC_n. In this regard, grafting of Nb-tagged benzenesulfonyl chloride **4.1.2** was successfully achieved on gram scale by using a previously described ROMP protocol, which afforded hybrid ROMP-derived magnetic benzenesulfonyl chloride NPs Co/C-OBSC **4.1.10** (Scheme 4.1.4).

Scheme 4.1.4. *Synthesis of Magnetic Co/C Hybrid ROMP Benzene Sulfonyl Chloride NPs Co/C-OBSC 4.1.10.*



The images were taken by transmission electron microscopy (TEM) to observe and evaluate the graphing of the corresponding Nb-tagged monomers onto the surface of the Co/C-particles nanoparticle.

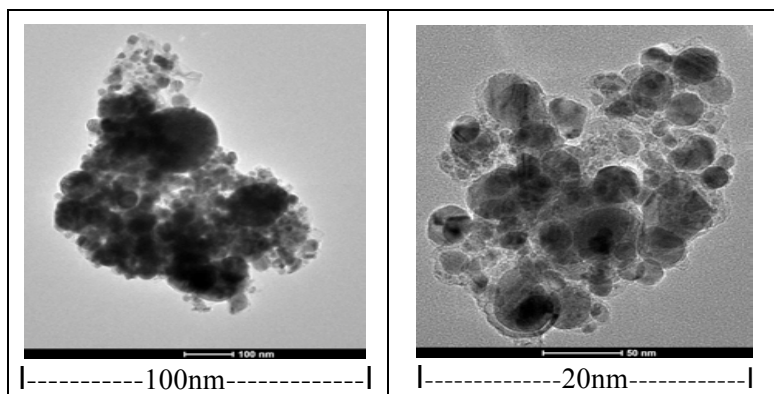


Figure 4.1.2 *TEM Images of Co/C-OBSE 4.1.8 and Co/C-OBSC 4.1.10.*

Direct methylations of carboxylic acids were successfully achieved by utilizing magnetic reagent **Co/C-OBSC_n 4.1.10** in the presence of a slight excess of MeOH (6–10 equiv.). Various simple aromatic and aliphatic carboxylic acids were subjected to methylation **4.1.11a–4.1.11h**, which afforded the majority of products in excellent yields (>90%) and purity (shown in Table 4.1.3). In addition, chemoselective methylation of a carboxylic acid group was observed in the presence of a phenolic hydroxyl group (entry 4).

Table 4.1.3. Methylation of Various Carboxylic Acids Utilizing Magnetic Co/C-OBSC_n

Reaction scheme: $\text{RCOOH} \xrightarrow[\text{Sonication, CH}_3\text{CN, 50 } ^\circ\text{C}]{\text{MeOH, K}_2\text{CO}_3, \text{4.1.10 (1.5 Equiv.)}} \text{RCOOMe}$ (4.1.11a–4.2.11h)

Structure of **Co/C-OBSC_n (4.1.10)**: Load = 2.1–2.2 mm/g

Entry	Product	Yield (%)	Entry	Product	Yield (%)
1	 4.1.11a	96	5	 4.1.11e	93
2	 4.1.11b	99	6	 4.1.11f	92
3	 4.1.11c	89	7	 4.1.11g	95
4	 4.1.11d	90	8	 4.1.11h	70

In light of the wide applications of esterification reactions in pharmaceutical, agrochemicals, plastics, perfumes, and biodiesels,¹⁴ we next directed studies to further explore the scope of the magnetic Co/C-OBSC reagent for alkylation of carboxylic acids with various alcohols. In this regard, reaction of carboxylic acids with deuterated methanol was successfully achieved in excellent yield 90–95 % and purity (Table 4.1.4). Alkylation in the presence of different alcohols afforded the desired alkylated ester in 72–82% yield. Moreover, the continued extensive alkylation studies with a variety of alcohols using a range of nucleophiles could further explore the scope of these magnetic reagents.

Table 4.1.4. Alkylation of Carboxylic Acids Utilizing Magnetic (Co/C-OBSC_n).

$$\text{RCOOH} \xrightarrow[\text{Sonication, CH}_3\text{CN, 50 } ^\circ\text{C}]{\text{ROH, K}_2\text{CO}_3, \text{Co/C-OBSC}_n \text{ 4.2.10}} \text{RCOOR}$$

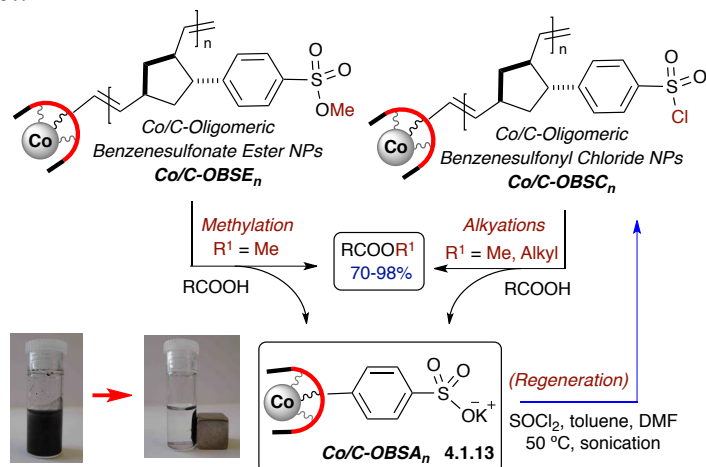
4.1.12a–4.1.12g

Co/C-Oligomeric Benzenesulfonyl Chloride NPs
Co/C-OBSC_n (4.1.10)

ROH	Product	Yield (%)	ROH	Product	Yield (%)
CD ₃ OD	<div style="display: flex; justify-content: space-between;"> <div> $\text{R}^1 =$ a) 3,5-OMe 93 b) <i>p</i>-NO₂ 95 </div> </div>		EtOH	<div style="display: flex; justify-content: space-between;"> <div> $\text{R}^1 =$ c) 3,5-OMe 72 d) <i>p</i>-NO₂ 75 </div> </div>	
				<div style="display: flex; justify-content: space-between;"> <div> $\text{R}^1 =$ c) 3,5-OMe 72 d) <i>p</i>-NO₂ 75 </div> </div>	
BnOH			HO-CH ₂ -CH=CH ₂	<div style="display: flex; justify-content: space-between;"> <div> $\text{R}^1 =$ c) 3,5-OMe 72 d) <i>p</i>-NO₂ 75 </div> </div>	
				<div style="display: flex; justify-content: space-between;"> <div> $\text{R}^1 =$ c) 3,5-OMe 72 d) <i>p</i>-NO₂ 75 </div> </div>	
BnOH			<i>n</i> BuOH	<div style="display: flex; justify-content: space-between;"> <div> $\text{R}^1 =$ c) 3,5-OMe 72 d) <i>p</i>-NO₂ 75 </div> </div>	
				<div style="display: flex; justify-content: space-between;"> <div> $\text{R}^1 =$ c) 3,5-OMe 72 d) <i>p</i>-NO₂ 75 </div> </div>	

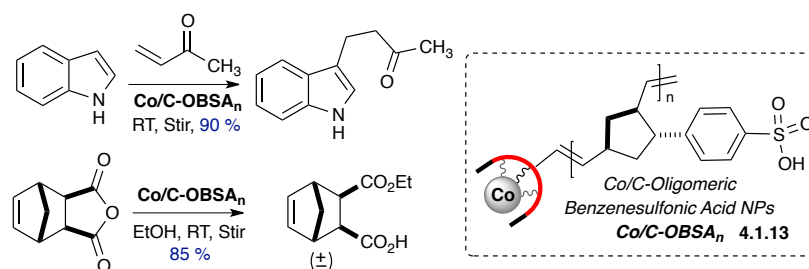
Our next focus was to regenerate the corresponding byproduct magnetic sulfonic acid NP salts, Co/C-OBSA **4.1.13**. To achieve this goal, the spent reagent was treated with SOCl₂ in toluene in the presence of a catalytic amount of DMF, which successfully afforded magnetic sulfonyl chloride NPs, Co/C-OBSC_n **4.1.10** (Scheme 4.1.5), without considerable loss of magnetic material. Multiple regenerations (up to ten times) were successfully achieved without any reduction in performance using the same protocol.

Scheme 4.1.5. Regeneration of Co/C Hybrid ROMP Benzenesulfonic acid NPs (Co/C-OBSA_n) byproduct.



This exciting result is currently being pursued in several related studies. In addition to successful regeneration, we further utilized the spent magnetic benzenesulfonic acid Co/C-OBAS for acid-catalyzed coupling of indole with methyl vinyl ketone, as well as for the alcoholysis of cyclic anhydride at room temperature (Scheme 4.1.6). The spent magnetic sulfonic acid was recovered by external magnet and the coupling products were achieved in 85–90 % yield.

Scheme 4.1.6. Acid Catalyzed Reactions Using Co/C Benzenesulfonic acid NPs (Co/C-OBSA_n).



In conclusion, we have demonstrated the utilization of high load magnetic Co/C ROMP-derived oligomeric benzenesulfonate ester Co/C-OBSE_n and benzenesulfonyl chloride Co/C-OBSC_n as an efficient methylating/alkylating reagent for a variety of carboxylic acids. These alkylations were achieved by simple decantation and filtrations of alkylated products in purification free protocols. The spent byproduct magnetic benzenesulfonic acid Co/C-OBSA_n has been successfully recycled and re-used multiple times without loss of activity.

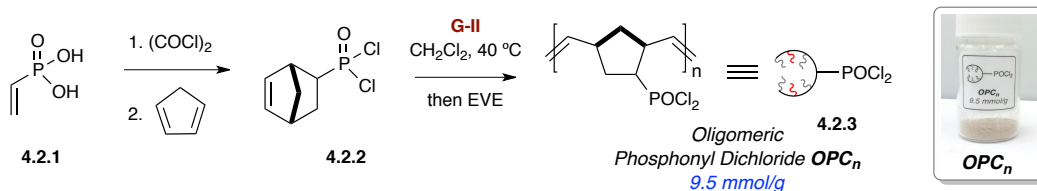
Section: 4.2 Synthesis of High-load, Hybrid Co/C-Oligomeric Phosphonyl Dichloride: Application to Scavenging Amines

4.2.1 Introduction:

The development of purification free protocols based on ROMP strategies in combination with magnetic Co/C tagging have recently introduced several efficient magnetic reagents and catalyst in the area of facilitated synthesis.⁴ Despite advances in this area, high-load Co/C hybrid ROMP reagents are still desired for its applications as a green, recyclable ligands/catalysts, reagents and scavengers. In Chapter 4 (Section 4.2) we describe the synthesis and utilization of Co/C ROMP-derived oligomeric phosphonyl dichlorides Co/C-OPC_n as an efficient magnetic scavenging agent for a variety of amines.

In 2006, Hanson and coworkers generated a ROMP-derived oligomeric soluble phosphonyl dichloride OPC_n as a scavenging agent for a variety of amines.¹⁵ The synthesis of Nb-tagged bicyclo[2.2.1]hept-5-en-2-ylphosphonic monomer (Nb-PC) **4.2.2** was conveniently achieved via Diels–Alder reaction of cyclopentadiene and vinyl phosphonic dichloride **4.2.1** which was derived from vinyl phosphonic acid **4.2.1** (Scheme 4.2.1). The soluble OPC reagent **4.2.3** was exploited in efficient room temperature scavenging of primary and secondary amines (present in excess) following a common benzoylation (30–60 min) or under microwave conditions in shorter duration (<5 min).

Scheme 4.2.1. Soluble High-load Oligomeric Phosphonyl Dichloride (OPC).

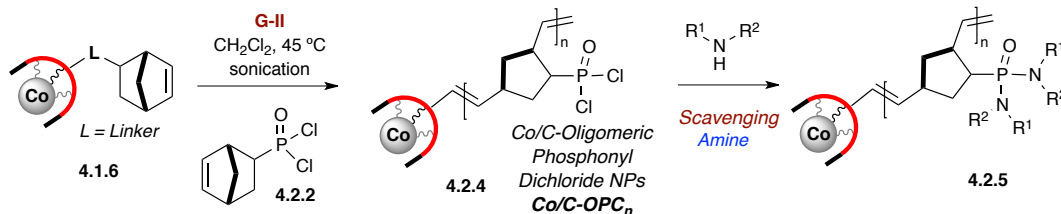


The inherent chemistry of phosphonyl dichlorides allowed efficient and exhaustive scavenging for a variety of amines (present in excess) in the reaction mixture. In this regard, we aimed to prepare a magnetic version of oligomeric phosphonyl chloride OPC_n as a scavenging agent for amines. It was envisioned that the magnetic version of this reagent could enable simple and rapid isolation through magnetic decantation.

4.2.2 Results and Discussion

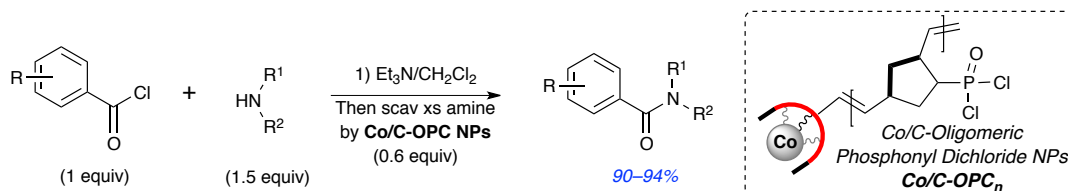
The Co/C magnetic variant **4.2.4** was generated *via* ROM polymerization of (Nb-PC) **4.2.2**, with Nb-tagged Co/C nanobeads linker **4.2.6** using the same protocol as outlined in Section 4.2. Under optimized conditions, Co/C-OPC_{n **4.2.4** was produced on gram scale with a load value of 4.4 mmol/g. The Co/C-OPC_n was developed as a magnetically recoverable scavenging agent with several attractive attributes, including: (i) exhaustive scavenging (ii) the facile and selective hydrolysis of phosphonamides and phosphonamidates, as well as (iii) potential regeneration. It should be noted that the superiority of the hydrolysis of phosphonamides vs sulfonamides and amides, provides a potential application in the recovery of precious amine components used in combinatorial library production.}

Scheme 4.2.2. *Synthesis of Magnetic Co/C Hybrid Oligomeric Phosphonyl Dichloride (Co/C-OPC_n).*



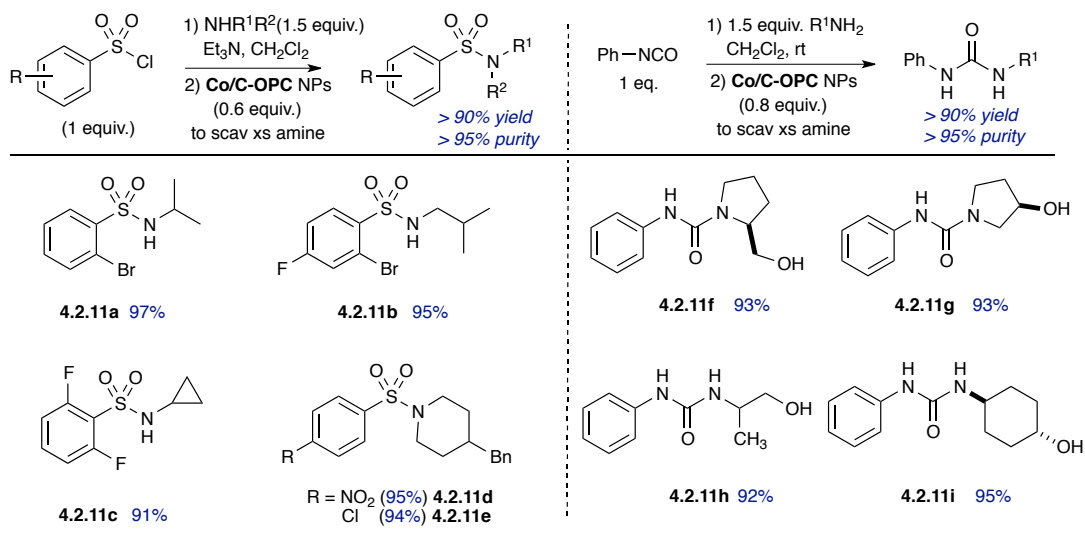
The Co/C-OPC_n **4.2.4** was produced on gram-scale (3 grams) and tested for efficient scavenging of various amines. In this regard, 0.6 equiv. of Co/C-OPC_n was found to be sufficient to scavenge excess amines after their reaction with acid chlorides. The resulting amides were isolated in high yield and good purity (Scheme 4.2.3).

Scheme 4.2.3. *Utilization of Magnetic Co/C-OPC_n for Amide Formations.*



In the next step, various sulfonylation reactions were achieved with an array of amines used in excess. In all cases, the excess amines were easily scavenged by magnetic Co/C-OPC, and the desired products were isolated with high yield and purity (Scheme 4.2.4). The magnetic Co/C-OPC was also tested for simple urea-forming reactions using an array of isocyanates in the presence of excess amine. It is noteworthy to mention that in the reaction with hydroxyl-amines, the magnetic Co/C-OPC displayed chemoselective scavenging, whereby it reacted with only the excess of starting amines at RT, leaving the carbinol-containing product in solution. The selective scavenging further highlights the scope and utility of this unique scavenging agent (Scheme 4.2.4).

Scheme 4.2.4 Utilization of Magnetic Co/C-OPC_n for Scavenging Amines in Sulfonylations and Urea Formations.



In conclusion, we have demonstrated the synthesis and utilization of high load hybrid magnetic oligomeric phosphonyl dichloride Co/C-OPC_n as an efficient chemoselective scavenger of amines (over alcohols) for use in a variety of coupling reactions. The magnetic Co/C-OPC_n scavenger is efficiently utilized in amide formations, sulfonylations and urea formations with a variety of primary and secondary amines. These coupling reactions were achieved by simple decantation and filtrations of desired products in purification free protocols. The spent magnetic scavenger is easily isolated through the use of external magnetic decantation and its regeneration is currently under study.

4.3 Special Acknowledgment

The author acknowledges that portions of this chapter, including the preliminary Introduction and Results and Discussion sections, are reprinted, in part, or adapted from the following publications, with permission from the corresponding publishers:

- [1] Maity, P. K.; Rolfe, A.; Samarakoon, T. B.; Faisal, S.; Kurtz, R. D.; Long, T. R.; Schatz, A.; Flynn, D. L.; Grass, R. N.; Stark, W. J.; Reiser, O.; Hanson, P. R. Monomer-on-Monomer (MoM) Mitsunobu Reaction: Facile Purification Utilizing Surface-Initiated Sequestration. *Org. Lett.* **2011**, *13*, 8–10. Copyright 2011 The Royal Society of Chemistry.

- [2] Maity, P. K.; Kainz, Q. M.; Faisal, S.; Rolfe, A.; Samarakoon, T. B.; Basha, F. Z.; Reiser, O.; Hanson, P. R. Intramolecular Monomer-on-Monomer (MoM) Mitsunobu Cyclization for the Synthesis of Thiadiazepine-dioxides. *Chem. Commun.* **2011**, *47*, 12524–12526. Copyright 2011, with permission from American Chemical Society publications.

References

- [1] (a) Kainz, Q. M.; Reiser, O. Polymer- and Dendrimer-Coated Magnetic Nanoparticles as Versatile Supports for Catalysts, Scavengers, and Reagents *Acc. Chem. Res.* **2014**, *47*, 667–677. (b) Ranjbar, S.; Riente, P.; Rodríguez-Esrich, C.; Yadav, J.; Ramineni, K.; Perica, M. A.; Polystyrene or Magnetic Nanoparticles as Support in Enantioselective Organocatalysis? A Case Study in Friedel–Crafts Chemistry *Org. Lett.* **2016**, *18*, 1602–1605. (c) Kainz, Q. M.; Späth, A.; Weiss, S.; Michl, T. D.; Schätz, A.; Stark, W. J.; König, B.; Reiser, O. Magnetic Nanobeads as Support for Zinc(II)–Cyclen Complexes: Selective and Reversible Extraction of Riboflavin. *Chem. Open.* **2012**, *1*, 125–129. (d) Kainz, Q. M.; Zeltner, M.; Rossier, M.; Stark, W. J.; Reiser, O. Synthesis of Trisubstituted Ureas by a Multistep Sequence Utilizing Recyclable Magnetic Reagents and Scavengers. *Chem. Eur. J.* **2013**, *19*, 10038–10045. (e) Jaita, S.; Phakhodee, W.; Pattarawarapan, M.; Ultrasound-Assisted Methyl Esterification of Carboxylic Acids Catalyzed by Polymer-Supported Triphenylphosphine *Synlett* **2015**, *26*, 2006–2008. (f) Zolfigol, M. A.; Ayazi-Nasrabadi, R. Synthesis of the first magnetic nano particles with thiourea dioxide-based sulfonic acid tag: Application at the one-pot synthesis of 1,1,3-tri(1H-indol-3-yl) alkanes under mild and green conditions. *RSC Adv.*, **2016**, *6*, 69595–69604.
- [2] (a) Long, T. R.; Maity, P. K.; Samarakoon, T. B.; Hanson, P. R. ROMP-Derived Oligomeric Phosphates for Application in Facile Benzylation. *Org. Lett.* **2010**, *12*, 2904–2907. (b) Long, T. R.; Faisal, S.; Maity, P. K.; Rolfe, A.; Kurtz, R. D.; Klimberg, S. V.; Najjar, M. R.; Basha, F. Z.; Hanson, P. R. “Click”-Capture, Ring-Opening Metathesis Polymerization (ROMP), Release: Facile Triazolation Utilizing ROMP-Derived Oligomeric Phosphates. *Org. Lett.* **2011**, *13*, 2038–2041. (c) Faisal, S.; Ullah, F.; Maity, P. K.; Rolfe, A.; Samarakoon, T. B.; Porubsky, P.; Neuenswander, B.; Lushington, G. H.; Basha, F. Z.; Organ, M. G.; Hanson, P. R. Facile (Triazolyl)methylation of MACOS-derived Benzofused Sultams Utilizing ROMP-derived OTP Reagents *ACS Comb. Sci.* **2012**, *14*, 268–272 (c) Stoianova, D.

- S.; Yao, L.; Rolfe, A.; Samarakoon, T.; Hanson, P. R. High-load, oligomeric phosphonyl dichloride: facile generation via ROM polymerization and application to scavenging amines *Tetrahedron Lett.* **2008**, *49*, 4553–4555. (d) Herpel, R. H.; Vedantham, P.; Flynn, D. L.; Hanson, P. R. High-load, Oligomeric Phosphonyl Dichloride: Facile Generation via ROM Polymerization and Applications to Scavenging Amines. *Tetrahedron Lett.* **2006**, *47*, 6429–6432. (e) Harned, A. M.; He Song, H.; Toy, P. H.; Flynn, D. L.; Hanson, P. R. Multipolymer Solution-Phase Reactions: Application to the Mitsunobu Reaction. *J. Am. Chem. Soc.* **2005**, *127*, 52–53.
- [3] (a) Rolfe, A.; Loh, J. K.; Maity, P. K.; Hanson, P. R. High-Load, Hybrid Si-ROMP Reagents. *Org. Lett.* **2011**, *13*, 4–7. (b) Maity, P. K.; Faisal, S.; Rolfe, A.; Stoianova, D.; Hanson, P. R. Silica-Supported Oligomeric Benzyl Phosphate (Si-OBP) and Triazole Phosphate (Si-OTP) Alkylating Reagents. *J. Org. Chem.* **2015**, *80*, 9942–9950 (c) Faisal, S.; Maity, P. K.; Zang, Q.; Samarakoon, T. B.; Sourk, R. L.; Hanson, P. R. Application of Silica-Supported Alkylating Reagents in a One-Pot, Sequential Protocol to Diverse Benzoxathiazepine 1,1-Dioxides. *ACS Comb. Sci.* **2016**, *18*, 387–393. (d) Faisal, S.; Maity, P. K.; Zang, Q.; Rolfe, A.; Hanson, P. R. Synthesis of High-Load, Hybrid Silica-Immobilized Heterocyclic Benzyl Phosphate (Si-OHBP) and Triazolyl Phosphate (Si-OHTP) Alkylating Reagents. *ACS Comb. Sci.* **2016**, *18*, 394–398.
- [4] (a) Schätz, A.; Long, T. R.; Grass, R. N.; Stark, W. J.; Hanson, P. R.; Reiser, O. Immobilization on a Nanomagnetic Co/C Surface using ROM Polymerization: Generation of a Novel Hybrid Material as Support for a Recyclable Palladium Catalyst. *Adv. Func. Mat.* **2010**, *20*, 4323–4328. (b) Kainz, Q. M.; Linhardt, R.; Maity, P. K.; Hanson, P. R.; Reiser, O. Ring-Opening Metathesis Polymerization-based Recyclable Magnetic Acylation Reagents. *ChemSusChem* **2013**, *6*, 721–729. (c) Maity, P. K.; Rolfe, A.; Samarakoon, T. B.; Faisal, S.; Kurtz, R. D.; Long, T. R.; Schatz, A.; Flynn, D. L.; Grass, R. N.; Stark, W. J.; Reiser, O.; Hanson, P. R. Monomer-on-Monomer (MoM) Mitsunobu Reaction: Facile Purification Utilizing

- Surface-Initiated Sequestration. *Org. Lett.* **2011**, *13*, 8–10. (d) Maity, P. K.; Kainz, Q. M.; Faisal, S.; Rolfe, A.; Samarakoon, T. B.; Basha, F. Z.; Reiser, O.; Hanson, P. R. Intramolecular Monomer-on-Monomer (MoM) Mitsunobu Cyclization for the Synthesis of Thiadiazepine-dioxides. *Chem. Commun.* **2011**, *47*, 12524–12526.
- [5] (a) Harned, A. M.; Song He, H.; Toy, P. H.; Flynn, D. L.; Hanson, P. R. Multipolymer Solution-Phase Reactions: Application to the Mitsunobu Reaction. *J. Am. Chem. Soc.* **2005**, *127*, 52–53. (b) Of notable importance is the seminal advances made by Barrett and co-workers demonstrating the concept of reagent annihilation (norbornenyl-tagged DEAD), see: (c) Barrett, A. G. M.; Roberts, R. S.; Schröder, J.; Impurity Annihilation: Chromatography-Free Parallel Mitsunobu Reactions *Org. Lett.*, **2000**, *2*, 2999–30001. For additional examples of in situ scavenging, see: (d) Moore, J. D.; Harned, A. M.; Henle, J.; Flynn, D. L.; Hanson, P. R. Scavenge–ROMP–Filter: A Facile Strategy for Soluble Scavenging via Norbornenyl Tagging of Electrophilic Reagents *Org. Lett.* **2002**, *4*, 1847–1849.
- [6] (a) Chu, Q.; Henry, C.; Curran, D. P. Second-generation tags for fluorous chemistry exemplified with a new fluorous Mitsunobu reagent. *Org. Lett.* **2008**, *10*, 2453–2456. (b) Starkey, G. W.; Parlow, J. J.; Flynn, D. L. Chemically-tagged Mitsunobu reagents for use in solution-phase chemical library synthesis. *Bioorg. Med. Chem. Lett.*, **1998**, *8*, 2385–2390. (d) Danapani, S.; Newsome, J. J.; Curran, D. P.; Separation tagging with cyclodextrin-binding groups: Mitsunobu reactions with bis-(2-(1-adamantyl)ethyl) azodicarboxylate (BadEAD) and bis-(1-adamantylmethyl) azodicarboxylate (BadMAD). *Tetrahedron Lett.* **2004**, *45*, 6653–6656. (e) Taft, B. R.; Swift, E. C.; Lipshutz, B. H. A convenient preparation of di-*p*-chlorobenzyl azodicarboxylate (DCAD) for Mitsunobu couplings. *Synthesis*, **2009**, *2*, 322–334. (g) Yang, J.; Dai, Wang, L. X.; Chen, Y.; Di-*p*-nitrobenzyl azodicarboxylate (DNAD): an alternative azo-reagent for the Mitsunobu reaction. *Tetrahedron*, **2011**, *67*, 1456–1462. (h) Figlus, M.; Tarruella, A. C.; Messer, A.; Sollis, S. L.; Hartley, R. C. Low molecular weight MPEG-assisted organic synthesis. *Chem. Commun.* **2010**, 4405–4206. (i) Figlus, M.; Wellaway, N.; Cooper, A. W. J.; Sollis, S. L.;

- Hartley, R. C.; Synthesis of Arrays Using Low Molecular Weight MPEG-Assisted Mitsunobu Reaction *ACS Comb. Sci.* **2011**, *13*, 280–285. (j) Bergbreiter, D. E.; Yang, Y.-C.; Hobbs, C. E. Polyisobutylene-Supported Phosphines as Recyclable and Regenerable Catalysts and Reagents. *J. Org. Chem.*, **2011**, *76*, 6912–6917.
- [7] (a) Buchmeiser, M. R.; Sinner, F.; Mupa, M. Wurst, K. Ring-Opening Metathesis Polymerization for the Preparation of Surface-Grafted Polymer Supports. *Macromolecules* **2000**, *33*, 32–39. (b) Krause, J. O.; Lubbad, S.; Nuyken, O.; Buchmeiser, M. R. Monolith- and Silica-Supported Carboxylate-Based Grubbs–Herrmann-Type Metathesis Catalysts. *Adv. Synth. Catal.* **2003**, *345*, 996–1004. (c) Kim, N. Y.; Jeon, N. L.; Choi, I. S.; Takami, S.; Harada, Y.; Finnie, K. R.; Girolami, G. S.; Nuzzo, R. G.; Whitesides, G. S.; Laibinis, P. E. Surface-Initiated Ring-Opening Metathesis Polymerization on Si/SiO₂. *Macromolecules*, **2000**, *33*, 2793–2795.
- [8] (a) Grass, R. N.; Athanassiou, E. K.; Stark, W. J. Magnetische Trennung von organischen Verbindungen durch kovalent funktionalisierte Cobaltnanopartikel. *Angew. Chem.* **2007**, *119*, 4996–4999. (b) Schätz, A.; Grass, R. N.; Stark, W. J.; Reiser, O. TEMPO Supported on Magnetic C/Co-Nanoparticles: A Highly Active and Recyclable Organocatalyst. *Chem. Eur. J.* **2008**, *14*, 8262–8266. (c) Wittmann, S.; Schätz, A. Grass, R. N.; Stark, W. J., Reiser O. A Recyclable Nanoparticle-Supported Palladium Catalyst for the Hydroxycarbonylation of Aryl Halides in Water. *Angew. Chem. Int. Ed. Engl.* **2010**, *49*, 1867–1870.
- [9] (a) Kemsley, J. N. Firm Fined For Chemist's Death *Chem. Eng. News* **2011**, *89* (19), 15. (b) Rippey, J. C. R.; Stallwood, M. I. Select this article Nine cases of accidental exposure to dimethyl sulphate—a potential chemical weapon. *Emerg. Med. J.* **2005**, *22*, 878–879. (c) Mileson, B. E.; Sweeney, L. M.; Gargas, M. L.; Kinzell, J. Iodomethane human health risk characterization. *Inhalation Toxicol.* **2009**, *21*, 583–605.
- [10] (a) Ji, Y.; Sweeney, J.; Zoglio, J.; Gorin, D. J. Highly Chemoselective Methylation and Esterification Reactions with Dimethyl Carbonate in the Presence of NaY

- Faujasite. The Case of Mercaptophenols, Mercaptobenzoic Acids, and Carboxylic Acids Bearing OH Substituents. *J. Org. Chem.* **2013**, 78, 11606–11611.
- (b) Crosignani, S.; White, P. D.; Linclau, B. Catalytic Methyl Transfer from Dimethylcarbonate to Carboxylic Acids *Org. Lett.* **2002**, 4, 1035–1037.
- (c) Chighine, A.; Crosignani, S.; Arnal, M.-C.; Bradley, M.; Linclau, B. Polymer-Supported *O*-Methylisourea: A New Reagent for the *O*-Methylation of Carboxylic Acids. *J. Org. Chem.* **2009**, 74, 4753–4762. (d) Yoshino, T.; Togo, H. Facile Preparation of Polymer-Supported Methyl Sulfonate and its Recyclable Use for Methylation of Carboxylic Acids and Amines. *Synlett* **2005**, 517–519.
- [11] Moore, J. D.; Herpel, R. H.; Lichtsinn, J. R.; Flynn, D. L.; Hanson, P. R. ROMP-Generated Oligomeric Sulfonyl Chlorides as Versatile Soluble Scavenging Agents. *Org. Lett.* **2003**, 5, 105–107.
- [12] Zhang, M.; Moore, J. D.; Flynn, D. L.; Hanson, P. R. Development of High-Load, Soluble, Oligomeric Sulfonate Esters via ROM Polymerization: Applications to the Benzoylation of Amines. *Org. Lett.* **2004**, 6, 2657–2660.
- [13] Harned, A. M.; Sherrill, W. M.; Flynn, D. L.; Hanson, P. R. High-load, soluble oligomeric benzenesulfonyl azide: Application to facile diazo-transfer reactions *Tetrahedron* **2005**, 61, 12093–12099.
- [14] (a) Mix, K. A.; Raines, R. T. Optimized diazo scaffold for protein esterification *Org. Lett.* **2015**, 17, 2358–2361. (b) Wei, G-Q.; Zheng, Y-N.; Li, W.; Liu, W-C.; Lin, T.; Zhang, W-Y.; Chen, H-F.; Zeng, J-Z.; hang, X-K.; Chen, Q-C. Structural modification of ginsenoside Rh₂ by fatty acid esterification and its detoxification property in antitumor. *Bioorg. Med. Chem. Lett.* **2012**, 22, 1082–1085. (c) Okuno, Y.; Isomura, S.; Sugamata, A.; Tamahori, K.; Fukuhara, A.; Kashiwagi, M.; Kitagawa, Y.; Kasai, E.; Takeda, K. Convenient and Simple Esterification in Continuous-Flow Systems using *g*-DMAP. *ChemSusChem* **2015**, 8, 3587–3589. (d) Carmo Jr., A. C.; de Souza, L. K. C.; da Costa, C. E. F.; Longo, E.; Zamian, J. R.; Filho, G. N. R. *Fuel*, **2009**, 88, 461–468. (e) Thombal, R. S.; Jadhav, A. R.; Jadhav, V. H. Biomass derived β -cyclodextrin-SO₃H as a solid acid catalyst for

- esterification of carboxylic acids with alcohols. *RSC Adv.* **2015**, *5*, 12981–12986.
- (f) Minakawa, M.; Baek, H.; Yamada, Y. M. A.; Han, W. J.; Uozumi, Y.; Direct Dehydrative Esterification of Alcohols and Carboxylic Acids with a Macroporous Polymeric Acid Catalyst *Org. Lett.* *15*, **2013**, 5798–5801.
- [15] Herpel, R. H.; Vedantham, P.; Flynn, D. L.; Hanson, P. R. High-load, oligomeric phosphonyl dichloride: facile generation via ROM polymerization and application to scavenging amines. *Tetrahedron Lett.* **2006**, *47*, 6429–6432.

Chapter 5

Supporting Information

Experimentals and Spectra for Chapter 2–4

5.1 General Experimental Methods

All air- and moisture-sensitive reactions were carried out in flame- or oven-dried glassware under argon atmosphere. Stirring was achieved with oven-dried magnetic stir bars. CH_2Cl_2 , THF, toluene, CH_3CN , and Et_2O were purified by passage through a Solv-Tek (www.solvtek.com) purification system employing activated Al_2O_3 (Grubbs, R. H.; Rosen, R. K.; Timmers, F. J. *Organometallics* **1996**, *15*, 1518–1520). CHCl_3 was passed through basic alumina and dried over molecular sieves. Et_3N was purified by passage through basic alumina or distilled over CaH_2 and stored over KOH. Flash column chromatography was performed with SiO_2 from Mallinckrodt Chemicals (V120-25, Silica gel, 60 Å, 40–63 μm). SPE purification was performed with SiO_2 purchased from Sorbent Technology (30930M-25, Silica Gel 60A, 40–63 μm) and 6 mL empty cartridges were purchased from Silicycle Inc. Thin layer chromatography was performed on silica gel 60F₂₅₄ plates (EMD-5715-7, Merck. For Celite-SPE 6 mL empty cartridges were purchased from Silicycle Inc. (www.silicycle.com/). Crude mixture was also purified using a Biotage® Isolera automated flash column chromatography system. TLC spots were observed using KMnO_4 stain. Deuterated solvents were purchased from Cambridge Isotope laboratories. ^1H , ^{13}C NMR spectra were recorded on a Bruker DRX-400 spectrometer operating at 400 MHz, 100 MHz respectively as well as a Bruker DRX-500 spectrometer operating at 500 MHz, 125 MHz respectively. Gas chromatography (GC) was performed using an Agilent Technologies 6890N with data processing on a Dell desktop. GC/mass spectrometry was performed using a Quattro micro GC (Micromass UK Limited). High-resolution mass spectrometry (HRMS) was recorded

on a LCT Premier Spectrometer (Micromass UK Limited) operating on ESI (MeOH). Silica and Magnetic nanoparticles were analyzed by transmission electron microscopy (CM30 ST-Philips, LaB₆ cathode, operated at 300 kV point resolution ~ 4 Å), scanning electron microscopy (Hitachi S-2700 equipped with a quartz PCI digital capture). FTIR spectroscopy on soluble compounds was performed using a Shimadzu FTIR-8400S instrument. Grubbs catalysts (G-I, G-II) were generously provided by Materia Inc. Azide bearing magnetic nanoparticles was purchased from Turbo Beads ETH Zurich. Observed rotations at 589 nm, 20 °C were measured using an AUTOPOL IV Model automatic polarimeter. All library syntheses were carried out in 1-dram vials utilizing Anton Parr ® Synthon 3000 microwave platform with parallel evaporations performed using a GeneVac EZ-2 plus evaporator. Samples were diluted in DMSO and purified utilizing an elution of water (modified to pH 9.8 through addition of NH₄OH) and CH₃CN, with a gradient increasing to 20% in CH₃CN over 4 minutes at a flow rate of 20 mL/min. The preparative gradient, triggering thresholds, and UV wavelength were selected based on the HPLC analysis of each crude sample. Analytical analysis of each sample after purification employed a Waters Acquity system with UV and mass detection (Waters LCT Premier). The analytical method utilized a Waters Aquity BEH C18 column (2.1 x 50 mm, 1.7 µm) eluting with a linear gradient of 5% water (modified to pH 9.8 through addition of NH₄OH) to 100% CH₃CN at 0.6 mL/min flow rate were purity was determined using UV peak area at 214 nm.

5.2 Experimentals for Chapter 2.1

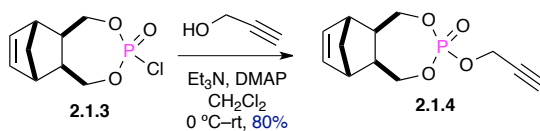
“Click”-Capture, Ring-Opening Metathesis Polymerization (ROMP), Release:

Facile Triazolation Utilizing ROMP-Derived Oligomeric Phosphates.

Experimental Section and Characterization data (SI-146–SI-173)

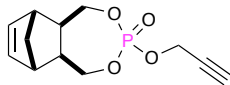
^1H , ^{13}C , Spectra for all Relevant Compounds (SI-174–SI-215)

General procedure A for phosphorylation of propargyl alcohol with Nb-tagged phosphoryl chloride.



To a flame-dried 25 mL RB flask under argon atmosphere was added Nb-tagged phosphoryl chloride **2.1.3** (1.55 g, 6.61 mmol) in CH_2Cl_2 (30 mL), followed by the addition of anhydrous Et_3N (2.3 mL, 16.5 mmol) and anhydrous DMAP (45 mg, 0.33 mmol) at $0\text{ }^\circ\text{C}$. To this mixture was added propargyl alcohol (0.63 mL, 10.6 mmol), which was stirred for 5 hrs at rt (TLC analysis). Upon completion, the reaction was concentrated *in vacuo* and purified by gradient flash chromatography (4:1 hexanes:EtOAc to 1:1 hexanes:EtOAc) to afford **2.1.4** as a white solid in 80% yield.

(5a*R*,6*R*,9*S*,9a*S*)-3-(prop-2-yn-1-yloxy)-1,5,5a,6,9,9a-hexahydro-6,9-methanobenzo[*e*][1,3,2]-dioxaphosphepine-3-oxide (2.1.4).



Utilizing general procedure **A**, **2.1.4** (1.36 g, 5.35 mmol, 80%) was isolated as a white solid.

Mp = 101 °C.

FTIR (neat): 3290, 2968, 2123, 1288, 1068, 1029 cm⁻¹;

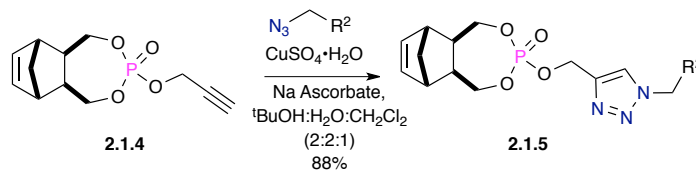
¹H NMR (400 MHz, CDCl₃): δ 6.23 (s, 2H), 4.74 (dd, *J* = 10.0, 2.5 Hz, 2H), 4.26-4.18 (m, 4H), 2.55-2.49 (m, 3H), 2.10-2.07 (m, 2H), 1.39-1.28 (m, 2H);

¹³C NMR (126 MHz, CDCl₃): δ 137.5, 76.4, 69.7 (d, *J*_{CP} = 8.0 Hz), 54.6 (d, *J*_{CP} = 4.4 Hz), 45.0, 43.8, 42.1;

³¹P NMR (CDCl₃, 162 MHz) δ 2.32, -3.84 (*dr* = 7.4:1);

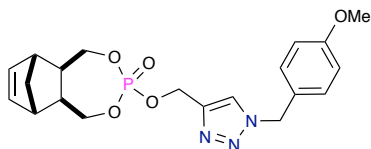
HRMS calculated for C₁₂H₁₅O₄PNa (M+Na)⁺ 277.0606; found 277.0612 (TOF MS ES+).

General procedure B for the [3+2] Huisgen “click” reaction for the generation of Monomers 2.1.5a–i.



To a stirring mixture of **2.1.4** (1 equiv.) and azide (2 equiv.) in CH_2Cl_2 was added $\text{CuSO}_4\cdot 5\text{H}_2\text{O}$ (0.3 equiv) and Na•ascorbate (0.3 equiv) in $t\text{BuOH:H}_2\text{O:CH}_2\text{Cl}_2$ (2:2:1) (0.2 M). The reaction mixture was stirred at rt for 14 hrs, after which the reaction mixture was quenched with water and extracted with CH_2Cl_2 . The combined organic layer was washed with brine, dried (Na_2SO_4), and concentrated in vacuo. The crude mixture was purified by gradient flash chromatography (8:2 EtOAc:hexane to 100% EtOAc) to afford the desired product **2.1.5a–2.1.5i**.

(5a*R*,6*R*,9*S*,9a*S*)-3-((1-(4-Methoxybenzyl)-1*H*-1,2,3-triazol-4-yl)methoxy)-1,5,5a,6,9, 9a-hexahydro-6,9-methanobenzo[*e*][1,3,2]-dioxaphosphepine-3-oxide (2.1.5a).



Utilizing general procedure **B**, **2.1.5a** (6.0 g, 14.38 mmol, 82%) was isolated as a white solid.

Mp = 128 °C

FTIR (neat): 3137, 2925, 1612, 1514, 1463, 1286, 1251, 1178, 1033 cm⁻¹;

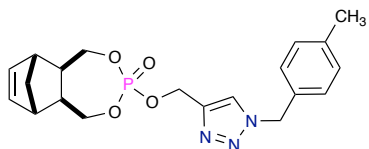
¹H NMR (400 MHz, CDCl₃): δ 7.65 (s, 1H), 7.27-7.25 (m, 2H), 6.92-6.90 (m, 2H), 6.21 (t, *J* = 1.8 Hz, 2H), 5.48 (s, 2H), 5.19 (d, *J* = 9.9 Hz, 2H), 4.14-4.01 (m, 4H), 3.82 (s, 3H), 2.51 (quin, *J* = 1.7 Hz, 2H), 2.11-2.05 (m, 2H), 1.39-1.29 (m, 2H);

¹³C NMR (126 MHz, CDCl₃): δ 160.1, 137.6, 137.4, 129.9, 126.4, 124.0, 114.6, 69.5 (d, *J*_{CP} = 7.9 Hz), 59.8 (d, *J*_{CP} = 5.0 Hz), 55.4, 53.9, 45.0, 43.7, 42.4;

³¹P NMR (CDCl₃, 162 MHz) δ ppm 2.03, -3.66 (*dr* = 6.3:1);

HRMS calculated for C₂₀H₂₄N₃O₅PNa (M+Na)⁺ 440.1351; found 440.1348 (TOF MS ES⁺).

(5a*R*,6*R*,9*S*,9a*S*)-3-((1-(4-Methylbenzyl)-1*H*-1,2,3-triazol-4-yl)methoxy)-1,5,5a,6,9,9a-hexahydro-6,9-methanobenzo[*e*][1,3,2]dioxaphosphepine 3-oxide (2.1.5b).



Utilizing general procedure **B**, **2.1.5b** (2.07 g, 5.16 mmol, 88%) was isolated as a colorless thick liquid.

FTIR (neat): 2925, 1455, 1284, 1120, 1064, 1033, 1008 cm⁻¹;

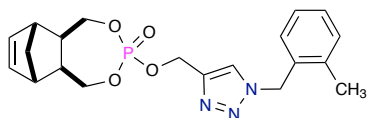
¹H NMR (400 MHz, CDCl₃): δ 7.65 (s, 1H), 7.18-7.15 (m, 4H), 6.19 (s, 2H), 5.48 (s, 2H), 5.16 (d, *J* = 9.9 Hz, 2H), 4.05-3.98 (m, 4H), 2.48 (m, 2H), 2.34 (s, 3H), 2.08-2.05 (m, 2H), 1.36-1.24 (m, 2H);

¹³C NMR (126 MHz, CDCl₃): δ 143.0, 139.0, 137.5, 131.4, 130.0, 128.4, 124.1, 69.5 (d, *J*_{CP} = 7.9 Hz), 59.9 (d, *J*_{CP} = 5.0 Hz), 54.3, 44.9, 43.7, 42.1, 21.3;

³¹P NMR (CDCl₃, 162 MHz) δ ppm 1.97, -3.67 (*dr* = 8.2:1);

HRMS calculated for C₂₀H₂₄N₃O₄PNa (M+Na)⁺ 424.1402; found 424.1398 (TOF MS ES⁺).

(5a*R*,6*R*,9*S*,9a*S*)-3-((1-(2-Methylbenzyl)-1*H*-1,2,3-triazol-4-yl)methoxy)-1,5,5a,6,9,9a-hexahydro-6,9-methanobenzo[*e*][1,3,2]dioxaphosphepine 3-oxide (2.1.5c).



Utilizing general procedure **B**, **2.1.5c** (1.7 g, 4.23 mmol, 77%) was isolated as a colorless thick liquid.

FTIR (neat): 2960, 1456, 1284, 1120, 1064, 1033, 1008 cm⁻¹;

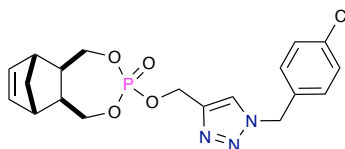
¹H NMR (400 MHz, CDCl₃): δ 7.57 (s, 1H), 7.30-7.15 (m, 4H), 6.20 (s, 2H), 5.53 (s, 2H), 5.16 (d, *J* = 9.9 Hz, 2H), 4.07-3.99 (m, 4H), 2.28 (s, 3H), 2.27-2.23 (m, 2H), 2.10-2.06 (m, 2H), 1.37-1.29 (m, 2H);

¹³C NMR (126 MHz, CDCl₃): δ 142.8, 137.3, 136.9, 132.2, 131.1, 129.5, 129.3, 126.8, 123.8, 69.5 (d, *J*_{CP} = 7.9 Hz), 59.7 (d, *J*_{CP} = 5.1 Hz), 52.4, 44.8, 43.6, 42.0, 19.0;

³¹P NMR (CDCl₃, 162 MHz) δ ppm 2.00, -3.74 (*dr* = 8.2:1);

HRMS calculated for C₂₀H₂₄N₃O₄PNa (M+Na)⁺ 424.1402; found 424.1407 (TOF MS ES⁺).

(5a*R*,6*R*,9*S*,9a*S*)-3-((1-(4-Chlorobenzyl)-1*H*-1,2,3-triazol-4-yl)methoxy)-1,5,5a,6,9,9a-hexahydro-6,9-methanobenzo[*e*][1,3,2]dioxaphosphepine 3-oxide (2.1.5d).



Utilizing general procedure **B**, **2.1.5d** (1.74 g, 4.13 mmol, 71%) was isolated as a white solid.

Mp = 125 °C

FTIR (neat): 3251, 2932, 1453, 1254, 1117, 1036, 1018 cm⁻¹;

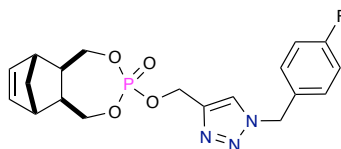
¹H NMR (400 MHz, CDCl₃): δ 7.72 (s, 1H), 7.36 (dt, *J* = 9.1, 2.5 Hz, 2H), 7.24 (dt, *J* = 9.1, 2.5 Hz, 2H), 6.21 (s, 2H), 5.50 (s, 2H), 5.22 (d, *J* = 9.9 Hz, 2H), 4.07-4.03 (m, 4H), 2.52-2.51 (m, 2H), 2.12-2.10 (m, 2H), 1.39-1.32 (m, 2H);

¹³C NMR (126 MHz, CDCl₃): δ 143.3, 137.3, 135.0, 132.9, 129.5, 129.4, 124.1, 69.4 (d, *J*_{CP} = 7.9 Hz), 59.7 (d, *J*_{CP} = 5.1 Hz), 53.6, 44.8, 43.6, 42.0;

³¹P NMR (CDCl₃, 162 MHz) δ ppm -3.66;

HRMS calculated for C₁₉H₂₂ClN₃O₄P (M+H)⁺ 422.1036; found 422.0971 (TOF MS ES+).

(5a*R*,6*R*,9*S*,9a*S*)-3-((1-(4-Fluorobenzyl)-1*H*-1,2,3-triazol-4-yl)methoxy)-1,5,5a,6,9,9a-hexahydro-6,9-methanobenzo[*e*][1,3,2]dioxaphosphepine 3-oxide (2.1.5e).



Utilizing general procedure **B**, **2.1.5e** (1.76 g, 4.34 mmol, 74%) was isolated as a white solid.

Mp = 147 °C

FTIR (neat): 2966, 1556, 1451, 1384, 1251, 1164, 1008 cm⁻¹;

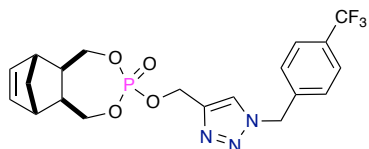
¹H NMR (400 MHz, CDCl₃): δ 7.71 (s, 1H), 7.31-7.28 (m, 2H), 7.10-7.06 (m, 2H), 6.21 (s, 2H), 5.50 (s, 2H), 5.22 (d, *J* = 9.9 Hz, 2H), 4.11-4.04 (m, 4H), 2.52-2.51 (m, 2H), 2.12-2.10 (m, 2H), 1.40-1.32 (m, 2H);

¹³C NMR (126 MHz, CDCl₃): δ 163.1 (d, ¹*J*_{CF} = 245 Hz), 161.9, 143.5, 137.3, 130.1 (³*J*_{C-F} = 8.4 Hz), 124.1, 116.2 (²*J*_{C-F} = 21.7 Hz), 69.6 (d, *J*_{CP} = 7.9 Hz), 59.8 (d, *J*_{CP} = 5.1 Hz), 53.8, 44.9, 43.7, 41.9;

³¹P NMR (CDCl₃, 162 MHz) δ ppm 2.14, -3.66 (*dr* = 10.3:1);

HRMS calculated for C₁₉H₂₂N₃O₄PF (M+H)⁺ 406.1332; found 406.1332 (TOF MS ES+).

(5a*R*,6*R*,9*S*,9a*S*)-3-((1-(4-(Trifluoromethyl)benzyl)-1*H*-1,2,3-triazol-4-yl)methoxy)-1,5,5a,6,9,9a-hexahydro-6,9-methanobenzo[*e*][1,3,2]dioxaphosphepine 3-oxide (2.1.5f).



Utilizing general procedure **B**, **2.1.5f** (2.6 g, 5.71 mmol, 73%) was isolated as a white solid.

Mp = 159 °C

FTIR (neat): 2967, 1456, 1367, 1284, 1120, 1064, 1033, 1008 cm⁻¹;

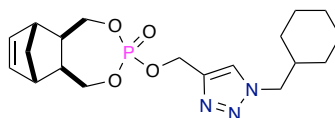
¹H NMR (400 MHz, CDCl₃): δ 7.79 (s, 1H), 7.65 (d, *J* = 8.1 Hz, 2H), 7.40 (d, *J* = 8.1 Hz, 2H), 6.22 (m, 2H), 5.60 (s, 2H), 5.23 (d, *J* = 10.1 Hz, 2H), 4.10-4.03 (m, 4H), 2.58-2.51 (m, 2H), 2.12-2.05 (m, 2H), 1.39-1.32 (m, 2H);

¹³C NMR (126 MHz, CDCl₃): δ 143.4, 138.3, 137.5, 137.3, 128.3, 126.2, 124.8, 123.5, 69.5 (d, *J*_{CP} = 7.9 Hz), 59.7 (d, *J*_{CP} = 5.1 Hz), 53.6, 44.8, 43.6, 42.0;

³¹P NMR (CDCl₃, 162 MHz) δ ppm 2.20, -3.66 (*dr* = 8.8:1);

HRMS calculated for C₂₀H₂₂N₃F₃O₄P (M+H)⁺ 456.1300; found 456.1297 (TOF MS ES⁺).

(5a*R*,6*R*,9*S*,9a*S*)-3-((1-(Cyclohexylmethyl)-1*H*-1,2,3-triazol-4-yl)methoxy)-1,5,5a,6,9,9a-hexahydro-6,9-methanobenzo[*e*][1,3,2]dioxaphosphepine 3-oxide (2.1.5g).



Utilizing general procedure **B**, **2.1.5g** (1.1 g, 2.79 mmol, 70%) was isolated as a white solid.

Mp = 148 °C

FTIR (neat): 2962, 1552, 1456, 1286, 1140, 1063, 1056, 1008 cm⁻¹;

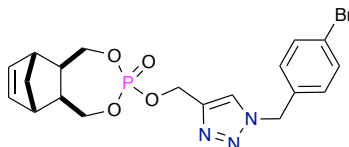
¹H NMR (400 MHz, CDCl₃): δ 7.71 (s, 1H), 6.21 (t, *J* = 1.8 Hz, 2H), 5.24 (d, *J* = 10.2 Hz, 2H), 4.19 (d, *J* = 7.5 Hz, 2H), 4.11-4.07 (m, 4H), 2.53-2.51 (m, 2H), 2.12-2.09 (m, 2H), 1.89-1.86 (m, 1H), 1.76-1.61 (m, 4H), 1.41-1.32 (m, 2H), 1.20-1.13 (m, 4H), 1.04-0.96 (m, 2H);

¹³C NMR (126 MHz, CDCl₃): δ 142.4, 137.3, 124.5, 69.4 (d, *J*_{CP} = 7.9 Hz), 59.8 (d, *J*_{CP} = 5.1 Hz), 56.6, 44.8, 43.6, 42.0, 38.7, 30.5, 26.0, 25.5;

³¹P NMR (CDCl₃, 162 MHz) δ ppm 1.95, -3.60 (*dr* = 8.4:1);

HRMS calculated for C₁₉H₂₉N₃O₄P (M+H)⁺ 394.1896; found 394.1875 (TOF MS ES+).

(5a*R*,6*R*,9*S*,9a*S*)-3-((1-(4-Bromobenzyl)-1*H*-1,2,3-triazol-4-yl)methoxy)-1,5,5a,6,9,9a-hexahydro-6,9-methanobenzo[*e*][1,3,2]dioxaphosphepine 3-oxide (2.1.5h).



Utilizing general procedure **B**, **2.1.5h** (1.31 g, 2.8 mmol, 89%) was isolated as a white solid.

Mp = 172 °C

FTIR (neat): 2925, 1452, 1287, 1250, 1164, 1037, 1018 cm⁻¹;

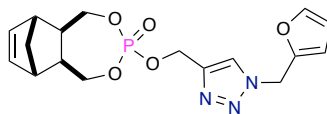
¹H NMR (400 MHz, CDCl₃): δ 7.73 (s, 1H), 7.54-7.52 (m, 2H), 7.20-7.18 (m, 2H), 6.21 (t, *J* = 1.8 Hz, 2H), 5.51 (s, 2H), 5.22 (d, *J* = 10.2 Hz, 2H), 4.10-4.03 (m, 4H), 2.53 (t, *J* = 1.7 Hz, 2H), 2.13-2.10 (m, 2H), 1.40-1.35 (m, 2H);

¹³C NMR (126 MHz, CDCl₃): δ 143.3, 137.3, 133.4, 132.4, 129.7, 124.1, 123.1, 69.4(d, *J*_{CP} = 7.9 Hz), 59.7 (*J*_{CP} = 5.0 Hz), 53.6, 44.8, 43.6, 41.9.

³¹P NMR (CDCl₃, 162 MHz) δ ppm -3.67;

HRMS calculated for C₁₉H₂₂N₃O₄BrP (M+H)⁺ 466.0531; found 488.0336 (TOF MS ES+).

(5a*R*,6*R*,9*S*,9a*S*)-3-((1-(Furan-2-ylmethyl)-1*H*-1,2,3-triazol-4-yl)methoxy)-1,5,5a,6,9,9a-hexahydro-6,9-methanobenzo[*e*][1,3,2]dioxaphosphepine 3-oxide (2.1.5i).



Utilizing general procedure **B**, **2.1.5i** (1.24 g, 3.28 mmol, 56%) was isolated as an off-white solid.

Mp = 143 °C.

FTIR (neat): 3139, 2962, 1461, 1286, 1064, 1033, 1008 cm⁻¹;

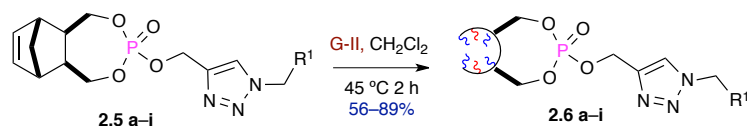
¹H NMR (400 MHz, CDCl₃): δ 7.77 (s, 1H), 6.48 (d, *J* = 3.2 Hz, 1H), 6.40 (dd, *J* = 3.2, 1.9 Hz, 2H), 6.21 (t, *J* = 1.8 Hz, 2H), 5.55 (s, 2H), 5.21 (d, *J* = 10.2 Hz, 2H), 4.13-4.03 (m, 4H), 2.52 (t, *J* = 1.7 Hz, 2H), 2.14-2.10 (m, 2H), 1.39-1.32 (m, 2H);

¹³C NMR (126 MHz, CDCl₃): δ 147.1, 144.0, 143.2, 137.5, 124.1, 111.1, 110.7, 69.6 (d, *J*_{CP} = 7.9 Hz), 59.9 (*J*_{CP} = 5.0 Hz), 47.0, 45.0, 43.8, 42.2;

³¹P NMR (CDCl₃, 162 MHz) δ ppm 1.82, -3.7 (*dr* = 11.2);

HRMS calculated for C₁₇H₂₀N₃O₅PNa (M+Na)⁺ 400.1038; found 400.1029 (TOF MS ES+).

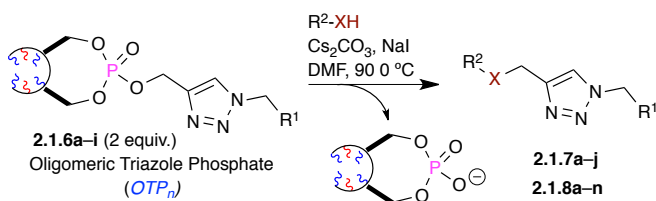
General procedure C for synthesis of OTP 2.1.6a–i via ROMP polymerization.



To a flame-dried flask under argon atmosphere was added OTP monomer **2.1.6a–i** (1 equiv.), which was solvated in anhydrous Ar-degassed CH_2Cl_2 (0.1M). To this stirring solution was added metathesis cat-**A** $[RuCl_2(PCy_3)_2=CHPh]$ (5 mol %). The reaction was stirred and heated at $45\text{ }^\circ C$ for 2–3 hours monitored by TLC (100 % EtOAc, product $R_f = 0$). Upon completion, the reaction was cooled and crude reaction quenched with ethyl vinyl ether (0.1 equiv.) and stirred for an additional 30 minutes. After such time Na_2CO_3 (1 equiv.) was added followed by the drop-wise addition of tetrakis(hydroxymethyl) phosphonium chloride (THPC) (1 equiv., 80% in H_2O). The reaction was then refluxed until complete disappearance of the purple color was observed. After which time the reaction was cooled to room temperature and washed with deionized water and sat. brine. The organic layer was dried ($MgSO_4$), filtered through a celite plug, and concentrated *in vacuo* until slight viscosity of the solution was observed. The resulting viscous solution was precipitated drop-wise in anhydrous Et_2O (1 L/ 5mmol) with stirring. Stirring was continued for 10 minutes after which time the oligomer was filtered and dried *in vacuo* to yield the desired oligomeric triazole phosphate (OTP) **2.1.6a–i** as a white powder in quantitative yield. Subsequent solubility tests (Table 1) confirmed the appropriate solvents to use for the different nucleophilic substitution reaction sequence.

Table 5.1: Solubility of OTP₂₀ 2.1.6a–i

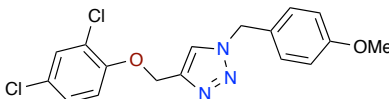
solvent	conditions	results
CH ₂ Cl ₂	RT w/ stirring	soluble
CHCl ₃	RT w/ stirring	soluble
THF	reflux w/ stirring	insoluble
DME	reflux w/ stirring	insoluble
1,3 dioxane	reflux w/ stirring	insoluble
DMF	RT w/ stirring	soluble
Toluene	reflux w/ stirring	insoluble
CH ₃ CN	reflux w/ stirring	insoluble

General procedure D for the triazolation of nucleophilic species with OTP₂₀**2.1.6a–i.**

To a 1-dram vial w/ teflon cap was added OTP₂₀ **2.1.6a–i** (1.5 equiv.) followed by addition of NaI (0.2 equiv), Cs₂CO₃ (3 equiv), and dry DMF (0.2M). The mixture was stirred rapidly until the oligomer dissolved (< 30 s) after which the corresponding nucleophile (1 equiv) was added. The reaction was heated to 90 °C for 2–14 hrs dependent on the nucleophile, after which time, DMF was removed in

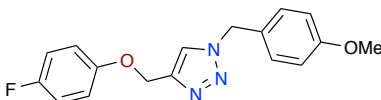
vacuo. The crude mixture was diluted in EtOAc, filtered through a SiO₂ SPE, rinsed several times with a mixture of EtOAc and concentrated *in vacuo* to yield the desired product.

4-((2,4-Dichlorophenoxy)methyl)-1-(4-methoxybenzyl)-1*H*-1,2,3-triazole (2.1.7a).



Utilizing general procedure **D**, **2.1.7a** (56 mg, 0.151 mmol, 98%) was isolated as a white solid, Mp = 73 °C. FTIR (neat): 2935, 2358, 1612, 1585, 1483, 1286 cm⁻¹; ¹H NMR (400 MHz, CDCl₃): δ 7.54 (s, 1H), 7.35 (d, *J* = 2.5 Hz, 2H), 7.25-7.22 (m, 2H), 7.16 (dd, *J* = 8.8, 2.5 Hz, 1H), 7.04 (m, 1H), 6.90 (m, 1H) 5.46 (s, 2H), 5.23 (s, 2H), 3.81 (s, 3H); ¹³C NMR (126 MHz, CDCl₃): δ 160.0, 152.6, 143.7, 130.0, 129.7, 127.7, 126.4, 126.3, 123.9, 122.7, 115.2, 114.5, 63.5, 55.4, 53.9; HRMS calculated for C₁₇H₁₅Cl₂N₃O₂Na (M+Na)⁺ 386.0439; found 386.0449 (TOF MS ES+).

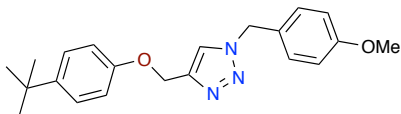
4-((4-fluorophenoxy)methyl)-1-(4-methoxybenzyl)-1*H*-1,2,3-triazole 2.1.7b.



Utilizing general procedure **D**, **2.1.7b** (46 mg, 0.147 mmol, 92%) was isolated as a white solid. Mp = 70 °C. FTIR (neat): 3001, 2935, 1612, 1504, 1249, 1205, 1031 cm⁻¹; ¹H NMR (400 MHz, CDCl₃): δ 7.50 (s, 1H), 7.35-7.18 (m, 2H), 7.00-6.95 (m, 2H), 6.93-6.90 (m, 4H), 5.48 (s, 2H), 5.14 (s, 2H), 3.83 (s, 3H); ¹³C NMR (126 MHz, CDCl₃): δ 160.0, 158.4, 156.6, 154.3 (d, *J* = 2.3 Hz), 144.3, 129.7, 126.4, 122.4,

115.9 (q, $J = 8.0$ Hz), 114.5, 62.7, 55.4, 53.8; HRMS calculated for $C_{17}H_{17}FN_3O_2$ (M+H)⁺ 314.1305; found 314.1293 (TOF MS ES+).

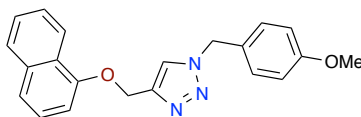
4-((4-(Tert-butyl)phenoxy)methyl)-1-(4-methoxybenzyl)-1*H*-1,2,3-triazole (2.1.7c).



Utilizing general procedure **D**, **2.1.7c** (50 mg, 0.142 mmol, 90%) was isolated as a white solid Mp = 88 °C. FTIR (neat): 2960, 2358, 1610, 1511, 1463, 1250, 1184, 1031 cm⁻¹;

¹H NMR (400 MHz, CDCl₃): δ 7.51 (s, 1H), 7.34-7.30 (m, 2H), 7.27-7.24 (m, 2H), 6.94-6.90 (m, 4H), 5.47 (s, 2H), 5.17 (s, 2H), 3.83 (s, 3H), 1.31 (s, 9H); ¹³C NMR (126 MHz, CDCl₃): δ 159.9, 156.0, 144.8, 143.9, 129.7, 126.5, 126.3, 122.3, 114.5, 114.2, 62.2, 55.4, 53.8, 34.1, 31.5; HRMS calculated for $C_{21}H_{25}N_3NaO_2$ (M+Na)⁺ 374.1844; found 374.1839 (TOF MS ES+).

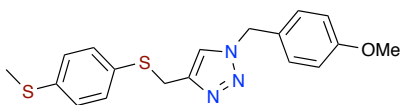
1-(4-Methoxybenzyl)-4-((naphthalen-1-yloxy)methyl)-1*H*-1,2,3-triazole (2.1.7d).



Utilizing general procedure **D**, **2.1.7d** (30 mg, 0.105 mmol, 70%) was isolated as a off-white solid, Mp = 94 °C. FTIR (neat): 3053, 2935, 2835, 1612, 1579, 1514, 1461, 1392, 1267, 1249, 1095 cm⁻¹; ¹H NMR (400 MHz, CDCl₃): δ 8.23 (d, $J = 8.3$ Hz, 1H), 7.81 (d, $J = 7.6$, 1H), 7.58 (s, 1H), 7.53-7.44 (m, 3H), 7.38 (t, $J = 8.0$ Hz, 1H), 7.25 (m, 2H), 6.96 (d, $J = 7.5$ Hz, 1H), 6.92 (m, 2H), 5.49 (s, 2H), 5.39 (s, 2H), 3.83

(s, 3H); ^{13}C NMR (126 MHz, CDCl_3): δ 160.0, 153.9, 144.7, 134.5, 129.7, 127.5, 126.5, 126.4, 125.8, 125.6, 125.2, 122.3, 122.0, 120.8, 114.5, 105.4, 62.5, 55.4, 53.8; HRMS calculated for $\text{C}_{21}\text{H}_{20}\text{N}_3\text{O}_2$ ($\text{M}+\text{H}$) $^+$ 346.1556; found 346.1554 (TOF MS ES+).

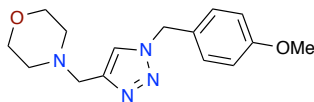
1-(4-Methoxybenzyl)-4-(((4-(methylthio)phenyl)thio)methyl)-1*H*-1,2,3-triazole (2.1.7e).



Utilizing general procedure **D**, **2.1.7e** (33 mg, 0.095 mmol, 60%) was isolated as an off-white solid, $\text{Mp} = 108\text{ }^\circ\text{C}$. FTIR (neat): 3109, 2916, 2837, 2358, 2341, 1612, 1515, 1251, 1178, 1027 cm^{-1} ; ^1H NMR (400 MHz, CDCl_3): δ 7.21-7.19 (m, 2H), 7.16-7.08 (m, 5H), 6.90-6.87 (m, 2H), 5.39 (s, 2H), 4.14 (s, 2H), 3.82 (s, 3H), 2.45 (s, 3H);

^{13}C NMR (126 MHz, CDCl_3): δ 159.9, 145.1, 137.4, 131.4, 131.1, 129.5, 126.9, 126.6, 121.8, 114.4, 55.4, 53.7, 29.6, 15.8; HRMS calculated for $\text{C}_{18}\text{H}_{20}\text{N}_3\text{O}_2\text{S}_2$ ($\text{M}+\text{H}$) $^+$ 358.1048 found 358.1059 (TOF MS ES+).

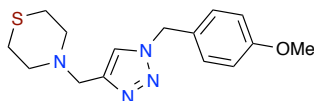
4-((1-(4-methoxybenzyl)-1*H*-1,2,3-triazol-4-yl)methyl)morpholine (2.1.7f).



Utilizing general procedure **D**, **2.1.7f** (35 mg, 0.121 mmol, 72%) was isolated as a brown solid, $\text{Mp} = 95\text{ }^\circ\text{C}$, FTIR (neat): 2927, 2852, 1612, 1514, 1454, 1249, 1178, 1114, 1003 cm^{-1} ; ^1H NMR (400 MHz, CDCl_3): δ 7.35 (s, 1H), 7.22-7.20 (m, 2H), 6.89-6.87 (m, 2H), 5.43 (s, 2H), 3.80 (s, 3H), 3.67 (t, $J = 4.7\text{ Hz}$, 4H), 3.61 (s, 2H),

2.47 (t, $J = 4.5$ Hz, 4H); ^{13}C NMR (126 MHz, CDCl_3): δ 159.9, 144.1, 129.7, 126.6, 124.4, 114.5, 66.7, 55.4, 53.7, 53.6, 53.3; HRMS calculated for $\text{C}_{15}\text{H}_{20}\text{N}_4\text{O}_2\text{Na}$ ($\text{M}+\text{Na}$) $^+$ 311.1484 found 311.1490 (TOF MS ES+).

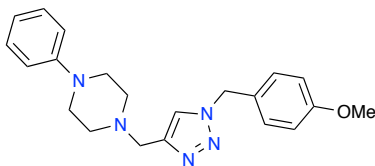
4-((1-(4-methoxybenzyl)-1*H*-1,2,3-triazol-4-yl)methyl)thiomorpholine (2.1.7g).



Utilizing general procedure **D**, **2.1.7g** (54 mg, 0.177 mmol, 75%) was isolated as a thick liquid. FTIR (neat): 2916, 2837, 2358, 1515, 1431, 1251, 1178, 1027 cm^{-1} ; ^1H NMR (400 MHz, CDCl_3): δ 7.34 (s, 1H), 7.25-7.23 (m, 2H), 6.92-6.90 (m 2H), 5.45 (s, 2H), 3.82 (s, 3H), 3.66 (s, 2H), 2.79-2.74 (m, 4H), 2.70-2.65 (m, 4H); ^{13}C NMR (126 MHz, CDCl_3): δ 159.9, 144.5, 129.7, 126.6, 122.2, 114.5, 55.6, 54.6, 54.2, 53.7, 27.8;

HRMS calculated for $\text{C}_{15}\text{H}_{21}\text{N}_4\text{OS}$ ($\text{M}+\text{H}$) $^+$ 305.1438 found 305.1421 (TOF MS ES+).

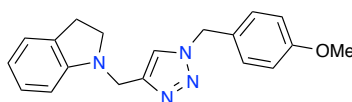
1-((1-(4-Methoxybenzyl)-1*H*-1,2,3-triazol-4-yl)methyl)-4-phenylpiperazine (2.1.7h).



Utilizing general procedure **D**, **2.1.7h** (85 mg, 0.234 mmol, 95%) was isolated as a off-white solid, $\text{Mp} = 137$ °C. FTIR (neat): 3132, 2939, 2833, 1600, 1514, 1454, 1326, 1301, 1251, 1178, 1143 cm^{-1} ; ^1H NMR (400 MHz, CDCl_3): δ 7.40 (s, 1H), 7.28-7.23 (m, 4H), 6.92-6.89 (m, 4H), 6.85 (t, $J = 7.3$ Hz 1H), 5.46 (s, 2H), 3.81 (s,

3H), 3.71 (s, 2H), 3.19 (t, $J = 5.0$ Hz, 4H), 2.66 (t, $J = 5.0$ Hz, 4H); ^{13}C NMR (126 MHz, CDCl_3): δ 159.8, 151.2, 144.5, 129.7, 129.0, 126.5, 122.3, 119.7, 116.0, 114.4, 55.3, 53.6, 53.3, 52.9, 48.9; HRMS calculated for $\text{C}_{21}\text{H}_{26}\text{N}_5\text{O}$ ($\text{M}+\text{H}$) $^+$ 364.2137; found 364.2134 (TOF MS ES+).

1-((1-(4-Methoxybenzyl)-1*H*-1,2,3-triazol-4-yl)methyl)indoline (2.1.7i)



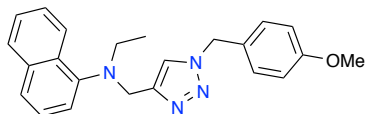
Utilizing general procedure **D**, **2.1.7i** (71 mg, 0.221 mmol, 88%) was isolated as a thick brown liquid.

FTIR (neat): 2952, 2931, 2835, 1608, 1514, 1487, 1460, 1249, 1178 cm^{-1} ;

^1H NMR (400 MHz, CDCl_3): δ 7.33 (s, 1H), 7.22-7.19 (m, 2H), 7.09-7.04 (m, 2H), 6.90-6.88 (m, 2H), 6.68 (t, $J = 7.6$ Hz, 1H), 6.53 (d, $J = 7.8$ Hz, 1H), 5.43 (s, 2H), 4.39 (s, 2H), 3.81 (s, 3H), 3.36 (t, $J = 8.3$, 2H), 2.94 (t, $J = 8.3$, 2H); ^{13}C NMR (126 MHz, CDCl_3): δ 159.8, 151.6, 145.1, 130.2, 129.5, 127.2, 126.6, 124.5, 121.6, 118.1, 114.4, 107.4, 55.3, 53.6, 53.4, 44.8, 28.5;

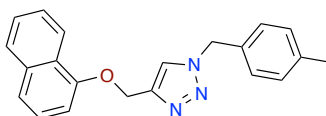
HRMS calculated for $\text{C}_{19}\text{H}_{20}\text{N}_4\text{ONa}$ ($\text{M}+\text{Na}$) $^+$ 343.1535; found 343.1530 (TOF MS ES+).

N-Ethyl-N-((1-(4-methoxybenzyl)-1*H*-1,2,3-triazol-4-yl)methyl)naphthalen-1-amine (2.1.7j).



Utilizing general procedure **D**, **2.1.7j** (53 mg, 0.143 mmol, 62%) was isolated as a thick brown liquid. FTIR (neat): 2966, 2931, 2835, 1612, 1573, 1514, 1461, 1249, 1178, 1045 cm^{-1} ; ^1H NMR (400 MHz, CDCl_3): δ 8.32-8.31 (m, 1H), 7.83-7.81 (m, 1H), 7.54 (d, $J = 8.2$ Hz 1H), 7.49-7.45 (m, 2H), 7.31 (t, $J = 7.6$ Hz, 1H), 7.06-7.00 (m, 3H), 6.94 (s, 1H), 6.84-6.81 (m, 2H), 5.33 (s, 2H), 4.46 (s, 2H), 3.81 (s, 3H), 3.19 (q, $J = 7.1$ Hz, 2H), 1.09 (t, $J = 7.1$ Hz, 3H). ^{13}C NMR (126 MHz, CDCl_3): δ 159.7, 146.8, 145.7, 134.8, 130.5, 129.2, 128.2, 126.9, 125.8, 125.4, 125.4, 123.8, 123.7, 122.0, 118.4, 114.3, 55.3, 53.5, 49.2, 47.8, 12.2; HRMS calculated for $\text{C}_{23}\text{H}_{25}\text{N}_4\text{O}$ ($\text{M}+\text{H}$) $^+$ 373.2028; found 373.2032 (TOF MS ES+).

1-(4-Methylbenzyl)-4-((naphthalen-1-yloxy)methyl)-1*H*-1,2,3-triazole (2.1.8b).

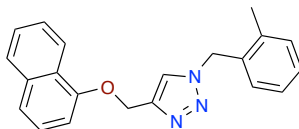


Utilizing general procedure **D**, **2.1.8b** (54 mg, 0.157 mmol, 90%) was isolated as an off-white solid, $\text{Mp} = 85$ $^{\circ}\text{C}$. FTIR (neat): 3053, 2923, 2358, 1595, 1579, 1508, 1461, 1392, 1267, 1238, 1095 cm^{-1} ; ^1H NMR (400 MHz, CDCl_3): δ 8.22 (d, $J = 8.3$ Hz, 1H), 7.80 (d, $J = 7.7$ Hz, 1H), 7.58 (s, 1H), 7.51-7.42 (m, 3H), 7.38 (t, $J = 7.9$ Hz, 1H), 7.19 (s, 4H), 6.96 (d, $J = 7.5$ Hz, 1H), 5.50 (s, 2H), 5.38 (s, 2H), 2.36 (s, 3H);

^{13}C NMR (126 MHz, CDCl_3): δ 153.7, 144.7, 138.8, 134.5, 131.5, 129.8, 128.2, 127.5, 126.5, 125.8, 125.6, 125.3, 122.5, 122.0, 120.8, 105.4, 62.5, 54.1, 21.2;

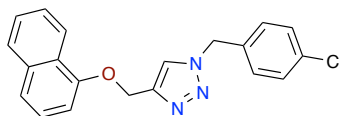
HRMS calculated for $\text{C}_{21}\text{H}_{20}\text{N}_3\text{O}$ ($\text{M}+\text{H}$) $^+$ 330.1606; found 330.1605 (TOF MS ES+).

1-(2-Methylbenzyl)-4-((naphthalen-1-yloxy)methyl)-1*H*-1,2,3-triazole(2.1.8c).



Utilizing general procedure **D**, **2.1.8c** (22 mg, 0.095 mmol, 55%) was isolated as a brown solid, Mp = 64 °C. FTIR (neat): 3053, 2925, 2355, 1577, 1509, 1460, 1392, 1267, 1238, 1095, 1047 cm^{-1} ; ^1H NMR (400 MHz, CDCl_3): δ 8.20 (d, J = 8.3 Hz, 1H), 7.80 (d, J = 7.7 Hz, 1H), 7.50-7.43 (m, 4H), 7.37 (t, J = 7.8 Hz, 1H), 7.34-7.29 (m, 1H), 7.25-7.21 (m, 2H), 7.18-7.15 (m, 1H), 6.96 (d, J = 7.4 Hz, 1H), 5.57 (s, 2H), 5.39 (s, 2H), 2.94 (s, 3H); ^{13}C NMR (126 MHz, CDCl_3): δ 153.9, 144.6, 136.9, 134.5, 132.4, 131.1, 129.4, 129.2, 127.5, 126.7, 126.4, 125.8, 125.6, 125.3, 122.5, 121.9, 120.9, 105.5, 62.5, 52.5, 19.0; HRMS calculated for $\text{C}_{21}\text{H}_{20}\text{N}_3\text{O}$ ($\text{M}+\text{H}$) $^+$ 330.1606; found 330.1597 (TOF MS ES+).

1-(4-Chlorobenzyl)-4-((naphthalen-1-yloxy)methyl)-1*H*-1,2,3-triazole (2.1.8d).



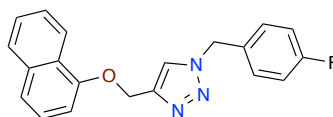
Utilizing general procedure **D**, **2.1.8d** (41 mg, 0.117 mmol, 68%) was isolated as an off-white solid. Mp = 116 °C. FTIR (neat): 3053, 2925, 1579, 1492, 1461, 1392, 1267, 1238, 1095, 1049, 1016 cm^{-1} ; ^1H NMR (400 MHz, CDCl_3): δ 8.21 (d, J = 8.2

Hz, 1H), 7.80 (d, $J = 8.2$ Hz, 1H), 7.60 (s, 1H), 7.51-7.43 (m, 3H), 7.39-7.35 (m, 3H), 7.22 (d, $J = 8.5$ Hz, 1H), 6.96 (d, $J = 7.5$ Hz, 1H), 5.52 (s, 2H), 5.40 (s, 2H);

^{13}C NMR (126 MHz, CDCl_3): δ 153.9, 145.0, 134.9, 134.5, 133.0, 129.4 (3C), 127.5, 126.5, 125.8, 125.6, 125.3, 122.5, 121.9, 120.9, 105.5, 62.5, 53.5;

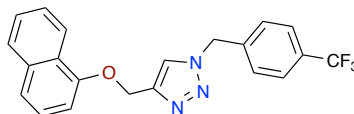
HRMS calculated for $\text{C}_{20}\text{H}_{17}\text{ClN}_3\text{O}$ ($\text{M}+\text{H}$) $^+$ 350.1060; found 350.1085 (TOF MS ES+).

1-(4-Fluorobenzyl)-4-((naphthalen-1-yloxy)methyl)-1*H*-1,2,3-triazole (2.1.8e).



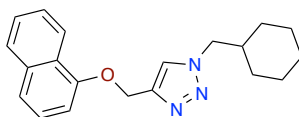
Utilizing general procedure **D**, **2.1.8e** (40 mg, 0.121 mmol, 70%) was isolated as an off-white solid, $\text{Mp} = 97$ °C. FTIR (neat): 2925, 1579, 1510, 1461, 1392, 1267, 1226, 1159, 1095, 1049 cm^{-1} ; ^1H NMR (400 MHz, CDCl_3): δ 8.22 (d, $J = 8.2$ Hz, 1H), 7.81 (d, $J = 8.2$ Hz, 1H), 7.60 (s, 1H), 7.51-7.43 (m, 3H), 7.38 (dd, $J = 8.1, 7.7$ Hz, 1H), 7.29-7.26 (m, 2H), 7.09-7.05 (m, 2H), 6.96 (d, $J = 7.5$ Hz, 1H), 5.52 (s, 2H), 5.40 (s, 2H); ^{13}C NMR (126 MHz, CDCl_3): δ 162.9 ($^1J_{\text{C-F}} = 248.2$ Hz), 153.9, 145.0, 134.5, 130.3 ($^4J_{\text{C-F}} = 3.3$ Hz), 129.9 ($^3J_{\text{C-F}} = 8.4$ Hz), 127.5, 126.5, 125.8, 125.6, 125.3, 122.5, 121.9, 120.9, 116.2, ($^2J_{\text{C-F}} = 21.9$ Hz), 105.4, 62.5, 53.5; HRMS calculated for $\text{C}_{20}\text{H}_{17}\text{FN}_3\text{O}$ ($\text{M}+\text{H}$) $^+$ 334.1356 found 334.1365 (TOF MS ES+).

4-((Naphthalen-1-yloxy)methyl)-1-(4-(trifluoromethyl)benzyl)-1H-1,2,3-triazole (2.1.8f).



Utilizing general procedure **D**, **2.1.8f** (30 mg, 0.113 mmol, 65%) was isolated as an off-white solid, Mp = 144 °C. FTIR (neat): 2924, 1595, 1579, 1508, 1461, 1392, 1325, 1267, 1164, 1124, 1066 cm⁻¹; ¹H NMR (400 MHz, CDCl₃): δ 8.22 (d, *J* = 8.2 Hz, 1H), 7.80 (d, *J* = 8.5 Hz, 1H), 7.65-7.63 (m, 3H), 7.51-7.42 (m, 3H), 7.39-7.35 (m, 3H), 6.96 (d, *J* = 7.4 Hz, 1H), 5.62 (s, 2H), 5.42 (s, 2H); ¹³C NMR (126 MHz, CDCl₃): δ 153.8, 145.2, 138.5, 134.5, 130.9, 128.2, 127.5, 126.5, 126.2, 126.1, 125.8, 125.6, 125.3, 122.7, 121.9, 121.0, 105.5, 62.5, 53.6; HRMS calculated for C₂₁H₁₇F₃N₃O (M+H)⁺ 384.1324; found 384.1322 (TOF MS ES+).

1-(cyclohexylmethyl)-4-((naphthalen-1-yloxy)methyl)-1H-1,2,3-triazole (2.1.8g).

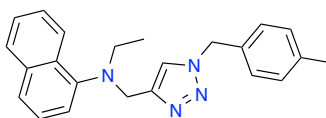


Utilizing general procedure **D**, **2.1.8g** (28mg, 0.084 mmol, 48%) was isolated as a brown solid, Mp = 67 °C. FTIR (neat): 3053, 2923, 2850, 2358, 1579, 1508, 1461, 1392, 1267, 1238, 1095 cm⁻¹; ¹H NMR (400 MHz, CDCl₃): δ 8.28-8.25 (m, 1H), 7.83-7.80 (m, 1H), 7.62 (s, 1H), 7.52-7.45 (m, 3H), 7.39 (t, *J* = 7.7 Hz, 1H), 6.98 (d, *J* = 7.3 Hz, 1H), 5.43 (s, 2H), 4.21 (d, *J* = 7.2 Hz, 2H), 1.92-1.84 (m, 1H), 1.77-1.73 (m, 2H), 1.70-1.62 (m, 2H), 1.31-1.18 (m, 4H), 1.05-0.96 (m, 2H);

^{13}C NMR (126 MHz, CDCl_3): δ 154.0, 144.2, 134.5, 127.5, 126.5, 125.8, 125.7, 125.3, 122.9, 122.0, 120.8, 105.5, 62.6, 56.6, 38.8, 30.5, 26.1, 25.5;

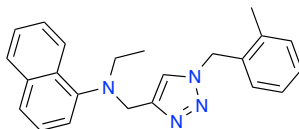
HRMS calculated for $\text{C}_{20}\text{H}_{24}\text{N}_3\text{O}$ ($\text{M}+\text{H}$) $^+$ 322.1919; found 322.1939 (TOF MS ES+).

N-Ethyl-N-((1-(4-methylbenzyl)-1H-1,2,3-triazol-4-yl)methyl)naphthalen-1-amine
(2.1.8i).



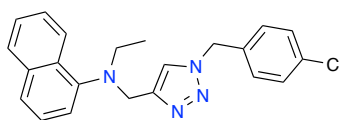
Utilizing general procedure **D**, **2.1.8i** (35 mg, 0.095 mmol, 55%) was isolated as a thick brown liquid. FTIR (neat): 2968, 2925, 2852, 1573, 1515, 1458, 1398, 1382, 1224, 1120, 1045 cm^{-1} ; ^1H NMR (400 MHz, CDCl_3): δ 8.31-8.29 (m, 1H), 7.83-7.81 (m, 1H), 7.53 (dd, J = 8.6, 3.6 Hz, 1H), 7.48-7.44 (m, 2H), 7.32-7.24 (m, 1H), 7.15-7.10 (m, 2H), 7.01-6.98 (m, 3H), 6.95 (s, 1H), 5.36 (d, J = 3.1 Hz, 2H), 4.46 (d, J = 2.9 Hz, 2H), 3.19 (q, J = 7.1 Hz, 2H), 2.34 (d, J = 3.4 Hz, 3H), 1.15 (m, 3H). ^{13}C NMR (126 MHz, CDCl_3): δ 146.8, 145.7, 138.4, 134.8, 131.8, 130.4, 129.6, 128.2, 127.7, 125.8, 125.4, 125.3, 123.8, 123.7, 122.1, 118.4, 53.7, 49.2, 47.8, 21.2, 12.2; HRMS calculated for $\text{C}_{23}\text{H}_{25}\text{N}_4$ ($\text{M}+\text{H}$) $^+$ 357.2079; found 357.2083 (TOF MS ES+).

N-ethyl-N-((1-(2-methylbenzyl)-1*H*-1,2,3-triazol-4-yl)methyl)naphthalen-1-amine (2.1.8j).



Utilizing general procedure **D**, **2.1.8j** (31 mg, 0.109 mmol, 63%) was isolated as a thick brown liquid. FTIR (neat): 3047, 2968, 2927, 1573, 1460, 1398, 1224, 1122, 1045 cm^{-1} ; ^1H NMR (400 MHz, CDCl_3): δ 8.31-8.29 (m, 1H), 7.83-7.80 (m, 1H), 7.52 (d, $J = 8.2$ Hz, 1H), 7.48-7.43 (m, 2H), 7.31-7.22 (m, 2H), 7.15-7.11 (m, 2H), 7.00 (d, $J = 7.3$ Hz, 1H), 6.90 (d, $J = 7.4$ Hz, 1H), 6.82 (s, 1H), 5.40 (s, 2H), 4.47 (s, 2H), 3.19 (q, $J = 7.1$ Hz, 2H), 2.10 (s, 3H), 1.10 (t, $J = 7.1$ Hz, 3H); ^{13}C NMR (126 MHz, CDCl_3): δ 146.7, 145.7, 136.6, 134.8, 132.6, 130.8, 130.5, 128.8 (2C), 128.2, 126.5, 125.8, 125.4, 125.3, 123.8, 123.7, 122.2, 118.5, 52.2, 49.2, 47.9, 18.8, 12.2; HRMS calculated for $\text{C}_{23}\text{H}_{25}\text{N}_4$ ($\text{M}+\text{H}$) $^+$ 357.2079; found 357.2073 (TOF MS ES+).

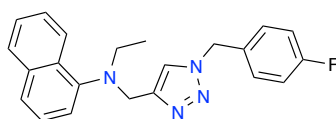
N-((1-(4-Chlorobenzyl)-1*H*-1,2,3-triazol-4-yl)methyl)-N-ethylnaphthalen-1-amine (2.1.8k).



Utilizing general procedure **D**, **2.1.8k** (22 mg, 0.115 mmol, 50%) was isolated as a thick brown liquid. FTIR (neat): 2968, 2925, 2358, 1573, 1492, 1400, 1224, 1089, 1045, 1016 cm^{-1} ; ^1H NMR (400 MHz, CDCl_3): δ 8.31 (m, 1H), 7.82 (m, 1H), 7.55 (d, $J = 8.2$ Hz, 1H), 7.48-7.45 (m, 2H), 7.31 (dd, $J = 8.0, 7.6$ Hz, 1H), 7.28-7.25 (m, 2H), 7.01 (d, $J = 7.3$ Hz, 1H), 6.97 (d, $J = 8.4$ Hz, 2H), 6.93 (s, 1H), 5.35 (s, 2H), 4.49 (s,

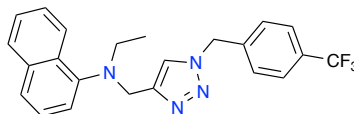
2H), 3.20 (q, $J = 7.1$ Hz, 2H), 1.11 (t, $J = 7.1$ Hz, 3H); ^{13}C NMR (126 MHz, CDCl_3): δ 146.7, 146.1, 134.8, 134.5, 133.3, 130.5, 129.2, 128.9, 128.3, 125.8, 125.5, 125.4, 123.9, 123.7, 122.2, 118.4, 53.1, 49.1, 48.2, 12.2; HRMS calculated for $\text{C}_{22}\text{H}_{22}\text{ClN}_4$ ($\text{M}+\text{H}$) $^+$ 377.1533; found 377.1547 (TOF MS ES+).

N-Ethyl-N-((1-(4-fluorobenzyl)-1H-1,2,3-triazol-4-yl)methyl)naphthalen-1-amine (2.1.8l).



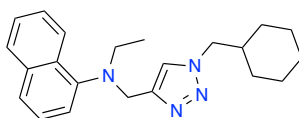
Utilizing general procedure **D**, **2.1.8l** (40 mg, 0.115 mmol, 50%) was isolated as a thick brown liquid. FTIR (neat): 3047, 2970, 2929, 1573, 1510, 1400, 1224, 1159, 1047 cm^{-1} ; ^1H NMR (400 MHz, CDCl_3): δ 8.33-8.30 (m, 1H), 7.83-7.81 (m, 1H), 7.54 (d, $J = 8.2$ Hz, 1H), 7.48-7.46 (m, 2H), 7.31 (dd, $J = 8.0, 7.6$ Hz, 1H), 7.06-6.96 (m, 5H), 6.93 (s, 1H), 5.36 (s, 2H), 4.49 (s, 2H), 3.20 (q, $J = 7.1$ Hz, 2H), 1.11 (t, $J = 7.1$ Hz, 3H); ^{13}C NMR (126 MHz, CDCl_3): δ 162.6 ($^1J_{\text{C-F}} = 248.2$ Hz), 146.7, 146.1, 134.8, 130.7, 130.5, 129.5 ($^3J_{\text{C-F}} = 8.4$ Hz), 128.3, 125.8, 125.5, 125.4, 123.8, 123.7, 122.1, 118.4, 116.0, ($^2J_{\text{C-F}} = 21.9$ Hz), 53.1, 49.1, 48.1, 12.2; HRMS calculated for $\text{C}_{22}\text{H}_{22}\text{FN}_4$ ($\text{M}+\text{H}$) $^+$ 361.1828 found 361.1838 (TOF MS ES+).

***N*-Ethyl-*N*-((1-(4-(trifluoromethyl)benzyl)-1*H*-1,2,3-triazol-4-yl)methyl)naphthalen-1-amine (2.1.8m).**



Utilizing general procedure **D**, **2.1.8m** (22 mg, 0.106 mmol, 60%) was isolated as a thick brown liquid. FTIR (neat): 2927, 1573, 1458, 1421, 1400, 1325, 1164, 1124, 1066, 1018 cm^{-1} ; ^1H NMR (400 MHz, CDCl_3): δ 8.32-8.30 (m, 1H), 7.83-7.80 (m, 1H), 7.55-7.52 (m, 3H), 7.49-7.44 (m, 2H), 7.30 (t, $J = 7.8$ Hz, 1H), 7.10 (d, $J = 8.1$ Hz, 2H), 7.03 (d, $J = 7.4$ Hz, 1H), 6.95 (s, 1H), 5.44 (s, 2H), 4.51 (s, 2H), 3.22 (q, $J = 7.1$ Hz, 2H), 1.12 (t, $J = 7.1$ Hz, 3H); ^{13}C NMR (126 MHz, CDCl_3): δ 146.6, 146.3, 138.8, 134.8, 130.6, 128.3, 128.2, 127.7, 126.2, 125.9, 125.8, 125.5, 123.9, 123.7, 122.4, 118.5, 116.6, 53.2, 48.9, 48.4, 12.2; HRMS calculated for $\text{C}_{23}\text{H}_{22}\text{F}_3\text{N}_3$ ($\text{M}+\text{H}$) $^+$ 411.1797; found 411.1771 (TOF MS ES+).

***N*-((1-(Cyclohexylmethyl)-1*H*-1,2,3-triazol-4-yl)methyl)-*N*-ethylnaphthalen-1-amine (2.1.8n)**



Utilizing general procedure **D**, **2.1.8n** (40 mg, 0.116 mmol, 66%) was isolated as a thick brown liquid. FTIR (neat): 2925, 2850, 1573, 1448, 1398, 1382, 1220, 1045 cm^{-1} ;

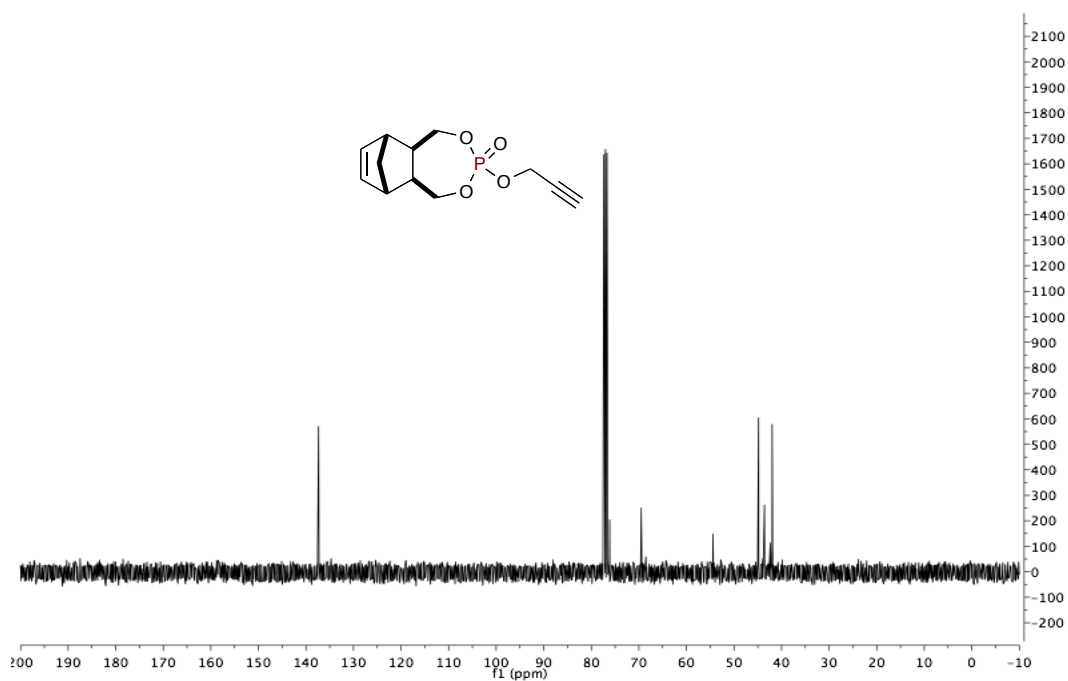
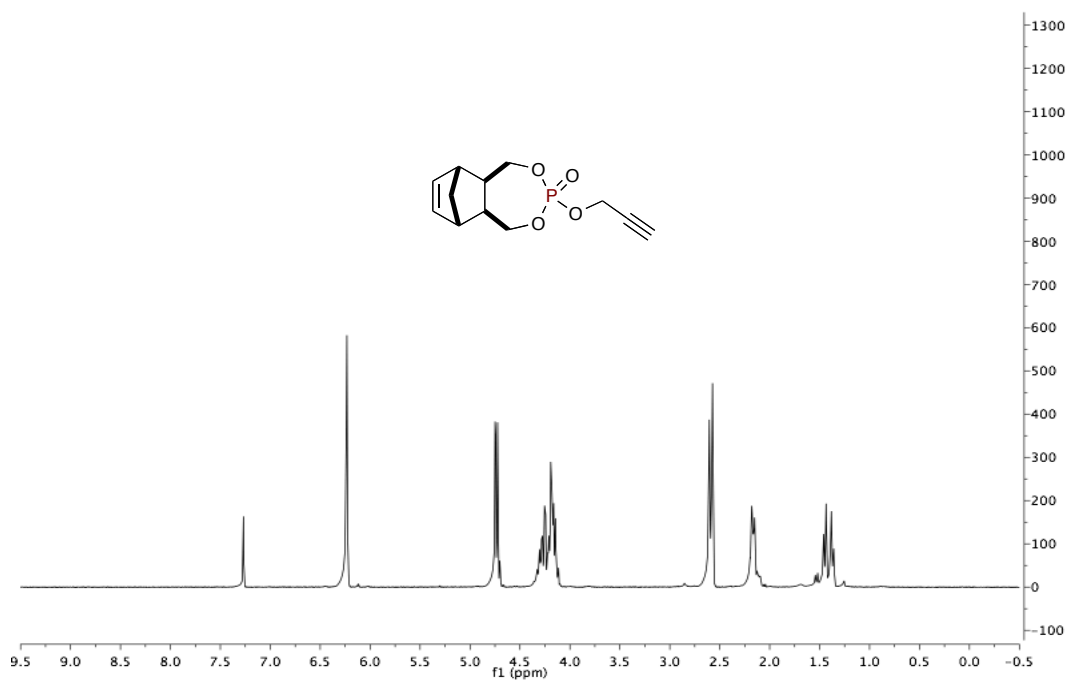
^1H NMR (400 MHz, CDCl_3): δ 8.37 (dd, $J = 8.1, 1.0$ Hz, 1H), 7.83 (dd, $J = 7.6, 1.5$ Hz, 1H), 7.56 (d, $J = 8.2$ Hz, 1H), 7.53-7.46 (m, 2H), 7.34 (dd, $J = 8.0, 7.6$ Hz, 1H),

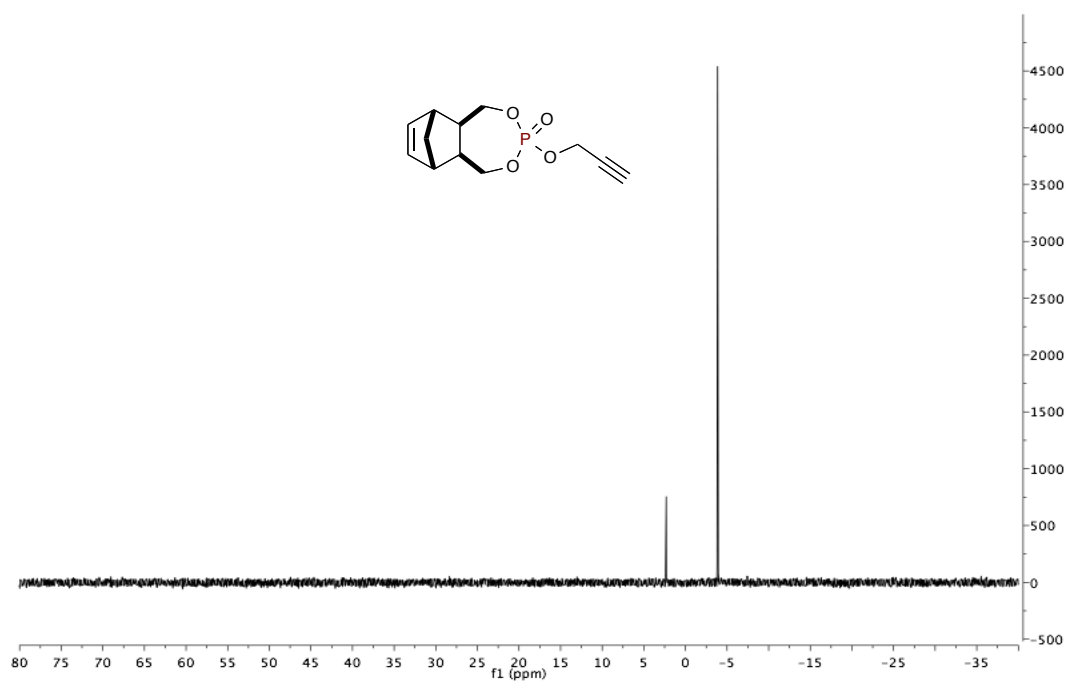
7.03 (d, $J = 7.4$ Hz, 1H), 6.92 (s, 1H), 4.50 (s, 2H), 4.02 (d, $J = 7.3$ Hz, 2H), 3.23 (q, $J = 7.1$ Hz, 2H), 1.73-1.65 (m, 5H), 1.44-1.40 (m, 2H), 1.16-1.11 (m, 2H), 1.14 (t, $J = 7.1$ Hz, 3H), 0.87-0.80 (m, 2H); ^{13}C NMR (126 MHz, CDCl_3): δ 146.8, 145.0, 134.8, 130.6, 128.3, 125.8, 125.5, 125.4, 123.9, 123.8, 122.6, 118.5, 56.2, 49.2, 48.0, 38.7, 30.3, 26.1, 25.5, 12.2; HRMS calculated for $\text{C}_{22}\text{H}_{29}\text{N}_4$ ($\text{M}+\text{H}$) $^+$ 349.2392; found 349.2386 (TOF MS ES+).

5.3 Spectra for Chapter 2.1

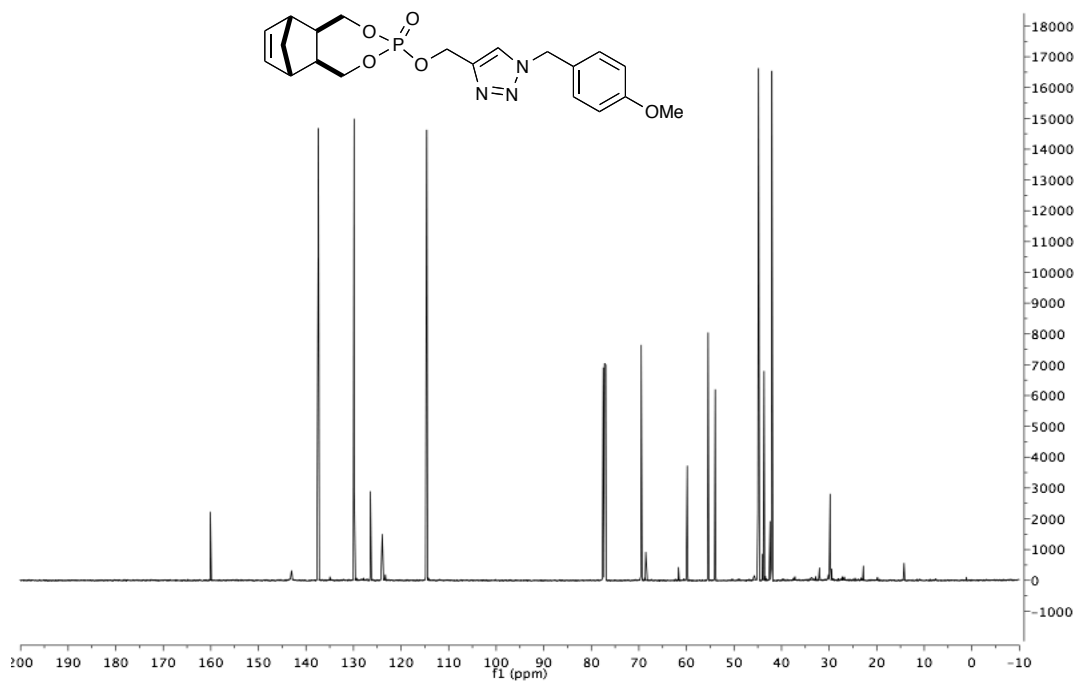
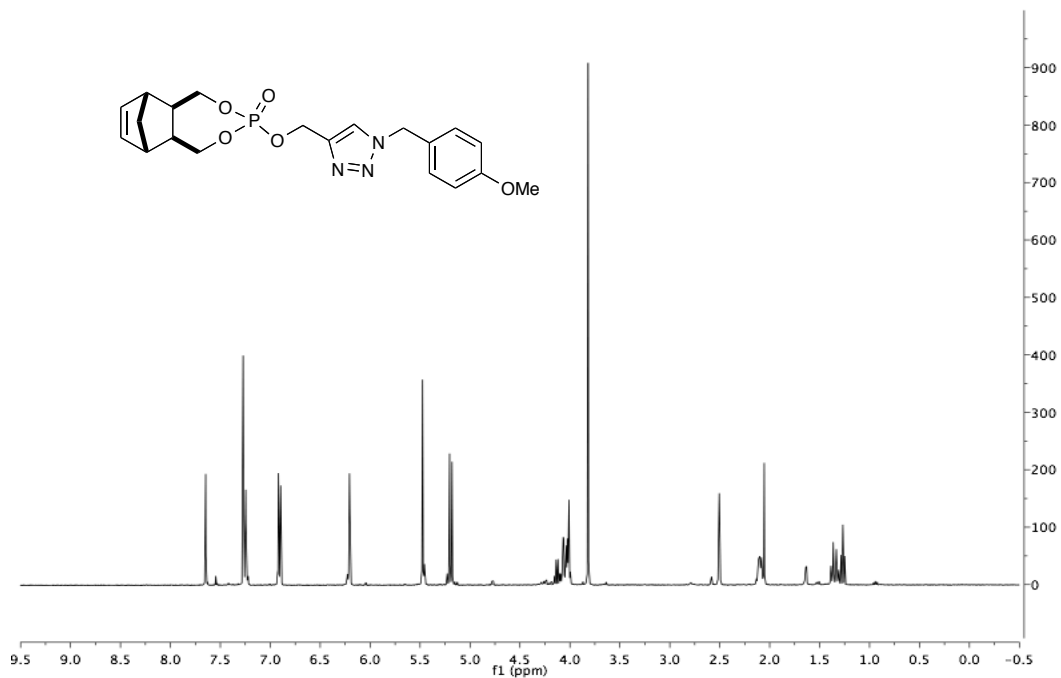
(5a*R*,6*R*,9*S*,9a*S*)-3-(prop-2-yn-1-yloxy)-1,5,5a,6,9,9a-hexahydro-

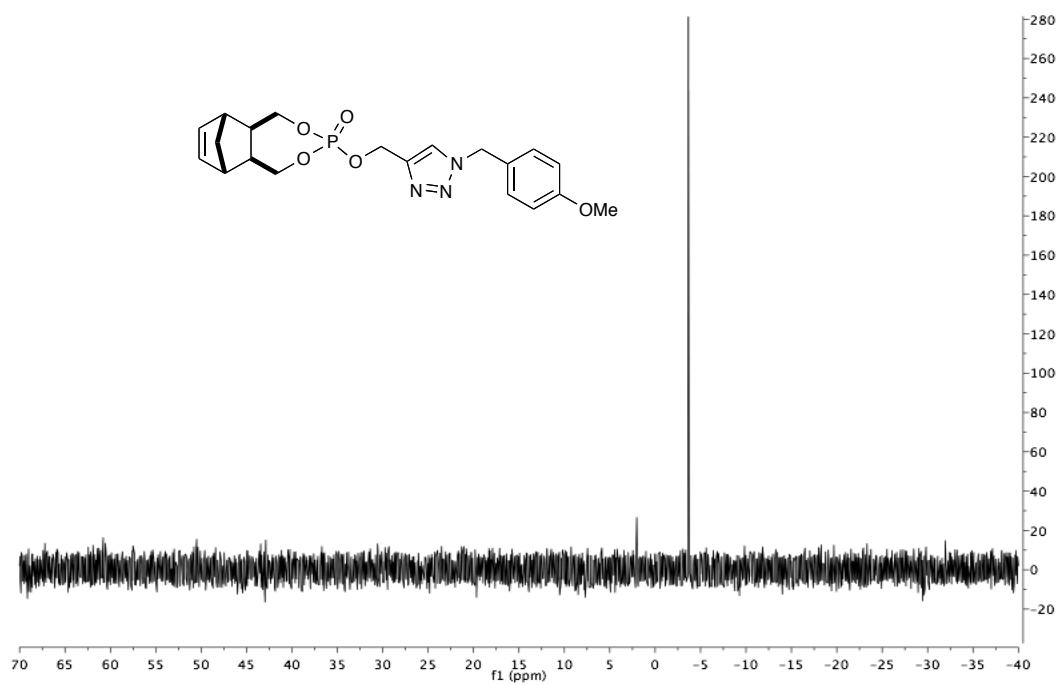
6,9methanobenzo[*e*][1,3,2]-dioxaphosphine-3-oxide (2.1.4)



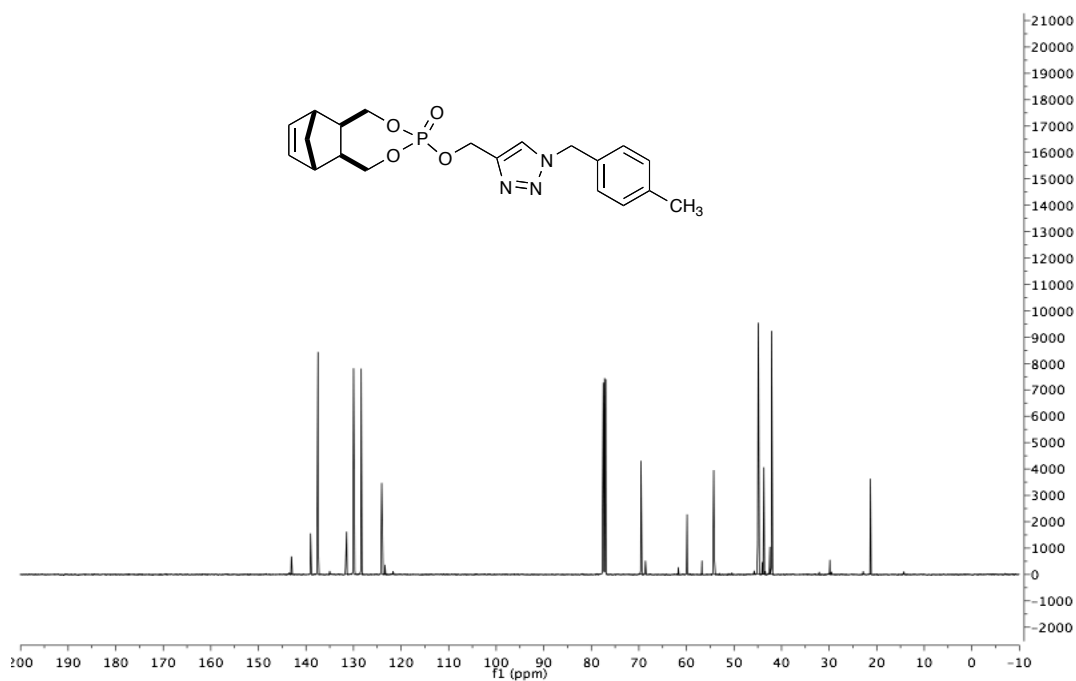
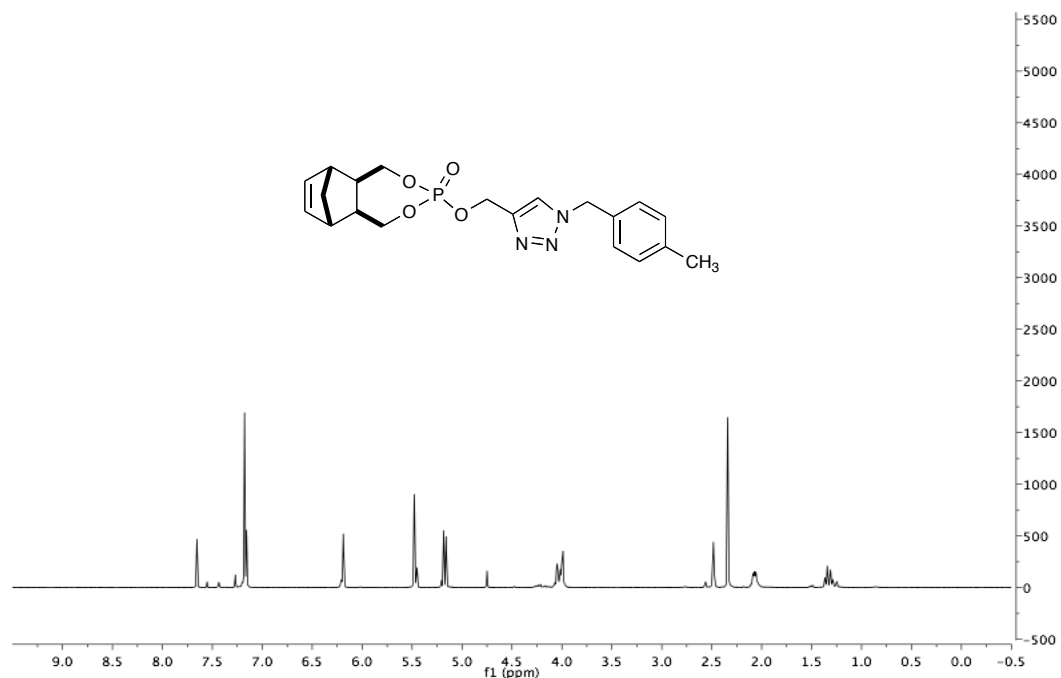


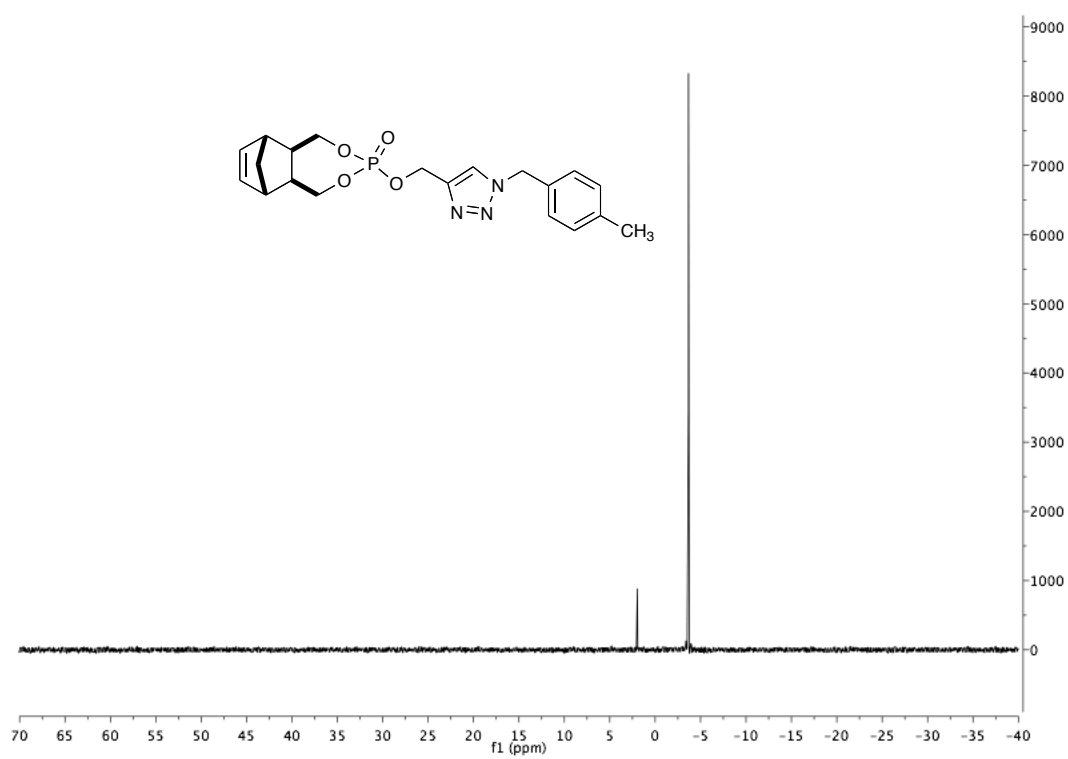
(5a*R*,6*R*,9*S*,9a*S*)-3-((1-(4-Methoxybenzyl)-1*H*-1,2,3-triazol-4-yl)methoxy)-1,5,5a,6,9, 9a - hexahydro-6,9-methanobenzo[*e*][1,3,2]dioxaphosphepine 3-oxide (2.1.5a).



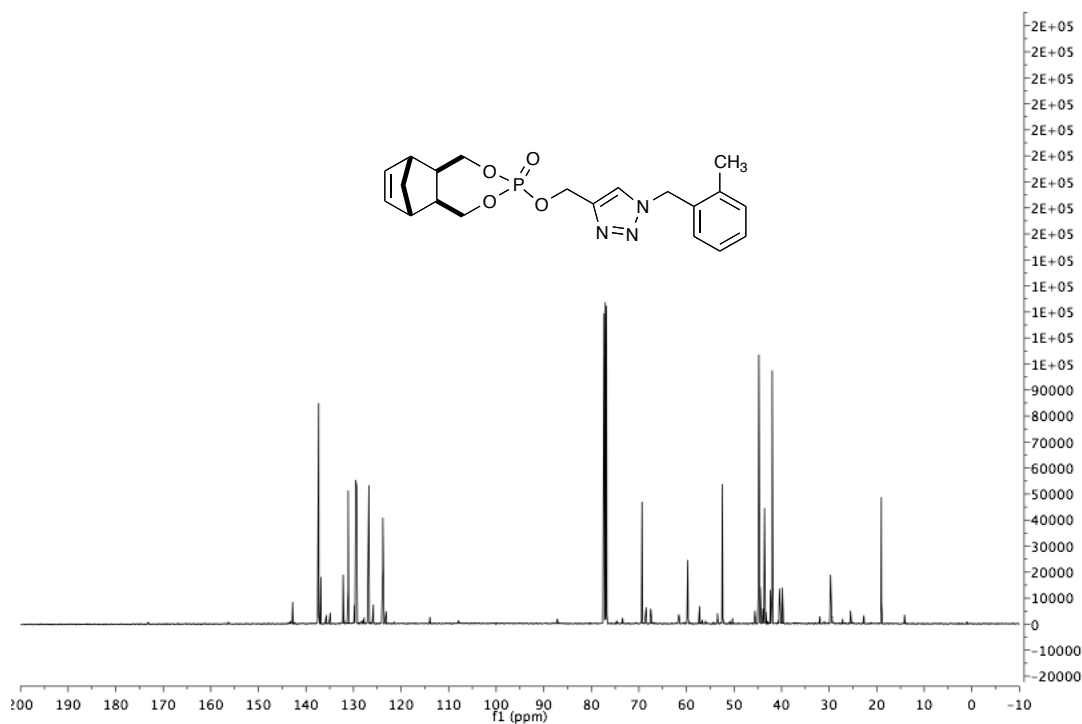
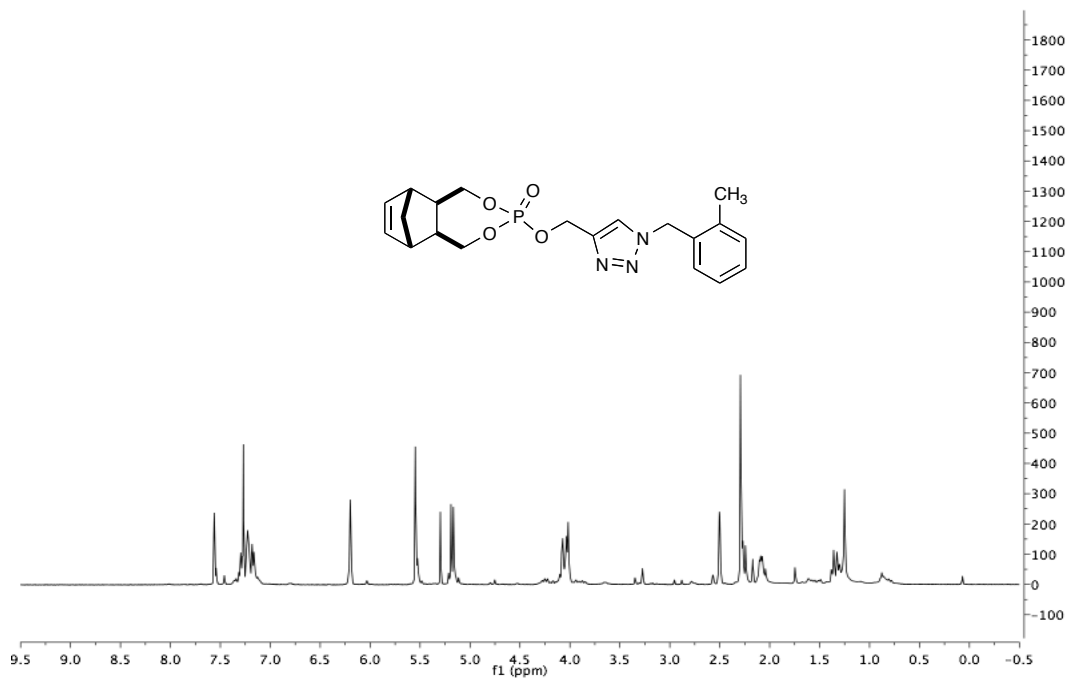


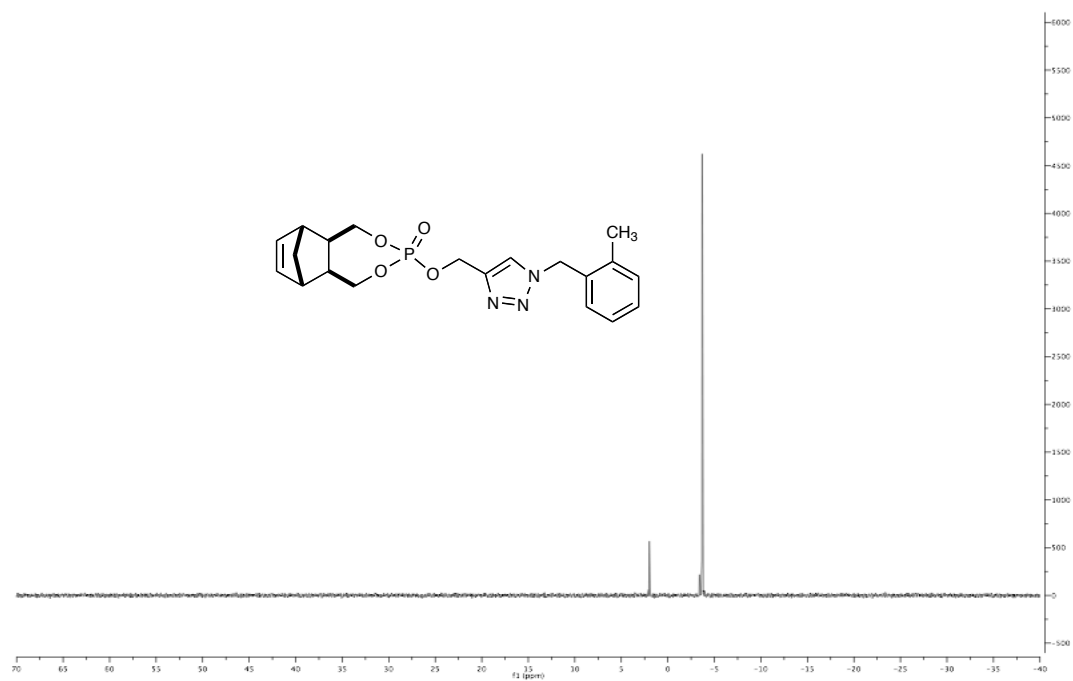
(5a*R*,6*R*,9*S*,9a*S*)-3-((1-(4-Methylbenzyl)-1*H*-1,2,3-triazol-4-yl)methoxy)-1,5,5a,6,9,9a-hexahydro-6,9-methanobenzo[*e*][1,3,2]dioxaphosphepine 3-oxide (2.1.5b).



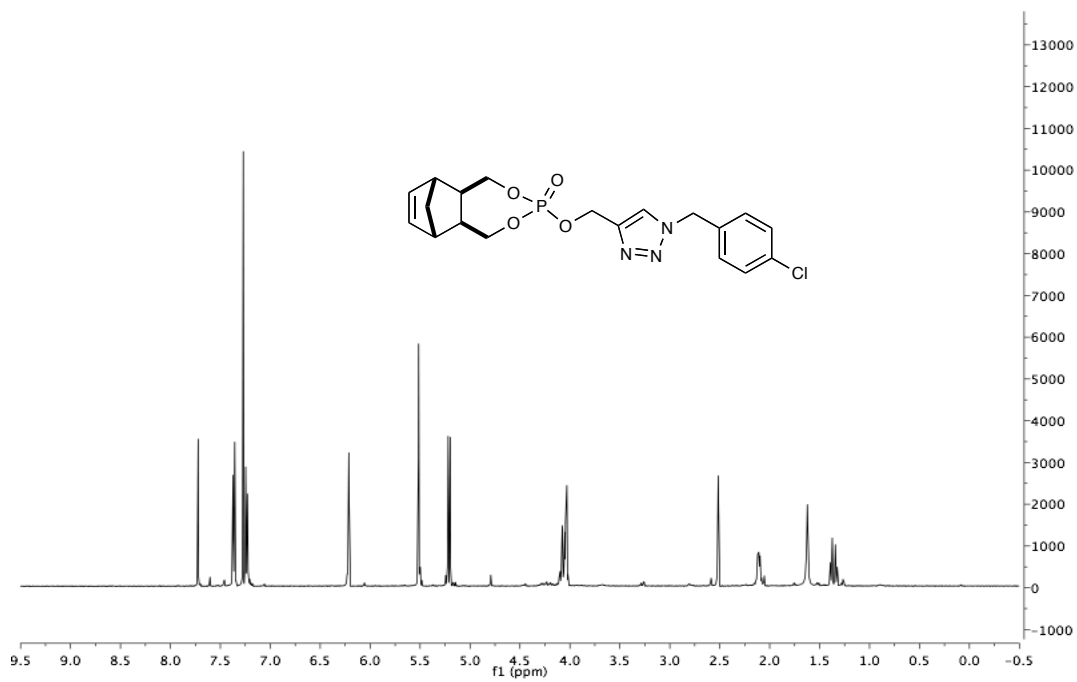
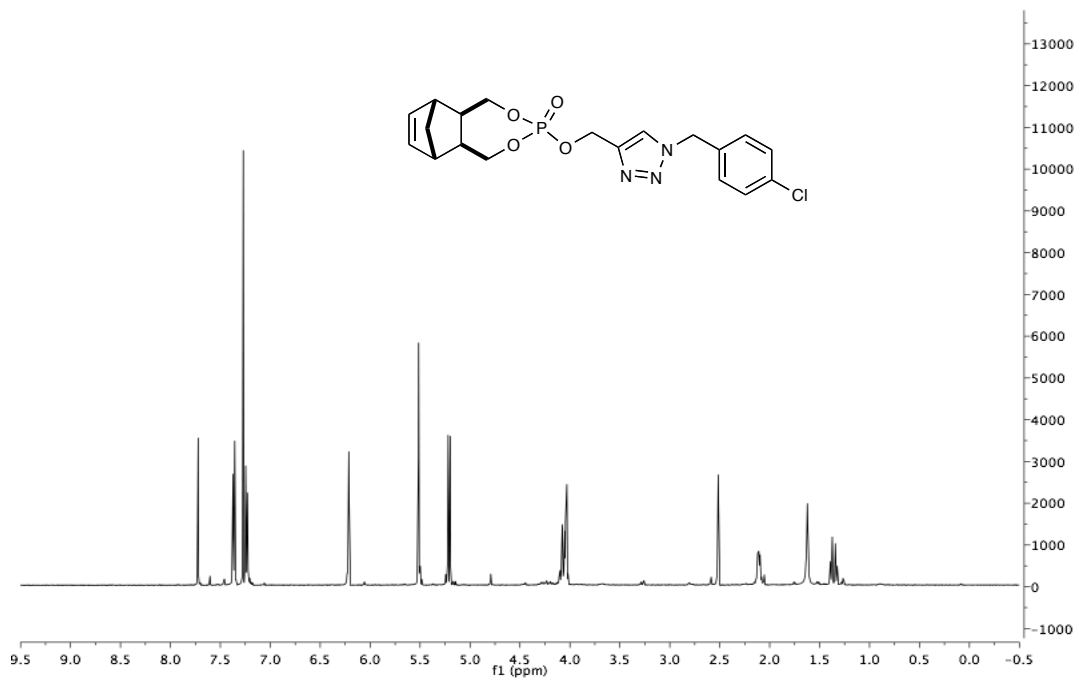


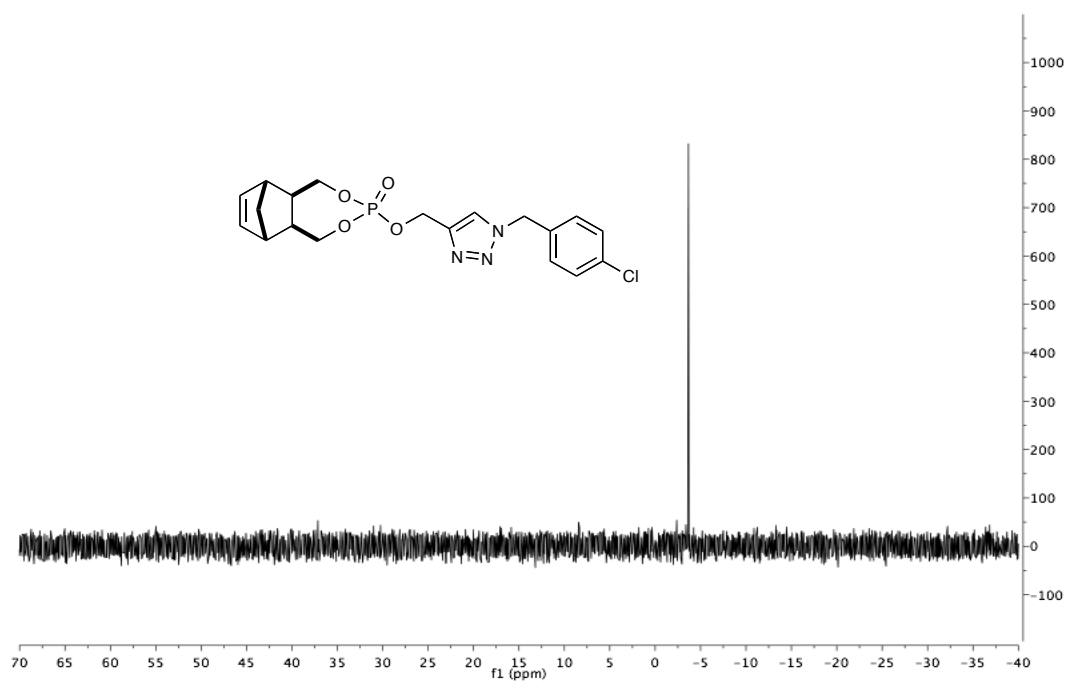
(5a*R*,6*R*,9*S*,9a*S*)-3-((1-(2-Methylbenzyl)-1*H*-1,2,3-triazol-4-yl)methoxy)-1,5,5a,6,9,9a-hexahydro-6,9-methanobenzo[*e*][1,3,2]dioxaphosphepine 3-oxide (2.1.5c).



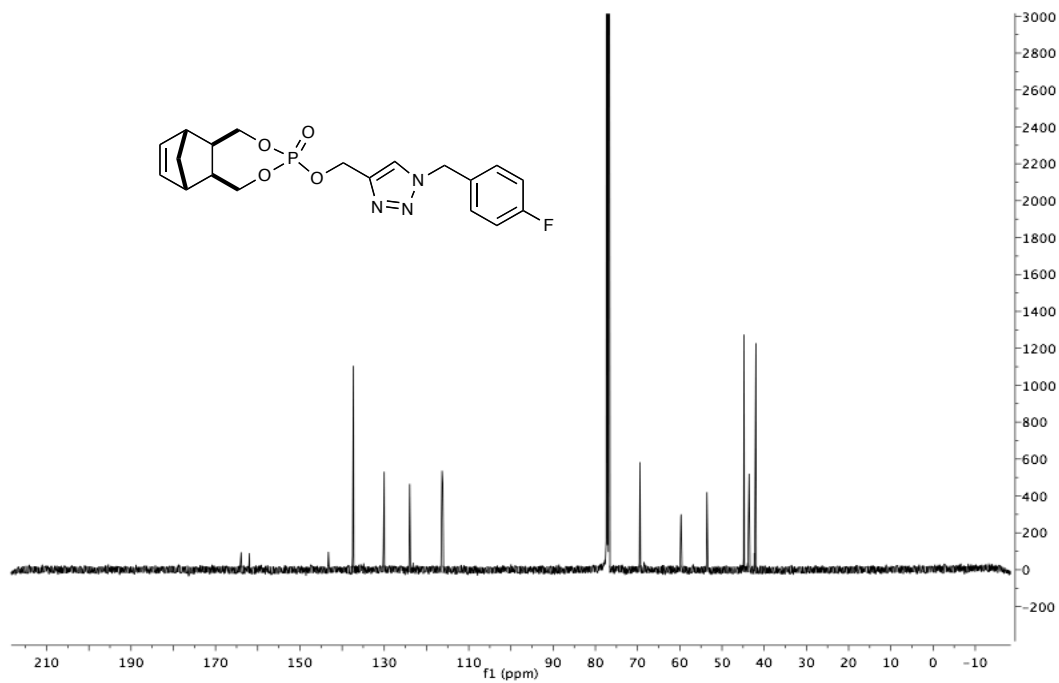
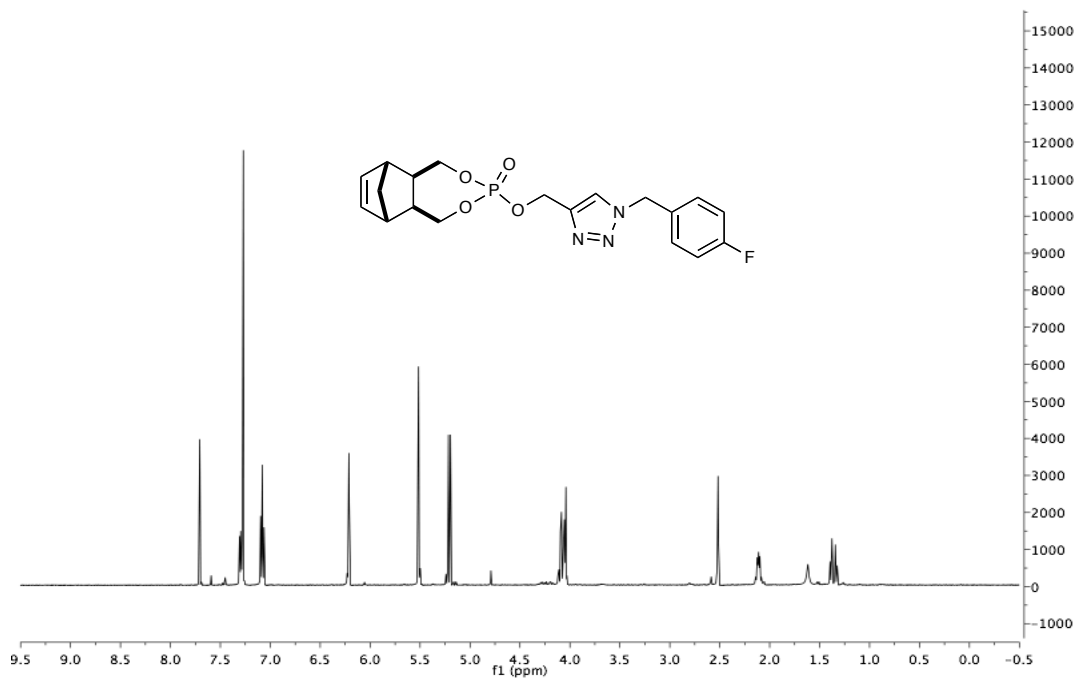


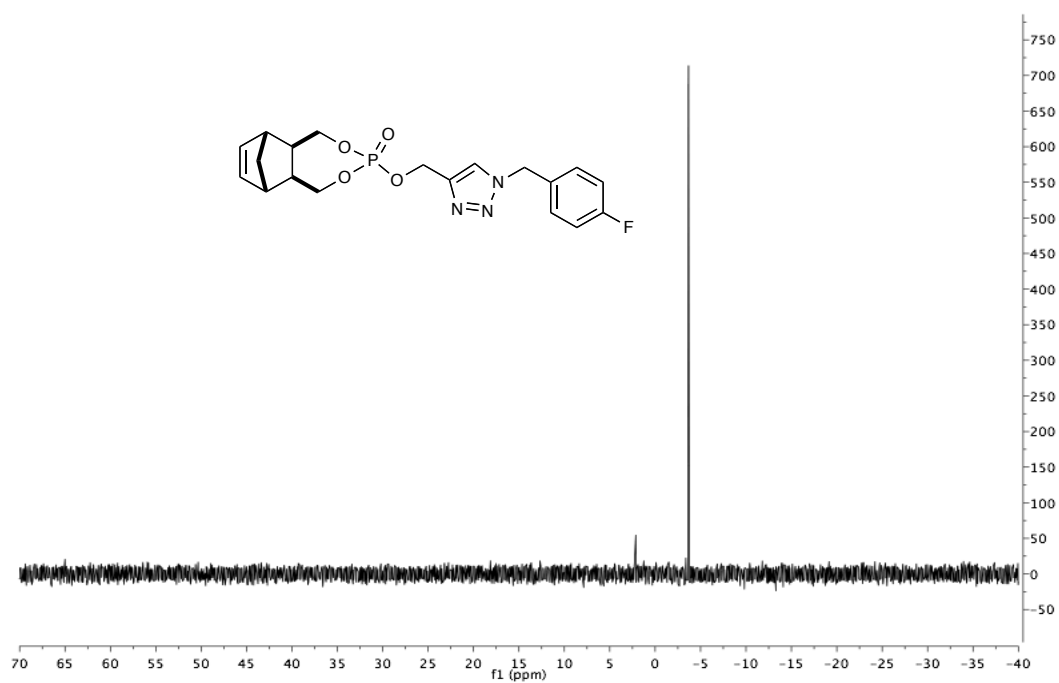
(5a*R*,6*R*,9*S*,9a*S*)-3-((1-(4-Chlorobenzyl)-1*H*-1,2,3-triazol-4-yl)methoxy)-1,5,5a,6,9,9a-hexahydro-6,9-methanobenzo[*e*][1,3,2]dioxaphosphepine 3-oxide (2.1.5d).



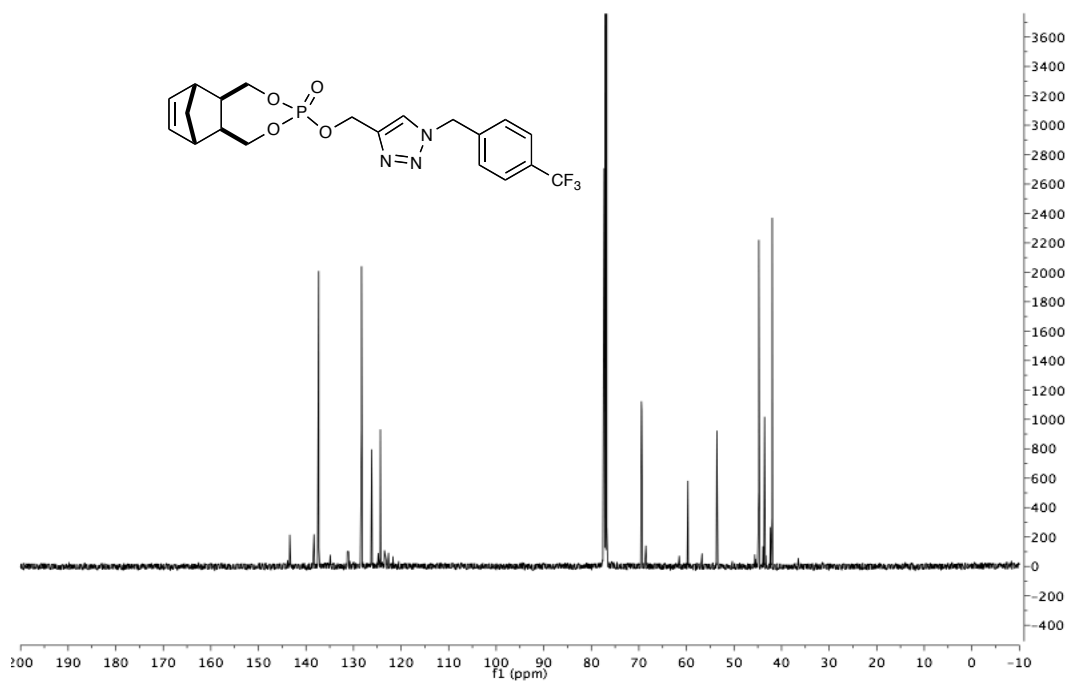
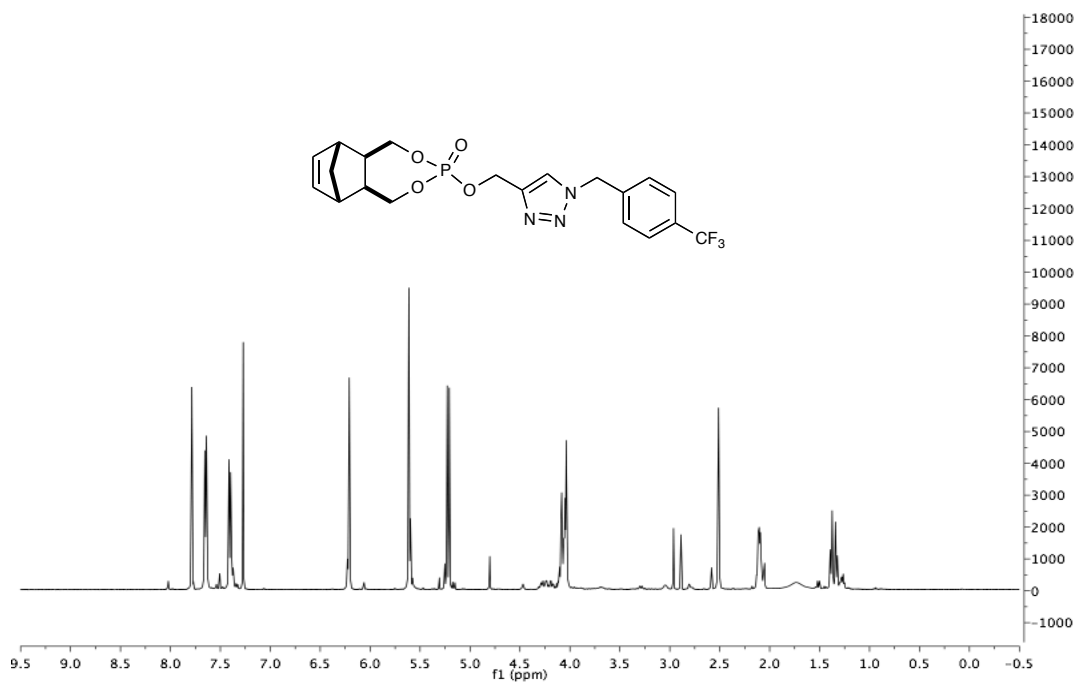


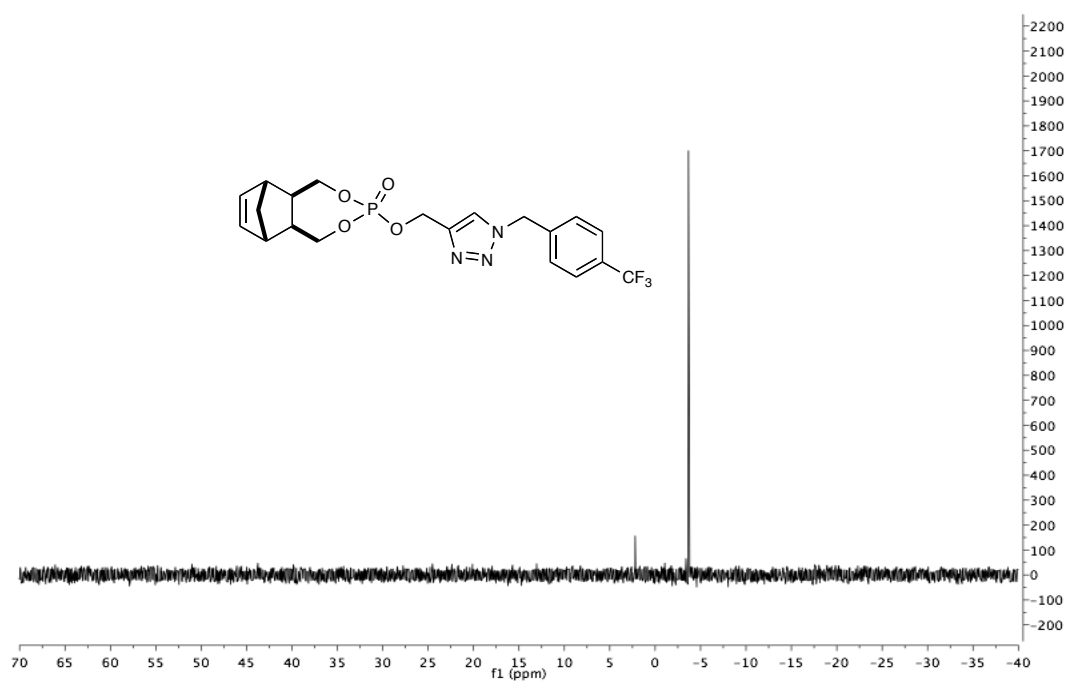
(5a*R*,6*R*,9*S*,9a*S*)-3-((1-(4-fluorobenzyl)-1*H*-1,2,3-triazol-4-yl)methoxy)-1,5,5a,6,9,9a-hexahydro-6,9-methanobenzo[*e*][1,3,2]dioxaphosphepine 3-oxide (2.1.5e)



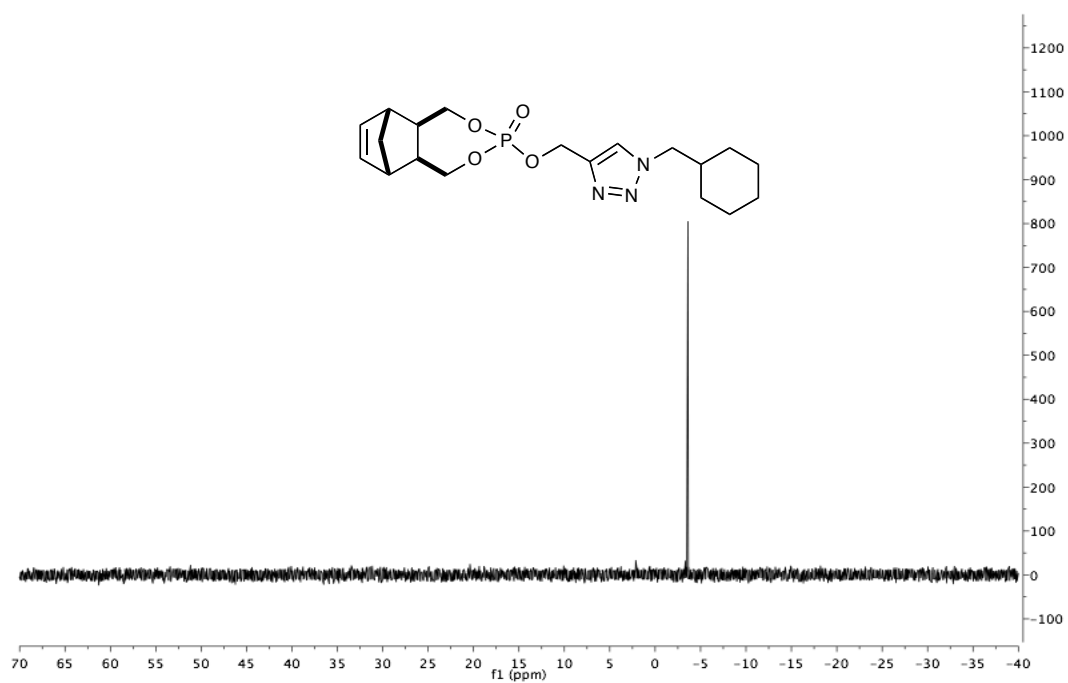


(5a*R*,6*R*,9*S*,9a*S*)-3-((1-(4-(trifluoromethyl)benzyl)-1*H*-1,2,3-triazol-4-yl)methoxy)-1,5,5a,6,9,9a-hexahydro-6,9-methanobenzo[*e*][1,3,2]dioxaphosphepine 3-oxide (2.1.5f)

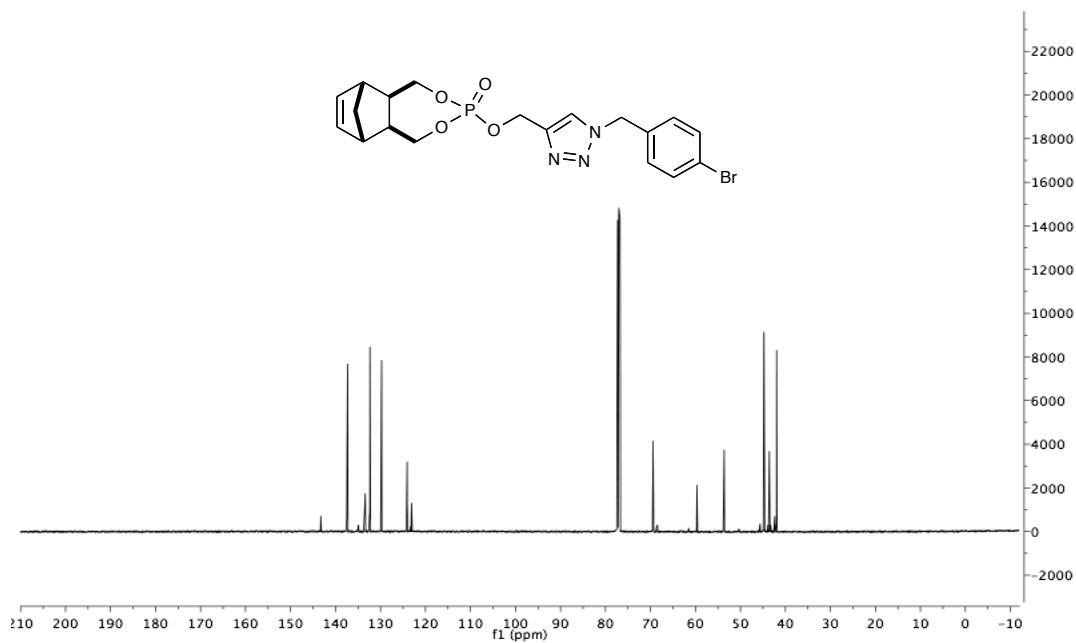
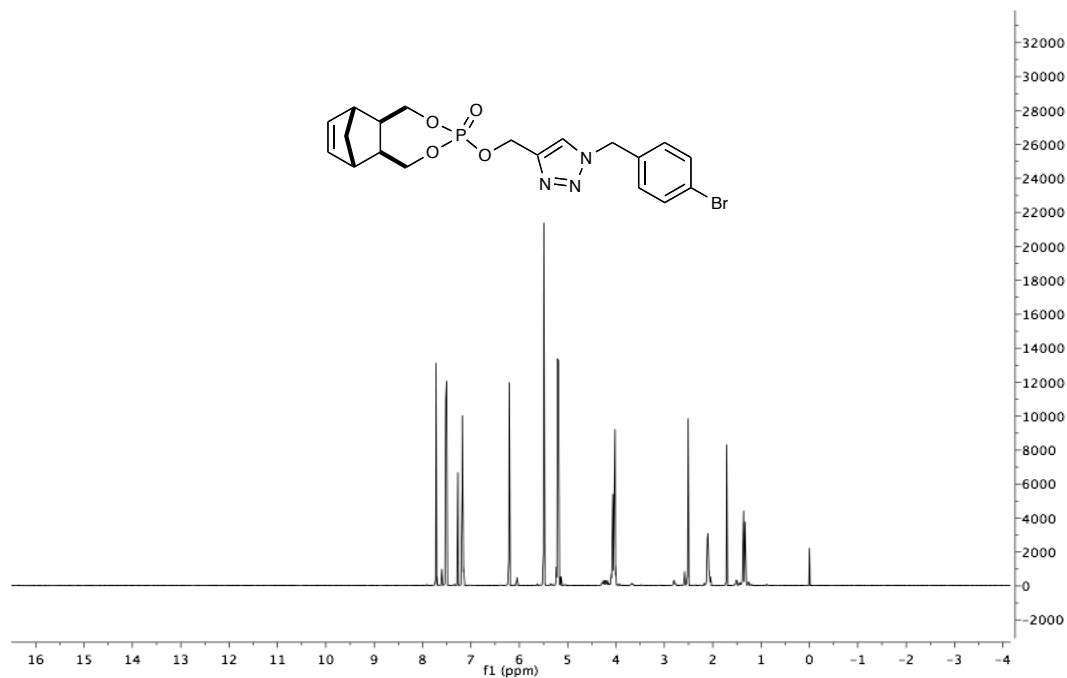


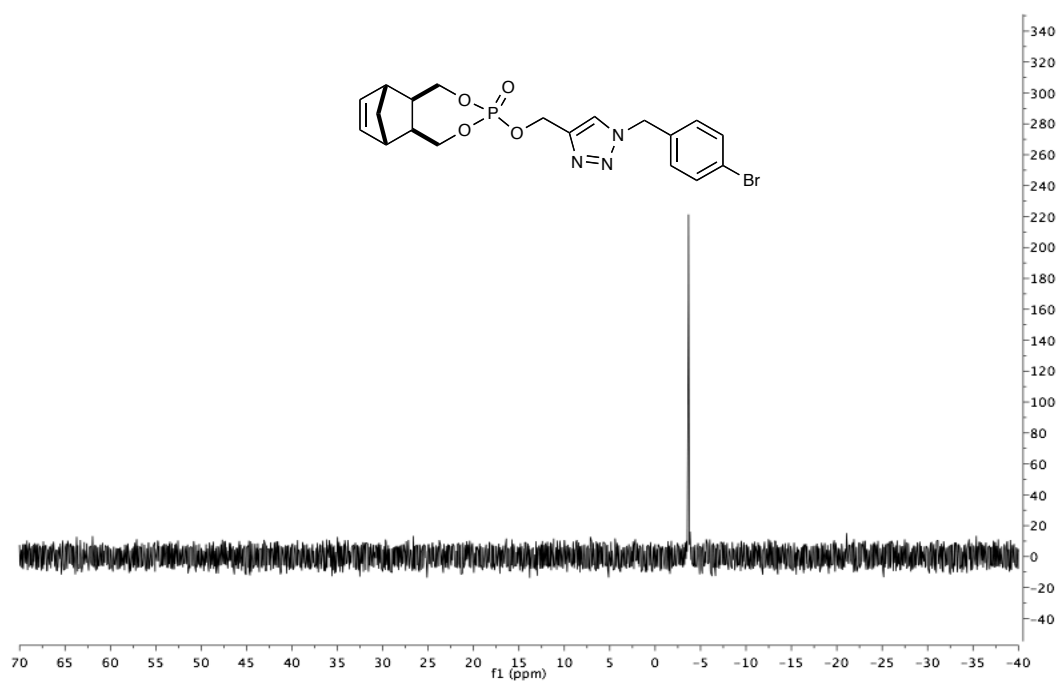


[illegible]

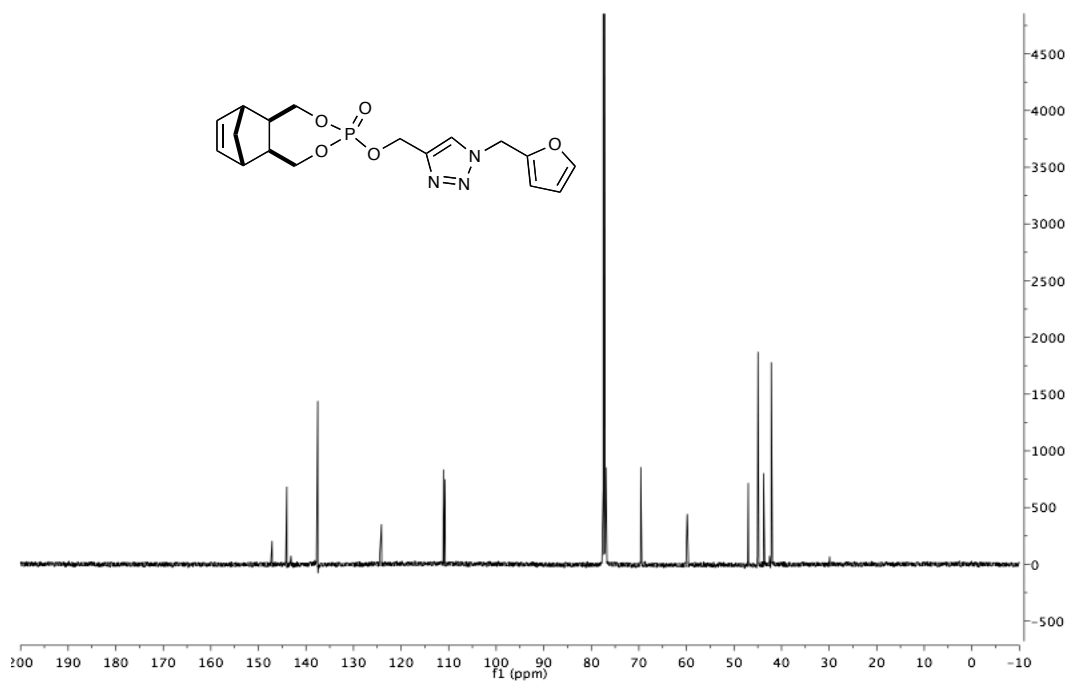
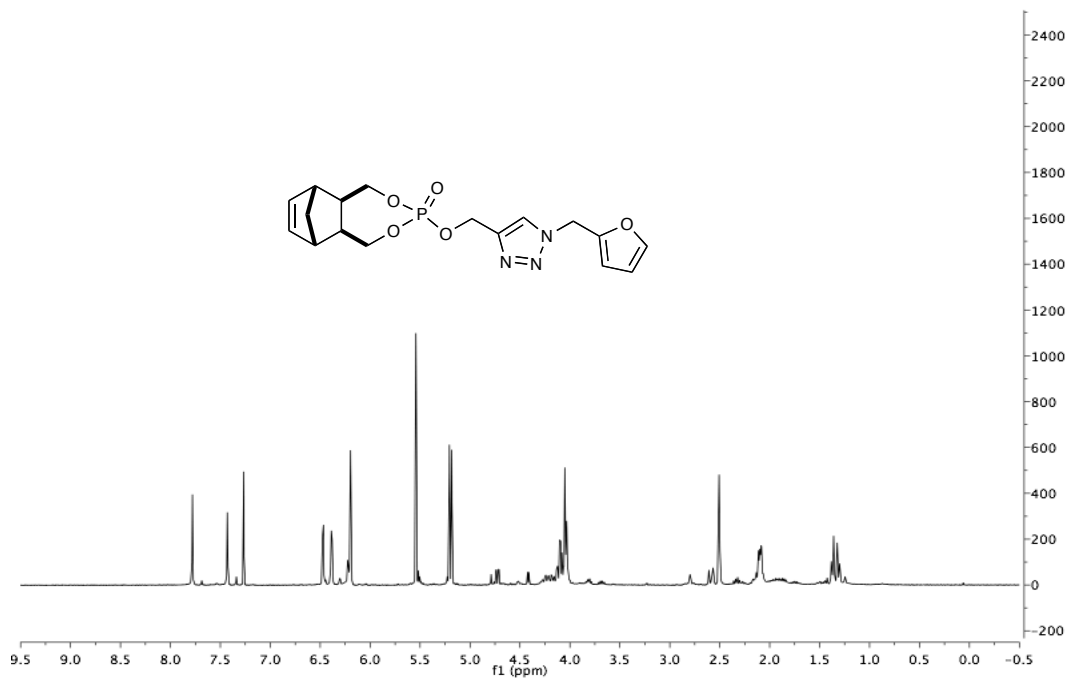


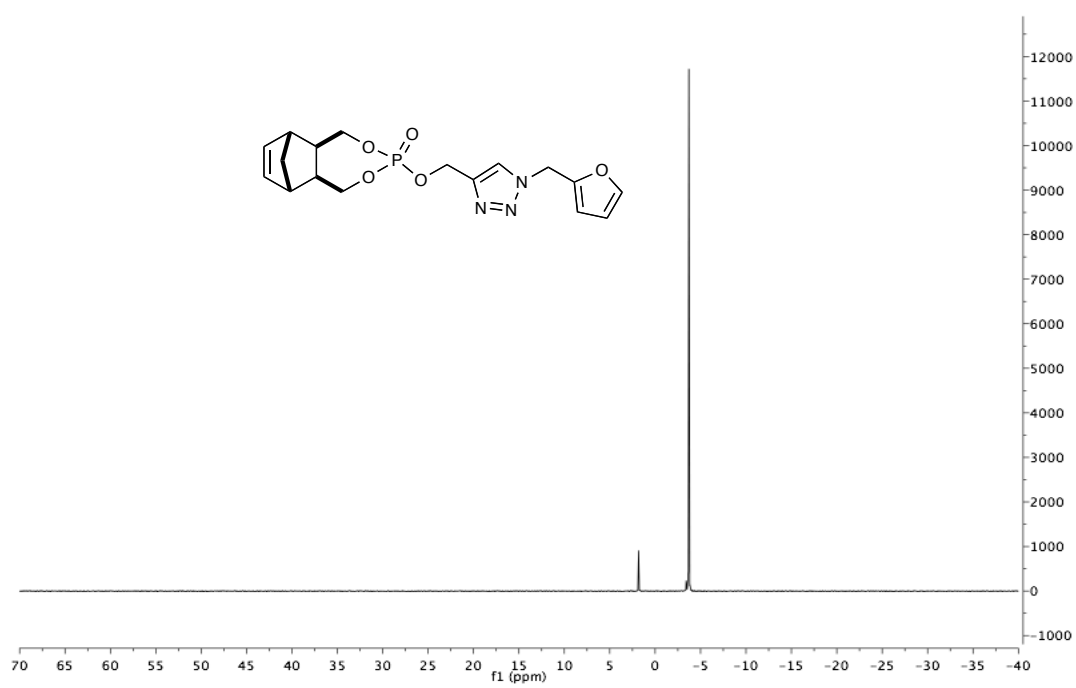
(5a*R*,6*R*,9*S*,9a*S*)-3-((1-(4-bromobenzyl)-1*H*-1,2,3-triazol-4-yl)methoxy)-1,5,5a,6,9,9a-hexahydro-6,9-methanobenzo[*e*][1,3,2]dioxaphosphepine 3-oxide (2.1.5h)



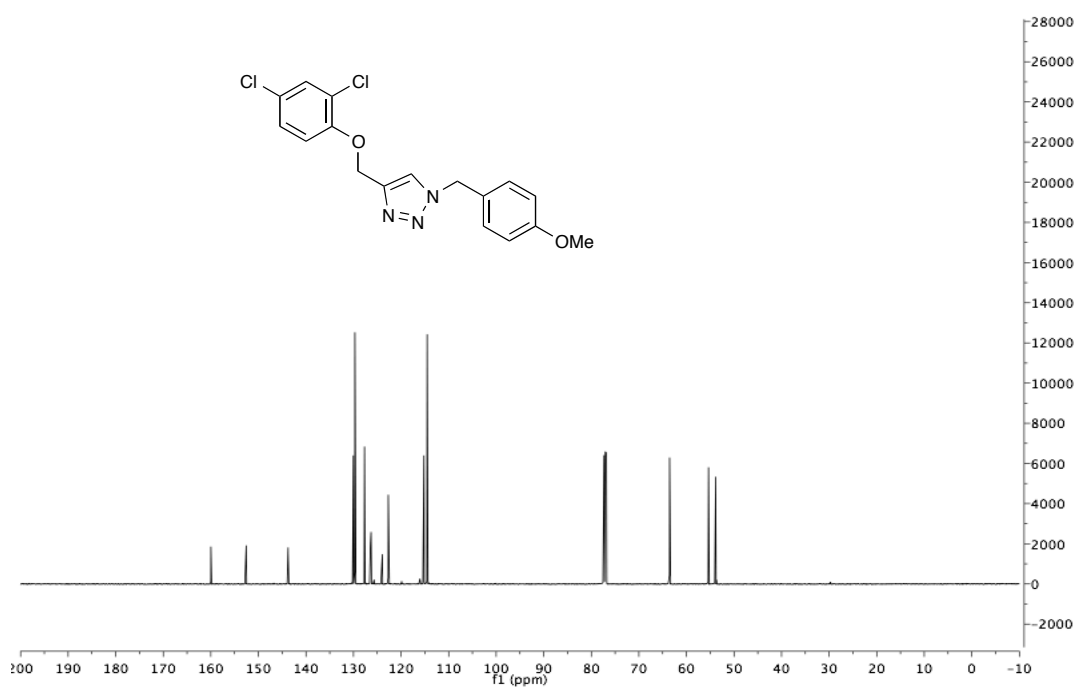
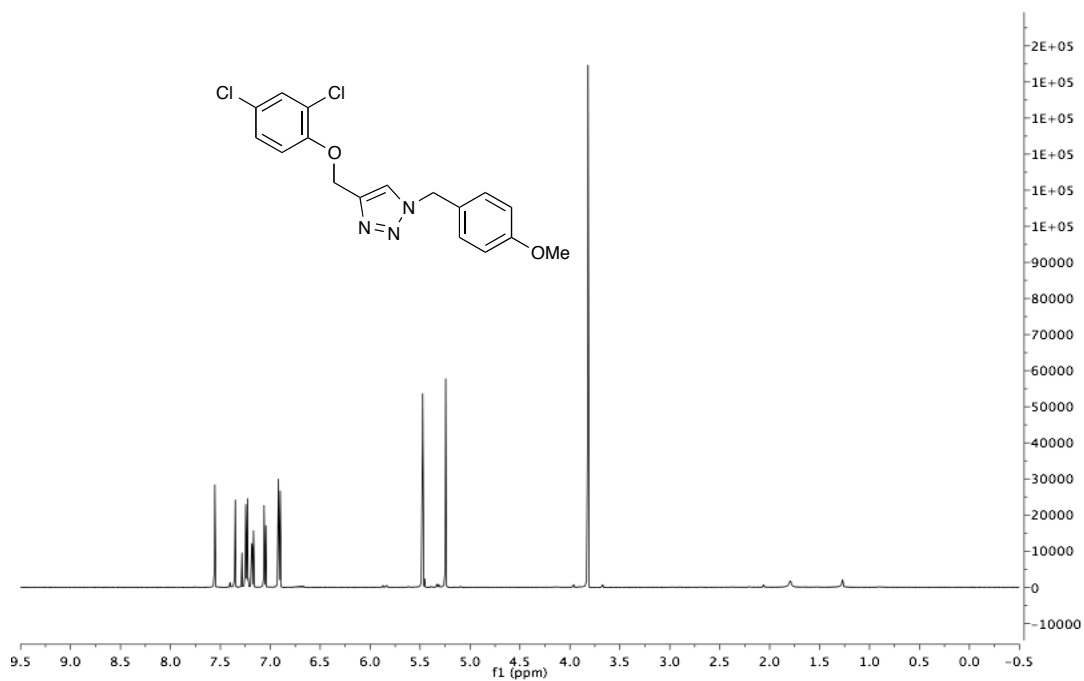


(5a*R*,6*R*,9*S*,9a*S*)-3-((1-(Furan-2-ylmethyl)-1*H*-1,2,3-triazol-4-yl)methoxy)-1,5,5a,6,9,9a-hexahydro-6,9-methanobenzo[*e*][1,3,2]dioxaphosphepine 3-oxide (2.1.5i).

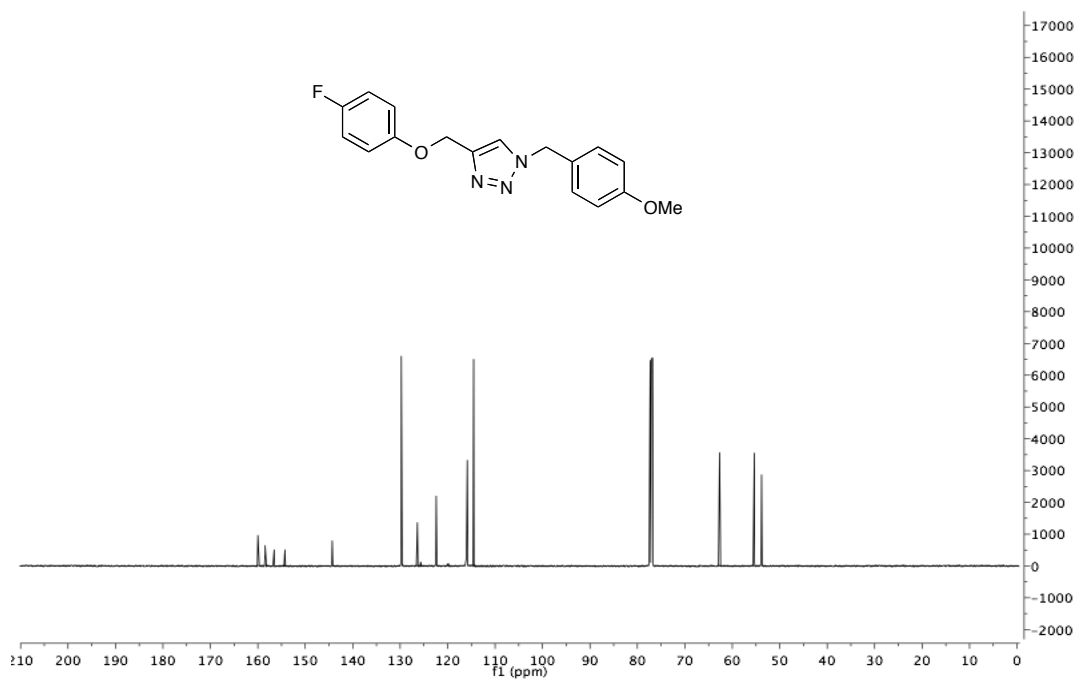
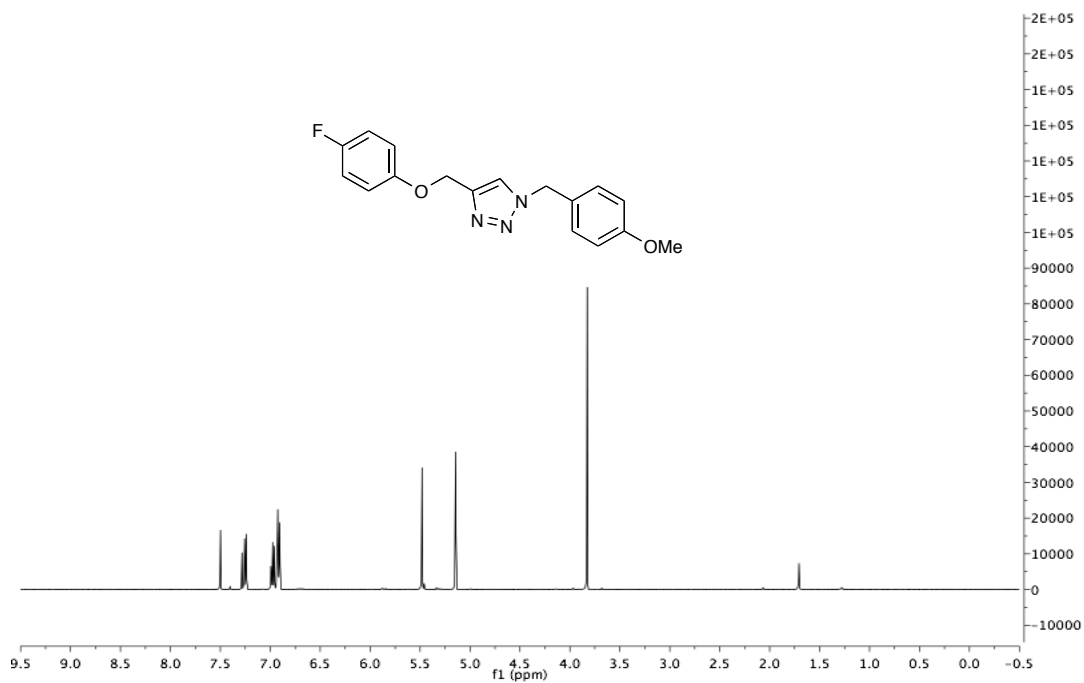




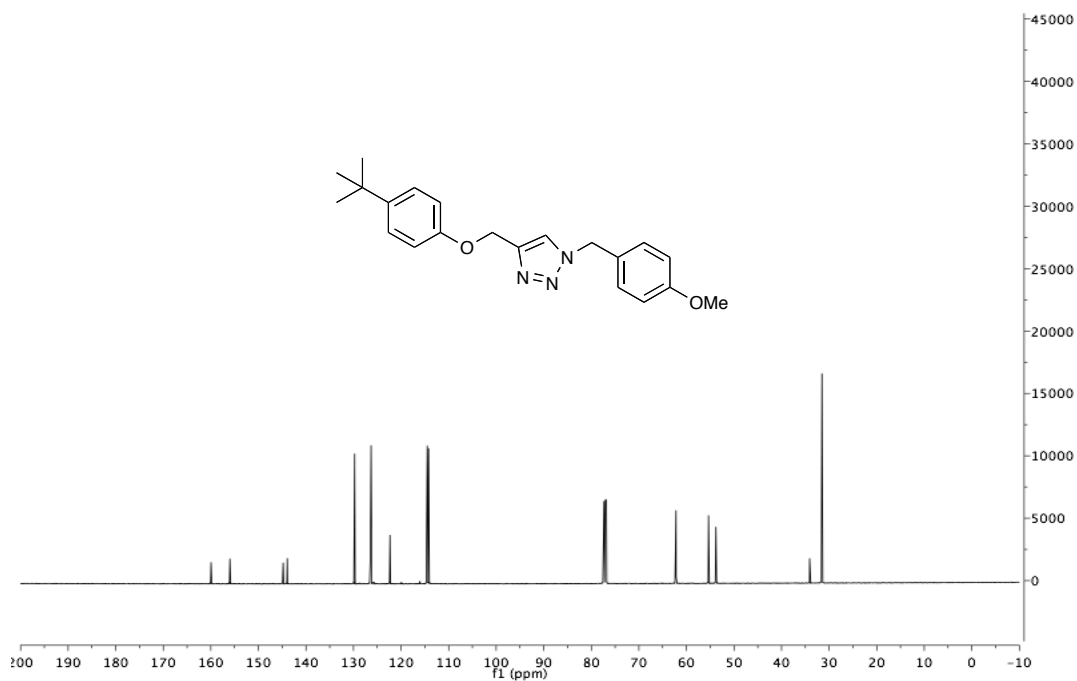
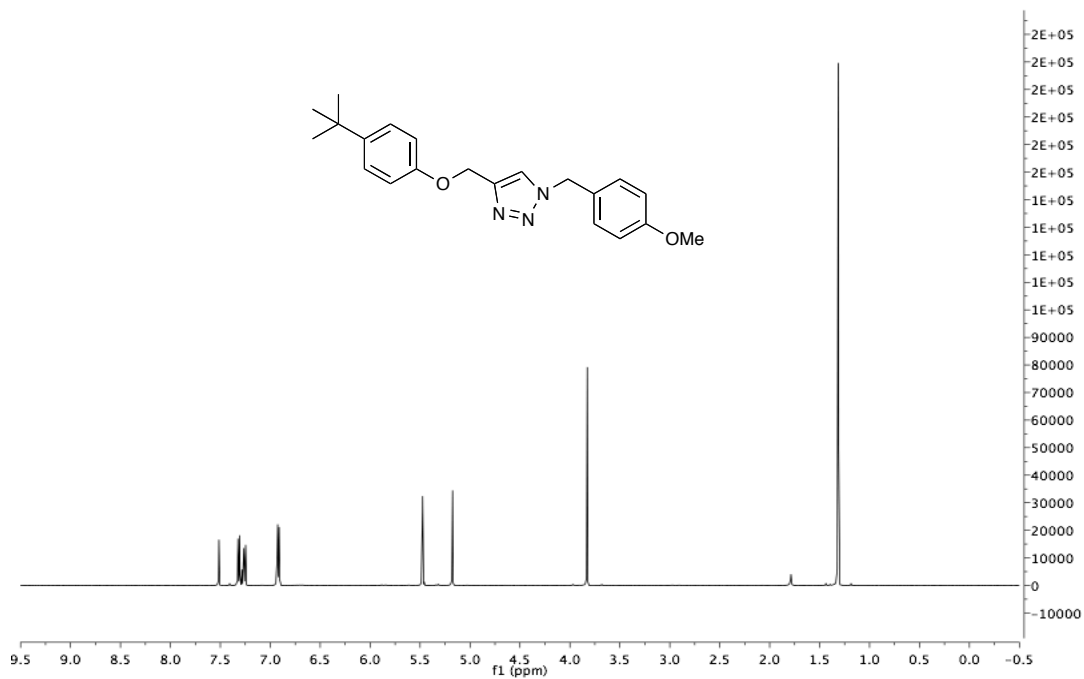
4-((2,4-Dichlorophenoxy)methyl)-1-(4-methoxybenzyl)-1H-1,2,3-triazole (2.1.7a).



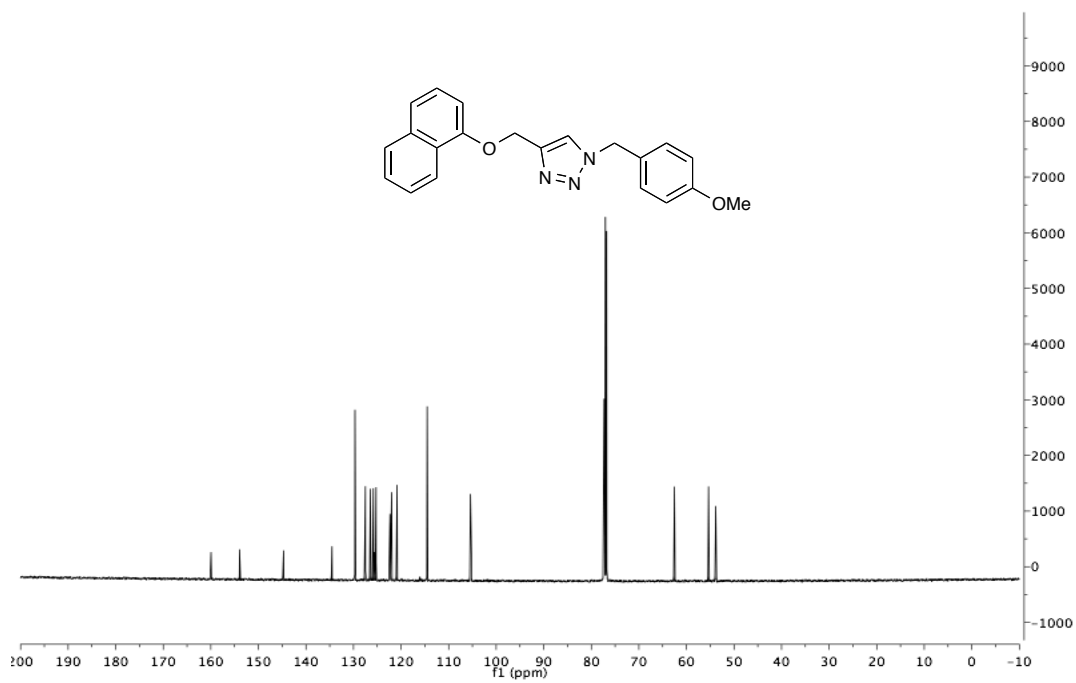
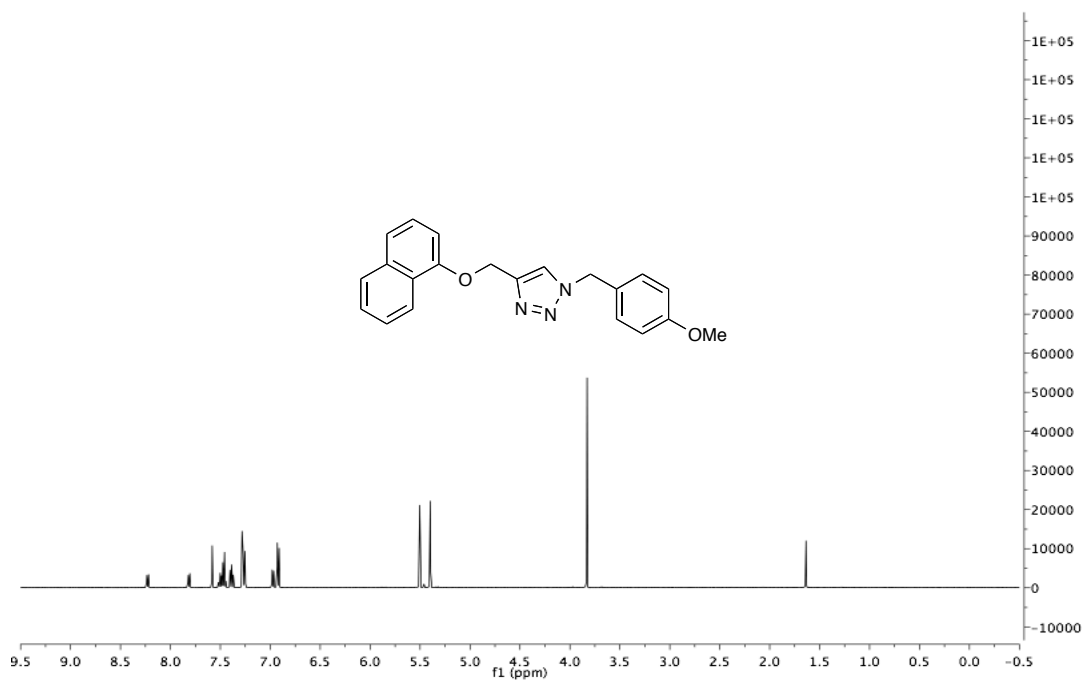
4-((4-Fluorophenoxy)methyl)-1-(4-methoxybenzyl)-1H-1,2,3-triazole (2.1.7b).



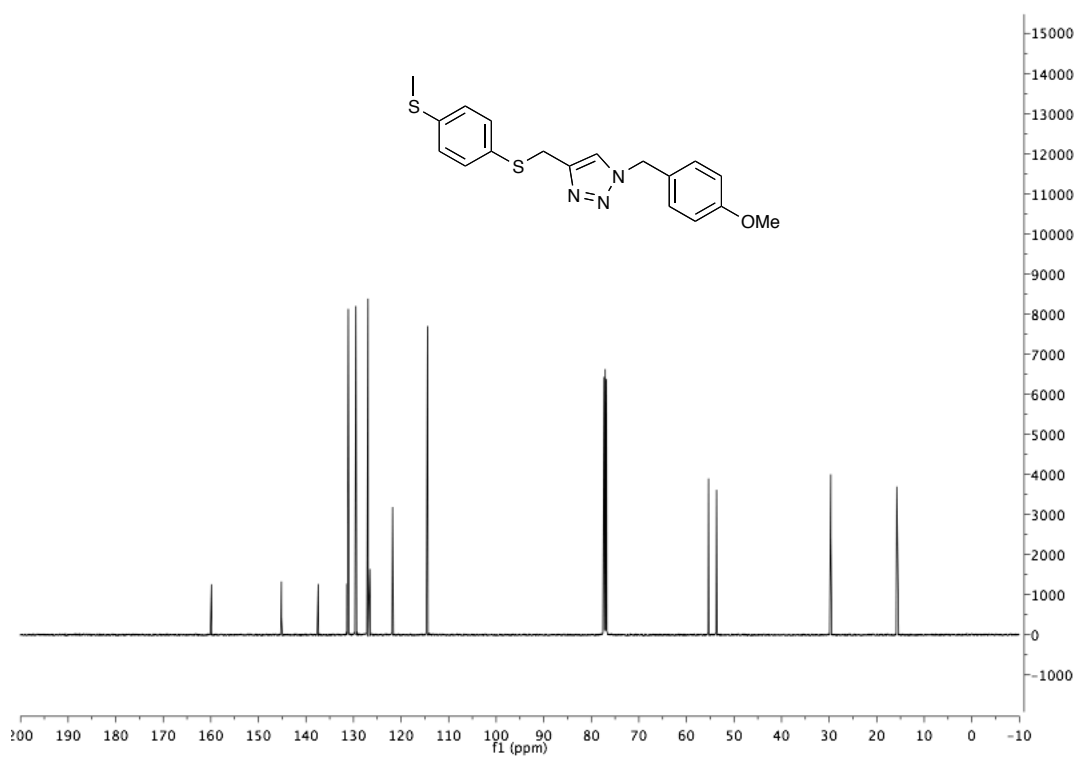
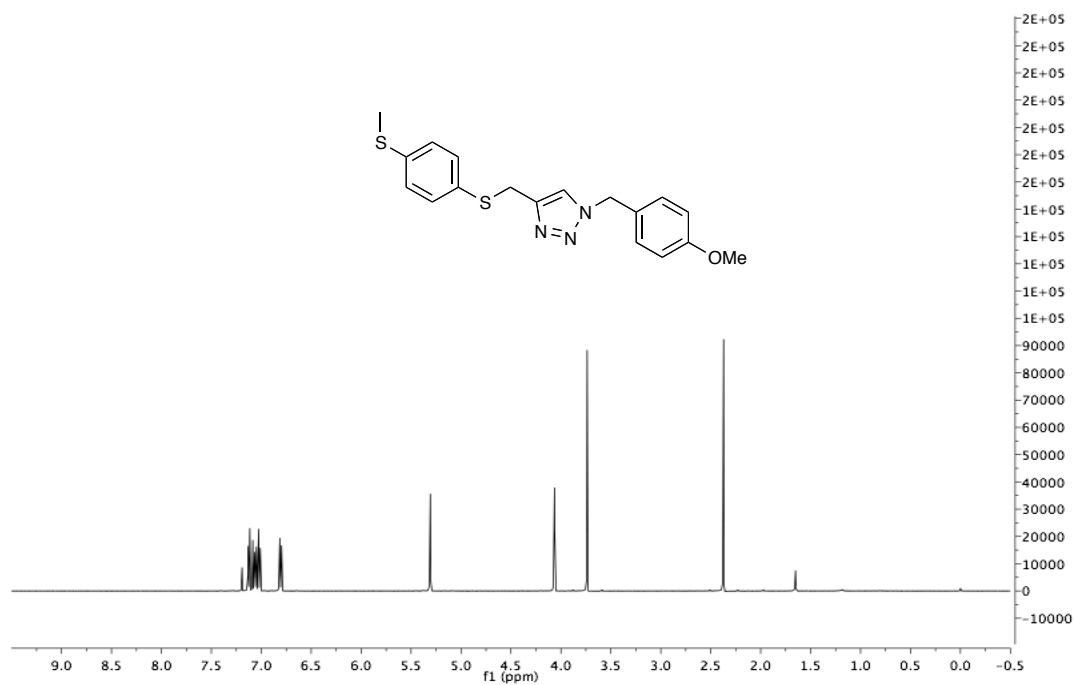
4-((4-(tert-butyl)phenoxy)methyl)-1-(4-methoxybenzyl)-1H-1,2,3-triazole (2.1.7c).



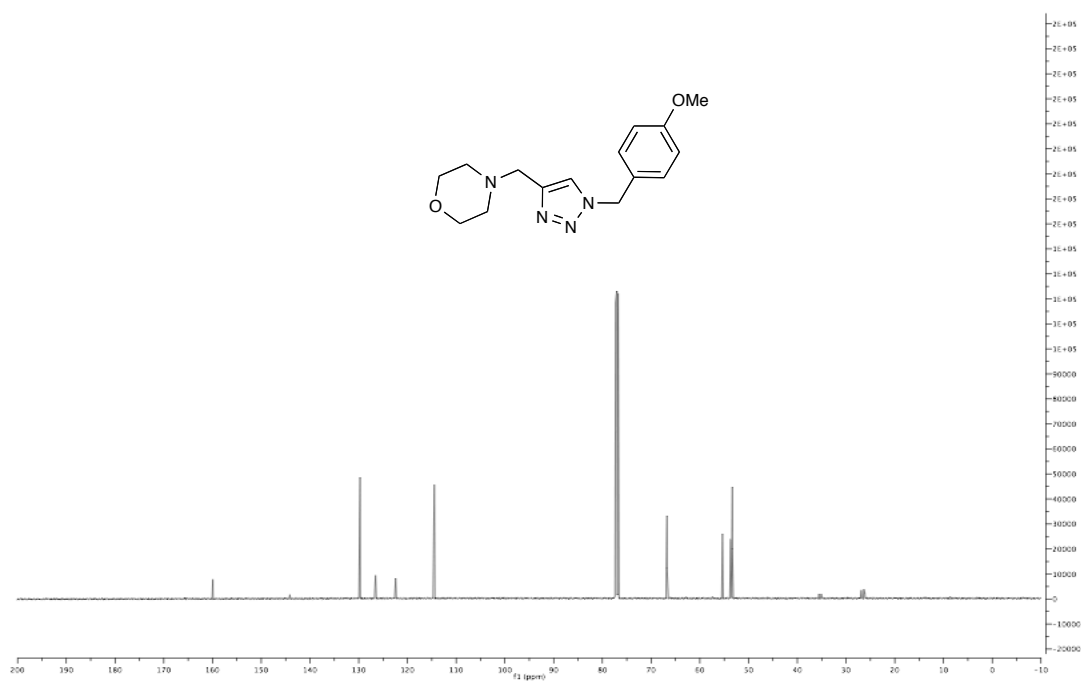
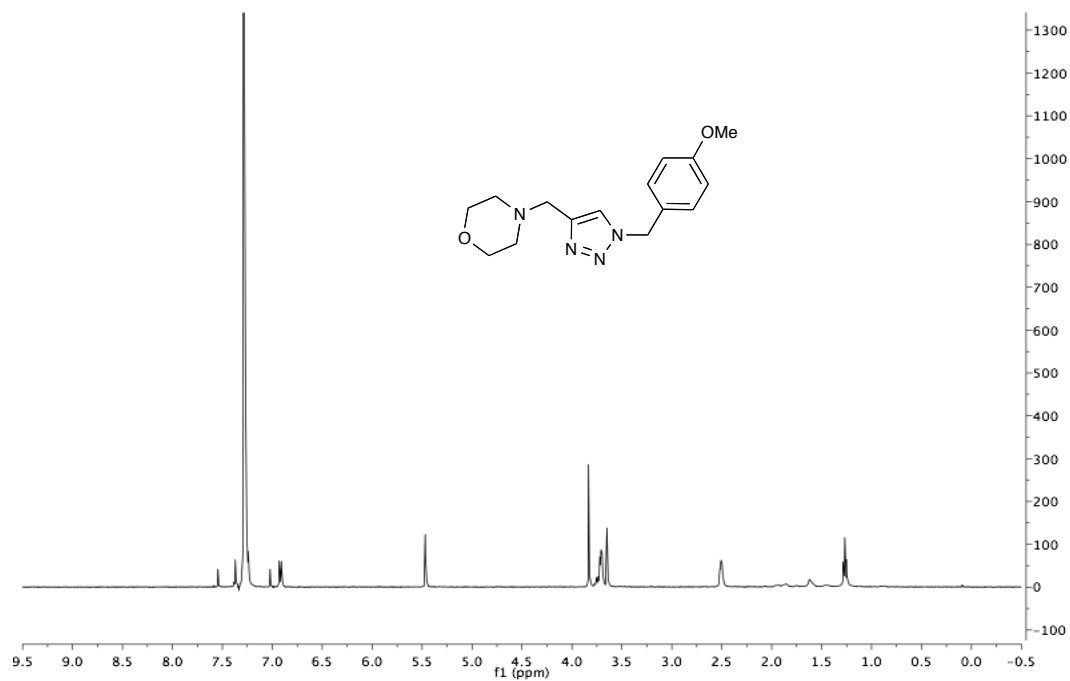
1-(4-Methoxybenzyl)-4-((naphthalen-1-yloxy)methyl)-1*H*-1,2,3-triazole (2.1.7d).



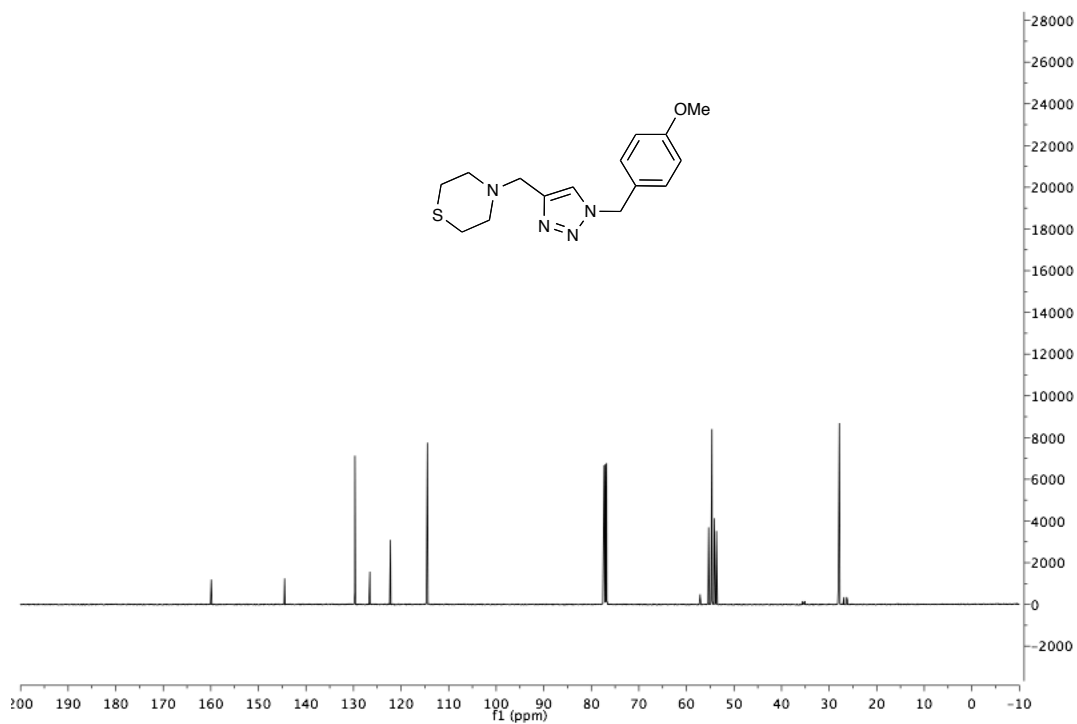
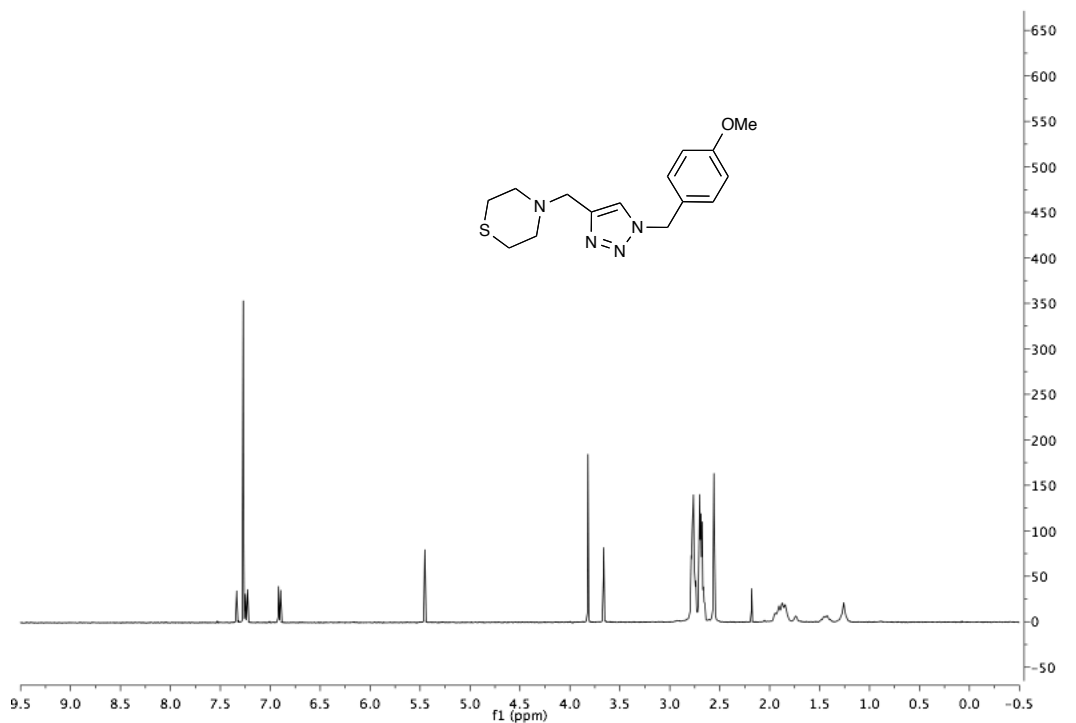
1-(4-Methoxybenzyl)-4-(((4-(methylthio)phenyl)thio)methyl)-1H-1,2,3-triazole (2.1.7e).



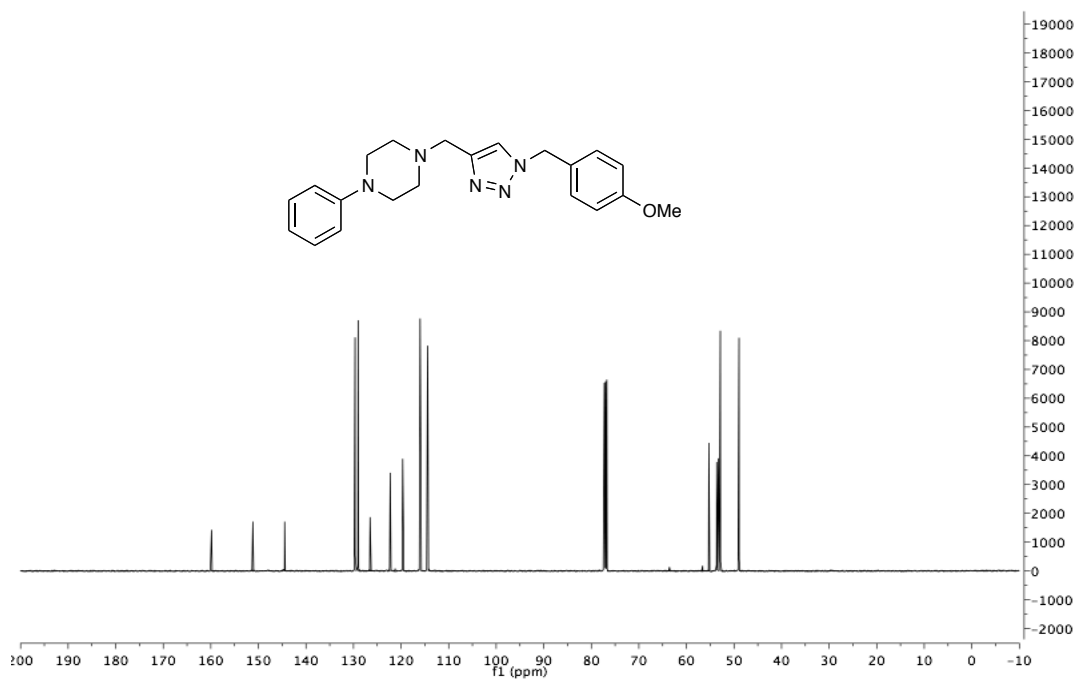
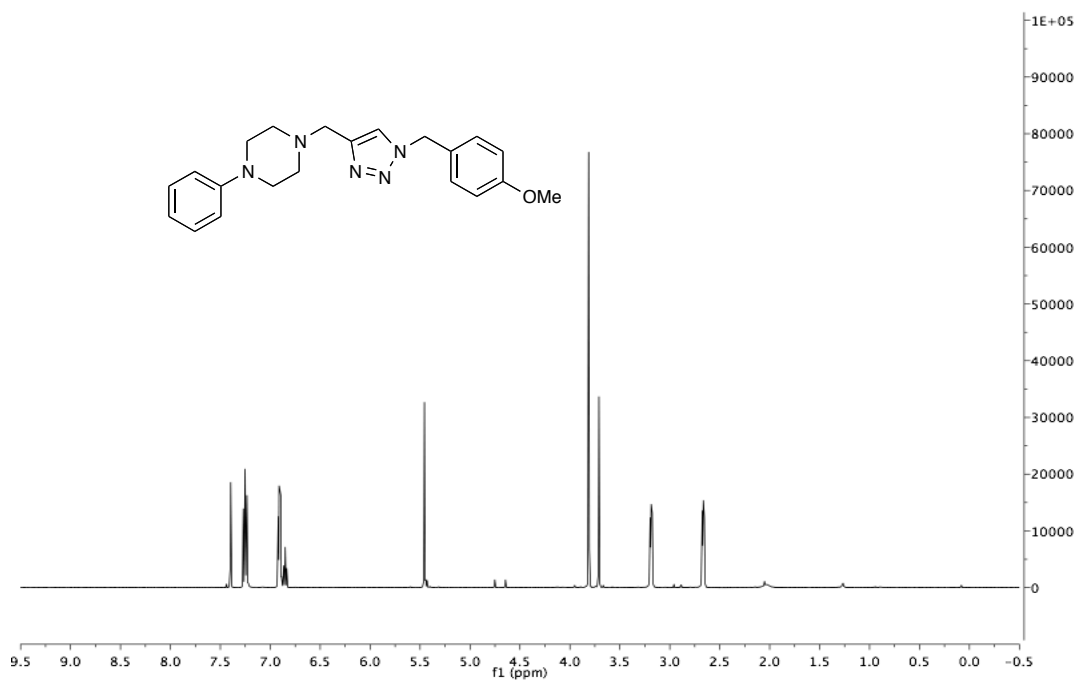
4-((1-(4-methoxybenzyl)-1*H*-1,2,3-triazol-4-yl)methyl)morpholine (2.1.7f)



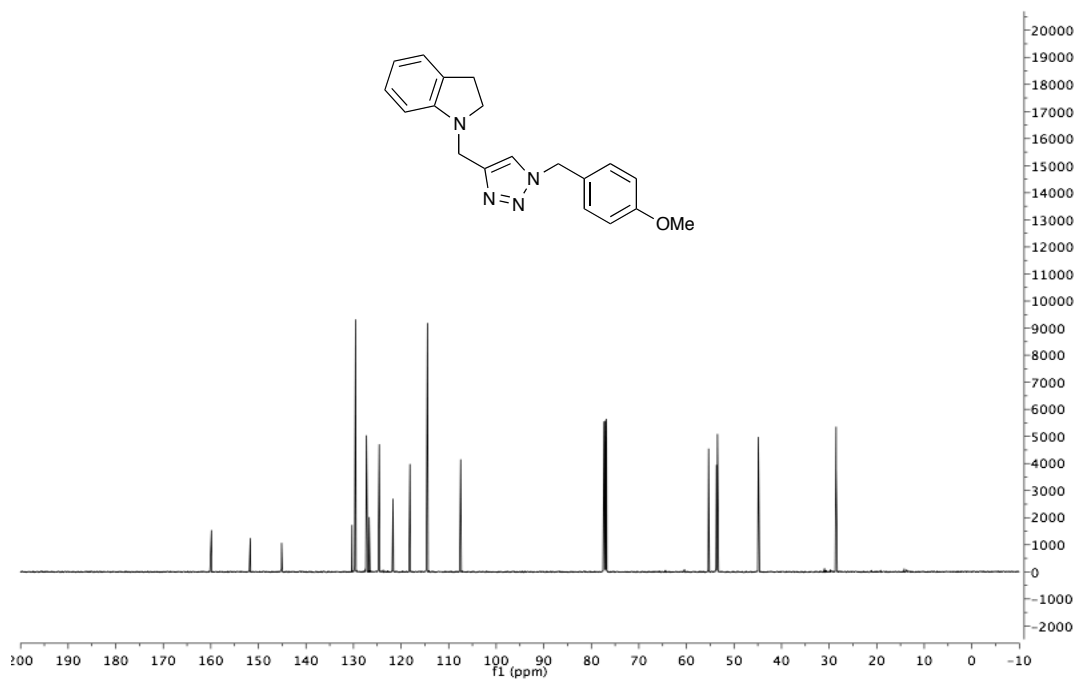
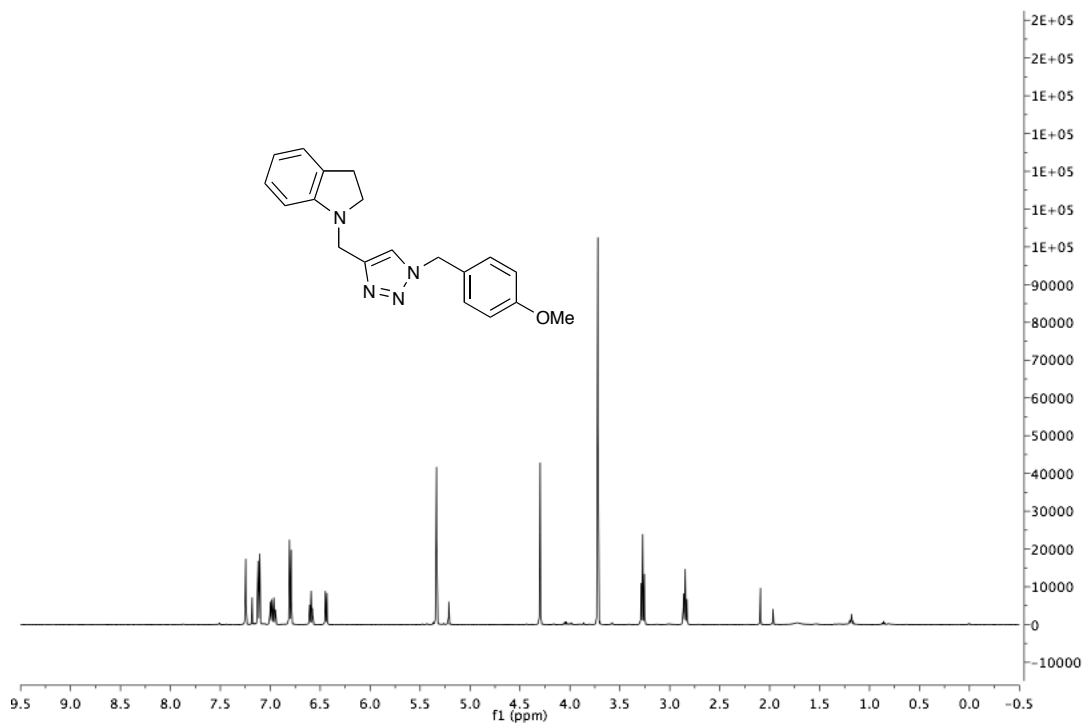
4-((1-(4-methoxybenzyl)-1*H*-1,2,3-triazol-4-yl)methyl)thiomorpholine (2.1.7g).



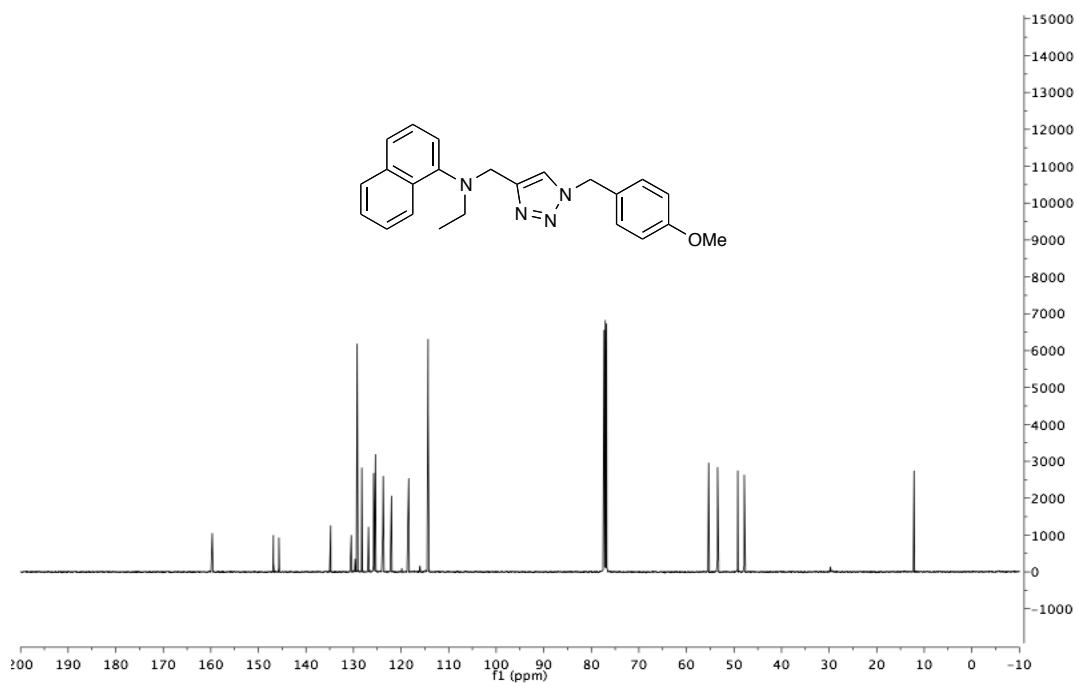
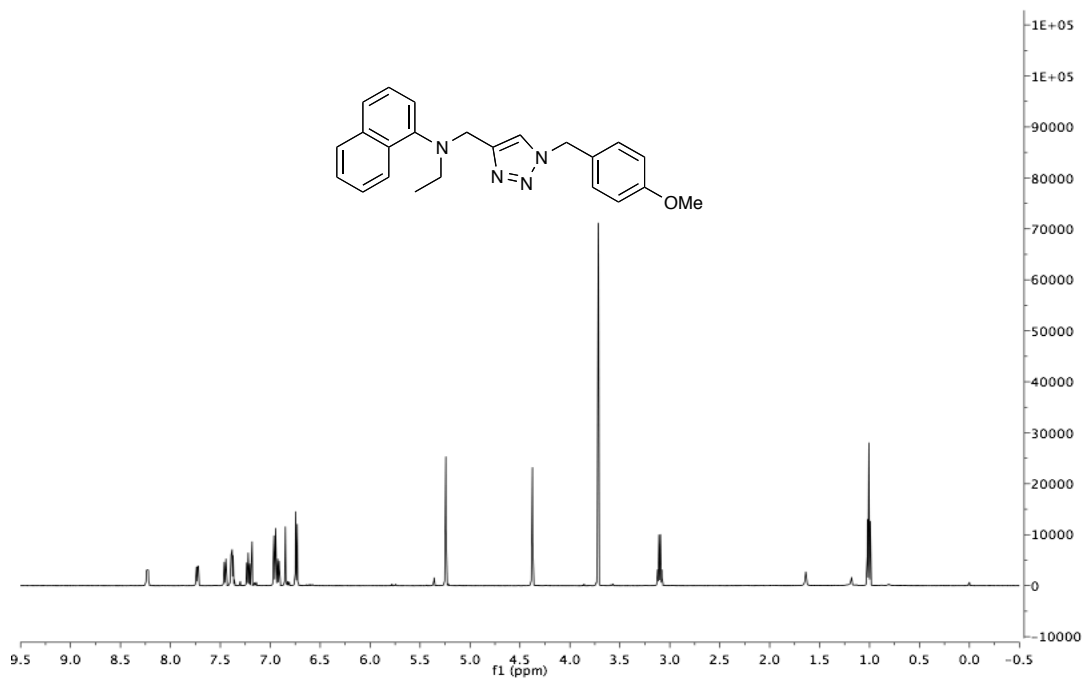
1-((1-(4-Methoxybenzyl)-1*H*-1,2,3-triazol-4-yl)methyl)-4-phenylpiperazine(2.1.7h)



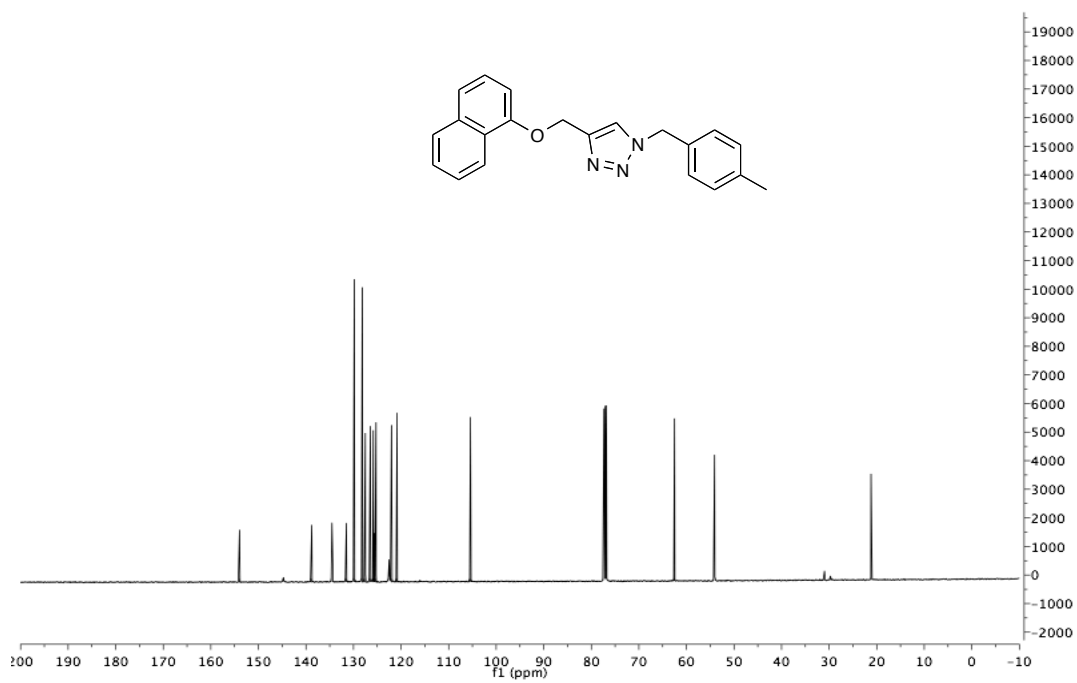
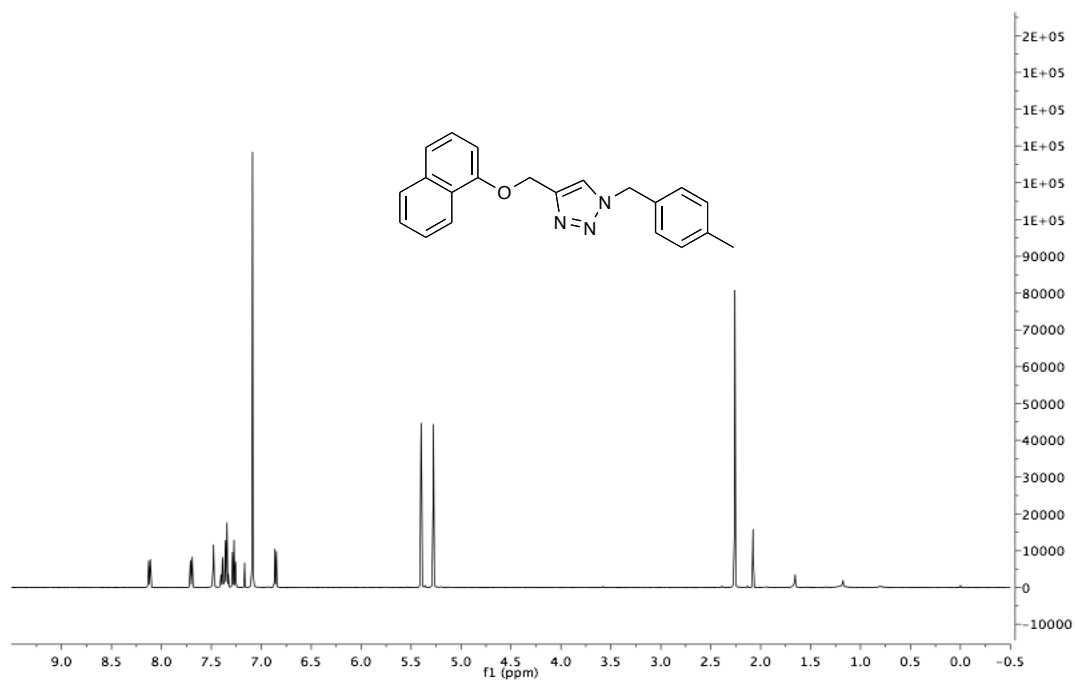
1-((1-(4-Methoxybenzyl)-1*H*-1,2,3-triazol-4-yl)methyl)indoline (2.17i).



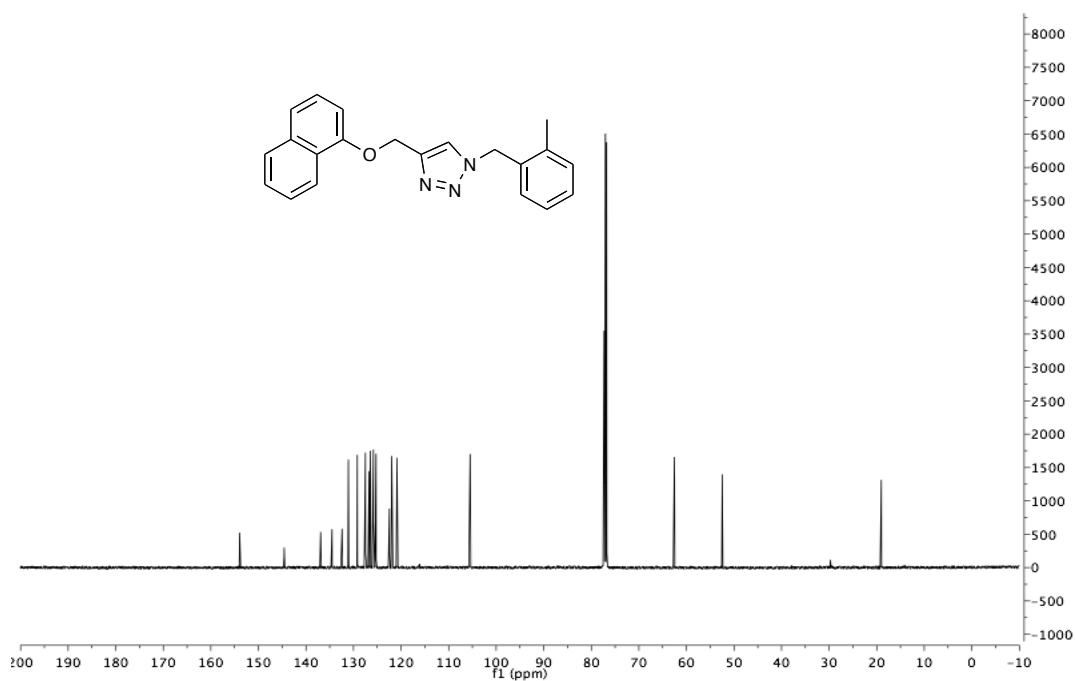
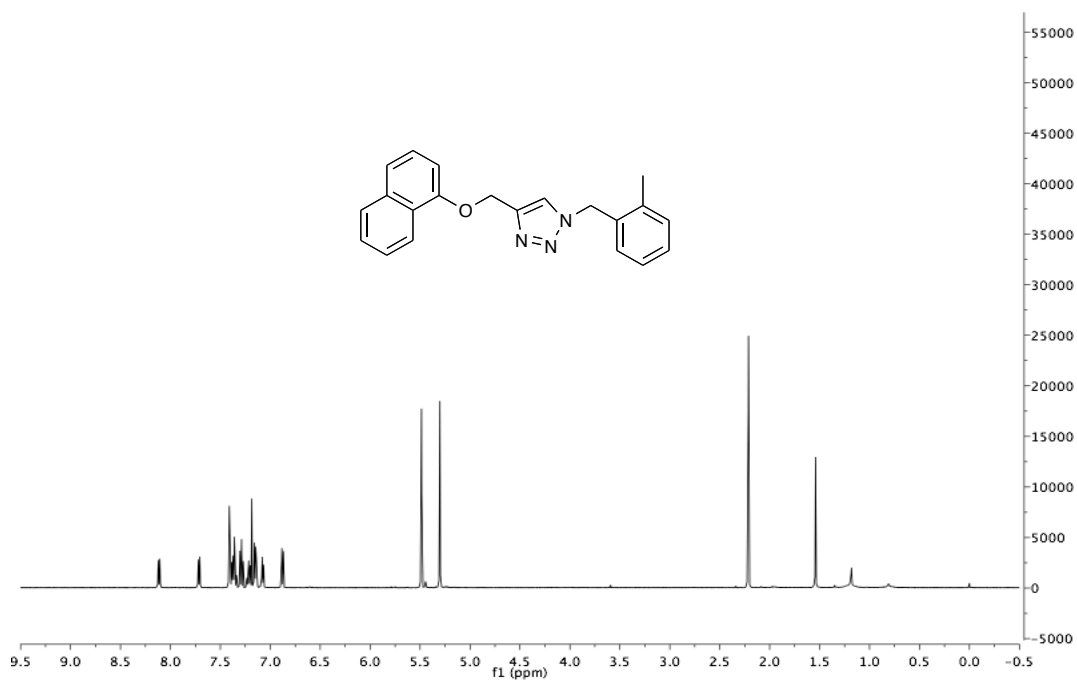
**N-ethyl-N-((1-(4-methoxybenzyl)-1H-1,2,3-triazol-4-yl)methyl)naphthalen-1-amine
(2.1.7j).**



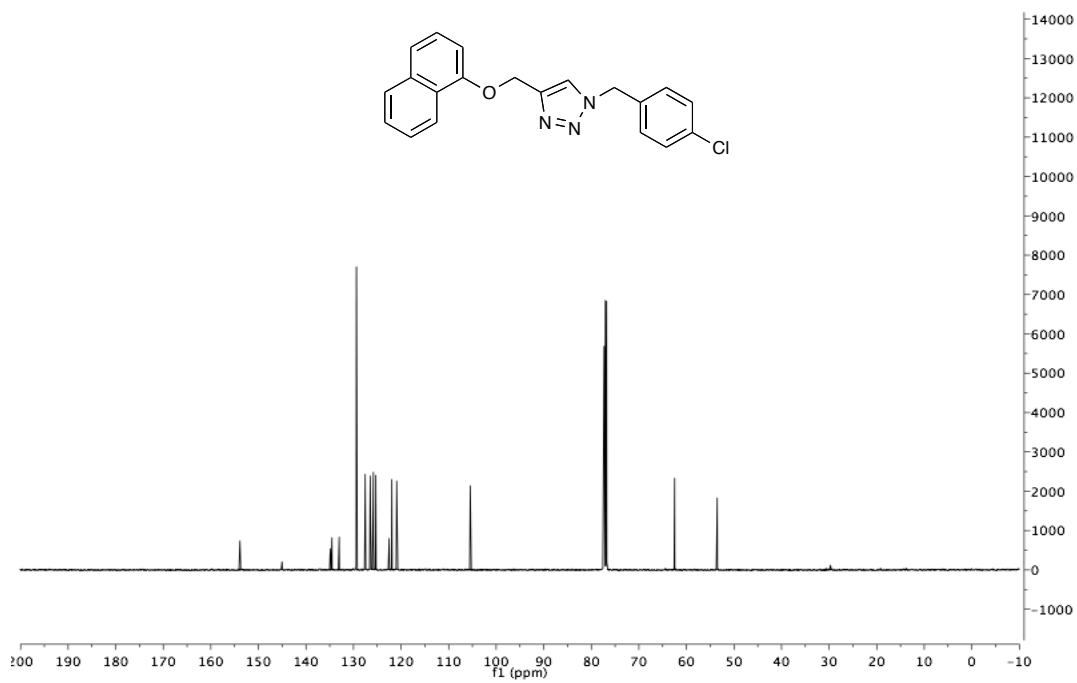
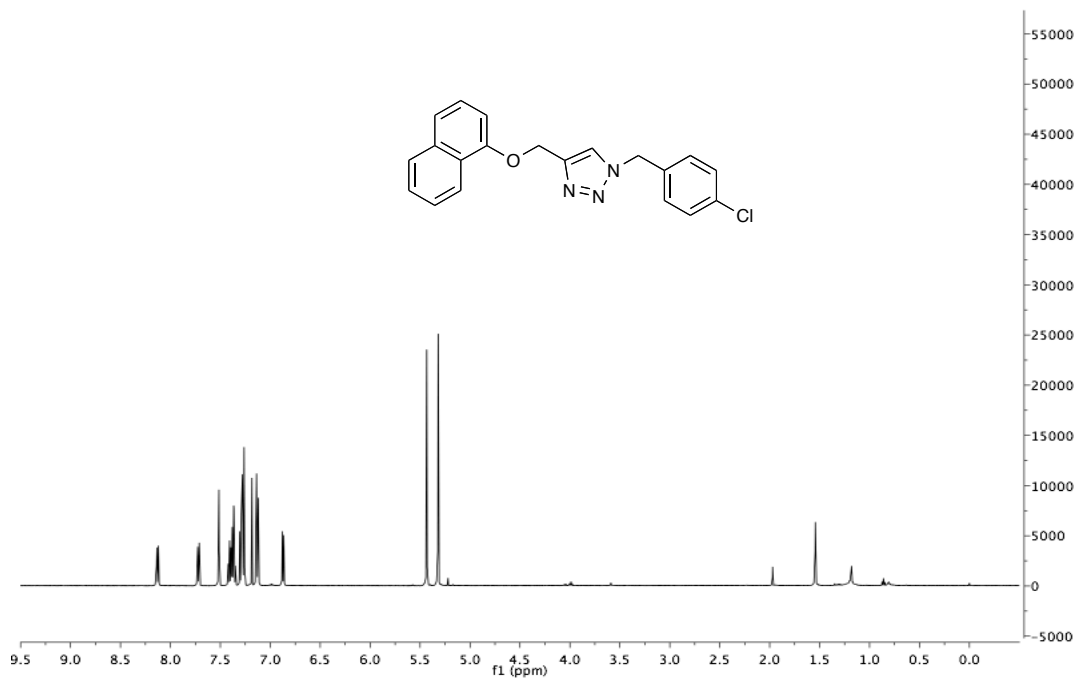
1-(4-Methylbenzyl)-4-((naphthalen-1-yloxy)methyl)-1H-1,2,3-triazole (2.1.8b).



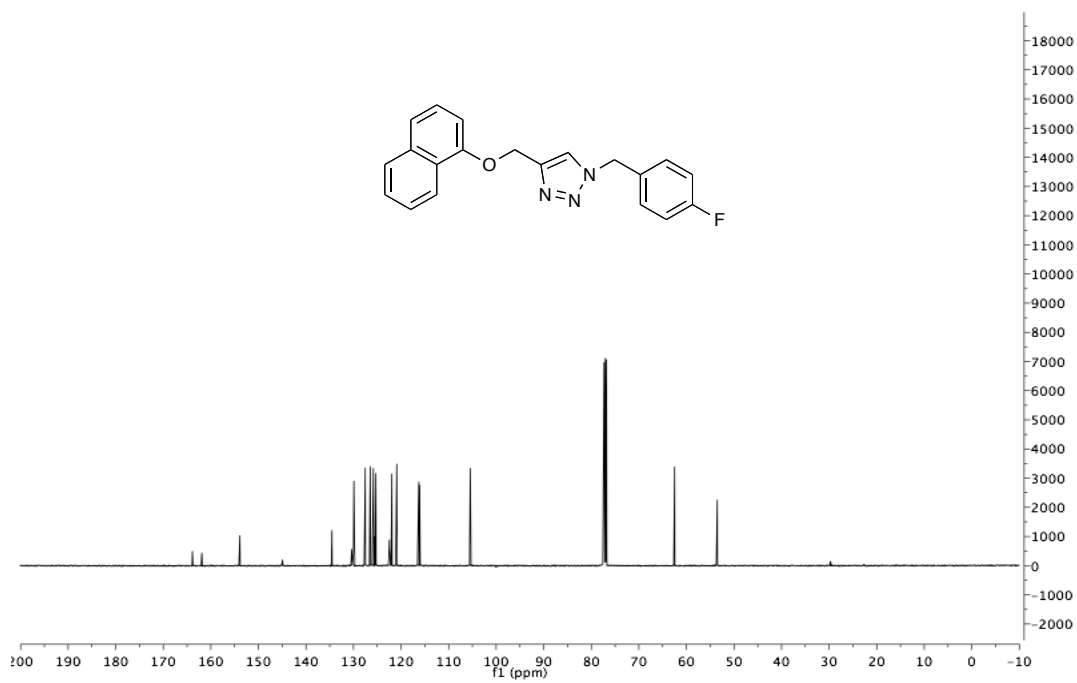
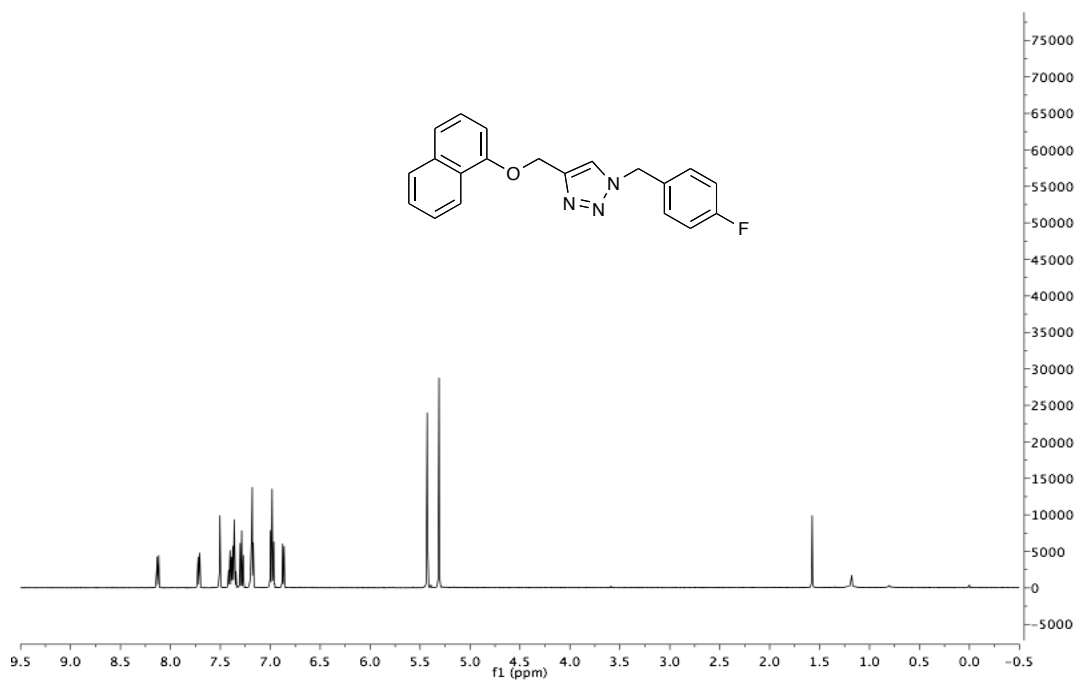
1-(2-Methylbenzyl)-4-((naphthalen-1-yloxy)methyl)-1H-1,2,3-triazole (2.1.8c).



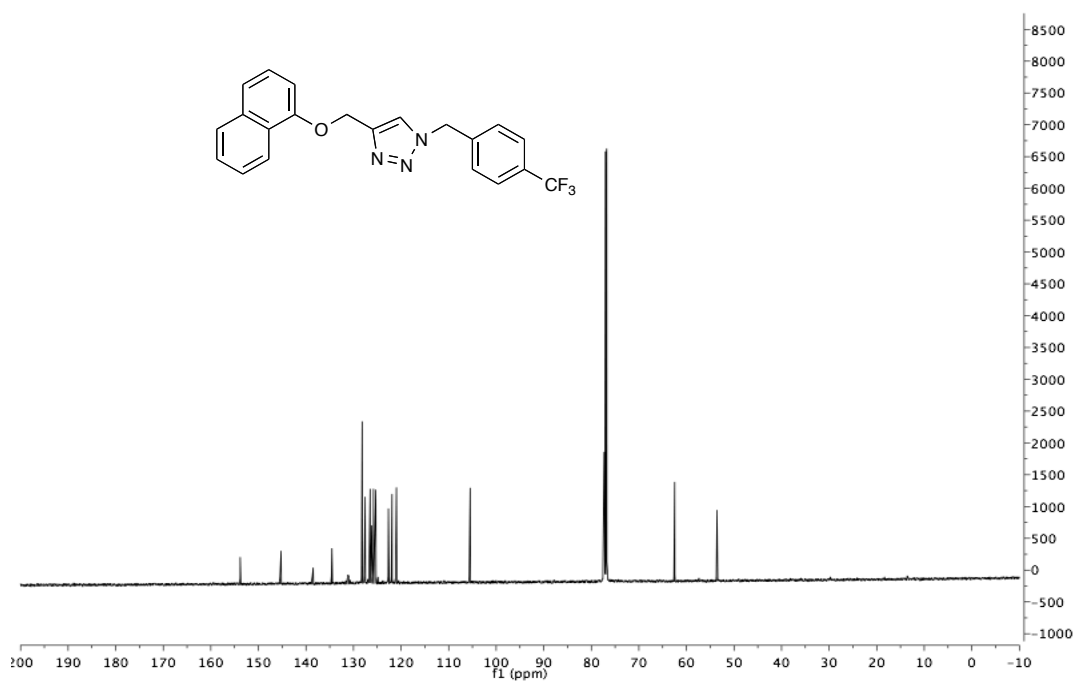
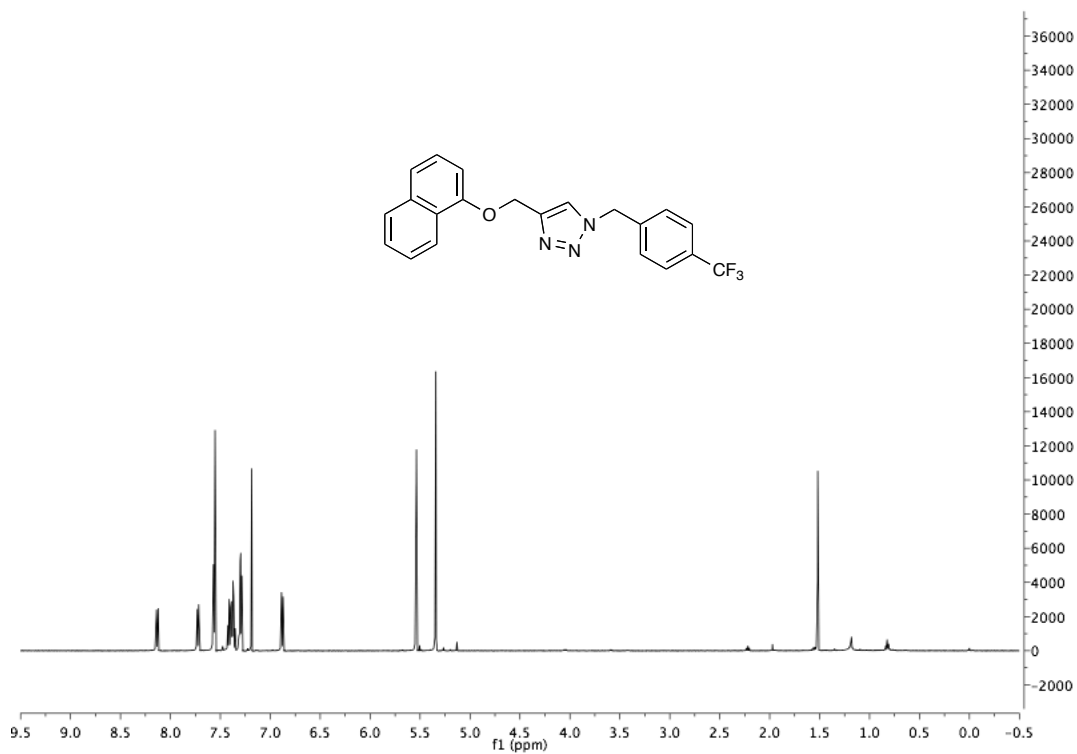
1-(4-Chlorobenzyl)-4-((naphthalen-1-yloxy)methyl)-1*H*-1,2,3-triazole (2.1.8d).



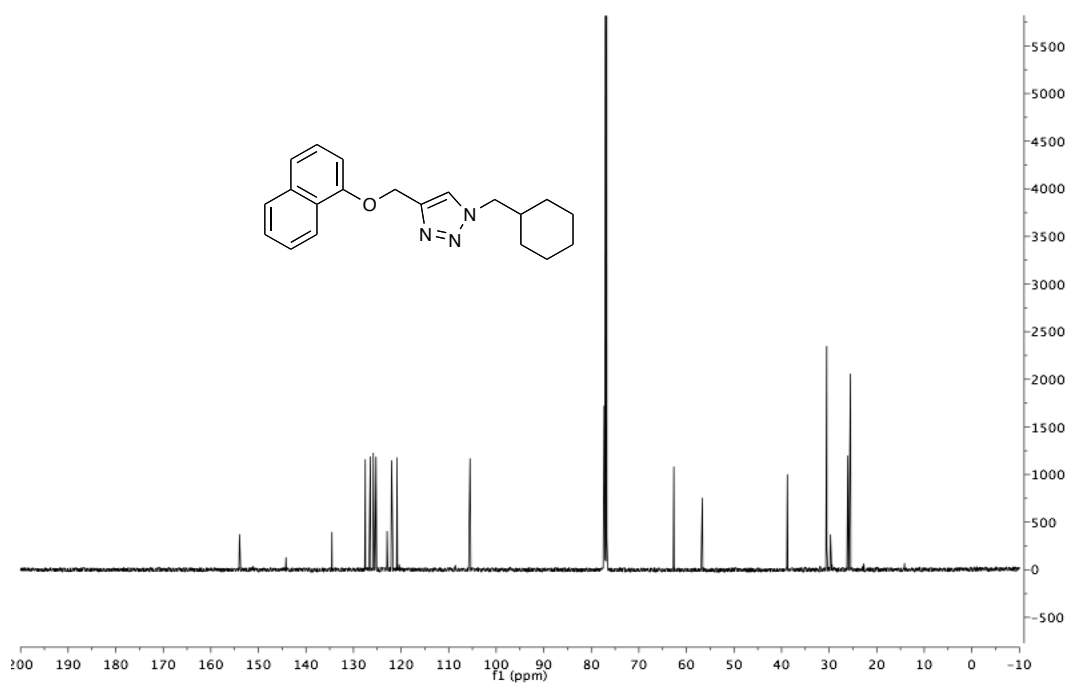
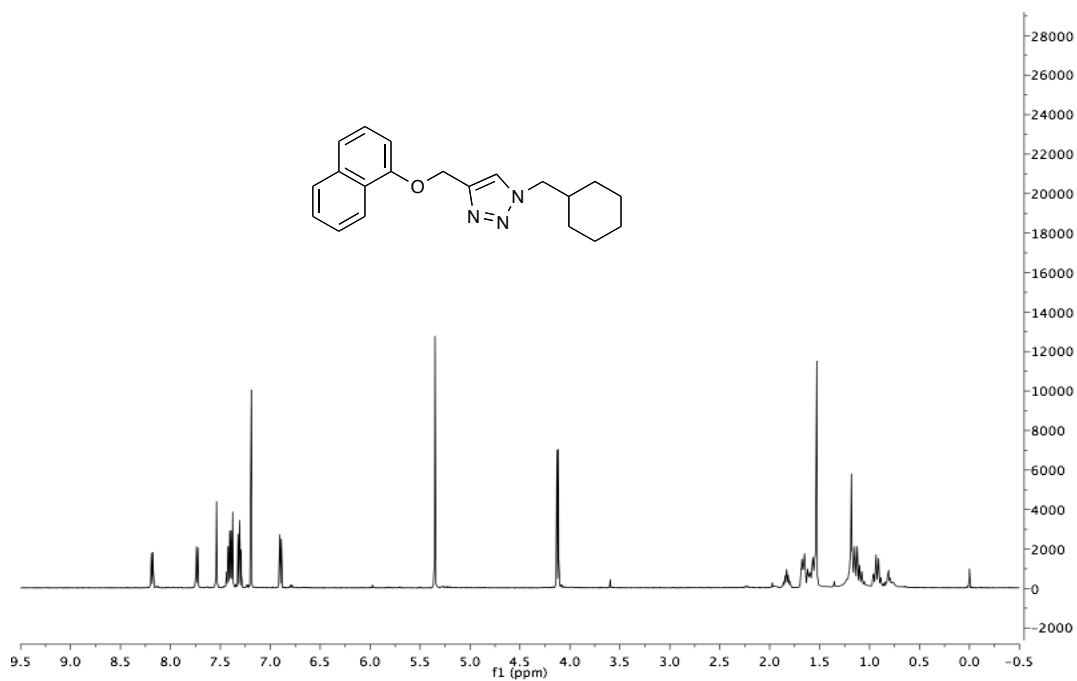
1-(4-Fluorobenzyl)-4-((naphthalen-1-yloxy)methyl)-1H-1,2,3-triazole (2.1.8e).



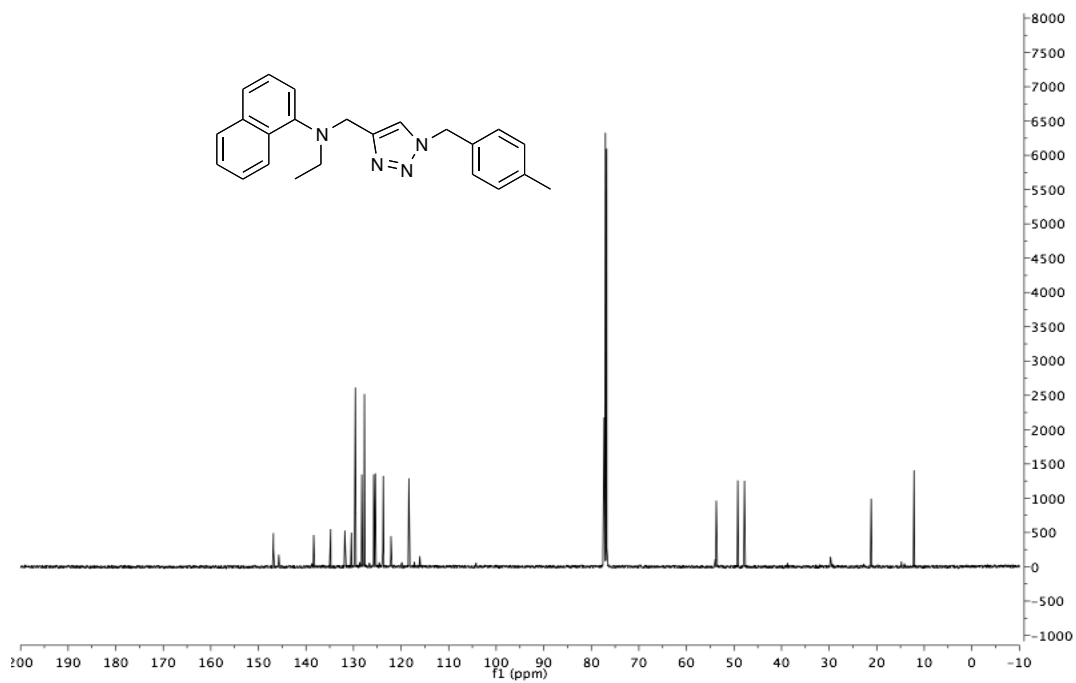
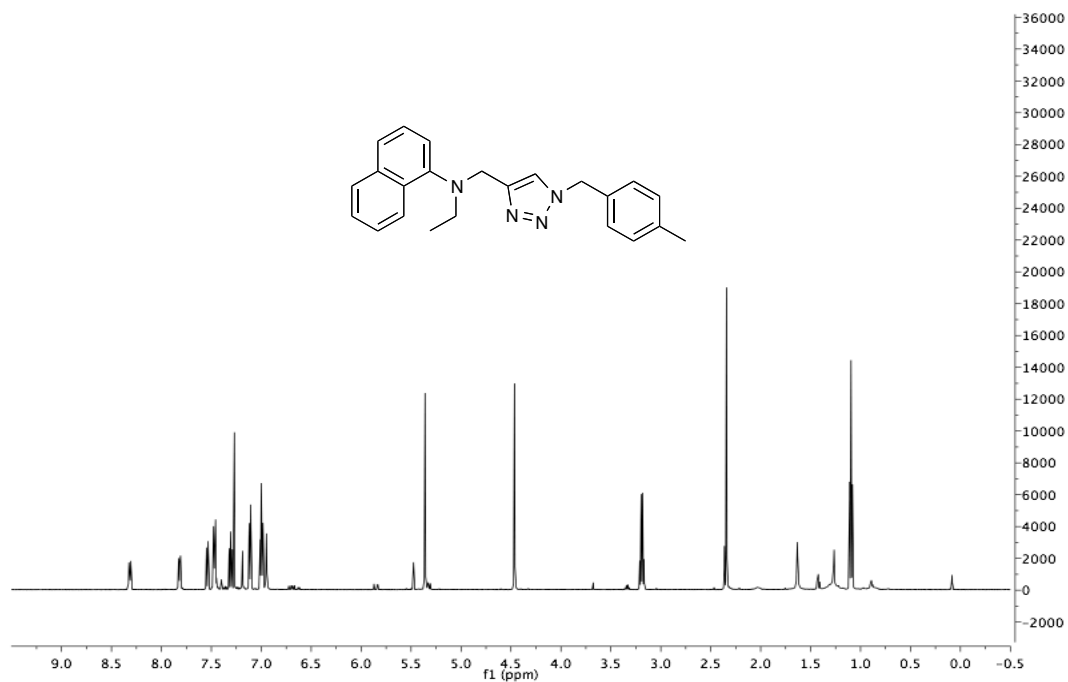
4-((naphthalen-1-yloxy)methyl)-1-(4-(trifluoromethyl)benzyl)-1H-1,2,3-triazole (2.1.8f).



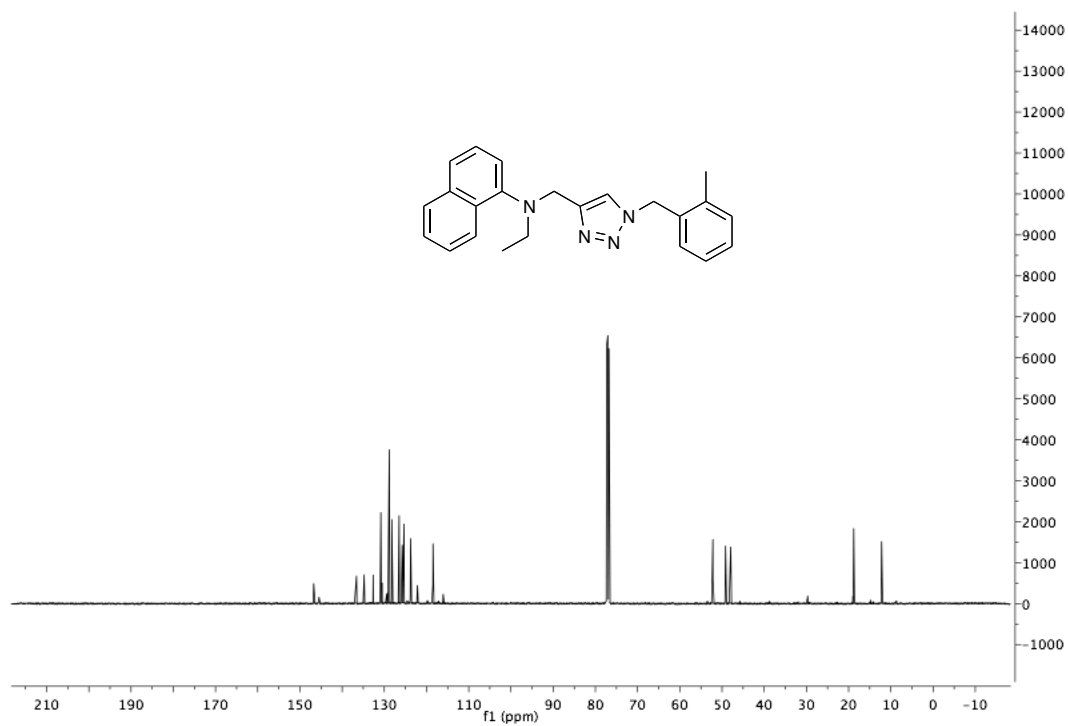
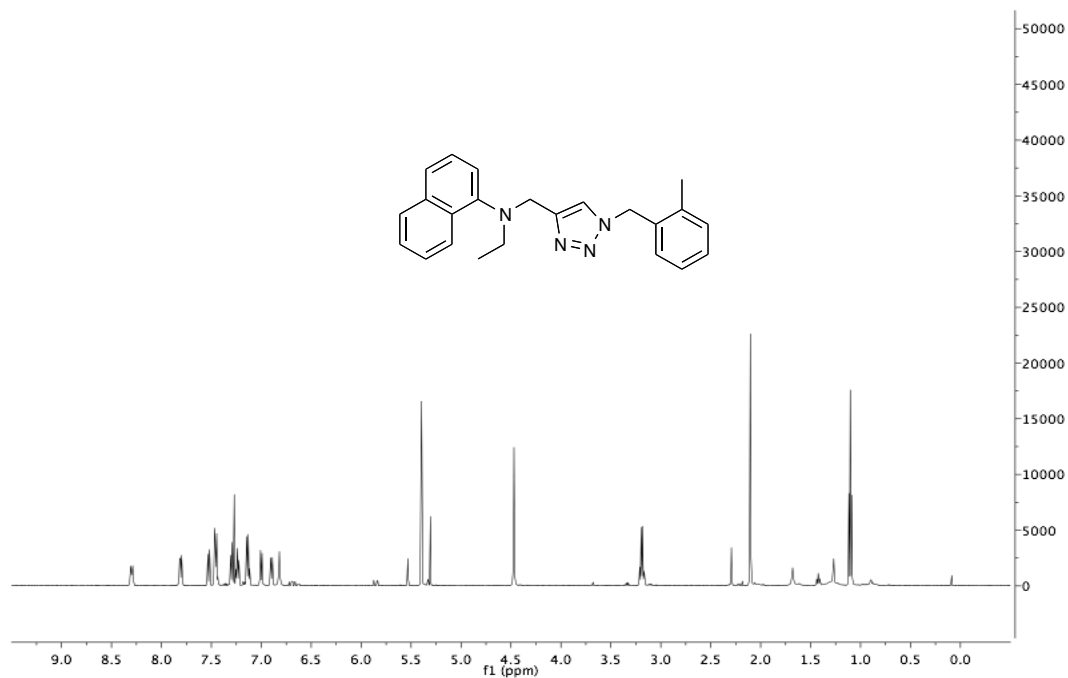
1-(Cyclohexylmethyl)-4-((naphthalen-1-yloxy)methyl)-1H-1,2,3-triazole (2.1.8g).



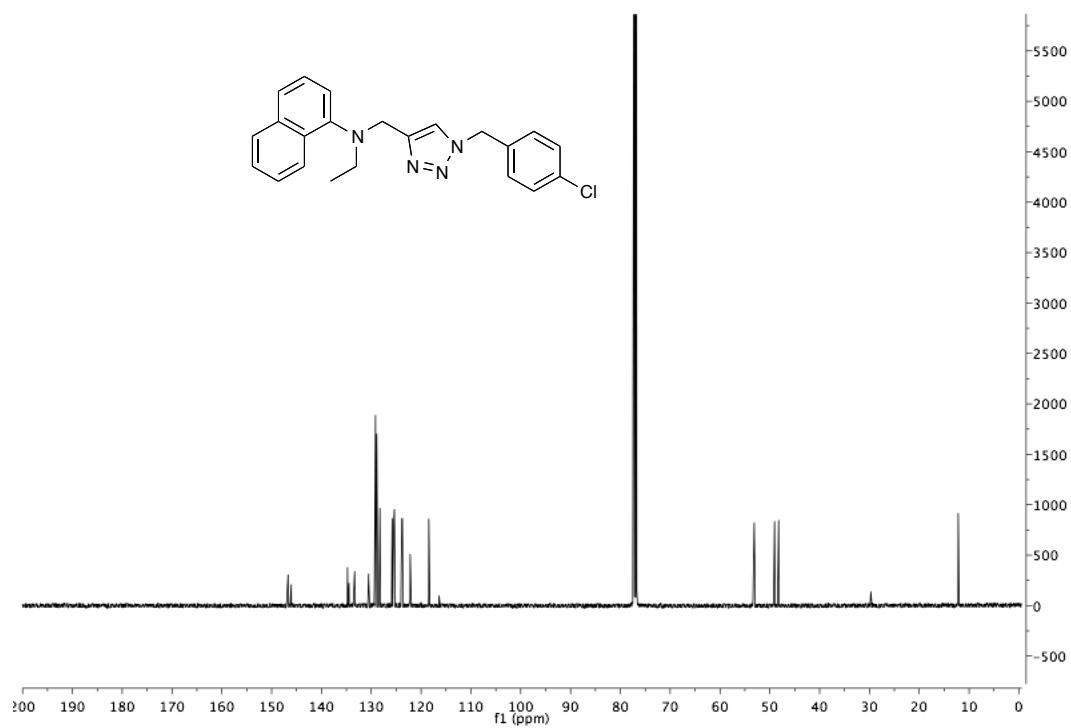
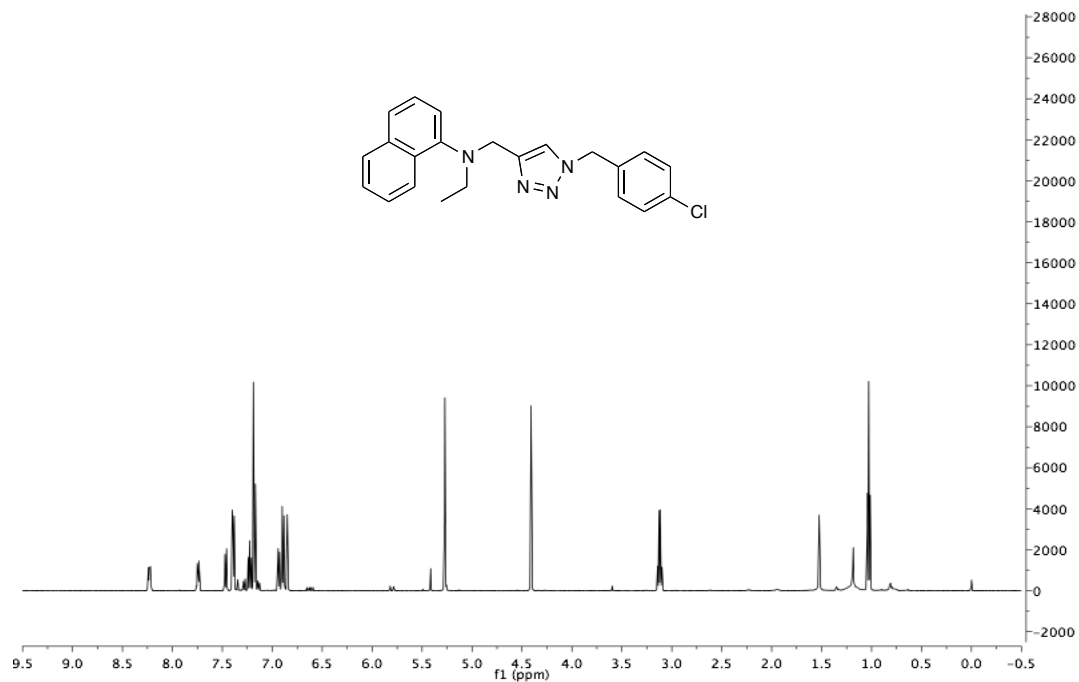
**N-Ethyl-N-((1-(4-methylbenzyl)-1H-1,2,3-triazol-4-yl)methyl)naphthalen-1-amine
(2.1.8i).**



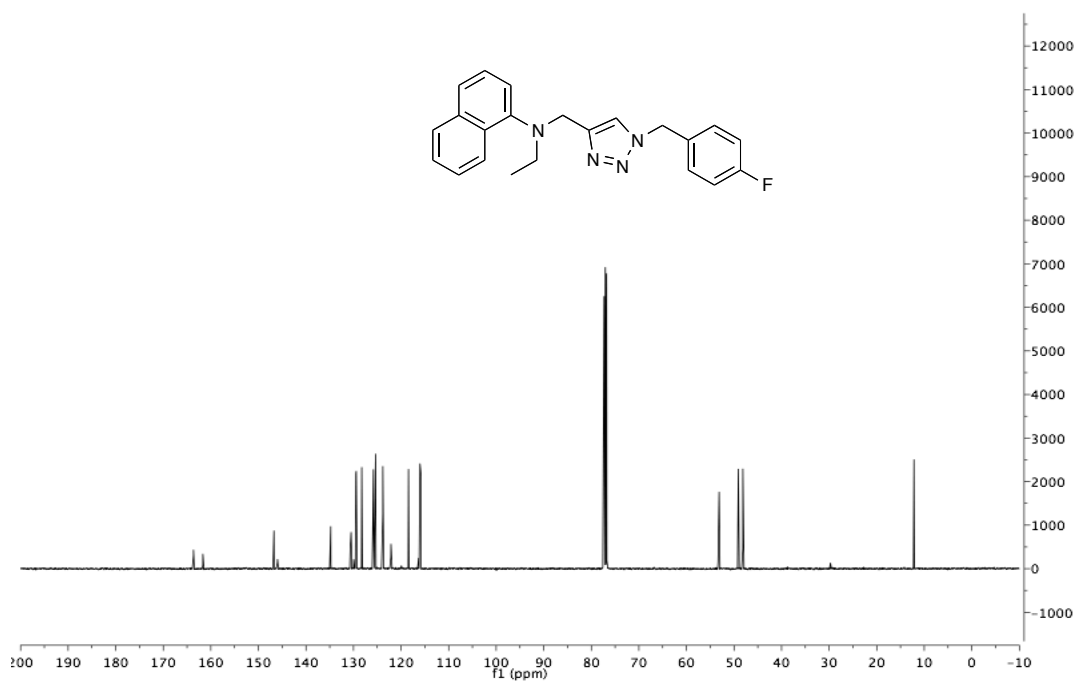
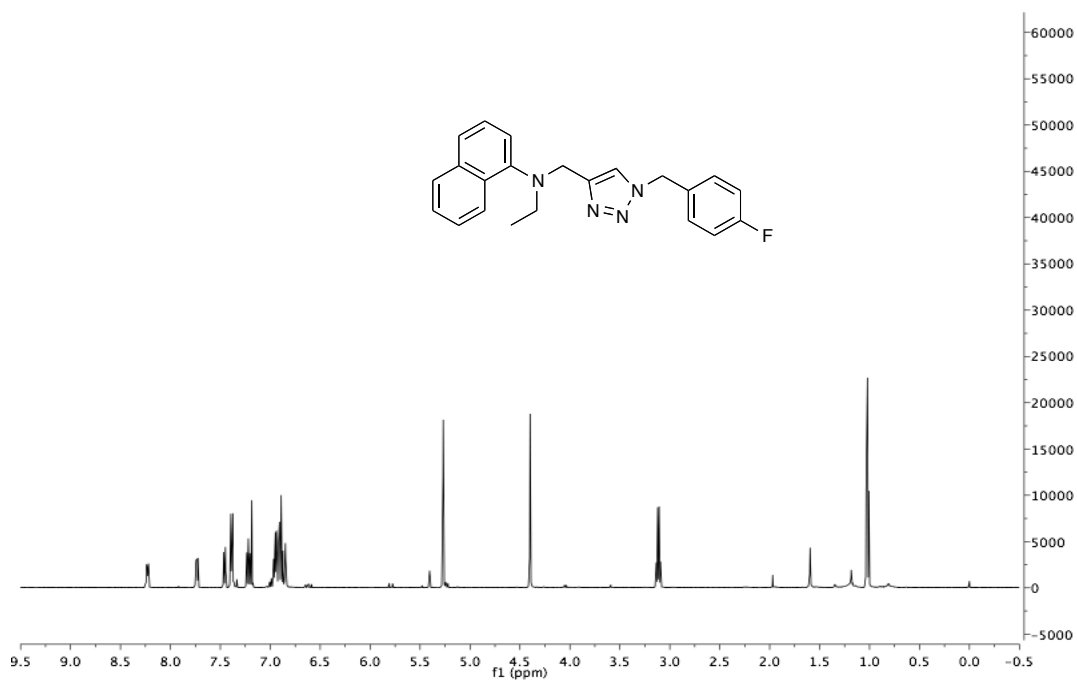
**N-Ethyl-N-((1-(2-methylbenzyl)-1H-1,2,3-triazol-4-yl)methyl)naphthalen-1-amine
(2.1.8j).**



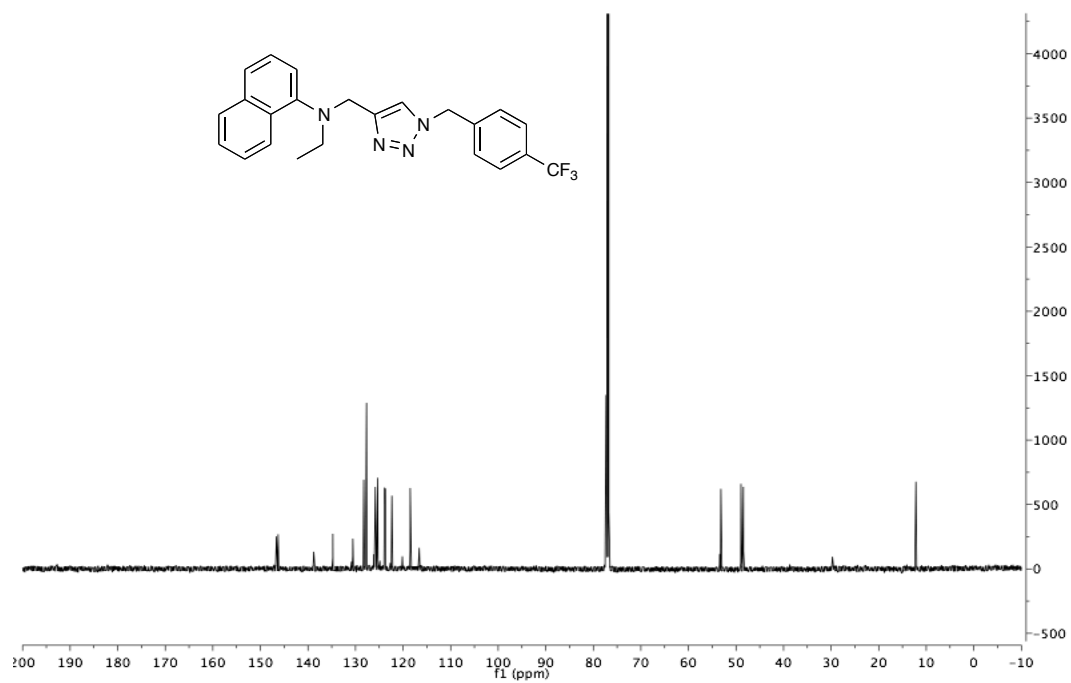
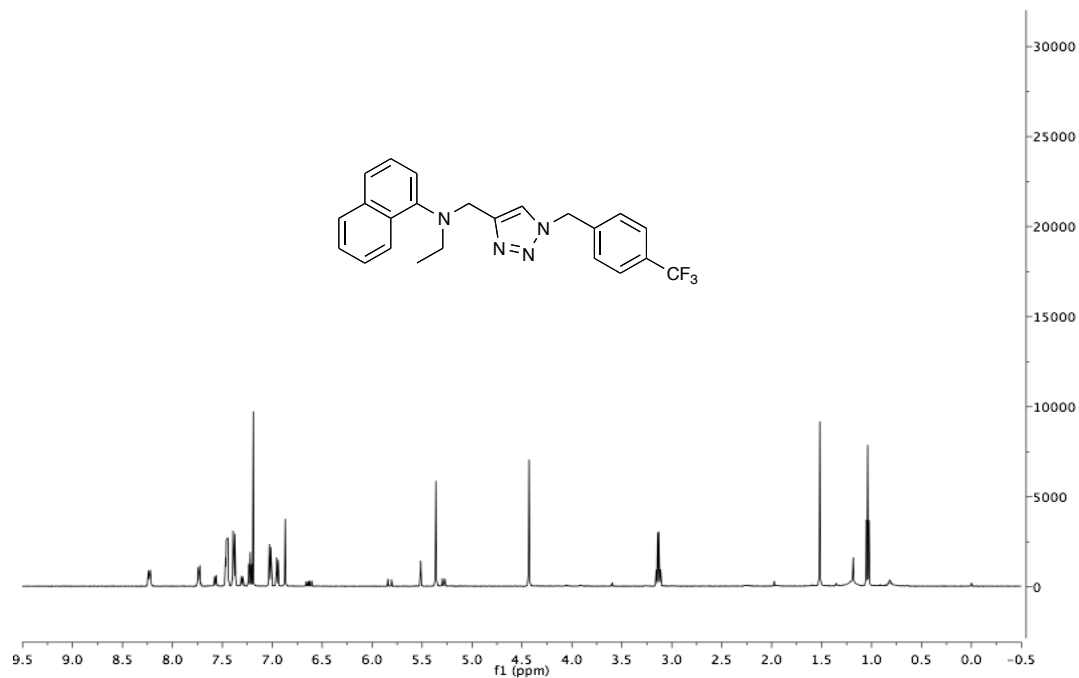
***N*-((1-(4-Chlorobenzyl)-1*H*-1,2,3-triazol-4-yl)methyl)-*N*-ethylnaphthalen-1-amine
(2.1.8k).**



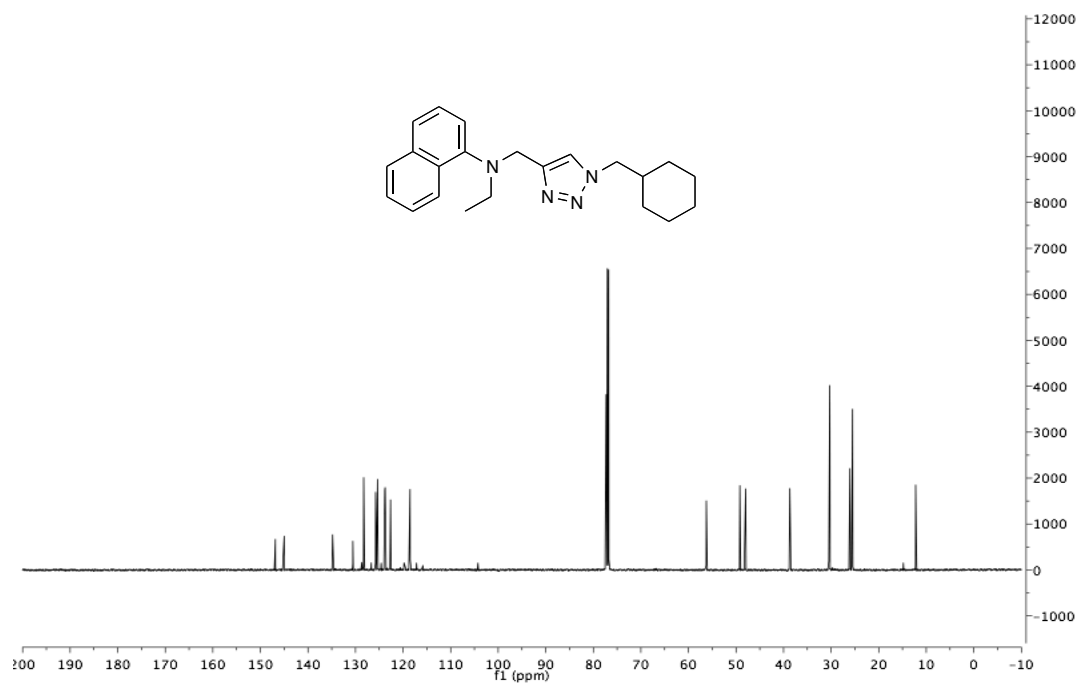
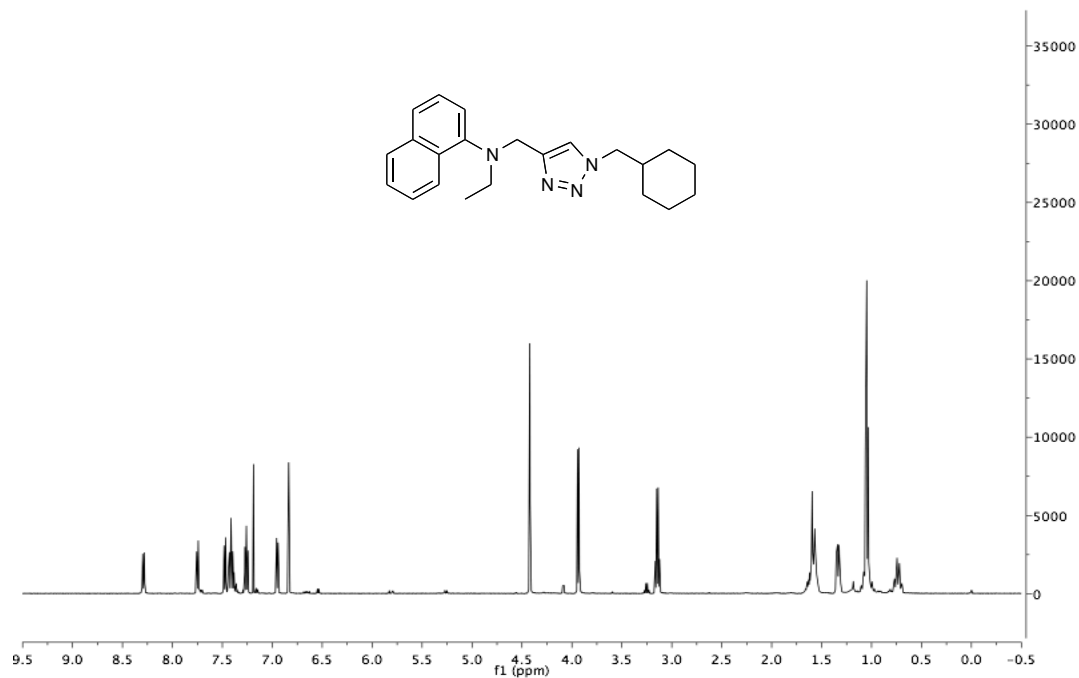
E-N-((1-(4-fluorobenzyl)-1H-1,2,3-triazol-4-yl)methyl)naphthalen-1-amine (2.1.8l).



N-Ethyl-N-((1-(4-(trifluoromethyl)benzyl)-1H-1,2,3-triazol-4-yl)methyl)naphthalen-1-amine (2.1.8m).



**N-((1-(Cyclohexylmethyl)-1H-1,2,3-triazol-4-yl)methyl)-N-ethylnaphthalen-1-amine
(2.1.8n).**



5.4 Experimental for Chapter 2.2

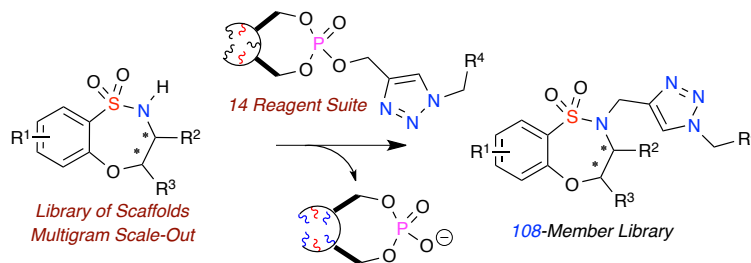
Facile (Triazolyl)methylation of MACOS-derived Benzofused Sultams

Utilizing ROMP-derived OTP Reagents.

Experimental Section and Characterization data (SI-216–SI-233)

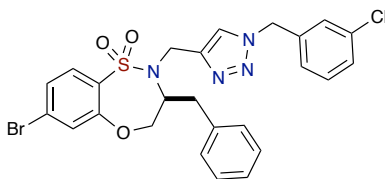
^1H , ^{13}C , Spectra for all Relevant Compounds (SI-234–SI-249)

General procedure A: Triazolation of nucleophilic species (2.2.1–2.2.10) with OTP₂₀ {2.2.1–2.2.14}.



To a 1-dram vial w/ teflon cap was added OTP₂₀ {2.2.1–2.2.14} (1.5 equiv) followed by addition of sodium iodide (0.2 equiv), Cs₂CO₃ (3 equiv), and dry DMF (0.2M). The mixture was stirred rapidly until the oligomer dissolved (< 30 s) after which the corresponding nucleophile (**2.2.1–2.2.10**) (1 equiv.) was added. The reaction was heated to 90 °C for 2–14 h dependent on the nucleophile, after which time, DMF was removed in *vacuo*. The crude mixture was diluted in EtOAc, filtered via SiO₂ SPE and rinsed several times with a mixture of EtOAc and concentrated in *vacuo* to yield the desired product.

(S)-3-Benzyl-7-bromo-2-((1-(3-chlorobenzyl)-1*H*-1,2,3-triazol-4-yl)methyl)-3,4-dihydro-2*H*-benzo[*b*][1,4,5]oxathiazepine 1,1-dioxide, Library Member 2.2.1{2.2.2I}.



Utilizing general procedure **A**, **2.2.1{2.2.2I}** (62 mg, 0.108 mmol, 85%) was isolated as an off white solid. $[\alpha]_D^{20} = -69.8^\circ$ ($c = 1.0$, CH_2Cl_2);

MP = 180 °C;

FTIR (neat): 3143, 2385, 2084, 1633, 1579, 1454, 1402, 1332, 1213, 1159, 1018 cm^{-1}

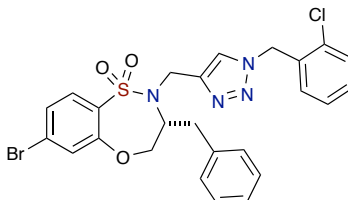
^1H NMR (400 MHz, CDCl_3): δ 7.63 (d, $J = 8.5$ Hz, 1H), 7.35–7.30 (m, 2H), 7.30–7.22 (m, 4H), 7.22–7.17 (m, 2H), 7.16 (s, 1H), 7.10 (d, $J = 1.7$ Hz, 1H), 7.03 (d, $J = 7.3$ Hz, 1H), 6.81 (s, 1H), 5.30 (d, $J = 15.0$ Hz, 1H), 5.25 (d, $J = 15.0$ Hz, 1H), 4.75 (t, $J = 11.8$ Hz, 1H), 4.39–4.23 (m, 3H), 4.19 (d, $J = 15.6$ Hz, 1H), 3.06 (dd, $J = 13.7$, 9.0 Hz, 1H), 2.81 (dd, $J = 13.7$, 6.4 Hz, 1H).

^{13}C NMR (126 MHz, CDCl_3): δ 156.0, 143.1, 137.1, 136.1, 135.0, 130.9, 130.4, 129.5 (2C), 129.0 (2C), 128.1, 127.3, 126.5, 126.3, 126.0, 124.6, 123.0, 73.0, 62.9, 53.3, 46.0, 36.6.

HRMS calculated for $\text{C}_{25}\text{H}_{22}\text{BrClN}_4\text{O}_3\text{SNa}$ ($\text{M}+\text{Na}$) $^+$ 595.0182; found 595.0161 (TOF MS ES+).

(R)-3-Benzyl-7-bromo-2-((1-(2-chlorobenzyl)-1H-1,2,3-triazol-4-yl)methyl)-3,4-dihydro-2H-benzo[b][1,4,5]oxathiazepine 1,1-dioxide, Library Member

2.2.2{2.2.22}.



Utilizing general procedure **A**, **2.2.2{2.2.22}** (45 mg, 0.076 mmol, 62%) was isolated as a yellow solid. $[\alpha]_D^{20} = +55.0^\circ$ ($c = 0.8$, CH_2Cl_2);

MP = 116 °C;

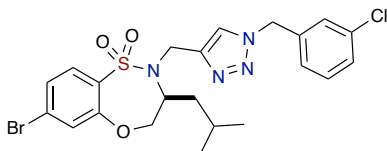
FTIR (neat): 3421, 2923, 2082, 1629, 1579, 1332, 1159, 1016 cm^{-1} ;

^1H NMR (400 MHz, CDCl_3): δ 7.65 (d, $J = 8.5$ Hz, 1H), 7.43 (d, $J = 7.1$ Hz, 1H), 7.37–7.17 (m, 8H), 7.10 (dd, $J = 14.5, 4.5$ Hz, 2H), 6.93 (s, 1H), 5.57–5.34 (m, 2H), 4.77 (t, $J = 11.5$ Hz, 1H), 4.41–4.24 (m, 3H), 4.20 (d, $J = 15.5$ Hz, 1H), 3.07 (dd, $J = 13.4, 8.7$ Hz, 1H), 2.83 (dd, $J = 13.7, 6.4$ Hz, 1H).

^{13}C NMR (126 MHz, CDCl_3): δ 156.0, 142.7, 137.0, 133.5, 132.1, 130.9, 130.3, 130.2, 129.9, 129.6, 129.5 (2C), 128.5 (2C), 127.7, 126.6, 126.3, 124.6, 123.2, 73.9, 62.8, 51.3, 45.9, 36.7, 29.7.

HRMS calculated for $\text{C}_{25}\text{H}_{22}\text{BrClN}_4\text{O}_3\text{SNa}$ ($\text{M}+\text{Na}$) $^+$ 595.0182; found 595.0160 (TOF MS ES $^+$).

(S)-7-Bromo-2-((1-(3-chlorobenzyl)-1H-1,2,3-triazol-4-yl)methyl)-3-isobutyl-3,4-dihydro-2H-benzo[*b*][1,4,5]oxathiazepine 1,1-dioxide, Library Member 2.2.3{2.2.21}.



Utilizing general procedure **A**, **2.2.3{2.2.21}** (74 mg, 0.137 mmol, 97%) was isolated as a white solid.

$[\alpha]_D^{20} = -84.7^\circ$ ($c = 0.9$, CH_2Cl_2);

MP = 169 °C;

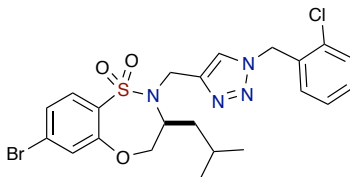
FTIR (neat): 2958, 2867, 2358, 2088, 1635, 1581, 1552, 1328, 1213, 1153 cm^{-1}

^1H NMR (400 MHz, CDCl_3): δ 7.63 (d, $J = 8.4$ Hz, 1H), 7.37–7.26 (m, 4H), 7.22 (s, 1H), 7.16 (s, 1H), 7.10 (d, $J = 7.1$ Hz, 1H), 5.46 (d, $J = 15.0$ Hz, 1H), 5.37 (d, $J = 15.0$ Hz, 1H), 4.43–4.29 (m, 3H), 4.28–4.15 (m, 2H), 1.69 (ddd, $J = 13.9, 8.8, 5.4$ Hz, 1H), 1.44 (dt, $J = 20.2, 6.6$ Hz, 1H), 1.28–1.16 (m, 1H), 0.81 (d, $J = 6.5$ Hz, 3H), 0.79 (d, $J = 6.6$ Hz, 3H).

^{13}C NMR (126 MHz, CDCl_3): δ 156.1, 144.2, 136.3, 135.1, 130.45, 130.4, 130, 129.1, 128.1, 127.5, 126.6, 126, 125.5, 123.4, 73.8, 59.8, 53.5, 44.1, 38.7, 24.6, 22.8, 21.9.

HRMS calculated for $\text{C}_{22}\text{H}_{25}\text{BrClN}_4\text{O}_3\text{SNa}$ ($\text{M}+\text{H}$) $^+$ 539.0519; found 539.0521 (TOF MS ES+).

(S)-7-Bromo-2-((1-(2-chlorobenzyl)-1*H*-1,2,3-triazol-4-yl)methyl)-3-isobutyl-3,4-dihydro-2*H*-benzo[*b*] [1,4,5]oxathiazepine 1,1-dioxide, Library Member 2.2.3{2.2.22}.



Utilizing general procedure **A**, **2.2.3{2.2.21}** (70 mg, 0.129 mmol, 92%) was isolated as a white solid.

$[\alpha]_D^{20} = -73.9^\circ$ ($c = 0.9$, CH_2Cl_2);

MP = 155 °C;

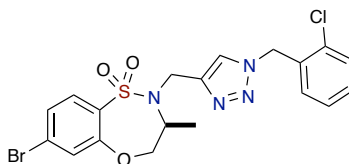
FTIR (neat): 3126, 2956, 2867, 2358, 2331, 1579, 1550, 1473, 1402, 1365, 1328, 1153, 1041 cm^{-1} ;

^1H NMR (400 MHz, CDCl_3): δ 7.63 (d, $J = 8.4$ Hz, 1H), 7.45 (dd, $J = 7.9$, 1.3 Hz, 1H), 7.39 (s, 1H), 7.34 (td, $J = 7.7$, 1.8 Hz, 1H), 7.31–7.25 (m, 2H), 7.17 (dt, $J = 4.1$, 1.9 Hz, 2H), 5.57 (q, $J = 15.0$ Hz, 2H), 4.48–4.34 (m, 3H), 4.27–4.19 (m, 2H), 1.71 (ddd, $J = 14.1$, 8.9, 5.6 Hz, 1H), 1.48–1.42 (m, 1H), 1.24 (ddd, $J = 13.9$, 6.9, 4.1 Hz, 1H), 0.81 (d, $J = 6.6$ Hz, 6H).

^{13}C NMR (126 MHz, CDCl_3): δ 156.1, 143.0, 133.6, 132.1, 131.6, 130.4, 130.3, 130.1, 129.9, 127.6, 127.5, 126.6, 125.3, 123.6, 73.9, 59.7, 51.5, 44.4, 38.8, 24.6, 22.8, 22.0.

HRMS calculated for $\text{C}_{22}\text{H}_{24}\text{BrClN}_4\text{O}_3\text{SNa}$ ($\text{M}+\text{Na}$) $^+$ 561.0339; found 561.0322 (TOF MS ES+).

(S)-7-Bromo-2-((1-(2-chlorobenzyl)-1*H*-1,2,3-triazol-4-yl)methyl)-3-methyl-3,4-dihydro-2*H*-benzo[*b*] [1,4,5]oxathiazepine 1,1-dioxide, Library Member 2.2.5{2.2.22}.



Utilizing general procedure **A**, **2.2.5{2.2.22}** (50 mg, 0.1004 mmol, 70%) was isolated as an off white solid.

$[\alpha]_D^{20} = -64.8^\circ$ ($c = 0.8$, CH_2Cl_2);

MP = 126 °C;

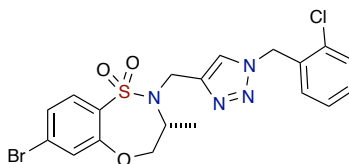
FTIR (neat): 3139, 2977, 2931, 1579, 1554, 1460, 1340, 1213, 1157, 1135, 1060, 1022 cm^{-1} ;

^1H NMR (400 MHz, CDCl_3): δ 7.62 (d, $J = 8.4$ Hz, 1H), 7.44 (dd, $J = 7.9, 1.3$ Hz, 1H), 7.37–7.35 (m, 1H), 7.34–7.29 (m, 1H), 7.28–7.23 (m, 2H), 7.16–7.13 (m, 2H), 5.56 (q, $J = 15.0$ Hz, 2H), 4.52–4.37 (m, 3H), 4.34–4.18 (m, 2H), 1.25 (d, $J = 6.8$ Hz, 3H).

^{13}C NMR (126 MHz, CDCl_3): δ 155.9, 143.9, 133.6, 132.0, 131.6, 130.5, 130.4, 130.0, 129.6, 127.6, 127.3, 126.4, 125.1, 123.3, 74.4, 56.9, 51.3, 30.9, 15.7.

HRMS calculated for $\text{C}_{19}\text{H}_{18}\text{BrClN}_4\text{O}_3\text{SNa}$ ($\text{M}+\text{Na}$) $^+$ 518.9869; found 518.9875 (TOF MS ES+).

(R)-7-Bromo-2-((1-(3-chlorobenzyl)-1*H*-1,2,3-triazol-4-yl)methyl)-3-methyl-3,4-dihydro-2*H*-benzo[*b*][1,4,5]oxathiazepine 1,1-dioxide, Library Member 2.2.6{2.2.21}.



Utilizing general procedure **A**, **2.2.6{2.2.21}** (78 mg, 0.157 mmol, 98%) was isolated as a white solid.

$[\alpha]_D^{20} = +71.7^\circ$ ($c = 1.0$, CH_2Cl_2);

MP = 137 °C;

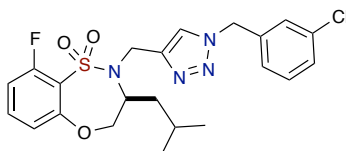
FTIR (neat): 3149, 3087, 2933, 1579, 1460, 1338, 1213, 1157, 1022 cm^{-1}

^1H NMR (400 MHz, CDCl_3): δ 7.63 (d, $J = 8.4$ Hz, 1H), 7.36–7.31 (m, 3H), 7.29–7.25 (m, 1H), 7.20 (s, 1H), 7.15 (d, $J = 1.8$ Hz, 1H), 7.09 (d, $J = 7.0$ Hz, 1H), 5.45 (d, $J = 15.0$ Hz, 1H), 5.38 (d, $J = 15.0$ Hz, 1H), 4.51–4.36 (m, 3H), 4.31–4.21 (m, 2H), 1.25 (d, $J = 6.8$ Hz, 3H).

^{13}C NMR (126 MHz, CDCl_3): δ 156.0, 144.4, 136.2, 135.0, 131.6, 130.4, 129.7, 129.1, 128.0, 127.4, 126.5, 126.0, 125.2, 123.1, 74.3, 57.1, 53.5, 43.7, 15.7.

HRMS calculated for $\text{C}_{19}\text{H}_{18}\text{BrClN}_4\text{O}_3\text{SNa}$ ($\text{M}+\text{Na}$) $^+$ 518.9869; found 518.9855 (TOF MS ES+).

(S)-2-((1-(3-Chlorobenzyl)-1H-1,2,3-triazol-4-yl)methyl)-9-fluoro-3-isobutyl-3,4-dihydro-2H-benzo[*b*][1,4,5]oxathiazepine 1,1-dioxide, Library Member 2.2.8{2.2.2I}



Utilizing general procedure **A**, **2.2.8{2.2.2I}** (63 mg, 0.131 mmol, 98%) was isolated as off white solid.

$[\alpha]_D^{20} = -78.0^\circ$ ($c = 0.7$, CH_2Cl_2);

MP = 153 °C;

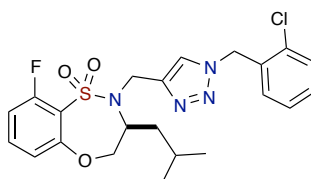
FTIR (neat): 3134, 3082, 2956, 2867, 1604, 1579, 1477, 1421, 1367, 1326, 1155, 1074 cm^{-1}

^1H NMR (400 MHz, CDCl_3): δ 7.77 (dd, $J = 8.8, 6.3$ Hz, 1H), 7.39 (s, 1H), 7.37–7.26 (m, 2H), 7.22 (s, 1H), 7.11 (d, $J = 7.2$ Hz, 1H), 6.84 (ddd, $J = 8.8, 7.6, 2.5$ Hz, 1H), 6.66 (dd, $J = 9.5, 2.4$ Hz, 1H), 5.44–5.39 (m, 2H), 4.43–4.31 (m, 3H), 4.28–4.15 (m, 2H), 1.75–1.64 (m, 1H), 1.48–1.35 (m, 1H), 1.25–1.18 (m, 1H), 0.81 (d, $J = 3.6$ Hz, 3H), 0.79 (d, $J = 3.8$ Hz, 3H).

^{13}C NMR (126 MHz, CDCl_3): δ 165.3 (d, $J = 255.2$ Hz), 157.5 (d, $J = 12.6$ Hz), 144.3, 136.3, 135.0, 130.9 (d, $J = 10.5$ Hz), 130.4, 129.1, 128.8, 128.1, 126.1, 123.4, 110.9 (d, $J = 22.3$ Hz), 109.6 (d, $J = 23.8$ Hz), 73.7, 59.7, 53.4, 44.3, 38.6, 24.6, 22.6, 21.9.

HRMS calculated for $C_{22}H_{24}ClFN_4O_3SNa$ ($M+Na$)⁺ 501.1139 found 501.1126 (TOF MS ES⁺).

(S)-2-((1-(2-Chlorobenzyl)-1*H*-1,2,3-triazol-4-yl)methyl)-9-fluoro-3-isobutyl-3,4-dihydro-2*H*-benzo[*b*] [1,4,5]oxathiazepine 1,1-dioxide, Library Member 2.2.8{2.2.22}



Utilizing general procedure **A**, **2.2.8{2.2.22}** (60 mg, 0.125 mmol, 94%) was isolated as a white solid.

$[\alpha]_D^{20} = -61.8^\circ$ ($c = 1.0$, CH_2Cl_2);

MP = 85 °C;

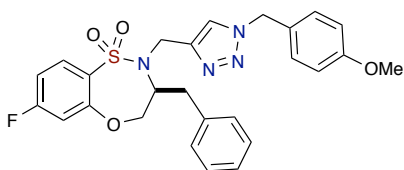
FTIR (neat): 2958, 2358, 1602, 1583, 1473, 1421, 1334, 1265, 1157, 1116, 1074, 1041 cm^{-1} ;

¹H NMR (400 MHz, $CDCl_3$): δ 7.76 (dd, $J = 8.8, 6.3$ Hz, 1H), 7.44 (dd, $J = 7.9, 1.3$ Hz, 1H), 7.41 (s, 1H), 7.34 (td, $J = 7.7, 1.8$ Hz, 1H), 7.29 (td, $J = 7.2, 1.4$ Hz, 1H), 7.18 (dd, $J = 7.6, 1.7$ Hz, 1H), 6.82 (ddd, $J = 8.8, 7.6, 2.5$ Hz, 1H), 6.64 (dd, $J = 9.5, 2.4$ Hz, 1H), 5.63–5.52 (m, 2H), 4.48–4.34 (m, 3H), 4.28–4.14 (m, 2H), 1.70 (ddd, $J = 14.1, 8.9, 5.6$ Hz, 1H), 1.46 (tt, $J = 13.1, 6.5$ Hz, 1H), 1.23 (ddd, $J = 13.9, 8.3, 5.4$ Hz, 1H), 0.80 (d, $J = 6.6$ Hz, 6H); ¹³C NMR (126 MHz, $CDCl_3$): δ 166.3 (d, $J = 254.3$ Hz), 157.5 (d, $J = 12.5$ Hz), 143.7, 133.6, 132.0 130.7 (d, $J = 10.4$ Hz), 130.5, 130.4,

130.0, 128.8, 127.7, 123.6, 110.9 (d, $J = 22.3$ Hz), 109.4 (d, $J = 23.7$ Hz), 73.8, 59.6, 51.5, 44.3, 38.8, 24.7, 22.7, 22.0;

HRMS calculated for $C_{22}H_{24}ClFN_4O_3SNa$ ($M+Na$)⁺ 501.1139; found 501.1156 (TOF MS ES⁺).

(S)-3-Benzyl-7-fluoro-2-((1-(4-methoxybenzyl)-1*H*-1,2,3-triazol-4-yl)methyl)-3,4-dihydro-2*H*-benzo[*b*][1,4,5]oxathiazepine 1,1-dioxide, Library Member 2.2.9{2.2.11}.



Utilizing general procedure **A**, **2.2.9{2.2.11}** (52 mg, 0.102 mmol, 63%) was isolated as an off white solid.

$[\alpha]_D^{20} = -67.4^\circ$ ($c = 1.0$, CH_2Cl_2);

MP = 176 °C;

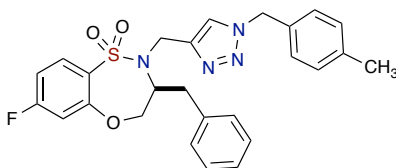
FTIR (neat): 2956, 2933, 2358, 1602, 1583, 1514, 1477, 1330, 1249, 1161, 1074, 1031 cm^{-1} ;

¹H NMR (400 MHz, $CDCl_3$): δ 7.76 (dd, $J = 8.9, 6.3$ Hz, 1H), 7.30–7.23 (m, 3H), 7.21–7.16 (m, 2H), 7.11 (d, $J = 8.6$ Hz, 2H), 6.90–6.84 (m, 2H), 6.84–6.78 (m, 2H), 6.57 (dd, $J = 9.6, 2.3$ Hz, 1H), 5.34–5.16 (m, 2H), 4.76 (t, $J = 11.6$ Hz, 1H), 4.38–4.22 (m, 3H), 4.17 (d, $J = 15.5$ Hz, 1H), 3.81 (s, 3H), 3.04 (dd, $J = 13.6, 8.6$ Hz, 1H), 2.81 (dd, $J = 13.7, 6.6$ Hz, 1H).

^{13}C NMR (126 MHz, CDCl_3): δ 165.1, (d, $J = 254.4$ Hz), 159.9, 157.3 (d, $J = 12.7$ Hz), 142.7, 137.1, 130.4 (d, $J = 10.6$ Hz), 129.6 (2C), 129.5 (2C), 128.5 (2C), 128.2, 126.5, 126.1, 122.6, 114.5 (2C), 110.6 (d, $J = 22.4$ Hz), 108.6 (d, $J = 23.8$ Hz), 73.8, 62.6, 55.3, 53.6, 45.9, 36.7;

HRMS calculated for $\text{C}_{26}\text{H}_{26}\text{FN}_4\text{O}_4\text{S}$ ($\text{M}+\text{H}$) $^+$ 509.1659, found 509.1628 (TOF MS ES+).

(S)-3-Benzyl-7-fluoro-2-((1-(4-methylbenzyl)-1*H*-1,2,3-triazol-4-yl)methyl)-3,4-dihydro-2*H*-benzo[*b*][1,4,5]oxathiazepine 1,1-dioxide, Library Member 2.2.9{2.2.12}.



Utilizing general procedure A, 2.2.9{2.2.12} (67 mg, 0.136 mmol, 89%) was isolated as a white solid.

$[\alpha]_D^{20} = -100.1^\circ$ ($c = 0.9$, CH_2Cl_2);

MP = 164 °C;

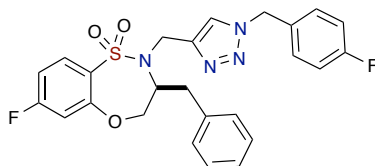
FTIR (neat): 3028, 2923, 2358, 1602, 1581, 1477, 1419, 1330, 1161, 1074 cm^{-1} ;

^1H NMR (400 MHz, CDCl_3): δ 7.76 (dd, $J = 8.8, 6.3$ Hz, 1H), 7.31–7.23 (m, 3H), 7.21–7.13 (m, 4H), 7.06 (d, $J = 8.0$ Hz, 2H), 6.84–6.78 (m, 2H), 6.57 (dd, $J = 9.6, 2.2$ Hz, 1H), 5.32 (d, $J = 14.6$ Hz, 1H), 5.22 (d, $J = 14.6$ Hz, 1H), 4.76 (t, $J = 11.5$ Hz, 1H), 4.39–4.23 (m, 3H), 4.18 (d, $J = 15.5$ Hz, 1H), 3.05 (dd, $J = 13.5, 8.5$ Hz, 1H), 2.82 (dd, $J = 13.6, 6.5$ Hz, 1H), 2.35 (s, 3H).

^{13}C NMR (126 MHz, CDCl_3): δ 166.1 (d, $J = 254.4$ Hz), 157.4 (d, $J = 12.7$ Hz), 142.7, 138.8, 137.1, 131.1, 130.5 (d, $J = 10.6$ Hz), 129.7 (2C), 129.5 (2C), 128.5 (2C), 128.1 (2C), 126.5, 122.7, 110.7, 110.6 (d, $J = 22.4$ Hz), 108.6 (d, $J = 24.3$ Hz), 73.8, 62.6, 53.4, 45.9, 36.7, 21.1.

HRMS calculated for $\text{C}_{26}\text{H}_{25}\text{FN}_4\text{O}_3\text{SNa}$ ($\text{M}+\text{Na}$) $^+$ 515.1529; found 515.1527 (TOF MS ES+).

(S)-3-Benzyl-7-fluoro-2-((1-(4-fluorobenzyl)-1*H*-1,2,3-triazol-4-yl)methyl)-3,4-dihydro-2*H*-benzo[*b*][1,4,5]oxathiazepine 1,1-dioxide, Library Member 2.2.9{2.2.14}.



Utilizing general procedure **A**, **2.2.9{2.2.14}** (62 mg, 0.124 mmol, 82%) was isolated as a white solid.

$[\alpha]_D^{20} = -75.8^\circ$ ($c = 0.8$, CH_2Cl_2);

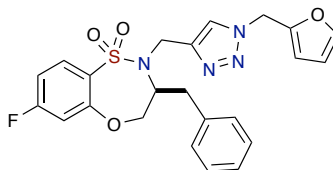
MP = 182 °C; FTIR (neat): 3136, 2952, 2339, 1602, 1512, 1419, 1328, 1265, 1224, 1161, 1074 cm^{-1} ;

^1H NMR (400 MHz, CDCl_3): δ 7.78 (dd, $J = 8.9, 6.2$ Hz, 1H), 7.32–7.24 (m, 3H), 7.23–7.15 (m, 4H), 7.08–7.02 (m, 2H), 6.86–6.80 (m, 2H), 6.59 (dd, $J = 9.6, 2.3$ Hz, 1H), 5.37–5.21 (m, 2H), 4.77 (t, $J = 11.8$ Hz, 1H), 4.40–4.24 (m, 3H), 4.23–4.16 (m, 1H), 3.07 (dd, $J = 13.7, 8.8$ Hz, 1H), 2.82 (dd, $J = 13.7, 6.5$ Hz, 1H).

^{13}C NMR (126 MHz, CDCl_3): δ 164.1 (d, $J = 254.5$ Hz), 161.1 (d, $J = 248.5$ Hz), 156.4 (d, $J = 12.6$ Hz), 142.0, 136.1, 129.5 (d, $J = 10.6$ Hz), 129.1 (d, $J = 3.3$ Hz), 128.9 (d, $J = 8.4$ Hz, 2C), 128.5 (2C), 127.5 (2C), 127.2, 125.5 (2C), 121.7, 115.1 (d, $J = 21.7$ Hz), 109.6 (d, $J = 22.3$ Hz), 107.5 (d, $J = 24.1$ Hz), 72.8, 61.7, 52.3, 44.8, 35.6.

HRMS calculated for $\text{C}_{25}\text{H}_{22}\text{F}_2\text{N}_4\text{O}_3\text{SNa}$ ($\text{M}+\text{Na}$) $^+$ 519.1278; found 519.1257 (TOF MS ES+).

(S)-3-Benzyl-7-fluoro-2-((1-(furan-2-ylmethyl)-1*H*-1,2,3-triazol-4-yl)methyl)-3,4-dihydro-2*H*-benzo[*b*][1,4,5]oxathiazepine 1,1-dioxide, Library Member 2.2.9{2.2.19}.



Utilizing general procedure **A**, **2.2.9{2.2.19}** (57 mg, 0.121 mmol, 79%) was isolated as a white solid.

$[\alpha]_D^{20} = -71.7^\circ$ ($c = 1.0$, CH_2Cl_2); MP = 145 °C;

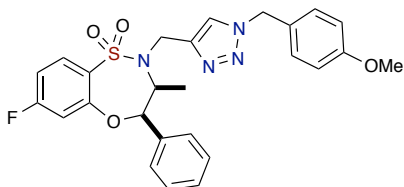
FTIR (neat): 2925, 2854, 2349, 1604, 1583, 1477, 1419, 1330, 1161, 1074 cm^{-1}

^1H NMR (400 MHz, CDCl_3): δ 7.78 (dd, $J = 8.9, 6.2$ Hz, 1H), 7.39 (t, $J = 1.3$ Hz, 1H), 7.30–7.22 (m, 3H), 7.23–7.18 (m, 2H), 6.93 (s, 1H), 6.82 (ddd, $J = 8.9, 7.6, 2.5$ Hz, 1H), 6.61 (dd, $J = 9.6, 2.4$ Hz, 1H), 6.37 (d, $J = 1.4$ Hz, 2H), 5.36 (d, $J = 15.4$ Hz, 1H), 5.27 (d, $J = 15.4$ Hz, 1H), 4.77 (t, $J = 11.8$ Hz, 1H), 4.38–4.23 (m, 3H), 4.19 (d, $J = 15.5$ Hz, 1H), 3.06 (dd, $J = 13.6, 8.7$ Hz, 1H), 2.81 (dd, $J = 13.7, 6.4$ Hz, 1H).

^{13}C NMR (126 MHz, CDCl_3): δ 165.1(d, $J = 254.4$ Hz), 157.4 (d, $J = 12.7$ Hz), 146.8, 143.7, 142.7, 137.1, 130.5 (d, $J = 10.6.4$ Hz), 129.5 (2C), 128.5 (2C), 128.1, 126.5, 122.8, 110.8, 110.6 (d, $J = 22.4$ Hz), 110.4, 108.6 (d, $J = 24.1$ Hz), 73.8, 62.7, 46.5, 45.9, 36.7;

HRMS calculated for $\text{C}_{23}\text{H}_{21}\text{FN}_4\text{O}_4\text{SNa}$ ($\text{M}+\text{Na}$) $^+$ 491.1165; found 491.1184 (TOF MS ES+).

(3*S*,4*R*)-7-Fluoro-2-((1-(4-methoxybenzyl)-1*H*-1,2,3-triazol-4-yl)methyl)-3-methyl-4-phenyl-3,4-dihydro-2*H*-benzo[*b*][1,4,5]oxathiazepine 1,1-dioxide, Library Member 2.2.10{2.2.11}.



Utilizing general procedure **A**, **2.2.10{2.2.11}** (58 mg, 0.114 mmol, 68%) was isolated as a thick liquid.

$[\alpha]_D^{20} = +218.1^\circ$ ($c = 1.0$, CH_2Cl_2);

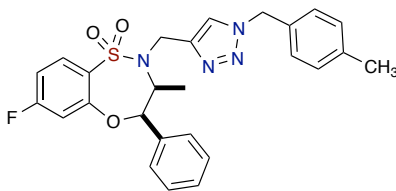
FTIR (neat): 3137, 2941, 1589, 1514, 1471, 1340, 1240, 1249, 1164, 1153, 1120, 1072, 1000 cm^{-1}

^1H NMR (400 MHz, CDCl_3): δ 7.81 (dd, $J = 8.7, 6.2$ Hz, 1H), 7.46–7.36 (m, 5H), 7.35–7.29 (m, 1H), 7.18–7.12 (m, 2H), 6.90–6.80 (m, 4H), 5.45 (d, $J = 14.6$ Hz, 1H), 5.33 (d, $J = 14.6$ Hz, 1H), 4.96 (s, 1H), 4.67 (d, $J = 15.5$ Hz, 1H), 4.53 (d, $J = 15.5$ Hz, 1H), 3.95–3.85 (m, 1H), 3.81 (s, 3H), 1.30 (d, $J = 7.2$ Hz, 3H).

^{13}C NMR (126 MHz, CDCl_3): δ 165.4 (d, $J = 255.9$ Hz), 160.0, 157.8 (d, $J = 12.2$ Hz), 143.6, 137.8, 131.9, 129.8 (d, $J = 254.4$ Hz), 129.6 (2C) 128.5 (2C), 127.8, 126.1, 125.4 (2C), 122.8, 114.5 111.7 (d, $J = 22.2$ Hz), 111.4 (d, $J = 23.3$ Hz, 2C), 83.3, 61.9, 53.8, 53.6, 46.1, 14.2;

HRMS calculated for $\text{C}_{26}\text{H}_{25}\text{FN}_4\text{O}_4\text{SNa}$ ($\text{M}+\text{Na}$) $^+$ 531.1478; found 531.1465 (TOF MS ES $^+$).

(3*S*,4*R*)-7-Fluoro-3-methyl-2-((1-(4-methylbenzyl)-1*H*-1,2,3-triazol-4-yl)methyl)-4-phenyl-3,4-dihydro-2*H*-benzo[*b*][1,4,5]oxathiazepine 1,1-dioxide, Library Member 2.2.10{2.2.12}.



Utilizing general procedure **A**, **2.2.10{2.2.12}** (56 mg, 0.113 mmol, 75%) was isolated as a thick liquid.

$[\alpha]_D^{20} = -79.3^\circ$ ($c = 1.0$, CH_2Cl_2); FTIR (neat): 3173, 2943, 2389, 2333, 1589, 1471, 1421, 1340, 1164, 1072, 1000 cm^{-1} ;

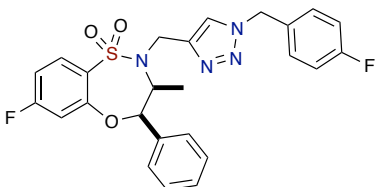
^1H NMR (400 MHz, CDCl_3): δ 7.84–7.78 (m, 1H), 7.47–7.38 (m, 5H), 7.33 (ddd, $J = 7.0, 3.8, 1.4$ Hz, 1H), 7.16 (d, $J = 8.0$ Hz, 2H), 7.10 (d, $J = 8.1$ Hz, 2H), 6.89–6.81 (m, 2H), 5.47 (d, $J = 14.7$ Hz, 1H), 5.36 (d, $J = 14.6$ Hz, 1H), 4.98 (d, $J = 1.5$ Hz, 1H), 4.68 (d, $J = 15.5$ Hz, 1H), 4.54 (d, $J = 15.5$ Hz, 1H), 3.93–3.90 (m, 1H), 2.37 (s, 3H), 1.30 (d, $J = 7.2$ Hz, 3H).

^{13}C NMR (126 MHz, CDCl_3): δ 165.4 (d, $J = 256.0$ Hz), 157.8 (d, $J = 12.2$ Hz), 143.7, 138.9, 137.8, 131.9, 131.1, 130.0 (2C), 129.8 (d, $J = 10.6$ Hz), 128.5 (2C), 128.1 (2C), 127.8, 125.4 (2C), 122.9, 111.7 (d, $J = 22.2$ Hz), 111.32 (d, $J = 23.4$ Hz), 83.3, 61.9, 54.2, 46.0, 21.2, 14.2.

HRMS calculated for $\text{C}_{26}\text{H}_{25}\text{FN}_4\text{O}_3\text{SNa}$ ($\text{M}+\text{Na}$) $^+$ 515.1529, found 515.1530 (TOF MS ES+).

(3*S*,4*R*)-7-Fluoro-2-((1-(4-fluorobenzyl)-1*H*-1,2,3-triazol-4-yl)methyl)-3-methyl-4-phenyl-3,4-dihydro-2*H*-benzo[*b*][1,4,5]oxathiazepine 1,1-dioxide, Library

Member 2.2.10{2.2.14}.



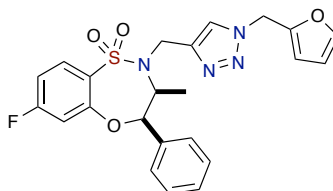
Utilizing general procedure **A**, **2.2.10{2.2.14}** (55 mg, 0.110 mmol, 72%) was isolated as a thick liquid. $[\alpha]_D^{20} = +80.0^\circ$ ($c = 0.9$, CH_2Cl_2);

FTIR (neat): 3070, 2943, 2358, 2341, 1589, 1512, 1473, 1421, 1224, 1164, 1072, 1000 cm^{-1}

^1H NMR (400 MHz, CDCl_3): δ 7.83 (dd, $J = 8.7, 6.2$ Hz, 1H), 7.48 (s, 1H), 7.46–7.37 (m, 4H), 7.35–7.30 (m, 1H), 7.24–7.17 (m, 2H), 7.07–6.98 (m, 2H), 6.88 (ddd, $J = 11.5, 8.5, 2.4$ Hz, 2H), 5.49 (d, $J = 14.8$ Hz, 1H), 5.39 (d, $J = 14.8$ Hz, 1H), 5.01 (d, $J = 1.2$ Hz, 1H), 4.69 (d, $J = 15.6$ Hz, 1H), 4.51 (d, $J = 15.5$ Hz, 1H), 3.90 (qd, $J = 7.2, 2.2$ Hz, 1H), 1.30 (d, $J = 7.2$ Hz, 3H). ^{13}C NMR (126 MHz, CDCl_3): δ 166.5 (d, $J = 256.1$ Hz), 162.9 (d, $J = 248.7$ Hz), 157.9 (d, $J = 12.2$ Hz), 157.8, 144.1, 137.7, 131.7, 130.1 (d, $J = 3.4$ Hz), 130.0, 129.9, 129.8, 128.5 (2C), 127.9, 125.9 (2C), 123.0, 116.2 (d, $J = 21.8$ Hz), 111.8 (d, $J = 22.2$ Hz), 111.3 (d, $J = 23.3$ Hz), 83.3, 62.0, 53.5, 45.9 14.3;

HRMS calculated for $\text{C}_{25}\text{H}_{22}\text{F}_2\text{N}_4\text{O}_3\text{S}$ ($\text{M}+\text{Na}$) $^+$ 519.1278; found 519.1277 (TOF MS ES+).

(3*S*,4*R*)-7-Fluoro-2-((1-(furan-2-ylmethyl)-1*H*-1,2,3-triazol-4-yl)methyl)-3-methyl-4-phenyl-3,4-dihydro-2*H*-benzo[*b*][1,4,5]oxathiazepine 1,1-dioxide, Library Member 2.2.10{2.2.19}.



Utilizing general procedure **A**, **2.2.10{2.2.19}** (53 mg, 0.113 mmol, 75%) was isolated as a thick liquid.

$[\alpha]_D^{20} = +96.8^\circ$ ($c = 0.8$, CH_2Cl_2);

FTIR (neat): 2943, 2358, 1589, 1473, 1340, 1164, 1153, 1118, 1164, 1153, 1074, 1010 cm^{-1}

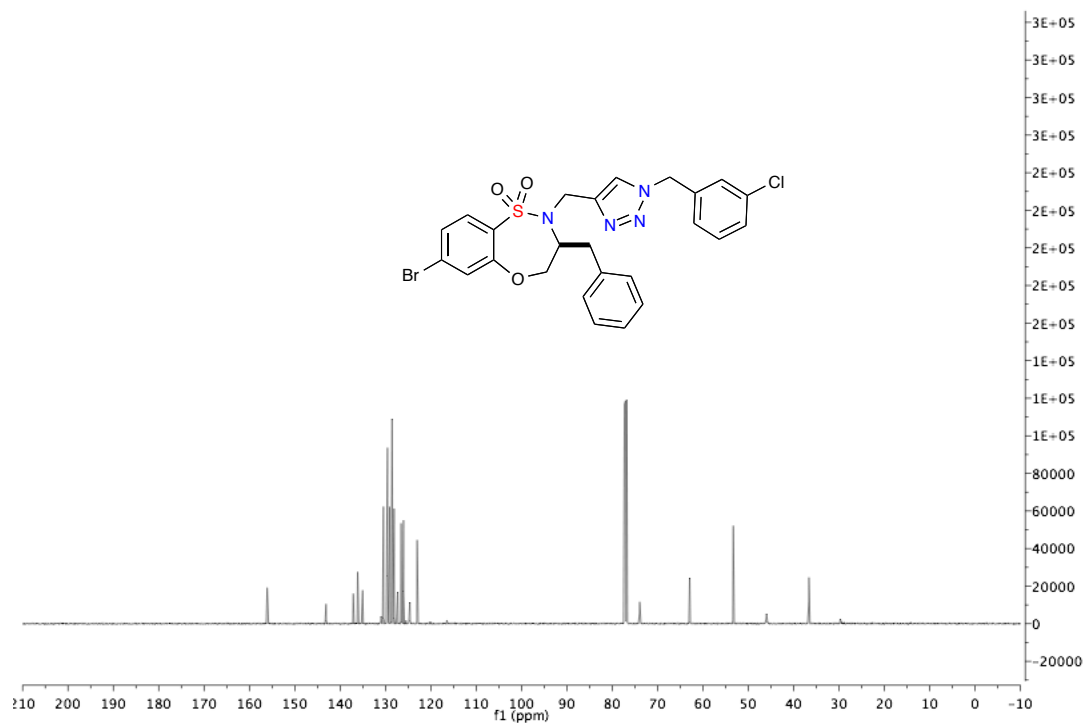
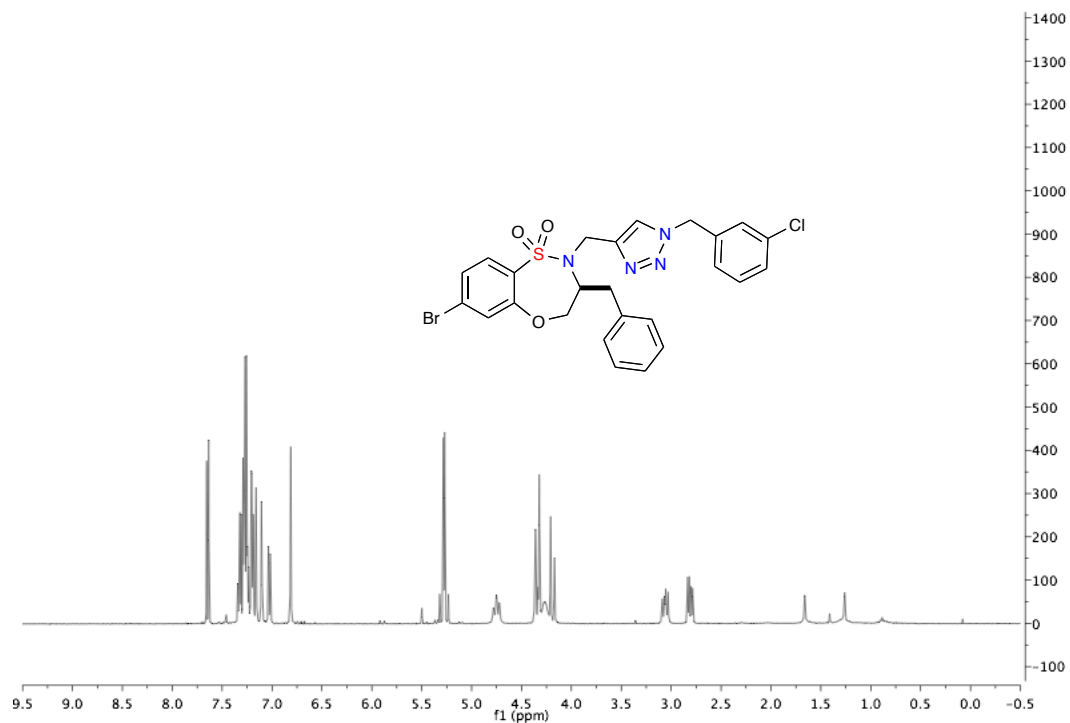
^1H NMR (400 MHz, CDCl_3): δ 7.84 (dd, $J = 8.7, 6.2$ Hz, 1H), 7.56 (s, 1H), 7.46–7.37 (m, 5H), 7.35–7.29 (m, 1H), 6.95–6.85 (m, 2H), 6.44–6.37 (m, 2H), 5.51 (d, $J = 15.5$ Hz, 1H), 5.44 (d, $J = 15.5$ Hz, 1H), 5.03 (s, 1H), 4.70 (d, $J = 15.5$ Hz, 1H), 4.52 (d, $J = 15.5$ Hz, 1H), 3.90 (qd, $J = 7.2, 2.3$ Hz, 1H), 1.31 (d, $J = 7.2$ Hz, 3H).

^{13}C NMR (126 MHz, CDCl_3): δ 166.5 (d, $J = 256.4$ Hz), 157.8 (d, $J = 12.1$ Hz), 146.7, 143.8, 143.7, 137.8, 131.8, 131.7, 129.8 (d, $J = 10.5$ Hz), 128.5 (2C), 127.8, 125.4 (2C), 123.0, 111.8, (d, $J = 22.2$ Hz), 111.4 (d, $J = 23.4$ Hz), 110.7 (d, $J = 42.7$ Hz), 83.2, 61.9, 46.8, 46.0, 14.3;

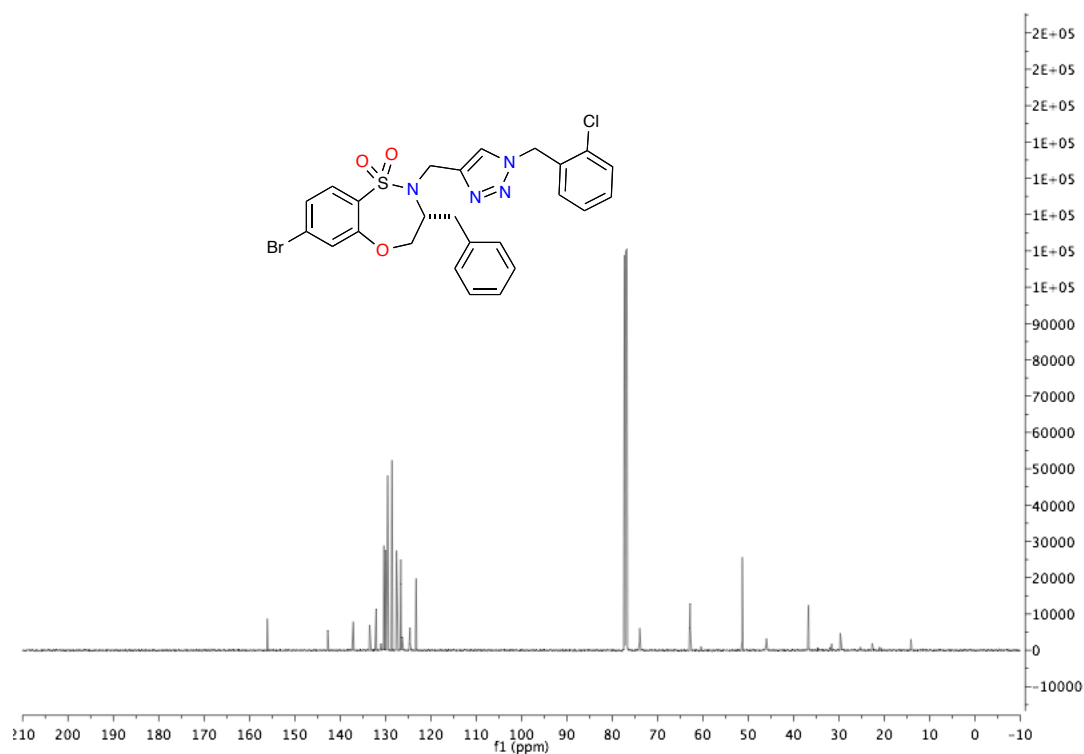
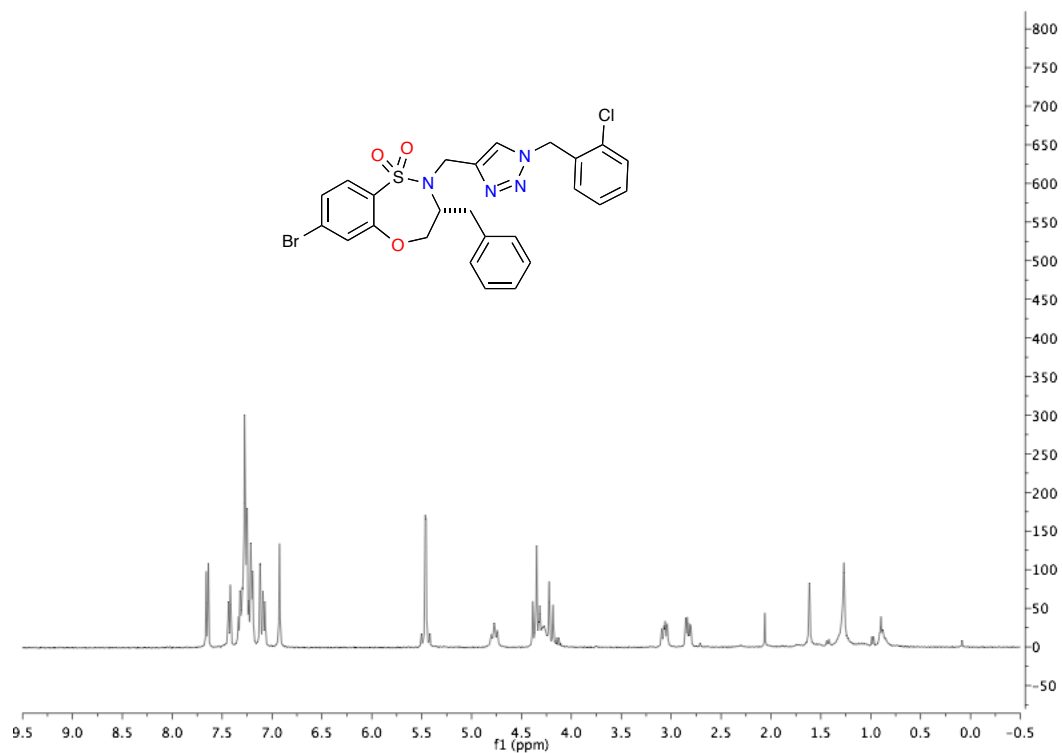
HRMS calculated for $\text{C}_{23}\text{H}_{21}\text{FN}_4\text{O}_4\text{SNa}$ ($\text{M}+\text{Na}$) $^+$ 491.1165; found 491.1131 (TOF MS ES+).

5.5 Spectra for Chapter 2.2

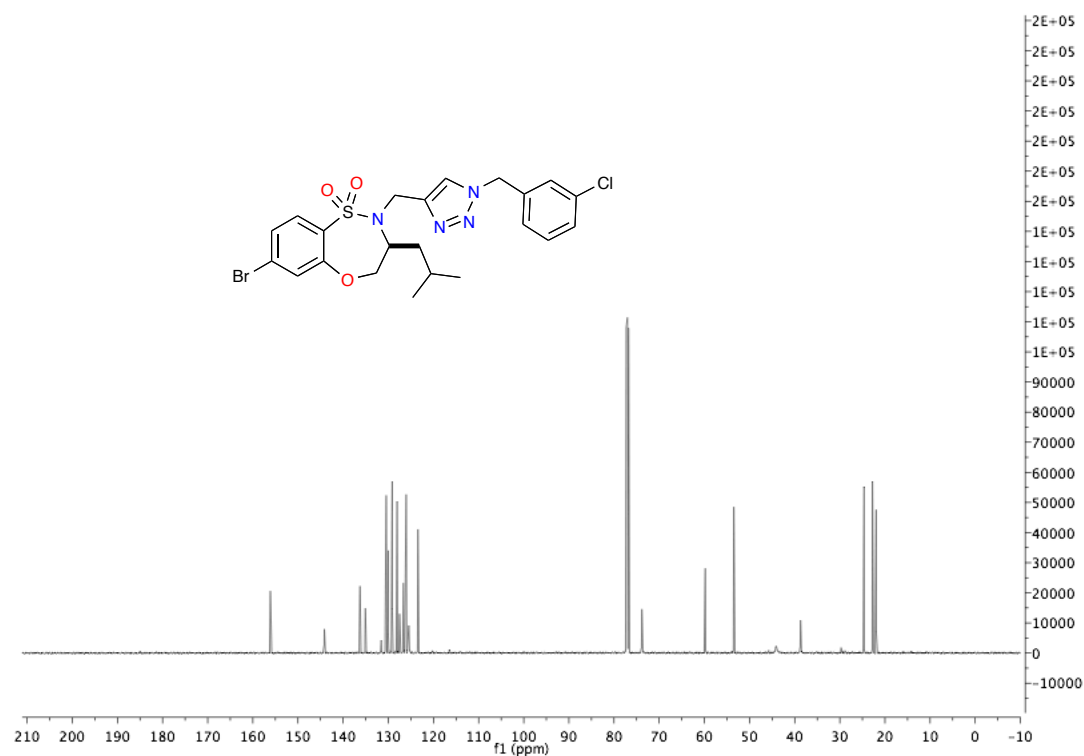
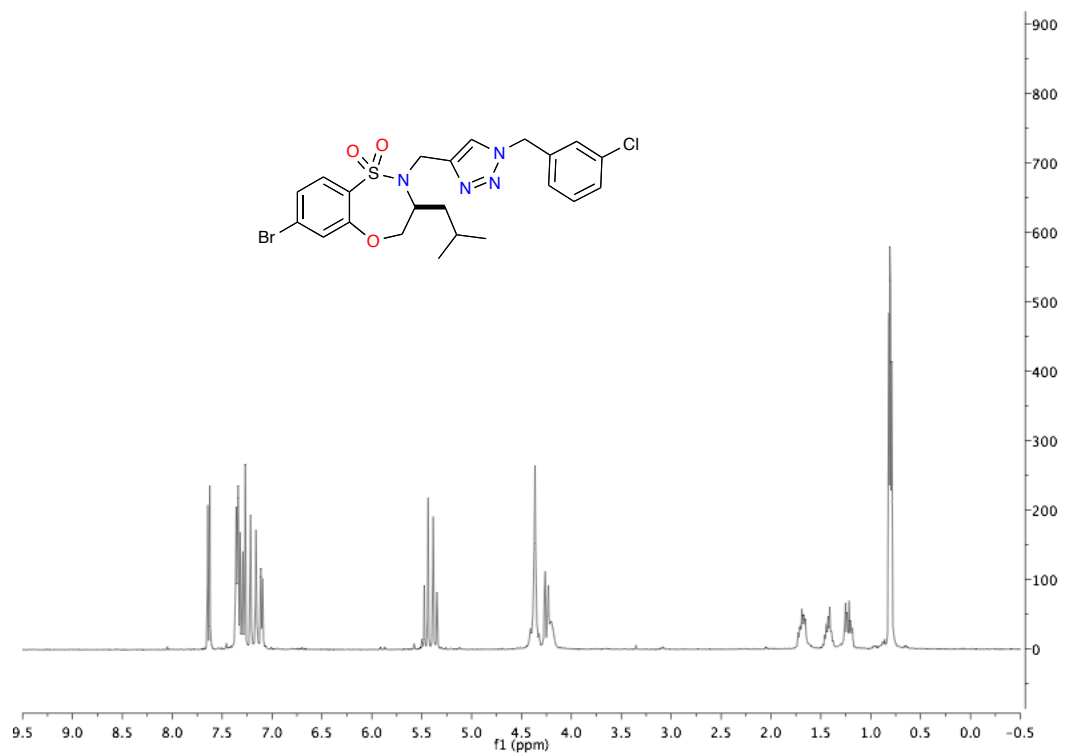
(*S*)-3-Benzyl-7-bromo-2-((1-(3-chlorobenzyl)-1*H*-1,2,3-triazol-4-yl)methyl)-3,4-dihydro-2*H*-benzo[*b*][1,4,5]oxathiazepine 1,1-dioxide, Library Member 2.2.1{2.2.2I}.



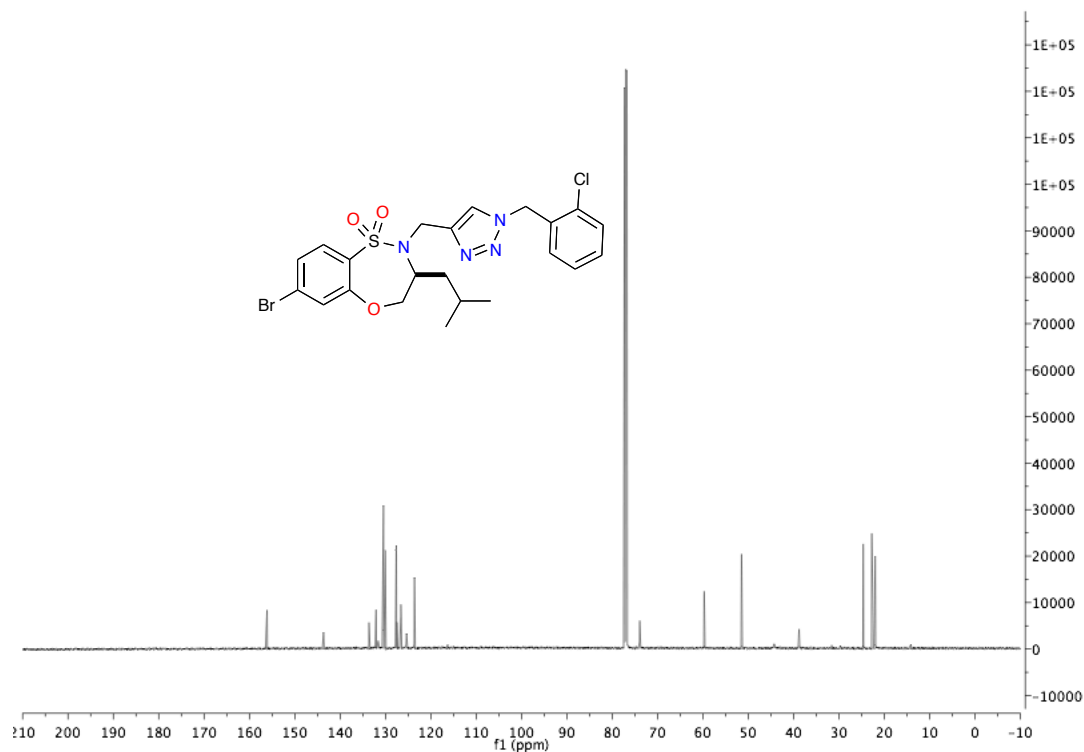
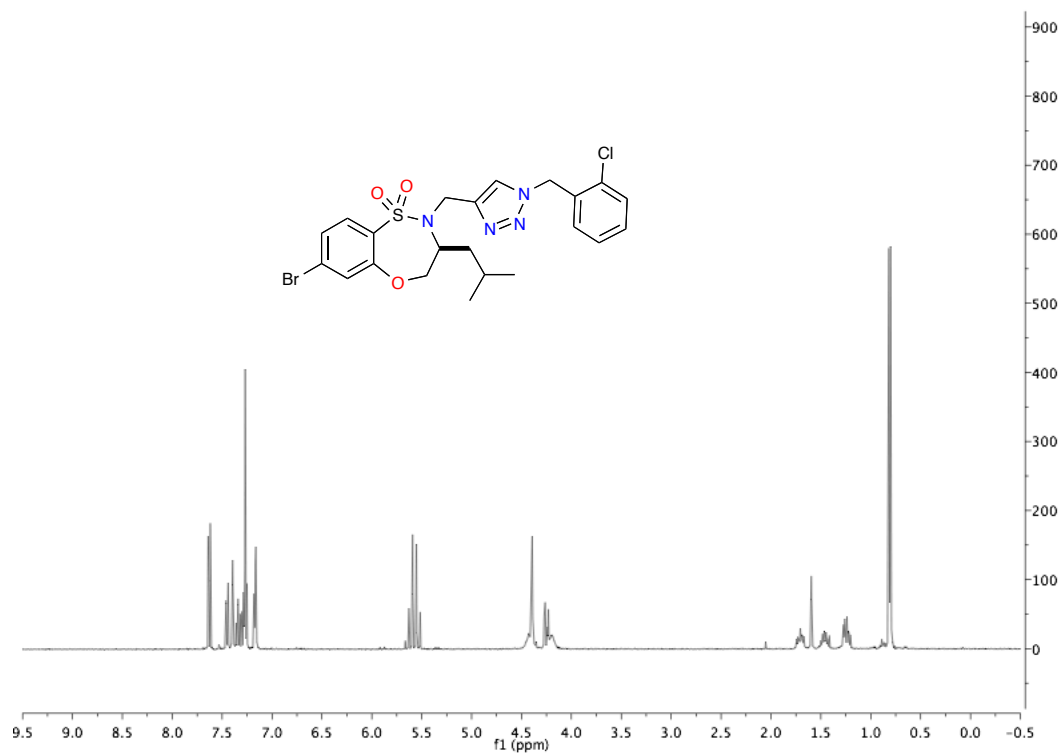
(R)-3-Benzyl-7-bromo-2-((1-(2-chlorobenzyl)-1H-1,2,3-triazol-4-yl)methyl)-3,4-dihydro-2H-benzo[b][1,4,5]oxathiazepine 1,1-dioxide, Library Member 2.2.2{2.2.22}.



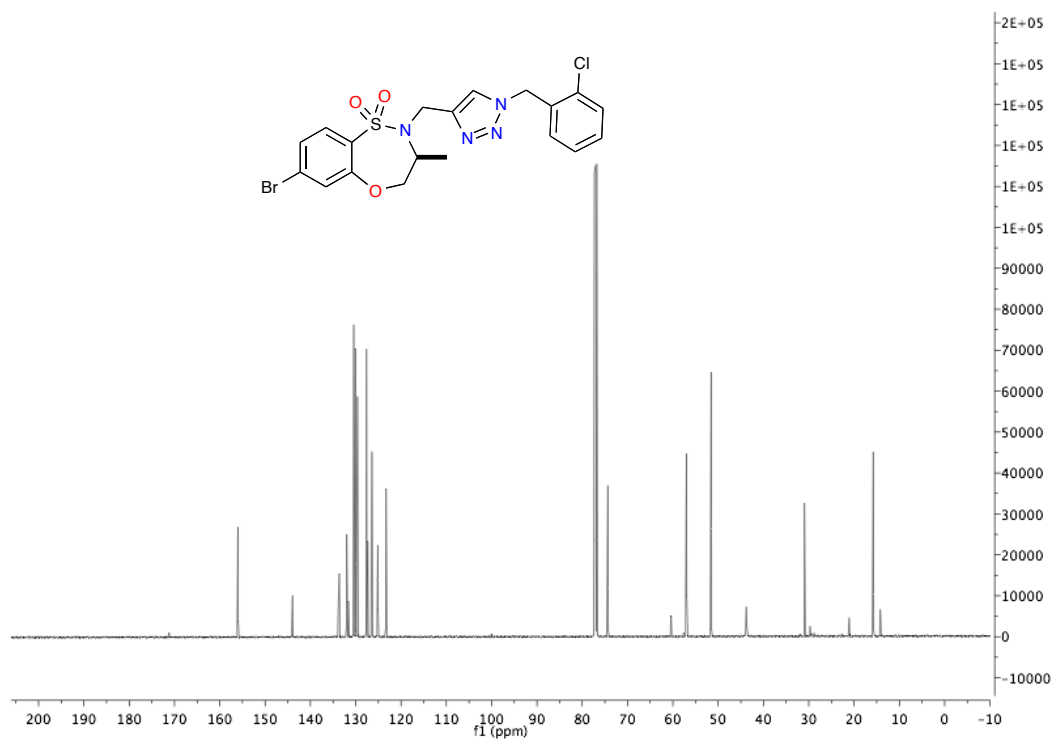
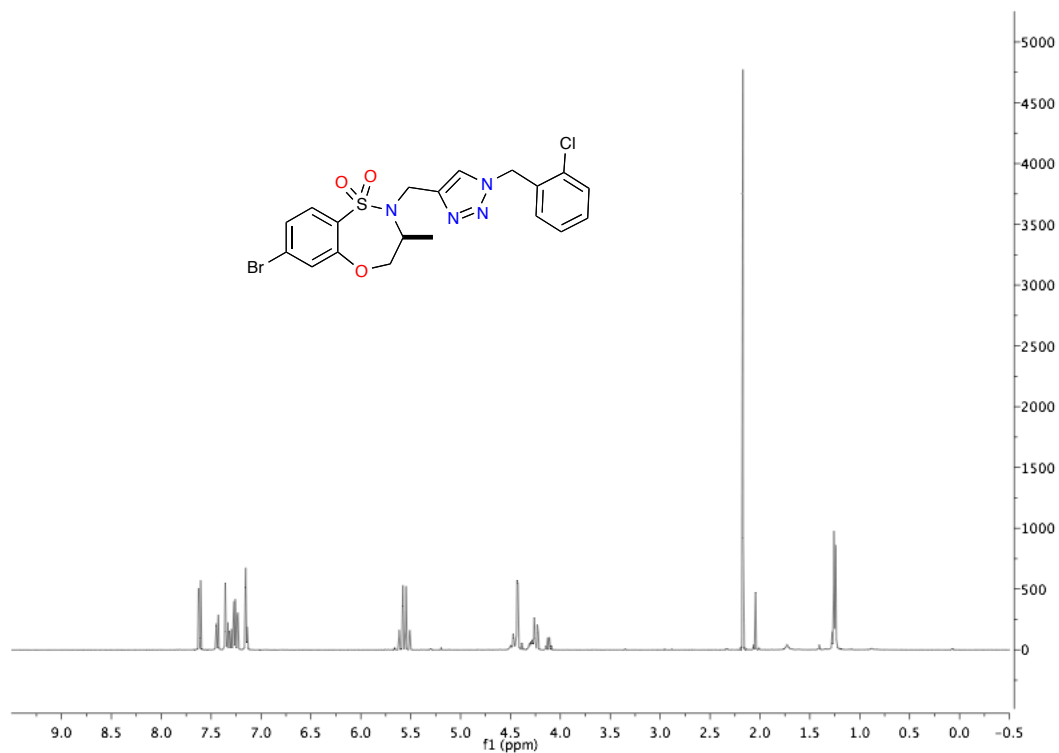
(S)-7-Bromo-2-((1-(3-chlorobenzyl)-1H-1,2,3-triazol-4-yl)methyl)-3-isobutyl-3,4-dihydro-2H-benzo[b][1,4,5]oxathiazepine 1,1-dioxide, Library Member 2.2.3{2.2.21}.



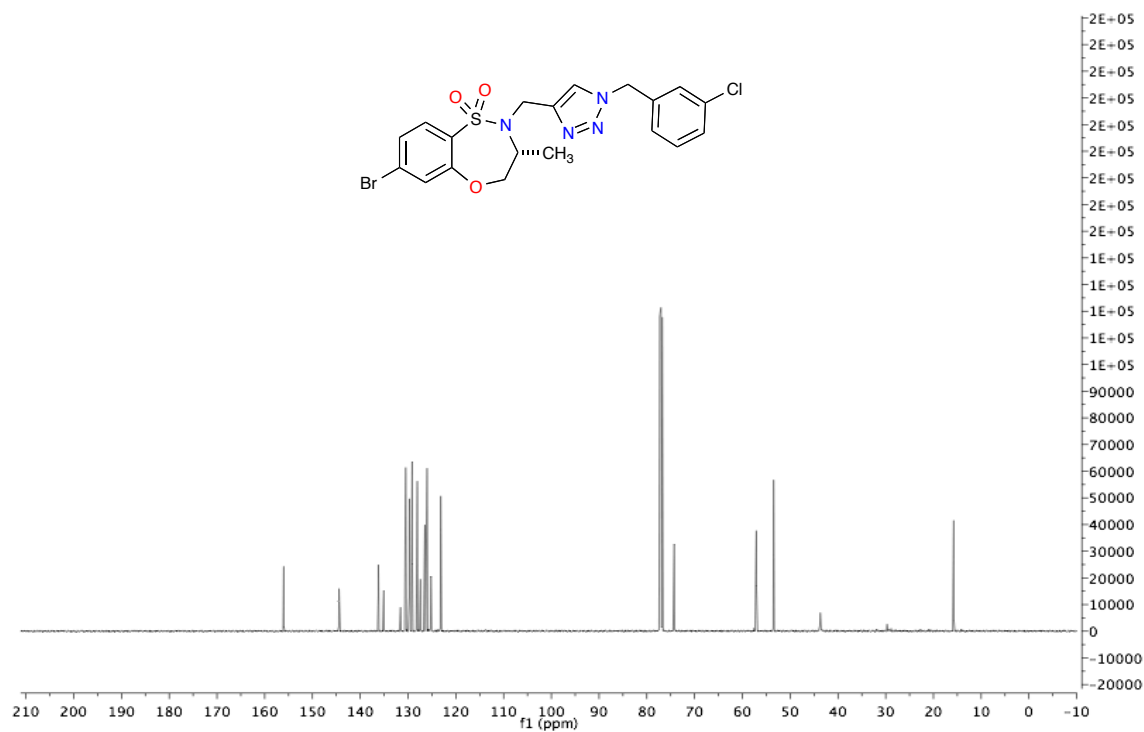
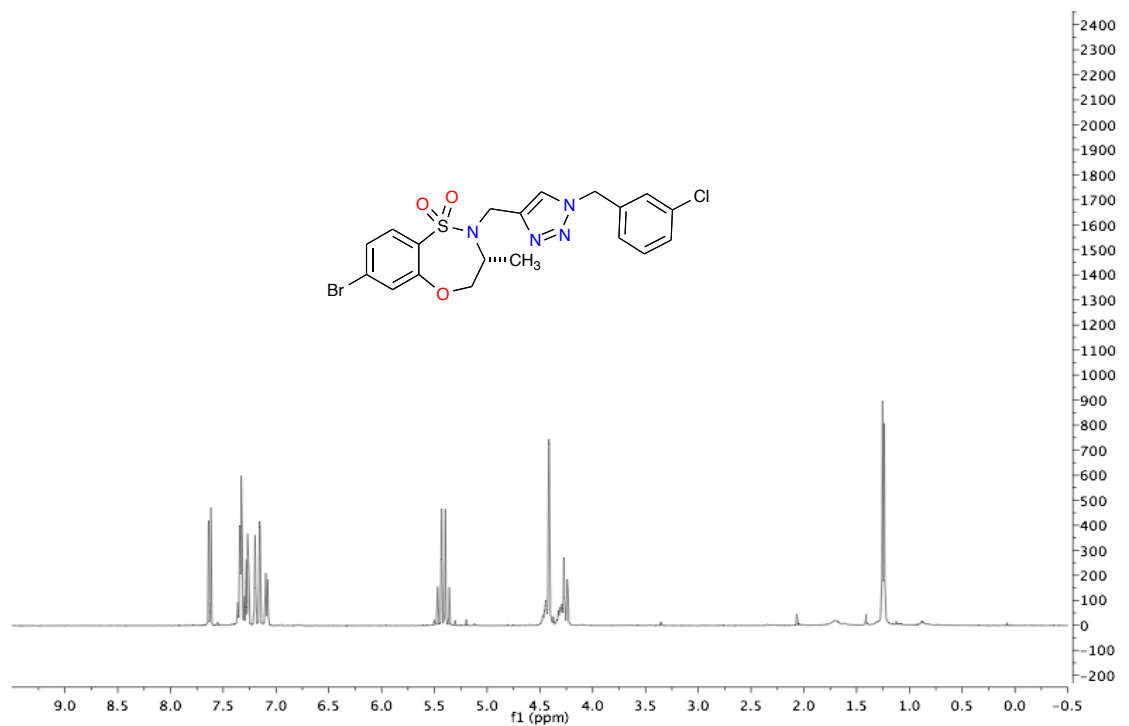
(S)-7-Bromo-2-((1-(2-chlorobenzyl)-1*H*-1,2,3-triazol-4-yl)methyl)-3-isobutyl-3,4-dihydro-2*H*-benzo[*b*][1,4,5]oxathiazepine 1,1-dioxide, Library Member 2.2.3{2.2.22}.



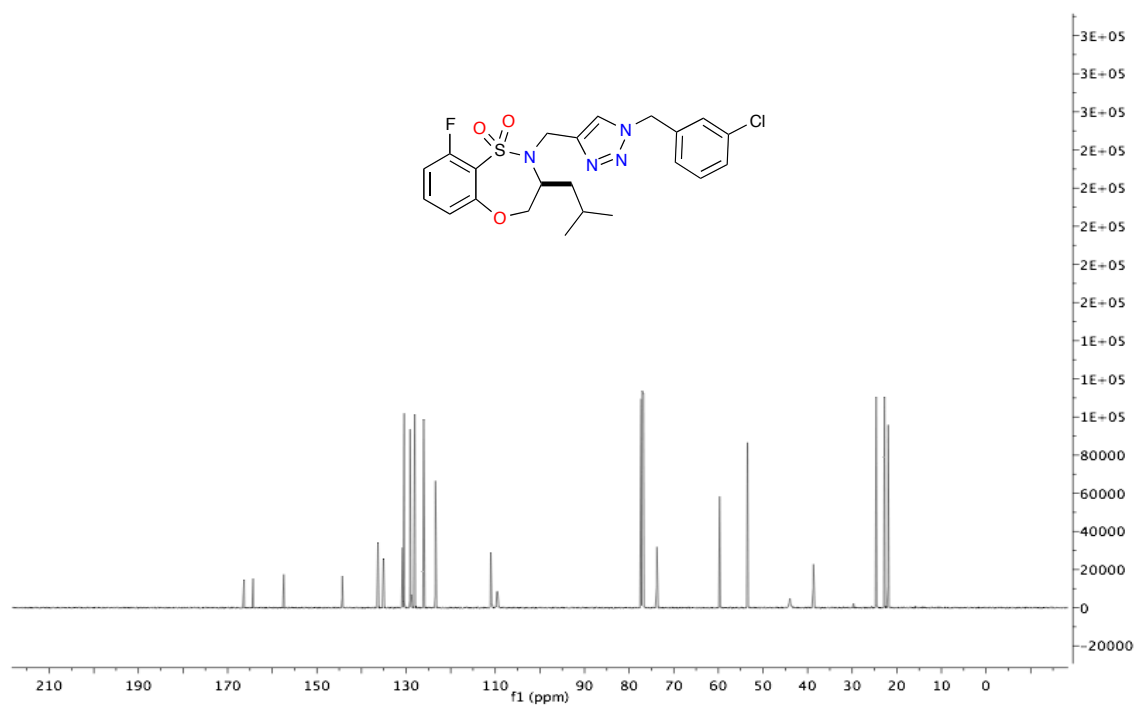
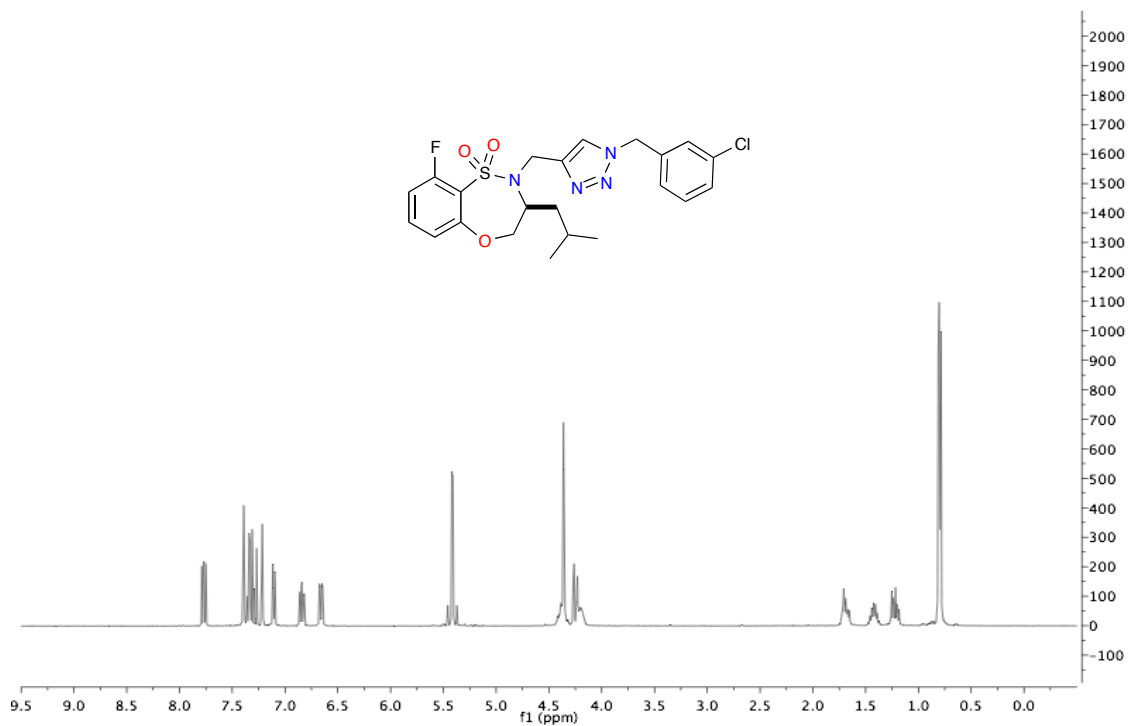
(S)-7-Bromo-2-((1-(2-chlorobenzyl)-1H-1,2,3-triazol-4-yl)methyl)-3-methyl-3,4-dihydro-2H-benzo[b][1,4,5]oxathiazepine 1,1-dioxide, Library Member 2.2.5{2.2.22}



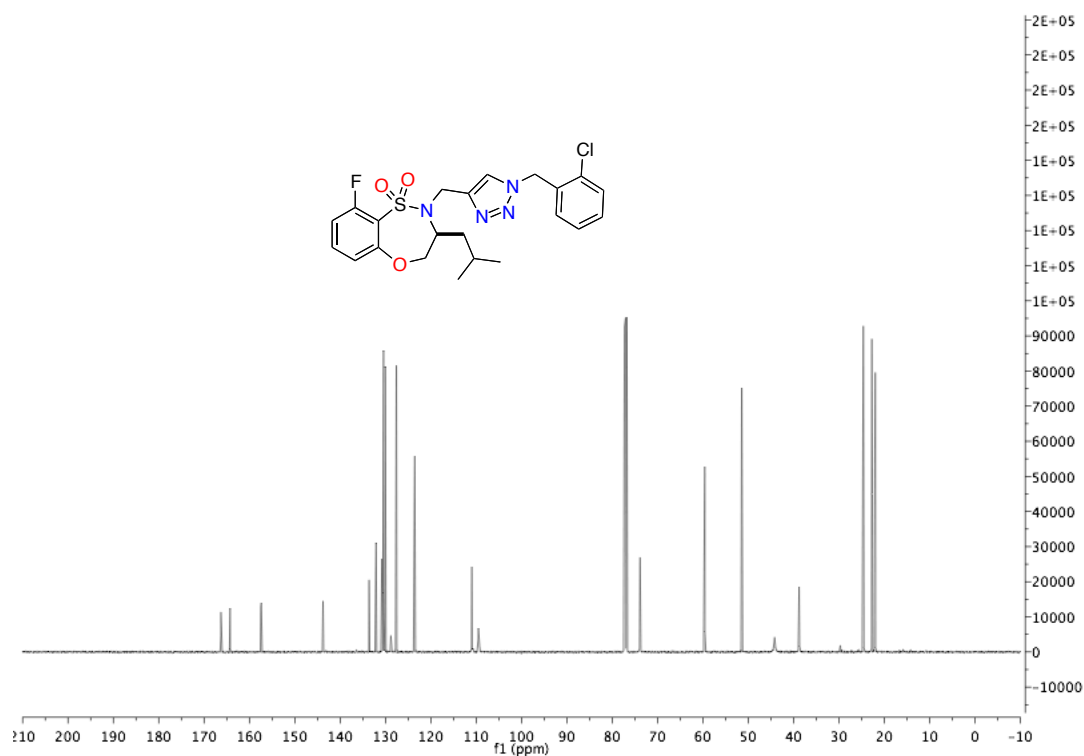
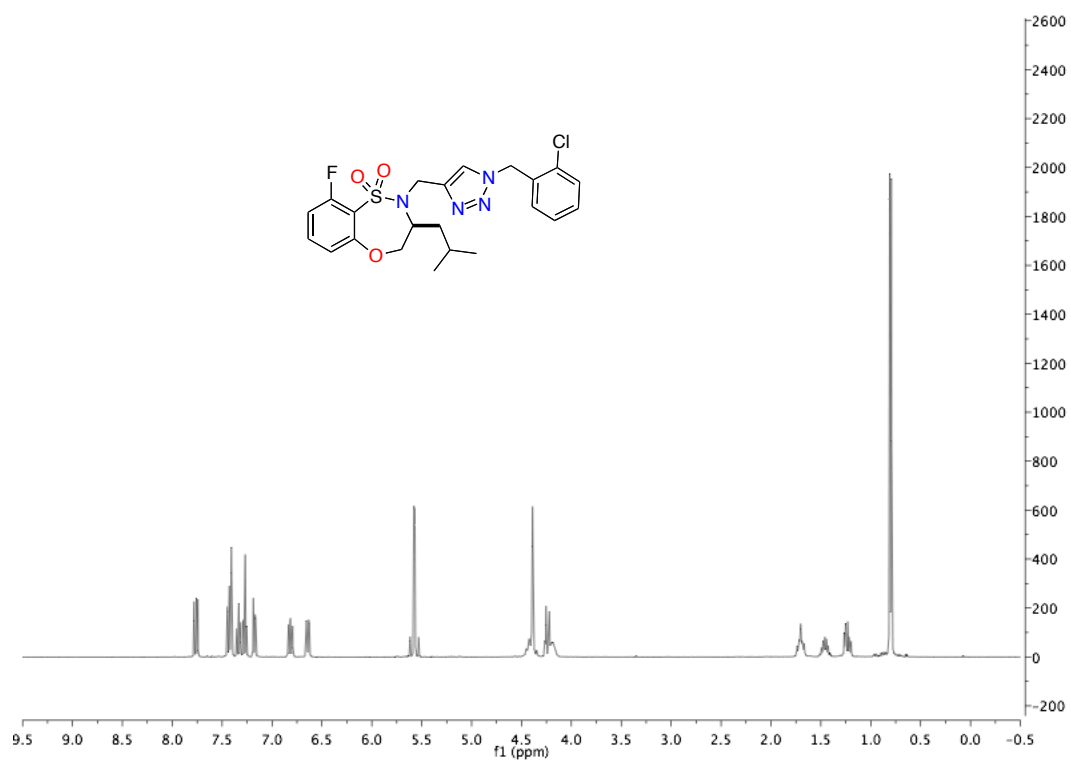
(R)-7-Bromo-2-((1-(3-chlorobenzyl)-1H-1,2,3-triazol-4-yl)methyl)-3-methyl-3,4-dihydro-2H-benzo[b][1,4,5]oxathiazepine 1,1-dioxide, Library Member 2.2.6{2.2.21}



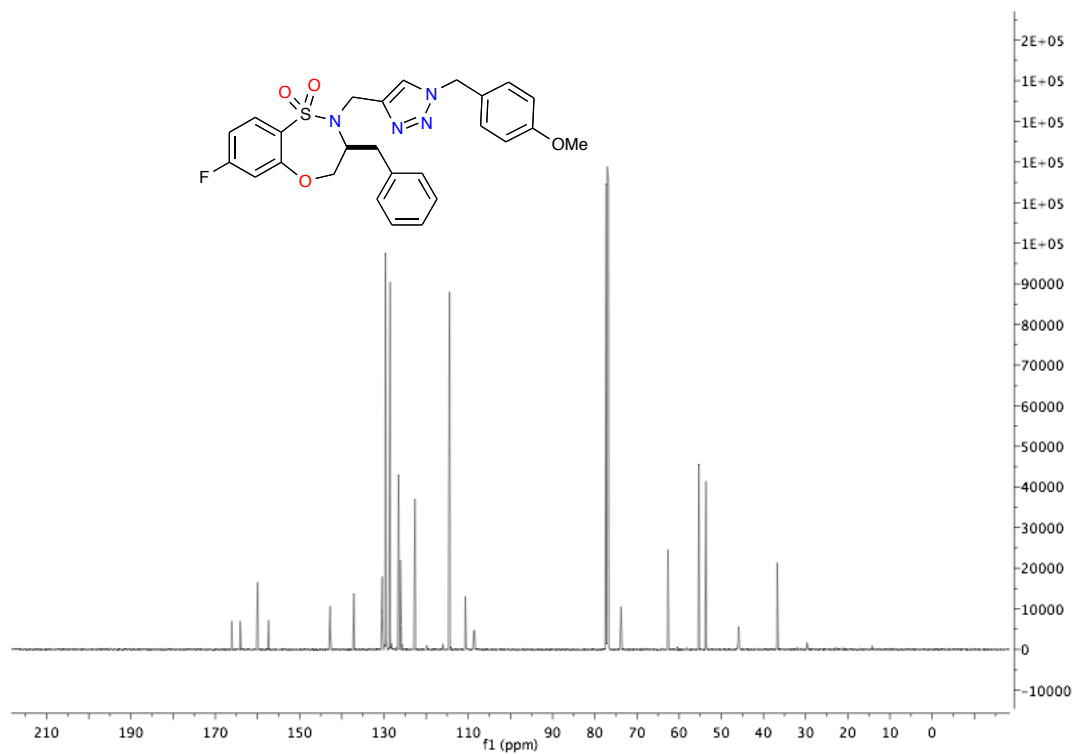
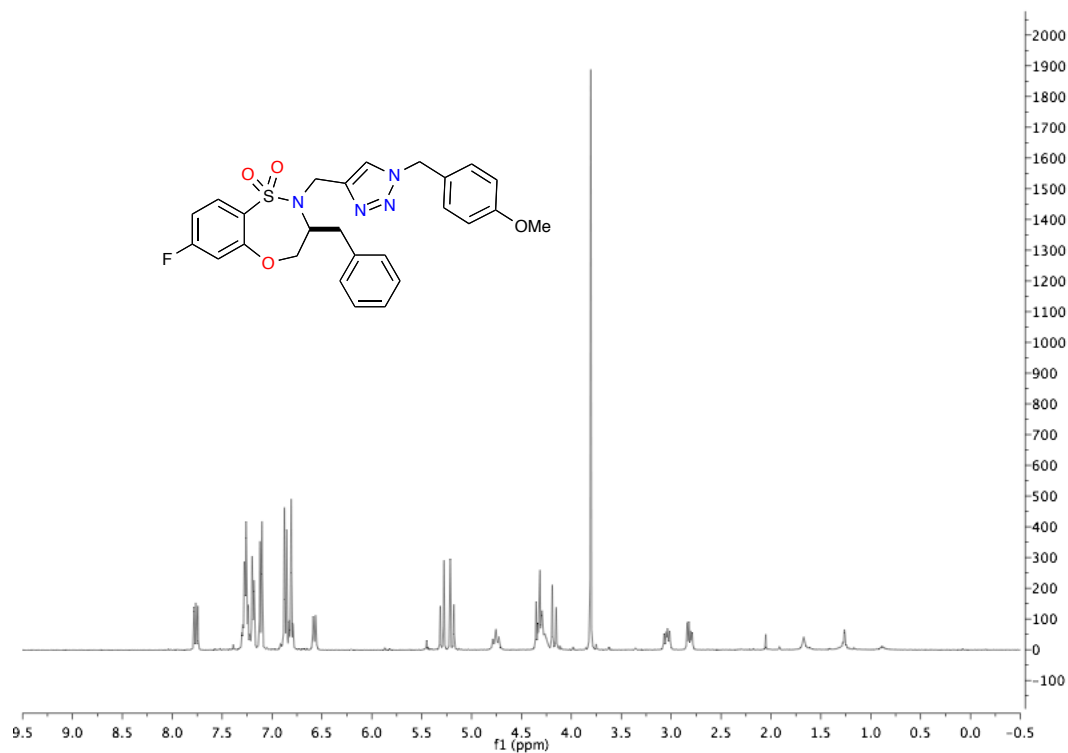
(S)-2-((1-(3-Chlorobenzyl)-1H-1,2,3-triazol-4-yl)methyl)-9-fluoro-3-isobutyl-3,4-dihydro-2H-benzo[b][1,4,5]oxathiazepine 1,1-dioxide, Library Member 2.2.8{2.2.21}



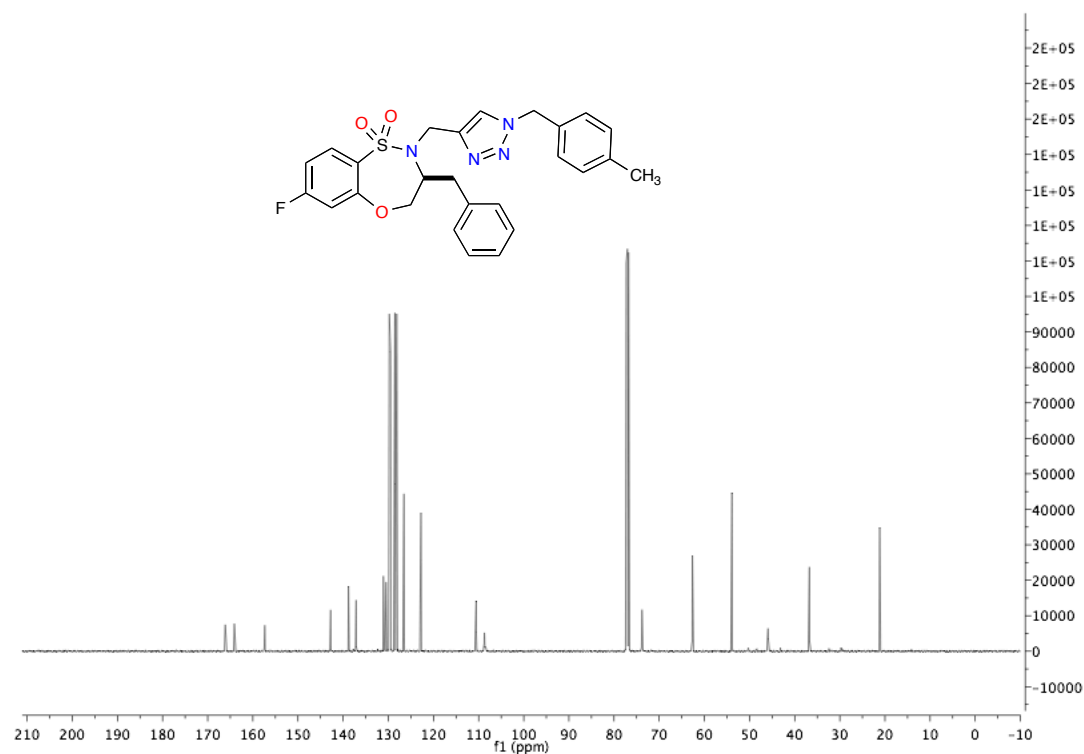
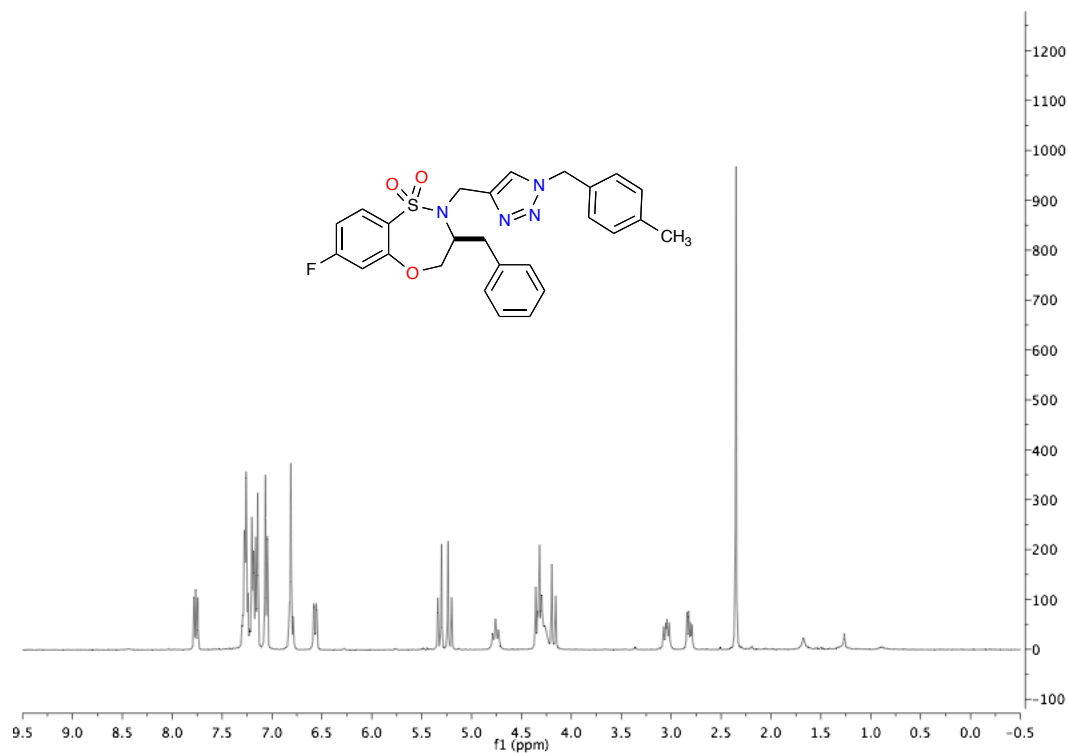
(S)-2-((1-(2-Chlorobenzyl)-1*H*-1,2,3-triazol-4-yl)methyl)-9-fluoro-3-isobutyl-3,4-dihydro-2*H*-benzo[*b*][1,4,5]oxathiazepine 1,1-dioxide, Library Member 2.2.8{2.2.22}



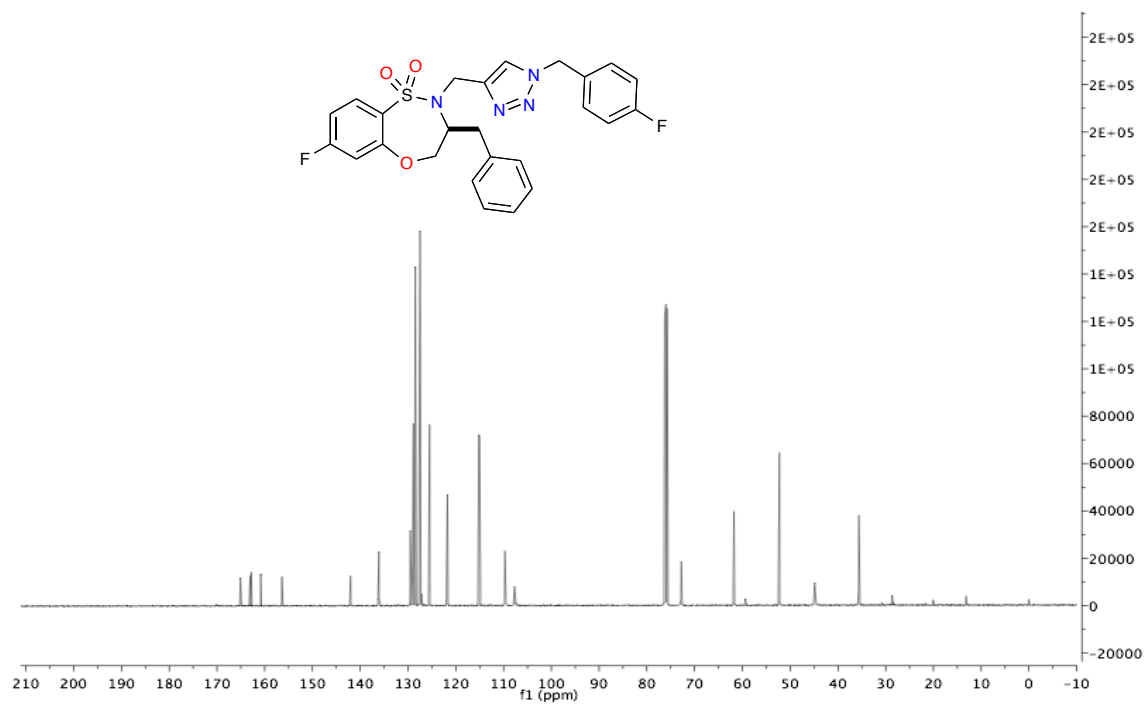
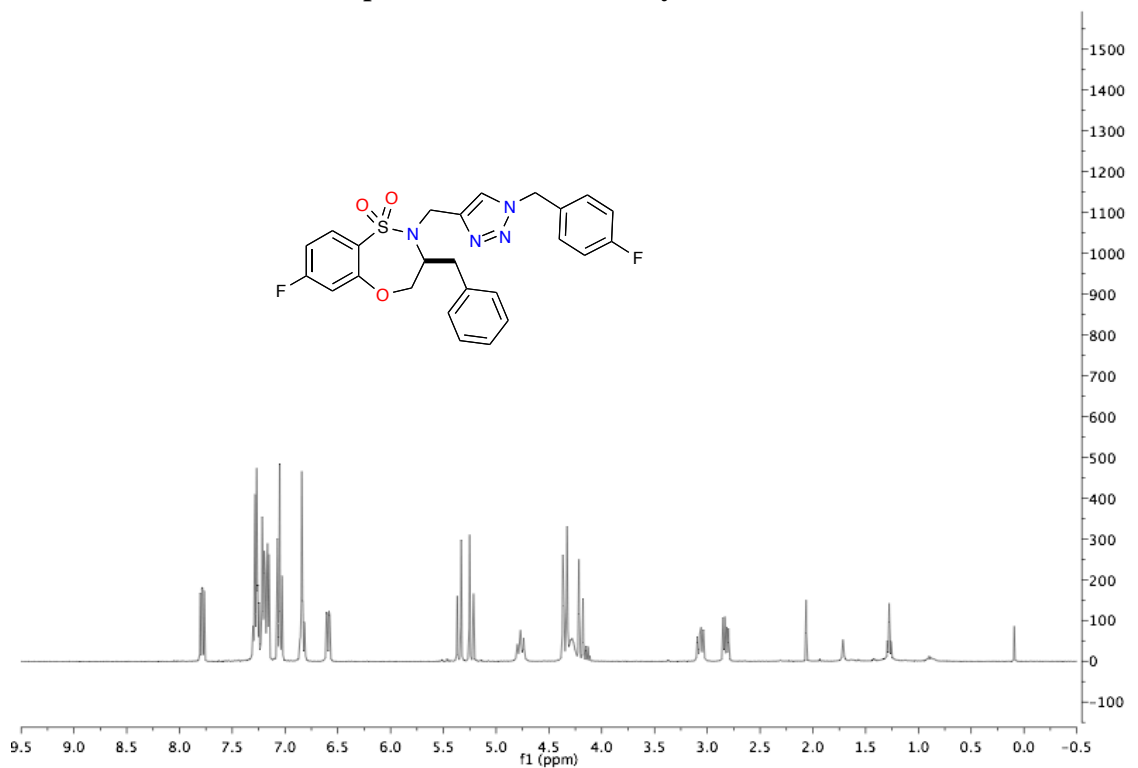
(S)-3-Benzyl-7-fluoro-2-((1-(4-methoxybenzyl)-1H-1,2,3-triazol-4-yl)methyl)-3,4-dihydro-2H-benzo[b][1,4,5]oxathiazepine 1,1-dioxide, Library Member 2.2.9{2.2.11}



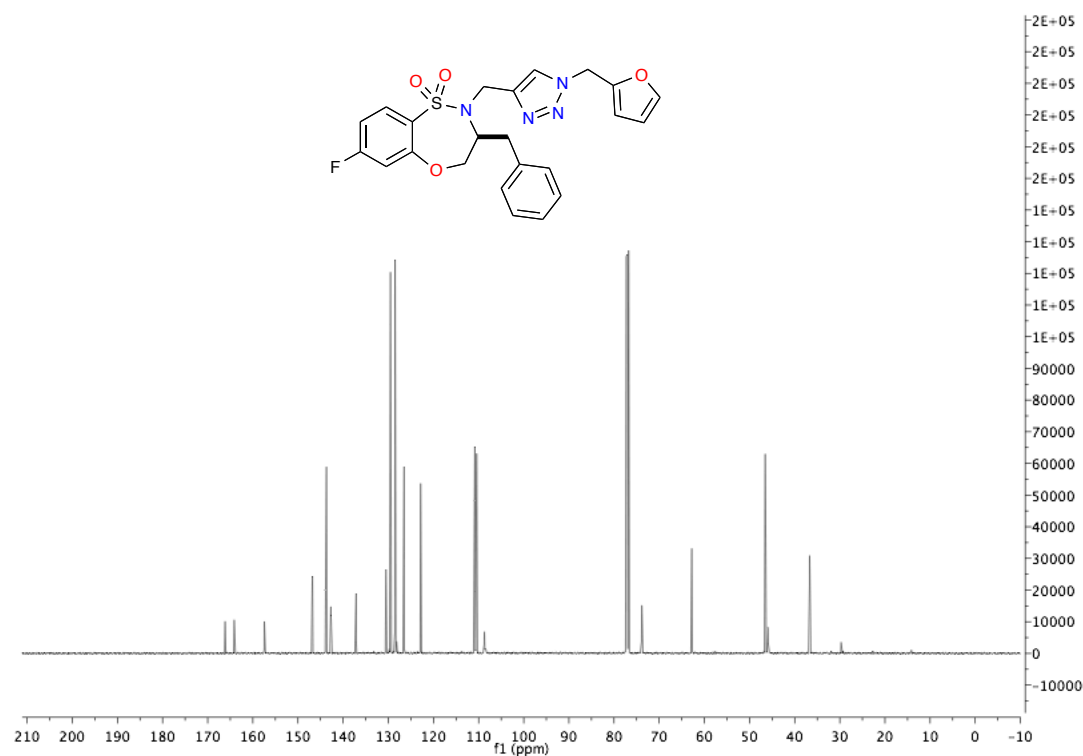
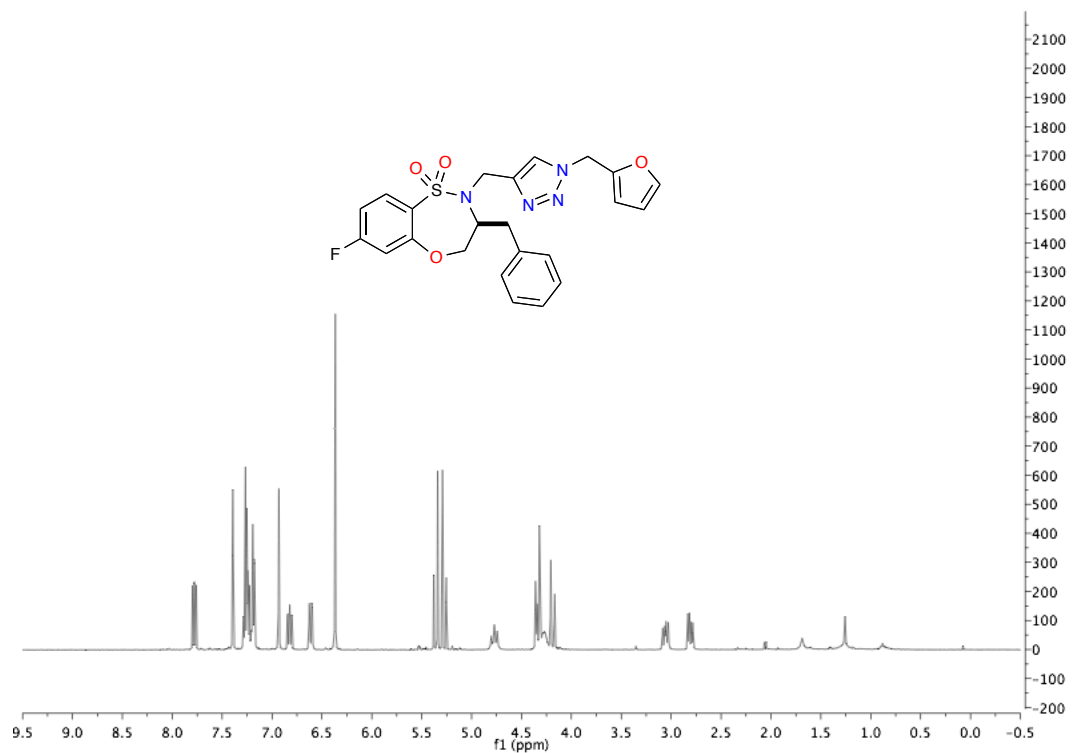
(S)-3-Benzyl-7-fluoro-2-((1-(4-methylbenzyl)-1*H*-1,2,3-triazol-4-yl)methyl)-3,4-dihydro-2*H*-benzo[*b*][1,4,5]oxathiazepine 1,1-dioxide, Library Member 2.2.9{2.2.12}



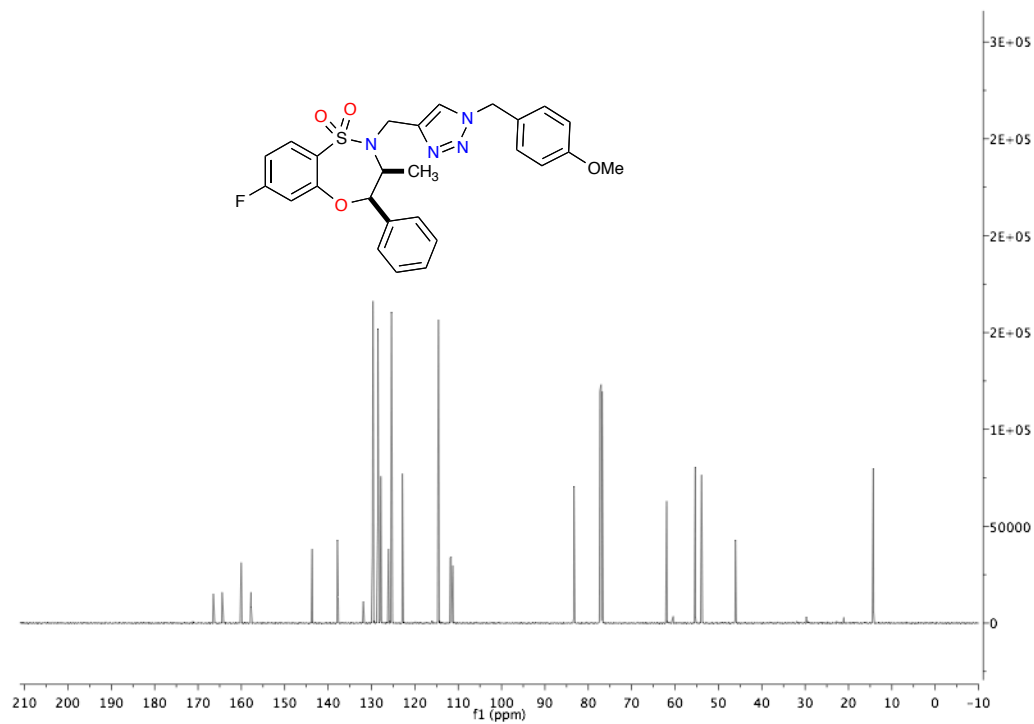
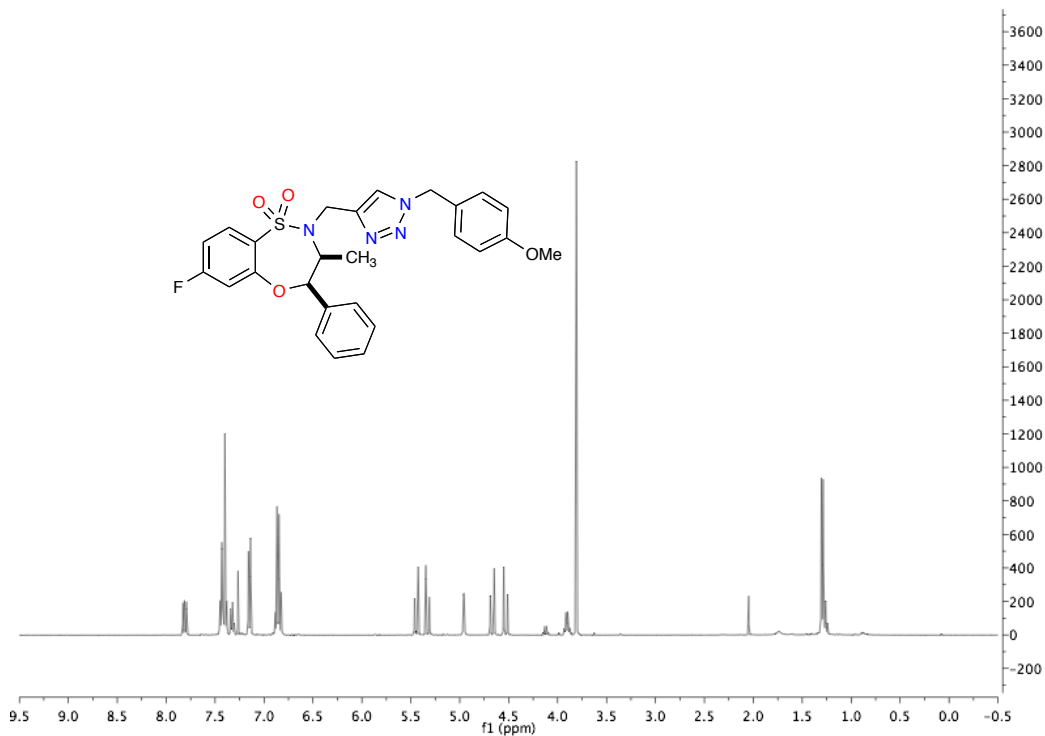
(S)-3-Benzyl-7-fluoro-2-((1-(4-fluorobenzyl)-1H-1,2,3-triazol-4-yl)methyl)-3,4-dihydro-2H-benzo[b][1,4,5]oxathiazepine 1,1-dioxide, Library Member 2.2.9{2.2.14}



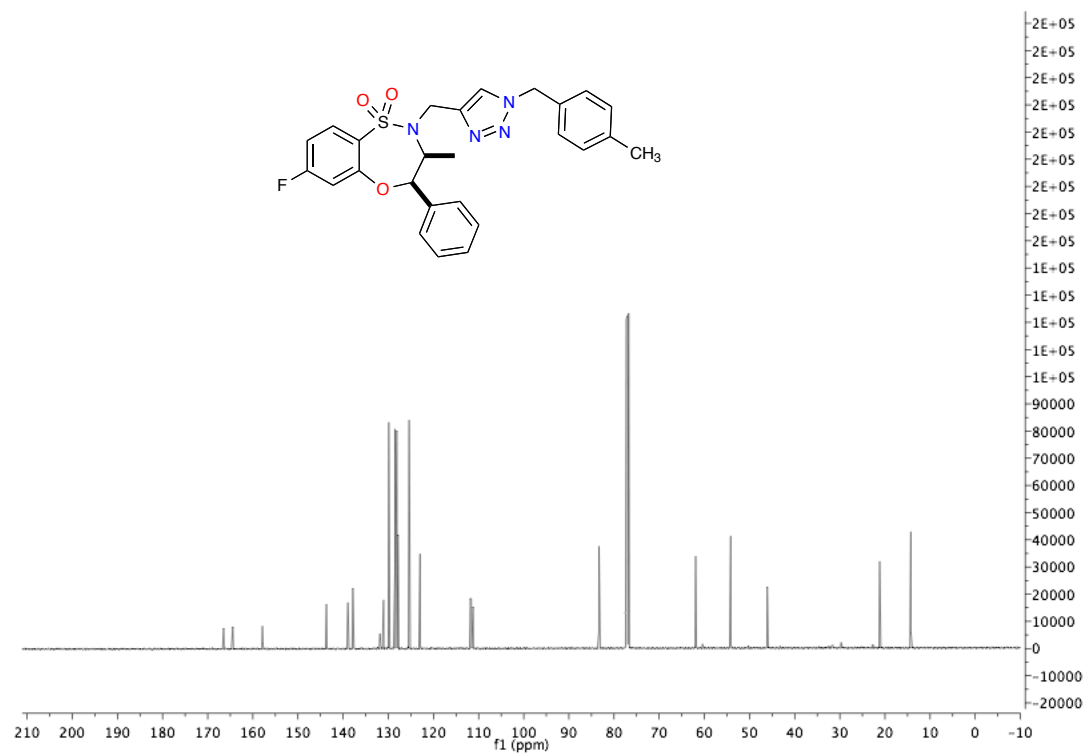
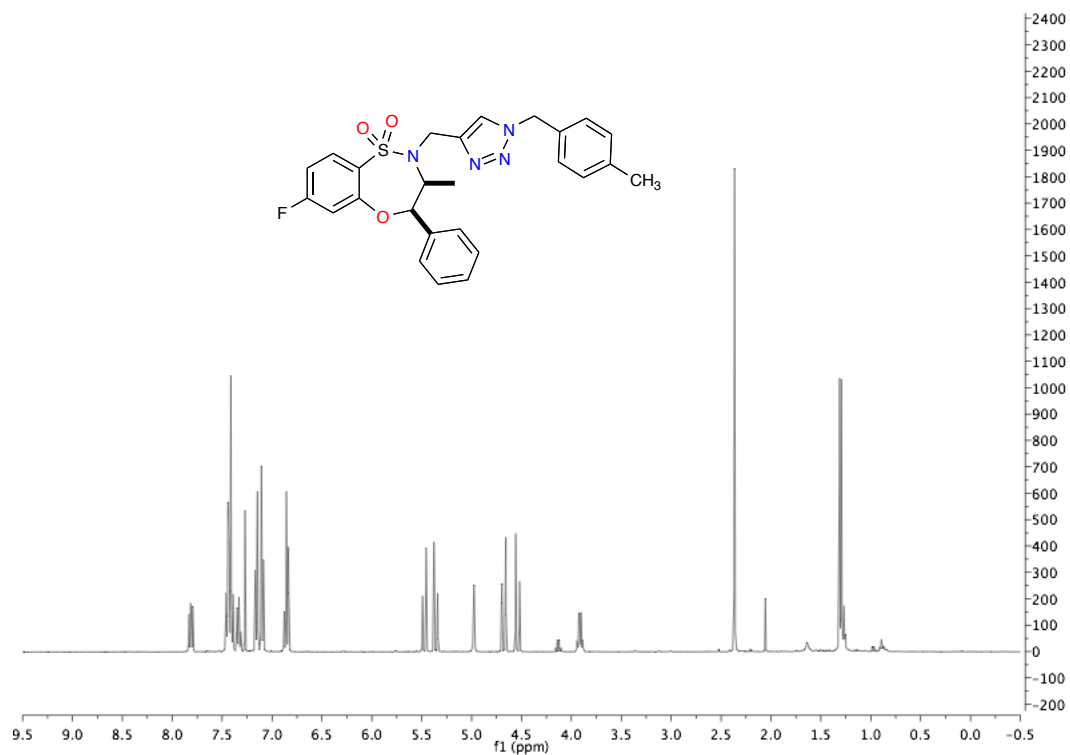
(S)-3-Benzyl-7-fluoro-2-((1-(furan-2-ylmethyl)-1H-1,2,3-triazol-4-yl)methyl)-3,4-dihydro-2H-benzo[b][1,4,5]oxathiazepine 1,1-dioxide, Library Member 2.2.9{2.2.19}



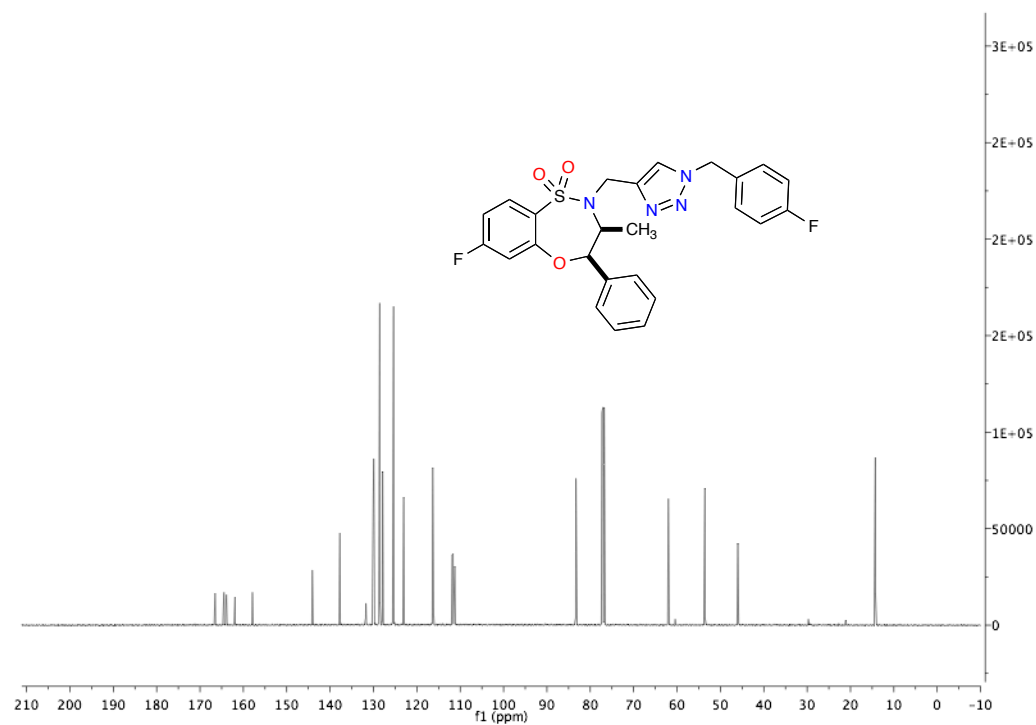
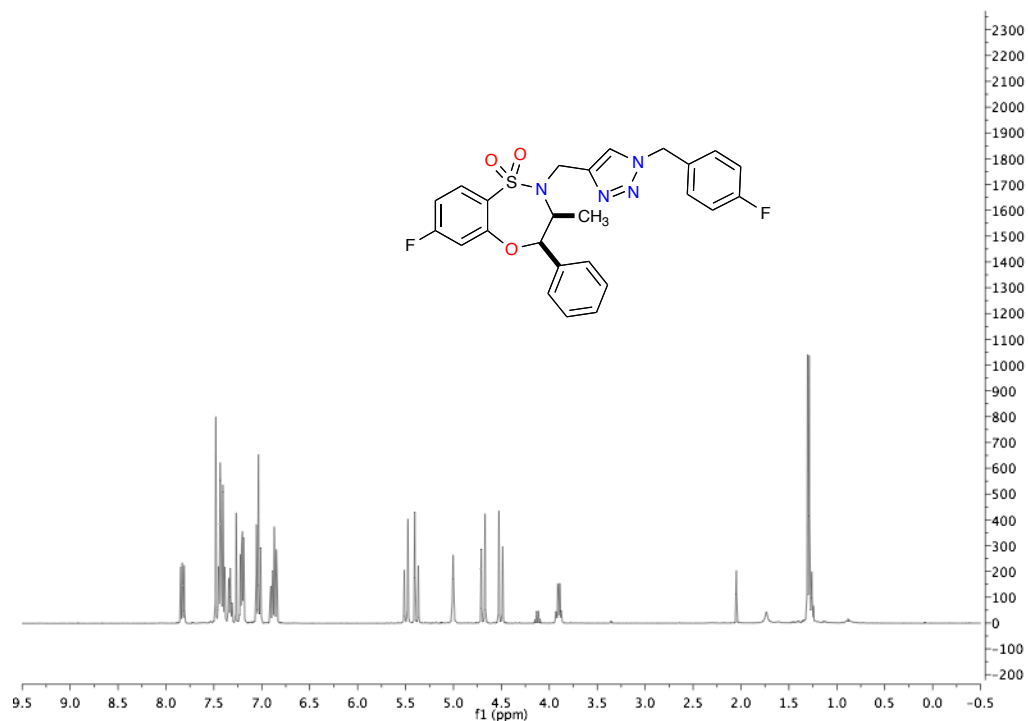
(3*S*,4*R*)-7-Fluoro-2-((1-(4-methoxybenzyl)-1*H*-1,2,3-triazol-4-yl)methyl)-3-methyl-4-phenyl-3,4-dihydro-2*H*-benzo[*b*][1,4,5]oxathiazepine 1,1-dioxide, Library Member 2.2.10{2.2.11}



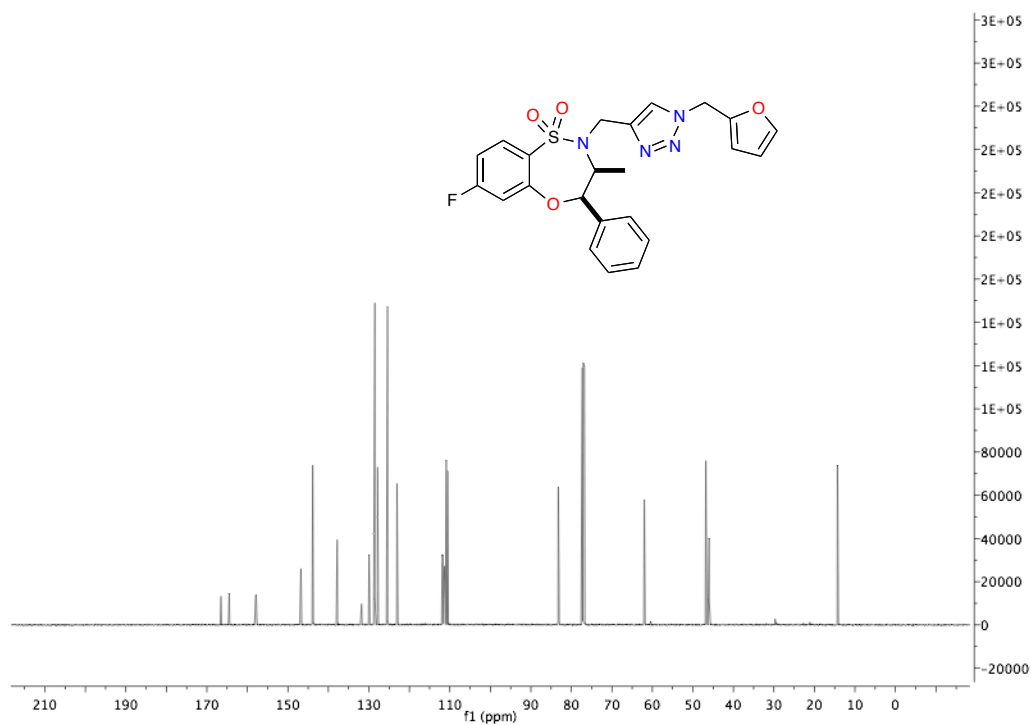
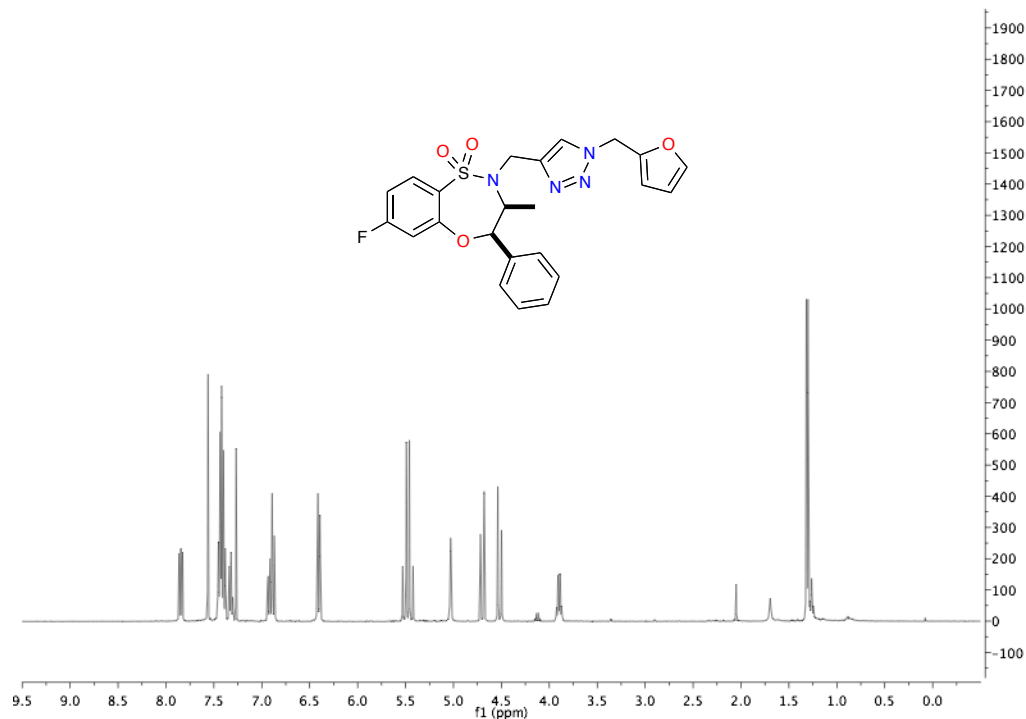
(3*S*,4*R*)-7-Fluoro-3-methyl-2-((1-(4-methylbenzyl)-1*H*-1,2,3-triazol-4-yl)methyl)-4-phenyl-3,4-dihydro-2*H*-benzo[*b*][1,4,5]oxathiazepine 1,1-dioxide, Library Member 10{2}



(3*S*,4*R*)-7-Fluoro-2-((1-(4-fluorobenzyl)-1*H*-1,2,3-triazol-4-yl)methyl)-3-methyl-4-phenyl-3,4-dihydro-2*H*-benzo[*b*][1,4,5]oxathiazepine 1,1-dioxide, Library Member 2.2.10{2.2.14}



(3*S*,4*R*)-7-Fluoro-2-((1-(furan-2-ylmethyl)-1*H*-1,2,3-triazol-4-yl)methyl)-3-methyl-4-phenyl-3,4-dihydro-2*H*-benzo[*b*][1,4,5]oxathiazepine 1,1-dioxide, Library Member 2.2.10{2.2.19}



5.5.1 Table 5.2 Library Data Set –Thiadiazepin-1,1-dioxide 4-ones

Comp.	HRMS Expected M/z (M)⁺	HRMS Found M/z (M+H)⁺	Mass (mg)	Yield (%)	Purity (%)
2.2.1{2.2.11}	568.0779	569.0867	24.0mg	32	99.1%
2.2.2{2.2.11}	568.0779	569.0857	44.7mg	60	98.9%
2.2.3{2.2.11}	534.0936	535.1046	21.3mg	30	100.0%
2.2.4{2.2.11}	534.0936	535.1015	20.0mg	28	100.0%
2.2.5{2.2.11}	492.0466	493.0539	53.1mg	70	100.0%
2.2.6{2.2.11}	492.0466	493.0520	54.1mg	72	100.0%
2.2.8{2.2.11}	490.1441	491.1516	9.0mg	11	100.0%
2.2.1{2.2.12}	552.0830	553.0902	14.1mg	19	100.0%
2.2.2{2.2.12}	552.0830	553.0913	56.9mg	76	97.6%
2.2.3{2.2.12}	518.0987	519.1038	37.1mg	48	100.0%
2.2.4{2.2.12}	518.0987	519.1068	39.9mg	52	97.9%
2.2.5{2.2.12}	476.0517	477.0577	50.9mg	63	100.0%
2.2.6{2.2.12}	476.0517	477.0612	55.0mg	68	99.2%
2.2.7{2.2.12}	538.0674	539.0788	11.0mg	15	92.4%
2.2.8{2.2.12}	458.1787	459.1893	21.1mg	29	97.3%
2.2.1{2.2.13}	552.0830	553.0891	54.9mg	74	100.0%
2.2.2{2.2.13}	552.0830	553.0861	60.0mg	80	97.9%
2.2.3{2.2.13}	518.0987	519.1070	32.2mg	42	100.0%
2.2.4{2.2.13}	518.0987	519.1078	35.4mg	46	98.6%
2.2.5{2.2.13}	476.0517	477.0608	56.4mg	70	99.6%
2.2.6{2.2.13}	476.0517	477.0594	63.0mg	77	100.0%
2.2.7{2.2.13}	538.0674	539.0767	40.2mg	55	71.2%
2.2.8{2.2.13}	458.1787	459.1848	46.6mg	62	98.5%
2.2.1{2.2.14}	556.0580	557.0670	48.1mg	64	98.3%
2.2.2{2.2.14}	556.0580	557.0622	56.9mg	76	98.4%
2.2.3{2.2.14}	522.0736	523.0776	34.6mg	44	98.7%

2.2.4{2.2.14}	522.0736	523.0817	37.4mg	48	100.0%
2.2.5{2.2.14}	480.0267	481.0358	58.6mg	79	99.5%
2.2.6{2.2.14}	480.0267	481.0338	59.0mg	80	98.7%
2.2.7{2.2.14}	542.0423	543.0486	36.5	49	65%
2.2.8{2.2.14}	462.1537	463.1593	43.2mg	57	100.0%
2.2.1{2.2.15}	544.1143	545.1255	55.2mg	75	100.0%
2.2.2{2.2.15}	544.1143	545.1237	43.2mg	60	97.5%
2.2.3{2.2.15}	510.1300	511.1394	30.1mg	40	98.0%
2.2.4{2.2.15}	510.1300	511.1376	19.3mg	26	97.9%
2.2.5{2.2.15}	468.083	469.0902	58.7mg	82	98.0%
2.2.6{2.2.15}	468.083	469.0927	56.2mg	78	99.2%
2.2.7{2.2.15}	530.098	531.1015	4.6mg	10	100.0%
2.2.8{2.2.15}	450.2100	451.2160	45.3mg	62	100.0%
2.2.1{2.2.16}	615.9779	616.9811	39.6mg	48	98.9%
2.2.3{2.2.16}	581.9935	583.0014	33.4mg	40	99.2%
2.2.4{2.2.16}	581.9935	583.0010	32.4mg	38	98.5%
2.2.5{2.2.16}	539.9466	540.9524	45.4mg	50	99.6%
2.2.6{2.2.16}	539.9466	540.9562	36.4mg	41	100.0%
2.2.7{2.2.16}	601.9622	602.9688	17.3mg	20	86.5%
2.2.1{2.2.17}	548.0729	549.0802	57.3mg	77	100.0%
2.2.2{2.2.17}	548.0729	549.0822	59.0mg	79	98.5%
2.2.3{2.2.17}	514.0885	515.0986	40.9mg	59	98.7%
2.2.4{2.2.17}	514.0885	515.0984	39.6mg	57	98.6%
2.2.5{2.2.17}	472.0416	473.0495	38.3mg	59	100.0%
2.2.6{2.2.17}	472.0416	473.0522	48.0mg	74	100.0%
2.2.7{2.2.17}	534.0572	535.0626	43.8mg	63	100.0%
2.2.8{2.2.17}	454.1686	455.1773	47.4mg	64	96.7%
2.2.1{2.2.18}	562.0885	563.0957	33.0mg	44	99.7%
2.2.2{2.2.18}	562.0885	563.0939	64.6mg	85	99.3%
2.2.3{2.2.18}	528.1042	529.1111	43.9mg	62	100.0%

2.2.4{2.2.18}	528.1042	529.1146	35.3mg	50	100.0%
2.2.5{2.2.18}	486.0572	487.0650	52.4mg	79	99.7%
2.2.6{2.2.18}	486.0572	487.0651	57.0mg	86	100.0%
2.2.7{2.2.18}	548.0729	549.0795	18.6mg	25	100.0%
2.2.8{2.2.18}	468.1842	469.1915	52.9mg	70	98.0%
2.2.2{2.2.19}	528.0466	529.0527	50.4mg	70	98.5%
2.2.3{2.2.19}	494.0623	495.0708	35.4mg	53	99.3%
2.2.4{2.2.19}	494.0623	495.0722	36.3mg	55	100.0%
2.2.5{2.2.19}	452.0153	453.0256	41.5mg	67	99.6%
2.2.7{2.2.19}	514.0310	515.0389	5.1mg	8	86.2%
2.2.8{2.2.19}	434.1424	435.1528	46.5mg	65	98.1%
2.2.1{2.2.20}	572.0284	573.0357	56.6mg	73	100.0%
2.2.2{2.2.20}	572.0284	573.0383	60.5mg	78	95.8%
2.2.3{2.2.20}	538.0441	539.0563	38.6mg	48	100.0%
2.2.4{2.2.20}	538.0441	539.0521	40.5mg	51	100.0%
2.2.5{2.2.20}	495.9971	497.0025	53.2mg	70	99.0%
2.2.6{2.2.20}	495.9971	497.0061	59.5mg	78	100.0%
2.2.7{2.2.20}	558.0128	559.023	3.9mg	5.1	66%
2.2.8{2.2.20}	478.1241	479.1340	46.8mg	60	96.4%
2.2.1{2.2.23}	538.0674	539.0740	57.9mg	79	97.7%
2.2.2{2.2.23}	538.0674	539.0745	59.1mg	81	95.6%
2.2.3{2.2.23}	504.08307	505.0896	16.6mg	22	99.5%
2.2.4{2.2.23}	504.08307	505.0960	44.4mg	65	99.3%
2.2.5{2.2.23}	462.03612	463.0403	49.4mg	63	99.4%
2.2.6{2.2.23}	462.03612	463.0405	64.0mg	81	99.2%
2.2.7{2.2.23}	524.0517	525.0556	52.5mg	70	99.3%
2.2.1{2.2.24}	606.0548	607.0640	30.0mg	37	97.9%
2.2.2{2.2.24}	606.0548	607.0630	53.8mg	66	97.8%
2.2.3{2.2.24}	572.0704	573.0773	31.0mg	39	100.0%
2.2.4{2.2.24}	572.0704	573.0762	35.7mg	44	100.0%

2.2.5 {2.2.24}	530.0235	531.0271	56.5mg	69	97.2%
2.2.6 {2.2.24}	530.0235	531.0343	40.5mg	50	97.5%
2.2.7 {2.2.24}	592.0339	593.0422	2.1mg	3	67%
2.2.8 {2.2.24}	512.1505	513.1599	31.2mg	37	99.1%

5.6 Experimental for Chapter 3.1

Silica-Supported Oligomeric Benzyl Phosphate (Si-OBP) and Triazole Phosphate (Si-OTP) Alkylating Reagents.

Experimental Section and Characterization data (SI-253–SI-269)

¹H, ¹³C, Spectra for all Relevant Compounds (SI-270–SI-294)

General Procedure for Synthesis of Silica Oligomeric Benzyl Phosphate (Si-OBP_n) and Triazole Phosphate (Si-OTP_n).

Si-Nb (load ~0.4 mmol/g, 1 equiv.) was heated with C848 (G-II, 0.2 equiv.) at 45 °C in dichloromethane for 2 hrs under argon. The OBP or OTP monomer was added (50 equiv. w/r to cat. G-II) in CH₂Cl₂ and toluene to the reaction mixture and heated at 45 °C for overnight. The reaction mixture was cooled to room temperature and EVE was added, with stirring for an additional 1 hour at room temperature. The reaction mixture was filtered and washed with mixture of toluene:CH₂Cl₂ (1:1), and dried over high vacuum pump.

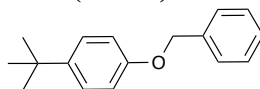
Procedure A: General procedure for different nucleophilic substitution with Si-OBP_n.

In a sealed pressure tube was added Si-OBP_n (1.5 equiv.), followed by addition of sodium iodide (0.2 equiv.), Cs₂CO₃ (3.0 equiv.), and solvent THF (0.2M). The mixture was stirred rapidly and then nucleophiles were added. The reaction was sealed under argon and heated to 80 °C with stirring for 12 h. After such time, the reaction was cooled to rt and the crude mixture was filtered via a Celite[®]-packed SPE and rinsed several times with a mixture of hexanes:EtOAc (1:2). The resulting eluent was concentrated *in vacuo* to yield the benzylated products in good to excellent yields and purities.

Procedure B: General procedure for different nucleophilic substitution with Si-OTP_n.

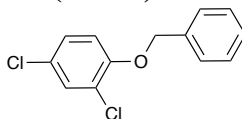
In a pressure tube was added Si-OTP_n (1.5 equiv.), followed by addition of NaI (0.2 equiv.), Cs₂CO₃ (3.0 equiv.), and solvent DMF (0.2M). The nucleophile was added and the resulting mixture was stirred rapidly. The reaction was sealed under argon and heated to 90 °C w/ stirring for (12–14 h) after which time, DMF was removed *in vacuo*. The crude mixture was filtered via celite[®]-SPE and rinsed with EtOAc. The resulting eluent was then concentrated *in vacuo* to yield the products in good to excellent yields and purities.

1-(benzyloxy)-4-(*tert*-butyl)benzene (3.1.8c).



Utilizing general procedure A, **3.1.8c** (18.5 mg, 0.077 mmol, 97%) was isolated as a white solid. MP: 65 °C; FTIR (neat): 3056, 3024, 2960, 2866, 1610, 1512, 1456, 1242, 1182, 1024 cm^{-1} ; ^1H NMR (400 MHz, CDCl_3): δ 7.46–7.43 (m, 2H), 7.42–7.38 (m, 2H), 7.36–7.30 (m, 3H), 6.92–6.96 (m, 2H), 5.06 (s, 2H), 1.33 (s, 9H); ^{13}C NMR (126 MHz, CDCl_3): δ 156.6, 143.7, 137.3, 128.5 (2C), 127.9, 127.5 (2C), 126.2 (2C), 114.2 (2C), 70.0, 34.1, 31.4 (3C); GC-MS (EI^+) calculated for $\text{C}_{17}\text{H}_{20}\text{O}$ 240.15; found 240.1 (M^+ 7), 91.0 (100).

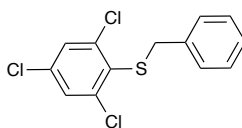
1-(benzyloxy)-2,4-dichlorobenzene (3.1.8d).



Utilizing general procedure A, **3.1.8d** (30 mg, 0.119 mmol, 98%) was isolated as a thick liquid.

FTIR (neat): 3031, 2931, 2835, 1597, 1481, 1452, 1382, 1290, 1249, 1060 cm^{-1} ; ^1H NMR (400 MHz, CDCl_3): δ 7.47–7.44 (m, 2H), 7.43–7.38 (m, 3H), 7.37–7.33 (m, 1H), 7.18 (dd, $J = 2.6, 8.7$ Hz, 1H), 6.90 (d, $J = 8.9$ Hz, 1H), 5.16 (s, 2H); ^{13}C NMR (126 MHz, CDCl_3): δ 153.0, 136.1, 130.1, 128.7 (2C), 128.1, 127.5, 127.1 (2C), 126.0, 124.1, 114.8, 71.2; GC-MS (EI^+) $\text{C}_{13}\text{H}_{10}\text{Cl}_2\text{O}$ calculated 252.01; found 251.9 (M^+ 4), 91.0 (100).

Benzyl(2,4,6-trichlorophenyl)sulfane (3.1.8e).



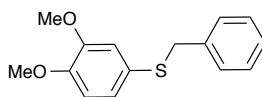
Utilizing general procedure A, **3.1.8e** (21 mg, 0.07 mmol, 98%) was isolated as a yellow solid. MP: 112 °C;

FTIR (neat): 3087, 2935, 2850, 1583, 1454, 1321, 1116, 1054 cm⁻¹.

¹H NMR (400 MHz, CDCl₃): δ 7.47 (s, 1 H), 7.37–7.33 (m, 4H), 7.32–7.39 (m, 2H), 4.15 (s, 2H);

¹³C NMR (126 MHz, CDCl₃): δ 136.3, 135.3, 132.0, 131.3, 130.6, 130.0, 129.5, 128.9 (2C), 128.8 (2C), 127.8, 37.6; GC-MS (EI⁺) C₁₃H₉Cl₃S calculated 301.95; found 301.9 (32), 169 (7), 91.0 (100).

Benzyl(3,4-dimethoxyphenyl)sulfane (3.1.8f).

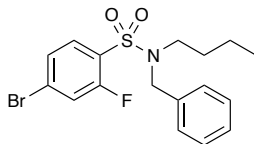


Utilizing general procedure A, **3.1.8f** (22 mg, 0.085 mmol, 98%) was isolated as a thick liquid.

FTIR (neat): 2933, 2833, 1595, 1504, 1251, 1228, 1135, 1026 cm⁻¹. ¹H NMR (400 MHz, CDCl₃): δ 7.31–7.19(m, 5 H), 6.95 (dd *J* = 8.3, 2.2 Hz, 1H), 6.0–6.74 (m, 2H), 4.02 (s, 2H), 3.88 (s, 3H), 3.75 (s, 3H);

¹³C NMR (126 MHz, CDCl₃): δ 148.7 (2C), 138.2, 129.0 (2C), 128.4 (2C), 127.0, 126.2, 125.3, 115.9, 111.3, 55.9, 55.8, 41.2; GC-MS (EI⁺) C₁₅H₁₆O₂S calculated 260.09; found 260.0 (32), 169 (30), 91.0 (100).

***N*-benzyl-4-bromo-*N*-butyl-2-fluorobenzenesulfonamide (3.1.8g).**

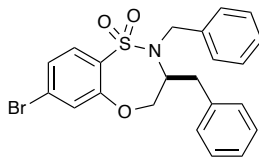


Utilizing general procedure A, **3.1.8g** (24 mg, 0.060 mmol, 99%) was isolated as a thick liquid. FTIR (neat): 3089, 3025, 2958, 2931, 1589, 1472, 1456, 1396, 1344, 1161, 1135 cm⁻¹.

¹H NMR (500 MHz, CDCl₃): δ 7.79 (t, *J* = 7.70 Hz, 1H), 7.43–7.38 (m, 2H), 7.34–7.28 (m, 5H), 4.47 (s, 2H), 3.19 (t, *J* = 7.60 Hz, 2H), 1.35–1.29 (m, 2H), 1.16–1.11 (m, 2H), 0.76 (t, *J* = 7.45 Hz, 3H).

¹³C NMR (126 MHz, CDCl₃): δ 158.44 (¹*J*_{C-F} = 259 Hz), 136.1, 131.8, 128.6 (2C), 128.2 (2C), 128.0, 127.8 (3C), 120.7 (²*J* = 25.0 Hz), 51.4, 47.3, 29.7, 19.7, 13.5. GC-MS (EI⁺) C₁₇H₁₉BrFNO₂S calculated 399.3; found 399.0 (M⁺ 3), 401.2 (M+2 2), 355.8 (60), 357.8 (60), 91 (100).

(*S*)-2,3-dibenzyl-7-bromo-3,4-dihydro-2*H*-benzo[*b*][1,4,5]oxathiazepine1,1-dioxide (3.1.8h).



Utilizing general procedure A, **3.1.8h** (30 mg, 0.066 mmol, 97%) was isolated as a white solid. MP: 170 °C.

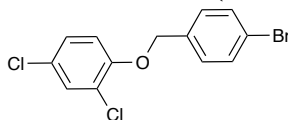
FTIR (neat): 3026, 2921, 2852, 1595, 1552, 1325, 1153, 700 cm⁻¹.

¹H NMR (500 MHz, CDCl₃): δ 7.74 (d, *J* = 8.5 Hz, 1H), 7.33–7.28 (m, 4H), 7.25–7.19 (m, 5H), 7.17 (d, *J* = 1.8 Hz, 1H), 6.92 (d, *J* = 7.5 Hz, 2H), 4.85 (t, *J* = 12.0 Hz,

1H), 4.40 (d, $J = 14.3$ Hz, 1H), 4.26 (dd, $J = 4.5, 13.42$ Hz, 1H), 4.09 (d, $J = 14.6$ Hz, 1H), 3.85 (m, 1H), 2.93 (m, 2H).

^{13}C NMR (126 MHz, CDCl_3): δ 156.1, 137.4, 135.2, 129.8, 130.8, 129.0 (2), 128.7 (2), 128.6 (2), 128.1 (2), 127.1 (2), 126.7, 126.4, 124.4, 73.7, 62.4, 55.2, 37.9. HRMS calculated for $\text{C}_{22}\text{H}_{20}\text{BrNO}_3\text{SNa}$ ($\text{M}+\text{Na}$) $^+$ 480.0245; found 480.0258 (TOF MS).

1-((4-bromobenzyl)oxy)-2,4-dichlorobenzene (3.1.8i).

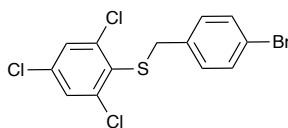


Utilizing general procedure A, **3.1.8i** (29 mg, 0.088 mmol, 98%) was isolated as a yellow solid. MP: 87 °C.

FTIR (neat) 3070, 2923, 2866, 1585, 1571, 1480, 1456, 1290, 1262, 1103 cm^{-1} . ^1H NMR (500 MHz, CDCl_3): δ 7.52–7.54 (m, $J = 8.4$ Hz, 2H), 7.40 (d, $J = 2.7$ Hz, 1H), 7.32–7.34 (m, 2H), 7.15–7.18 (dd, $J = 8.6, 2.4$ Hz, 1H), 6.85 (d, $J = 8.8$, 1H), 5.10 (s, 2H).

^{13}C NMR (126 MHz, CDCl_3): δ 152.7, 135.0, 131.8 (2C), 130.1, 128.7 (2C), 127.5, 126.3, 124.1, 122.1, 114.7, 70.3. GC-MS (EI^+) $\text{C}_{13}\text{H}_9\text{BrCl}_2\text{O}$ calculated 329.92; found 331.9 ($\text{M}+2$, 2), 169 (100), 90 (25).

(4-bromobenzyl)(2,4,6-trichlorophenyl)sulfane (3.1.8j).

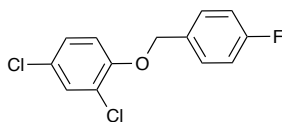


Utilizing general procedure A, **3.1.8j** (25 mg, 0.066 mmol, 94%) was isolated as a white solid. MP: 54 °C. FTIR (neat) 2923, 1590, 1487, 1452, 1433, 1323, 1116, 1058, 1012 cm^{-1} .

^1H NMR (500 MHz, CDCl_3): δ 7.44–7.47 (m, 3H), 7.27 (s, 1H), 7.20–7.22 (m, 2H), 4.08 (s, 2H).

^{13}C NMR (126 MHz, CDCl_3): δ 135.6, 134.5, 132.4, 131.9 (2C), 131.4, 130.7, 130.5 (2C), 130.4, 129.9, 121.7, 37.1. GC-MS (EI^+) $\text{C}_{13}\text{H}_8\text{Cl}_3\text{BrS}$ calculated 379.86; found 379.8 (M^+ 5), 381.8 ($\text{M}+2$, 7), 169 (100), 90 (25).

2,4-dichloro-1-((4-fluorobenzyl)oxy)benzene (3.1.8k).



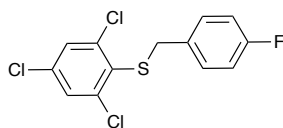
Utilizing general procedure A, **3.1.8k** (24 mg, 0.088 mmol, 96%) is isolated as a thick liquid.

FTIR (neat) 2931, 1604, 1510, 1483, 1379, 1226, 1060, 823, 730 cm^{-1} .

^1H NMR (500 MHz, CDCl_3): δ 7.41–7.45 (m, 2H), 7.40 (d, $J = 2.5$ Hz, 1H), 7.15–7.18 (dd, $J = 8.6, 2.5$ Hz, 1H), 7.07–7.11 (m, 2H), 6.88 (d, $J = 7.5$, 1H), 5.10 (s, 2H).

^{13}C NMR (126 MHz, CDCl_3): δ 162.5 ($^1J_{\text{C-F}} = 246.5$ Hz) 152.8, 131.8, 130.1, 129.1 ($^3J = 8.4$ Hz, 2), 127.5, 126.6, 124.2, 115.6 ($^2J = 21.6$ Hz, 2) 114.9, 70.5. GC-MS (EI^+) $\text{C}_{13}\text{H}_9\text{Cl}_2\text{FO}$ calculated 270.00; found 269.9 (M^+ 2), 109 (100).

4-fluorobenzyl)(2,4,6-trichlorophenyl)sulfane (3.1.8l).

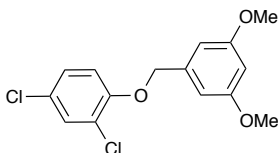


Utilizing general procedure A, **3.1.8l** (21 mg, 0.065 mmol, 95%) was isolated as a thick liquid.

FTIR (neat) 2933, 1600, 1505, 1433, 1323, 1228, 1116, 1058, 837 cm^{-1} . ^1H NMR (500 MHz, CDCl_3): δ 7.49 (s, 1H), 7.31–7.34 (m, 2H), 7.29 (s, 1H), 7.01–7.05 (m, 2H), 4.13 (s, 2H).

^{13}C NMR (126 MHz, CDCl_3): δ 163.3, ($^1J_{\text{C-F}} = 247.5$ Hz) 135.8, 132.3, 131.3, 131.1 ($^4J_{\text{C-F}} = 3.6$ Hz), 130.7, 130.5 ($^3J = 8.5$ Hz, 2) 130.4, 129.9, 115.7 ($^2J = 22.3$ Hz, 2), 36.9. GC-MS (EI^+). $\text{C}_{13}\text{H}_8\text{Cl}_3\text{FS}$ calculated 319.94; found 319.9 (M^+ 5), 109 (100).

2,4-dichloro-1-((3,5-dimethoxybenzyl)oxy)benzene (3.1.8m).

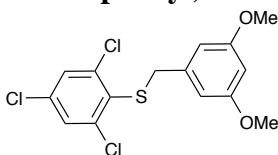


Utilizing general procedure A, **3.1.8m** (28 mg) 0.089 mmol, 98%) was isolated as a yellow solid. MP: 55 $^{\circ}\text{C}$; FTIR (neat): 2935, 2825, 1598, 1483, 1456, 1292, 1157, 1060 cm^{-1} ;

^1H NMR (500 MHz, CDCl_3): δ 7.38 (d, $J = 2.5$ Hz, 1H), 7.14–7.16 (dd, $J = 8.7, 2.4$ Hz, 1H), 6.88–6.85 (d, $J = 7.8$ Hz, 1H), 6.60 (d, $J = 2.2$ Hz, 2H), 6.42 (t, $J = 2.5$ Hz, 1H), 5.09 (s, 1H), 3.80 (s, 6H);

^{13}C NMR (126 MHz, CDCl_3): δ 161.0 (2C), 152.9, 138.5, 130.0, 127.5, 126.1, 124.0, 114.8, 104.7 (2C), 99.8, 70.9, 55.3 (2C). GC-MS (EI^+). $\text{C}_{15}\text{H}_{13}\text{Cl}_3\text{O}_2\text{S}$, calculated 312.03; found 312.0 (M^+ , 3), 151.1 (100).

(3,5-dimethoxybenzyl)(2,4,6-trichlorophenyl)sulfane (3.1.8n).

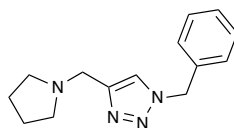


Utilizing general procedure A, **3.1.8n** (20 mg, 0.055 mmol, 94%) was isolated as a white solid. MP: 84 °C; FTIR (neat): 2956, 2931, 2830, 1610, 1596, 1454, 1431, 1323, 1205, 1157, 1158 cm^{-1} ;

^1H NMR (500 MHz, CDCl_3): δ 7.46 (s, 1H), 7.30 (s, 1H), 6.51 (d, $J = 2.25$ Hz, 2H), 6.38 (t, $J = 2.3$, Hz 1H), 4.08 (s, 2H), 3.79 (s, 6H).

^{13}C NMR (126 MHz, CDCl_3): δ 160.1 (2C), 137.5, 136.3, 131.9, 131.3, 130.6, 130.0, 129.4, 106.9 (2C), 99.8, 55.4 (2C), 37.8. GC-MS (EI^+). $\text{C}_{15}\text{H}_{13}\text{Cl}_3\text{O}_2\text{S}$, calculated 361.97 found 361.9 (M^+ 3), 151.1 (100).

1-benzyl-4-(pyrrolidin-1-ylmethyl)-1H-1,2,3-triazole (3.1.11a).

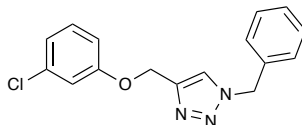


Utilizing general procedure B, **3.1.11a** (48 mg, 0.198 mmol, 84%) was isolated as a light brown thick liquid. FTIR (neat): 3307, 2923, 1581, 1448, 1420, 1396, 1238, 1215, 1121, 1008 cm^{-1} ;

^1H NMR (400 MHz, CDCl_3): δ 7.59 (s, 1H), 7.41–7.33 (m, 3H), 7.30–7.26 (m, 2H), 5.52 (s, 2H), 3.87 (s, 2H), 2.74–2.67 (m, 4H), 1.89–1.81 (m, 4H). ^{13}C NMR (126

MHz, CDCl₃): δ 144.6, 134.6, 129.1 (2C), 128.7, 128.1 (2C), 122.9, 54.2, 53.9 (2C), 50.5, 23.4 (2C). HRMS calculated for C₁₄H₁₉N₄ (M+H)⁺ 243.1610; found 243.1631 (TOF MS ES+).

1-benzyl-4-((3-chlorophenoxy)methyl)-1*H*-1,2,3-triazole (3.1.11c).

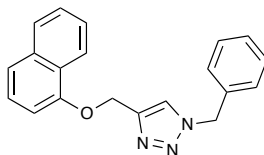


Utilizing general procedure B, 1-benzyl-4-((3-chlorophenoxy)methyl)-1*H*-1,2,3-triazole **3.1.11c** (50 mg, 0.167 mmol, 91%) was isolated as a white solid. MP: 96 °C; FTIR (neat): 2960, 2358, 1610, 1511, 1463, 1250, 1184, 1031 cm⁻¹;

¹H NMR (400 MHz, CDCl₃): δ 7.53 (s, 1H), 7.43 – 7.35 (m, 3H), 7.29 (dd, *J* = 4.8, 2.8 Hz, 2H), 7.20 (t, *J* = 8.1 Hz, 1H), 6.98 – 6.93 (m, 2H), 6.89 – 6.84 (m, 1H), 5.55 (s, 2H), 5.17 (s, 2H).

¹³C NMR (126 MHz, CDCl₃): δ 158.9, 144.1, 134.9, 134.4, 130.3, 129.2 (2C), 128.9, 128.2 (2C), 122.7, 121.5, 115.4, 113.1, 62.2, 54.3. HRMS calculated for C₁₆H₁₅ClN₃O (M+H)⁺ 300.0904; found 300.0906 (TOF MS ES+).

1-benzyl-4-((naphthalen-1-yloxy)methyl)-1*H*-1,2,3-triazole (3.1.11d).

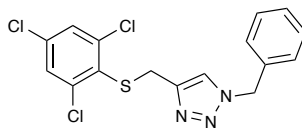


Utilizing general procedure B, **3.1.11d** (53 mg, 0.168 mmol, 90%) was isolated as a light brown solid. MP: 94 °C;

FTIR (neat): 3409, 2918, 1583, 1458, 1390, 1267, 1238, 1155, 1095 cm⁻¹; ¹H NMR (400 MHz, CDCl₃): δ 8.23 (d, *J* = 8.1 Hz, 1H), 7.82 (d, *J* = 7.6 Hz, 1H), 7.62 (s, 1H), 7.54–7.44 (m, 3H), 7.43–7.36 (m, 4H), 7.34 – 7.25 (m, 2H), 6.98 (d, *J* = 7.6 Hz, 1H), 5.57 (s, 2H), 5.41 (s, 2H).

¹³C NMR (126 MHz, CDCl₃): δ 153.9, 144.8, 134.5, 129.2 (2C), 128.8, 128.1 (2C), 127.5, 126.5, 125.8, 125.6, 125.3, 122.6, 122.0, 120.9, 105.4, 62.5, 54.3. HRMS calculated for C₂₀H₁₈N₃O (M+H)⁺ 316.1450; found 316.1427 (TOF MS ES+).

1-benzyl-4-(((2,4,6-trichlorophenyl)thio)methyl)-1*H*-1,2,3-triazole (3.1.11e).

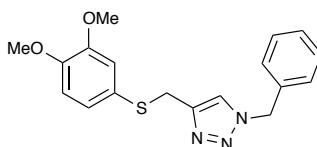


Utilizing general procedure A, **3.1.11e** (63 mg, 0.164 mmol, 92%) was isolated as a white solid. MP: 137 °C; FTIR (neat): 3369, 2923, 1699, 1456, 1433, 1363, 1242, 1116, 1049, 721 cm⁻¹;

¹H NMR (400 MHz, CDCl₃): δ 7.44 (s, 1H), 7.41–7.34 (m, 5H), 7.24–7.20 (m, 2H), 5.52 (s, 2H), 4.25 (s, 2H).

¹³C NMR (126 MHz, CDCl₃): δ 143.8, 135.1, 134.4, 132.3, 131.5, 130.7, 130.6, 130.0, 129.2 (2C), 128.9, 128.0 (2C), 122.1, 54.3, 27.8. HRMS calculated for C₁₆H₁₃Cl₃N₃S (M+H)⁺ 383.9896; found 383.9912 (TOF MS ES+).

1-benzyl-4-(((3,4-dimethoxyphenyl)thio)methyl)-1*H*-1,2,3-triazole (3.1.11f).



Utilizing general procedure B, **3.1.11f** (53 mg, 0.155 mmol, 94%) was isolated as a white solid. MP: 101 °C;

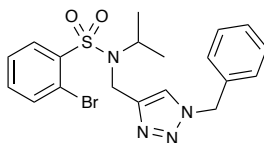
FTIR (neat): 2952, 1581, 1502, 1438, 1253, 1228, 1135, 1024 cm⁻¹;

¹H NMR (400 MHz, CDCl₃): δ 7.58–7.32 (m, 3H), 7.20 (dd, *J* = 6.7, 2.7 Hz, 2H), 7.17 (s, 1H), 6.89 (dt, *J* = 5.1, 2.1 Hz, 2H), 6.72 (d, *J* = 8.2 Hz, 1H), 5.47 (s, 2H), 4.14 (s, 2H), 3.86 (s, 3H), 3.79 (s, 3H).

¹³C NMR (126 MHz, CDCl₃): δ 149.0, 148.7, 145.5, 134.6, 129.1 (2C), 128.7, 127.9 (2C), 125.7, 124.8, 121.9, 115.2, 111.4, 55.9, 55.9, 54.1, 30.8.

HRMS calculated for C₁₈H₁₉N₃O₂S (M+Na)⁺ 364.1096; found 364.1063 (TOF MS ES⁺).

***N*-((1-benzyl-1*H*-1,2,3-triazol-4-yl)methyl)-2-bromo-*N*-isopropylbenzenesulfonamide (3.1.11g).**



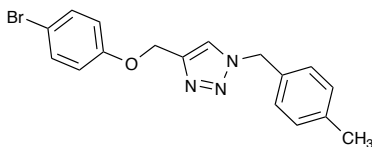
Utilizing general procedure B, **3.1.11g** (47 mg, 0.104 mmol, 89%) was isolated as a colorless thick liquid. FTIR (neat): 3134, 2923, 2846, 1703, 1604, 1487, 1456, 1411, 1328, 1220, 1049 cm⁻¹;

^1H NMR (400 MHz, CDCl_3): δ 8.14 (dd, $J = 7.8, 1.8$ Hz, 1H), 7.2923, (dd, $J = 7.7, 1.4$ Hz, 1H), 7.65 (s, 1H), 7.48 – 7.32 (m, 5H), 7.27 – 7.20 (m, 2H), 5.52 (d, $J = 5.1$ Hz, 2H), 4.71 (s, 2H), 4.03 – 3.82 (m, 1H), 1.09 (d, $J = 6.8$ Hz, 6H).

^{13}C NMR (126 MHz, CDCl_3): δ 147.1, 139.3, 135.6, 134.7, 133.5, 132.5, 129.1 (2C), 128.7, 127.9 (2C), 127.5, 123.6, 120.3, 54.2, 49.9, 38.6, 21.1 (2C).

HRMS calculated for $\text{C}_{19}\text{H}_{21}\text{BrN}_4\text{NaO}_2\text{S}$ ($\text{M}+\text{H}$) $^+$ 471.0466; found 471.0478 (TOF MS ES+)

4-((4-bromophenoxy)methyl)-1-(4-methylbenzyl)-1H-1,2,3-triazole (3.1.11h).



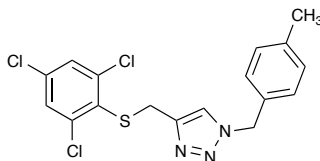
Utilizing general procedure B, **3.1.11h** (52 mg, 0.145 mmol, 85%) was isolated as a white solid. MP: 103 °C; FTIR (neat): 3087, 2920, 1589, 1490, 1384, 1282, 1242, 1022, 825, 757 cm^{-1} .

^1H NMR (400 MHz, CDCl_3): δ 7.49 (s, 1H), 7.37 (d, $J = 8.8$ Hz, 2H), 7.19 (m, 4H), 6.85 (d, $J = 8.8$ Hz, 2H), 5.49 (s, 1H), 5.14 (s, 1H), 2.36 (s, 1H).

^{13}C NMR (126 MHz, CDCl_3): δ 157.3, 144.1, 138.8, 132.3 (2C), 131.3, 129.8 (2C), 128.2 (2C), 122.6, 116.6 (2C), 113.5, 62.2, 54.1, 21.2.

HRMS calculated for $\text{C}_{17}\text{H}_{17}\text{BrN}_3\text{O}$ ($\text{M}+\text{H}$) $^+$ 358.0555; found 358.0558 (TOF MS ES+).

1-(4-methylbenzyl)-4-(((2,4,6-trichlorophenyl)thio)methyl)-1H-1,2,3-triazole (3.1.11i).



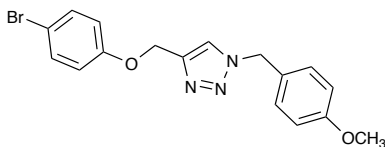
Utilizing general procedure B, **3.1.11i** (48 mg, 0.120 mmol, 87%) was isolated as a white solid. MP: 136 °C; FTIR (neat): 3083, 2920, 1515, 1434, 1323, 1151, 1116, 1058, 871 cm⁻¹.

¹H NMR (400 MHz, CDCl₃): δ 7.43 (s, 1H), 7.38 (s, 1H), 7.31 (s, 1H), 7.18 (d, *J* = 7.9 Hz, 2H), 7.12 (d, *J* = 8.0 Hz, 2H), 5.45 (s, 2H), 4.23 (s, 2H), 2.36 (s, 3H).

¹³C NMR (126 MHz, CDCl₃): δ 143.7, 138.2, 135.1, 132.3, 131.5, 131.3, 130.7, 130.5, 130.0, 129.8 (2C), 128.0 (2C), 122.0, 54.1, 27.9, 21.2.

HRMS calculated for C₁₇H₁₅Cl₃N₃S (M+H)⁺ 398.0052; found 398.0063 (TOF MS ES+).

4-((4-bromophenoxy)methyl)-1-(4-methoxybenzyl)-1H-1,2,3-triazole (3.1.11j).



Utilizing general procedure B, **3.1.11j** (67 mg, 0.179 mmol, 89%) was isolated as a white solid. MP: 98 °C

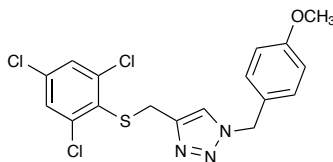
FTIR (neat): 3137, 2933, 1612, 1514, 1487, 1461, 1247, 1176, 1049, 1031, 821 cm⁻¹.

^1H NMR (400 MHz, CDCl_3): δ 7.48 (s, 1H), 7.36 (dd, J = 9.6, 2.5 Hz, 2H), 7.23 (d, J = 8.6 Hz, 2H), 6.91 (d, J = 8.6 Hz, 2H), 6.85 (d, J = 8.9 Hz, 2H), 5.47 (s, 2H), 5.14 (s, 2H), 3.82 (s, 3H).

^{13}C NMR (126 MHz, CDCl_3): δ 160.0, 157.3, 144.1, 132.3 (2C), 129.8 (2C), 126.3, 122.4, 116.6 (2C), 114.5 (2C), 113.5, 62.2, 55.4, 53.9.

HRMS calculated for $\text{C}_{17}\text{H}_{16}\text{BrN}_3\text{NaO}_2$ ($\text{M}+\text{Na}$) $^+$ 396.0324; found 396.0331 (TOF MS ES+).

1-(4-methoxybenzyl)-4-(((2,4,6-trichlorophenyl)thio)methyl)-1H-1,2,3-triazole(3.1.11k).



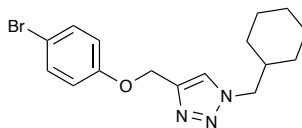
Utilizing general procedure B, **3.1.11k** (50 mg, 0.120 mmol, 86%) was isolated as a yellow solid.

FTIR (neat): 3082, 2931, 1612, 1514, 1434, 1323, 1249, 1176, 1118, 1058 cm^{-1} ; MP: 88 $^{\circ}\text{C}$ ^1H NMR (400 MHz, CDCl_3): δ 7.35 (m, 1H), 7.31 (m, 1H), 7.22 (s, 1H), 7.20–7.17 (m, 1H), 7.09 (dd, J = 8.5, 1.8 Hz, 2H), 6.82 (dd, J = 8.4, 2.1 Hz, 2H), 5.34 (s, 2H), 4.14 (s, 2 H), 3.74 (s, 3H).

^{13}C NMR (126 MHz, CDCl_3): δ 160.0, 143.6, 135.2, 132.3, 131.5, 130.7, 130.5, 130.0, 129.6 (2C), 126.3, 121.9, 114.5 (2C), 55.4, 53.8, 27.9.

HRMS calculated for $\text{C}_{17}\text{H}_{15}\text{Cl}_3\text{N}_3\text{OS}$ ($\text{M}+\text{H}$) $^+$ 414.0001; found 414.0007 (TOF MS ES+).

4-((4-bromophenoxy)methyl)-1-(cyclohexylmethyl)-1*H*-1,2,3-triazole (3.1.11l).



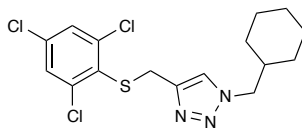
Utilizing general procedure B, **3.1.11l** (52 mg, 0.148 mmol, 86%) was isolated as a white solid. FTIR (neat): 2921, 2852, 1488, 1446, 1384, 1244, 1224, 1112, 1054 cm⁻¹; MP: 90 °C;

¹H NMR (400 MHz, CDCl₃): 7.54 (s, 1H), 7.41–7.35 (ddd, *J* = 10.2, 3.4, 2.2, 2H), 6.91–6.85 (ddd, *J* = 10.2, 3.4, 2.2, 2H), 5.19 (s, 2H), 4.18 (d, *J* = 7.2 Hz, 2H), 1.94–1.83 (m, 1H), 1.76–1.61 (m, 5H), 1.29–1.14 (m, 3H), 1.04–0.94 (m, 2H).

¹³C NMR (126 MHz, CDCl₃): δ 157.3, 143.5, 132.3, 123.1, 116.7, 113.5, 62.3, 56.6, 38.7, 30.5 (2C), 26.0, 25.5 (2C).

HRMS calculated for C₁₆H₂₁BrN₃O (M+H)⁺ 350.0868; found 350.0870 (TOF MS ES+).

1-(cyclohexylmethyl)-4-(((2,4,6-trichlorophenyl)thio)methyl)-1*H*-1,2,3-triazole (3.1.11m).



Utilizing general procedure B, **3.1.11m** (48 mg, 0.122 mmol, 88%) was isolated as a white solid.

FTIR (neat): 2925, 2852, 1450, 1427, 1215, 1153, 1116 cm⁻¹; MP: 141 °C.

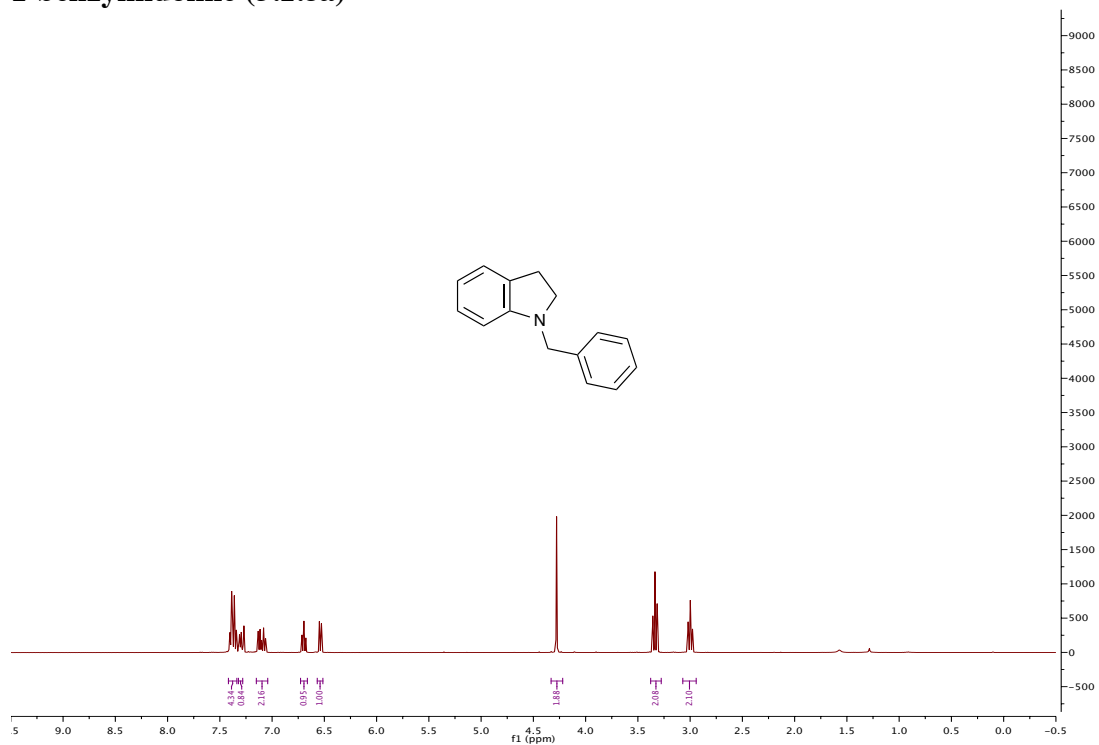
^1H NMR (500 MHz, CDCl_3): δ 7.46 (s, 1H), 7.39 (d, $J = 5.3$ Hz, 2H), 4.27 (s, 2H), 4.14 (d, $J = 7.2$ Hz, 2H), 1.89–1.79 (m, 1H), 1.76–1.61 (m, 4H), 1.58–1.50 (m, 2H), 1.28–1.09 (m, 4H), 0.95 (qd, $J = 12.2, 3.2$ Hz, 2H).

^{13}C NMR (126 MHz, CDCl_3): δ 143.1, 135.2, 132.3, 131.5, 130.7, 130.5, 130.0, 122.6, 56.6, 38.7, 30.4 (2C), 27.8, 26.0, 25.5 (2C).

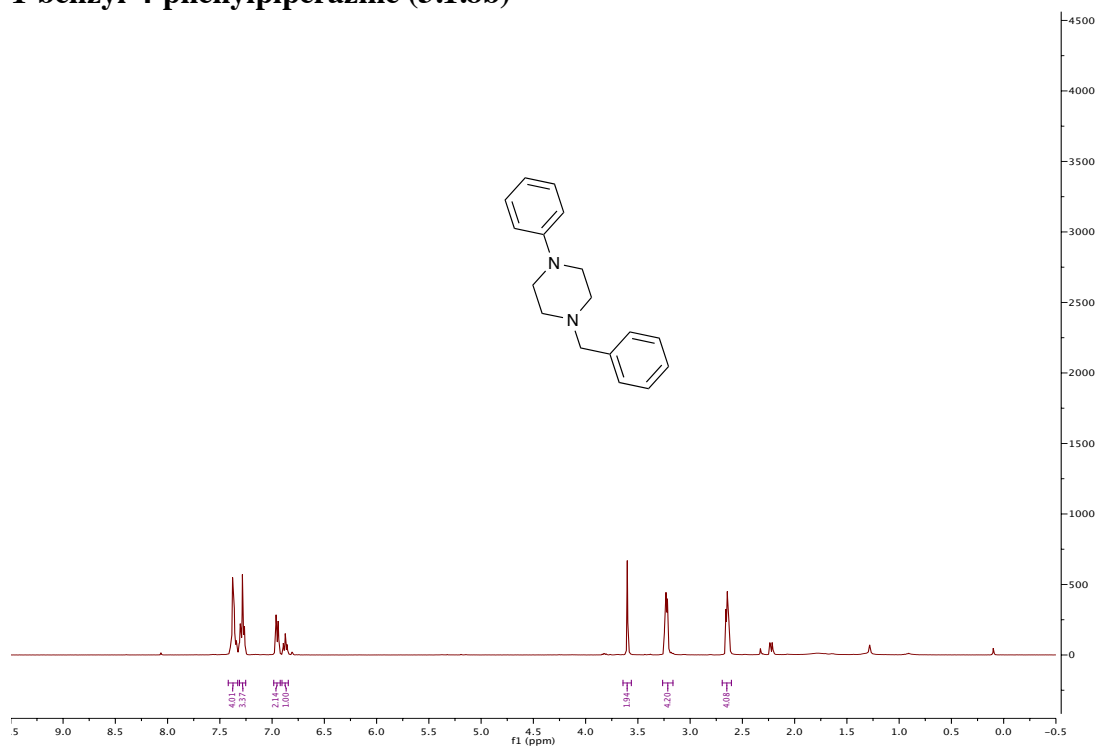
HRMS calculated for $\text{C}_{16}\text{H}_{19}\text{Cl}_3\text{N}_3\text{S}$ ($\text{M}+\text{H}$) $^+$ 390.0365; found 390.0377 (TOF MS ES+).

5.7 Spectra for Chapter 3.1.

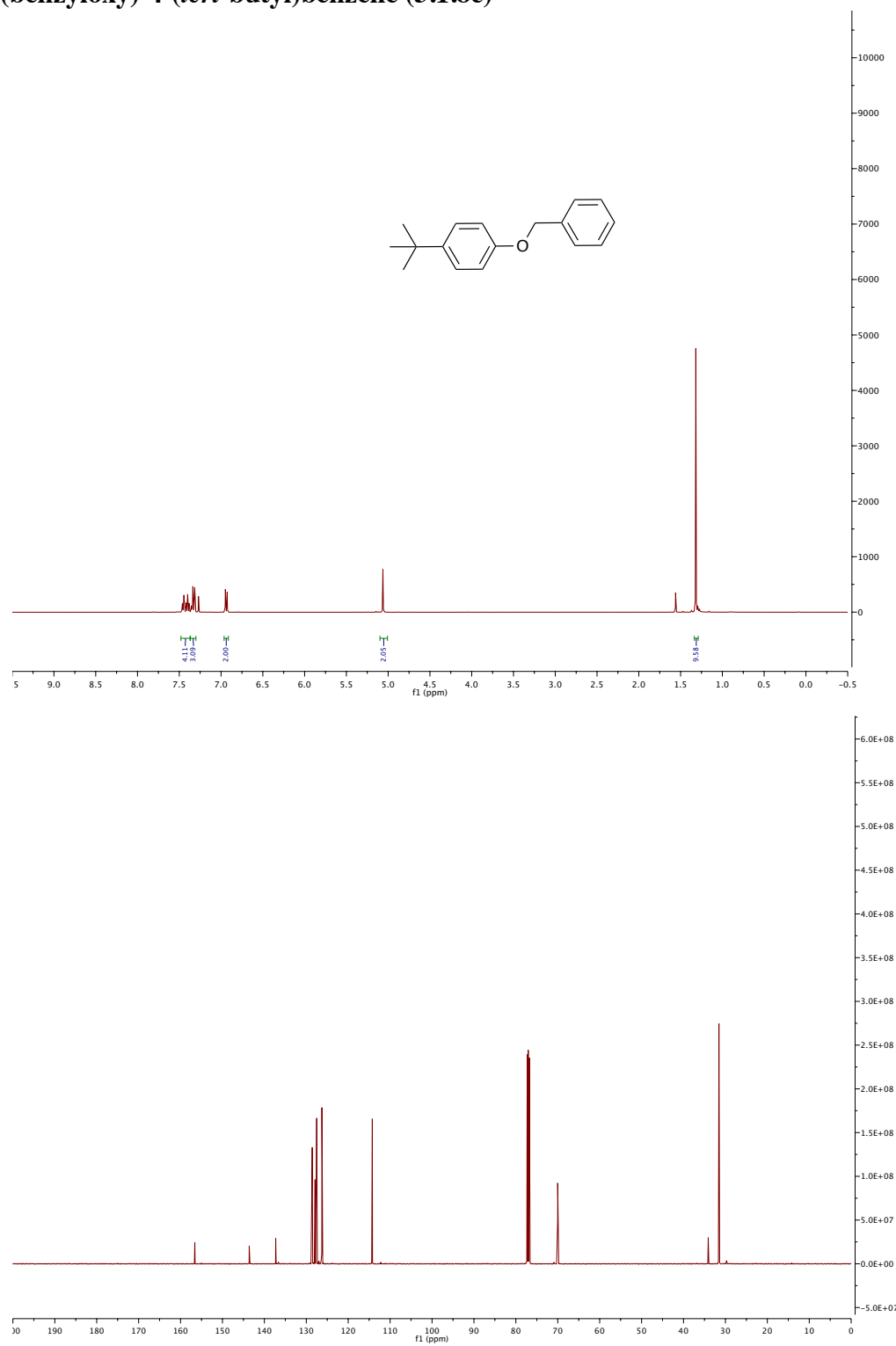
1-benzylindoline (3.1.8a)



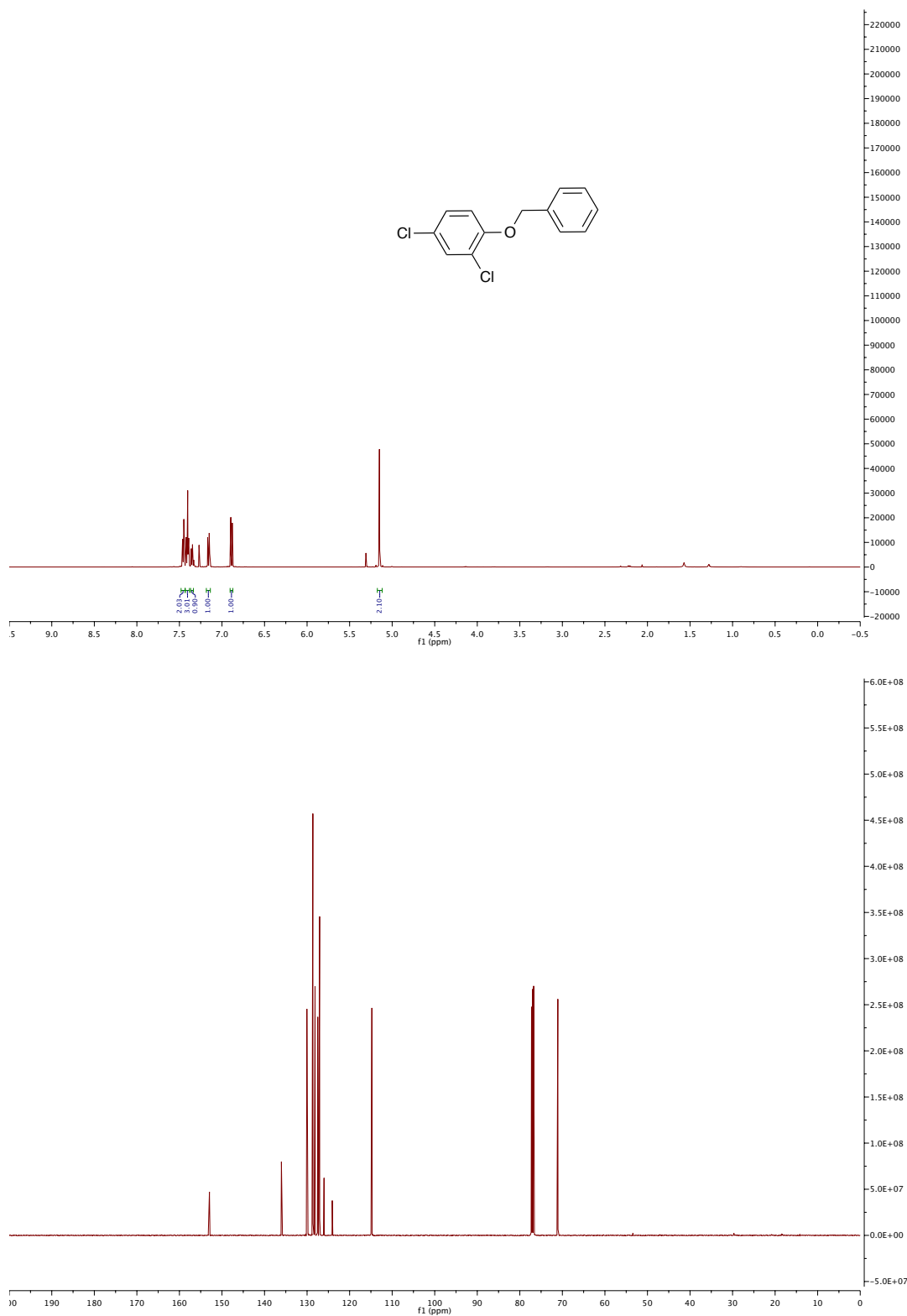
1-benzyl-4-phenylpiperazine (3.1.8b)



1-(benzyloxy)-4-(*tert*-butyl)benzene (3.1.8c)

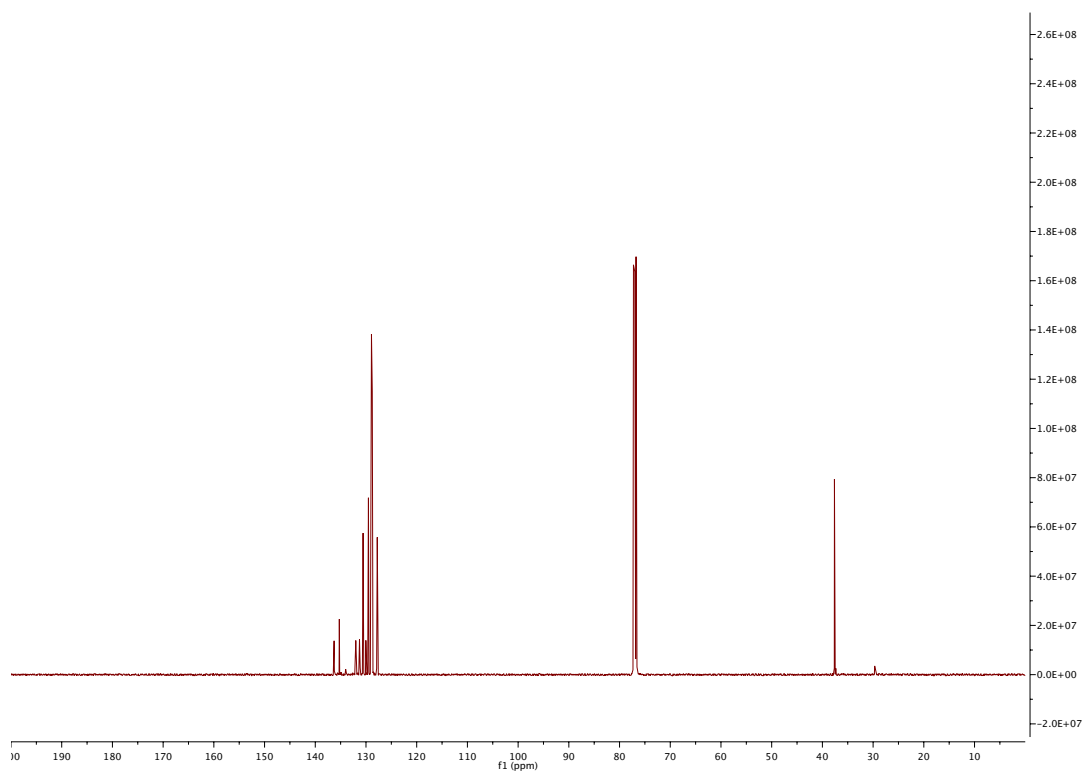


1-(benzyloxy)-2,4-dichlorobenzene (3.1.8d)

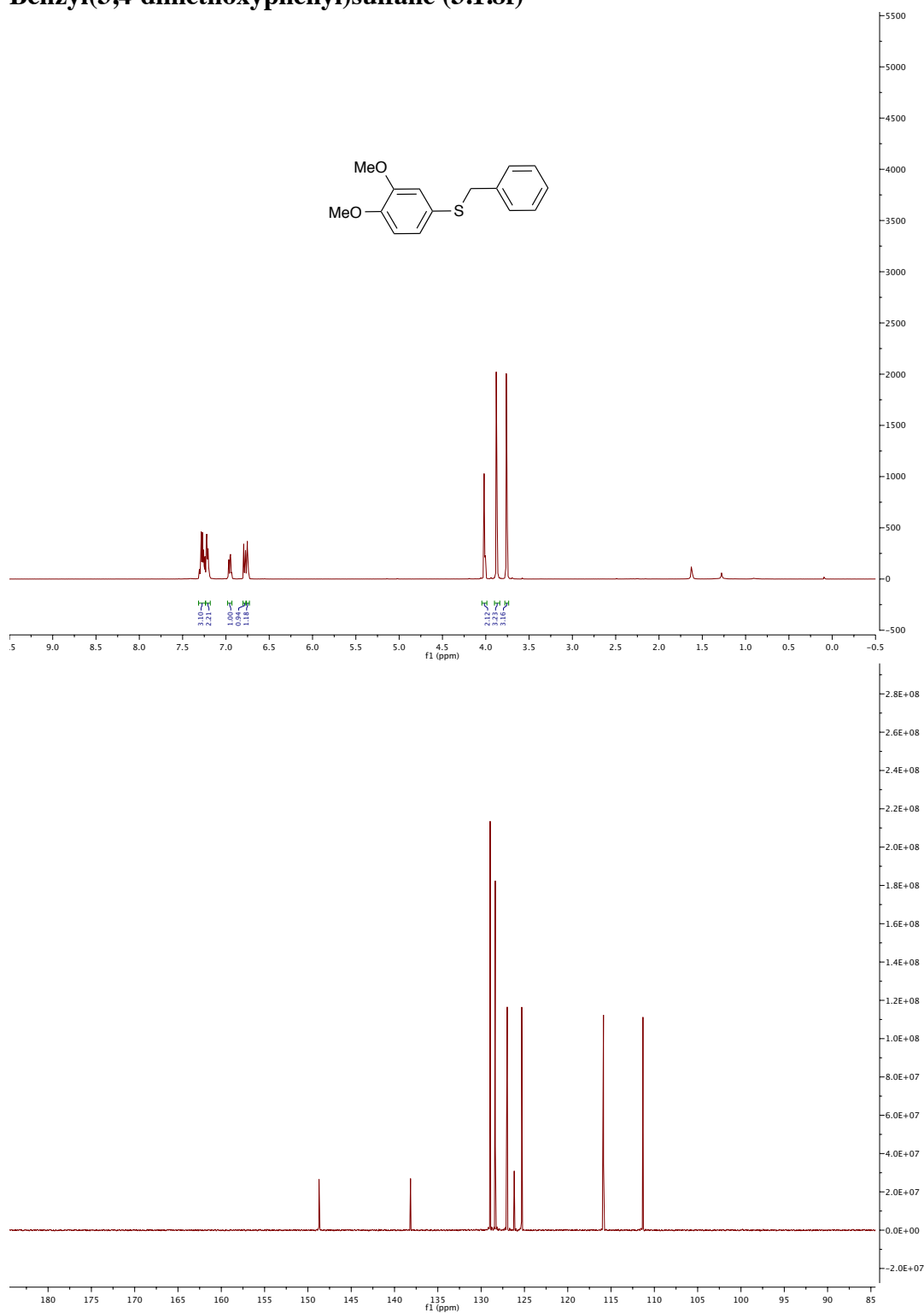


Chemical structure: Clc1cc(Cl)c(SCc2ccccc2)c(Cl)c1

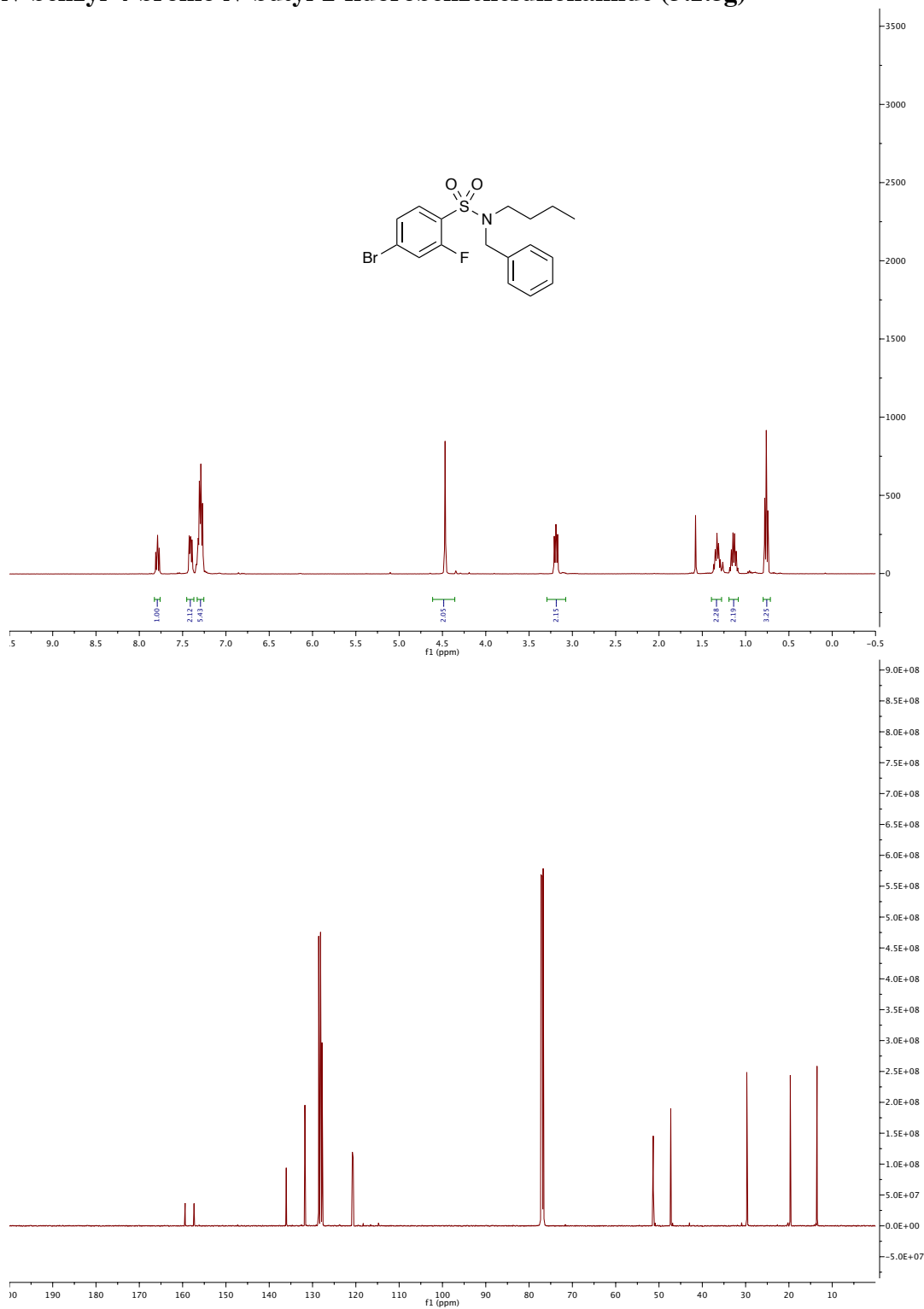
¹H NMR spectrum (CDCl₃) showing peaks at approximately 7.5 ppm (multiplet, integration 1.00, 3.09, 2.02), 4.1 ppm (singlet, integration 2.25), and 1.5 ppm (singlet).



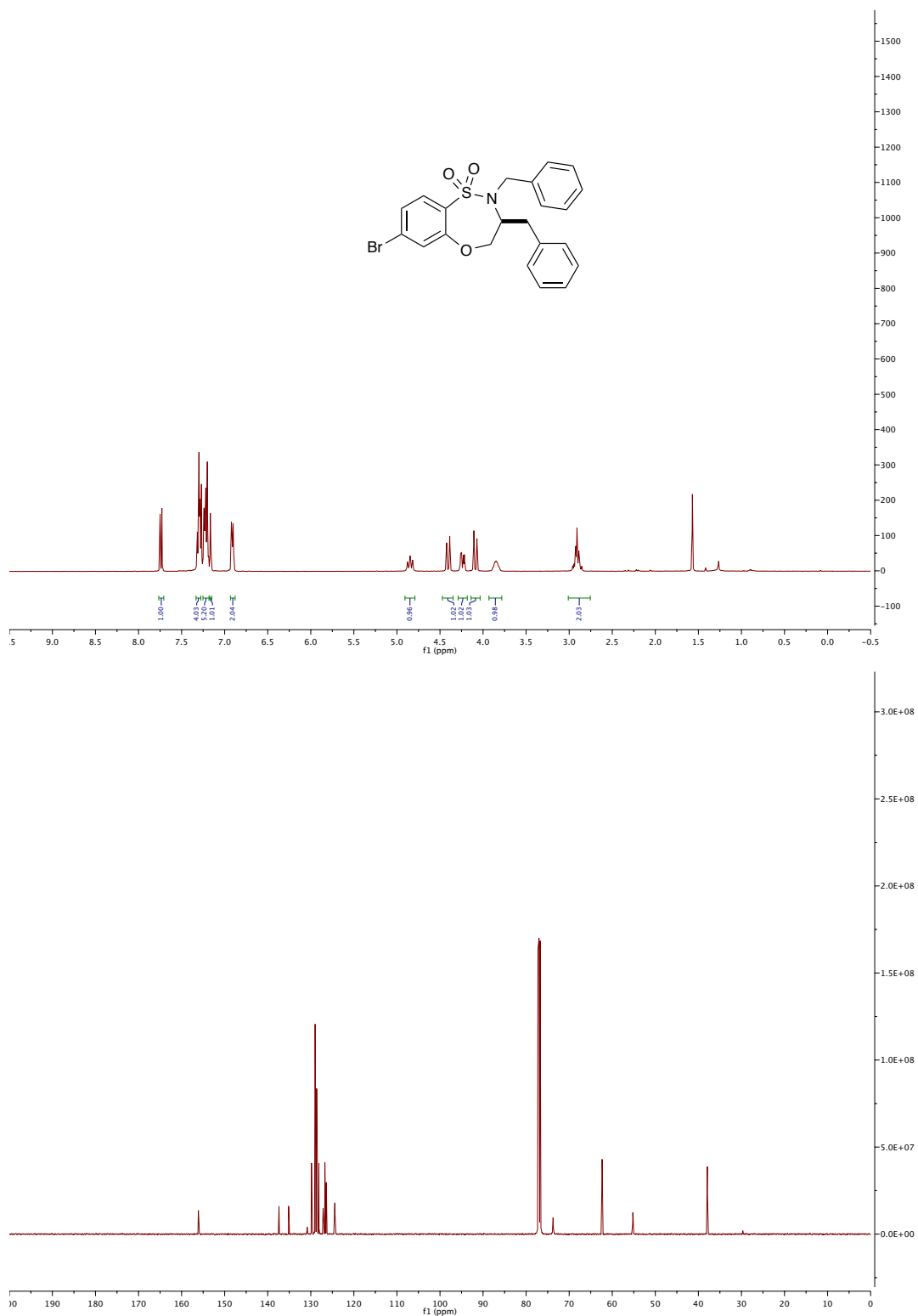
Benzyl(3,4-dimethoxyphenyl)sulfane (3.1.8f)



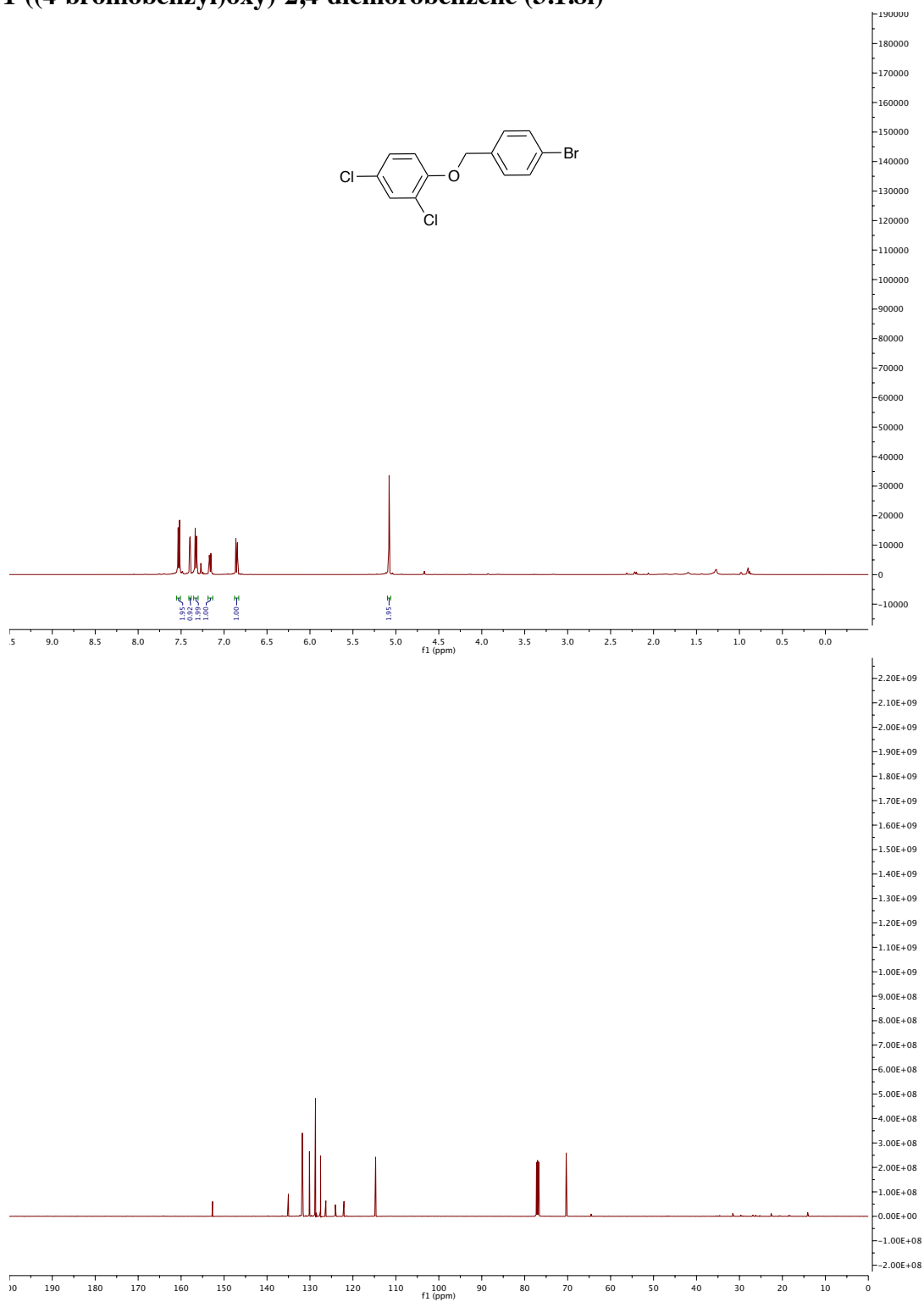
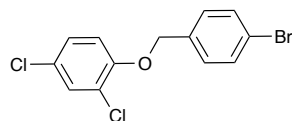
***N*-benzyl-4-bromo-*N*-butyl-2-fluorobenzenesulfonamide (3.1.8g)**



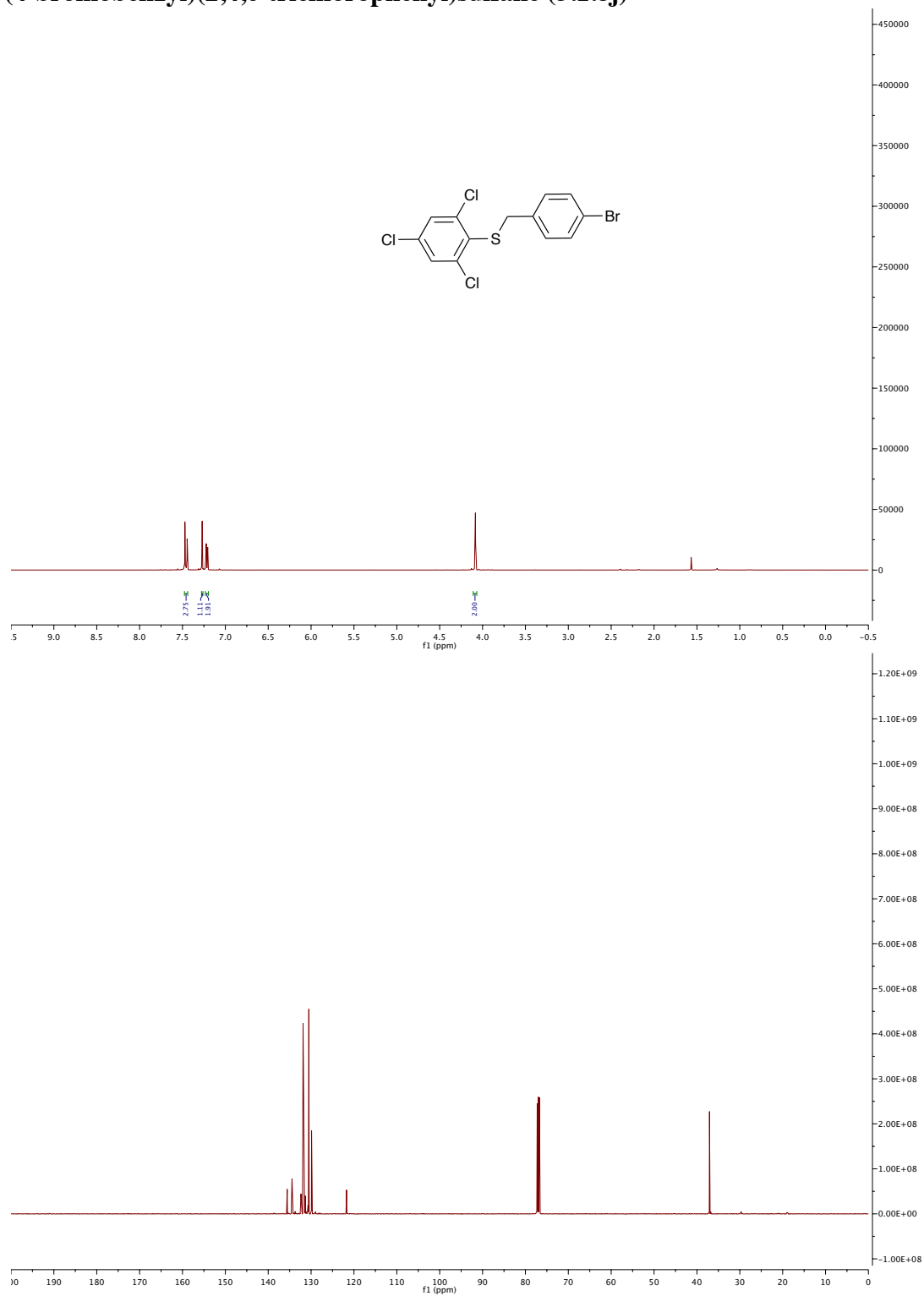
**2,3-dibenzyl-7-bromo-3,4-dihydro-2H-benzo[b][1,4,5]oxathiazepine 1,1-dioxide
(3.1.8h)**



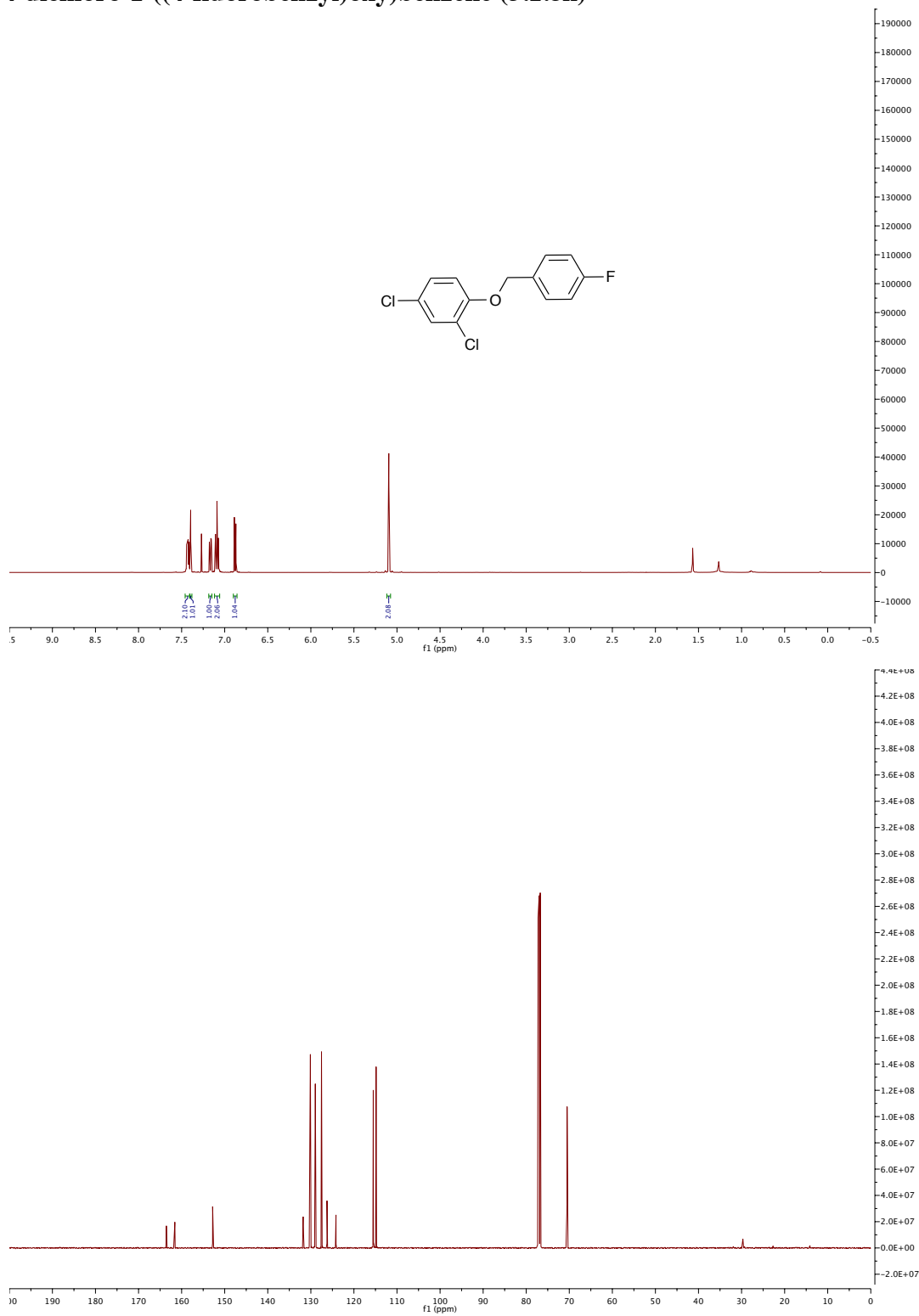
1-((4-bromobenzyl)oxy)-2,4-dichlorobenzene (3.1.8i)



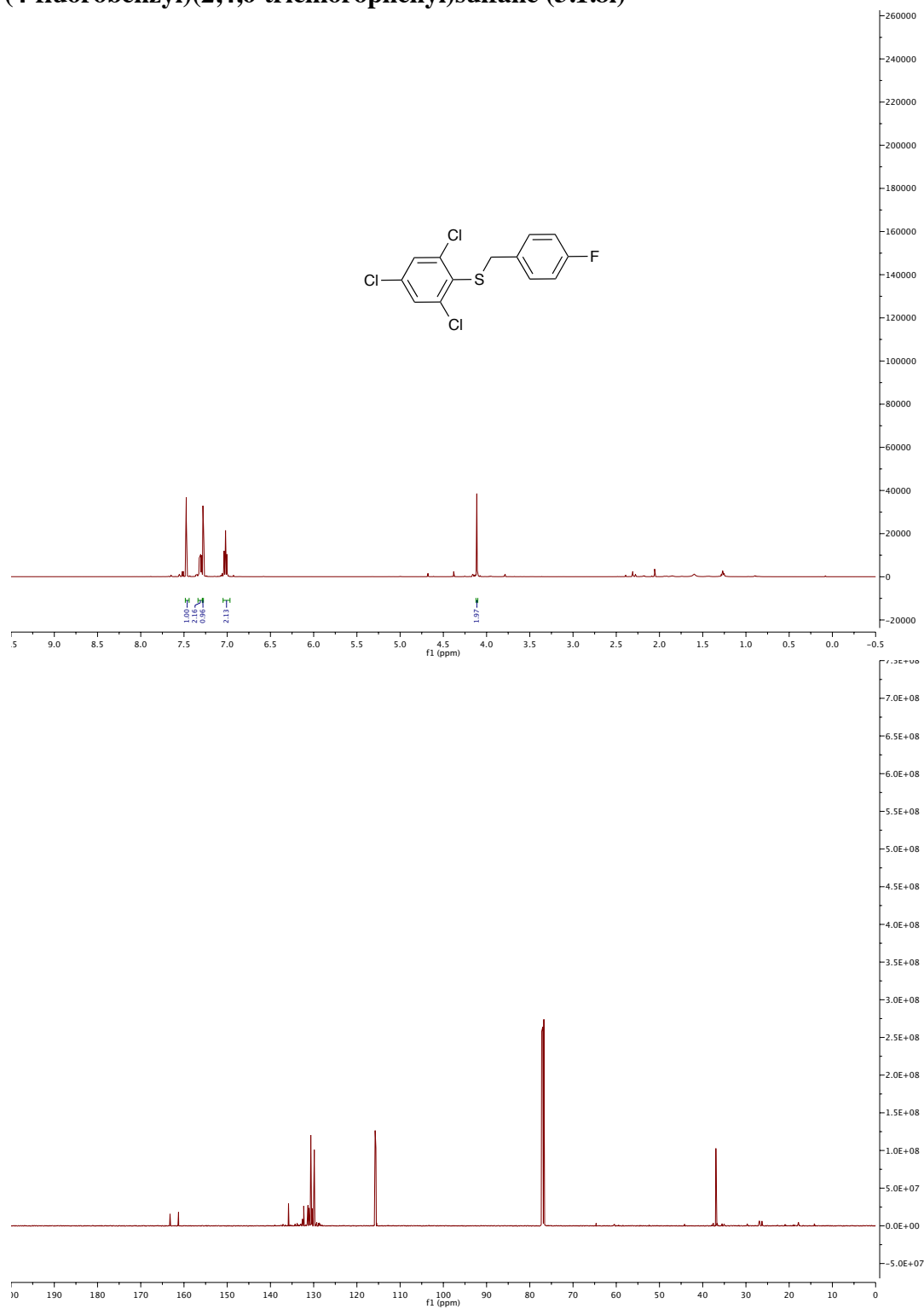
(4-bromobenzyl)(2,4,6-trichlorophenyl)sulfane (3.1.8j)



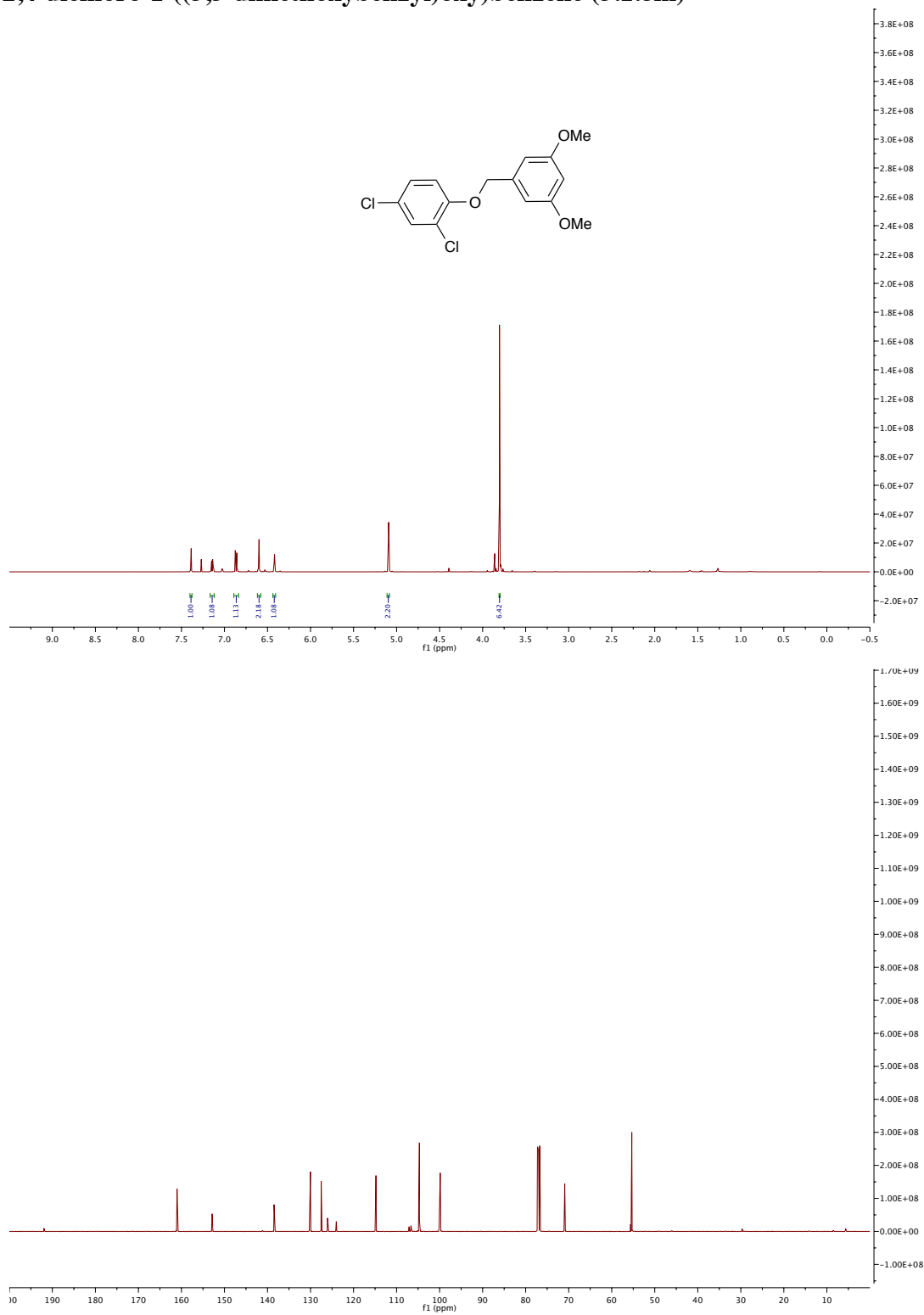
4-dichloro-1-((4-fluorobenzyl)oxy)benzene (3.1.8k)



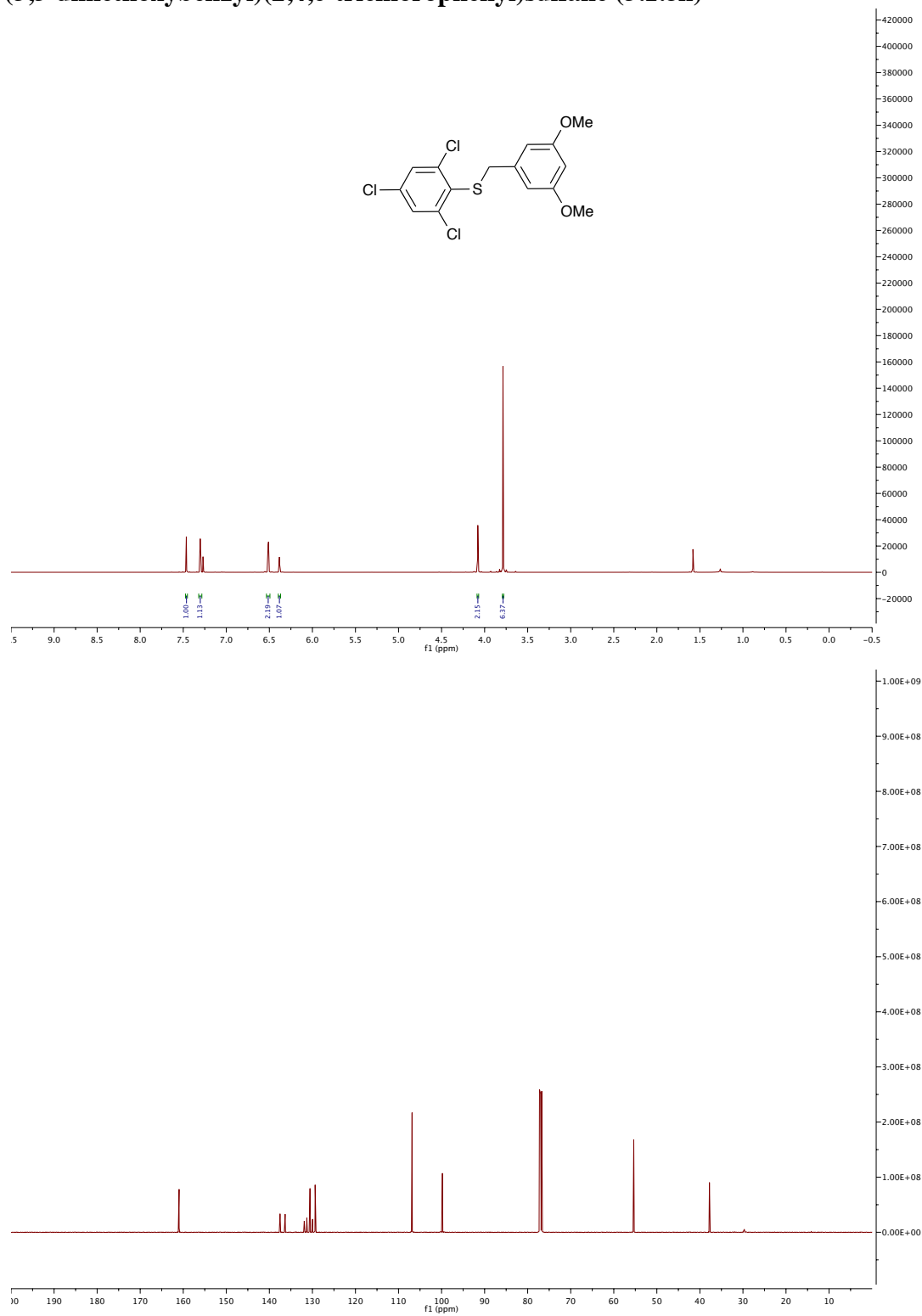
(4-fluorobenzyl)(2,4,6-trichlorophenyl)sulfane (3.1.8l)



2,4-dichloro-1-((3,5-dimethoxybenzyl)oxy)benzene (3.1.8m)



(3,5-dimethoxybenzyl)(2,4,6-trichlorophenyl)sulfane (3.1.8n)



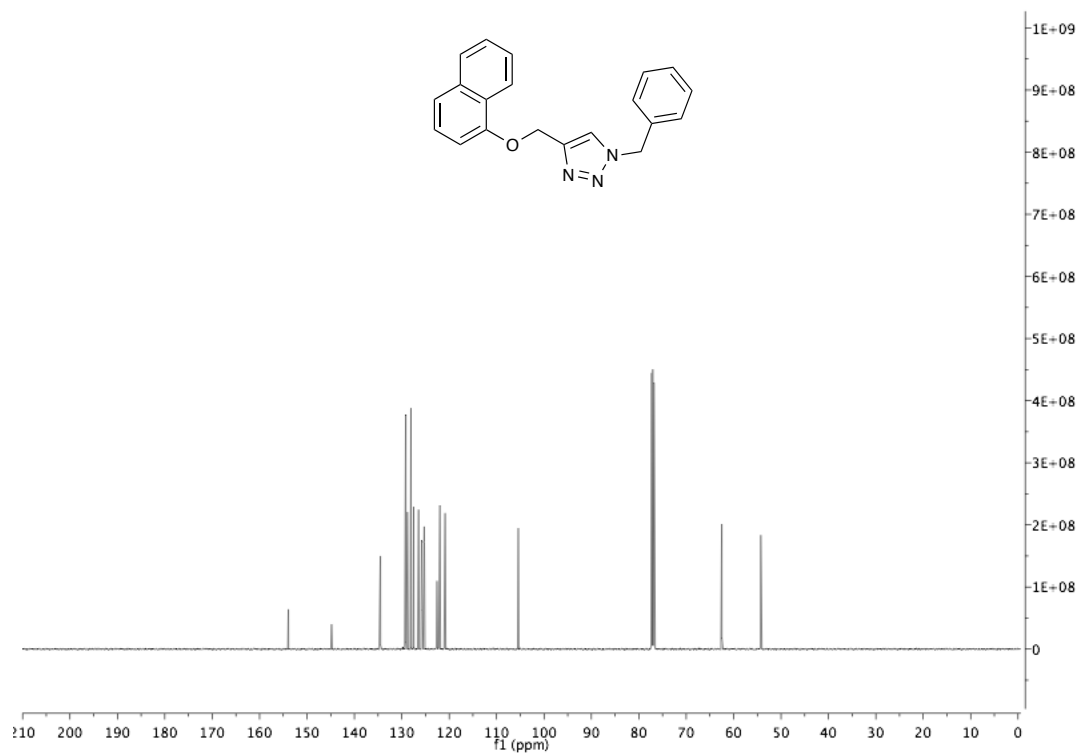
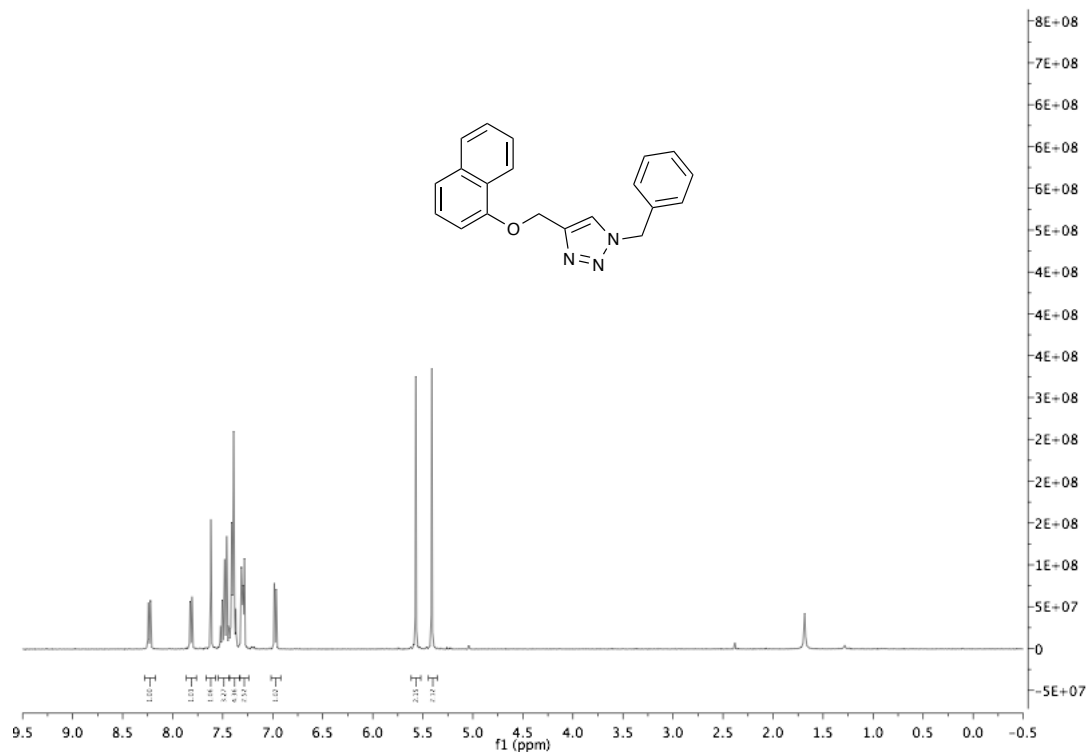
Chemical structure: c1ccc(cc1)N2C=CC(OC3=CC=C(C=C3)Cl)=N2

¹H NMR spectrum (ppm):

- 7.45 (d, 2H, integration 1.00)
- 7.35 (d, 2H, integration 1.00)
- 7.25 (t, 2H, integration 0.97)
- 7.15 (t, 2H, integration 0.96)
- 7.05 (d, 2H, integration 1.00)
- 6.95 (d, 2H, integration 1.00)
- 5.45 (s, 2H, integration 2.01)
- 5.15 (s, 2H, integration 2.02)

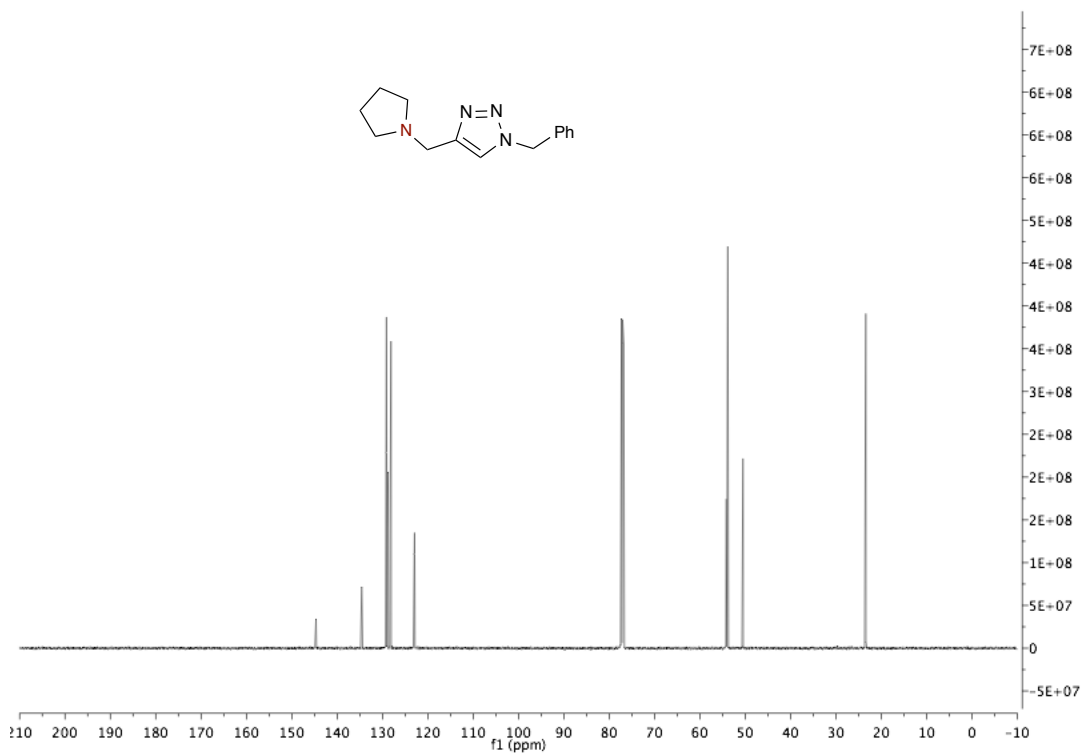


1-benzyl-4-((naphthalen-1-yloxy)methyl)-1*H*-1,2,3-triazole (3.1.11b)

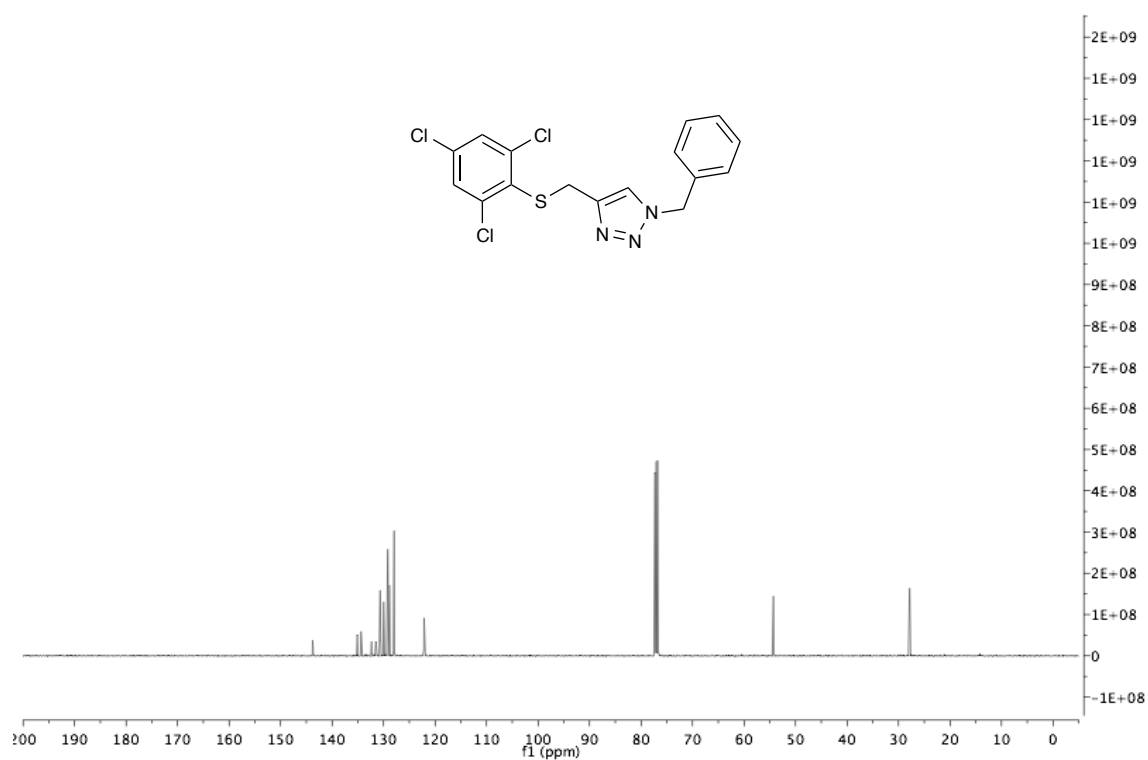
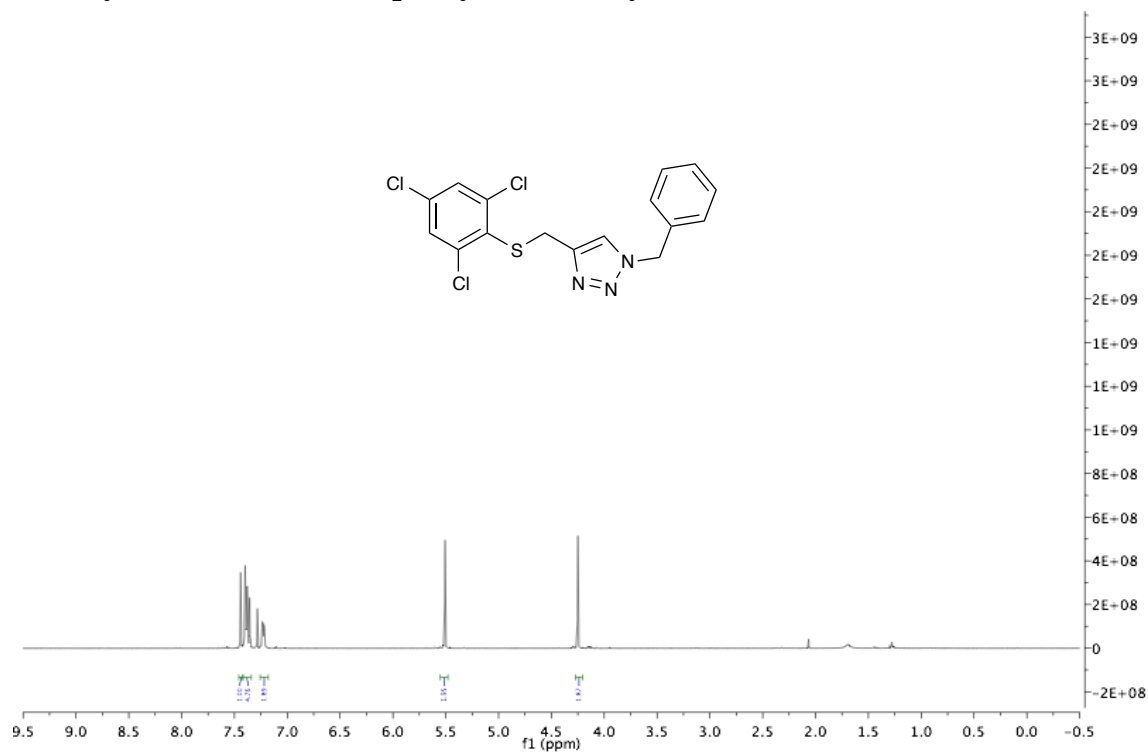


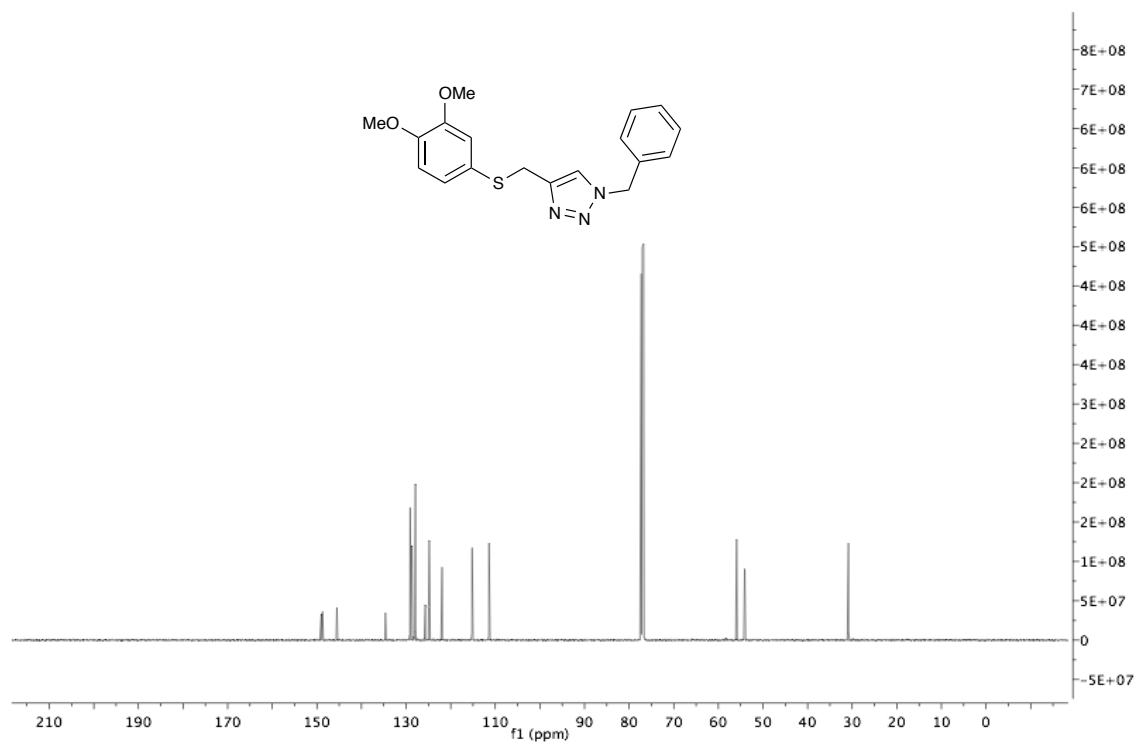
Chemical structure of 1-(cyclopentylmethyl)-4-(benzylamino)-1H-1,2,4-triazole is shown above the corresponding ¹H NMR spectrum (400 MHz, CDCl₃). The spectrum displays characteristic peaks for the compound, with integration values provided below the baseline.

Chemical Shift (ppm)	Integration
~7.3	1.00
~7.2	1.00
~7.1	2.73
~5.4	2.04
~4.0	2.40
~2.6	6.54
~1.9	4.25

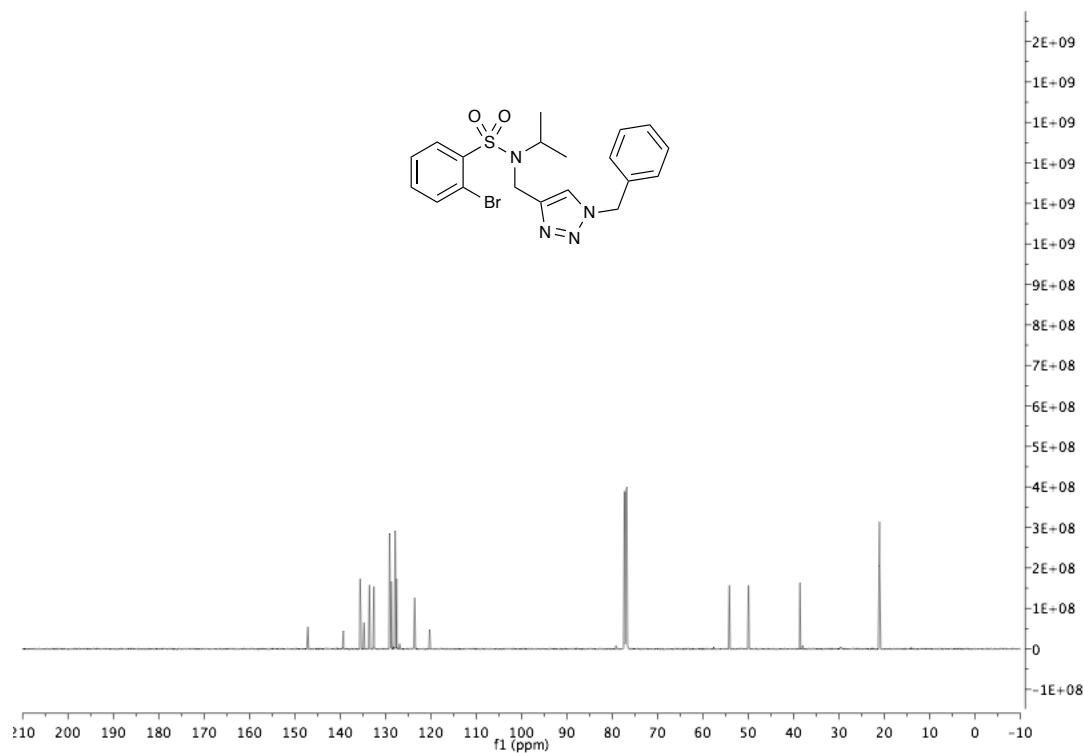
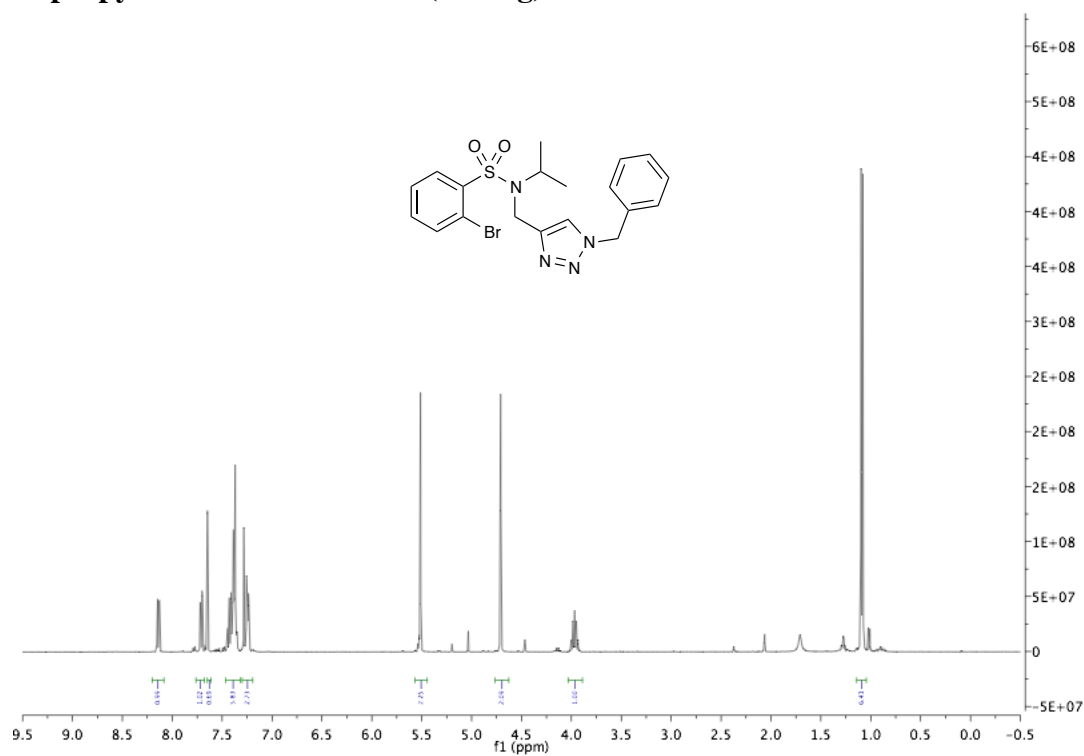


1-benzyl-4-(((2,4,6-trichlorophenyl)thio)methyl)-1*H*-1,2,3-triazole (3.1.11e)

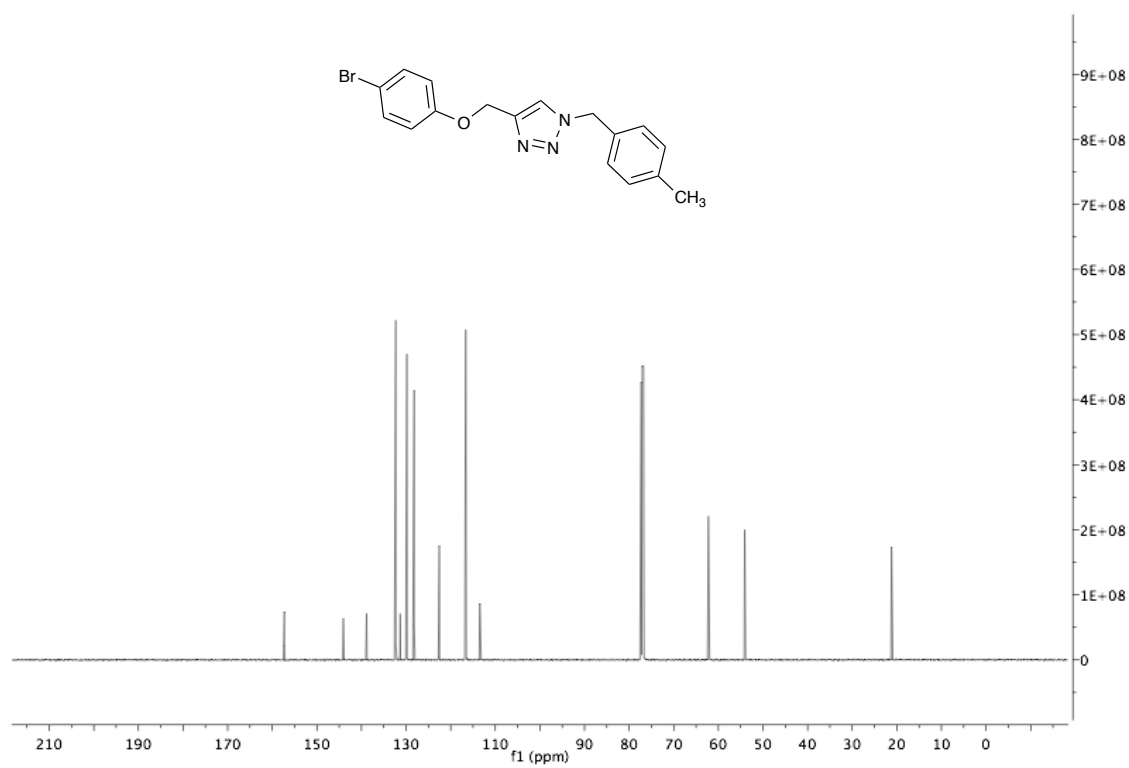
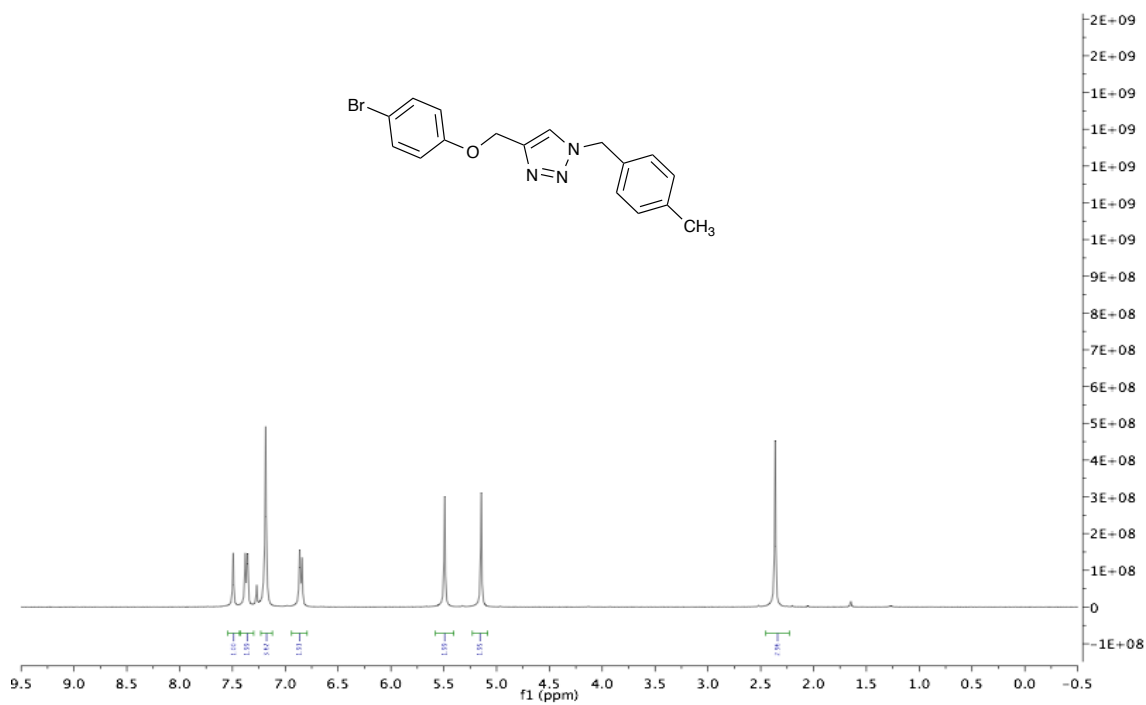


[illegible]

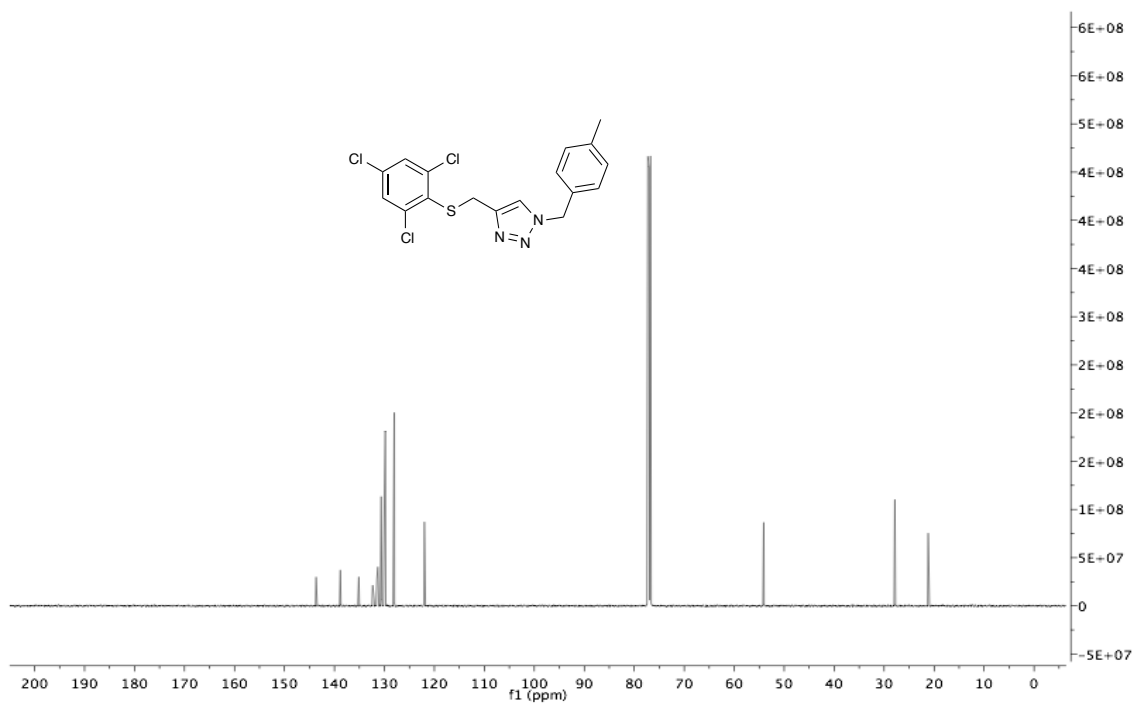
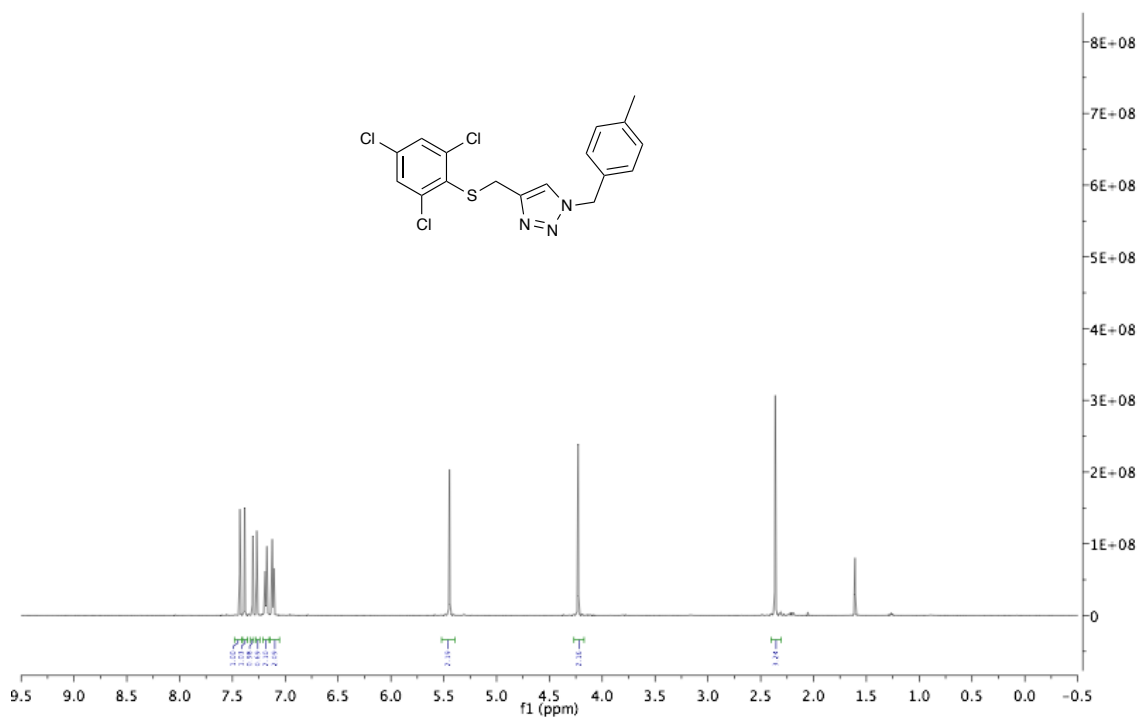
***N*-((1-benzyl-1*H*-1,2,3-triazol-4-yl)methyl)-2-bromo-*N*-isopropylbenzenesulfonamide (3.1.11g)**



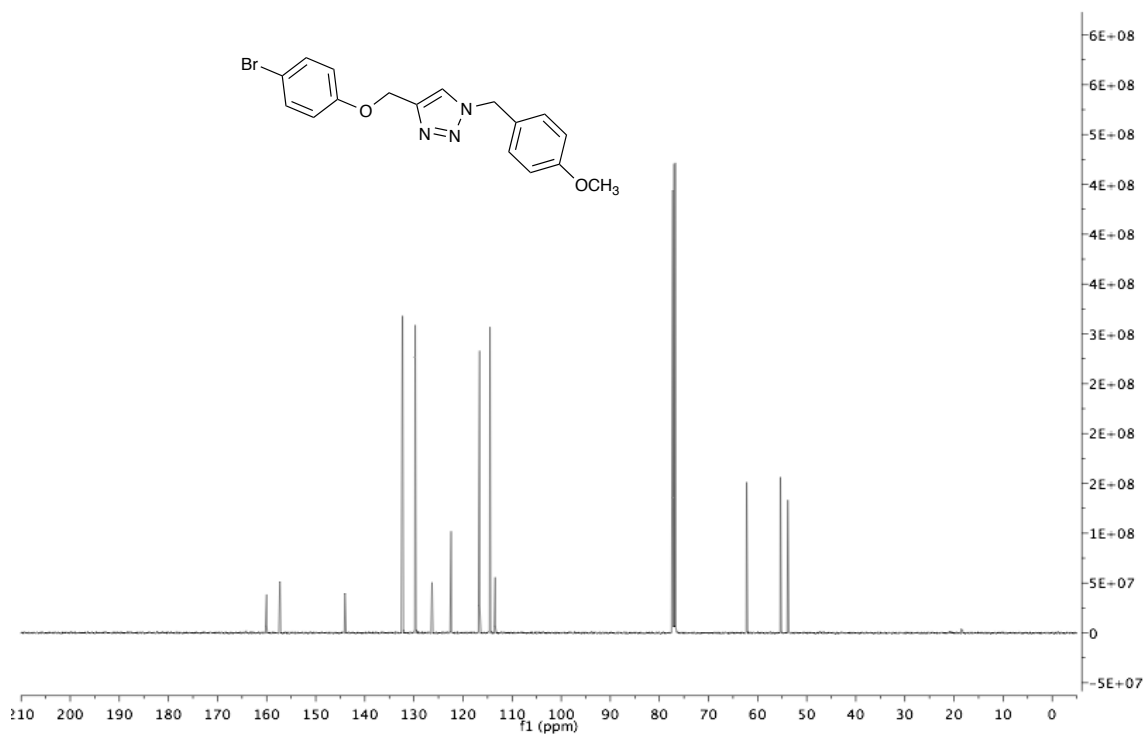
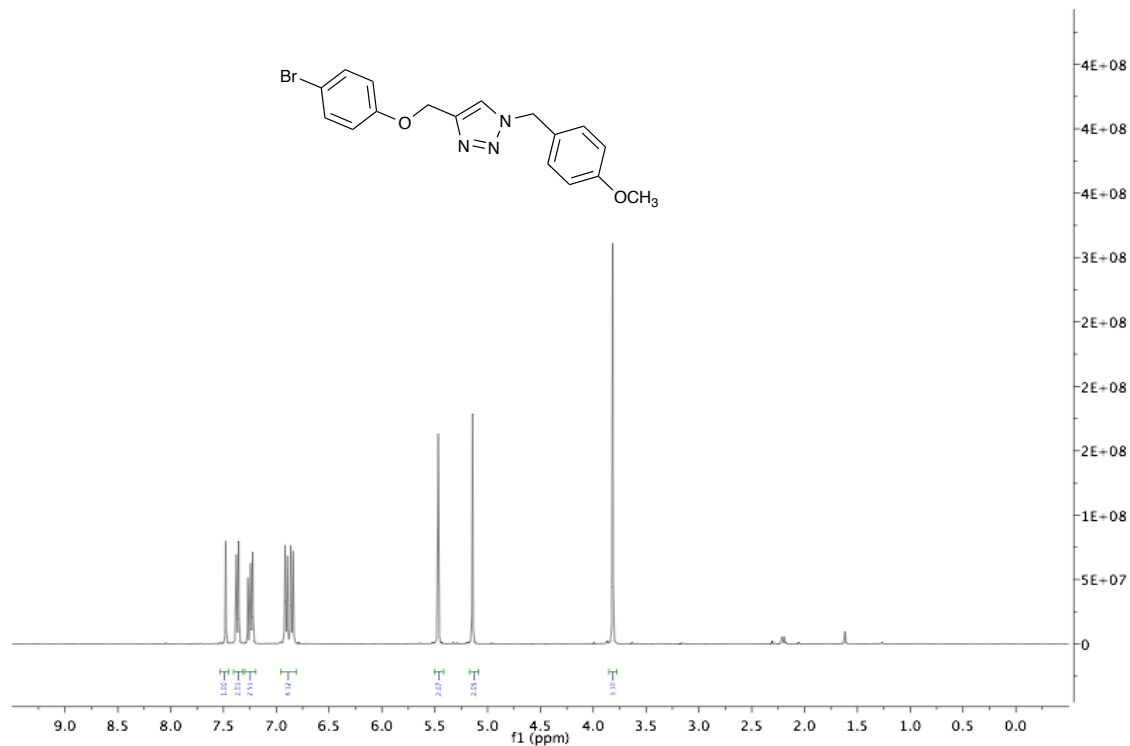
4-((4-bromophenoxy)methyl)-1-(4-methylbenzyl)-1H-1,2,3-triazole (3.1.11h)



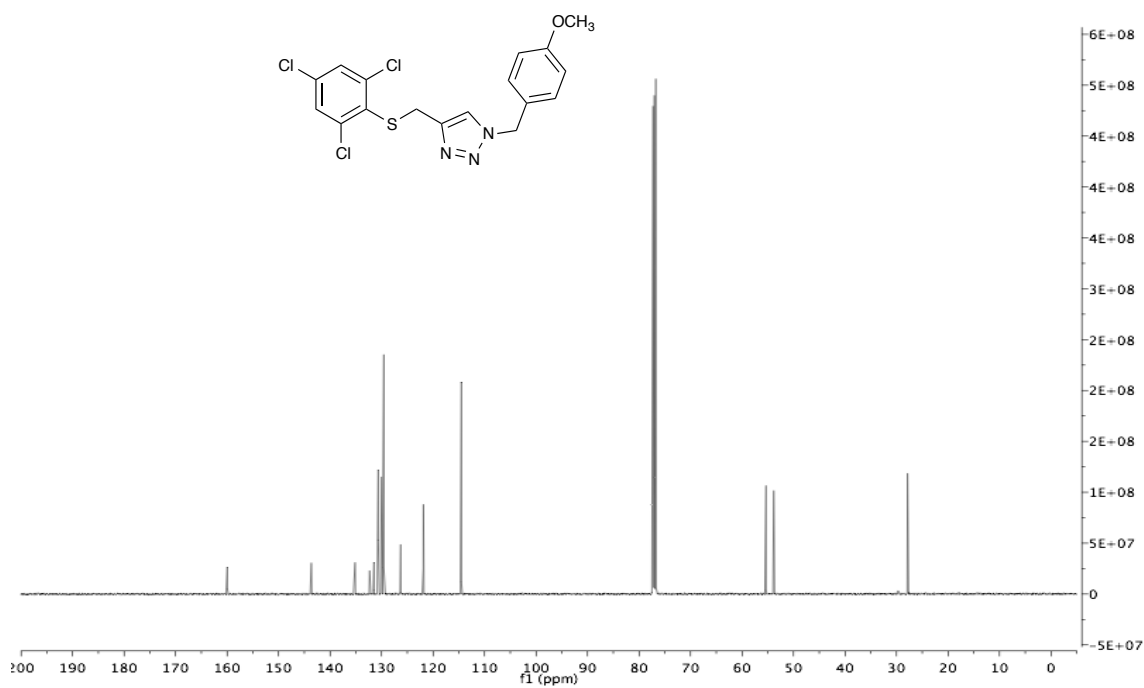
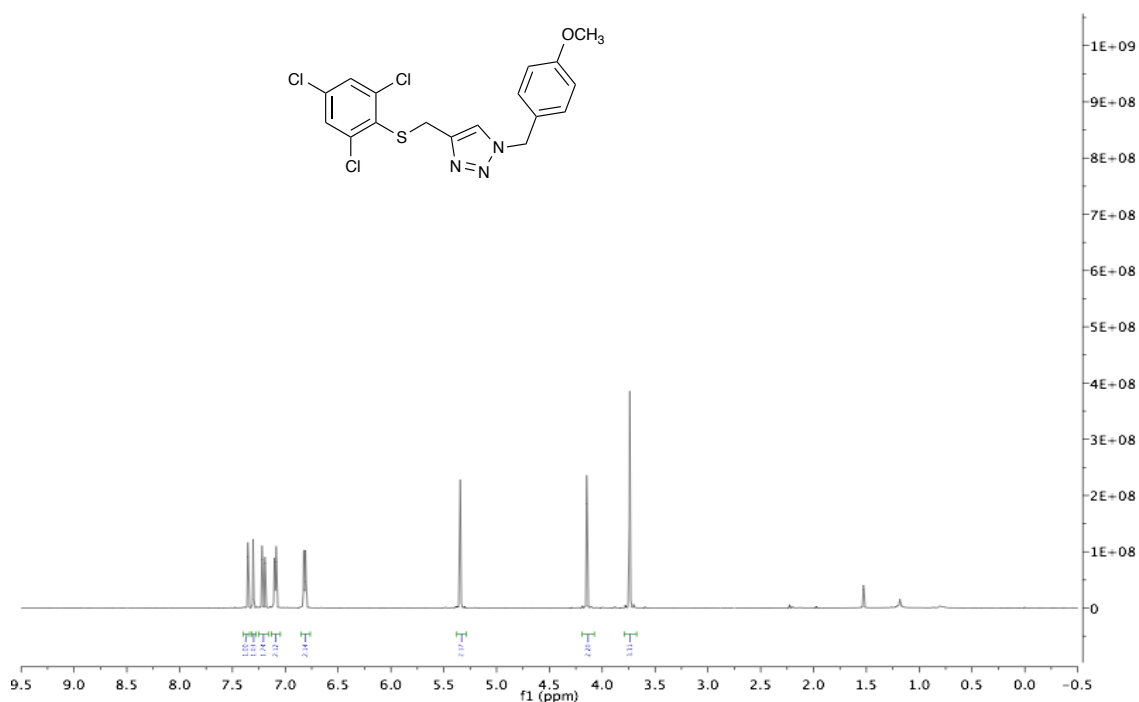
**1-(4-methylbenzyl)-4-(((2,4,6-trichlorophenyl)thio)methyl)-1H-1,2,3-triazole
(3.1.11i)**



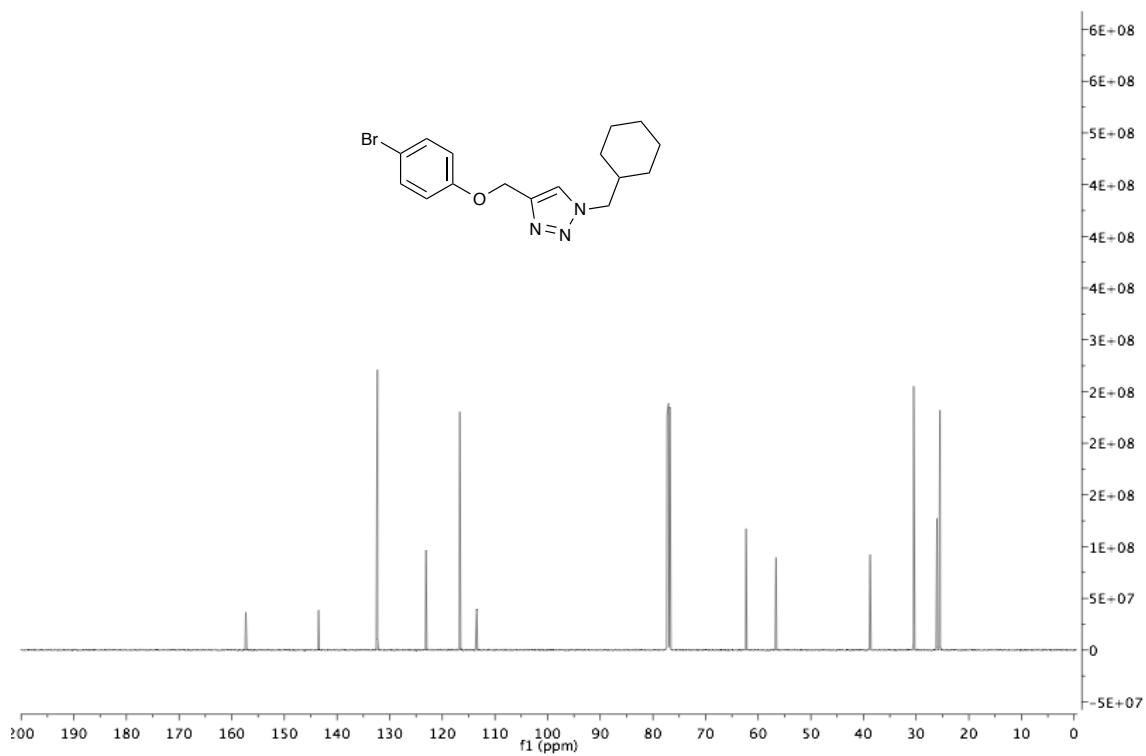
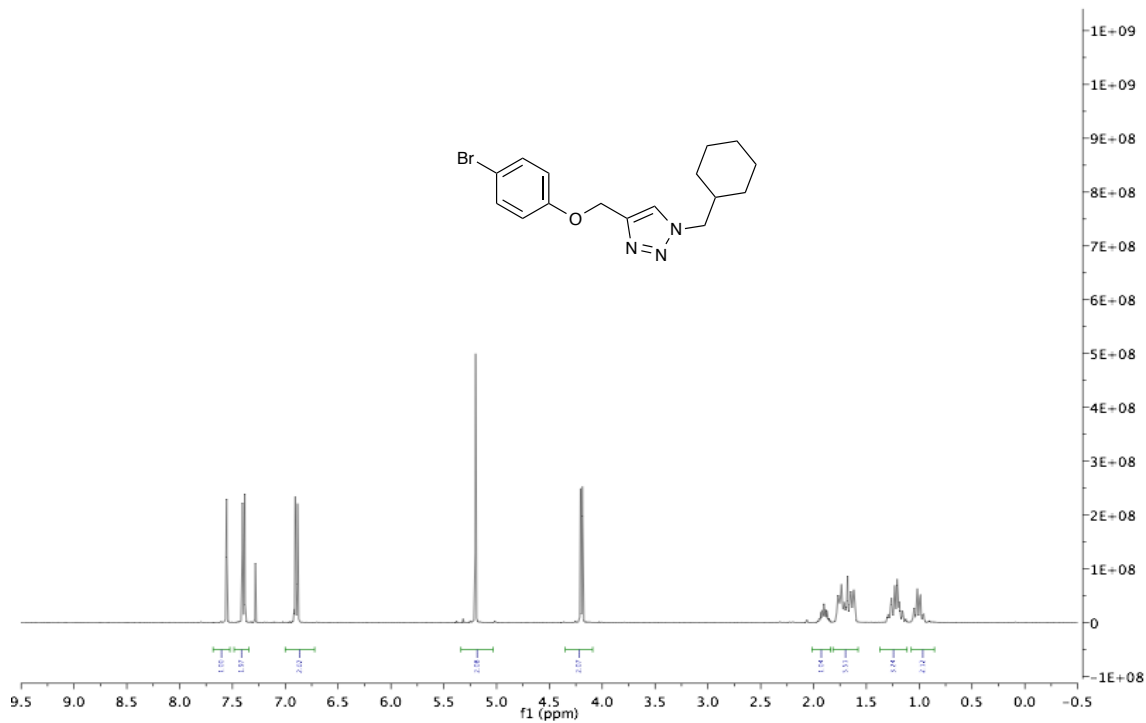
4-((4-bromophenoxy)methyl)-1-(4-methoxybenzyl)-1*H*-1,2,3-triazole (3.1.11j)



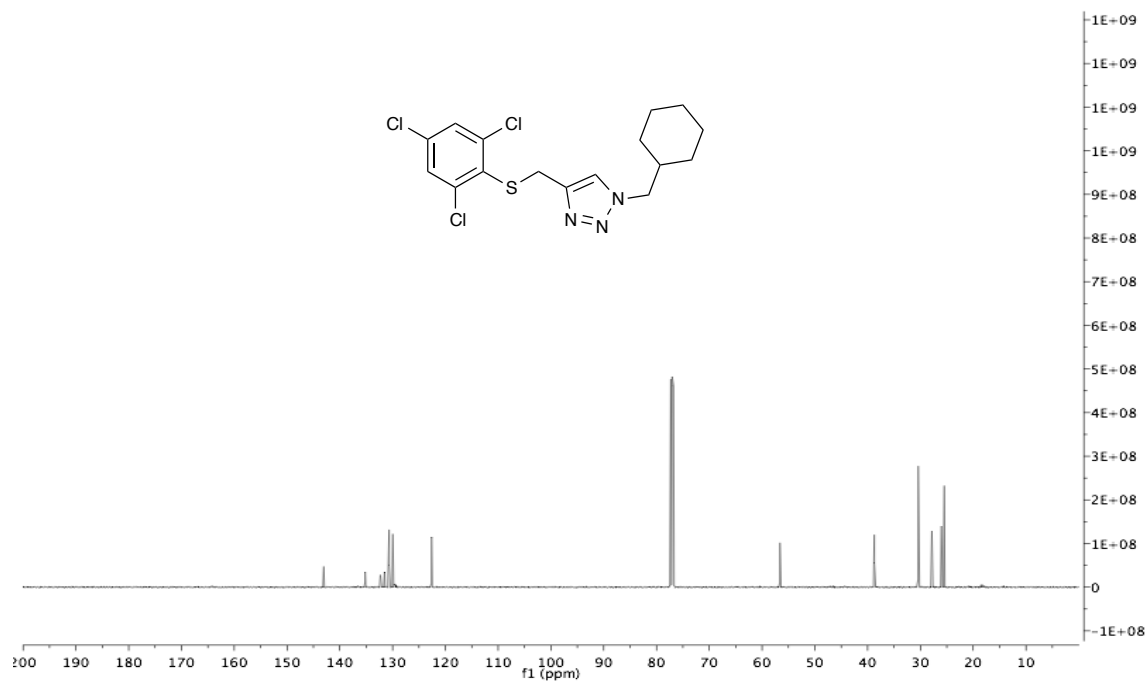
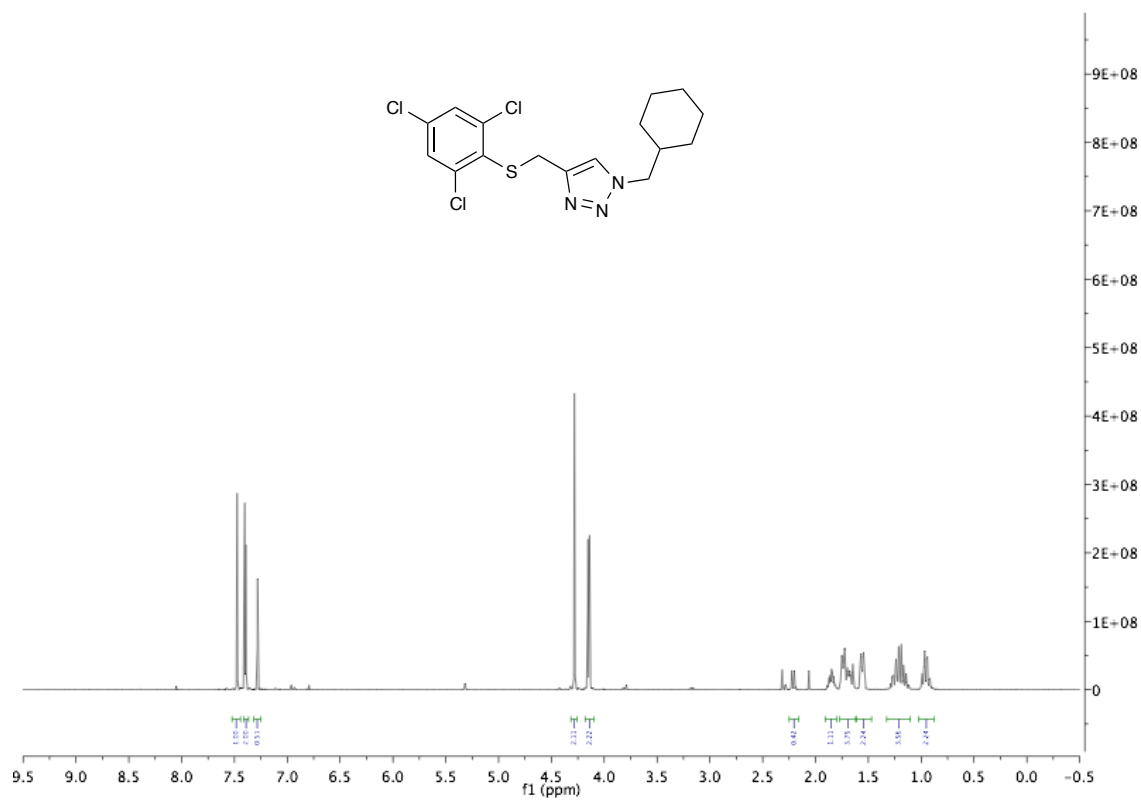
**1-(4-methoxybenzyl)-4-(((2,4,6-trichlorophenyl)thio)methyl)-1*H*-1,2,3-triazole
(3.1.11k)**



4-((4-bromophenoxy)methyl)-1-(cyclohexylmethyl)-1H-1,2,3-triazole (3.1.11l)



**1-(cyclohexylmethyl)-4-(((2,4,6-trichlorophenyl)thio)methyl)-1H-1,2,3-triazole
(3.1.11m)**



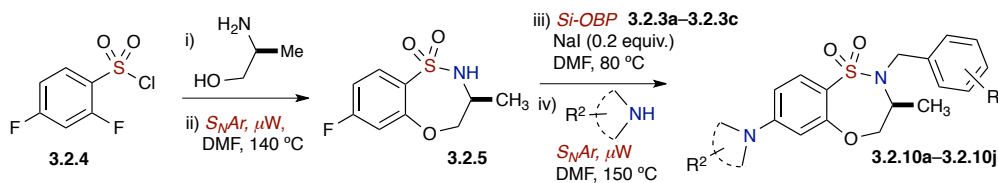
5.8 Experimental for Chapter 3.2.

Application of Silica-supported Alkylating Reagents in a One-Pot, Sequential Protocol to Diverse Benzoxathiazepine 1,1-Dioxides.

Experimental Section and Characterization data (SI-295–SI-310)

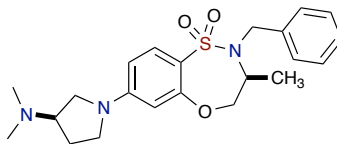
^1H , ^{13}C , Spectra for all Relevant Compounds (SI-311–SI-325)

Procedure A: General procedure for the synthesis of benzoxathiazepine 1,1-dioxides in one pot sequential protocol.



To a microwave vial (0.5–2.0 mL) vial w/ teflon cap was added 2,4-difluorobenzenesulfonyl chloride **3.2.4** (1.0 equiv.) in solvent DMF (0.2 M) followed by addition of chiral amino alcohol **3.2.5** (1.1 equiv.) and Et_3N (1.2 equiv.). The reaction was sealed under argon and stirred for 4–5 hours at RT. Next, Cs_2CO_3 (2.5 equiv.) was added and the reaction mixture was heated to 140 °C under microwave conditions for 30 min to generate compound **3.2.7**. The reaction was monitored by TLC, and upon disappearance of SM, the corresponding Si-Reagent [Si-ROMP benzylating Si-OBP_n **3.2.3a–c** ($n \sim 50$) and triazolating Si-OTP_n **3.2.3d–e** ($n \sim 50$)] was added to the resulting mixture, followed by the addition of NaI (0.2 equiv.) and the mixture was heated to 80 °C for 12–14 hrs. Then the amine component (2.5 equiv.) was added neat, and the final intermolecular S_NAr reaction was achieved at 150 °C under microwave irradiations in the same pot. The mixture was concentrated in *vacuo* and purified by flash chromatography. The resulting final products (**3.2.10–3.2.11**) were isolated in 70–92% overall yields.

(S)-2-benzyl-7-((R)-3-(dimethylamino)pyrrolidin-1-yl)-3-methyl-3,4-dihydro-2H-benzo[*b*][1,4,5]oxathiazepine 1,1-dioxide (3.2.10a)



Utilizing general procedure **A**, **3.2.10a** (34 mg, 0.082 mmol, 71%) was isolated after chromatography (5% MeOH in EtOAc) as a yellow solid.

MP: 131 °C.

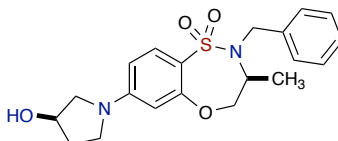
FTIR (neat, cm^{-1}): 2975, 2929, 2864, 2773, 1600, 1514, 1481, 1330, 1143, 1076.

^1H NMR (400 MHz, CDCl_3) δ 7.65 (d, J = 8.8 Hz, 1H), 7.41 (d, J = 7.1 Hz, 2H), 7.36–7.30 (m, 2H), 7.30–7.24 (m, 1H), 6.29 (dd, J = 8.9, 2.4 Hz, 1H), 6.17 (d, J = 2.4 Hz, 1H), 4.40 (dd, J = 13.1, 10.5 Hz, 1H), 4.28 (d, J = 15.4 Hz, 1H), 4.20 (dd, J = 13.1, 3.8 Hz, 1H), 4.08 (d, J = 15.4 Hz, 1H), 3.57–3.44 (m, 2H), 3.34 (td, J = 9.8, 6.7 Hz, 1H), 3.19 (t, J = 8.8 Hz, 1H), 2.94–2.82 (m, 1H), 2.33 (s, 6H), 2.25 (dd, J = 12.1, 5.8 Hz, 1H), 2.05–1.91 (m, 1H), 1.28–1.21 (m, 1H), 1.10 (d, J = 7.0 Hz, 3H).

^{13}C NMR (126 MHz, CDCl_3) δ 157.2, 151.4, 137.5, 130.5, 128.5 (2C), 127.9, 127.9, 127.5, 118.6, 106.5, 103.1, 77.3, 73.9, 65.3, 56.5, 52.0, 46.9, 44.2, 44.1, 29.9, 16.2.

HRMS calculated for $\text{C}_{22}\text{H}_{30}\text{N}_3\text{O}_3\text{S}$ ($\text{M}+\text{H}$) $^+$ 416.2008; found 416.1975 (TOF MS ES $^+$)

(S)-2-benzyl-7-((R)-3-hydroxypyrrolidin-1-yl)-3-methyl-3,4-dihydro-2H-benzo[*b*][1,4,5]oxathiazepine 1,1-dioxide (3.2.10b)



Utilizing general procedure **A**, **3.2.10b** (33 mg, 0.085 mmol, 90%) was isolated after chromatography (2:8 Hex/EtOAc) as a light brown solid.

MP: 95 °C.

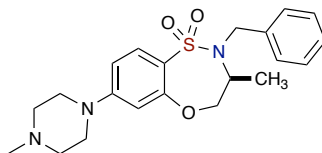
FTIR (neat, cm^{-1}): 2929, 2854, 1600, 1504, 1388, 1325, 1139, 1080.

^1H NMR (400 MHz, CDCl_3) δ 7.64 (d, J = 8.8 Hz, 1H), 7.44–7.38 (m, 2H), 7.36–7.31 (m, 2H), 7.31–7.22 (m, 1H), 6.29 (dd, J = 8.8, 2.4 Hz, 1H), 6.18 (d, J = 2.3 Hz, 1H), 4.63 (m, 1H), 4.37 (dd, J = 13.2, 10.4 Hz, 1H), 4.30–4.24 (m, 1H), 4.21 (dd, J = 13.1, 3.7 Hz, 1H), 4.15–4.04 (m, 2H), 3.58–3.49 (m, 2H), 3.40 (td, J = 9.1, 3.1 Hz, 1H), 3.29 (dt, J = 10.8, 1.6 Hz, 1H), 2.16 (m, 1H), 2.10 (m, 1H), 1.27 (t, J = 7.2 Hz, 1H), 1.10 (d, J = 7.0 Hz, 3H).

^{13}C NMR (126 MHz, CDCl_3) δ 157.1, 151.6, 137.5, 130.5, 128.5 (2C), 127.9 (2C), 127.5, 118.4, 106.8, 103.4, 73.9, 70.8, 56.5, 56.1, 51.7, 45.6, 34.0, 16.2.

HRMS calculated for $\text{C}_{20}\text{H}_{24}\text{N}_2\text{O}_4\text{S}$ ($\text{M}+\text{Na}$) $^+$ 411.1354; found 411.1349 (TOF MS ES $^+$).

(S)-2-benzyl-3-methyl-7-(4-methylpiperazin-1-yl)-3,4-dihydro-2H-benzo[*b*][1,4,5]oxathiazepine 1,1-dioxide (3.2.10c)



Utilizing general procedure A, **3.2.10c** (30 mg, 0.076 mmol, 79%) was isolated after chromatography (5% MeOH in EtOAc) as a yellow solid.

MP: 136 °C.

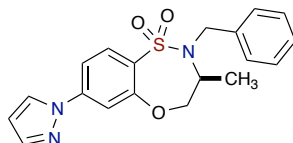
FTIR (neat, cm^{-1}): 2935, 2844, 2796, 1596, 1550, 1425, 1330, 1147, 1076.

^1H NMR (400 MHz, CDCl_3) δ 7.68 (d, J = 8.9 Hz, 1H), 7.40 (d, J = 7.5 Hz, 2H), 7.37–7.28 (m, 3H), 6.64 (dd, J = 9.0, 2.5 Hz, 1H), 6.50 (d, J = 2.4 Hz, 1H), 4.48 (t, J = 12.0 Hz, 1H), 4.36 (d, J = 15.3 Hz, 1H), 4.22 (dd, J = 13.1, 4.0 Hz, 1H), 4.09 (d, J = 15.3 Hz, 1H), 4.01 (m, 1H), 3.37 – 3.28 (m, 4H), 2.56 (t, J = 5.1 Hz, 4H), 2.37 (s, 3H), 1.11 (d, J = 7.0 Hz, 3H).

^{13}C NMR (126 MHz, CDCl_3) δ 157.1, 154.8, 137.2, 130.2 (2C), 128.5 (2C), 128.0, 127.6, 121.1, 109.3, 106.6, 77.2, 74.2, 56.7, 54.6 (2C), 47.3 (2C), 46.0, 16.2.

HRMS calculated for $\text{C}_{21}\text{H}_{28}\text{N}_3\text{O}_3\text{S}$ ($\text{M}+\text{H}$) $^+$ 402.1851; found 402.1869 (TOF MS ES+).

(S)-2-benzyl-3-methyl-7-(1*H*-pyrazol-1-yl)-3,4-dihydro-2*H*-benzo[*b*][1,4,5]oxathiazepine 1,1-dioxide (3.2.10d)



Utilizing general procedure **A**, **3.2.10d** (31.5 mg, 0.085 mmol, 90%) was isolated after chromatography (1:1, Hex/EtOAc) as a white solid.

MP: 149 °C.

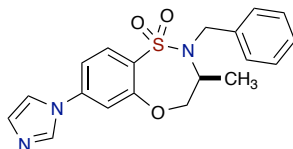
FTIR (neat, cm⁻¹): 2979, 2923, 1600, 1521, 1334, 1159, 1076.

¹H NMR (500 MHz, CDCl₃) δ 7.99–7.96 (m, 1H), 7.94 (d, *J* = 8.5 Hz, 1H), 7.77 (d, *J* = 1.7 Hz, 1H), 7.53–7.48 (m, 2H), 7.41–7.38 (m, 2H), 7.35 (tt, *J* = 6.3, 1.0 Hz, 2H), 7.32–7.29 (m, 1H), 6.52 (dd, *J* = 2.6, 1.7 Hz, 1H), 4.73–4.61 (m, 1H), 4.48 (d, *J* = 15.1 Hz, 1H), 4.32 (dd, *J* = 13.2, 4.4 Hz, 1H), 4.16 (d, *J* = 15.0 Hz, 1H), 4.06–3.96 (m, 1H), 1.16 (d, *J* = 6.9 Hz, 3H).

¹³C NMR (126 MHz, CDCl₃) δ 156.8, 143.8, 142.9, 136.4, 130.4, 128.6 (2C), 129.5, 128.2 (2C), 127.9, 126.9, 113.1, 111.7, 108.7, 74.8, 56.9, 53.3, 16.1.

HRMS calculated for C₁₉H₂₀N₃O₃S (M+H)⁺ 370.1225; found 370.1194 (TOF MS ES+).

(S)-2-benzyl-7-(1*H*-imidazol-1-yl)-3-methyl-3,4-dihydro-2*H*-benzo[*b*][1,4,5]oxathiazepine 1,1-dioxide (3.2.10e)



Utilizing general procedure **A**, **3.2.10e** (32 mg, 0.087 mmol, 91%) was isolated after chromatography (1:1, Hex/EtOAc) as a yellow liquid.

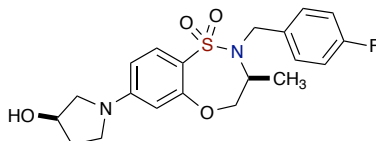
FTIR (neat, cm^{-1}): 2929, 2852, 1602, 1575, 1328, 1498, 1334, 1203, 1161, 1076.

^1H NMR (400 MHz, CDCl_3) δ 7.97 (d, $J = 8.5$ Hz, 1H), 7.92 (s, 1H), 7.40–7.29 (m, 6H), 7.26–7.19 (m, 2H), 7.11–7.07 (m, 1H), 4.75 (t, $J = 12.2$ Hz, 1H), 4.53 (d, $J = 14.9$ Hz, 1H), 4.33 (dd, $J = 13.2, 4.5$ Hz, 1H), 4.18 (d, $J = 14.9$ Hz, 1H), 3.98 (m, 1H), 1.17 (d, $J = 6.9$ Hz, 3H).

^{13}C NMR (126 MHz, CDCl_3) δ 156.9, 141.1, 136.1, 135.3, 131.2, 130.9, 130.6, 128.6 (2C), 128.3 (2C), 128.0, 117.7, 115.3, 113.6, 75.1, 57.1, 53.8, 16.1.

HRMS calculated for $\text{C}_{19}\text{H}_{20}\text{N}_3\text{O}_3\text{S}$ ($\text{M}+\text{H}$) $^+$ 370.1225; found 370.1212 (TOF MS ES $^+$).

(S)-2-(4-fluorobenzyl)-7-((R)-3-hydroxypyrrolidin-1-yl)-3-methyl-3,4-dihydro-2H-benzo[b][1,4,5]oxathiazepine 1,1-dioxide (3.2.10f)



Utilizing general procedure **A**, **3.2.10f** (34.5 mg, 0.085 mmol, 90%) was isolated after chromatography (2:8, Hex/EtOAc) as a yellow liquid.

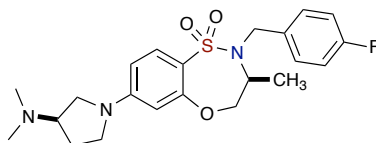
FTIR (neat, cm^{-1}): 2975, 2929, 2918, 2854, 1600, 1508, 1388, 1325, 1139, 1078.

^1H NMR (400 MHz, CDCl_3) δ 7.63 (d, $J = 8.8$ Hz, 1H), 7.43–7.32 (m, 2H), 7.09–6.95 (m, 2H), 6.29 (dd, $J = 8.8, 2.4$ Hz, 1H), 6.17 (d, $J = 2.3$ Hz, 1H), 4.68–4.55 (m, 1H), 4.40–4.29 (m, 1H), 4.20 (dt, $J = 14.3, 4.0$ Hz, 2H), 4.07 (t, $J = 13.4$ Hz, 2H), 3.59–3.48 (m, 2H), 3.39 (ddd, $J = 9.4, 8.4, 3.2$ Hz, 1H), 3.29 (dt, $J = 10.9, 1.6$ Hz, 1H), 2.23–2.03 (m, 3H), 1.09 (d, $J = 7.0$ Hz, 3H).

^{13}C NMR (126 MHz, CDCl_3) δ 162.2 ($^1J_{\text{C-F}} = 245.6$ Hz), 157.1, 151.6, 133.3 ($^4J_{\text{C-F}} = 3.1$ Hz), 130.5, 129.5 ($^3J_{\text{C-F}} = 8.1$ Hz), 118.3, 115.3 ($^2J_{\text{C-F}} = 21.6$ Hz, 2C), 106.5, 103.1, 73.8, 70.8, 60.4, 56.6, 56.1, 50.8, 45.6, 34.0, 16.2.

HRMS calculated for $\text{C}_{20}\text{H}_{24}\text{FN}_2\text{O}_4\text{S}$ ($\text{M}+\text{H}$) $^+$ 407.1441; found 407.1417 (TOF MS ES+).

(S)-7-((R)-3-(dimethylamino)pyrrolidin-1-yl)-2-(4-fluorobenzyl)-3-methyl-3,4-dihydro-2H-benzo[b][1,4,5]oxathiazepine 1,1-dioxide (3.2.10g)



Utilizing general procedure **A**, **3.2.10g** (36 mg, 0.083 mmol, 90%) was isolated after chromatography (5% MeOH in EtOAc)

as a light brown solid.

MP: 132 °C.

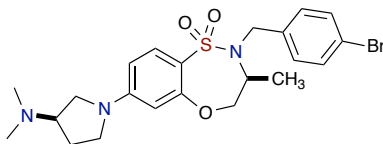
FTIR (neat, cm^{-1}): 2975, 2948, 2866, 2773, 1600, 1508, 1330, 1143, 1076.

^1H NMR (400 MHz, CDCl_3) δ 7.64 (d, $J = 8.8$ Hz, 1H), 7.41–7.33 (m, 2H), 7.06–6.92 (m, 2H), 6.29 (dd, $J = 8.8, 2.4$ Hz, 1H), 6.16 (d, $J = 2.4$ Hz, 1H), 4.42–4.32 (m, 1H), 4.26–4.16 (m, 2H), 4.16–4.01 (m, 2H), 3.56–3.43 (m, 2H), 3.34 (td, $J = 9.8, 6.8$ Hz, 1H), 3.18 (dd, $J = 9.3, 8.2$ Hz, 1H), 2.92–2.79 (m, 1H), 2.33 (s, 6H), 2.29–2.21 (m, 1H), 2.00–1.90 (m, 1H), 1.09 (d, $J = 7.1$ Hz, 3H).

^{13}C NMR (126 MHz, CDCl_3) δ 162.2 ($^1J_{\text{C-F}} = 245.6$) Hz, 157.1, 151.4, 133.3 ($^4J_{\text{C-F}} = 3.2$ Hz), 130.4, 129.6, 129.5 ($^3J_{\text{C-F}} = 8.1$ Hz), 118.4, 115.3 ($^2J_{\text{C-F}} = 21.4$ Hz, 2C), 106.5, 103.1, 73.9, 65.3, 56.5, 52.2, 51.0, 46.9, 44.2 (2C), 30.1, 16.2.

HRMS calculated for $\text{C}_{22}\text{H}_{29}\text{FN}_3\text{O}_3\text{S}$ ($\text{M}+\text{H}$) $^+$ 433.1835; found 434.1891 (TOF MS ES $^+$).

(3*S*)-2-(4-bromobenzyl)-7-((*R*)-3-(dimethylamino)pyrrolidin-1-yl)-3-methyl-3,4-dihydro-2*H*-benzo[*b*][1,4,5]oxathiazepine 1,1-dioxide (3.2.10h)



Utilizing general procedure **A**, **3.2.10h** (33 mg, 0.067 mmol, 72%) was isolated after chromatography (5% MeOH in EtOAc) as a white solid.

MP: 158 °C.

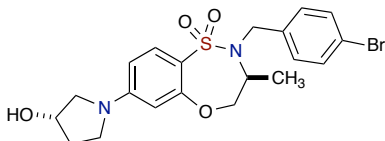
FTIR (neat, cm⁻¹): 2975, 2947, 2835, 2773, 1600, 1546, 1485, 1330, 1143, 1074.

¹H NMR (400 MHz, CDCl₃) 7.63 (d, *J* = 8.8 Hz, 1H), 7.47–7.43 (m, 2H), 7.29 (d, *J* = 1.9 Hz, 1H), 7.28, (d, *J* = 1.9 Hz, 1H) 6.29 (dd, *J* = 8.8, 2.4 Hz, 1H), 6.16 (d, *J* = 2.4 Hz, 1H), 4.39–4.29 (m, 1H), 4.20 (dd, *J* = 13.1, 3.8 Hz, 1H), 4.13 (d, *J* = 21.3 Hz, 2H), 4.06 (d, *J* = 15.7 Hz, 1H), 3.61–3.43 (m, 2H), 3.34 (td, *J* = 9.9, 6.8 Hz, 1H), 3.18 (dd, *J* = 9.3, 8.1 Hz, 1H), 2.93–2.79 (m, 1H), 2.33 (s, 6H), 2.24 (ddt, *J* = 12.8, 6.6, 2.8 Hz, 1H), 2.02–1.87 (m, 1H), 1.09 (d, *J* = 7.0 Hz, 3H).

¹³C NMR (126 MHz, CDCl₃) δ 157.1, 151.5, 136.7, 131.6 (2C), 130.5, 129.6 (2C), 121.4, 118.4, 106.6, 103.2, 73.8, 65.3, 56.7, 52.1, 51.0, 46.9, 44.2 (2C), 30.1, 16.2.

HRMS calculated for C₂₂H₂₉BrN₃O₃S (M+H)⁺ 494.1113; found 494.1125 (TOF MS ES⁺).

(S)-2-(4-bromobenzyl)-7-((S)-3-hydroxypyrrolidin-1-yl)-3-methyl-3,4-dihydro-2H-benzo[b][1,4,5]oxathiazepine 1,1-dioxide (3.2.10i)



Utilizing general procedure A, **3.2.10i** (37 mg, 0.079 mmol, 84%) was isolated after chromatography (100% EtOAc) as a yellow liquid.

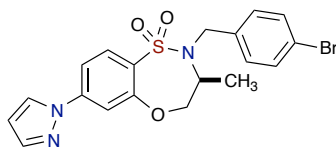
FTIR (neat, cm^{-1}): 2933, 2916, 2848, 1600, 1487, 1386, 1326, 1141, 1078.

^1H NMR (400 MHz, CDCl_3) δ 7.61 (dd, $J = 8.8, 2.1$ Hz, 1H), 7.47–7.42 (m, 2H), 7.31–7.24 (m, 2H), 6.28 (dt, $J = 8.9, 2.3$ Hz, 1H), 6.17 (t, $J = 2.2$ Hz, 1H), 4.66–4.58 (m, 1H), 4.38–4.26 (m, 1H), 4.24–4.00 (m, 4H), 3.57–3.46 (m, 2H), 3.40 (td, $J = 8.9, 3.2$ Hz, 1H), 3.29 (dt, $J = 10.9, 1.7$ Hz, 1H), 2.21–2.07 (m, 1H), 1.95 (bs, 1H), 1.26 (td, $J = 7.2, 2.1$ Hz, 1H), 1.09 (dd, $J = 7.3, 2.1$ Hz, 3H).

^{13}C NMR (126 MHz, CDCl_3) δ 157.1, 151.7, 136.7, 131.6 (2C), 130.5, 129.6, 129.5, 121.4, 118.3, 106.8, 103.5, 77.3, 73.7, 70.8, 56.6, 56.1, 45.6, 34.0, 16.1.

HRMS calculated for $\text{C}_{20}\text{H}_{23}\text{BrN}_2\text{O}_4\text{SNa}$ ($\text{M}+\text{Na}$) $^+$ 489.0460; found 489.0452 (TOF MS ES $^+$).

(S)-2-(4-bromobenzyl)-3-methyl-7-(1*H*-pyrazol-1-yl)-3,4-dihydro-2*H*-benzo[*b*][1,4,5]oxathiazepine 1,1-dioxide (3.2.10j)



Utilizing general procedure A, **3.2.10j** (29.5 mg, 0.066 mmol, 70%) was isolated after chromatography (1:1, Hex/EtOAc) as a white solid.

MP: 192 °C.

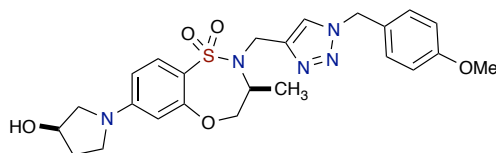
FTIR (neat, cm⁻¹): 2972, 2848, 1600, 1575, 1487, 1514, 1388, 1334, 1159, 1076.

¹H NMR (400 MHz, CDCl₃) δ 7.95 (d, *J* = 2.5 Hz, 1H), 7.90 (d, *J* = 8.5 Hz, 1H), 7.75 (d, *J* = 1.7 Hz, 1H), 7.52–7.43 (m, 4H), 7.25–7.16 (m, 2H), 6.53–6.48 (m, 1H), 4.61 (dd, *J* = 13.3, 10.9 Hz, 1H), 4.43–4.25 (m, 2H), 4.11 (d, *J* = 15.3 Hz, 1H), 4.00 (dt, *J* = 11.8, 5.6 Hz, 1H), 1.15 (d, *J* = 6.9 Hz, 3H).

¹³C NMR (126 MHz, CDCl₃) δ 156.8, 143.9, 142.2, 135.7, 131.8 (2C), 130.5, 129.8 (2C), 129.3, 126.9, 121.8, 113.2, 111.8, 108.8, 74.6, 57.3, 52.5, 16.1.

HRMS calculated for C₁₉H₁₉BrN₃O₃S (M+H)⁺ 448.0330; found 448.0335 (TOF MS ES⁺).

(S)-7-((R)-3-hydroxypyrrolidin-1-yl)-2-((1-(4-methoxybenzyl)-1*H*-1,2,3-triazol-4-yl)methyl)-3-methyl-3,4-dihydro-2*H*-benzo[*b*][1,4,5]oxathiazepine 1,1-dioxide (3.2.11a)



Utilizing general procedure **A**, **3.2.11a** (33 mg, 0.066 mmol, 70%) was isolated after chromatography (100% EtOAc) as a brown liquid.

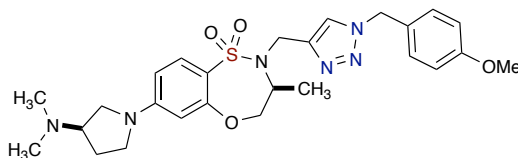
FTIR (neat, cm^{-1}): 2933, 2916, 2848, 1600, 1514, 1328, 1249, 1078.

^1H NMR (400 MHz, CDCl_3) δ 7.57 (d, $J = 8.8$ Hz, 1H), 7.45 (s, 1H), 7.20–7.16 (m, 2H), 6.91–6.85 (m, 2H), 6.26 (dd, $J = 8.9, 2.4$ Hz, 1H), 6.14 (d, $J = 2.4$ Hz, 1H), 5.54–5.27 (m, 2H), 4.63 (tt, $J = 4.6, 2.0$ Hz, 1H), 4.41–4.29 (m, 1H), 4.24–4.17 (m, 2H), 4.17–4.08 (m, 2H), 3.85–3.78 (m, 4H), 3.58–3.47 (m, 2H), 3.38 (td, $J = 8.9, 3.2$ Hz, 1H), 3.28 (dt, $J = 10.8, 1.6$ Hz, 1H), 2.15–2.09 (m, 2H), 1.16 (d, $J = 7.1$ Hz, 3H).

^{13}C NMR (126 MHz, CDCl_3) δ 159.9, 157.1, 151.8, 130.4, 129.8, 129.7, 129.6, 126.4, 123.1, 118.4, 114.5 (2C), 106.6, 103.9, 73.3, 70.7, 56.5, 56.2, 55.4, 53.7, 45.6, 42.0, 34.0, 15.7.

HRMS calculated for $\text{C}_{24}\text{H}_{30}\text{N}_5\text{O}_5\text{S}$ ($\text{M}+\text{H}$) $^+$ 500.1968; found 500.1987 (TOF MS ES $^+$).

(S)-7-((R)-3-(dimethylamino)pyrrolidin-1-yl)-2-((1-(4-methoxybenzyl)-1H-1,2,3-triazol-4-yl)methyl)-3-methyl-3,4-dihydro-2H-benzo[b][1,4,5]oxathiazepine 1,1-dioxide (3.2.11b)



Utilizing general procedure A, **3.2.11b** (35.5 mg, 0.067 mmol, 72%) was isolated after chromatography (5% MeOH in EtOAc) as a brown liquid.

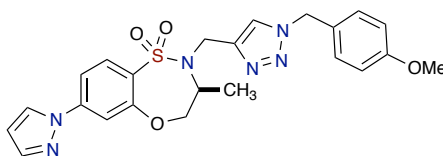
FTIR (neat, cm^{-1}): 2950, 2852, 2773, 1600, 1514, 1330, 1251, 1143, 1076.

^1H NMR (400 MHz, CDCl_3) δ 7.58 (d, $J = 8.8$ Hz, 1H), 7.46 (s, 1H), 7.23–7.11 (m, 2H), 6.92–6.78 (m, 2H), 6.26 (dd, $J = 8.8, 2.4$ Hz, 1H), 6.14 (d, $J = 2.4$ Hz, 1H), 5.46–5.31 (m, 2H), 4.39–4.29 (m, 1H), 4.24–4.17 (m, 4H), 3.81 (s, 3H), 3.58–3.43 (m, 2H), 3.32 (td, $J = 9.8, 6.8$ Hz, 1H), 3.18 (dd, $J = 9.4, 8.1$ Hz, 1H), 2.94–2.82 (m, 1H), 2.33 (s, 6H), 2.27–2.21 (m, 1H), 1.97 (dt, $J = 12.0, 9.3$ Hz, 1H), 1.16 (d, $J = 7.1$ Hz, 3H).

^{13}C NMR (126 MHz, CDCl_3) δ 159.9, 157.2, 151.6, 145.7, 130.4, 129.6 (2C), 126.4, 123.1, 118.6, 114.5 (2C), 106.4, 103.8, 73.4, 65.2, 56.5, 55.4, 53.7, 52.0, 46.9, 44.1 (2C), 42.0, 29.9, 15.7.

HRMS calculated for $\text{C}_{26}\text{H}_{35}\text{N}_6\text{O}_4\text{S}$ ($\text{M}+\text{H}$) $^+$ 527.2440; found 527.2400 (TOF MS ES+).

(S)-2-((1-(4-methoxybenzyl)-1*H*-1,2,3-triazol-4-yl)methyl)-3-methyl-7-(1*H*-pyrazol-1-yl)-3,4-dihydro-2*H*-benzo[*b*][1,4,5]oxathiazepine 1,1-dioxide (3.2.11c)



Utilizing general procedure A, **3.2.11c** (33 mg, 0.069 mmol, 73%) was isolated after chromatography (1:2, Hex/EtOAc) as a yellow solid.

MP: 86 °C.

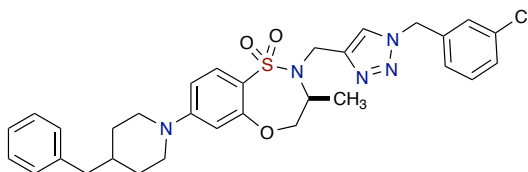
FTIR (neat, cm^{-1}): 2954, 2935, 2848, 1600, 1514, 1336, 1159, 1076.

^1H NMR (400 MHz, CDCl_3) δ 7.95 (d, $J = 2.6$, 1H), 7.83 (d, $J = 8.7$ Hz, 1H), 7.77 (dd, $J = 1.7$, 0.6 Hz, 1H), 7.48 (dd, $J = 8.6$, 2.2 Hz, 1H), 7.38 (d, $J = 2.2$ Hz, 1H), 7.28 (s, 1H), 7.16–7.08 (m, 2H), 6.90–6.78 (m, 2H), 6.53 (dd, $J = 2.6$, 1.7 Hz, 1H), 5.47–5.22 (m, 2H), 4.50–4.42 (m, 1H), 4.40 (d, $J = 2.7$ Hz, 2H), 4.34 (ddd, $J = 14.3$, 7.6, 3.8 Hz, 1H), 4.28 (dd, $J = 12.8$, 3.7 Hz, 1H), 3.80 (s, 3H), 1.25 (dd, $J = 7.0$, 2.6 Hz, 3H).

^{13}C NMR (126 MHz, CDCl_3) δ 159.9, 156.7, 144.2, 143.9, 142.3, 130.1, 129.7 (2C), 129.6, 126.9, 126.1, 122.9, 114.5 (2C), 113.0, 111.8, 108.9, 74.2, 57.0, 55.4, 53.8, 43.5, 15.8.

HRMS calculated for $\text{C}_{23}\text{H}_{25}\text{N}_6\text{O}_4\text{S}$ ($\text{M}+\text{H}$) $^+$ 481.1658; found 481.1655 (TOF MS ES+).

(S)-7-(4-benzylpiperidin-1-yl)-2-((1-(3-chlorobenzyl)-1*H*-1,2,3-triazol-4-yl)methyl)-3-methyl-3,4-dihydro-2*H*-benzo[*b*][1,4,5]oxathiazepine 1,1-dioxide (3.2.11d)



Utilizing general procedure **A**, **3.2.11d** (45 mg, 0.079 mmol, 80%) was isolated after chromatography (1:1, Hex/EtOAc) as a brownish red liquid.

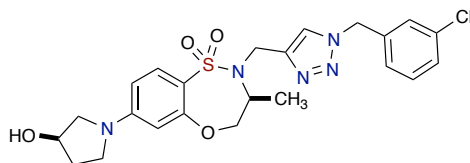
FTIR (neat, cm^{-1}): 2927, 2848, 1596, 1332, 1153, 1143, 1076.

^1H NMR (400 MHz, CDCl_3) δ 7.58 (d, $J = 8.9$ Hz, 1H), 7.49 (s, 1H), 7.34–7.31 (m, 2H), 7.30 (dd, $J = 7.7, 1.6$ Hz, 2H), 7.22–7.20 (m, 2H), 7.19–7.13 (m, 2H), 7.12–7.09 (m, 1H), 6.59 (dd, $J = 9.1, 2.4$ Hz, 1H), 6.44 (d, $J = 2.4$ Hz, 1H), 5.48–5.38 (m, 2H), 4.30–4.23 (m, 2H), 4.20–4.15 (m, 2H), 3.82–3.75 (m, 2H), 2.82–2.74 (m, 2H), 2.57 (d, $J = 6.7$ Hz, 2H), 1.77–1.68 (m, 3H), 1.34–1.22 (m, 3H), 1.19 (d, $J = 7.0$ Hz, 3H).

^{13}C NMR (126 MHz, CDCl_3) δ 157.1, 155.1, 145.9, 140.0, 136.4, 135.0, 130.4, 130.2, 129.1 (2C), 129.0, 128.3 (2C), 128.1, 126.1, 126.0, 123.4, 120.1, 109.1, 106.5, 73.4, 57.0, 56.7, 53.5, 48.0, 47.9, 43.0, 37.9, 31.4, 31.4, 15.8.

HRMS calculated for $\text{C}_{31}\text{H}_{35}\text{ClN}_5\text{O}_3\text{S}$ ($\text{M}+\text{H}$) $^+$ 592.2149; found 592.2158 (TOF MS ES $^+$).

(S)-2-((1-(3-chlorobenzyl)-1*H*-1,2,3-triazol-4-yl)methyl)-7-((*R*)-3-hydroxypyrrolidin-1-yl)-3-methyl-3,4-dihydro-2*H*-benzo[*b*][1,4,5]oxathiazepine 1,1-dioxide (3.2.11e)



Utilizing general procedure **A**, **3.2.11e** (43 mg, 0.085 mmol, 92%) was isolated after chromatography (1:2, Hex/EtOAc) as a yellow liquid.

FTIR (neat, cm^{-1}): 3404, 3141, 2939, 2854, 1600, 1388, 1326, 1141, 1078.

^1H NMR (500 MHz, CDCl_3) δ 7.57 (d, $J = 8.8$ Hz, 1H), 7.52 (s, 1H), 7.34–7.28 (m, 2H), 7.20 (t, $J = 1.8$ Hz, 1H), 7.10 (dt, $J = 7.1, 1.6$ Hz, 1H), 6.26 (dd, $J = 8.8, 2.4$ Hz, 1H), 6.14 (d, $J = 2.3$ Hz, 1H), 5.48–5.33 (m, 2H), 4.63 (dt, $J = 4.6, 2.6$ Hz, 1H), 4.41–4.30 (m, 1H), 4.27–4.14 (m, 3H), 4.13–4.02 (m, 1H), 3.58–3.45 (m, 2H), 3.37 (ddd, $J = 9.4, 8.3, 3.2$ Hz, 1H), 3.27 (dt, $J = 10.9, 1.4$ Hz, 1H), 2.32 (bs, 1H) 2.19–2.10 (m, 2H), 1.17 (d, $J = 7.1$ Hz, 3H).

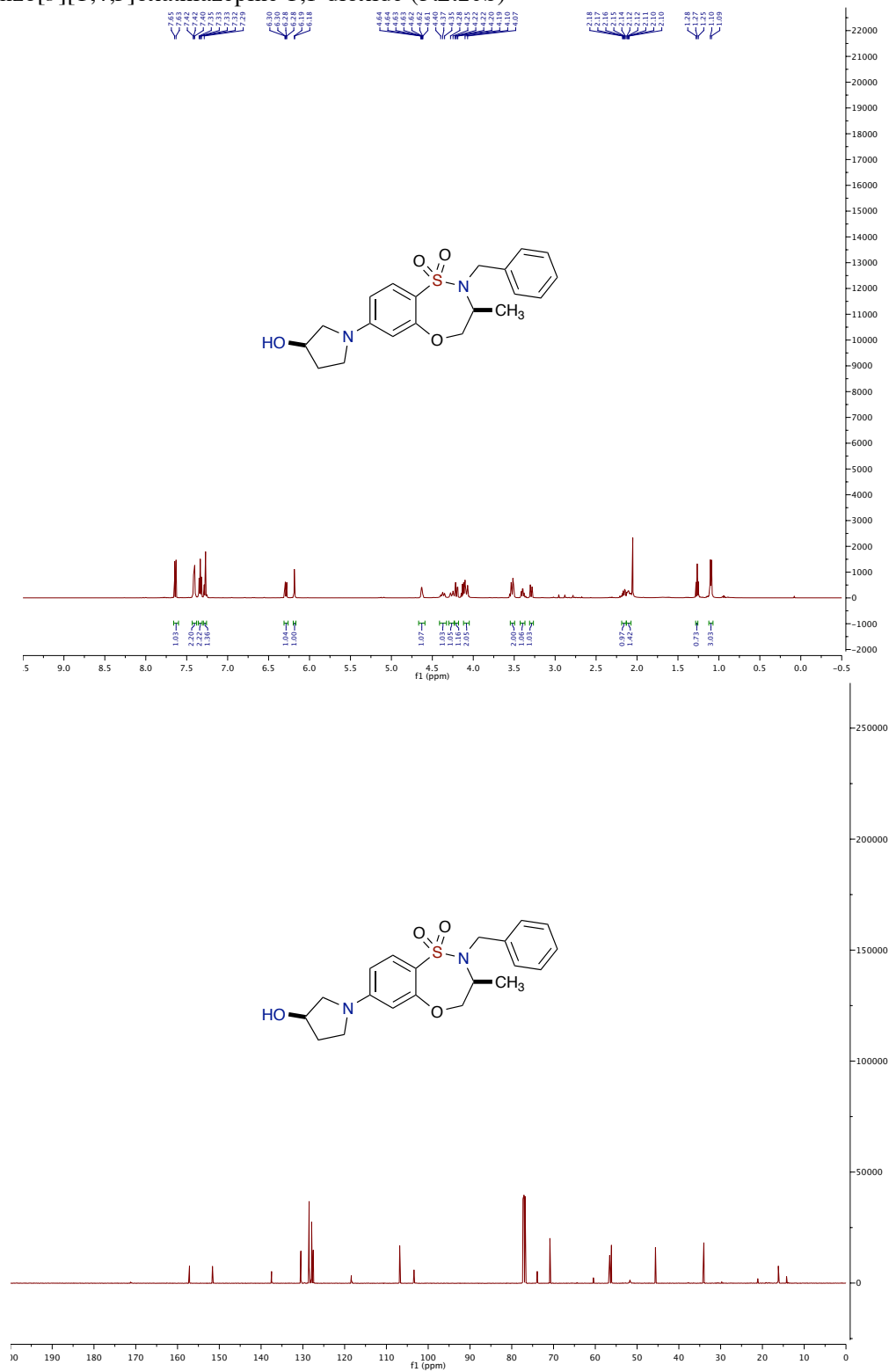
^{13}C NMR (126 MHz, CDCl_3) δ 157.1, 151.9, 136.4, 134.9, 130.5, 130.4, 129.0, 128.9, 128.0, 126.0, 123.5, 118.3, 106.7, 103.9, 73.3, 70.7, 56.6, 56.5, 53.5, 45.6, 41.9, 34.0, 15.8.

HRMS calculated for $\text{C}_{23}\text{H}_{27}\text{ClN}_5\text{O}_4\text{S}$ ($\text{M}+\text{H}$) $^+$ 504.1472; found 504.1458 (TOF MS ES $^+$).

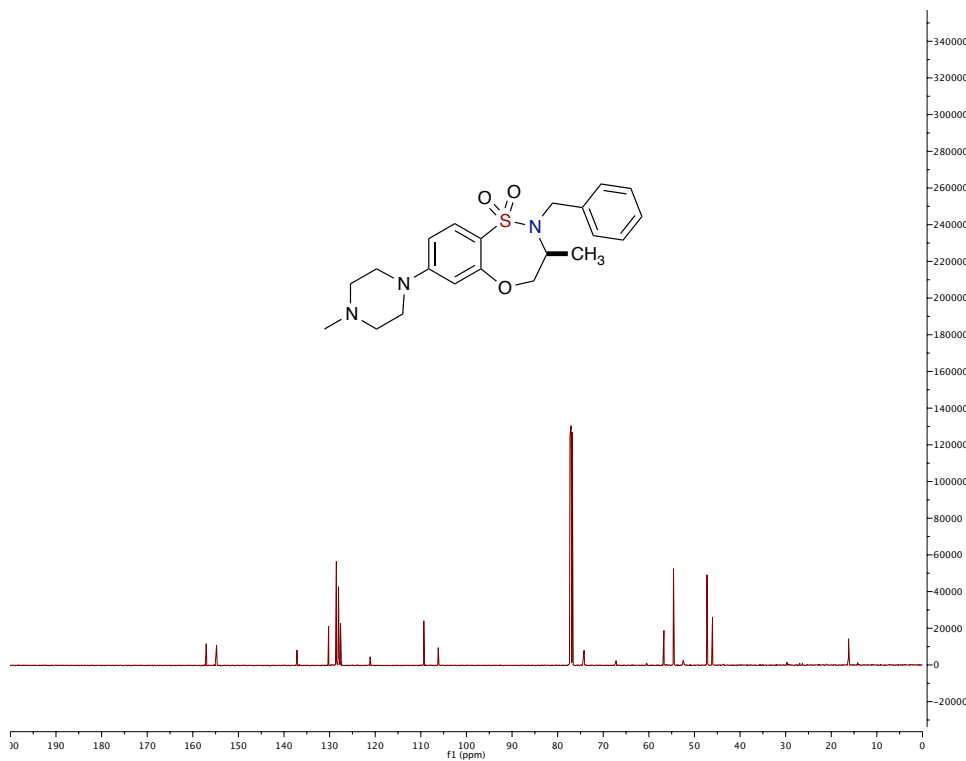
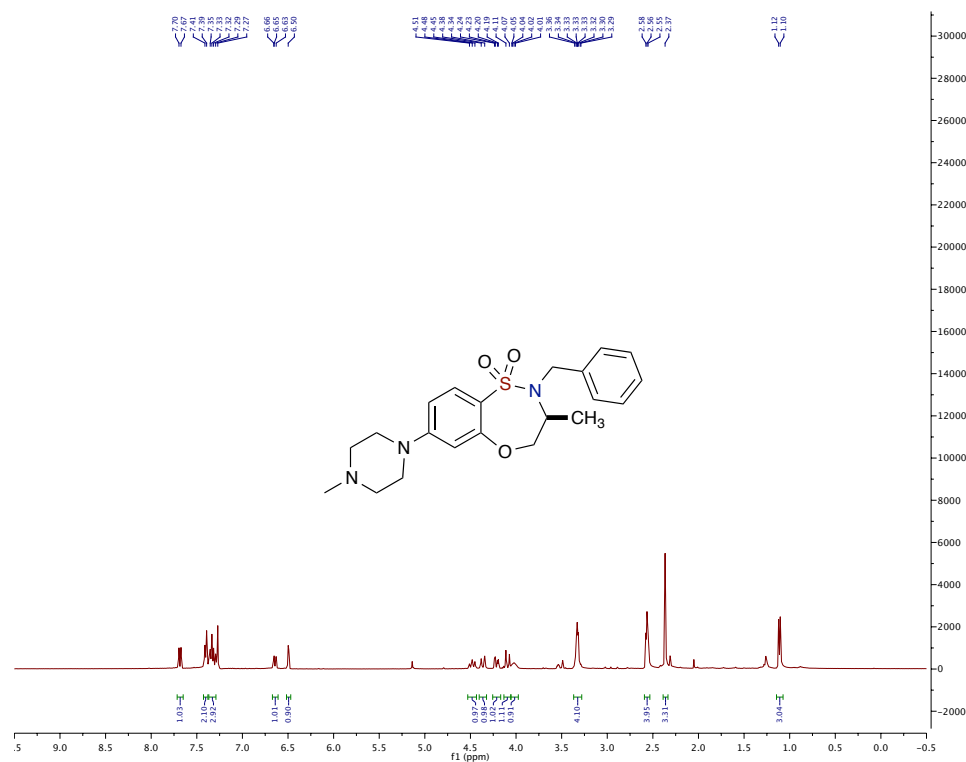
(*S*)-2-benzyl-7-((*R*)-3-(dimethylamino)pyrrolidin-1-yl)-3-methyl-3,4-dihydro-2*H*-benzo[*b*][1,4,5]oxathiazepine 1,1-dioxide (**3.2.10a**)



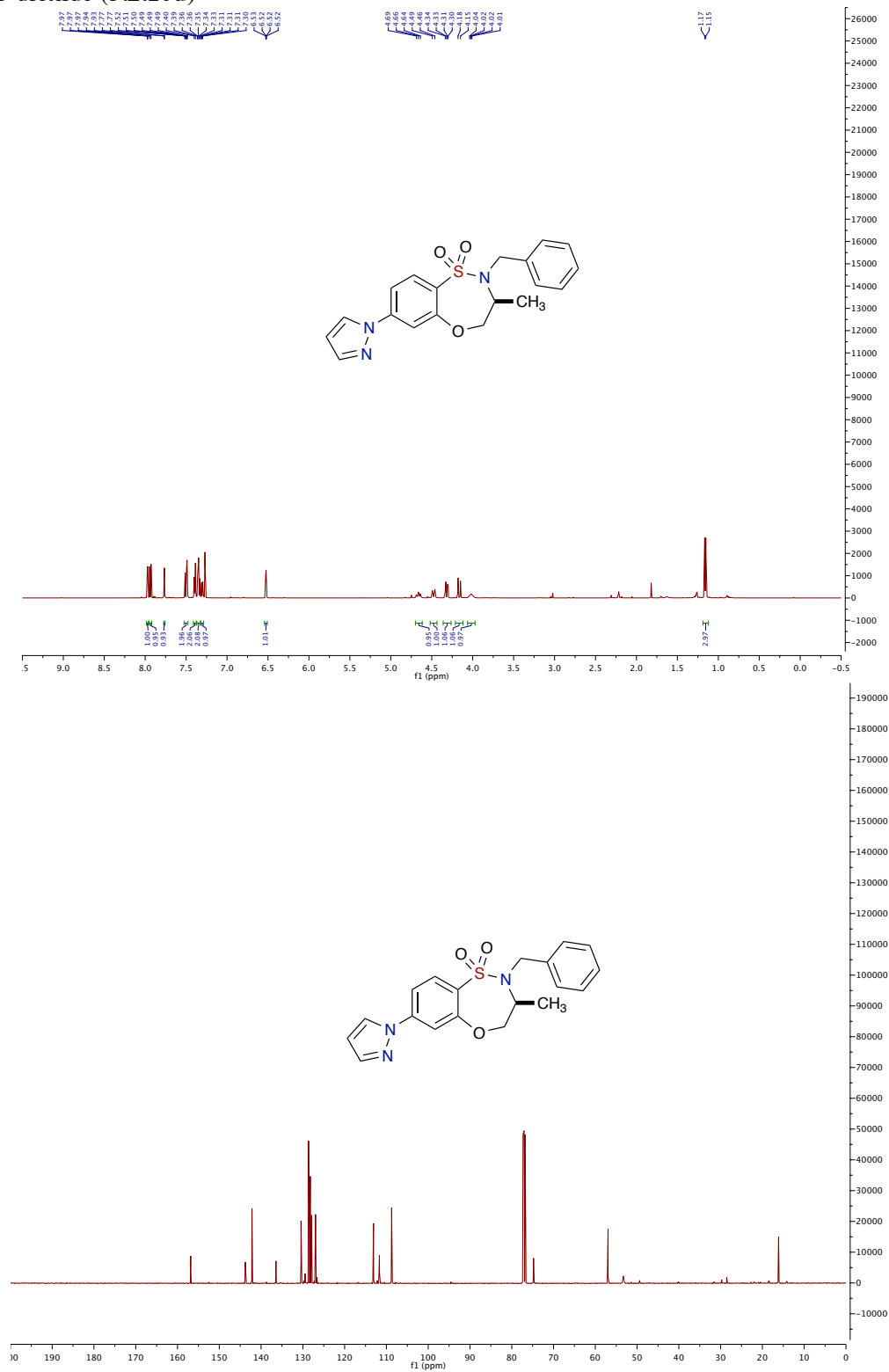
(S)-2-benzyl-7-((R)-3-hydroxypyrrolidin-1-yl)-3-methyl-3,4-dihydro-2H-benzo[b][1,4,5]oxathiazepine 1,1-dioxide (**3.2.10b**)



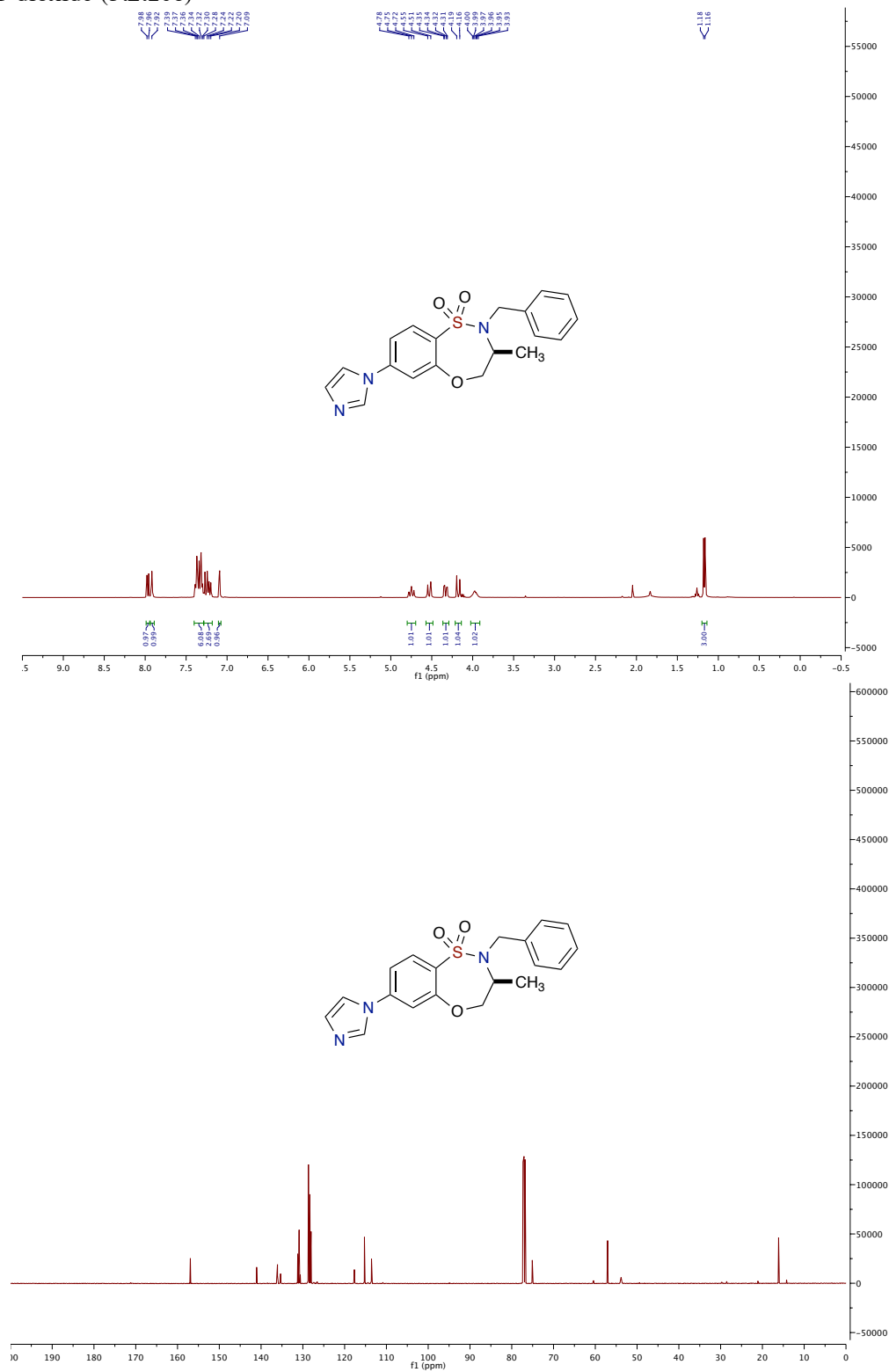
((*S*)-2-benzyl-3-methyl-7-(4-methylpiperazin-1-yl)-3,4-dihydro-2*H*-benzo[*b*][1,4,5]oxathiazepine 1,1-dioxide (**3.2.10c**))



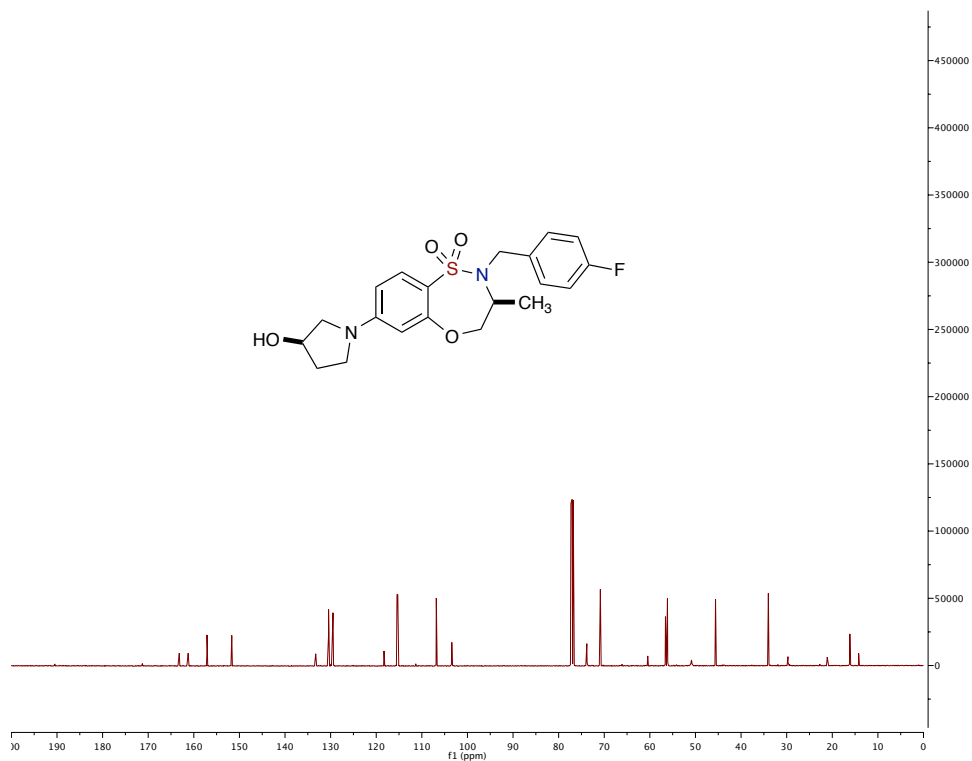
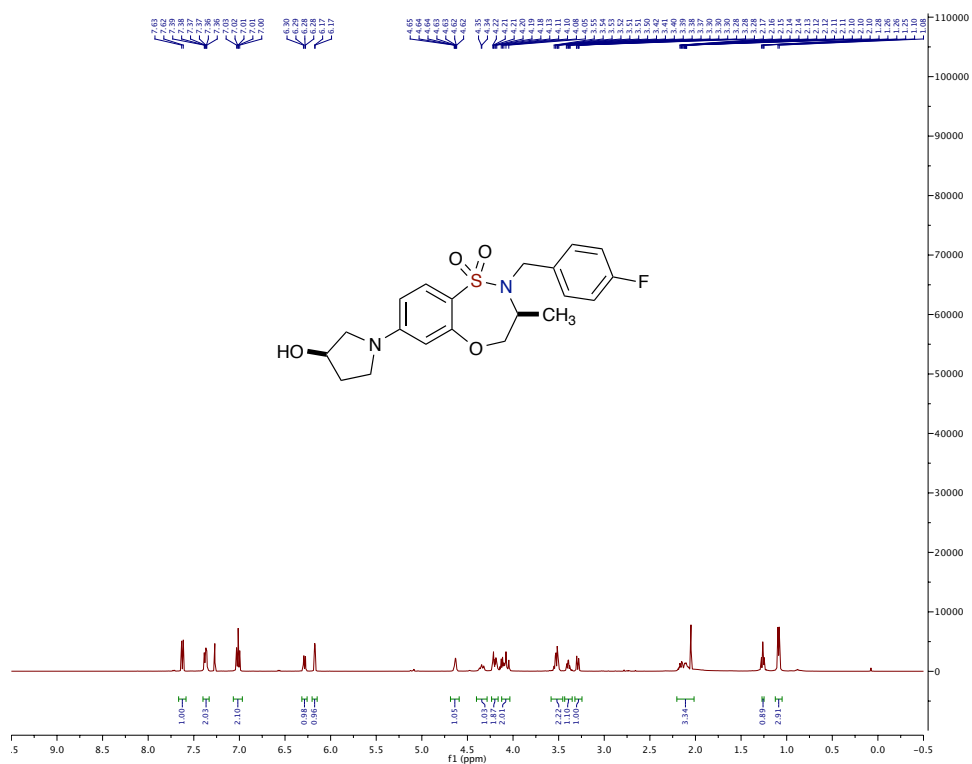
(*S*)-2-benzyl-3-methyl-7-(1*H*-pyrazol-1-yl)-3,4-dihydro-2*H*-benzo[*b*][1,4,5]oxathiazepine 1,1-dioxide (**3.2.10d**)



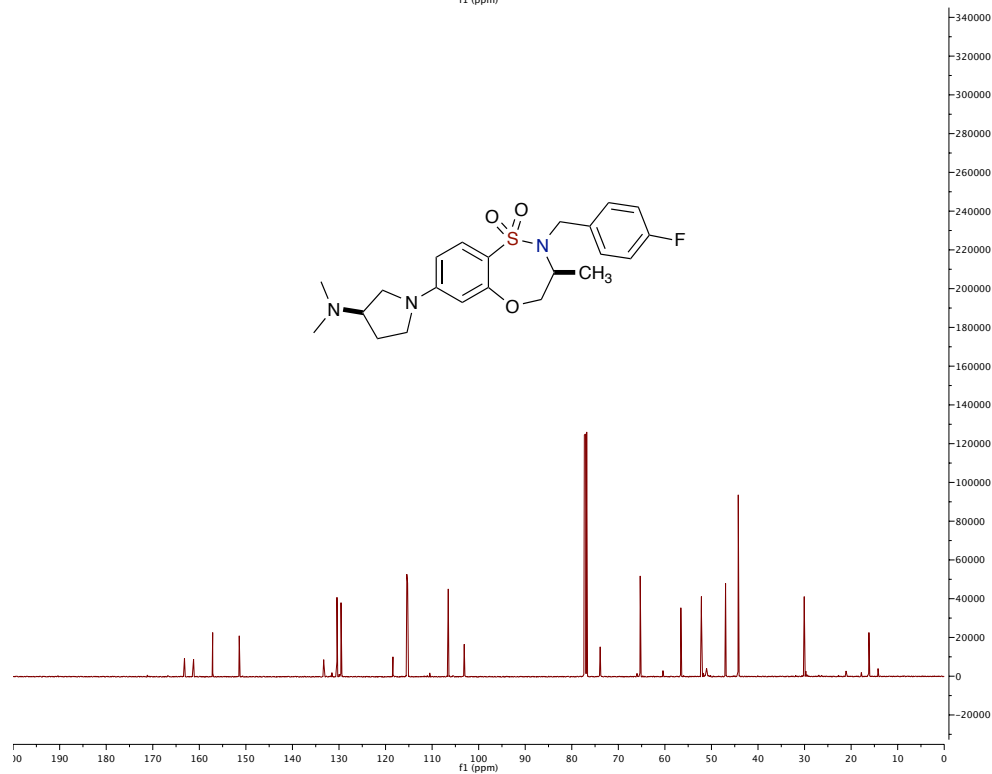
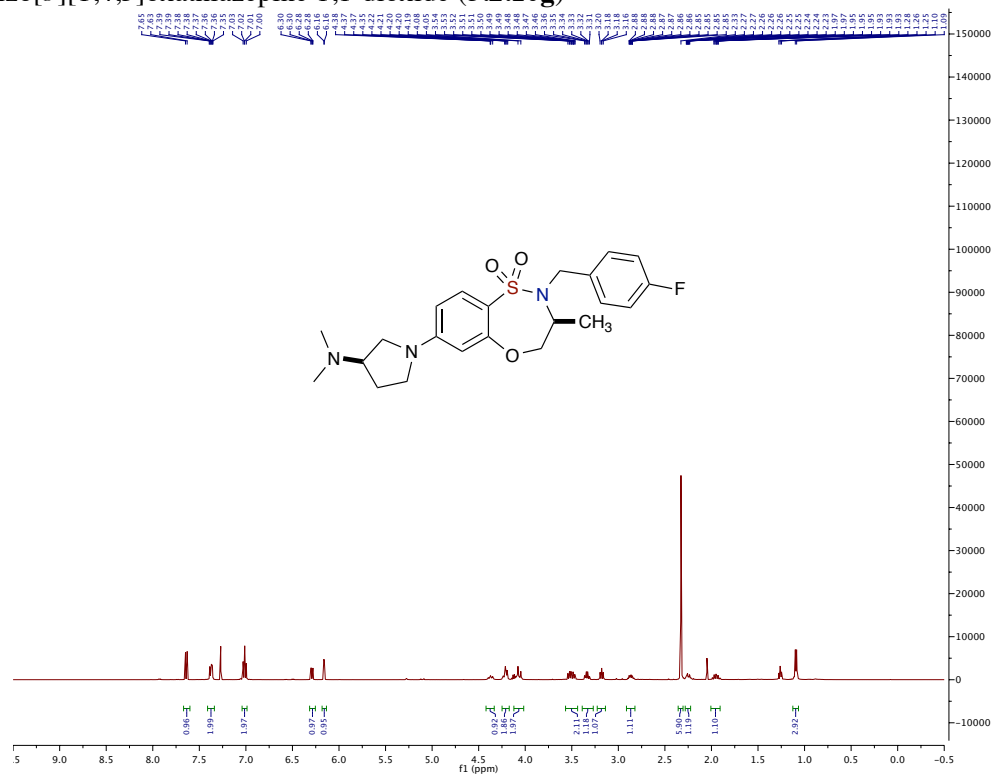
(*S*)-2-benzyl-7-(1*H*-imidazol-1-yl)-3-methyl-3,4-dihydro-2*H*-benzo[*b*][1,4,5]oxathiazepine 1,1-dioxide (**3.2.10e**)



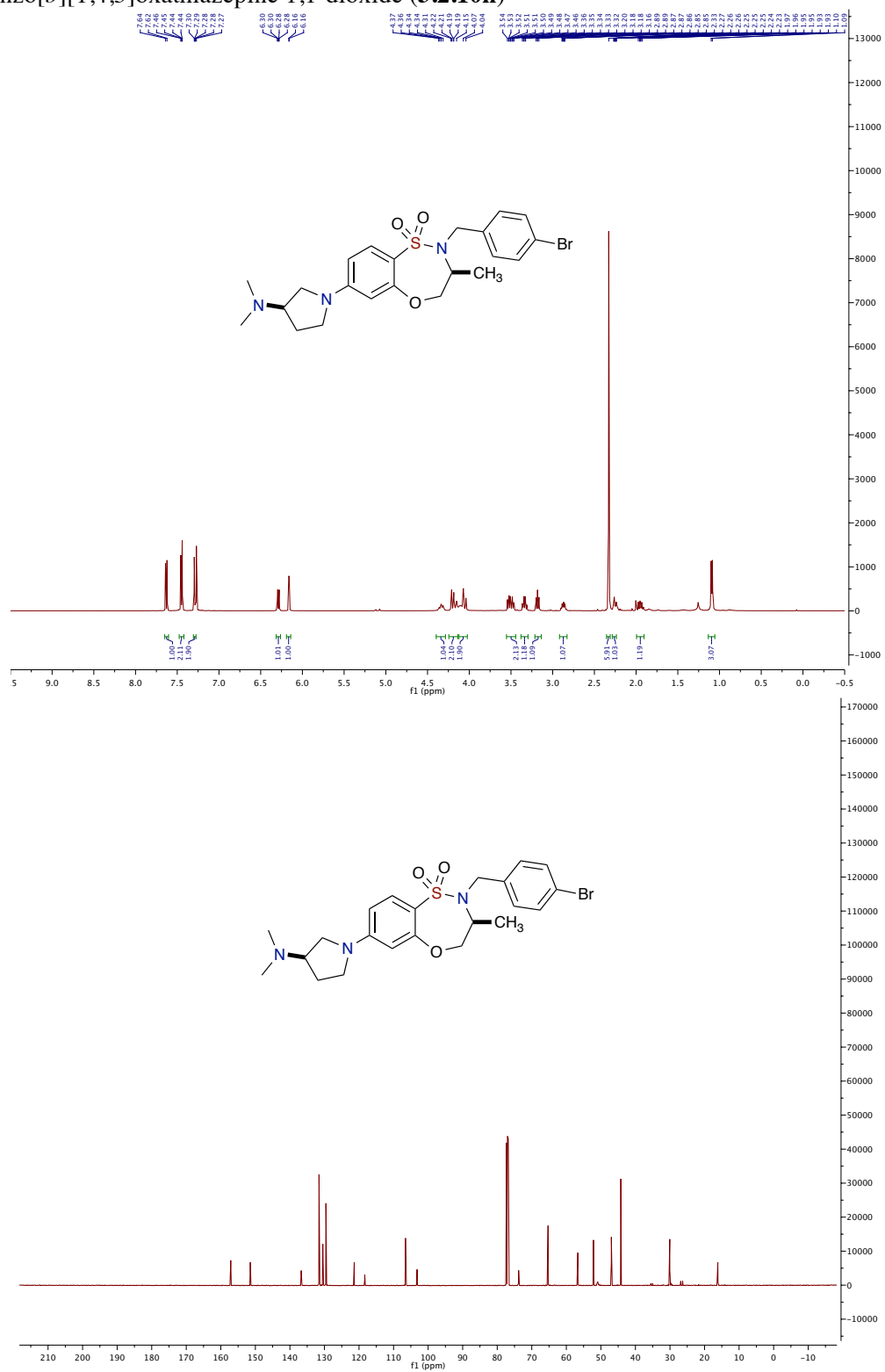
(S)-2-(4-fluorobenzyl)-7-((R)-3-hydroxypyrrolidin-1-yl)-3-methyl-3,4-dihydro-2H-benzo[b][1,4,5]oxathiazepine 1,1-dioxide (**3.2.10f**)



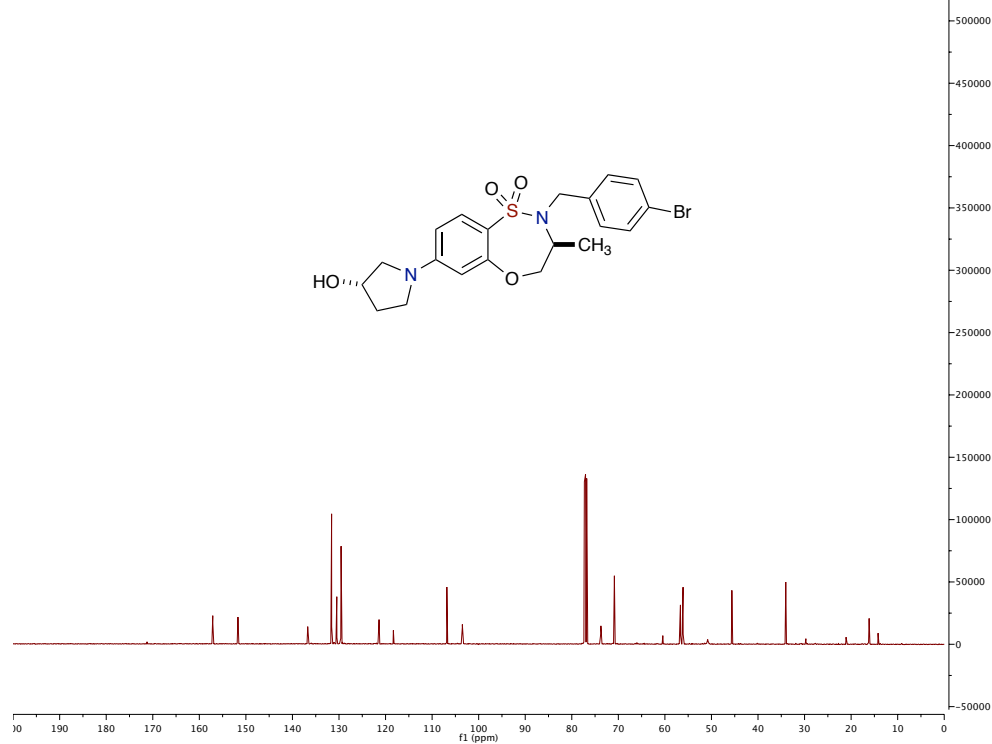
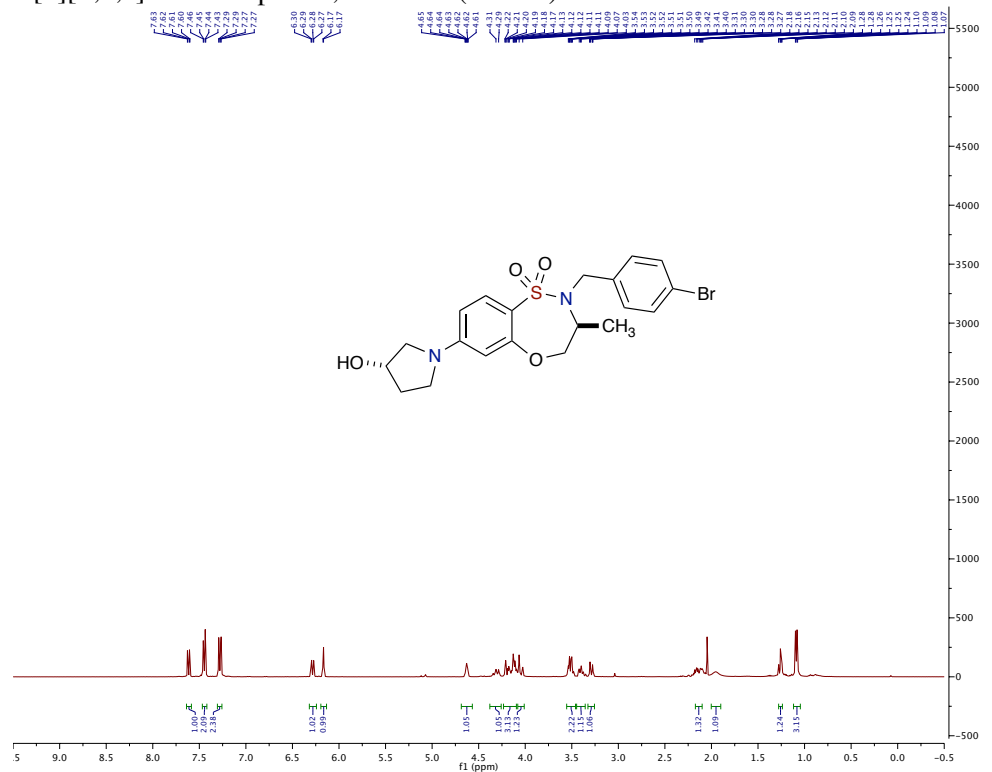
(S)-7-((R)-3-(dimethylamino)pyrrolidin-1-yl)-2-(4-fluorobenzyl)-3-methyl-3,4-dihydro-2H-benzo[b][1,4,5]oxathiazepine 1,1-dioxide (**3.2.10g**)



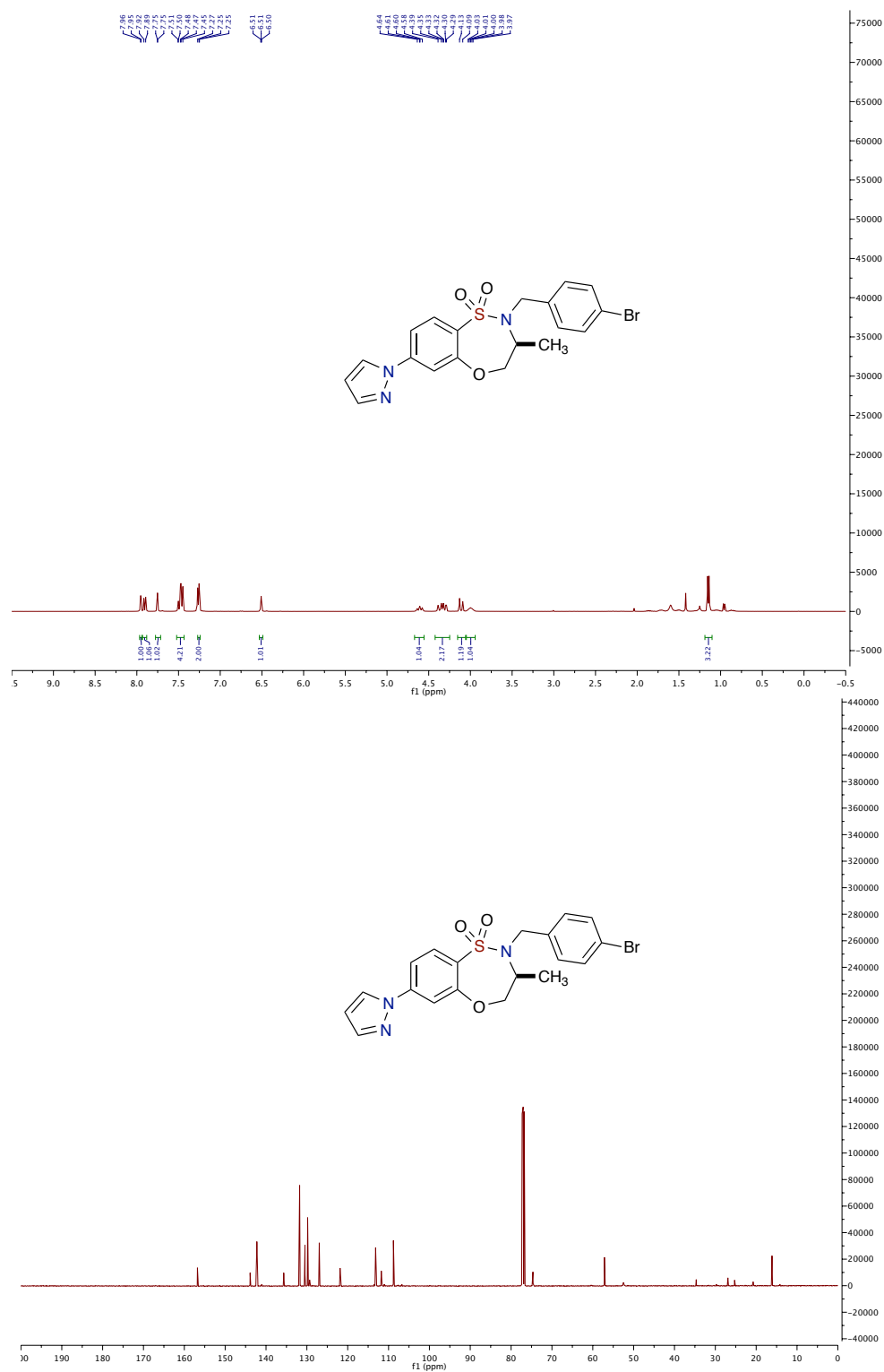
(3*S*)-2-(4-bromobenzyl)-7-(3-(dimethylamino)pyrrolidin-1-yl)-3-methyl-3,4-dihydro-2*H*-benzo[*b*][1,4,5]oxathiazepine 1,1-dioxide (**3.2.10h**)



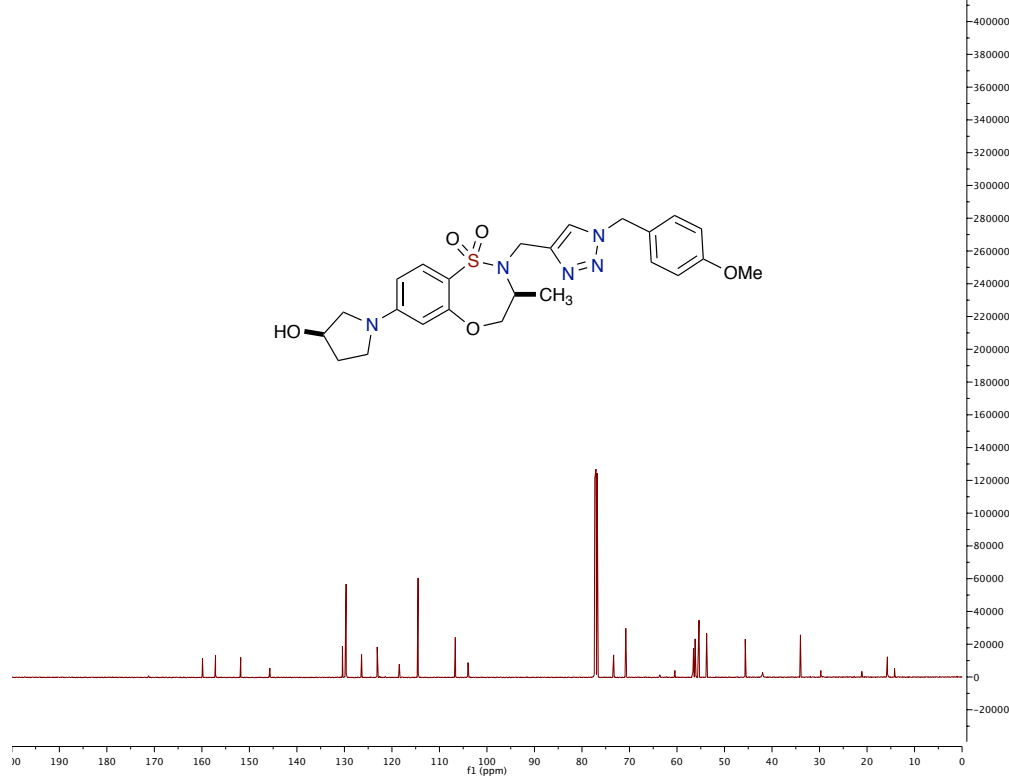
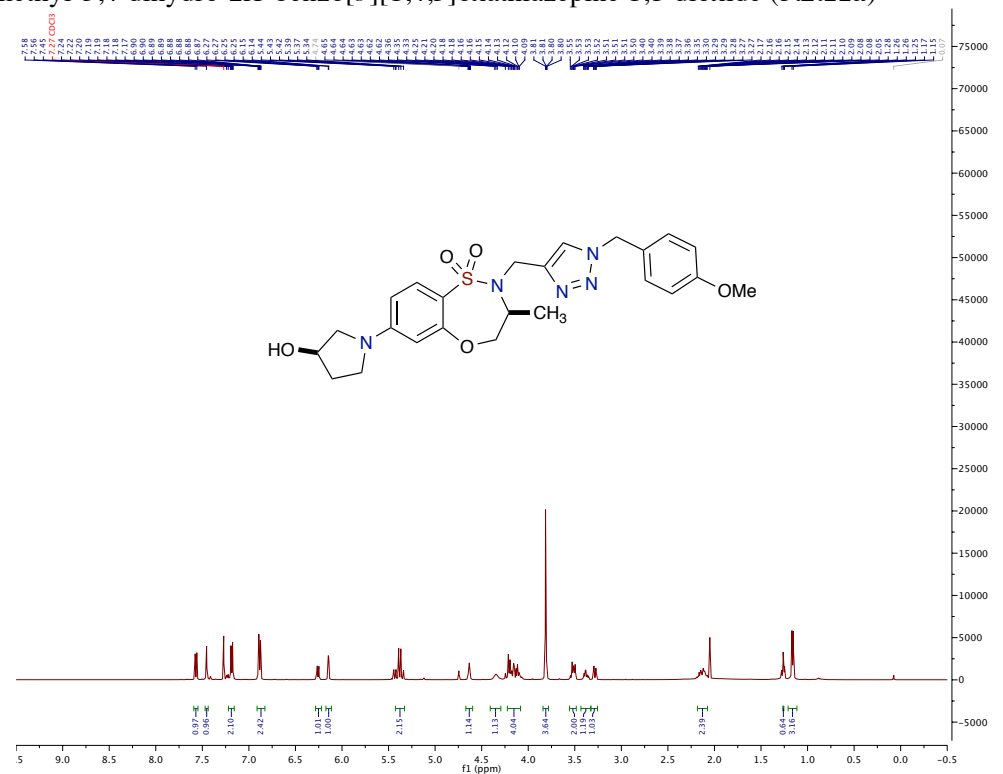
(*S*)-2-(4-bromobenzyl)-7-((*S*)-3-hydroxypyrrolidin-1-yl)-3-methyl-3,4-dihydro-2*H*-benzo[*b*][1,4,5]oxathiazepine 1,1-dioxide (**3.2.10i**)



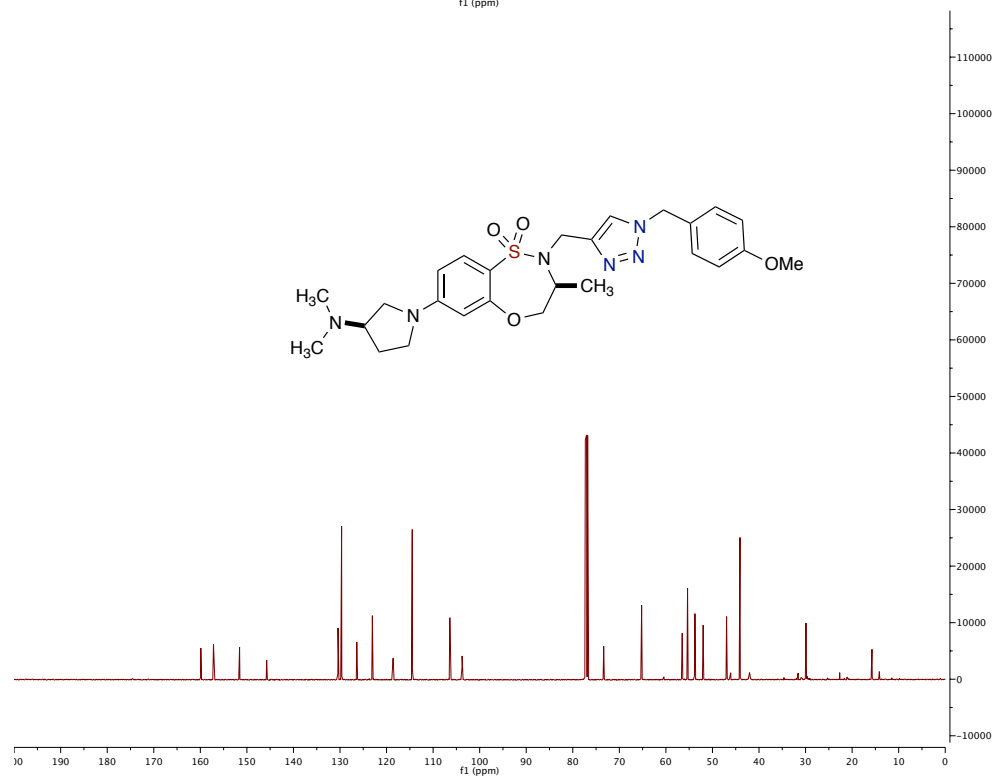
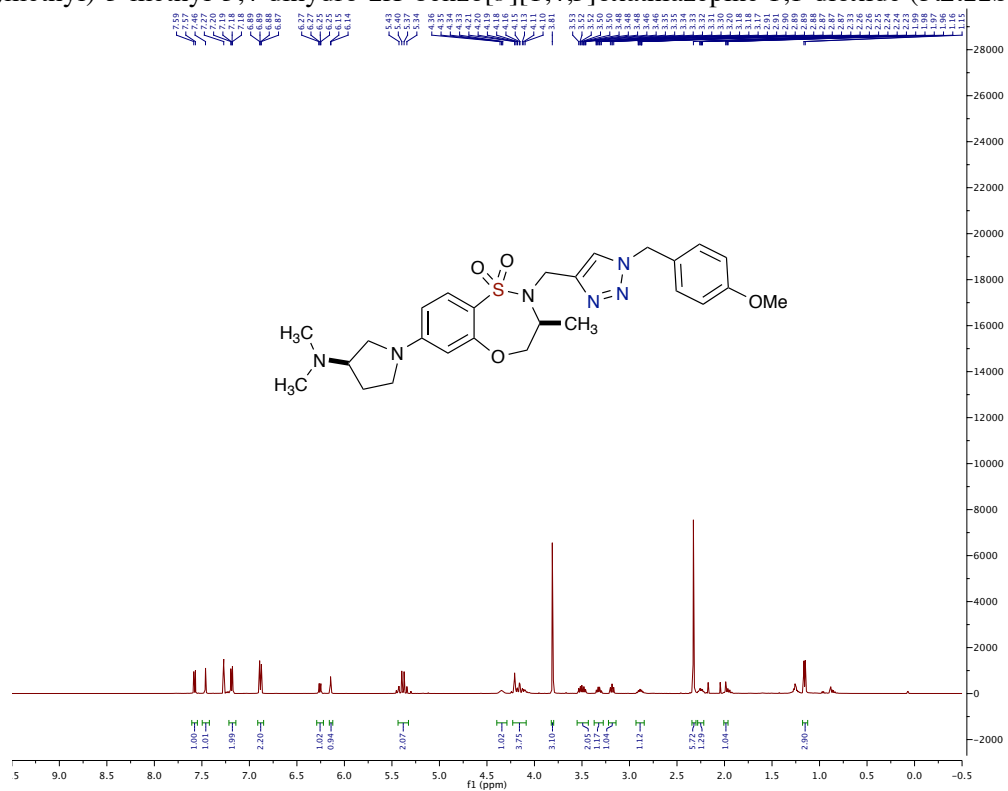
(S)-2-(4-bromobenzyl)-3-methyl-7-(1*H*-pyrazol-1-yl)-3,4-dihydro-2*H*-benzo[*b*][1,4,5]oxathiazepine 1,1-dioxide (**3.2.10j**)



(*S*)-7-((*R*)-3-hydroxypyrrolidin-1-yl)-2-((1-(4-methoxybenzyl)-1*H*-1,2,3-triazol-4-yl)methyl)-3-methyl-3,4-dihydro-2*H*-benzo[*b*][1,4,5]oxathiazepine 1,1-dioxide (**3.2.11a**)



(*S*)-7-((*R*)-3-(dimethylamino)pyrrolidin-1-yl)-2-((1-(4-methoxybenzyl)-1*H*-1,2,3-triazol-4-yl)methyl)-3-methyl-3,4-dihydro-2*H*-benzo[*b*][1,4,5]oxathiazepine 1,1-dioxide (**3.2.11b**)



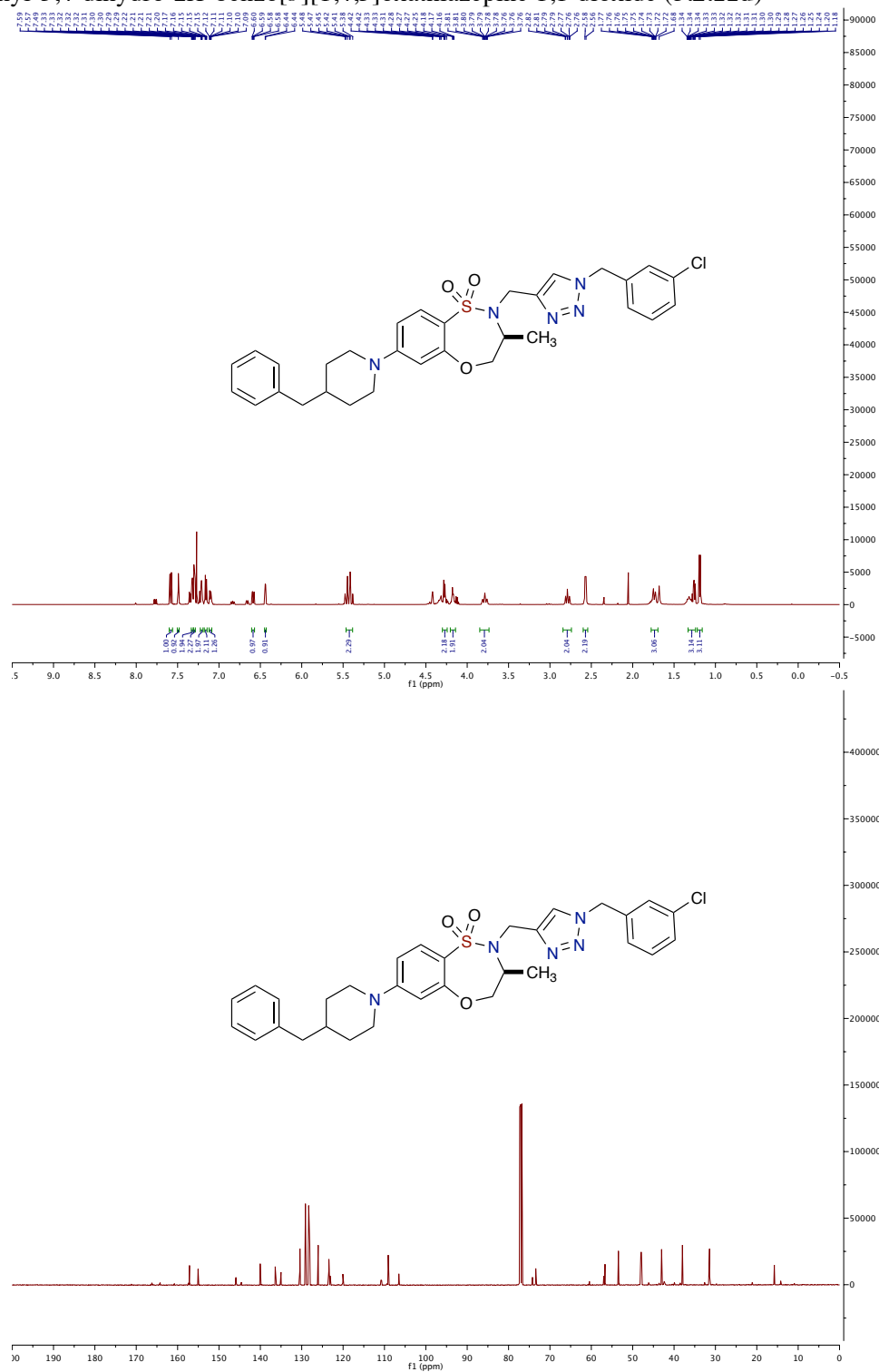
Chemical structure of compound 10 is shown above the spectrum. The spectrum displays peaks from 0 to 8 ppm with corresponding integrations and a list of chemical shifts on the right.

Chemical shifts (ppm): 7.95, 7.94, 7.94, 7.84, 7.84, 7.77, 7.77, 7.76, 7.69, 7.69, 7.67, 7.38, 7.38, 7.28, 7.28, 7.13, 7.13, 7.12, 7.11, 6.95, 6.95, 6.83, 6.83, 6.53, 6.53, 6.52, 6.52, 5.39, 5.32, 5.32, 4.46, 4.46, 4.41, 4.41, 4.36, 4.36, 4.35, 4.35, 4.33, 4.33, 4.29, 4.29, 4.27, 4.27, 3.80, 3.80, 1.26, 1.26, 1.24, 1.24.

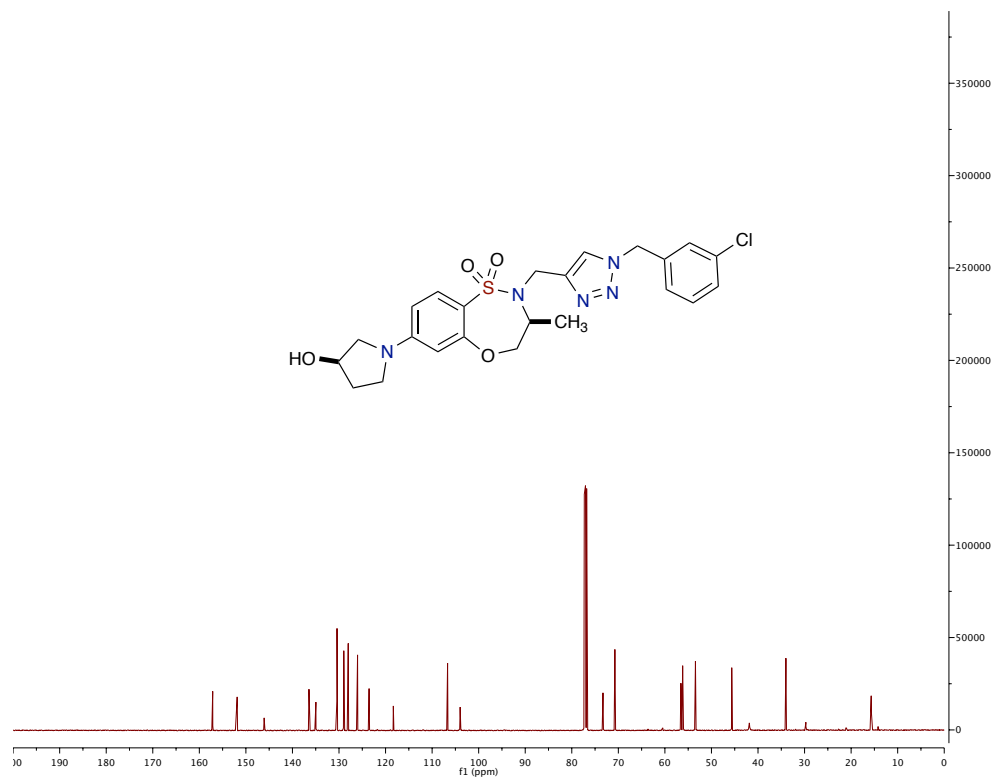
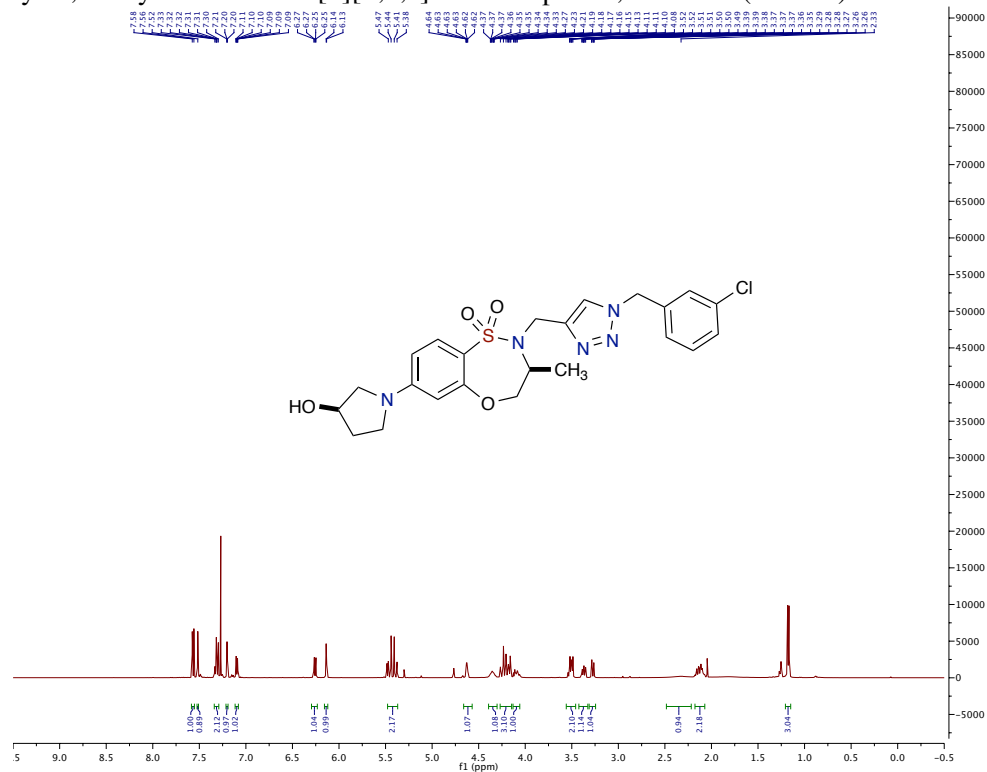
Integrations: 1.00, 0.99, 0.95, 1.10, 0.97, 1.99, 1.98, 1.03, 2.18, 0.99, 1.80, 1.11, 1.17, 3.17, 3.15.



(*S*)-7-(4-benzylpiperidin-1-yl)-2-((1-(3-chlorobenzyl)-1*H*-1,2,3-triazol-4-yl)methyl)-3-methyl-3,4-dihydro-2*H*-benzo[*b*][1,4,5]oxathiazepine 1,1-dioxide (**3.2.11d**)



(*S*)-2-((1-(3-chlorobenzyl)-1*H*-1,2,3-triazol-4-yl)methyl)-7-((*R*)-3-hydroxypyrrolidin-1-yl)-3-methyl-3,4-dihydro-2*H*-benzo[*b*][1,4,5]oxathiazepine 1,1-dioxide (**3.2.11e**)



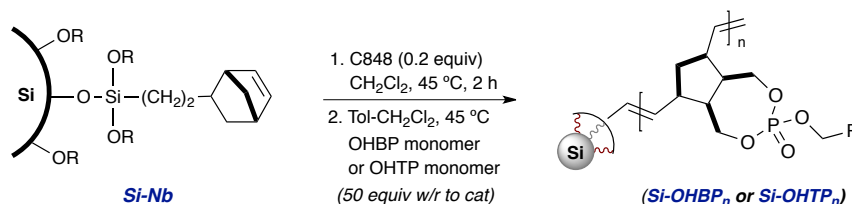
5.10 Experimental for Chapter 3.3.

Synthesis of High-load, Hybrid Silica-immobilized Heterocyclic Benzyl Phosphate (Si-OHBP) and Triazolyl Phosphate (Si-OHTP) Alkylating Reagents.

Experimental Section and Characterization data (SI-326–SI-337)

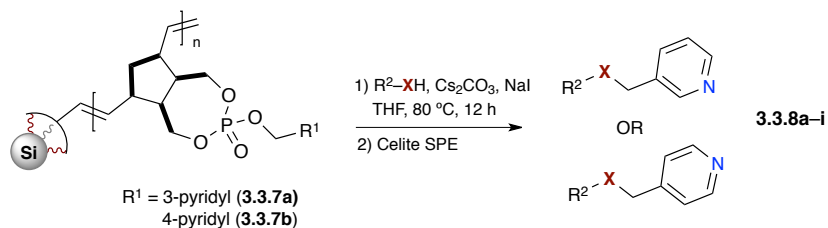
^1H , ^{13}C , Spectra for all Relevant Compounds (SI-338–SI-356)

General procedure for silica oligomeric heterocyclic benzyl phosphate (Si-OHBP_n) and triazole phosphate (Si-OHTP_n).



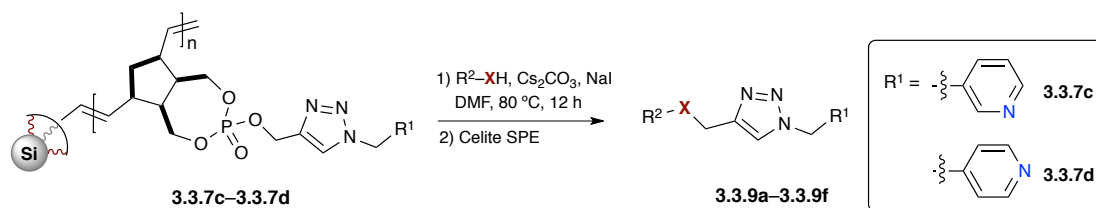
Si-Nb (load ~0.4 mmol/g, 1 equiv.) was heated with C848 (**G-II**) (0.2 equiv.) at 45 °C in dichloromethane for 2 h under argon. The OHBP or OHTP monomer was added (50 equiv. w/r to cat. **G-II**) in CH₂Cl₂ and toluene to the reaction mixture and heated at 45 °C for overnight. The reaction mixture was cooled to room temperature and EVE was added, and then stirred for an additional 1 hour at room temperature. The reaction mixture was filtered and washed with mixture of toluene:CH₂Cl₂ (1:1), and dried over high *vacuo* pump.

Procedure A: General procedure for different nucleophilic substitution with Si-OHBP_n



To a 1-dram vial w/teflon cap was added Si-OHBP **3.1.7a** or **3.1.7b** (1.5 equiv.) followed by addition of sodium iodide (0.2 equiv.), Cs₂CO₃ (3.0 equiv.), and solvent THF (0.2 M). The mixture was stirred rapidly followed by subsequent addition of different nucleophiles. The reaction was sealed under argon and heated to 80 °C w/stirring for 12–14 hrs. After such time the reaction was cooled to rt and crude mixture was then filtered via celite packed 6 mL SPE and rinsed several times with a mixture of hexanes:EtOAc (1:2). The resulting eluent was then concentrated *in vacuo* to yield the hetero-benzylated products in good to excellent yields and purities.

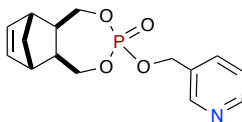
Procedure B: General procedure for different nucleophilic substitution with Si-OHTP_n



To a 1-dram vial w/ teflon cap was added Si-OHTP **3.3.7c** or **3.3.7d** (1.5 equiv.) followed by addition of sodium iodide (0.2 equiv.), Cs₂CO₃ (3.0 equiv.), and solvent DMF (0.2 M). To the mixture nucleophile was added and stirred rapidly. The reaction was sealed under argon and heated to 80 °C w/ stirring for 12–14 hrs. The resulting eluent was then concentrated *in vacuo*. The crude mixture of either case was then filtered via celite-SPE and rinsed with a mixture of hexanes:EtOAc (1:2).

The resulting eluent was then concentrated *in vacuo* to yield the products in good to excellent yields and purities.

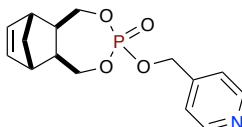
(5aR,6R,9S,9aS)-3-(pyridin-3-ylmethoxy)-1,5,5a,6,9,9a-hexahydro-6,9-methanobenzo[e][1,3,2]dioxaphosphepine 3-oxide (3.3.3a)



Compound **3.3.3a** (2.6 g, 8.4 mmol, 66%) was isolated as a light brown solid.

MP = 101 °C. FTIR (neat, cm^{-1}): 3446, 3058, 2960, 2850, 1577, 1429, 1284, 1060, 1035, 1010; ^1H NMR (500 MHz, CDCl_3) δ 8.69 (d, J = 2.5 Hz, 1H), 8.63, (m, 1H), 7.82 (dt, J = 8.0, 2.0 Hz, 1H), 7.36 (dd, J = 7.9, 4.8 Hz, 1H), 6.22 (t, J = 1.9 Hz, 2H), 5.15 (d, J = 8.2 Hz, 2H), 4.17 (ddd, J = 25.5, 12.1, 3.7 Hz, 2H), 4.08–3.94(m, 2H), 2.54 (s, 2H), 2.15 (m, 2H), 1.34 (m, 2H). ^{13}C NMR (126 MHz, CDCl_3) δ 150.9, 149.3, 137.4, 137.3, 136.2, 123.6, 69.4, 69.3, 66.3, 66.2, 44.8 (2C), 43.6, 41.9 (2C). HRMS calculated for $\text{C}_{15}\text{H}_{19}\text{NO}_4\text{P}$ ($\text{M}+\text{H}$) $^+$ 308.1052; found 308.0931 (TOF MS ES+).

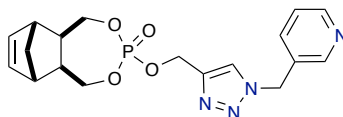
(5aR,6R,9S,9aS)-3-(pyridin-4-ylmethoxy)-1,5,5a,6,9,9a-hexahydro-6,9-methanobenzo[e][1,3,2]dioxaphosphepine 3-oxide (3.3.3b)



Compound **3.3.3b** (1.9 g, 6.1mmol, 60%) was isolated as a brown solid.

MP = 110 °C. FTIR (neat, cm^{-1}): 3446, 3058, 2966, 2850, 1604, 1564, 1415, 1288, 1064, 1035, 1012; ^1H NMR (500 MHz, CDCl_3) δ 8.63 (d, J = 5.1 Hz, 2H), 7.31 (m, 2H), 6.21 (t, J = 2.2 Hz, 2H), 5.11 (d, J = 7.7 Hz, 2H), 4.21(ddd, J = 25.7, 12.0, 3.8 Hz, 2H), 4.12–3.99 (m, 2H), 2.54 (s, 2H), 2.15 (ddd, J = 8.9, 4.5, 2.2 Hz, 2H), 1.35 (m, 2H). ^{13}C NMR (126 MHz, CDCl_3) δ 150.1 (2C), 144.7, 137.4, 137.3 (2C), 121.6, 69.4, 69.3, 66.5, 44.8 (2C), 43.6, 41.9 (2C). HRMS calculated for $\text{C}_{15}\text{H}_{19}\text{NO}_4\text{P}$ ($\text{M}+\text{H}$) $^+$ 308.1052; found 308.1053 (TOF MS ES+).

(5aR,6R,9S,9aS)-3-((1-(pyridin-3-ylmethyl)-1H-1,2,3-triazol-4-yl)methoxy)-1,5,5a,6,9,9a-hexahydro-6,9-methanobenzo[e][1,3,2]dioxaphosphepine 3-oxide (3.3.4a)



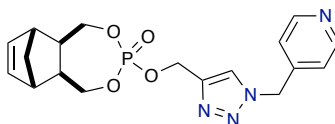
Compound **3.3.4a** (0.38 g, 0.978 mmol, 83%) was isolated as white solid.

MP = 154 °C. FTIR (neat): 2683, 2358, 2104, 1635, 1429, 1340, 1274, 1176, 1120, 1006 cm⁻¹. ¹H NMR (400 MHz, CDCl₃): δ 8.58 (brs, 2H), 7.81–7.71 (m, 1H), 7.61–7.50 (m, 1H), 7.39–7.27 (m, 1H), 6.25–6.18 (m, 2H), 5.64–5.49 (m, 2H), 5.26–5.14 (m, 2H), 4.18–3.97 (m, 4H), 2.60–2.42 (m, 2H), 2.15–1.92 (m, 2H), 1.38 (m, 2H).

¹³C NMR (126 MHz, CDCl₃): δ 150.4, 149.2, 143.5, 137.5, 137.3, 135.7, 130.2, 124.1, 123.9, 69.5, 69.4, 59.7, 51.7, 44.8 (2C), 43.6, 42.0 (2C).

HRMS calculated for C₁₈H₂₂N₄O₄P (M+H)⁺ 389.1379; found 389.1265 (TOF MS ES⁺).

(5aR,6R,9S,9aS)-3-((1-(pyridin-4-ylmethyl)-1H-1,2,3-triazol-4-yl)methoxy)-1,5,5a,6,9,9a-hexahydro-6,9-methanobenzo[e][1,3,2]dioxaphosphepine 3-oxide (3.3.4b)

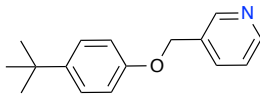


Compound **3.3.4b** (1.81 g, 4.63 mmol, 79%) was isolated as a white solid.

MP = 149 °C. FTIR (neat): 2964, 2358, 2341, 1645, 1591, 1488, 1419, 1323, 1249, 1207, 1093 cm⁻¹. ¹H NMR (400 MHz, CDCl₃): δ 8.62 (d, *J* = 5.3 Hz, 2H), 7.83 (s, 1H), 7.12 (d, *J* = 5.3 Hz, 2H), 6.25–6.19 (m, 2H), 5.58 (s, 2H), 5.23 (d, *J* = 10.4 Hz, 2H), 4.09 (dd, *J* = 20.6, 6.4 Hz, 4H), 2.52 (s, 2H), 2.12–2.03 (m, 2H), 1.40–1.32 (m, 2H). ¹³C NMR (126 MHz, CDCl₃): δ 150.6, 143.8, 143.3, 137.3 (2C), 124.7, 122.2 (2C), 122.1, 69.5, 69.4, 59.7, 52.8, 44.8, 44.7, 43.5, 42.3, 41.9.

HRMS calculated for C₁₈H₂₂N₄O₄P (M+H)⁺ 389.1379; found 389.1313 (TOF MS ES⁺).

3-((4-(tert-butyl)phenoxy)methyl)pyridine (3.3.8a)



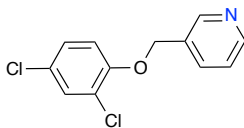
Utilizing general procedure **A**, **3.3.8a** (19.5 mg, 0.08mmol, 97%) was isolated as a light brown solid.

MP = 53 °C. FTIR (neat, cm^{-1}): 2958, 1605, 1585, 1518, 1294, 1242, 1182, 827;

^1H NMR (400 MHz, CDCl_3) δ 8.72 (s, 1 H), 8.61 (s, 1H), 7.84 (dd, J = 7.9, 4.9 Hz, 1H), 7.38 (dd, J = 7.9, 4.9 Hz, 1H), 7.35–7.31 (m, 2H), 6.92 (d, J = 8.8 Hz, 2H), 5.10 (m, 2H), 1.31 (s, 9H). ^{13}C NMR (126 MHz, CDCl_3) δ 156.1, 148.7, 148.3, 144.2, 135.9, 133.2, 126.4 (2C), 123.8, 114.3 (2C), 67.4, 34.1, 31.5 (3C).

HRMS calculated for $\text{C}_{16}\text{H}_{20}\text{NO}$ ($\text{M}+\text{H}$) $^+$ 242.1545; found 242.1551 (TOF MS ES+).

3-((2,4-dichlorophenoxy)methyl)pyridine (3.3.8b)

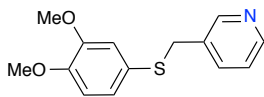


Utilizing general procedure **A**, **3.3.8b** (16.5 mg, 0.065mmol, 72%) was isolated as a yellow solid

MP = 105 °C. FTIR (neat, cm^{-1}): 2918, 1595, 1490, 1461, 1431, 1298, 1066, 802;

^1H NMR (400 MHz, CDCl_3) δ 8.74 (s, 1 H), 8.64 (s, 1H), 7.89 (d, J = 7.9 Hz, 1H), 7.42–7.36 (m, 2H), 7.20 (dt, J = 8.8, 2.4 Hz, 1H), 6.93 (d, J = 8.8 Hz, 1H), 5.17 (m, 2H). ^{13}C NMR (126 MHz, CDCl_3) δ 152.6, 149.1, 148.1, 135.6, 132.1, 130.3, 127.7, 126.8, 124.3, 123.8, 114.9, 68.7. HRMS calculated for $\text{C}_{12}\text{H}_{10}\text{Cl}_2\text{NO}$ ($\text{M}+\text{H}$) $^+$ 254.0139; found 254.0112 (TOF MS ES+).

3-(((3,4-dimethoxyphenyl)thio)methyl)pyridine (3.3.8c)



Utilizing general procedure A, **3.3.8c** (16 mg, 0.061 mmol, 70%) was isolated as a yellow thick liquid.

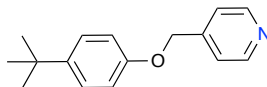
FTIR (neat, cm^{-1}): 2997, 2954, 2848, 1581, 1504, 1461, 1253, 1135, 1024, 1035;

^1H NMR (500 MHz, CDCl_3): δ 8.49 (s, 1H), 8.39 (s, 1H), 7.51(d, $J = 8.0$ Hz, 1H), 7.24 (m, 1H), 6.90 (dd, $J = 8.3$ Hz, 2.1 Hz, 1H), 6.77 (dd, $J = 5.2, 3.1$ Hz, 2H), 3.98 (s, 2H), 3.87 (s, 3H), 3.79 (s, 3H).

^{13}C NMR (126 MHz, CDCl_3) δ 149.6, 149.2, 148.9, 147.8, 136.8, 134.4, 126.2, 124.7, 123.5, 116.3, 111.4, 55.9 (2C), 38.4.

HRMS calculated for $\text{C}_{14}\text{H}_{16}\text{NO}_2\text{S}$ ($\text{M}+\text{H}$) $^+$ 262.0902; found 262.0890 (TOF MS ES+).

4-(((4-(tert-butyl)phenoxy)methyl)pyridine (3.3.8d)



Utilizing general procedure A, **3.3.8d** (19 mg, 0.078 mmol, 98%) was isolated as a brown liquid.

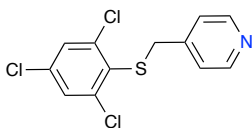
FTIR (neat, cm^{-1}): 2958, 2904, 2866, 1606, 1502, 1413, 1244, 1182, 827;

^1H NMR (400 MHz, CDCl_3) δ 8.63–8.64 (m, 2H), 7.42 (d, $J = 5.3$ Hz, 2H), 7.34–7.32 (m, 2H), 6.91–6.89 (m, 2H), 5.12 (s, 2H), 1.31 (s, 9H).

^{13}C NMR (126 MHz, CDCl_3) δ 155.8, 149.3 (2C), 147.4, 144.3, 126.4 (2C), 121.7, 114.9, 114.2 (2C), 68.1, 34.1, 31.5 (3C).

HRMS calculated for $\text{C}_{16}\text{H}_{20}\text{NO}$ ($\text{M}+\text{H}$) $^+$ 242.1403; found 242.1403 (TOF MS ES+).

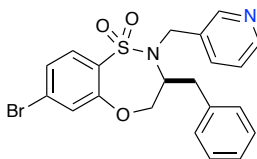
4-(((2,4,6-trichlorophenyl)thio)methyl)pyridine (3.3.8e)



Utilizing general procedure A, **3.3.8e** (16.5 mg, 0.054 mmol, 97%) was isolated as a white solid

MP = 86 °C. FTIR (neat, cm^{-1}): 3070, 3028, 2956, 2921, 1598, 1560, 1433, 1413, 1323, 1116, 1018; ^1H NMR (400 MHz, CDCl_3) δ 8.59 (d, J = 54.1 Hz, 2H), 7.49 (s, 1H), 7.29 (d, J = 5.8 Hz, 2H), 7.26 (s, 1H), 4.12 (s, 2H). ^{13}C NMR (126 MHz, CDCl_3) δ 149.7 (2C), 145.6, 134.4, 133.1, 131.5, 131.3, 130.9 (2C), 130.7, 123.9, 36.7. HRMS calculated for $\text{C}_{12}\text{H}_9\text{Cl}_3\text{NS}$ ($\text{M}+\text{H}$) $^+$ 383.9521; found 383.9430 (TOF MS ES+).

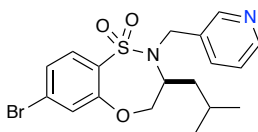
(S)-3-benzyl-7-bromo-2-(pyridin-3-ylmethyl)-3,4-dihydro-2H-benzo[b][1,4,5]oxathiazepine 1,1-dioxide (3.3.8f)



Utilizing general procedure A, **3.3.8f** (25mg, 0.054 mmol, 99%) was isolated as a white solid.

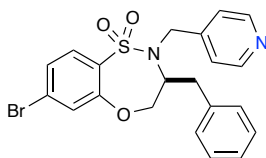
MP = 175 °C. FTIR (neat, cm^{-1}): 3085, 3026, 2954, 2921, 1579, 1550, 1452, 1326, 1155, 1027; ^1H NMR (500 MHz, CDCl_3) δ 8.48 (d, J = 4.1 Hz, 1H), 8.37 (s, 1H), 7.72 (d, J = 8.5 Hz, 1H), 7.46 (d, J = 7.9 Hz, 1H), 7.33 (dd, J = 8.5, 1.8 Hz, 1H), 7.23–7.17 (m, 4H), 7.11 (dd, J = 7.9, 4.8 Hz, 1H), 7.01 (m, J = 7.3, 1.9 Hz, 2H), 4.85 (t, J = 12.2 Hz, 1H), 4.37 (dd, J = 13.3, 4.8 Hz, 1H), 4.29 (d, J = 15.1 Hz, 1H), 4.15–4.07 (m, 1H), 3.89 (m, 1H), 3.00 (dd, J = 14.1, 8.0 Hz, 1H), 2.81 (dd, J = 13.8, 7.0 Hz, 1H). ^{13}C NMR (126 MHz, CDCl_3) δ 156.0, 148.7, 148.6, 137.2, 136.8, 131.4, 129.9, 129.3 (2C), 129.1, 128.8 (2C), 127.6, 126.9, 126.7, 124.7, 123.8, 74.2, 63.5, 52.5, 37.0. HRMS calculated for $\text{C}_{21}\text{H}_{19}\text{BrN}_2\text{OS}$ ($\text{M}+\text{H}$) $^+$ 459.0378; found 459.0282 (TOF MS ES+).

(S)-7-bromo-3-isobutyl-2-(pyridin-3-ylmethyl)-3,4-dihydro-2H-benzo[b][1,4,5]oxathiazepine 1,1-dioxide (3.3.8g)



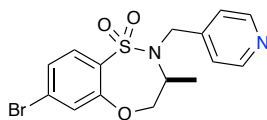
Utilizing general procedure **A**, **3.3.8g** (21.5 mg, 0.050 mmol, 84%) was isolated as a white solid. MP: 173 °C. FTIR (neat, cm^{-1}): 2954, 2923, 2958, 2875, 1579, 1550, 11471, 1325, 1153, 1024; ^1H NMR (500 MHz, CDCl_3) δ 8.59 (s, 2H), 7.89 (d, $J = 7.8$ Hz, 1H), 7.71 (d, $J = 8.4$ Hz, 1H), 7.39–7.31 (m, 2H), 7.26 (d, $J = 1.9$ Hz, 1H), 4.56 (t, $J = 11.9$ Hz, 1H), 4.46–4.28 (m, 2H), 4.25–4.08 (m, 1H), 3.89 (s, 1H), 1.37 (m, 1H), 1.31–1.19 (m, 2H), 0.70 (d, $J = 6.5$ Hz, 3H), 0.67 (d, $J = 6.4$ Hz, 3H). ^{13}C NMR (126 MHz, CDCl_3) δ 156.1, 148.8 (2C), 137.5, 130.9, 130.2 (2C), 127.7, 126.9, 125.2, 123.3, 74.2, 60.2, 39.5, 29.7, 24.7, 22.9, 22.0. HRMS calculated for $\text{C}_{18}\text{H}_{22}\text{BrN}_2\text{O}_3\text{S}$ ($\text{M}+\text{H}$) $^+$ 425.0535; found 425.0536 (TOF MS ES+).

(S)-3-benzyl-7-bromo-2-(pyridin-4-ylmethyl)-3,4-dihydro-2H-benzo[b][1,4,5]oxathiazepine 1,1-dioxide (3.3.8h)



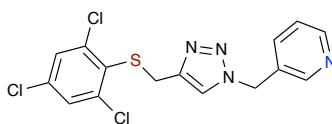
Utilizing general procedure **A**, **3.3.8h** (18 mg, 0.039 mmol, 97%) was isolated as a yellow solid. MP = 179 °C. FTIR (neat, cm^{-1}): 3085, 3026, 2958, 2921, 1602, 1579, 1538, 1323, 1153, 1018; ^1H NMR (500 MHz, CDCl_3) δ 8.43 (s, 2H), 7.71 (d, $J = 8.5$ Hz, 1H), 7.35 (dd, $J = 8.5, 2.0$ Hz, 1H), 7.25 (d, $J = 1.9$ Hz, 1H), 7.24–7.19 (m, 3H), 7.09 (m, 2H), 7.04–6.99 (m, 2H), 4.79 (t, $J = 12.2$ Hz, 1H), 4.44–4.28 (m, 2H), 4.07 (d, $J = 15.6$ Hz, 1H), 3.95–3.88 (m, 1H), 3.06 (dd, $J = 14.0, 8.2$ Hz, 1H), 2.85 (dd, $J = 13.9, 7.5$ Hz, 1H). ^{13}C NMR (126 MHz, CDCl_3) δ 155.9, 148.3 (2C), 146.4, 136.7, 130.1, 129.2 (2C), 129.1, 128.9, 128.8, 127.8, 127.3, 127.1, 126.9, 124.9, 123.5, 74.2, 64.3, 53.9, 36.9. HRMS calculated for $\text{C}_{21}\text{H}_{20}\text{BrN}_2\text{O}_3\text{S}$ ($\text{M}+\text{H}$) $^+$ 459.0378; found 459.0282 (TOF MS ES+).

(S)-7-bromo-3-methyl-2-(pyridin-3-ylmethyl)-3,4-dihydro-2H-benzo[b][1,4,5]oxathiazepine-1,1-dioxide (3.3.8i)



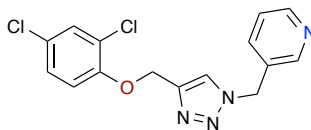
Utilizing general procedure **A**, **3.3.8i** (14 mg, 0.036 mmol, 72%) was isolated as a yellow solid MP = 164 °C. FTIR (neat, cm^{-1}): 2960, 2852, 2358, 1600, 1577, 1538, 1460, 1340, 1161, 1024, 1006; ^1H NMR (500 MHz, CDCl_3) δ 8.67–8.58 (m, 2H), 7.70 (d, J = 8.4 Hz, 1H), 7.42 (d, J = 5.1 Hz, 2H), 7.36 (dd, J = 8.4, 1.9 Hz, 1H), 7.31 (d, J = 1.9 Hz, 1H), 4.47 (t, J = 12.0 Hz, 1H), 4.40–4.29 (m, 2H), 4.21 (d, J = 16.4 Hz, 1H), 4.15–4.04 (m, 1H), 1.19 (d, J = 7.0 Hz, 3H). ^{13}C NMR (126 MHz, CDCl_3) δ 156.0, 148.9, 147.6, 131.1, 130.1 (2C), 127.9, 127.1 (2C), 125.5, 122.9, 74.5, 51.4, 57.7, 15.9. HRMS calculated for $\text{C}_{16}\text{H}_{15}\text{BrN}_2\text{O}_3\text{S}$ ($\text{M}+\text{H}$) $^+$ 383.0065; found 382.0039 (TOF MS ES+).

3-(((4-(((2,4,6-trichlorophenyl)thio)methyl)-1H-1,2,3-triazol-1-yl)methyl)pyridine (3.3.9a)



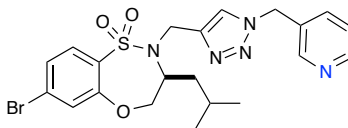
Utilizing general procedure **B**, **3.3.9a** (47 mg, 0.121 mmol, 88%) was isolated as a brown thick liquid. FTIR (neat): 2358, 2341, 1629, 1473, 1321, 1274, 1259, 1116, 1058 cm^{-1} ; ^1H NMR (500 MHz, CDCl_3): δ 8.63 (dd, J = 4.8, 1.5 Hz, 1H), 8.60 (d, J = 2.1 Hz, 1H), 7.55–7.50 (m, 1H), 7.45 (s, 1H), 7.41 (s, 1H), 7.39 (s, 1H), 7.34–7.31 (m, 1H), 5.53 (s, 2H), 4.25 (s, 2H). ^{13}C NMR (126 MHz, CDCl_3): δ 150.4, 149.1, 144.3, 135.6, 134.9, 132.4, 131.5, 130.7, 130.7, 130.3, 129.9, 124.0, 122.1, 51.7, 27.7. HRMS calculated for $\text{C}_{15}\text{H}_{12}\text{Cl}_3\text{N}_4\text{S}$ ($\text{M}+\text{H}$) $^+$ 384.9848; found 384.9813 (TOF MS ES+).

3-((4-((2,4-dichlorophenoxy)methyl)-1*H*-1,2,3-triazol-1-yl)methyl)pyridine (3.3.9b)



Utilizing general procedure **B**, **3.3.9b** (57 mg, 0.170 mmol, 93%) was isolated as a colorless thick liquid. FTIR (neat): 2925, 2358, 2341, 1635, 1375, 1261, 1118, 1026 cm^{-1} ; ^1H NMR (400 MHz, CDCl_3): δ 8.65 (brs, 2H), 7.65 (s, 1H), 7.61 (d, $J = 7.9$ Hz, 1H), 7.37 (d, $J = 2.5$ Hz, 1H), 7.35 – 7.32 (m, 1H), 7.19 (dd, $J = 8.8, 2.5$ Hz, 1H), 7.05 (d, $J = 8.8$ Hz, 1H), 5.59 (s, 2H), 5.27 (s, 2H). ^{13}C NMR (126 MHz, CDCl_3): δ 152.5, 150.4, 149.1, 144.3, 135.7, 130.3, 130.1, 127.7, 126.6, 124.1, 124.0, 122.8, 115.1, 63.5, 51.7. HRMS calculated for $\text{C}_{15}\text{H}_{13}\text{Cl}_2\text{N}_4\text{O}$ ($\text{M}+\text{H}$) $^+$ 335.0466; found 335.0421 (TOF MS ES $^+$).

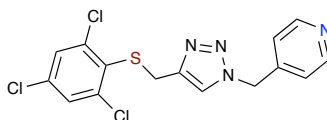
(*S*)-7-bromo-3-isobutyl-2-((1-(pyridin-3-ylmethyl)-1*H*-1,2,3-triazol-4-yl)methyl)-3,4-dihydro-2*H*-benzo[*b*][1,4,5]oxathiazepine 1,1-dioxide (3.3.9c)



Utilizing general procedure **B**, **3.3.9c** (36 mg, 0.071 mmol, 81%) was isolated as a thick liquid. FTIR (neat): 2958, 2358, 2341, 1579, 1558, 1458, 1423, 1373, 1323, 1164, 1081 cm^{-1} ; ^1H NMR (400 MHz, CDCl_3): δ 8.64 (d, $J = 8.4$ Hz, 1H), 8.58 (s, 1H), 7.64 (d, $J = 8.4$ Hz, 1H), 7.55 (d, $J = 7.9$ Hz, 1H), 7.38 (s, 1H), 7.35–7.31 (m, 1H), 7.30–7.27 (m, 1H), 7.16 (s, 1H), 5.47 (dd, $J = 34.4, 15.1$ Hz, 2H), 4.45–4.29 (m, 3H), 4.28–4.20 (m, 2H), 1.75 – 1.64 (m, 1H), 1.49–1.38 (m, 1H), 1.26–1.20 (m, 1H), 0.82 (dd, $J = 6.4, 3.5$ Hz, 6H). ^{13}C NMR (126 MHz, CDCl_3): δ 156.1, 150.4, 149.2, 144.3, 135.6, 131.6, 130.2, 130.0, 127.5, 126.6, 125.4, 123.9, 123.4, 77.2, 73.8, 59.9, 51.6, 38.7, 24.6,

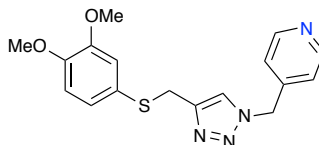
22.8, 22.0. HRMS calculated for $C_{21}H_{25}BrN_5O_3S$ ($M+H$)⁺ 506.0861; found 506.0868 (TOF MS ES⁺).

4-((4-(((2,4,6-trichlorophenyl)thio)methyl)-1H-1,2,3-triazol-1-yl)methyl)pyridine (3.3.9d)



Utilizing general procedure **B**, **3.3.9d** (45 mg, 0.116 mmol, 84%) was isolated as a brown thick liquid. FTIR (neat): 2923, 2850, 2283, 1635, 1473, 1274, 1259, 1110, 1024 cm^{-1} ; 1H NMR (400 MHz, $CDCl_3$): δ 8.51 (d, $J = 4.7$ Hz, 1H), 7.61 (t, $J = 7.7$ Hz, 1H), 7.54 (s, 1H), 7.36 (s, 1H), 7.31 (s, 1H), 7.20 (t, $J = 6.2$ Hz, 1H), 7.05 (d, $J = 7.8$ Hz, 1H), 5.54 (s, 2H), 4.19 (s, 2H). ^{13}C NMR (126 MHz, $CDCl_3$): δ 154.2, 149.8, 143.8, 137.4, 135.1, 132.4, 131.5, 130.7, 130.5, 129.9, 123.5, 122.9, 122.3, 55.7, 27.8. HRMS calculated for $C_{15}H_{12}Cl_3N_4S$ ($M+H$)⁺ 384.9848; found 384.9810 (TOF MS ES⁺).

4-((4-(((3,4-dimethoxyphenyl)thio)methyl)-1H-1,2,3-triazol-1-yl)methyl)pyridine (3.3.9e)



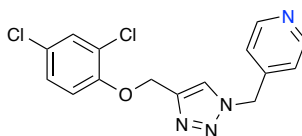
Utilizing general procedure **B**, **3.3.9e** (53 mg, 0.155 mmol, 89%) was isolated as a white solid.

FTIR (neat): 2952, 1581, 1502, 1438, 1253, 1228, 1135, 1024 cm^{-1} .

1H NMR (400 MHz, $CDCl_3$): δ 7.58–7.32 (m, 2H), 7.26–7.18 (m, 2H), 7.17 (s, 1H), 6.92–6.85 (m, 2H), 6.72 (d, $J = 8.2$ Hz, 1H), 5.47 (s, 2H), 4.14 (s, 2H), 3.86 (s, 3H), 3.79 (s, 3H). ^{13}C NMR (126 MHz, $CDCl_3$): δ 149.4, 148.6, 145.2, 134.9, 129.1, 128.7, 127.6 (2C), 125.6, 124.7, 121.4, 115.8, 111.7, 55.9, 55.8, 54.2, 30.6.

HRMS calculated for $C_{17}H_{19}N_4O_2S$ ($M+H$)⁺ 343.1229; found 343.1258 (TOF MS ES⁺).

4-((4-((2,4-dichlorophenoxy)methyl)-1*H*-1,2,3-triazol-1-yl)methyl)pyridine (3.3.9f)



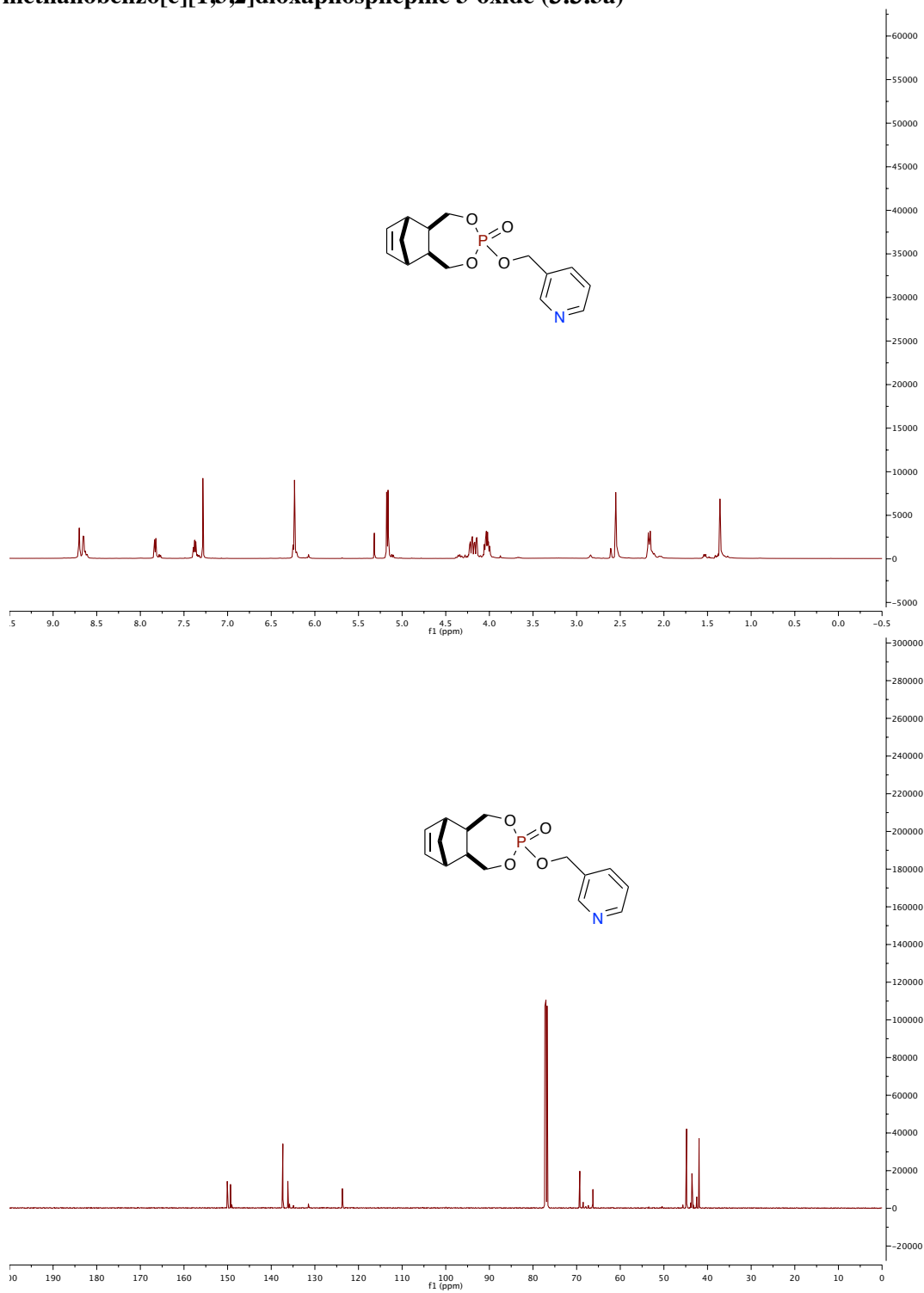
Utilizing general procedure **B**, **3.3.9f** (53 mg, 0.158 mmol, 87%) was isolated as a colorless thick liquid.

FTIR (neat): 2929, 2850, 2358, 2088, 1639, 1448, 1274, 1259, 1135, 1105, 1049 cm⁻¹; ¹H NMR (400 MHz, CDCl₃): δ 8.52 (d, *J* = 4.6 Hz, 1H), 7.76 (s, 1H), 7.62 (t, *J* = 7.7 Hz, 1H), 7.28 (s, 1H), 7.21–7.18 (m, 1H), 7.13–7.09 (m, 2H), 6.98 (d, *J* = 8.8 Hz, 1H), 5.59 (s, 2H), 5.20 (s, 2H). ¹³C NMR (126 MHz, CDCl₃): δ 154.2, 152.6, 149.9, 143.9, 137.4, 130.1, 127.7, 126.5, 124.0, 123.6, 123.6, 122.5, 115.2, 63.5, 55.7.

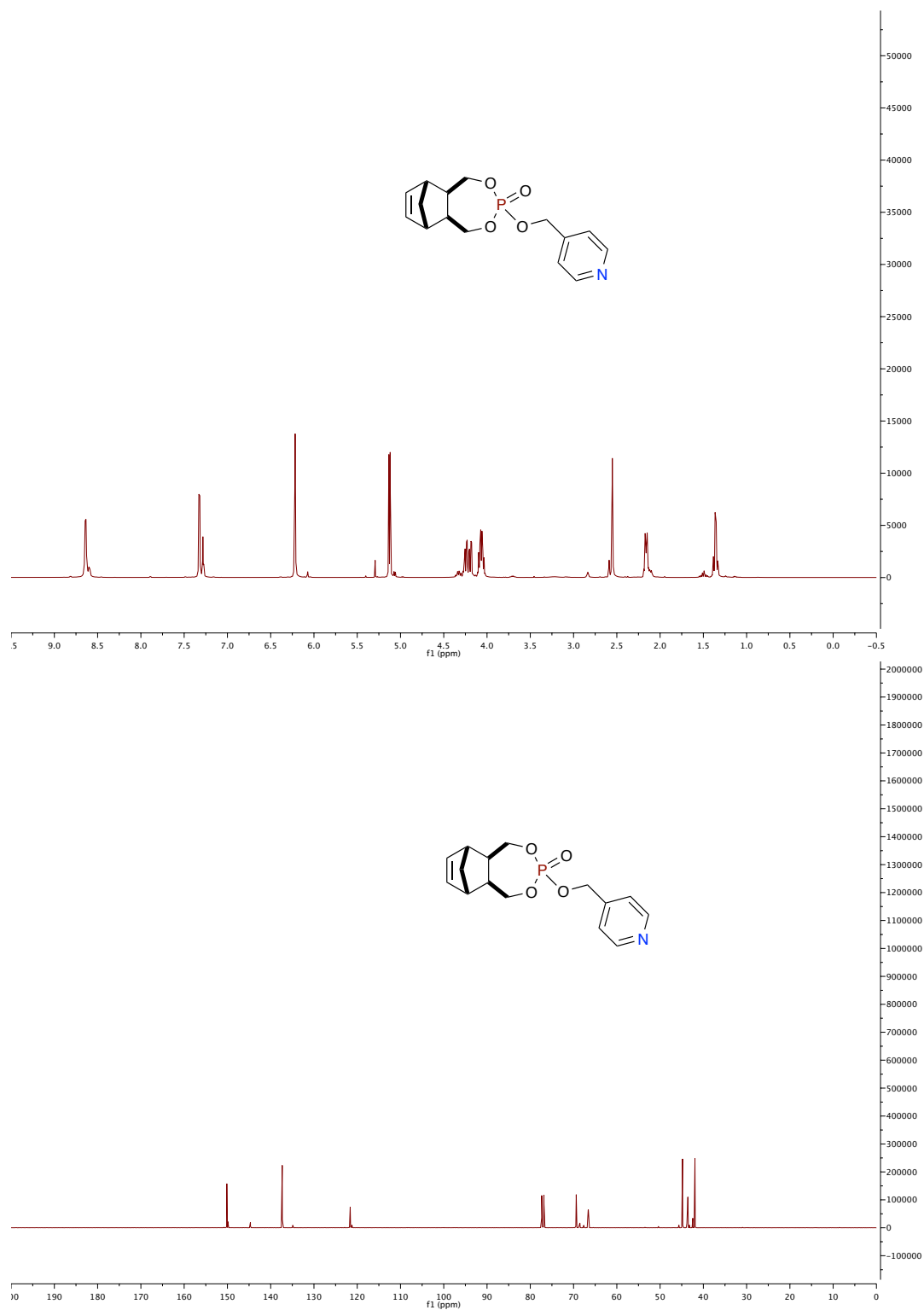
HRMS calculated for C₁₅H₁₃Cl₂N₄O (M+H)⁺ 335.0466; found 335.0422 (TOF MS ES⁺).

5.11 Spectra for Chapter 3.3

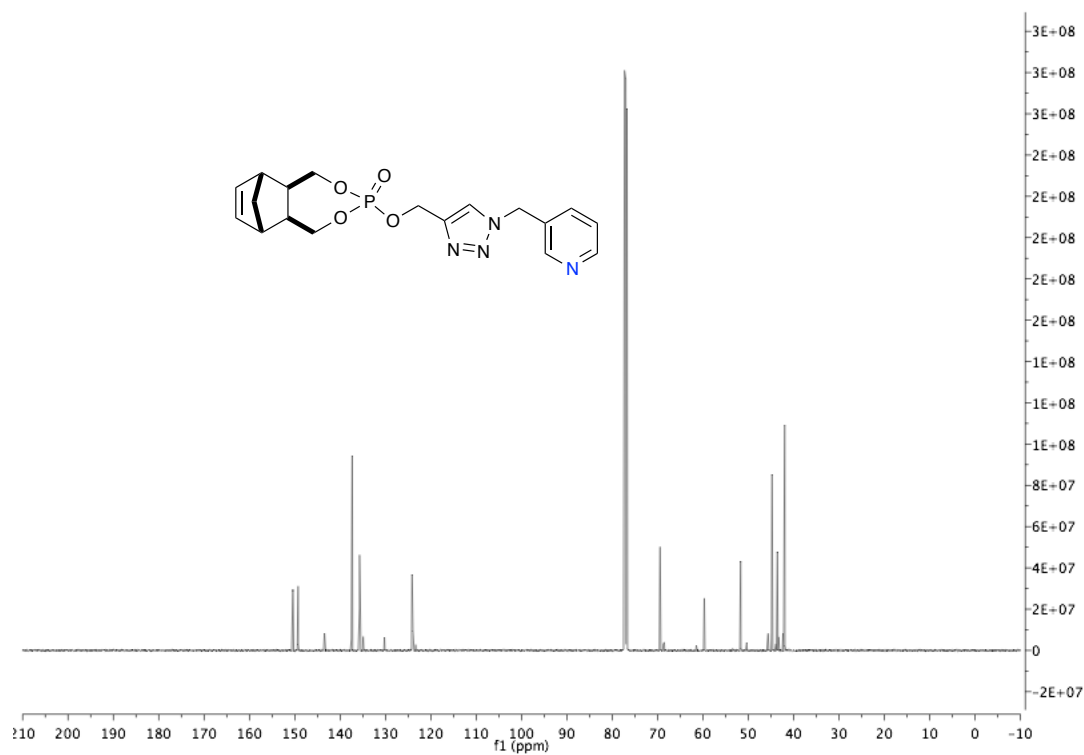
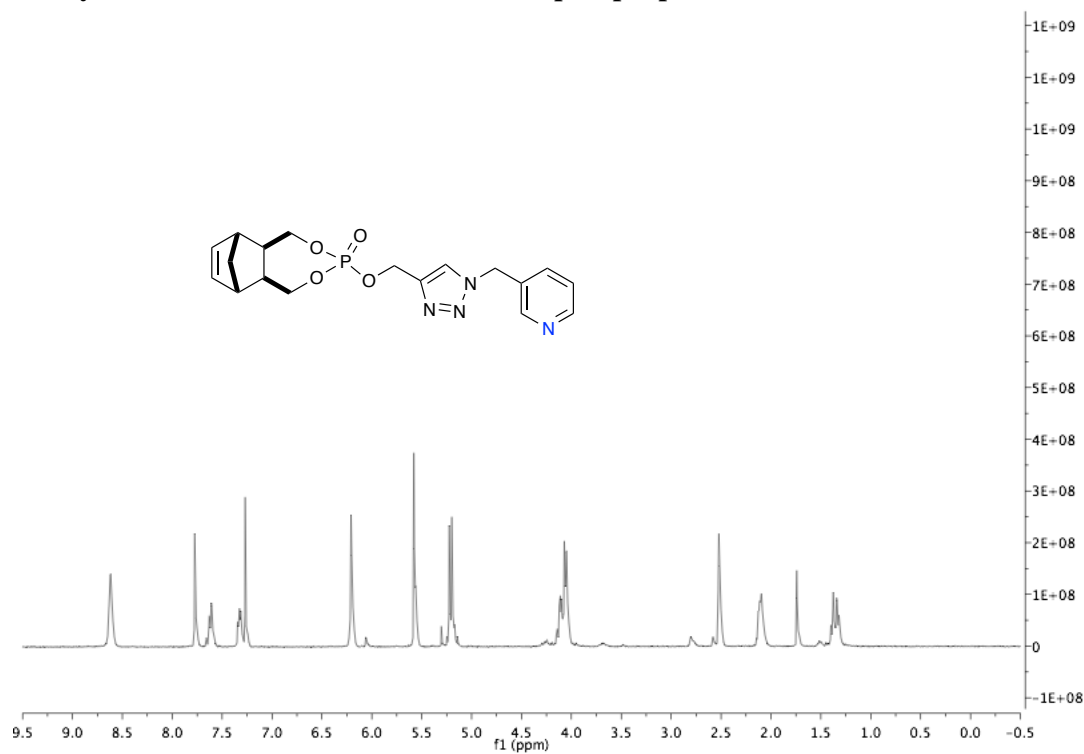
(5aR,6R,9S,9aS)-3-(pyridin-3-ylmethoxy)-1,5,5a,6,9,9a-hexahydro-6,9-methanobenzo[e][1,3,2]dioxaphosphepine 3-oxide (3.3.3a)



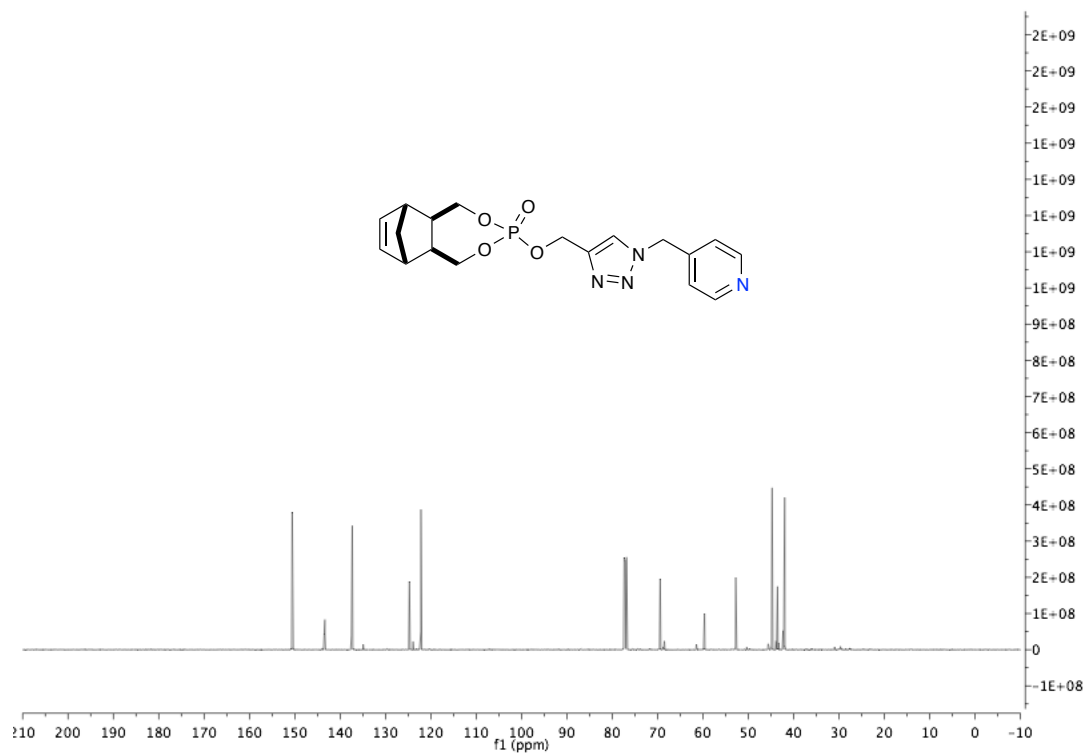
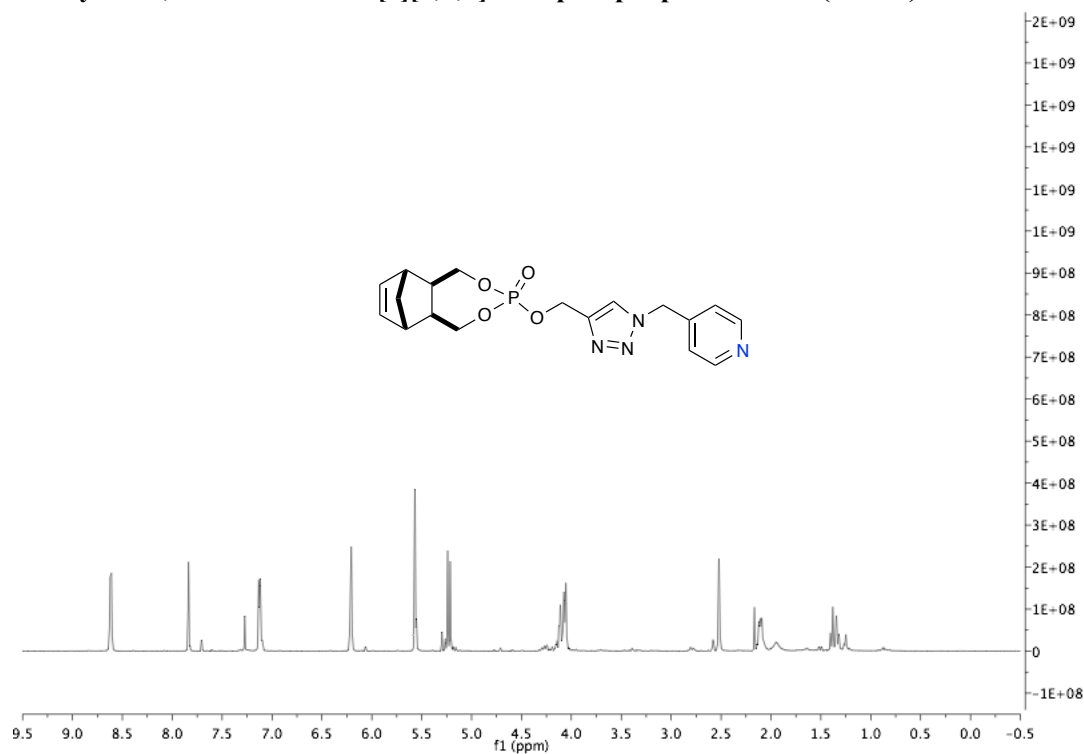
(5aR,6R,9S,9aS)-3-(pyridin-4-ylmethoxy)-1,5,5a,6,9,9a-hexahydro-6,9-methanobenzo[e][1,3,2]dioxaphosphepine 3-oxide (3.3.3b)



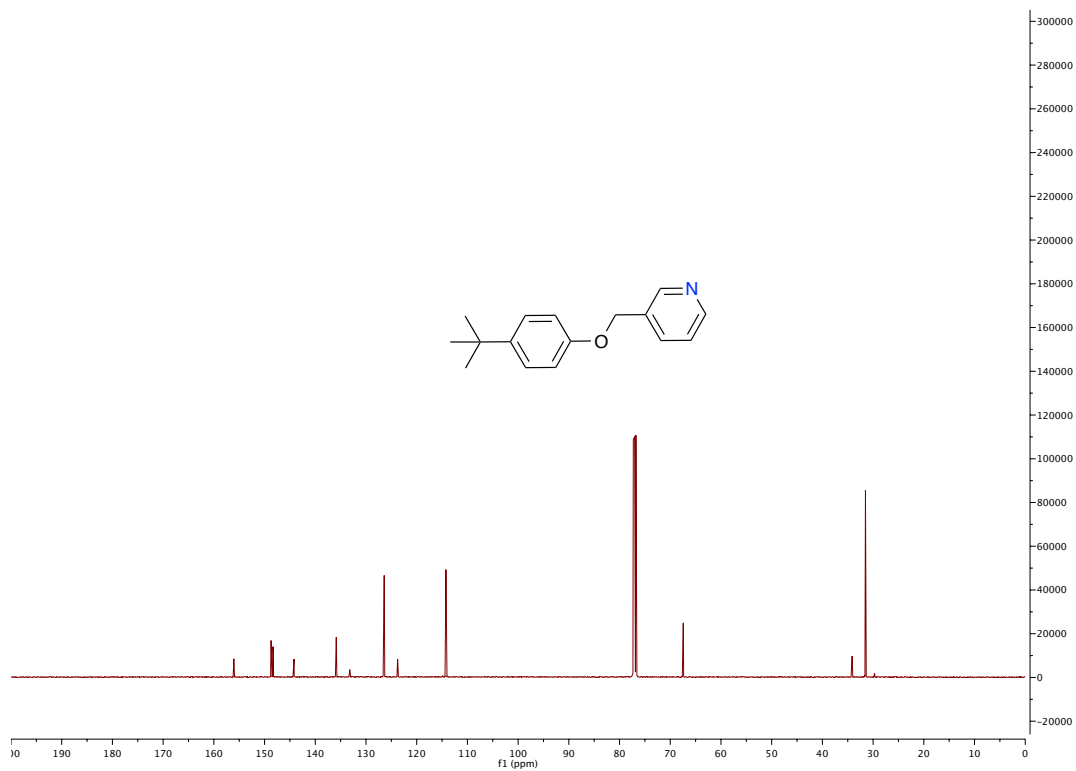
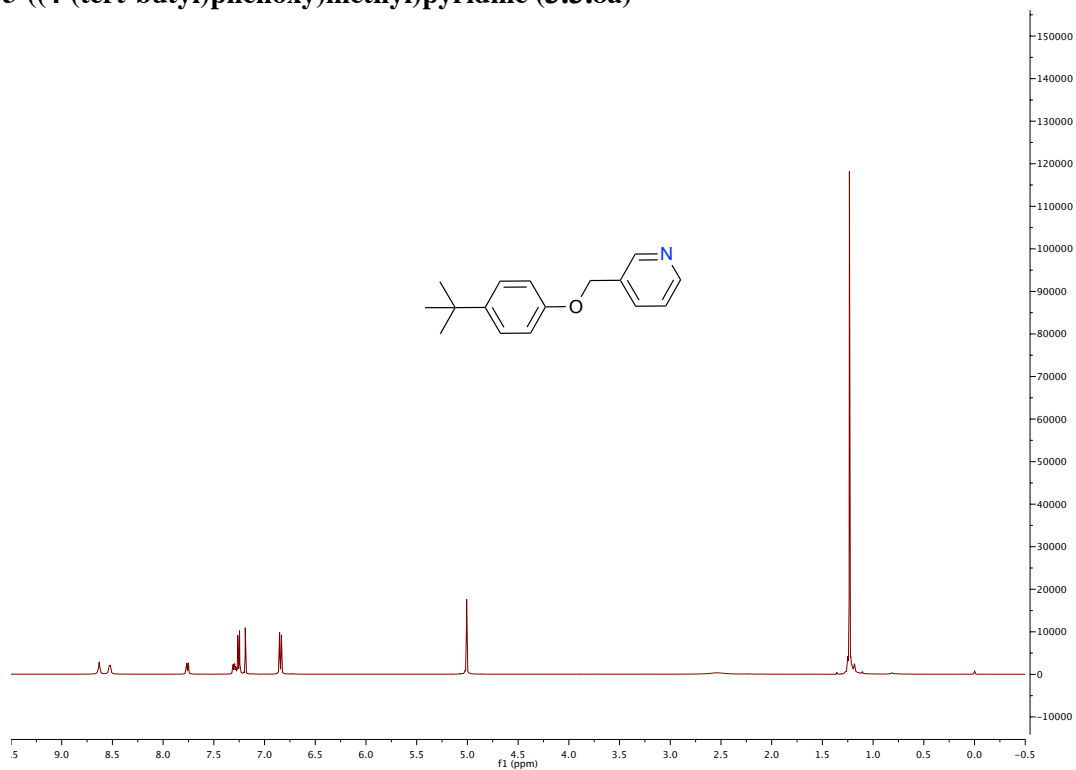
(5a*R*,6*R*,9*S*,9a*S*)-3-((1-(pyridin-3-ylmethyl)-1*H*-1,2,3-triazol-4-yl)methoxy)1,5,5a,6,9,9a-hexahydro-6,9 methanobenzo[*e*][1,3,2]dioxaphosphine 3-oxide (3.3.4a)



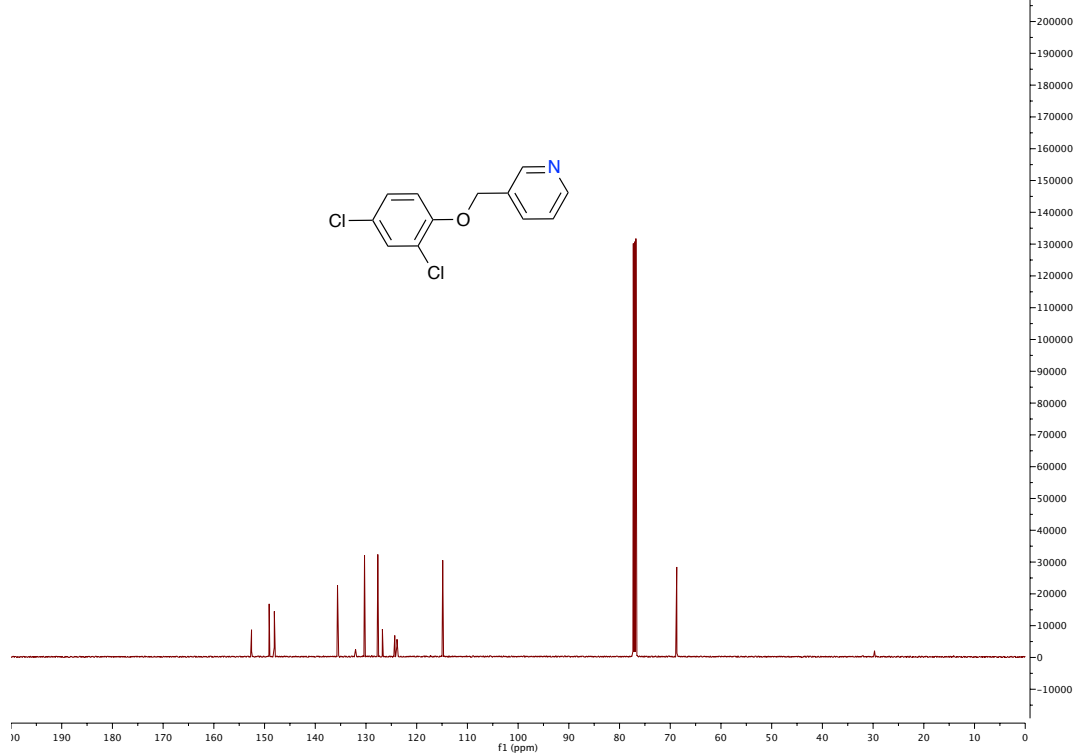
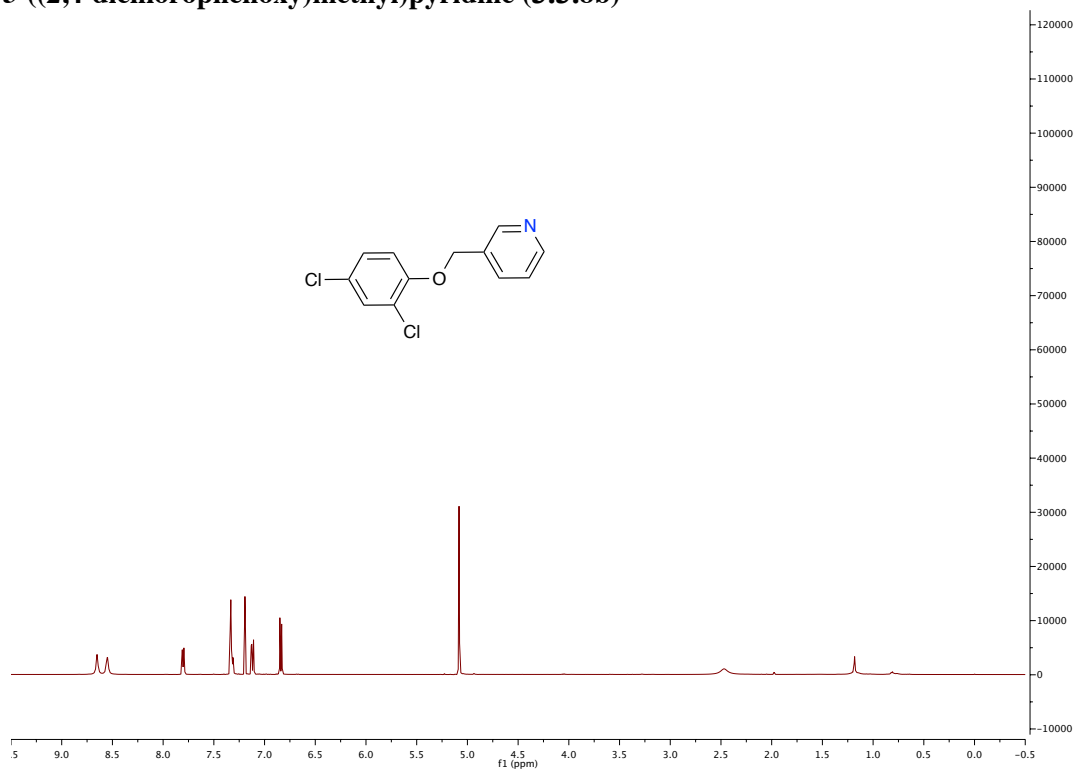
(5a*R*,6*R*,9*S*,9a*S*)-3-((1-(pyridin-4-ylmethyl)-1*H*-1,2,3-triazol-4-yl)methoxy)-1,5,5a,6,9,9a-hexahydro-6,9-methanobenzo[*e*][1,3,2]dioxaphosphepine 3-oxide (3.3.4b)



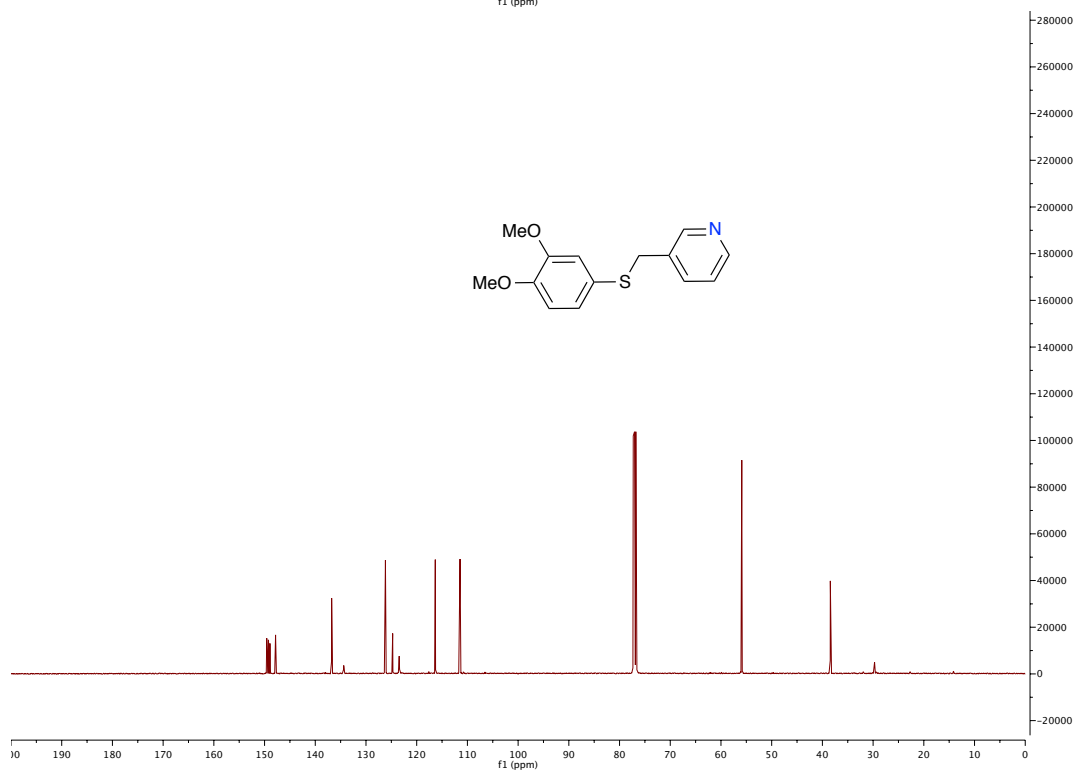
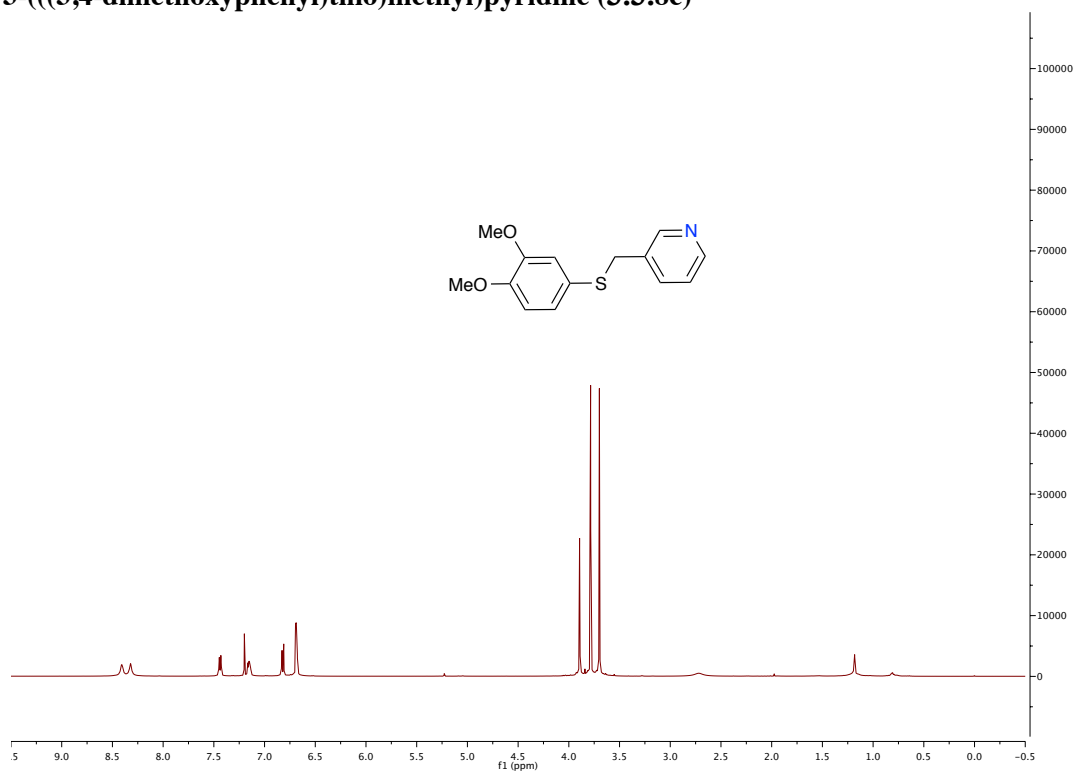
3-((4-(tert-butyl)phenoxy)methyl)pyridine (3.3.8a)



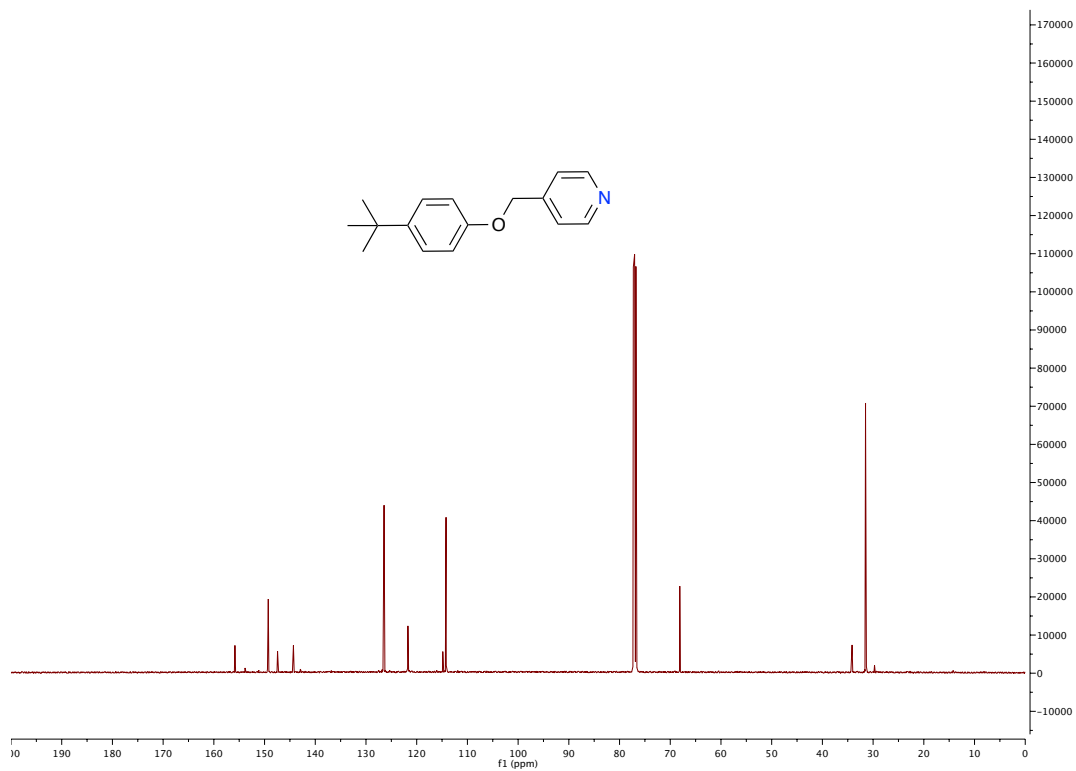
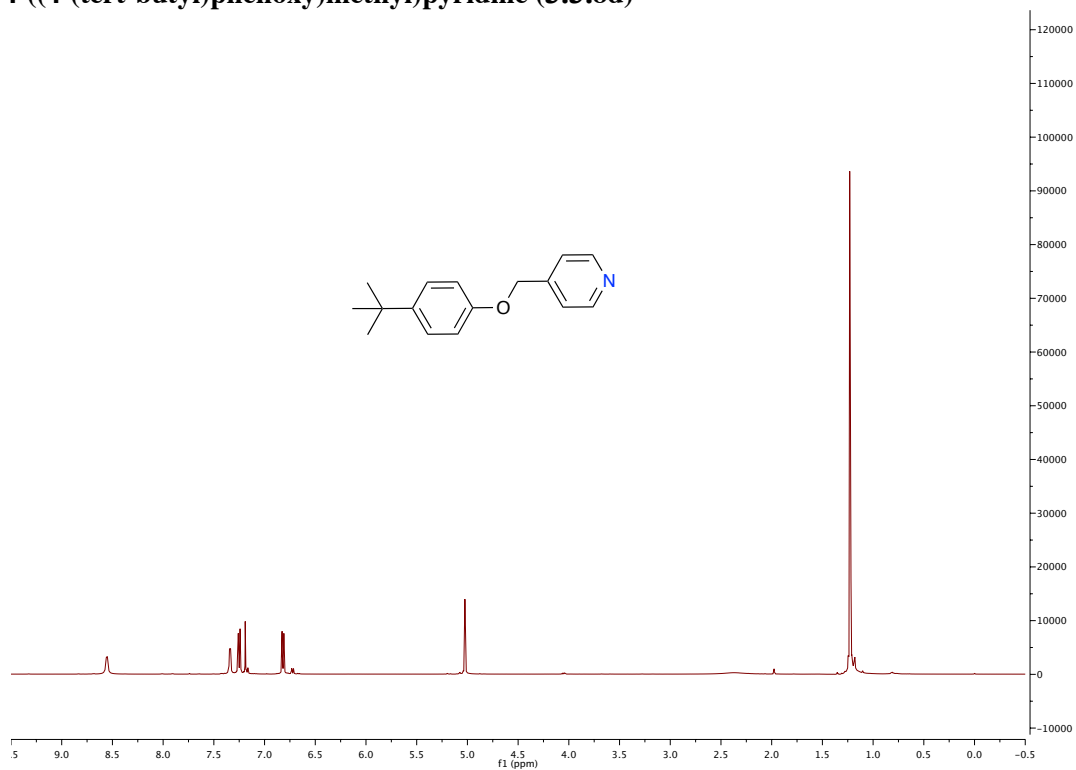
3-((2,4-dichlorophenoxy)methyl)pyridine (3.3.8b)



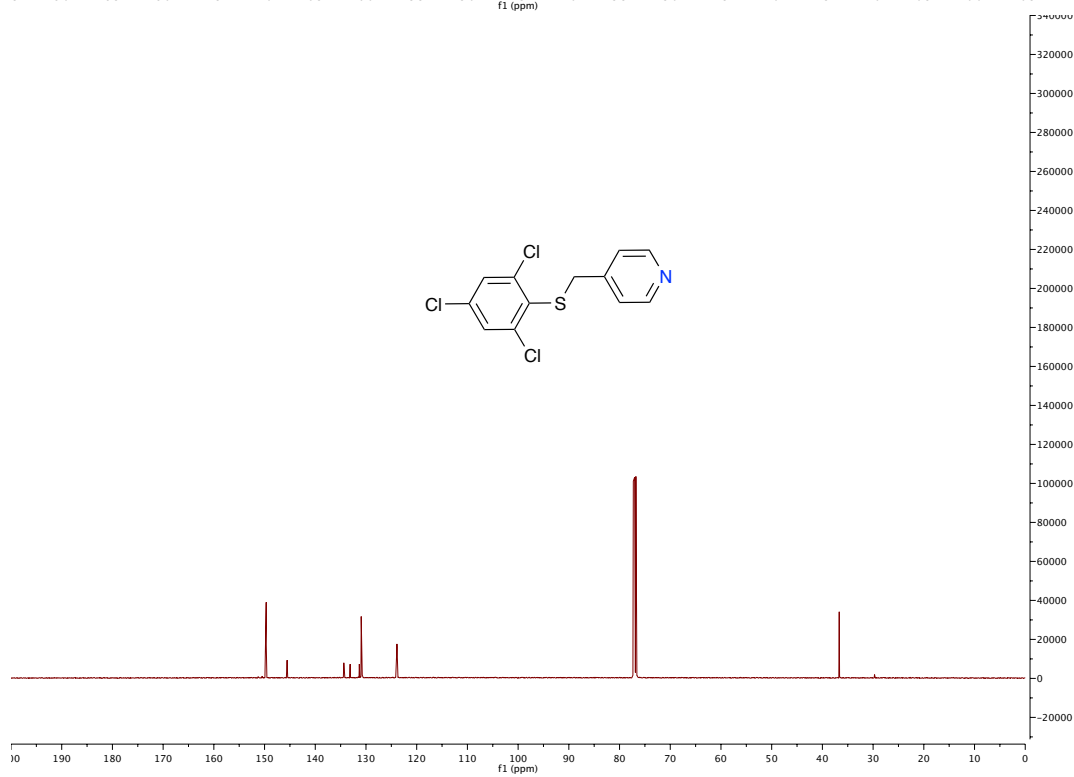
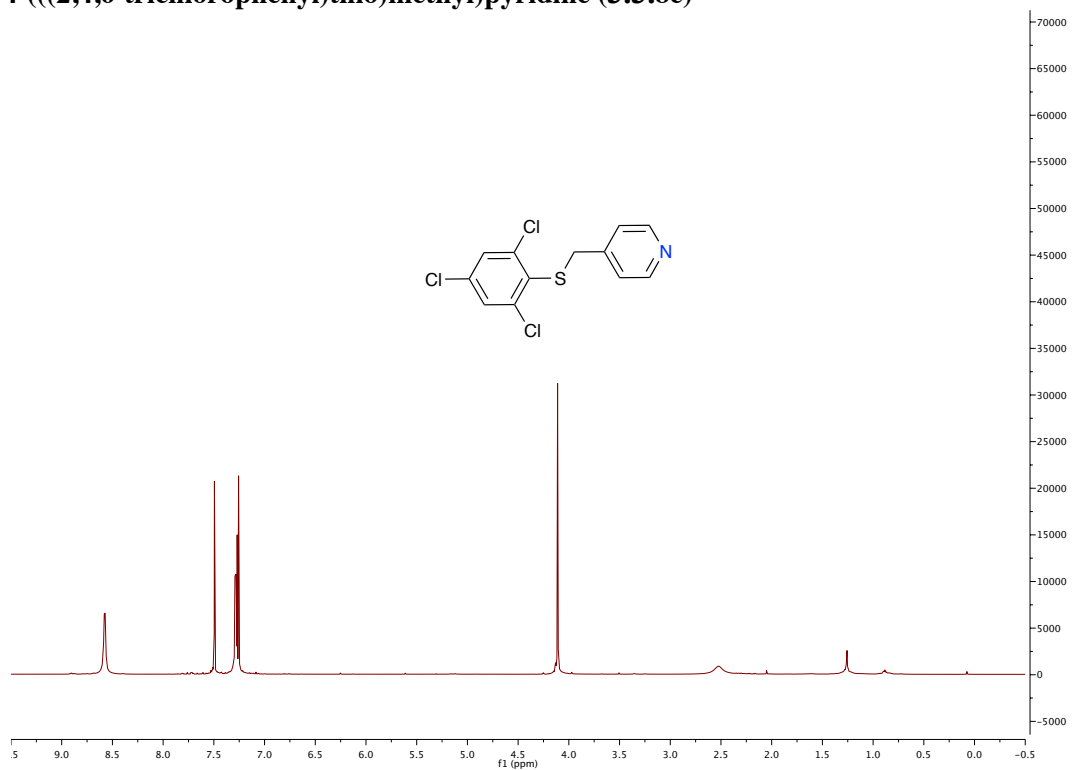
3-(((3,4-dimethoxyphenyl)thio)methyl)pyridine (3.3.8c)



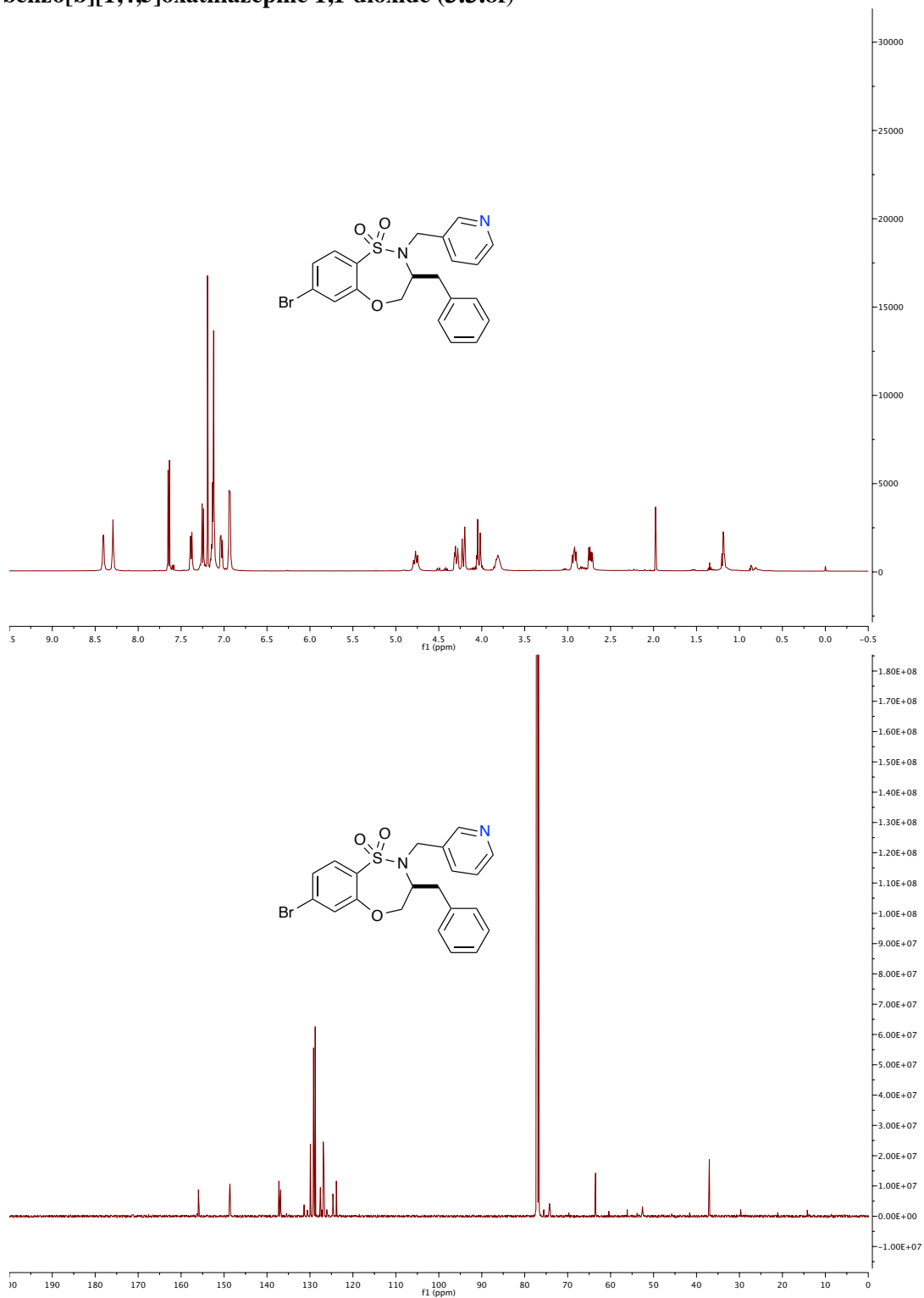
4-((4-(tert-butyl)phenoxy)methyl)pyridine (3.3.8d)



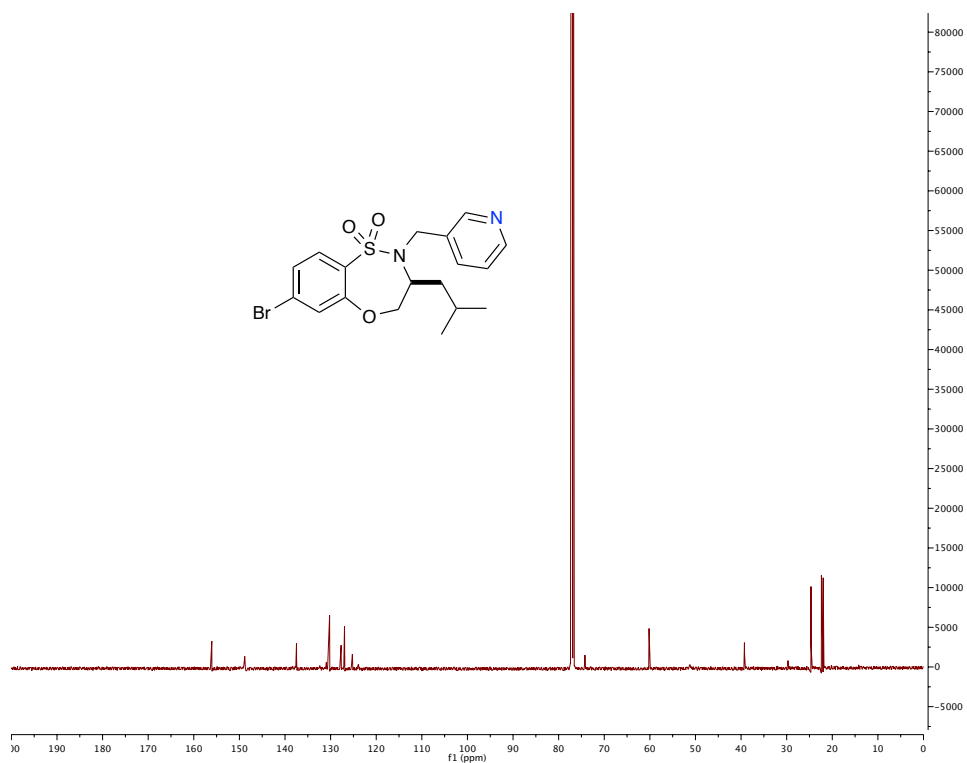
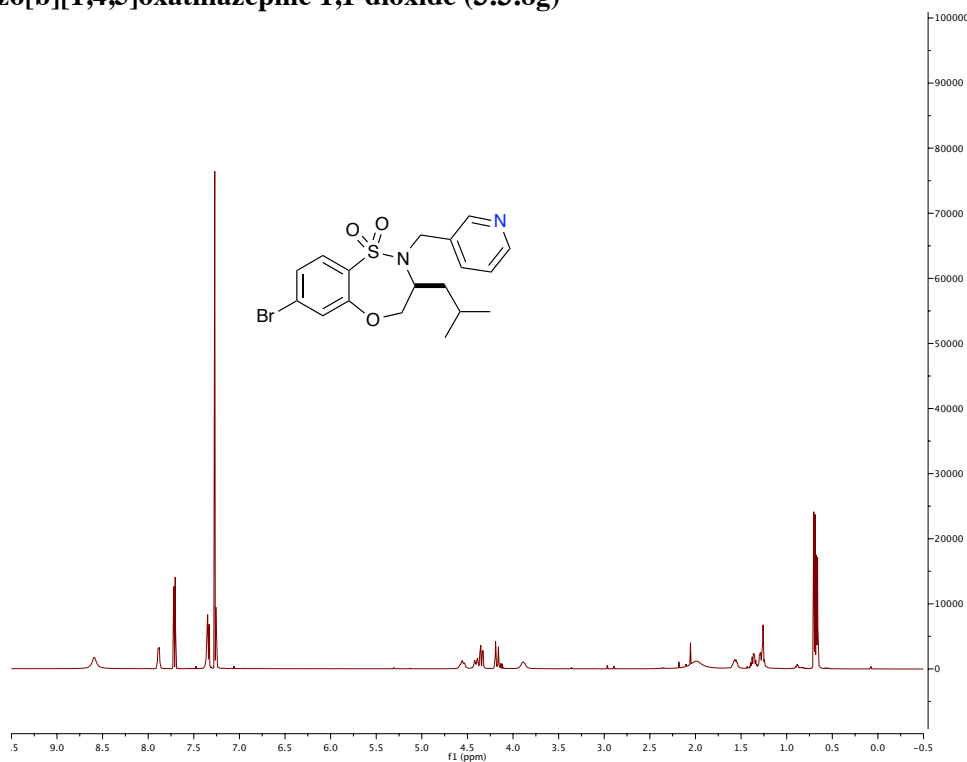
4-(((2,4,6-trichlorophenyl)thio)methyl)pyridine (3.3.8e)



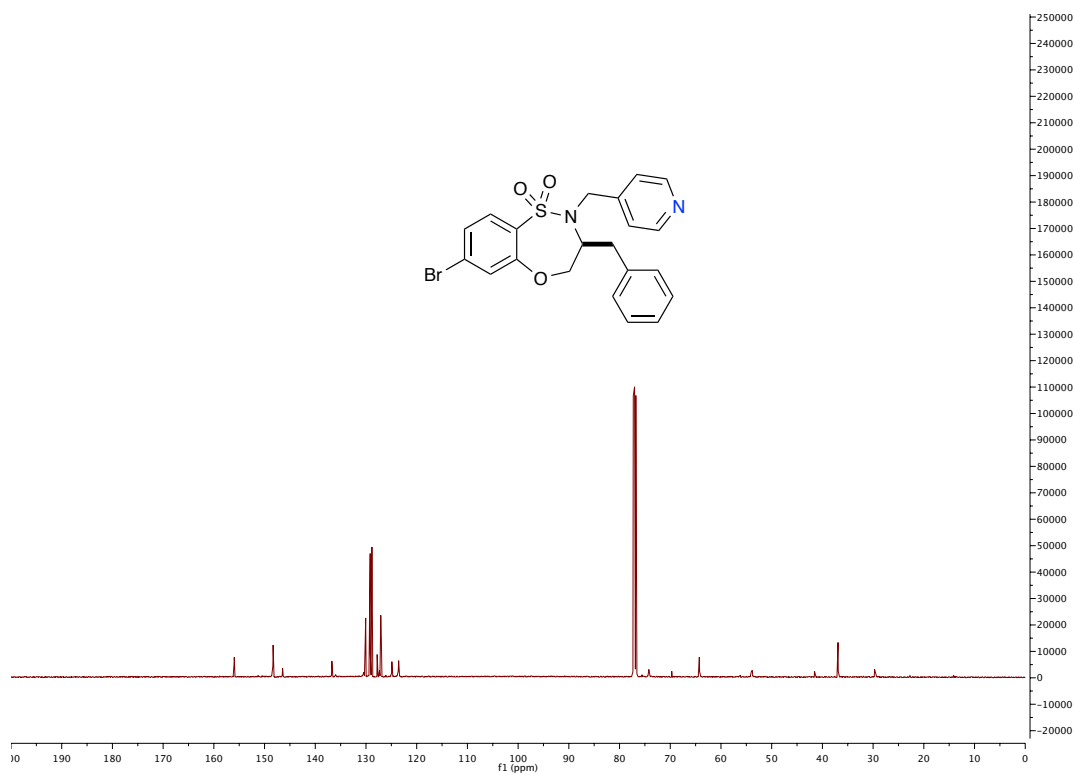
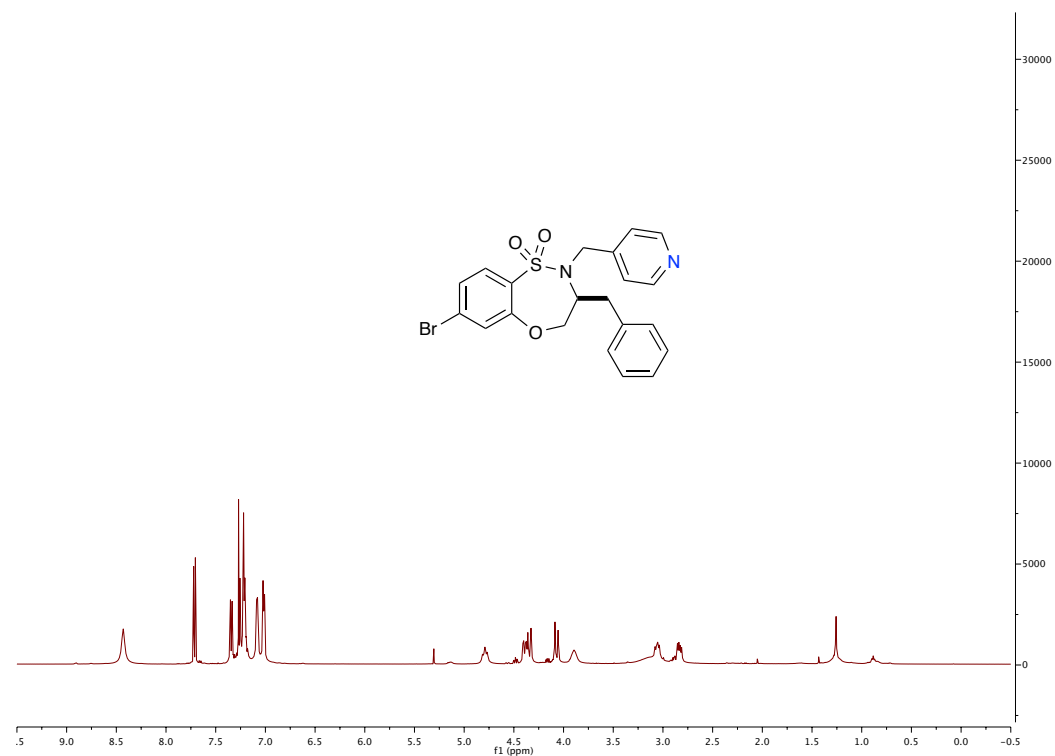
(S)-3-benzyl-7-bromo-2-(pyridin-3-ylmethyl)-3,4-dihydro-2H-benzo[b][1,4,5]oxathiazepine 1,1-dioxide (3.3.8f)



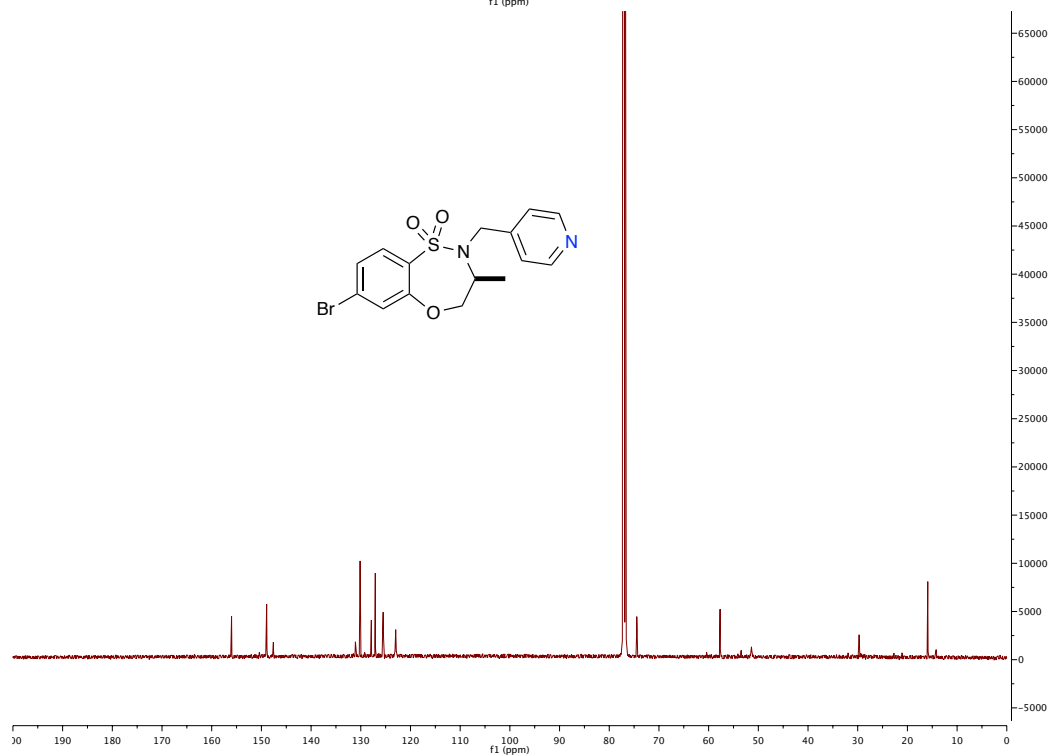
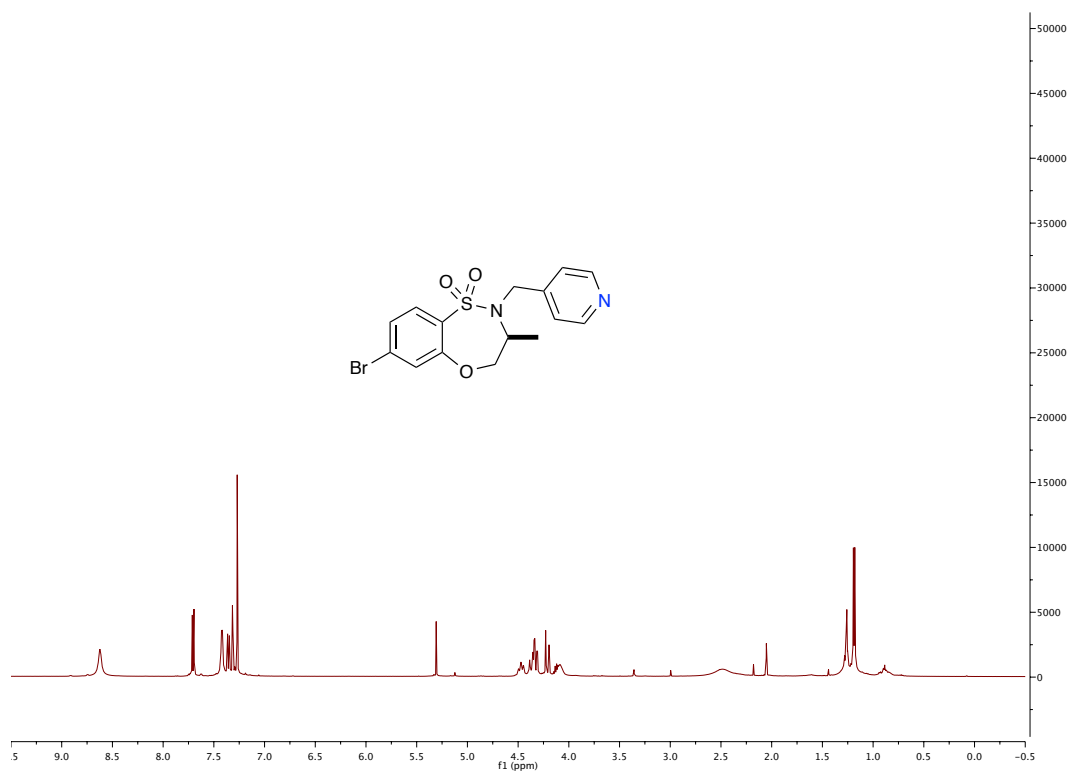
(S)-7-bromo-3-isobutyl-2-(pyridin-3-ylmethyl)-3,4-dihydro-2H-benzo[b][1,4,5]oxathiazepine 1,1-dioxide (3.3.8g)



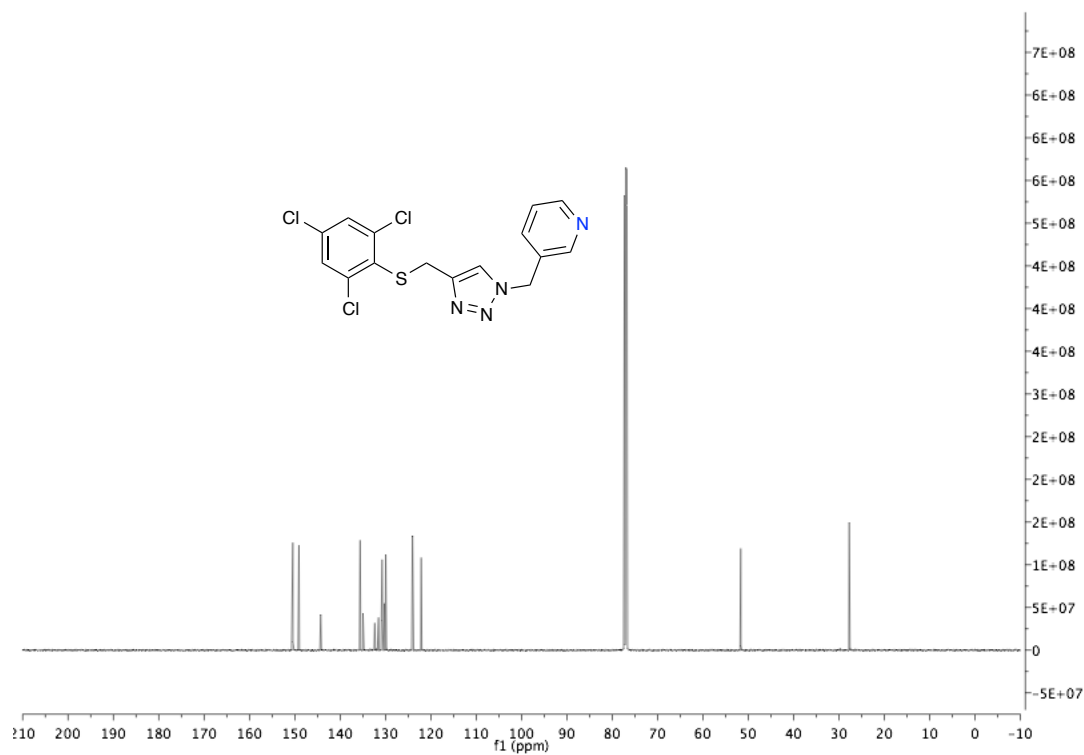
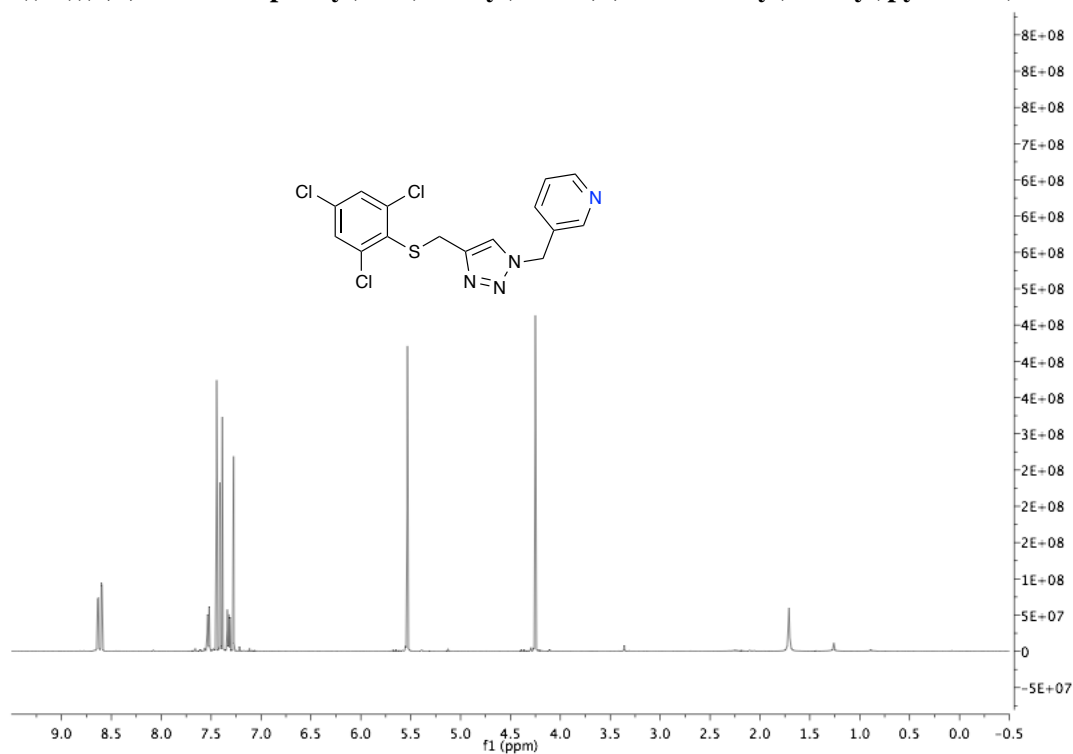
(S)-7-bromo-3-methyl-2-(pyridin-3-ylmethyl)-3,4-dihydro-2H-benzo[b][1,4,5]oxathiazepine-1,1-dioxide (3.3.8i)



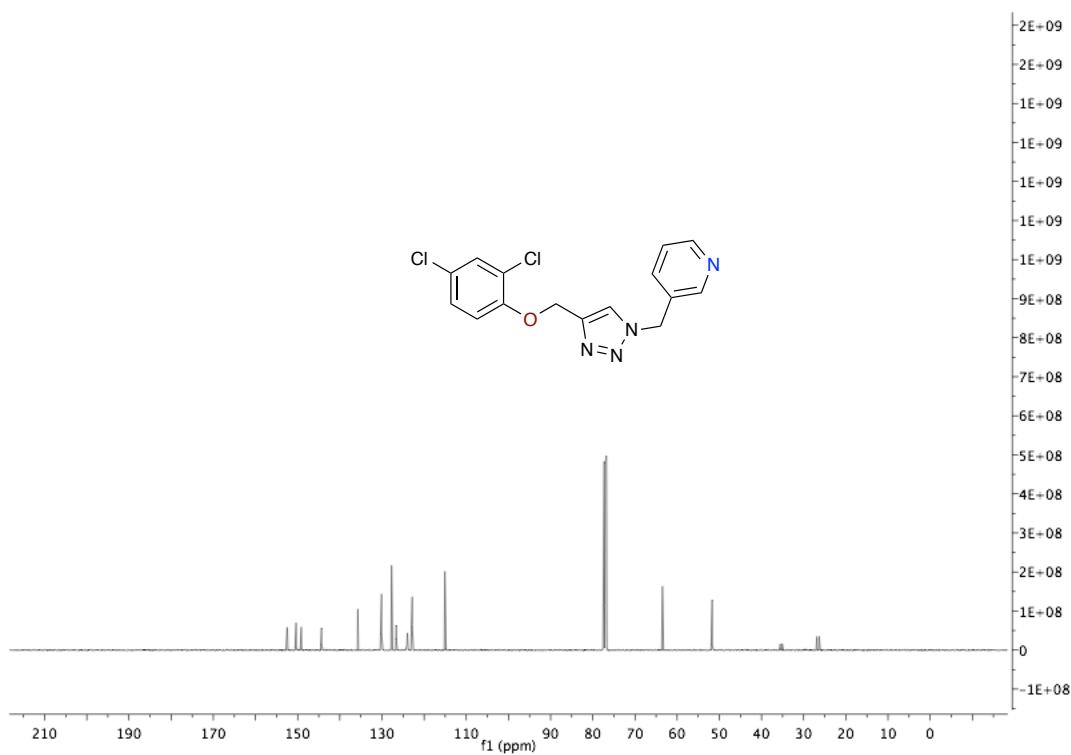
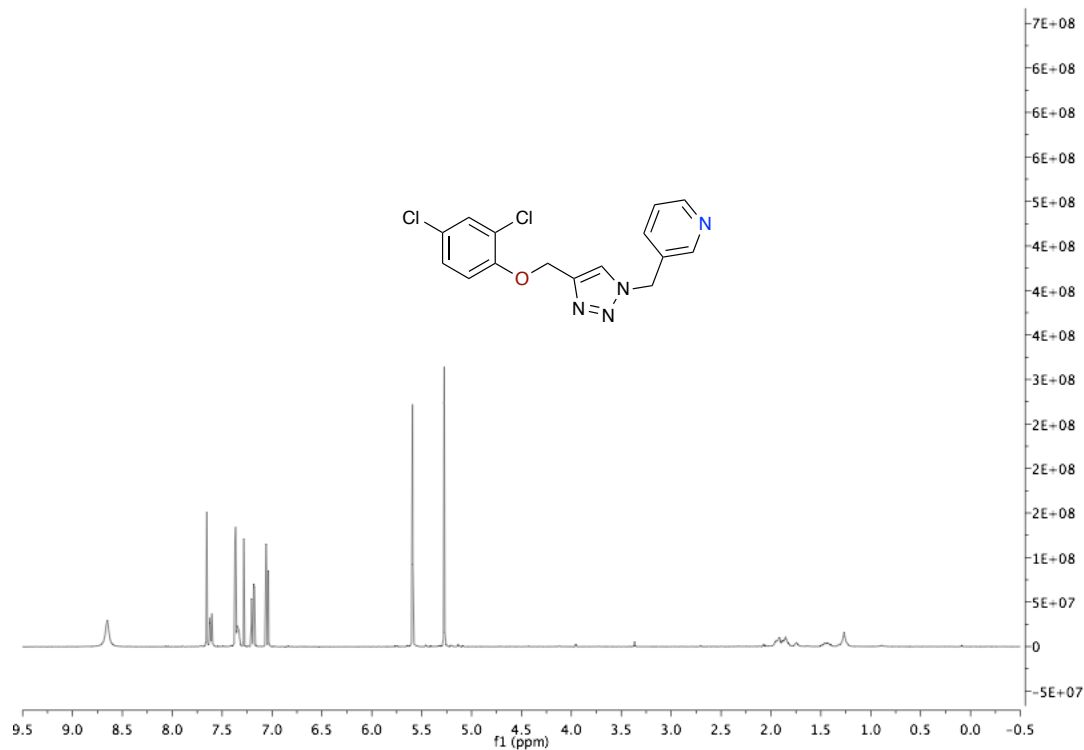
(S)-7-bromo-3-methyl-2-(pyridin-3-ylmethyl)-3,4-dihydro-2H-benzo[b][1,4,5]oxathiazepine-1,1-dioxide (3.3.8i)



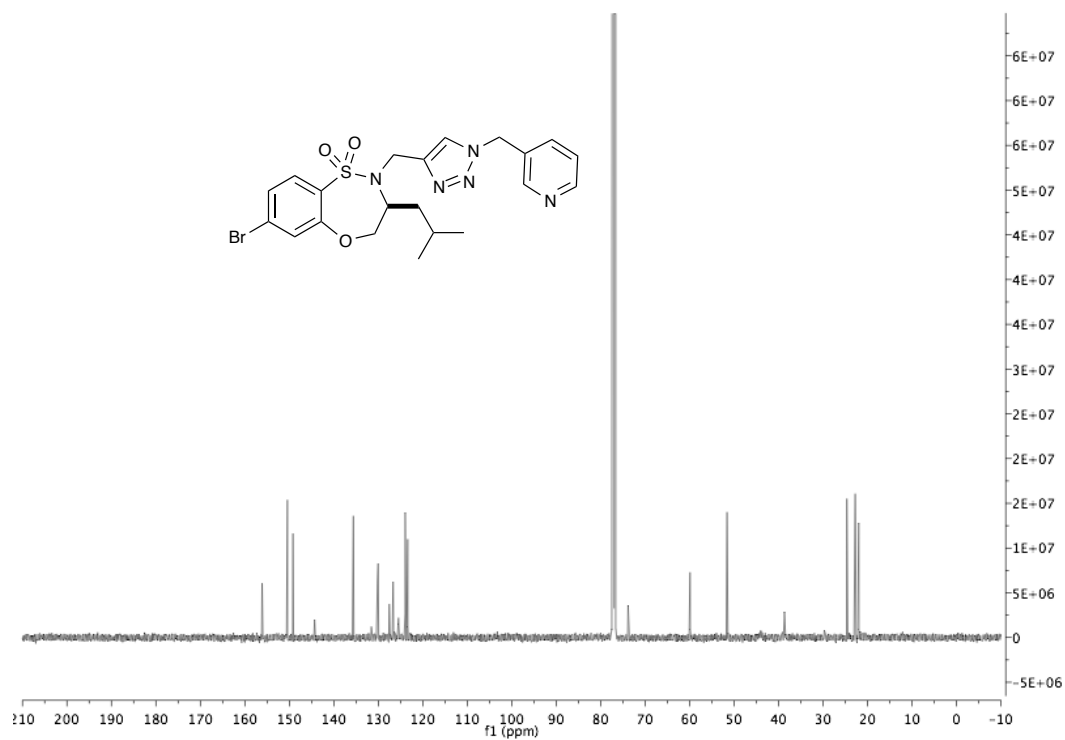
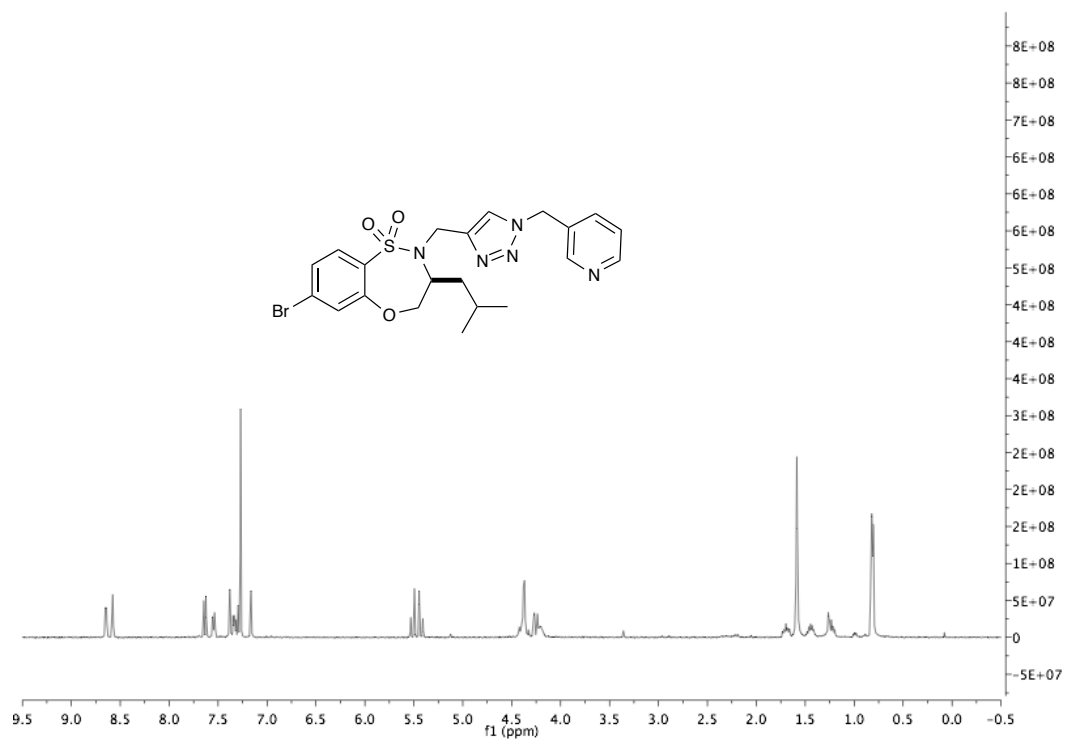
3-((4-(((2,4,6-trichlorophenyl)thio)methyl)-1H-1,2,3-triazol-1-yl)methyl)pyridine (3.3.9a)



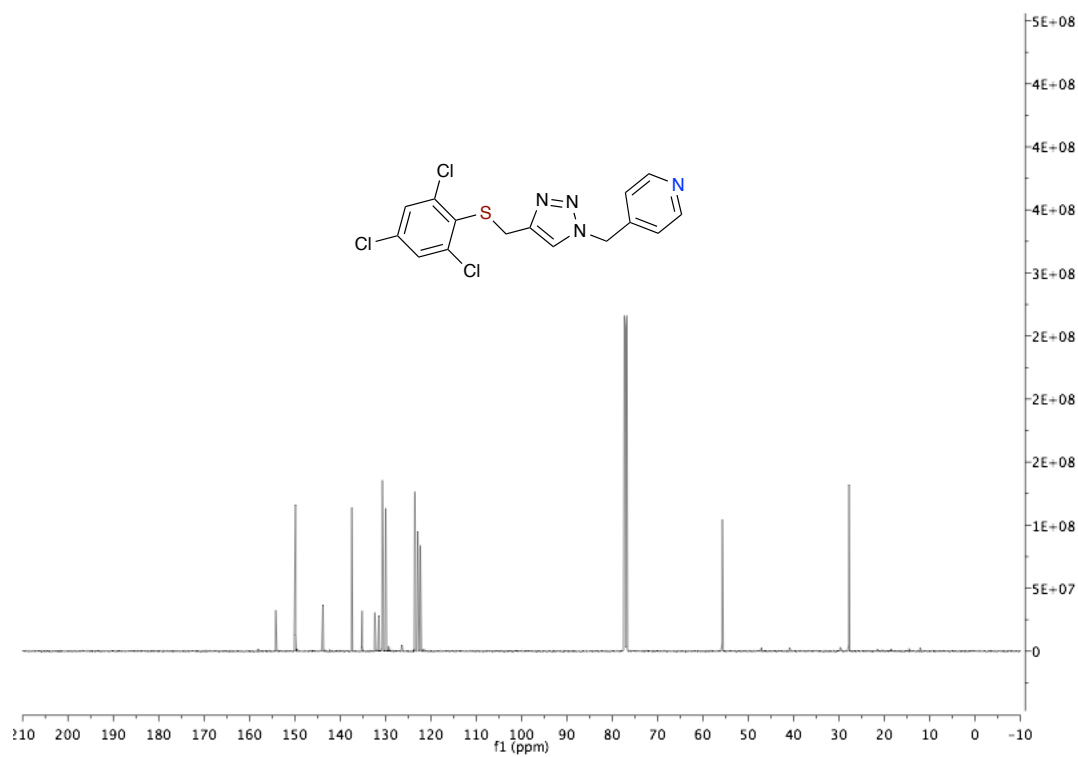
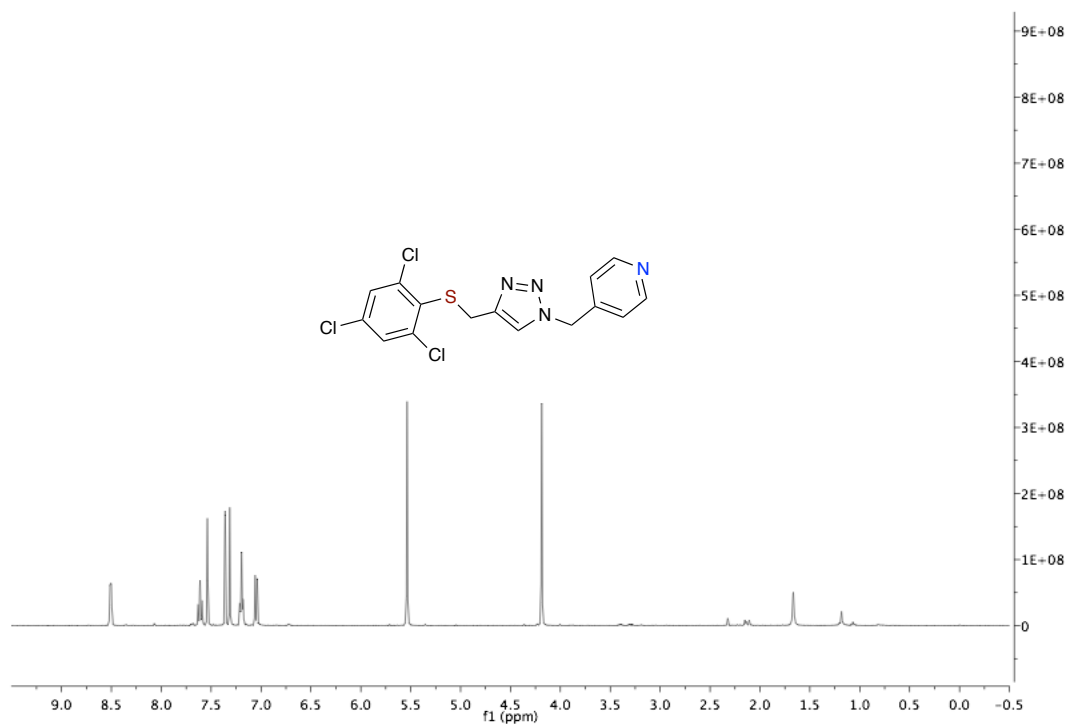
3-((4-((2,4-dichlorophenoxy)methyl)-1H-1,2,3-triazol-1-yl)methyl)pyridine (3.3.9b)



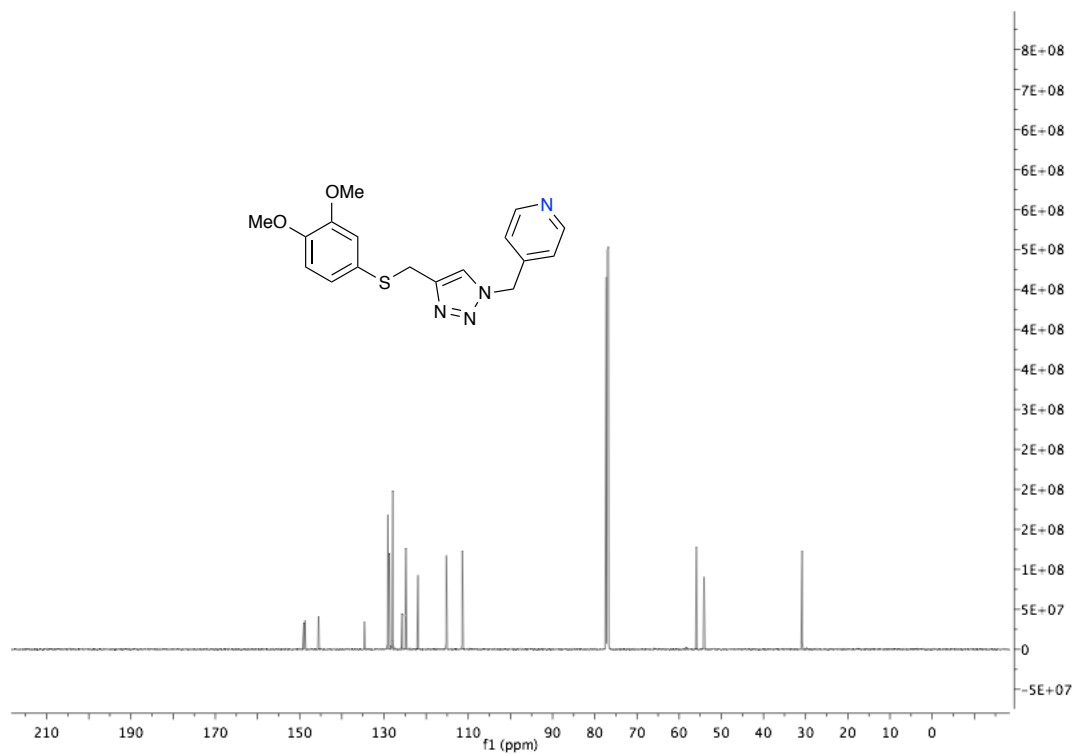
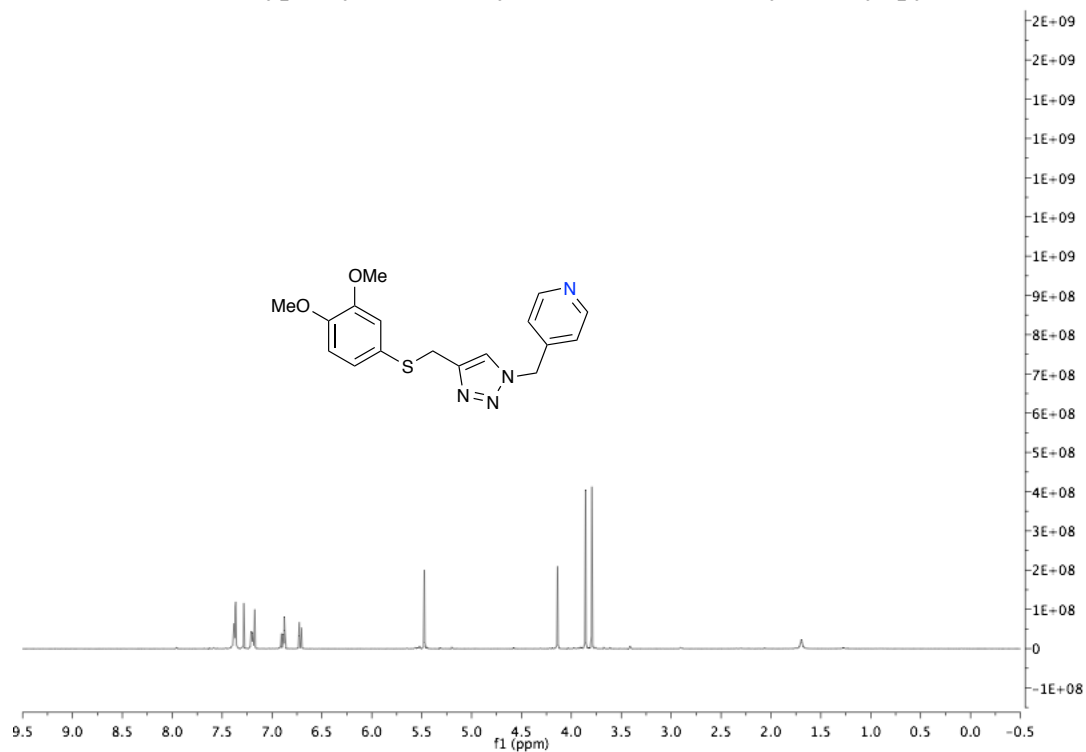
(S)-7-bromo-3-isobutyl-2-((1-(pyridin-3-ylmethyl)-1*H*-1,2,3-triazol-4-yl)methyl)-3,4-dihydro-2*H*-benzo[*b*][1,4,5]oxathiazepine 1,1-dioxide (3.3.9c)



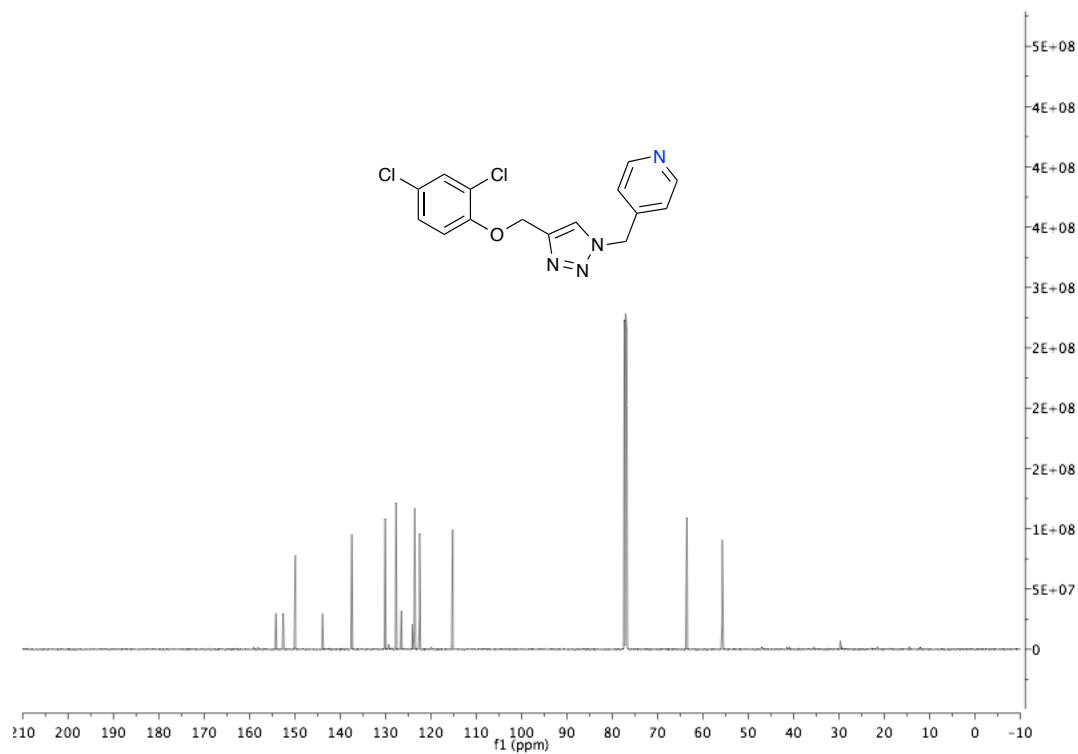
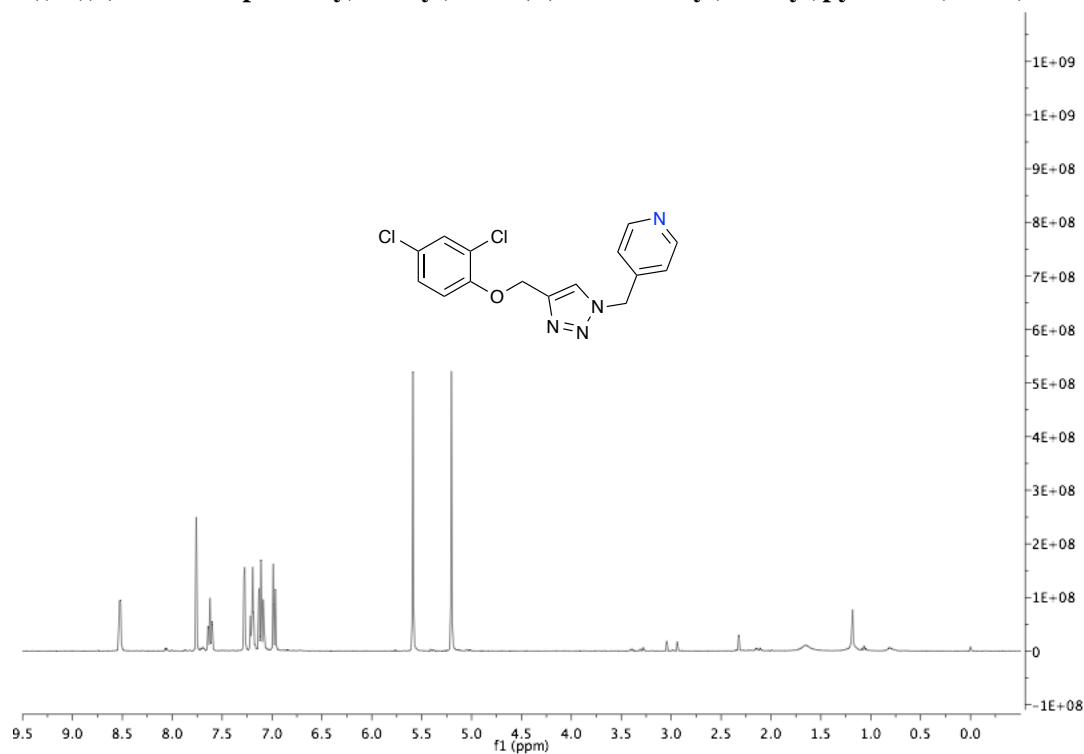
**4-(((4-((2,4,5-trichlorophenyl)thio)methyl)-1H-1,2,3-triazol-1-yl)methyl)pyridine
(3.3.9d)**



4-(((4-(3,4-dimethoxyphenyl)thio)methyl)-1*H*-1,2,3-triazol-1-yl)methyl)pyridine (3.3.9e)



4-((4-((2,4-dichlorophenoxy)methyl)-1H-1,2,3-triazol-1-yl)methyl)pyridine (3.3.9f)



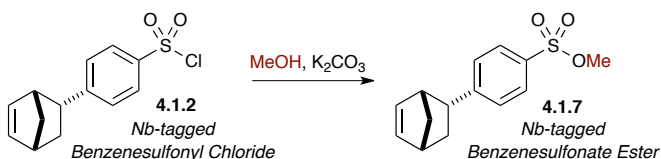
5.12 Experimental for Chapter 4.1.

Recyclable Magnetic Co/C Hybrid ROMP Benzene Sulfonate Ester (Co/C-OBSE) and Sulfonyl Chloride (Co/C-OBSC) Nanoparticles (NPs) as Facile Methylating/Alkylating Reagents: Development and Applications.

Experimental Section and Characterization data (SI-357–SI-362)

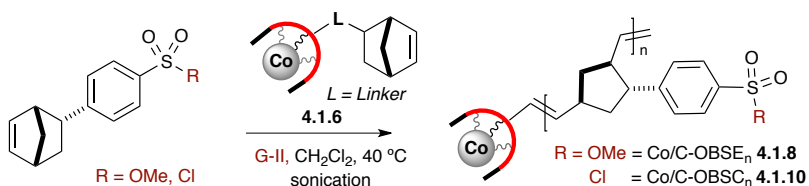
^1H , ^{13}C , Spectra for all Relevant Compounds (SI-363–SI-372)

Procedure A: General procedure for the synthesis of Nb-tagged Benzenesulfonate Ester.



To a dry Mortar Nb-tagged benzenesulfonyl chloride **4.1.2** and K_2CO_3 (2.5 equiv.) was added and mechanically grinded in wet methanol for 3-5 min. The resulting product is monitored by TLC analysis, and upon disappearance of SM, the resulting mixture was extracted with $\text{CH}_2\text{Cl}_2/\text{H}_2\text{O}$. The combined organic layer was washed with brine, dried (Na_2SO_4) and concentrated in *vacuo*, which afforded the desired norbornenyl-tagged benzene sulfonate ester **4.1.7** (90% yield) as a white solid in high purity without any flash chromatography.

Procedure B: General procedure for synthesis Co/C Hybrid ROMP Benzenesulfonate Ester (Co/C-OBSE) and Benzenesulfonyl Chloride (Co/C-OBSC).



To initiate ROMP on the surface of the nanobeads, Nb-tagged Co/C nanobeads linker **4.1.6** were dispersed in degassed toluene/CH₂Cl₂ in a sealed pressure tube under argon atmosphere using sonicator. A solution of Grubbs-II catalyst (1.0 equiv. with respect to the loading of Co/C-Nb **4.1.6**) was sonicated at 45 °C to generate an active ruthenium carbene species on the surface of the nano-beads. Then Nb-tagged sulfonate or sulfonyl chloride (50 equiv.) monomer was added in solution and heated further 6-8 hours under sonication, which afforded a ROMPgel grafted onto the nano-beads. After quenching with ethyl vinyl ether EVE, the solvent was decanted with the help of neodymium magnet, washed with CH₂Cl₂ and the lump was dried well under vacuum and crushed for further use. Based on the gain in mass of magnetic polymers **4.1.8** or **4.1.10**, greater than 95% of monomer was incorporated into the hybrid material.

Procedure C: General procedure for methylation/alkylation of various carboxylic acids.

To a Pyrex pressure tube (5.0 mL) w/teflon cap was added carboxylic acid (1.0 equiv.) in CH₃CN (0.5 M) followed by addition of K₂CO₃ (2.0 equiv.), MeOH (5.0 equiv.) and Co/C-OBSE or Co/C-OBSC (1.5 equiv.). The reaction was sealed under argon and sonicated for 4–6 hours at 50 °C. Further it was monitored by TLC, and upon disappearance of SM, the reaction mixture was decanted with the help of neodymium magnet, and filtered with celite to remove K₂CO₃ and concentrated in *vacuo*. The resulting methylated/alkylated products were isolated in 70–99% overall yields.

Procedure D: Regeneration of Co/C ROMP Benzenesulfonic Acid (Co/C-OBSA_n) to Benzenesulfonyl Chloride (Co/C-OBSC_n)

To a Pyrex pressure tube (5.0 mL) w/ Teflon cap was added Co/C-OBSA (1.0 equiv.) in toluene (0.5 M) followed by addition of SOCl₂ (5.0 equiv.), and sonicated for 30 minutes. After such time catalytic DMF (0.1 equiv.) was added and the reaction was sonicated additional for 8–10 hours at 40 °C. The reaction mixture is cooled to room temperature and washed with toluene. Then subsequently washed with water and acetone with the help of neodymium magnet, dried in *vacuo*, and re-used for next reactions.

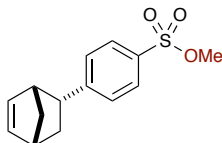
Procedure E: Acid Catalyzed reactions using Co/C Benzene Sulfonic acid NPs (Co/C-OBSA_n).

Coupling Reaction: To a 1-dram vial w/teflon cap was added indole (1.0 equiv.) followed by addition of methyl vinyl ketone (3 equiv.), Co/C-OBSA **4.1.13** (20 mol%), and solvent CH₃CN (0.5 M). The mixture was stirred at room temperature for 12–14 hrs. After such time the reaction mixture was decanted to R.B.F with the help of neodymium magnet and the solvent is evaporated in *vacuo*. Further crude product is filtered via celite SPE and rinsed with a mixture of Hexane:EtOAc (1:1). The resulting eluent was then concentrated *in vacuo* to yield the desired Michael adduct in 90% yield.

Alcoholysis: To a 1-dram vial w/teflon cap was added carbic anhydride (1.0 equiv.) followed by addition of EtOH (5 equiv.), Co/C-OBSA **4.1.13** (20 mol%), and solvent CH₃CN (0.5 M). The mixture was stirred at room temperature for 12–14 hrs. After such time the reaction mixture was decanted to R.B.F with the help of neodymium

magnet and the solvent is evaporated in *vacuo*. Further the crude product is filtered via celite SPE and rinsed with a mixture of Hexane:EtOAc (1:1). The resulting eluent was then concentrated *in vacuo* and afforded alcoholysis product in 85% yield.

Methyl 4-((1*R*,2*R*,4*R*)-bicyclo[2.2.1]hept-5-en-2-yl)benzenesulfonate 4.1.7.



Utilizing general procedure **A**, **7** (200 mg, 0.758 mmol, 98%) was isolated as a yellow solid.

MP: 51-53 °C.

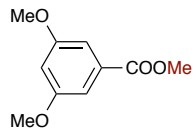
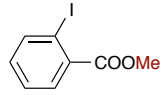
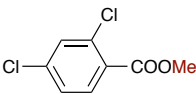
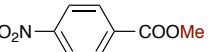
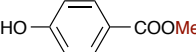
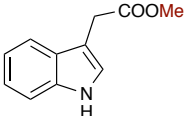
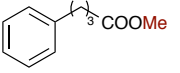
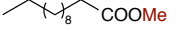
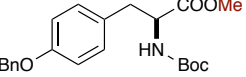
FTIR (neat, cm^{-1}): 3058, 2958, 2877, 1693, 1595, 1454, 1402, 1359, 1178, 1095, 989.

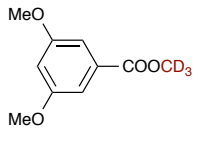
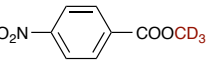
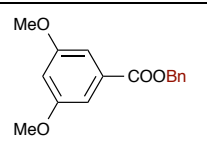
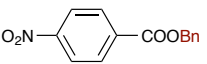
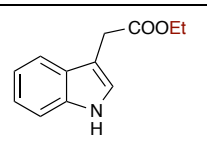
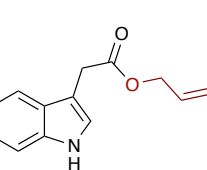
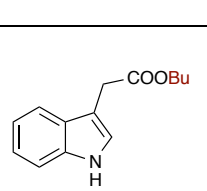
^1H NMR (400 MHz, CDCl_3) δ 7.78–7.74 (m, 2H), 7.34–7.30 (m, 2H), 6.31 (dd, $J = 5.6, 3.1$ Hz, 1H), 5.76 (dd, $J = 5.7, 2.9$ Hz, 1H), 3.75 (s, 3H), 3.52–3.43 (m, 1H), 3.12 (q, $J = 2.2, 1.8$ Hz, 1H), 3.02 (s, 1H), 2.25 (ddd, $J = 12.0, 9.3, 3.8$ Hz, 1H), 1.59–1.47 (m, 2H), 1.33 (ddd, $J = 12.0, 4.8, 2.5$ Hz, 1H).

^{13}C NMR (126 MHz, CDCl_3) δ 152.1, 137.8, 132.3, 132.2, 128.9 (2C), 127.5 (2C), 56.2, 50.4, 48.8, 43.8, 43.3, 33.1.

HRMS calculated for $\text{C}_{14}\text{H}_{17}\text{O}_3\text{S}$ ($\text{M}+\text{Na}$) $^+$ 287.0718; found 287.0734 (TOF MS ES+).

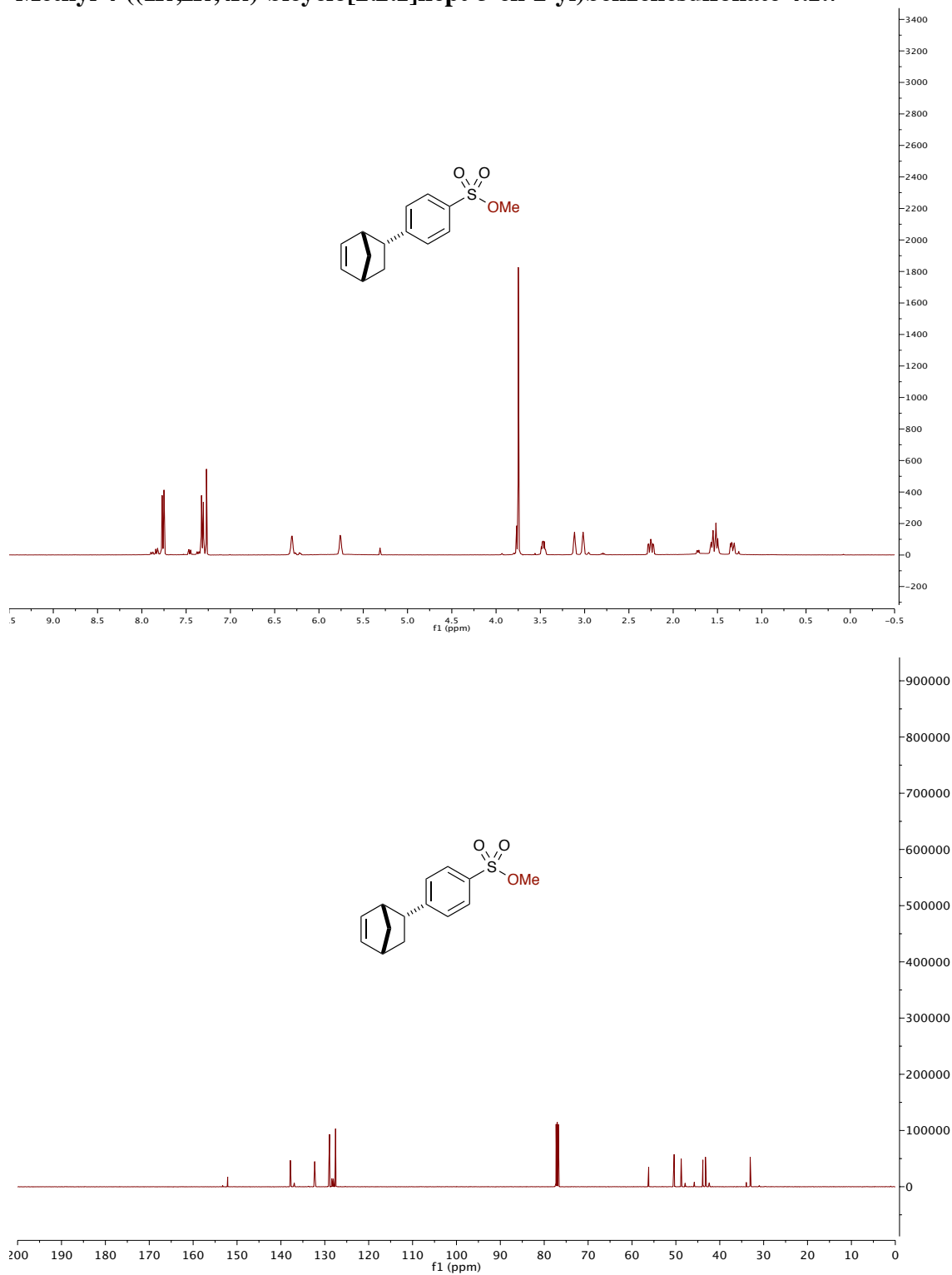
Table 5.3. Alkylation of Carboxylic Acids Utilizing Magnetic (Co/C-OBSC_n).

Compd. #	Product	¹ H-NMR
4.1.9a 4.1.11a		(400 MHz, CDCl ₃) δ 7.20 (d, <i>J</i> = 2.4 Hz, 2H), 6.66 (t, <i>J</i> = 2.4 Hz, 1H), 3.92 (s, 3H), 3.84 (s, 6H).
4.1.9b 4.1.11c		(400 MHz, CDCl ₃) δ 8.01 (dd, <i>J</i> = 8.0, 1.2 Hz, 1H), 7.81 (dd, <i>J</i> = 7.8, 1.7 Hz, 1H), 7.41 (td, <i>J</i> = 7.6, 1.2 Hz, 1H), 7.16 (td, <i>J</i> = 7.7, 1.7 Hz, 1H), 3.94 (s, 3H).
4.1.9c		(400 MHz, CDCl ₃) δ 7.82 (d, <i>J</i> = 8.4 Hz, 1H), 7.49 (d, <i>J</i> = 2.0 Hz, 1H), 7.31 (dd, <i>J</i> = 8.5, 2.0 Hz, 1H), 3.94 (s, 3H).
4.1.9d 4.1.11b		(400 MHz, CDCl ₃) δ 8.34–8.26 (m, 1H), 8.26–8.20 (m, 1H), 3.99 (d, <i>J</i> = 1.0 Hz, 2H).
4.1.11d		(400 MHz, CDCl ₃) δ 8.00–7.91 (m, 2H), 6.90–6.82 (m, 2H), 5.32 (s, 1H), 3.90 (s, 3H).
4.1.9e 4.1.11e		(400 MHz, CDCl ₃) δ 8.09 (s, 1H), 7.70–7.60 (m, 1H), 7.41–7.35 (m, 1H), 7.25–7.12 (m, 2H), 3.80 (d, <i>J</i> = 0.9 Hz, 1H), 3.71 (s, 2H).
4.1.11f		(400 MHz, CDCl ₃) δ 7.32–7.27 (m, 2H), 7.18–7.22 (m, 3H), 3.68 (s, 3H), 2.66 (t, <i>J</i> = 7.6 Hz, 2H), 2.35 (t, <i>J</i> = 7.5 Hz, 2H), 2.02–1.92 (m, 2H).
4.1.11g		(400 MHz, CDCl ₃) δ 3.68 (s, 3H), 2.31 (t, <i>J</i> = 7.6 Hz, 2H), 1.62 (m, 2H), 1.28 (m, 16H), 0.89 (t, <i>J</i> = 6.8 Hz, 3H).
4.1.11h		(400 MHz, CDCl ₃) δ 3.68 (s, 3H), 2.31 (t, <i>J</i> = 7.6 Hz, 2H), 1.62 (m, 2H), 1.28 (m, 16H), 0.89 (t, <i>J</i> = 6.8 Hz, 3H).

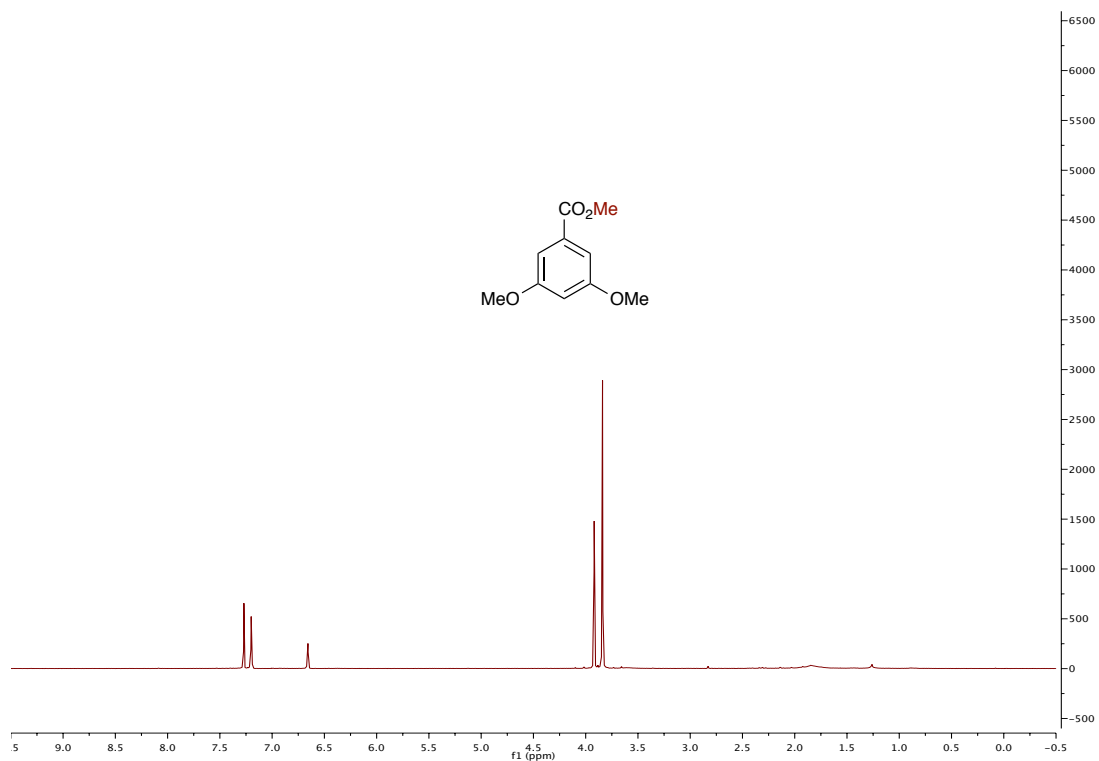
4.1.12a		400 MHz, CDCl ₃ δ 7.21–7.17 (m, 2H), 6.66 (td, <i>J</i> = 2.5, 1.0 Hz, 1H), 3.83 (dd, <i>J</i> = 5.4, 2.3 Hz, 6H).
4.1.12b		400 MHz, CDCl ₃ δ 8.33–8.28 (m, 2H), 8.25–8.20 (m, 2H).
4.1.12c		(400 MHz, CDCl ₃) δ 7.47–7.43 (m, 2H), 7.42–7.35 (m, 3H), 7.23 (d, <i>J</i> = 2.3 Hz, 2H), 6.66 (t, <i>J</i> = 2.4 Hz, 1H), 5.37 (s, 2H), 3.83 (s, 6H).
4.1.12d		(400 MHz, CDCl ₃) δ 8.27 (q, <i>J</i> = 8.9 Hz, 4H), 7.50–7.38 (m, 5H), 5.42 (s, 2H).
4.1.12e		(400 MHz, CDCl ₃) δ 8.09 (bs, 1H), 7.64 (d, <i>J</i> = 7.8 Hz, 1H), 7.38 (d, <i>J</i> = 8.0 Hz, 1H), 7.24–7.10 (m, 3H), 4.18 (q, <i>J</i> = 7.1 Hz, 2H), 3.78 (s, 2H), 1.27 (t, <i>J</i> = 7.1 Hz, 3H).
4.1.12f		(400 MHz, CDCl ₃) δ 8.09 (bs, 1H), 7.41–7.34 (m, 1H), 7.25–7.12 (m, 3H), 5.93 (ddt, <i>J</i> = 16.4, 10.9, 5.7 Hz, 1H), 5.35–5.15 (m, 2H), 4.68–4.57 (m, 2H), 3.83 (s, 2H).
4.1.12g		(400 MHz, CDCl ₃) δ 8.09 (bs, 1H), 7.64 (d, <i>J</i> = 7.8 Hz, 1H), 7.40–7.33 (m, 1H), 7.25–7.10 (m, 3H), 4.12 (dd, <i>J</i> = 7.2, 6.2 Hz, 2H), 3.79 (d, <i>J</i> = 1.1 Hz, 2H), 1.68–1.58 (m, 2H), 1.36 (h, <i>J</i> = 7.4 Hz, 2H), 0.96–0.86 (m, 3H).

5.13 Spectra for Chapter 4.1

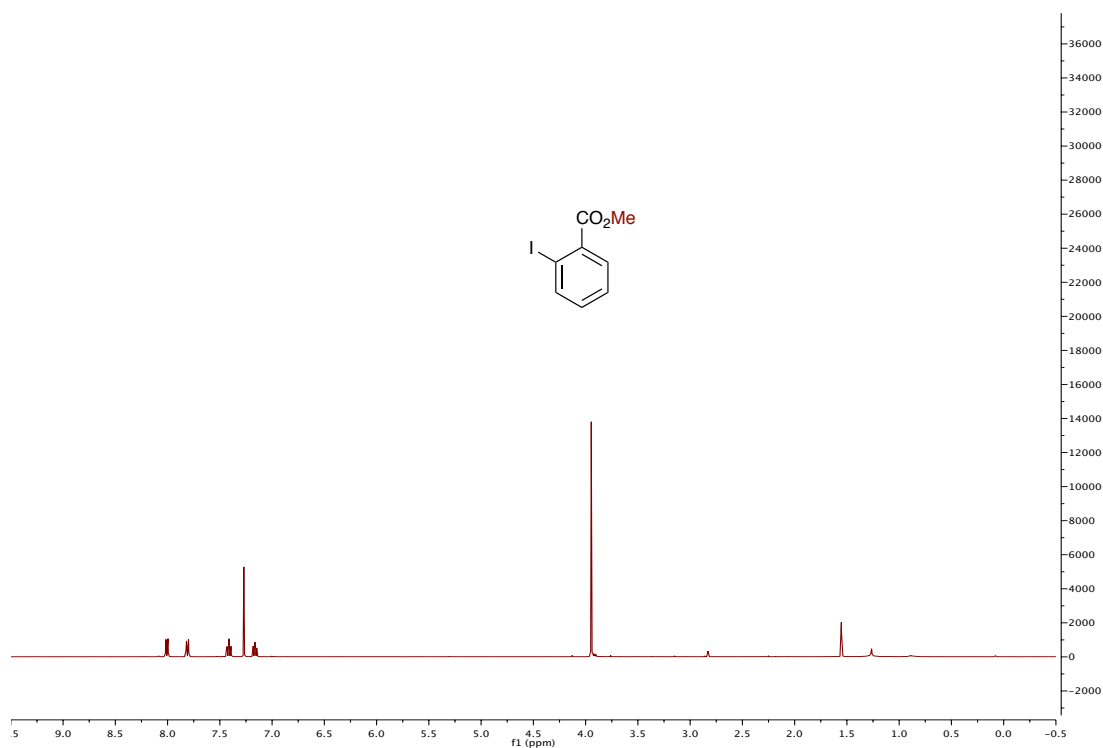
Methyl 4-((1*R*,2*R*,4*R*)-bicyclo[2.2.1]hept-5-en-2-yl)benzenesulfonate 4.1.7



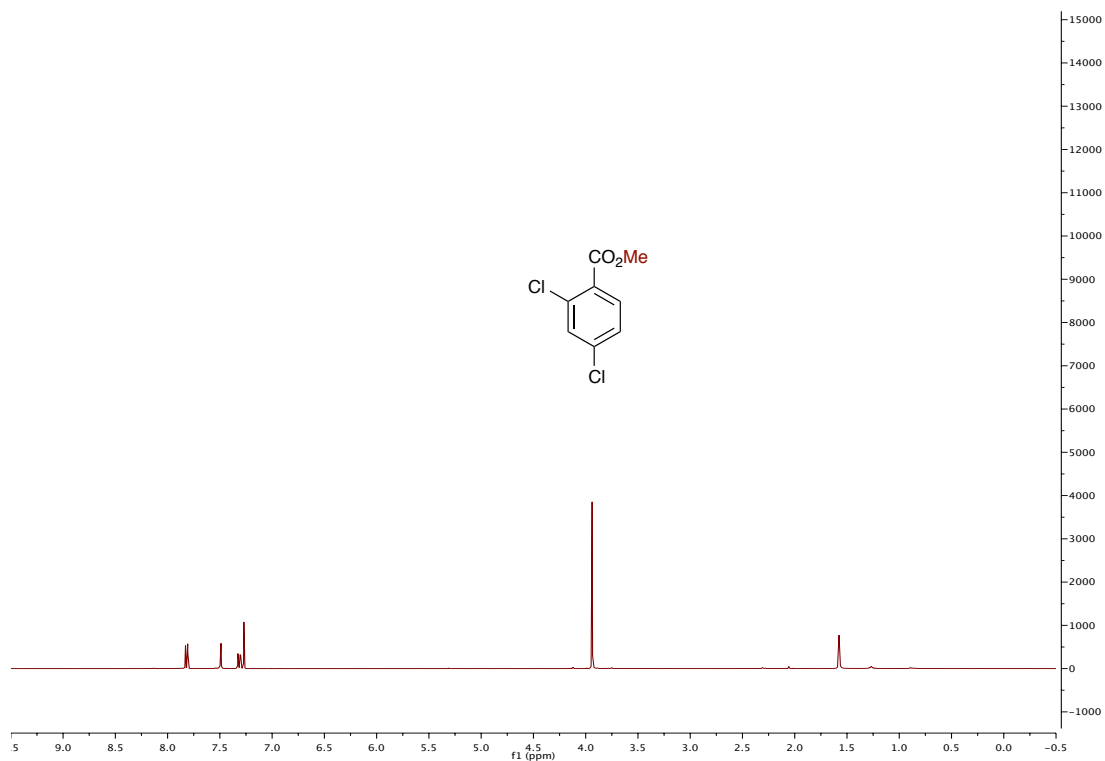
Methyl 3,5-dimethoxybenzoate 4.1.9a



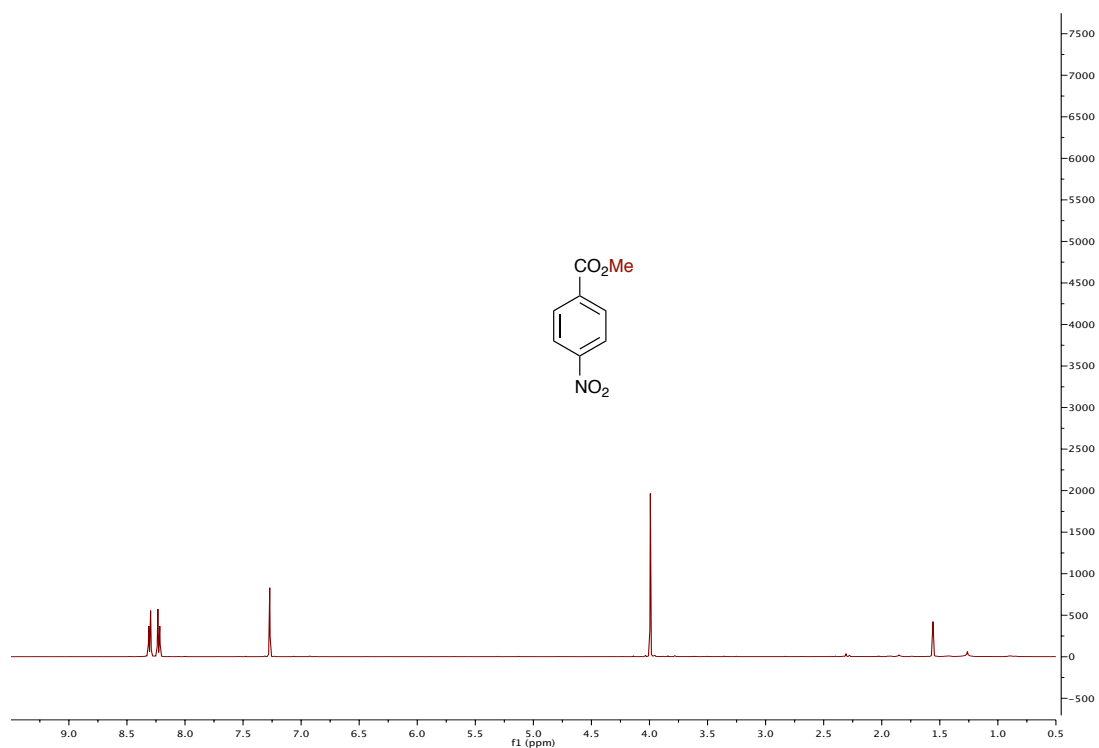
Methyl 2-iodobenzoate 4.1.9b



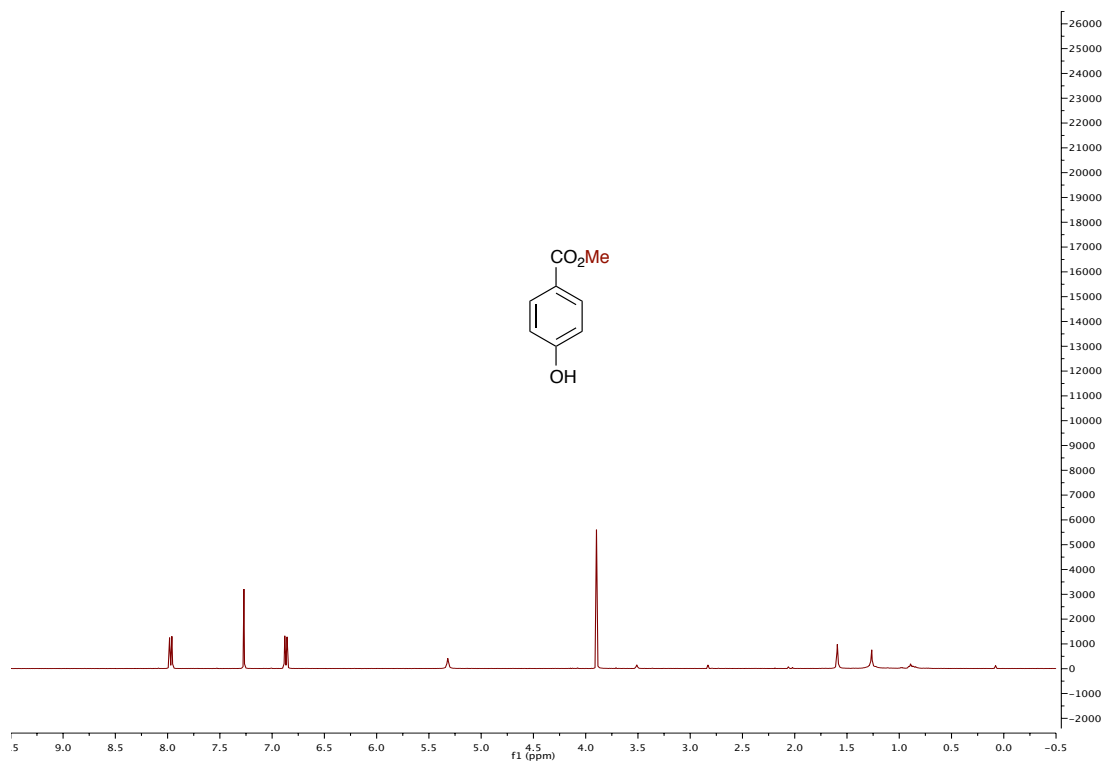
Methyl 2,4-dichlorobenzoate 4.1.9c



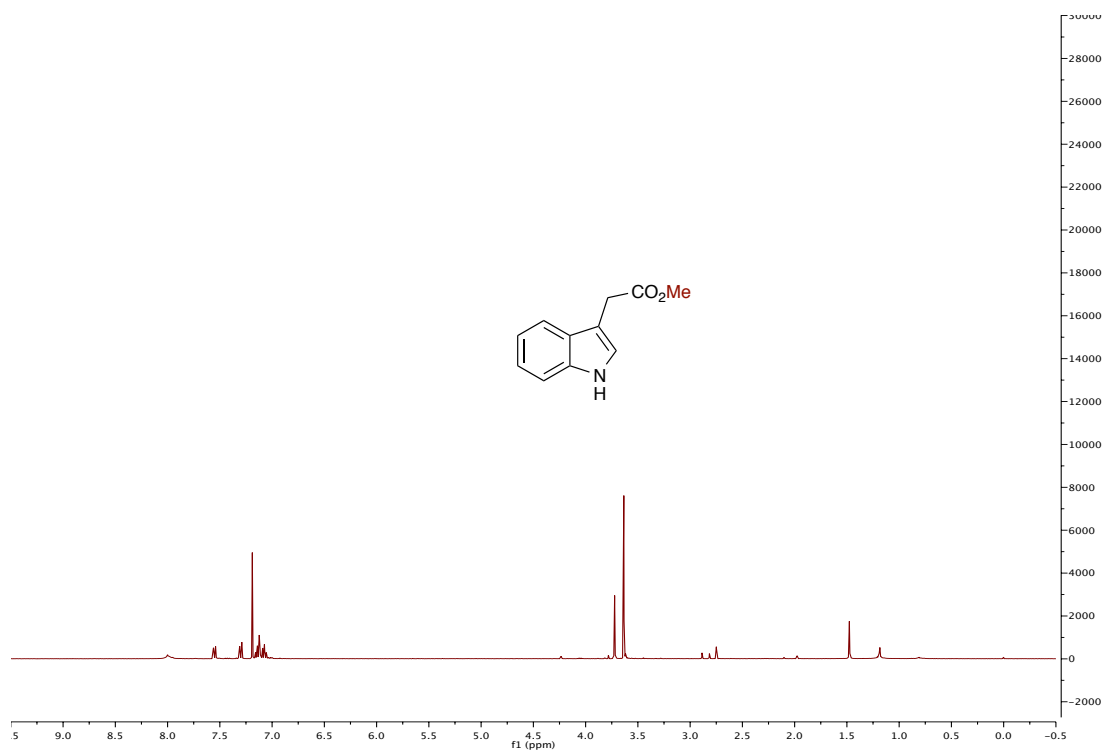
Methyl 4-nitrobenzoate 4.1.9d



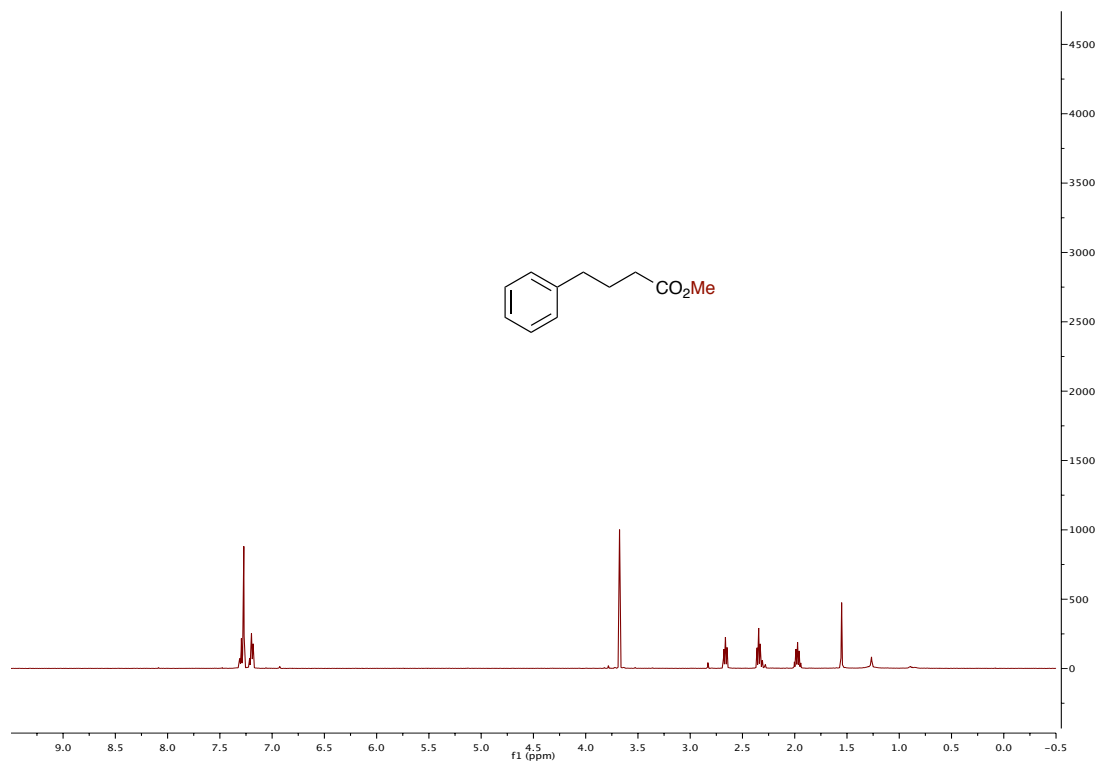
Methyl 4-hydroxybenzoate 4.1.11d



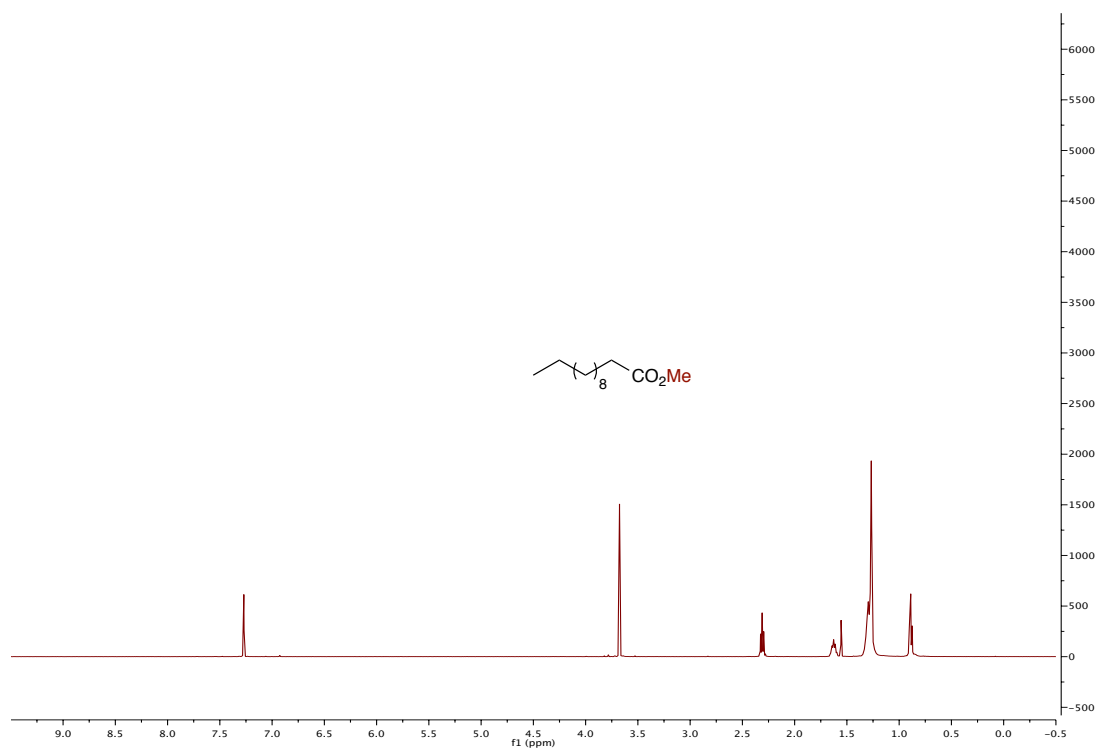
Methyl 2-(1*H*-indol-3-yl)acetate 4.1.9e



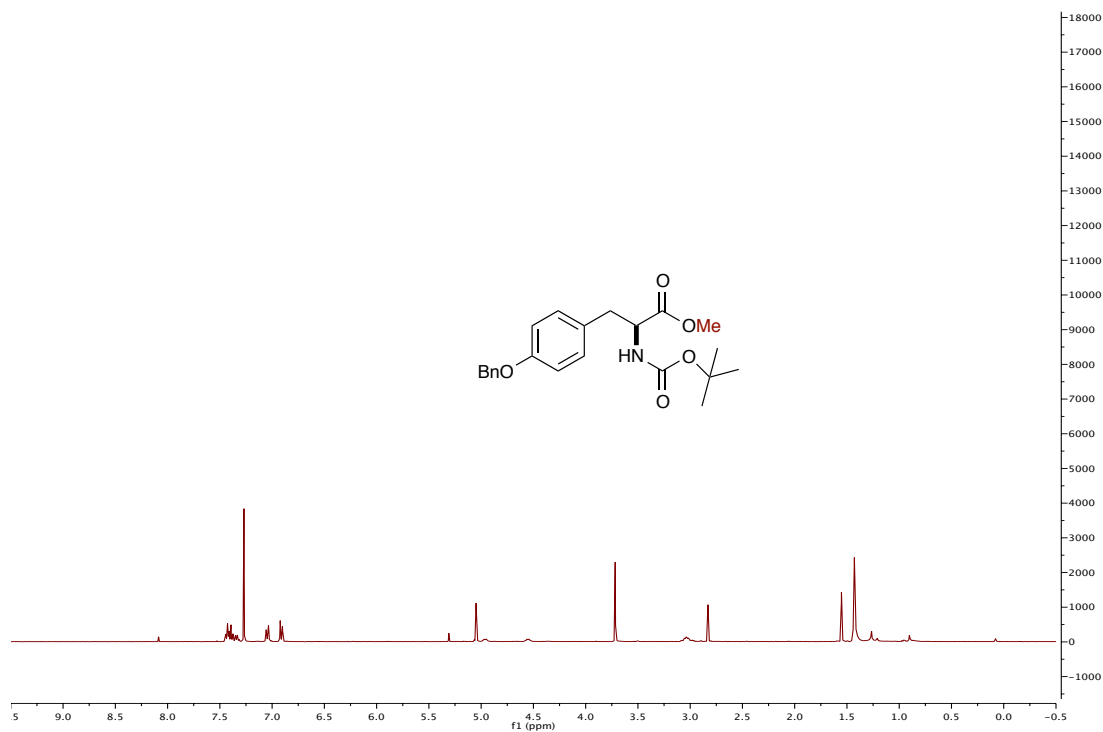
Methyl 4-phenylbutanoate 4.1.11f



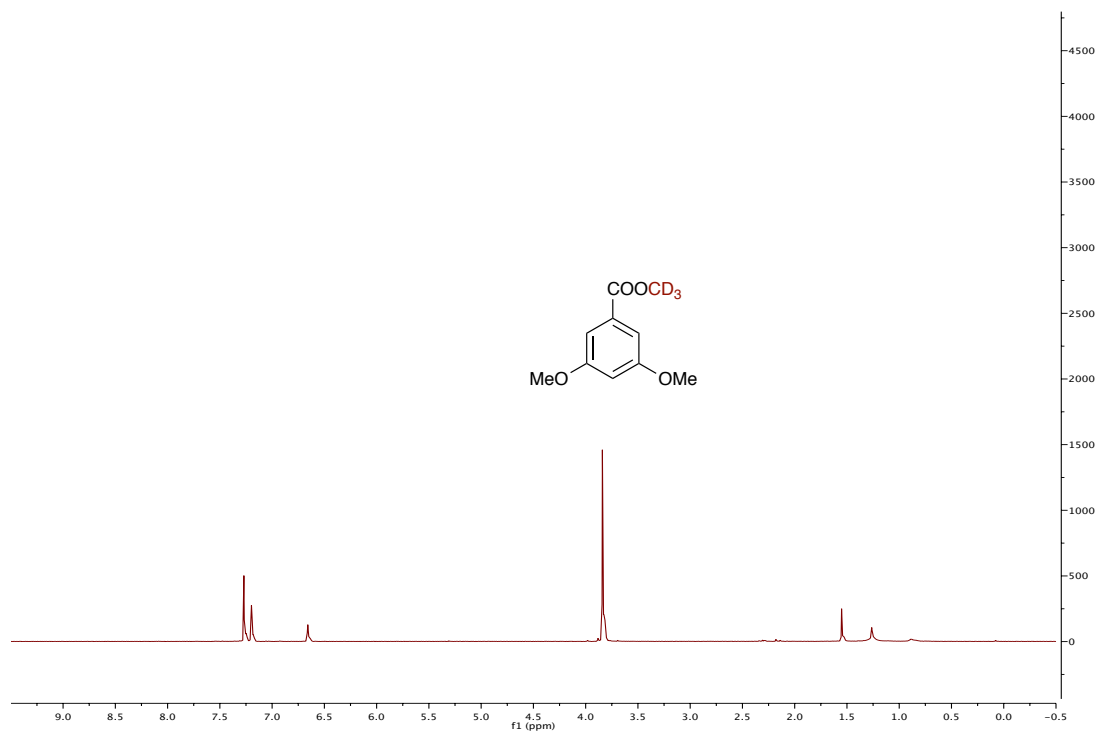
Methyl dodecanoate 4.1.11g



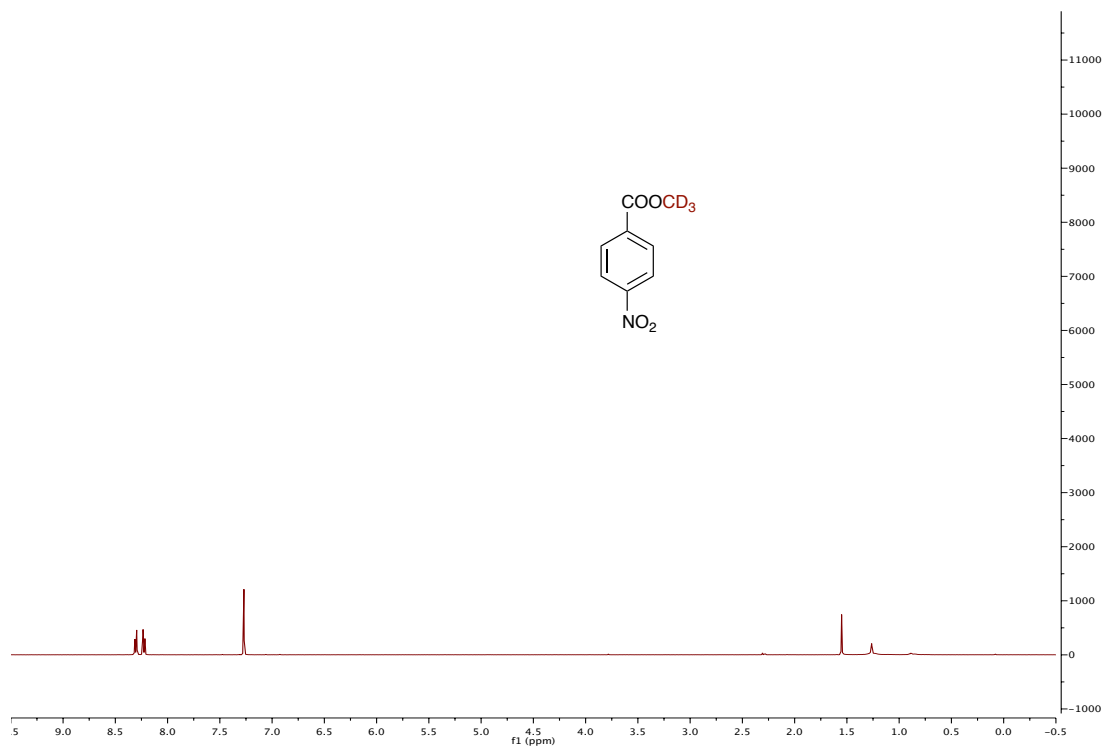
(S)-methyl 3-(4-(benzyloxy)phenyl)-2-((*tert*-butoxycarbonyl)amino)propanoate
4.1.11h



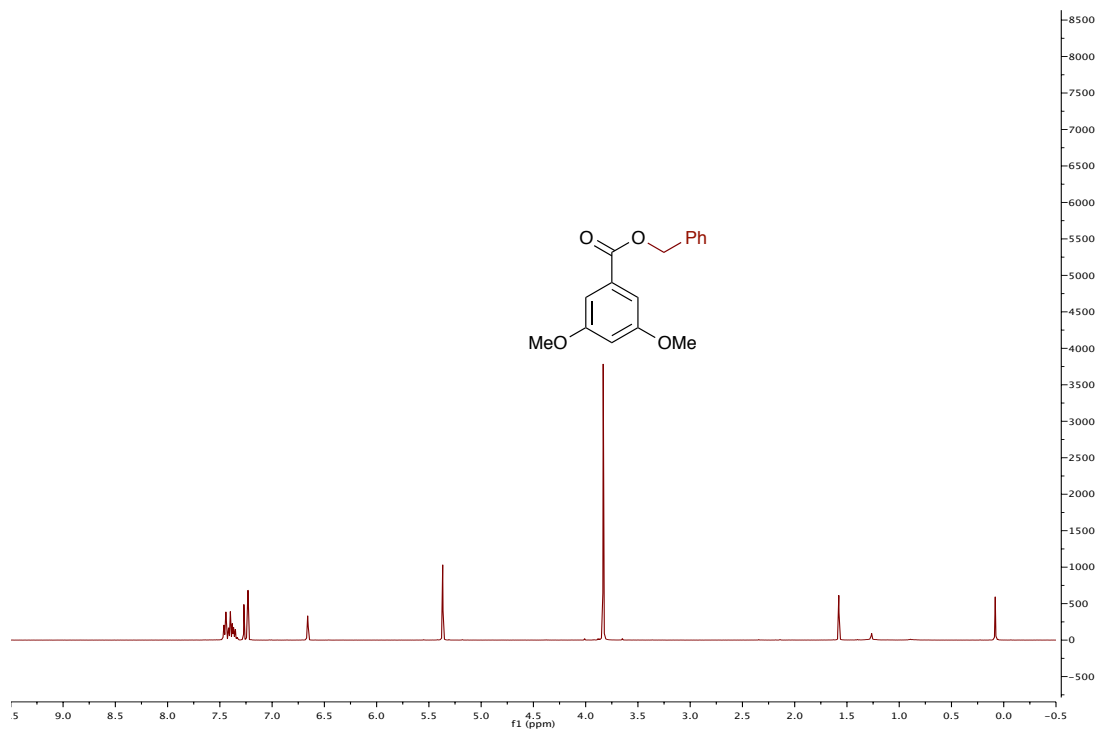
Deuterated methyl 3,5-dimethoxybenzoate 4.1.12a



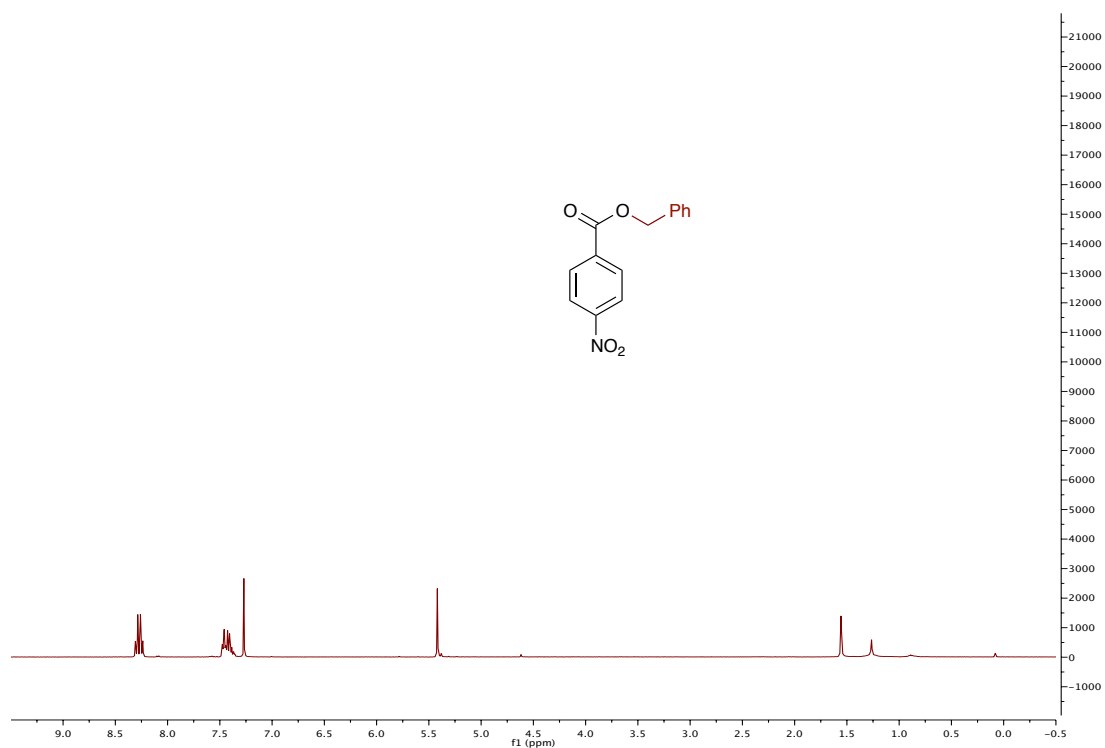
Deuterated methyl 4-nitrobenzoate 4.1.12b



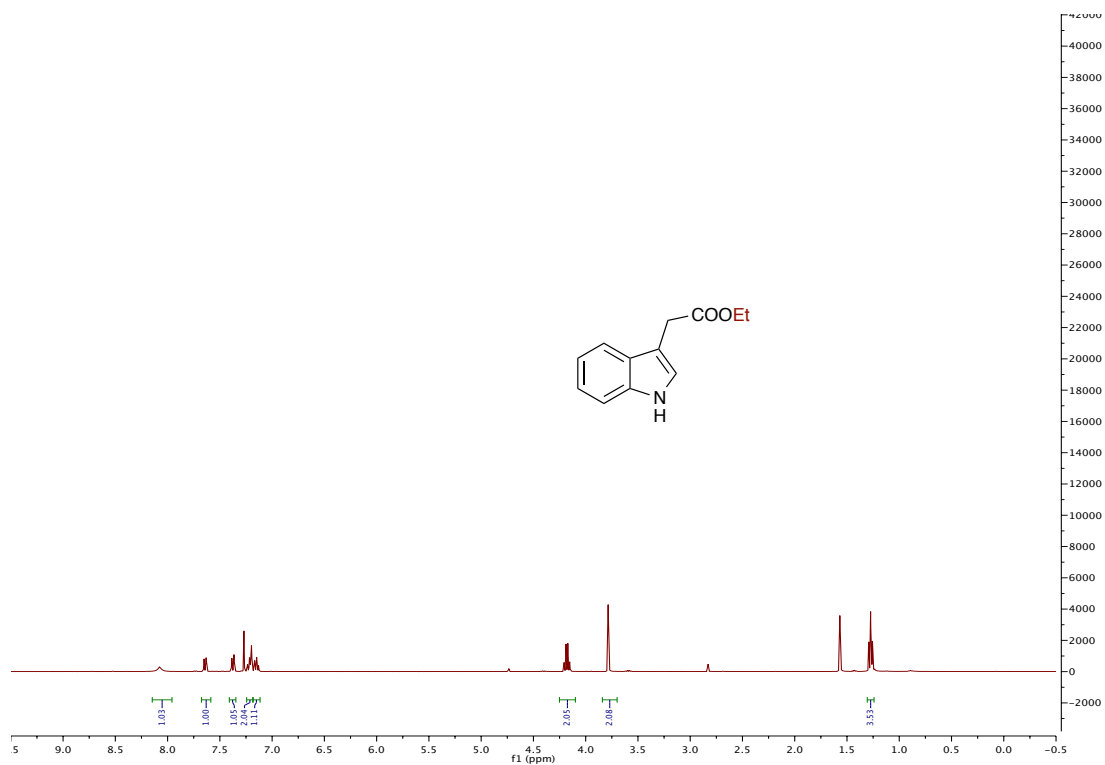
Benzyl 3,5-dimethoxybenzoate 4.1.12c



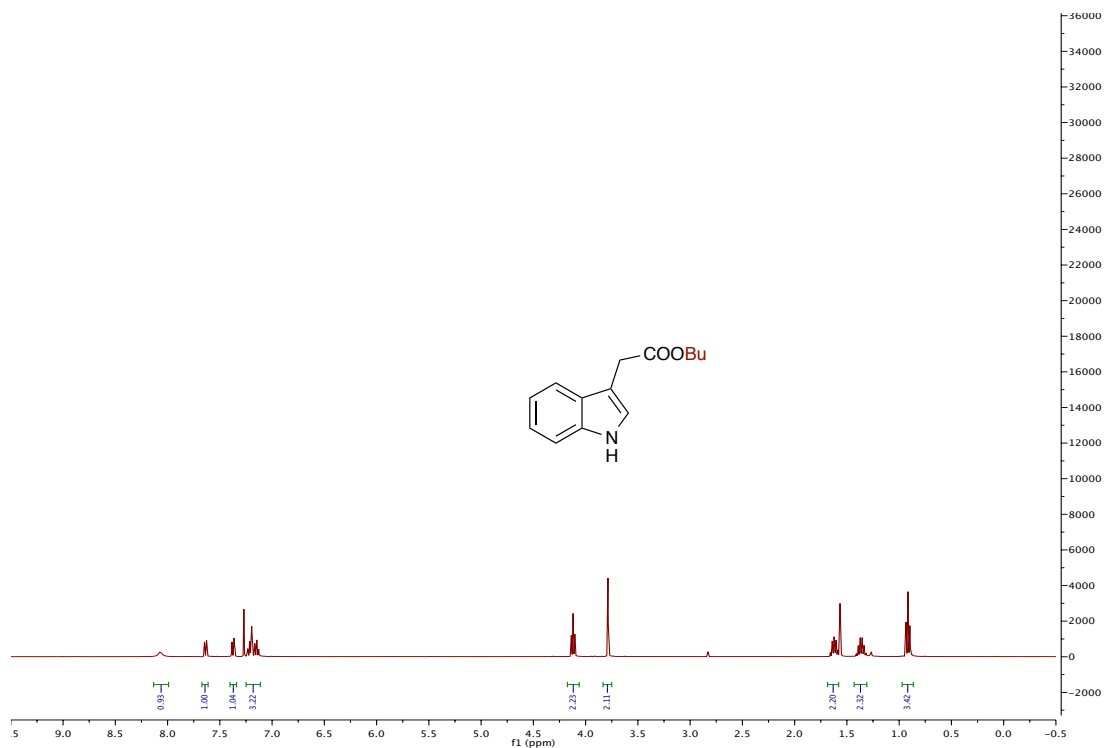
Benzyl 4-nitrobenzoate 4.1.12d



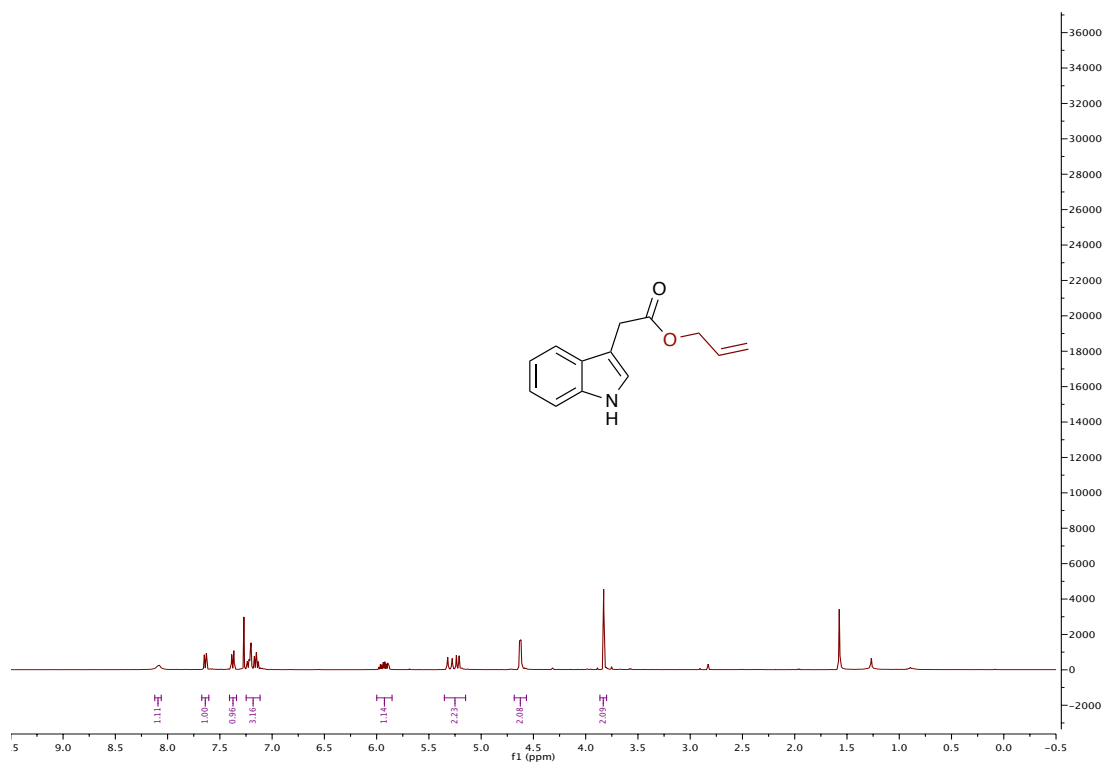
Ethyl 2-(1H-indol-3-yl)acetate 4.1.12e



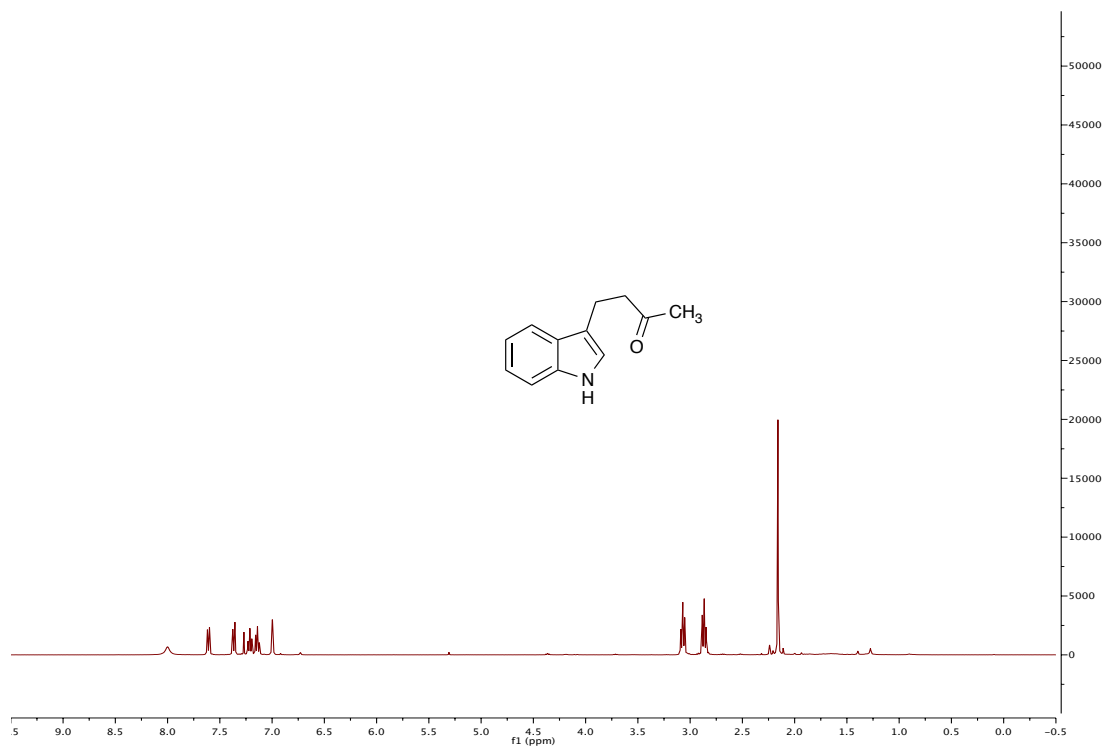
Butyl 2-(1*H*-indol-3-yl)acetate 4.1.12f



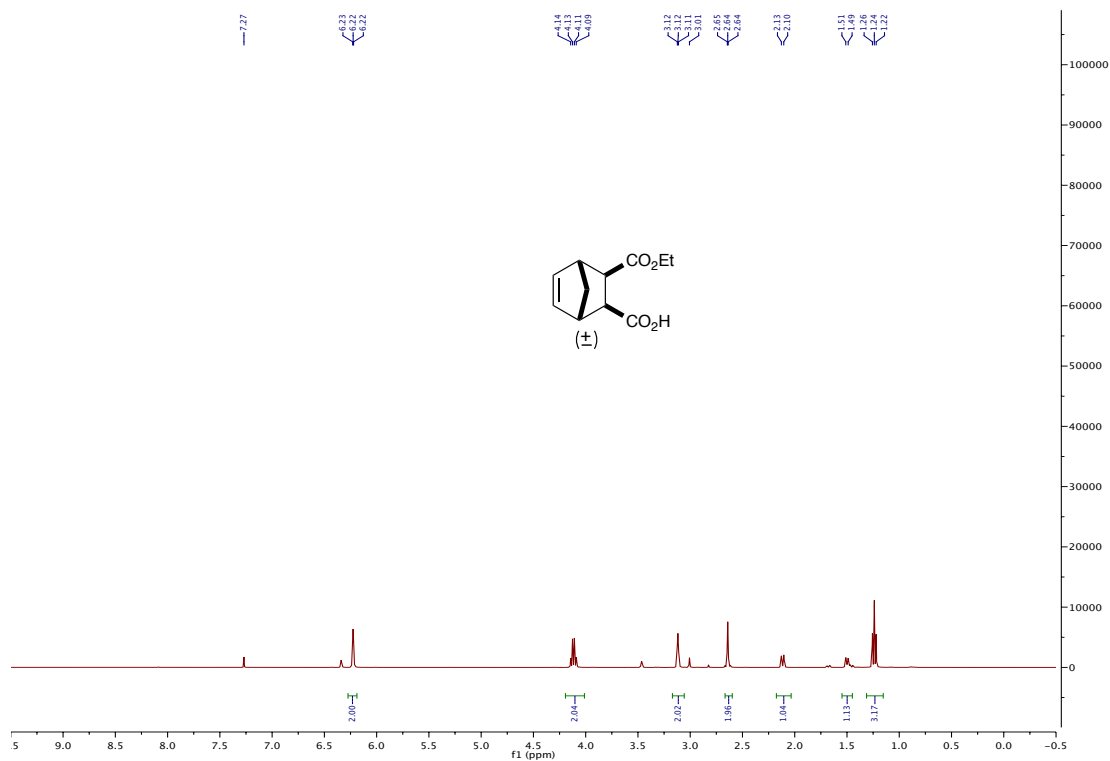
Allyl 2-(1*H*-indol-3-yl)acetate 4.1.12g



4-(1*H*-indol-3-yl)butan-2-one 4.1.14



3-(ethoxycarbonyl)bicyclo[2.2.1]hept-5-ene-2-carboxylic acid 4.15



5.14 Experimental for Chapter 4.2

Synthesis of High-load, Hybrid Co/C-Oligomeric Phosphonyl Dichloride:

Application to Scavenging Amines.

Experimental Section and Characterization data (SI-373–SI-377)

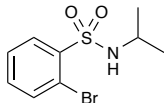
^1H , ^{13}C , Spectra for all Relevant Compounds (SI-378–SI-386)

General Procedure:

Sulfonamide Reaction: In a sealed pressure tube was added sulfonyl chloride (1 equiv.) in CH_2Cl_2 (0.1M), followed by addition of amine (1.5 equiv.) and Et_3N (2.0 equiv.). The mixture was stirred rapidly at room temperature for 6–8 h. After completion of reaction, Co/C-OPC (0.6 equiv.) was added and stirred for another 4 h to scavenge the excess amine. Then the reaction mixture was decanted using external magnet and filtered via Celite-packed SPE. The resulting eluent was concentrated *in vacuo* which afforded the desired sulfonylated products in good to excellent yields and purities.

Urea formation Reaction: In a sealed pressure tube was taken isocyanate (1 equiv.) in CH_2Cl_2 (0.1M), followed by addition of amino alcohol (1.5 equiv.) and Et_3N (2.0 equiv.). The mixture was stirred rapidly at room temperature for 8–10 h. After such time, Co/C-OPC (0.8 equiv.) was added and stirred for another 4 h to scavenge the excess amino alcohol. Then the reaction mixture was decanted using external magnet and filtered via Celite SPE. The resulting eluent was concentrated *in vacuo* to yield the urea products in good to excellent yields and purities.

2-bromo-*N*-isopropylbenzenesulfonamide (4.2.11a)



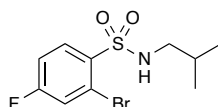
Utilizing general procedure B, 2-bromo-*N*-isopropylbenzenesulfonamide **4.2.11a** (28 mg, 0.101 mmol, 97%) was isolated as a white solid.

^1H NMR (500 MHz, CDCl_3): δ 8.21–8.14 (m, 1H), 7.77–7.69 (m, 1H), 7.50–7.46 (m, 1H), 7.42–7.38 (m, 1H), 5.03 (d, J = 7.1 Hz, 1H), 3.47–3.38 (m, 1H), 1.12 (s, 3H), 1.10 (s, 3H).

^{13}C NMR (126 MHz, CDCl_3): δ 139.8, 135.1, 133.6, 131.4, 127.9, 119.8, 46.6, 23.5.

HRMS calculated for $\text{C}_9\text{H}_{12}\text{BrNO}_2\text{SNa}$ ($\text{M}+\text{Na}$) $^+$ 299.9670; found 299.9643 (TOF MS ES+).

2-bromo-4-fluoro-*N*-isobutylbenzenesulfonamide (4.2.11b)



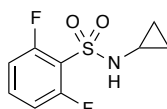
Utilizing general procedure B, 2-bromo-4-fluoro-*N*-isobutylbenzenesulfonamide **4.2.11a** (26 mg, 0.083 mmol, 93%) was isolated as a white solid.

^1H NMR (500 MHz, CDCl_3): δ 8.17 (dd, J = 8.8, 5.8 Hz, 1H), 7.50 (dd, J = 7.9, 2.5 Hz, 1H), 7.20 (ddd, J = 8.9, 7.6, 2.5 Hz, 1H), 5.14 (t, J = 6.2 Hz, 1H), 2.72 (t, J = 6.6 Hz, 2H), 1.77–1.71 (m, 1H), 0.91 (d, J = 6.7 Hz, 6H).

^{13}C NMR (126 MHz, CDCl_3): δ 164.2 (d, J = 258.8 Hz), 135.1 (d, J = 3.6 Hz), 133.6 (d, J = 9.2 Hz), 122.5 (d, J = 25.1 Hz), 120.8 (d, J = 10.0 Hz), 115.0 (d, J = 21.1 Hz), 50.7, 28.4, 19.9.

HRMS calculated for $\text{C}_{10}\text{H}_{13}\text{BrFNNaO}_2\text{S}$ ($\text{M}+\text{Na}$) $^+$ 331.9732; found 331.9675 (TOF MS ES+).

N-cyclopropyl-2,6-difluorobenzenesulfonamide (4.2.11c)



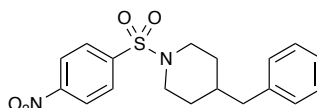
Utilizing general procedure B, *N*-cyclopropyl-2,6 difluorobenzenesulfonamide **4.2.11a** (32 mg, 0.137 mmol, 91%) was isolated as a white solid.

^1H NMR (500 MHz, CDCl_3): δ 7.60–7.51 (m, 1H), 7.10–7.01 (m, 2H), 5.42 (brs, 1H), 2.43–2.36 (m, 1H), 0.79–0.72 (m, 2H), 0.72–0.66 (m, 2H).

^{13}C NMR (126 MHz, CDCl_3): δ 160.7 (d, $J = 3.8$ Hz), 158.7 (d, $J = 4.0$ Hz), 134.6 (t, $J = 11.2$ Hz), 117.6 (t, $J = 15.8$ Hz), 113.3 (d, $J = 3.7$ Hz), 113.1 (d, $J = 3.9$ Hz), 24.4, 6.9.

HRMS calculated for $\text{C}_9\text{H}_9\text{F}_2\text{NNaO}_2\text{S}$ ($\text{M}+\text{Na}$) $^+$ 256.0220; found 256.0211 (TOF MS ES $^+$).

4-benzyl-1-((4-nitrophenyl)sulfonyl)piperidine (4.2.11d)



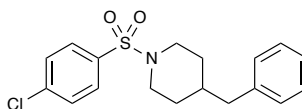
Utilizing general procedure B, 4-benzyl-1-((4-nitrophenyl)sulfonyl)piperidine **4.2.11d** (37 mg, 0.102 mmol, 95%) was isolated as a light yellow solid.

^1H NMR (400 MHz, CDCl_3) δ 8.37 (d, $J = 8.8$ Hz, 2H), 7.94 (d, $J = 8.8$ Hz, 2H), 7.30–7.24 (m, 2H), 7.22–7.18 (m, 1H), 7.09 (d, $J = 7.1$ Hz, 2H), 3.85 (d, $J = 11.7$ Hz, 2H), 2.54 (d, $J = 7.0$ Hz, 2H), 2.30 (td, $J = 11.9, 2.0$ Hz, 2H), 1.72 (d, $J = 13.2$ Hz, 2H), 1.54–1.45 (m, 1H), 1.41–1.31 (m, 2H).

^{13}C NMR (126 MHz, CDCl_3): δ 150.1, 142.6, 139.4, 129.0 (2C), 128.7 (2C), 128.4 (2C), 126.2, 124.3 (2C), 46.5 (2C), 42.5, 37.2, 31.2 (2C).

HRMS calculated for $\text{C}_{18}\text{H}_{21}\text{N}_2\text{O}_4\text{S}$ ($\text{M}+\text{H}$) $^+$ 361.1222; found 361.1243 (TOF MS ES $^+$).

4-benzyl-1-((4-chlorophenyl)sulfonyl)piperidine (4.2.11e)



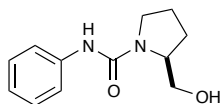
Utilizing general procedure B, 4-benzyl-1-((4-chlorophenyl)sulfonyl)piperidine **4.2.11a** (33 mg, 0.094 mmol, 94%) was isolated as a white solid.

^1H NMR (400 MHz, CDCl_3) δ 7.69 (d, $J = 8.5$ Hz, 2H), 7.51 (d, $J = 8.5$ Hz, 2H), 7.34–7.25 (m, 2H), 7.22–7.15 (m, 1H), 7.10 (d, $J = 7.1$ Hz, 2H), 3.78 (d, $J = 11.7$ Hz, 2H), 2.54 (d, $J = 6.9$ Hz, 2H), 2.29–2.05 (m, 2H), 1.71 (d, $J = 12.7$ Hz, 2H), 1.52–1.45 (m, 1H), 1.43–1.32 (m, 2H).

^{13}C NMR (126 MHz, CDCl_3): δ 139.7, 139.2, 134.7, 129.3 (2C), 129.1 (2C), 129.0 (2C), 128.3 (2C), 126.1, 46.5 (2C), 42.6, 37.3, 31.2 (2C).

HRMS calculated for $\text{C}_{18}\text{H}_{21}\text{ClNO}_2\text{S}$ ($\text{M}+\text{H}$) $^+$ 350.0982; found 350.0993 (TOF MS ES+).

(S)-2-(hydroxymethyl)-N-phenylpyrrolidine-1-carboxamide (4.2.11f)



Utilizing general procedure B, (S)-2-(hydroxymethyl)-N-phenylpyrrolidine-1-carboxamide **4.2.11f** (28 mg, 0.127 mmol, 91%) was isolated as a thick liquid.

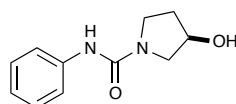
FTIR (neat): cm^{-1} ;

^1H NMR (400 MHz, CDCl_3): δ 7.37–7.33 (m, 2H), 7.29–2.25 (m, 2H), 7.03 (t, $J = 7.3$ Hz, 1H), 4.53 (brs, 1H), 4.13 (t, $J = 8.4$ Hz, 1H), 3.74–3.68 (m, 1H), 3.66–3.58 (m, 2H), 3.49–3.39 (m, 1H), 2.11–2.02 (m, 1H), 1.99–1.88 (m, 2H), 1.67–1.58 (m, 2H).

^{13}C NMR (126 MHz, $\text{DMSO}-d_6$): δ 155.2, 140.9, 128.8 (2C), 121.9, 119.6 (2C), 64.1, 59.3, 47.0, 28.2, 23.8.

HRMS calculated for $\text{C}_{12}\text{H}_{16}\text{N}_2\text{NaO}_2$ ($\text{M}+\text{Na}$) $^+$ 243.1109; found 243.1089 (TOF MS ES+).

(R)-3-hydroxy-N-phenylpyrrolidine-1-carboxamide (4.2.11g)



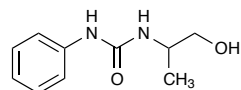
Utilizing general procedure B, (R)-3-hydroxy-N-phenylpyrrolidine-1-carboxamide **4.2.11g** (25 mg, 0.121 mmol, 93%) was isolated as a brown thick liquid.

^1H NMR (400 MHz, CDCl_3): δ 7.38–7.32 (m, 2H), 7.20–7.13 (m, 2H), 6.93–6.86 (m, 1H), 6.66 (brs, 1H), 4.38 (brs, 1H), 4.16 (brs, 1H), 3.59–3.35 (m, 4H), 1.99–1.86 (m, 2H).

^{13}C NMR (126 MHz, $\text{DMSO}-d_6$): δ 159.1, 144.3, 133.4 (2C), 127.2, 124.4 (2C), 74.8, 58.9, 48.6, 38.7.

HRMS calculated for $C_{11}H_{14}N_2NaO_2$ ($M+Na$)⁺ 229.0953; found 229.0965 (TOF MS ES+).

1-(1-hydroxypropan-2-yl)-3-phenylurea (4.2.11h)



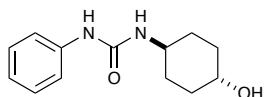
Utilizing general procedure B, 1-(1-hydroxypropan-2-yl)-3-phenylurea **11a** (21 mg, 0.108 mmol, 89%) was isolated as a colorless thick liquid.

¹H NMR (400 MHz, DMSO-*d*₆): δ 8.00 (s, 1H), 7.51 (d, *J* = 7.9 Hz, 2H), 7.25 (t, *J* = 7.8 Hz, 2H), 6.94 (t, *J* = 7.3 Hz, 1H), 5.79 (brs, 1H), 4.11 (brs, 1H), 3.96–3.86 (m, 1H), 3.56 (d, *J* = 4.6 Hz, 2H), 1.19 (d, *J* = 6.7 Hz, 3H).

¹³C NMR (126 MHz, DMSO-*d*₆): δ 155.3, 140.9, 129.1 (2C), 121.5, 117.9 (2C), 65.1, 47.1, 18.3.

HRMS calculated for $C_{10}H_{14}N_2NaO_2$ ($M+Na$)⁺ 217.0953; found 217.0964 (TOF MS ES+).

1-((1*R*,4*R*)-4-hydroxycyclohexyl)-3-phenylurea (4.2.11i)



Utilizing general procedure B, 1-((1*R*,4*R*)-4-hydroxycyclohexyl)-3-phenylurea **4.2.11i** (35mg, 0.149 mmol, 92%) was isolated as a brown thick solid.

¹H NMR (400 MHz, DMSO-*d*₆): δ 8.00 (s, 1H), 7.51 (d, *J* = 7.9 Hz, 2H), 7.25 (t, *J* = 7.8 Hz, 2H), 6.94 (t, *J* = 7.3 Hz, 1H), 5.79 (brs, 1H), 4.11 (brs, 1H), 3.96 – 3.86 (m, 1H), 3.56 (d, *J* = 4.6 Hz, 2H), 1.19 (d, *J* = 6.7 Hz, 3H).

¹³C NMR (126 MHz, DMSO-*d*₆): δ 155.1, 140.8, 129.1 (2C), 121.5, 118.0 (2C), 68.5, 48.0, 34.2, 31.2.

HRMS calculated for $C_{13}H_{18}N_2NaO_2$ ($M+Na$)⁺ 257.1266; found 257.1294 (TOF MS ES+).

2-bromo-*N*-isopropylbenzenesulfonamide (4.2.11a)



The figure displays two NMR spectra for the compound N-(2-bromo-4-fluorophenyl)isopropylsulfonamide.

Top Spectrum: The ¹H NMR spectrum shows peaks from 0 to 9 ppm. Aromatic protons appear as a multiplet between 7.0 and 8.2 ppm. The sulfonamide NH proton is at approximately 5.1 ppm. Aliphatic protons include a doublet for the isopropyl methyl groups around 1.2 ppm and a septet for the methine proton around 2.6 ppm. Integration values are provided below the baseline.

Bottom Spectrum: The ¹³C NMR spectrum shows peaks from 20 to 170 ppm. Key signals include carbonyl carbons at ~165 ppm, aromatic carbons between 110 and 140 ppm, the isopropyl methine carbon at ~70 ppm, and methyl carbons at ~25 ppm. Solvent peaks for DMSO-d₆ are visible at 40 and 50 ppm.

¹H NMR (400 MHz, CDCl₃)

Chemical structure: O=[N+]([O-])c1ccc(cc1)S(=O)(=O)N2CCCC2Cc3ccccc3

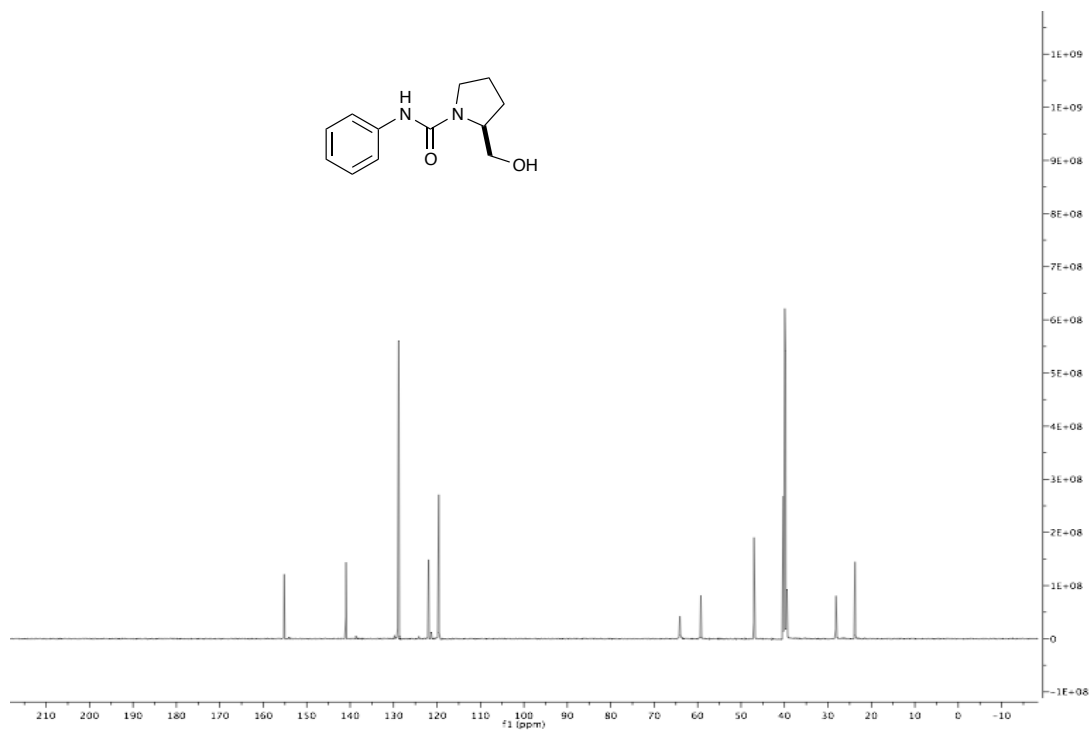
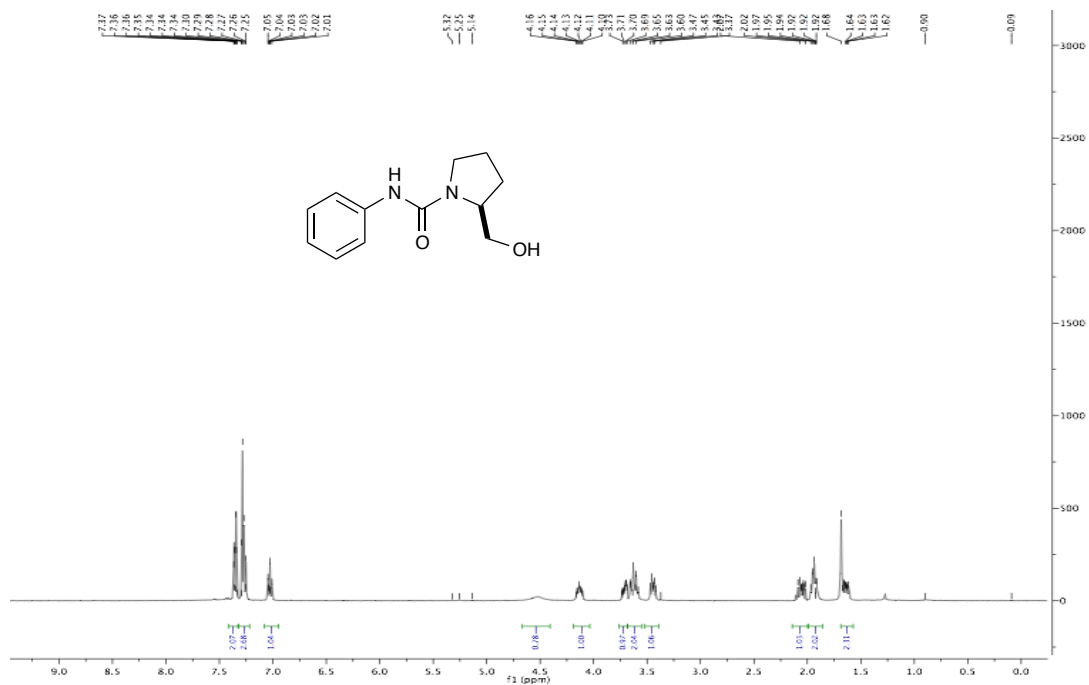
Peak list (ppm): 8.39, 8.36, 7.95, 7.93, 7.29, 7.28, 7.27, 7.26, 7.25, 7.24, 7.23, 7.22, 7.21, 7.20, 7.19, 7.18, 7.17, 7.16, 7.15, 7.14, 7.13, 7.12, 7.11, 7.10, 7.09, 7.08, 7.07, 7.06, 7.05, 7.04, 7.03, 7.02, 7.01, 7.00, 6.99, 6.98, 6.97, 6.96, 6.95, 6.94, 6.93, 6.92, 6.91, 6.90, 6.89, 6.88, 6.87, 6.86, 6.85, 6.84, 6.83, 6.82, 6.81, 6.80, 6.79, 6.78, 6.77, 6.76, 6.75, 6.74, 6.73, 6.72, 6.71, 6.70, 6.69, 6.68, 6.67, 6.66, 6.65, 6.64, 6.63, 6.62, 6.61, 6.60, 6.59, 6.58, 6.57, 6.56, 6.55, 6.54, 6.53, 6.52, 6.51, 6.50, 6.49, 6.48, 6.47, 6.46, 6.45, 6.44, 6.43, 6.42, 6.41, 6.40, 6.39, 6.38, 6.37, 6.36, 6.35, 6.34, 6.33, 6.32, 6.31, 6.30, 6.29, 6.28, 6.27, 6.26, 6.25, 6.24, 6.23, 6.22, 6.21, 6.20, 6.19, 6.18, 6.17, 6.16, 6.15, 6.14, 6.13, 6.12, 6.11, 6.10, 6.09, 6.08, 6.07, 6.06, 6.05, 6.04, 6.03, 6.02, 6.01, 6.00, 5.99, 5.98, 5.97, 5.96, 5.95, 5.94, 5.93, 5.92, 5.91, 5.90, 5.89, 5.88, 5.87, 5.86, 5.85, 5.84, 5.83, 5.82, 5.81, 5.80, 5.79, 5.78, 5.77, 5.76, 5.75, 5.74, 5.73, 5.72, 5.71, 5.70, 5.69, 5.68, 5.67, 5.66, 5.65, 5.64, 5.63, 5.62, 5.61, 5.60, 5.59, 5.58, 5.57, 5.56, 5.55, 5.54, 5.53, 5.52, 5.51, 5.50, 5.49, 5.48, 5.47, 5.46, 5.45, 5.44, 5.43, 5.42, 5.41, 5.40, 5.39, 5.38, 5.37, 5.36, 5.35, 5.34, 5.33, 5.32, 5.31, 5.30, 5.29, 5.28, 5.27, 5.26, 5.25, 5.24, 5.23, 5.22, 5.21, 5.20, 5.19, 5.18, 5.17, 5.16, 5.15, 5.14, 5.13, 5.12, 5.11, 5.10, 5.09, 5.08, 5.07, 5.06, 5.05, 5.04, 5.03, 5.02, 5.01, 5.00, 4.99, 4.98, 4.97, 4.96, 4.95, 4.94, 4.93, 4.92, 4.91, 4.90, 4.89, 4.88, 4.87, 4.86, 4.85, 4.84, 4.83, 4.82, 4.81, 4.80, 4.79, 4.78, 4.77, 4.76, 4.75, 4.74, 4.73, 4.72, 4.71, 4.70, 4.69, 4.68, 4.67, 4.66, 4.65, 4.64, 4.63, 4.62, 4.61, 4.60, 4.59, 4.58, 4.57, 4.56, 4.55, 4.54, 4.53, 4.52, 4.51, 4.50, 4.49, 4.48, 4.47, 4.46, 4.45, 4.44, 4.43, 4.42, 4.41, 4.40, 4.39, 4.38, 4.37, 4.36, 4.35, 4.34, 4.33, 4.32, 4.31, 4.30, 4.29, 4.28, 4.27, 4.26, 4.25, 4.24, 4.23, 4.22, 4.21, 4.20, 4.19, 4.18, 4.17, 4.16, 4.15, 4.14, 4.13, 4.12, 4.11, 4.10, 4.09, 4.08, 4.07, 4.06, 4.05, 4.04, 4.03, 4.02, 4.01, 4.00, 3.99, 3.98, 3.97, 3.96, 3.95, 3.94, 3.93, 3.92, 3.91, 3.90, 3.89, 3.88, 3.87, 3.86, 3.85, 3.84, 3.83, 3.82, 3.81, 3.80, 3.79, 3.78, 3.77, 3.76, 3.75, 3.74, 3.73, 3.72, 3.71, 3.70, 3.69, 3.68, 3.67, 3.66, 3.65, 3.64, 3.63, 3.62, 3.61, 3.60, 3.59, 3.58, 3.57, 3.56, 3.55, 3.54, 3.53, 3.52, 3.51, 3.50, 3.49, 3.48, 3.47, 3.46, 3.45, 3.44, 3.43, 3.42, 3.41, 3.40, 3.39, 3.38, 3.37, 3.36, 3.35, 3.34, 3.33, 3.32, 3.31, 3.30, 3.29, 3.28, 3.27, 3.26, 3.25, 3.24, 3.23, 3.22, 3.21, 3.20, 3.19, 3.18, 3.17, 3.16, 3.15, 3.14, 3.13, 3.12, 3.11, 3.10, 3.09, 3.08, 3.07, 3.06, 3.05, 3.04, 3.03, 3.02, 3.01, 3.00, 2.99, 2.98, 2.97, 2.96, 2.95, 2.94, 2.93, 2.92, 2.91, 2.90, 2.89, 2.88, 2.87, 2.86, 2.85, 2.84, 2.83, 2.82, 2.81, 2.80, 2.79, 2.78, 2.77, 2.76, 2.75, 2.74, 2.73, 2.72, 2.71, 2.70, 2.69, 2.68, 2.67, 2.66, 2.65, 2.64, 2.63, 2.62, 2.61, 2.60, 2.59, 2.58, 2.57, 2.56, 2.55, 2.54, 2.53, 2.52, 2.51, 2.50, 2.49, 2.48, 2.47, 2.46, 2.45, 2.44, 2.43, 2.42, 2.41, 2.40, 2.39, 2.38, 2.37, 2.36, 2.35, 2.34, 2.33, 2.32, 2.31, 2.30, 2.29, 2.28, 2.27, 2.26, 2.25, 2.24, 2.23, 2.22, 2.21, 2.20, 2.19, 2.18, 2.17, 2.16, 2.15, 2.14, 2.13, 2.12, 2.11, 2.10, 2.09, 2.08, 2.07, 2.06, 2.05, 2.04, 2.03, 2.02, 2.01, 2.00, 1.99, 1.98, 1.97, 1.96, 1.95, 1.94, 1.93, 1.92, 1.91, 1.90, 1.89, 1.88, 1.87, 1.86, 1.85, 1.84, 1.83, 1.82, 1.81, 1.80, 1.79, 1.78, 1.77, 1.76, 1.75, 1.74, 1.73, 1.72, 1.71, 1.70, 1.69, 1.68, 1.67, 1.66, 1.65, 1.64, 1.63, 1.62, 1.61, 1.60, 1.59, 1.58, 1.57, 1.56, 1.55, 1.54, 1.53, 1.52, 1.51, 1.50, 1.49, 1.48, 1.47, 1.46, 1.45, 1.44, 1.43, 1.42, 1.41, 1.40, 1.39, 1.38, 1.37, 1.36, 1.35, 1.34, 1.33, 1.32, 1.31, 1.30, 1.29, 1.28, 1.27, 1.26, 1.25, 1.24, 1.23, 1.22, 1.21, 1.20, 1.19, 1.18, 1.17, 1.16, 1.15, 1.14, 1.13, 1.12, 1.11, 1.10, 1.09, 1.08, 1.07, 1.06, 1.05, 1.04, 1.03, 1.02, 1.01, 1.00, 0.99, 0.98, 0.97, 0.96, 0.95, 0.94, 0.93, 0.92, 0.91, 0.90, 0.89, 0.88, 0.87, 0.86, 0.85

¹H NMR Spectrum (Top):

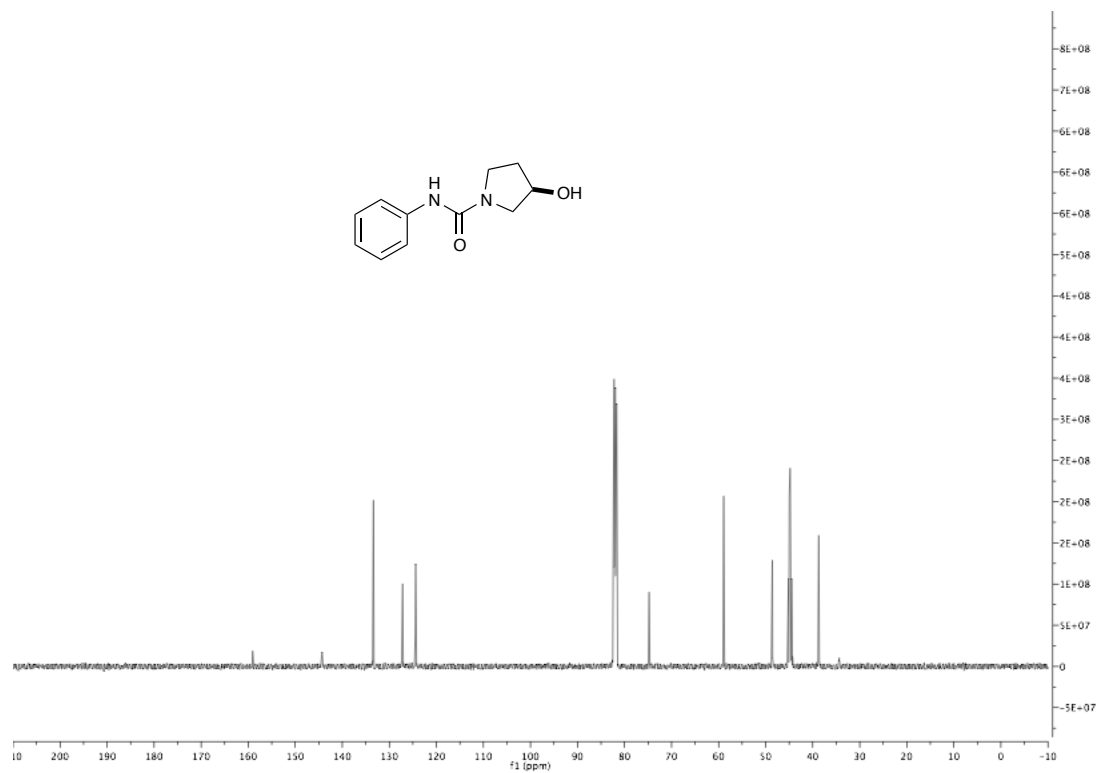
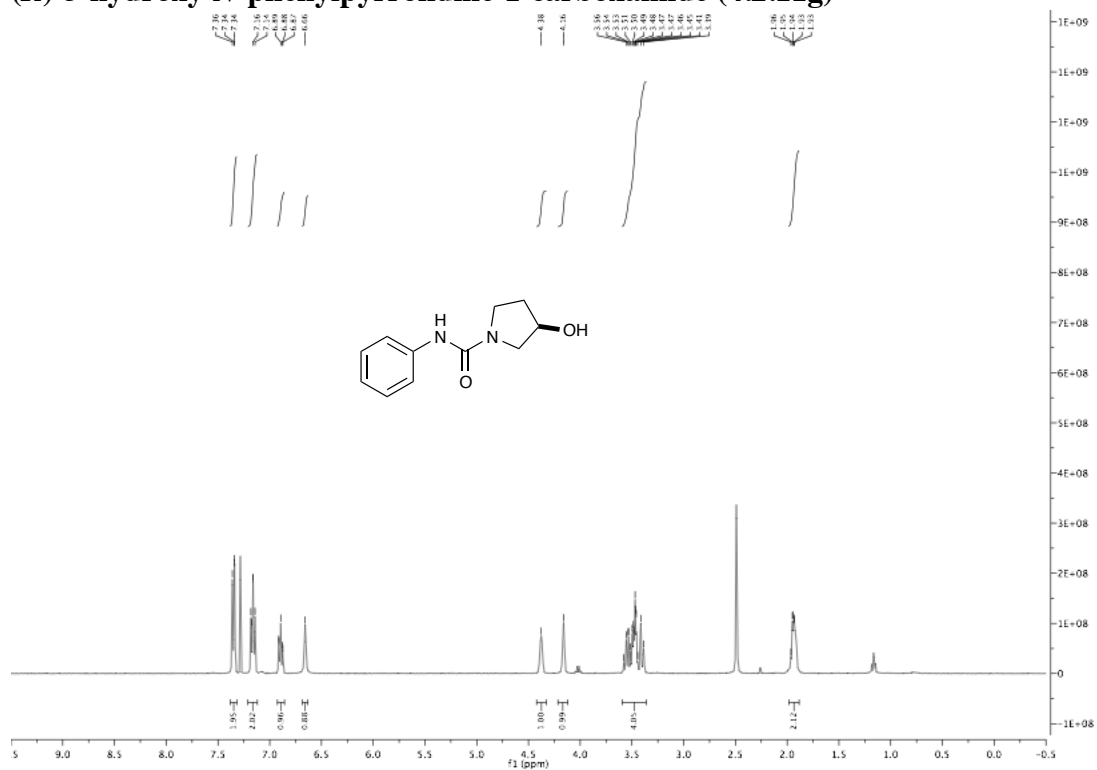
Chemical structure: Clc1ccc(cc1)S(=O)(=O)N1CCCC(C1)Cc2ccccc2

Peak list (ppm): 7.78, 7.68, 7.49, 7.32, 7.30, 7.28, 7.26, 7.24, 7.22, 7.20, 7.18, 7.16, 7.14, 7.12, 7.10, 7.08, 7.06, 7.04, 7.02, 7.00, 6.98, 6.96, 6.94, 6.92, 6.90, 6.88, 6.86, 6.84, 6.82, 6.80, 6.78, 6.76, 6.74, 6.72, 6.70, 6.68, 6.66, 6.64, 6.62, 6.60, 6.58, 6.56, 6.54, 6.52, 6.50, 6.48, 6.46, 6.44, 6.42, 6.40, 6.38, 6.36, 6.34, 6.32, 6.30, 6.28, 6.26, 6.24, 6.22, 6.20, 6.18, 6.16, 6.14, 6.12, 6.10, 6.08, 6.06, 6.04, 6.02, 6.00, 5.98, 5.96, 5.94, 5.92, 5.90, 5.88, 5.86, 5.84, 5.82, 5.80, 5.78, 5.76, 5.74, 5.72, 5.70, 5.68, 5.66, 5.64, 5.62, 5.60, 5.58, 5.56, 5.54, 5.52, 5.50, 5.48, 5.46, 5.44, 5.42, 5.40, 5.38, 5.36, 5.34, 5.32, 5.30, 5.28, 5.26, 5.24, 5.22, 5.20, 5.18, 5.16, 5.14, 5.12, 5.10, 5.08, 5.06, 5.04, 5.02, 5.00, 4.98, 4.96, 4.94, 4.92, 4.90, 4.88, 4.86, 4.84, 4.82, 4.80, 4.78, 4.76, 4.74, 4.72, 4.70, 4.68, 4.66, 4.64, 4.62, 4.60, 4.58, 4.56, 4.54, 4.52, 4.50, 4.48, 4.46, 4.44, 4.42, 4.40, 4.38, 4.36, 4.34, 4.32, 4.30, 4.28, 4.26, 4.24, 4.22, 4.20, 4.18, 4.16, 4.14, 4.12, 4.10, 4.08, 4.06, 4.04, 4.02, 4.00, 3.98, 3.96, 3.94, 3.92, 3.90, 3.88, 3.86, 3.84, 3.82, 3.80, 3.78, 3.76, 3.74, 3.72, 3.70, 3.68, 3.66, 3.64, 3.62, 3.60, 3.58, 3.56, 3.54, 3.52, 3.50, 3.48, 3.46, 3.44, 3.42, 3.40, 3.38, 3.36, 3.34, 3.32, 3.30, 3.28, 3.26, 3.24, 3.22, 3.20, 3.18, 3.16, 3.14, 3.12, 3.10, 3.08, 3.06, 3.04, 3.02, 3.00, 2.98, 2.96, 2.94, 2.92, 2.90, 2.88, 2.86, 2.84, 2.82, 2.80, 2.78, 2.76, 2.74, 2.72, 2.70, 2.68, 2.66, 2.64, 2.62, 2.60, 2.58, 2.56, 2.54, 2.52, 2.50, 2.48, 2.46, 2.44, 2.42, 2.40, 2.38, 2.36, 2.34, 2.32, 2.30, 2.28, 2.26, 2.24, 2.22, 2.20, 2.18, 2.16, 2.14, 2.12, 2.10, 2.08, 2.06, 2.04, 2.02, 2.00, 1.98, 1.96, 1.94, 1.92, 1.90, 1.88, 1.86, 1.84, 1.82, 1.80, 1.78, 1.76, 1.74, 1.72, 1.70, 1.68, 1.66, 1.64, 1.62, 1.60, 1.58, 1.56, 1.54, 1.52, 1.50, 1.48, 1.46, 1.44, 1.42, 1.40, 1.38, 1.36, 1.34, 1.32, 1.30, 1.28, 1.26, 1.24, 1.22, 1.20, 1.18, 1.16, 1.14, 1.12, 1.10, 1.08, 1.06, 1.04, 1.02, 1.00, 0.98, 0.96, 0.94, 0.92, 0.90, 0.88, 0.86, 0.84, 0.82, 0.80, 0.78, 0.76, 0.74, 0.72, 0.70, 0.68, 0.66, 0.64, 0.62, 0.60, 0.58, 0.56, 0.54, 0.52, 0.50, 0.48, 0.46, 0.44, 0.42, 0.40, 0.38, 0.36, 0.34, 0.32, 0.30, 0.28, 0.26, 0.24, 0.22, 0.20, 0.18, 0.16, 0.14, 0.12, 0.10, 0.08, 0.06, 0.04, 0.02, 0.00, -0.02, -0.04, -0.06, -0.08, -0.10, -0.12, -0.14, -0.16, -0.18, -0.20, -0.22, -0.24, -0.26, -0.28, -0.30, -0.32, -0.34, -0.36, -0.38, -0.40, -0.42, -0.44, -0.46, -0.48, -0.50, -0.52, -0.54, -0.56, -0.58, -0.60, -0.62, -0.64, -0.66, -0.68, -0.70, -0.72, -0.74, -0.76, -0.78, -0.80, -0.82, -0.84, -0.86, -0.88, -0.90, -0.92, -0.94, -0.96, -0.98, -1.00, -1.02, -1.04, -1.06, -1.08, -1.10, -1.12, -1.14, -1.16, -1.18, -1.20, -1.22, -1.24, -1.26, -1.28, -1.30, -1.32, -1.34, -1.36, -1.38, -1.40, -1.42, -1.44, -1.46, -1.48, -1.50, -1.52, -1.54, -1.56, -1.58, -1.60, -1.62, -1.64, -1.66, -1.68, -1.70, -1.72, -1.74, -1.76, -1.78, -1.80, -1.82, -1.84, -1.86, -1.88, -1.90, -1.92, -1.94, -1.96, -1.98, -2.00, -2.02, -2.04, -2.06, -2.08, -2.10, -2.12, -2.14, -2.16, -2.18, -2.20, -2.22, -2.24, -2.26, -2.28, -2.30, -2.32, -2.34, -2.36, -2.38, -2.40, -2.42, -2.44, -2.46, -2.48, -2.50, -2.52, -2.54, -2.56, -2.58, -2.60, -2.62, -2.64, -2.66, -2.68, -2.70, -2.72, -2.74, -2.76, -2.78, -2.80, -2.82, -2.84, -2.86, -2.88, -2.90, -2.92, -2.94, -2.96, -2.98, -3.00, -3.02, -3.04, -3.06, -3.08, -3.10, -3.12, -3.14, -3.16, -3.18, -3.20, -3.22, -3.24, -3.26, -3.28, -3.30, -3.32, -3.34, -3.36, -3.38, -3.40, -3.42, -3.44, -3.46, -3.48, -3.50, -3.52, -3.54, -3.56, -3.58, -3.60, -3.62, -3.64, -3.66, -3.68, -3.70, -3.72, -3.74, -3.76, -3.78, -3.80, -3.82, -3.84, -3.86, -3.88, -3.90, -3.92, -3.94, -3.96, -3.98, -4.00, -4.02, -4.04, -4.06, -4.08, -4.10, -4.12, -4.14, -4.16, -4.18, -4.20, -4.22, -4.24, -4.26, -4.28, -4.30, -4.32, -4.34, -4.36, -4.38, -4.40, -4.42, -4.44, -4.46, -4.48, -4.50, -4.52, -4.54, -4.56, -4.58, -4.60, -4.62, -4.64, -4.66, -4.68, -4.70, -4.72, -4.74, -4.76, -4.78, -4.80, -4.82, -4.84, -4.86, -4.88, -4.90, -4.92, -4.94, -4.96, -4.98, -5.00, -5.02, -5.04, -5.06, -5.08, -5.10, -5.12, -5.14, -5.16, -5.18, -5.20, -5.22, -5.24, -5.26, -5.28, -5.30, -5.32, -5.34, -5.36, -5.38, -5.40, -5.42, -5.44, -5.46, -5.48, -5.50, -5.52, -5.54, -5.56, -5.58, -5.60, -5.62, -5.64, -5.66, -5.68, -5.70,

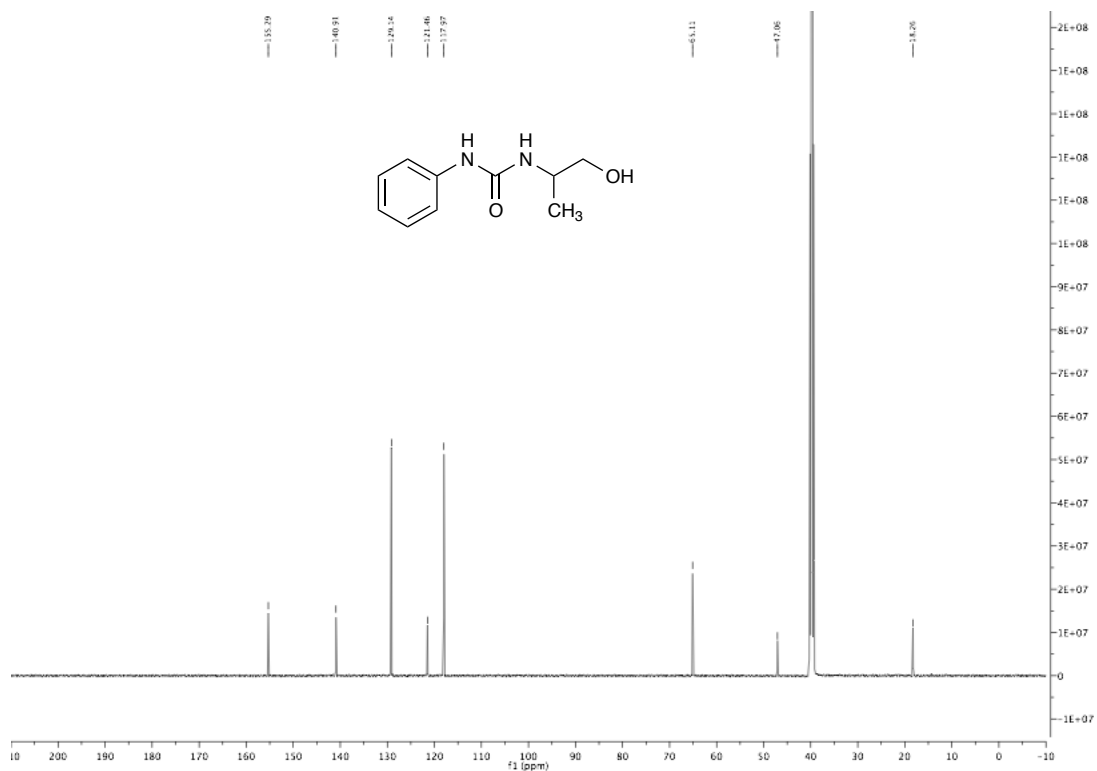
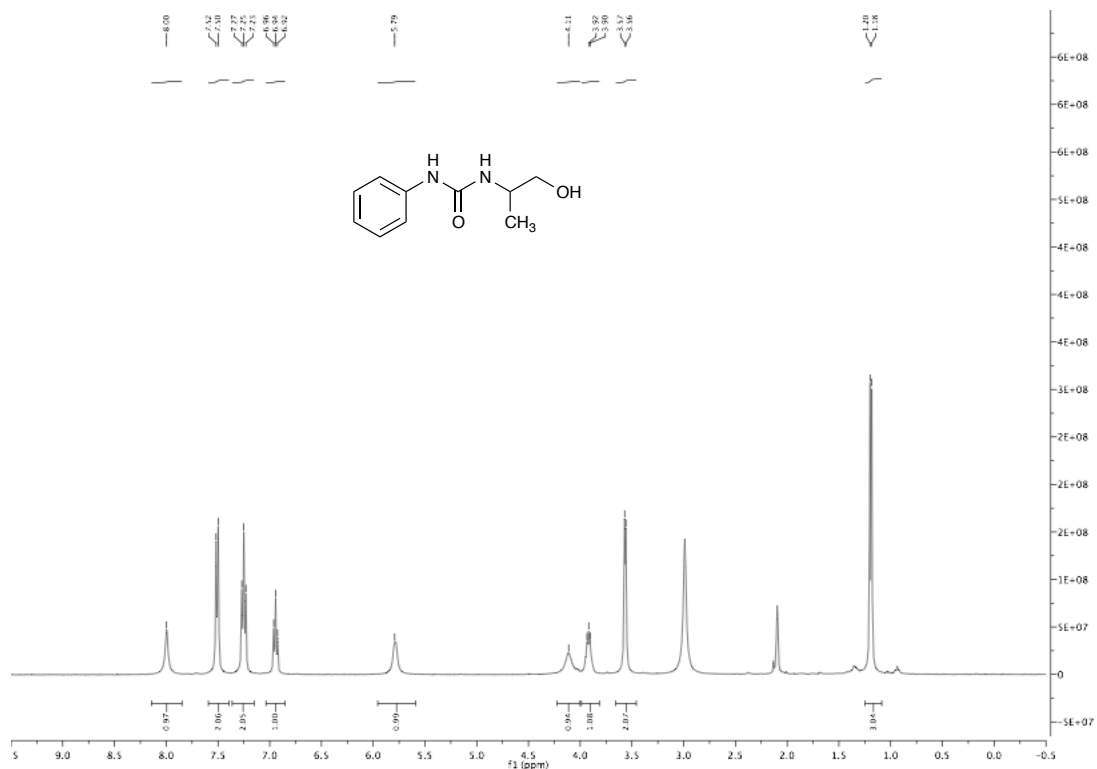
(S)-2-(hydroxymethyl)-N-phenylpyrrolidine-1-carboxamide (4.2.11f)



(R)-3-hydroxy-N-phenylpyrrolidine-1-carboxamide (4.2.11g)



1-(1-hydroxypropan-2-yl)-3-phenylurea (4.2.11h)



Chemical structure of (S)-1-(benzylideneamino)-2-hydroxycyclohexane (1a) is shown above its ¹H NMR spectrum (400 MHz, CDCl₃). The spectrum displays characteristic peaks for the compound, including aromatic protons (7.3-7.5 ppm), the amide NH (5.1 ppm), the cyclohexane protons (1.5-2.5 ppm), and the hydroxyl group (1.0 ppm).

